THE UNIVERSITY of York

Exploiting imidate ligand effects in transition metal-mediated C-C bond forming processes

Jonathan Paul Reeds

PhD

University of York

Chemistry

August 2010

Abstract

The effects of substituting (pseudo)halide for imidate ligands in Au(I) and Au(III) ([AuBr(NHC)] and [$AuBr_3$(NHC)]), Ru(II) ([$RuCl_2$(CHR)(L_2)]) and Pd(II) ([$Pd(OAc)_2$]) complexes has been investigated. The activity of these complexes as (pre)catalysts in enyne cycloisomerisation and propargylic nucleophilic substitution, diene ring-closing metathesis and ring-opening metathesis polymerisation and direct arylation reactions, respectively, has been determined.

[Au(*N*-imidate)(NHC)] and [$AuBr_2$(*N*-imidate)(NHC)] complexes were prepared and the structure and bonding of the complexes examined spectroscopically and crystallographically. The [$AuBr_2$(*N*-imidate)(NHC)] complexes, in combination with co-catalytic silver salts, were tested for activity in the cycloisomerisation of 1,5- and 1,6-enynes and found to be more effective than tribromide analogues. Kinetic analysis of the reactions showed subtle changes to the imidate structure had a pronounced effect on the activity of the complexes and the use of the silver salt Ag[$Al(OC(CF_3)_3)_4$] as a co-catalyst greatly increased catalytic activity. The complexes were also found to catalyse a unique tandem nucleophilic substitution-cycloisomerisation of propargyl alcohols and allylsilanes. [$AuBr_2$(*N*-tfs)(I^tPe)] was found to be an effective precatalyst for this reaction whilst Au(III) tribromide and Au(I) complexes were ineffective. 1,3-Diarylbicyclo[3.1.0]hexenes products were found to undergo a post-reaction ambient temperature 1,3-carbon shift isomerisation.

The complex [Ru(*N*-tfs)$_2$(*o*-^{i}PrO-CHPh)($IMesH_2$)] was prepared and characterised spectroscopically and crystallographically. The complex was found to be inactive in the ring-closing metathesis and ring-opening metathesis polymerisation of alkenes. Attempts to selectively substitute chloride for imidate ligands derived from imides with higher pKa's of 8.3-9.7 (in water) resulted in decomposition of the alkylidene or benzylidene ligand.

[$Pd(imidate)_2$(MeCN)] and [$Pd(imidate)_2$(THT)] complexes were prepared and analysed by NMR and infra-red spectroscopy. The complexes were tested for activity in the direct arylation of imidazole with iodoarenes without added base or neutral ligands. The activity of the complexes was to some degree dependant on the structure of the imidate ligand, possessing moderate activity in comparison with [$Pd(OAc)_2$]. The activity of other palladium sources and conditions for this reaction were investigated and it was found that the formation of Pd nanoparticles may be key to reaction progression.

Acknowledgements

The results contained in the thesis could not have been obtained without the contributions of many people. I would firstly like to thank the technical staff of the elemental analysis, NMR and mass spectroscopy services at the University of York for running many spectra and for technical advice. The ESPRC national solid state NMR service technicians at the University of Durham for spectra and very helpful analysis. Adrian Whitworth and Rob Thatcher for the crystallographic information contained within this thesis. John Slattery and Zhenyang Lin for carrying out computational calculations and for the explanation of them. Ellie Hurst for mentoring when I first arrived in York and initial studies on Au(I) imidate complexes and Anant Kapdi for initial studies on Pd bis imidate complexes. Ben Moulton and Amanda Jarvis for helping to run NMR experiments. Mark for his supervision and advice and (along with the staff at GSK) for his help and support whilst I worked at GSK Harlow. Many thanks to Ian for his supervision over the last three years, for advice and corrections during the writing of this thesis and his ideas. Tom, Tony, Mike, Amanda, Sara and the rest of the Fairlamb group for making the lab an interesting place to work. My parents for supporting me during the compilation of this thesis. And Jillian for understanding, support, encouragement and motivation throughout my PhD.

Author's declaration

I declare that all the work presented in this thesis is my own, and that any material not my own is clearly referenced or acknowledged in the main body of the text. The work was conducted between October 2006 and May 2010.

Jonathan Paul Reeds

August 2010

Abbreviations

Ac	acetyl
app.	apparent
Ar	aryl
aq.	aqueous
asym.	asymmetric
br	broad
Bu	butyl
cat.	catalyst
COD	cyclooctadiene
conc.	concentrated
Conv.	conversion
Cp	cyclopentadienyl
Cy	cyclohexyl
d	doublet
dbs	2,3-dibromosuccinimidate
DCM	dichloromethane
DFT	density functional theory
DMA	dimethylacetamide
DMF	dimethylformamide
DMSO	dimethylsulfoxide
ee	enantiomeric excess
EI	electron impact
equiv.	equivalents
ESI	electrospray ionisation
Et	ethyl
h	hours
HMPA	hexamethylphosphoramide
HRMS	high resolution mass spectrometry
Hz	hertz
IR	infra-red
LDA	lithium diisopropylamide
Lit.	literature
LUMO	lowest unoccupied molecular orbital
m (IR)	medium
m (NMR)	multiplet

M	molar
mal	maleimidate
Me	methyl
Mes	mesityl
mg	milligrams
MHz	mega hertz
mol	moles
mmol	millimoles
Ms	mesyl
MS	mass spectrum
NMR	nuclear magnetic resonance
obs	*o*-benzoic sulfimidate
Pe	pentyl
Ph	phenyl
Pr	propyl
ptm	phthalimidate
Py	pyridine
q	quartet
r.t.	room temperature
s (IR)	strong
s (NMR)	singlet
succ	succinimidate
t	triplet
^{t}Bu	*tert*-butyl
temp.	temperature
Tf	triflate
tfs	tetrafluorosuccinimidate
THF	tetrahydrofuran
TLC	thin layer chromatography
TMS	trimethylsilyl
^{t}Pe	*tert*-pentyl
sym.	symmetric
UV	ultra-violet
w	weak
w.r.t.	with respect to

Contents

Chapter 1. Introduction

1.1. Halide ligands in organometallic chemistry

Metal halogen bonds are prevalent throughout organometallic chemistry and appear in a significant number of homogenous transition metal catalysts. Optimisation of these anionic ligands is often neglected despite there being many examples of the nature of the anionic ligand affecting catalytic efficiency. Halide ligands can influence a catalyst in a number of ways, principally electronically, but also by polarisability, nucleophilicity, the *trans* effect and sterics.[1] The effects of changing a halide ligand is not always easily predictable due to their σ and π donor properties, for example although fluorine is the weakest σ donor due to electronegativity, it is the strongest π donor as it possesses more contracted p orbitals.[2] Also, the ligand effect in catalysis will depend upon the electronic structure of the metal atom, as π donation can stabilise (for low electron counts) or destabilise (for high electron counts) the reaction transition states and intermediates. The combination of hard and soft ligands and metals will also significantly effect metal halide bond strengths.

The nature of the halide ligand can effect many aspects of the reactivity of a transition metal complex. For example, the rate and mechanism of the phosphine catalysed isomerisation of *cis*-$[PtX_2(PR_3)_2]$ (where R is Me, Et or *o*-tolyl and X is halide) to *trans*-$[PtX_2(PR_3)_2]$ is dependant on the halide ligand. The rate of isomerisation is in the order: I>Br>Cl. This reflects the stability of the proposed five coordinate $[PtX_2(PR_3)_3]$ intermediates.[3] Similar effects are observed in analogous Pd(II) complexes.[4]

Variation of halide ligands cannot only affect the rate and yield of a reaction it can also have less expected results, such as affecting product distribution and enantiomeric excess (*ee*). Zhang and co-workers[5] have observed a significant halide effect in the Rh(I) catalysed enantioselective hydrogenation of ketones (Scheme 1). For example, with acetophenone **1** it was found that using a $[\{Rh(1,5\text{-}COD)Cl\}_2]$ catalyst, in combination with chiral phosphane ligand **3**, 45% conversion to **2** in 57% *ee* was observed, which was improved to 67% *ee* (44% conversion) using a LiCl additive (one equivalent relative to Rh). However, with KBr both conversion (89%) and *ee* (92%) improved dramatically. The bromide is speculated to replace the chloride ligand in the Rh complex to generate a more active catalyst.

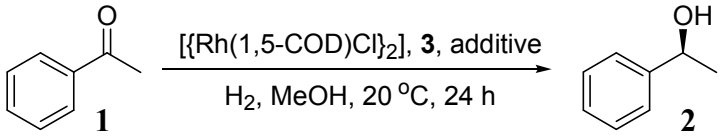

Entry	Additive	Conversion (%)	*ee* (%)
1	-	45	57
2	LiCl	44	67
3	KBr	89	92

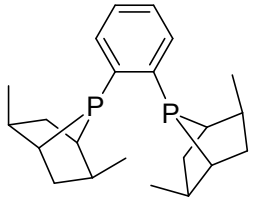

3

Scheme 1. Effect of halide salt additives on the outcome of the Rh(I) catalysed asymmetric hydrogenation of acetophenone (**1**).

Cooper and Caulton[6] have studied the effect of halide ligand variation on the Ir(III) catalysed isomerisation of 3-phenylprop-1-ene (**4**) to 1-phenylprop-1-ene (**5**) (Scheme 2). They found that the use of a fluoride ligand increased the reaction rate 55.4 times relative to iodide and that pseudohalide OCH_2CF_3 and OH ligands were 35.4 and 10.0 times more efficient than iodide, respectively. The authors concluded that stronger π donor ligands stabilised a coordinatively unsaturated 14 electron active catalytic species (believed to be $[IrH(\eta^2\text{-}C_6H_4P^tBu_2)(X)]$). This demonstrates the significant effect imparted by π-donating halide ligands on the outcome of a reaction.

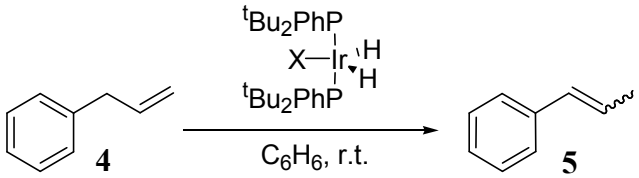

Entry	X	Relative rate
1	I	1
2	Br	2.5
3	Cl	6.2
4	OH	10.0
5	OCH_2CF_3	35.4
6	F	55.4

Scheme 2. The effect of changing the nature of the halide ligand in an $[IrX(H)_2(P^tBu_2Ph)_2]$ catalysed isomerisation reaction.

Ashimori *et al.*[7] have studied the effect of adding halide and pseudohalide salts to the palladium catalysed asymmetric Heck reaction of **6** to **7** (Scheme 3). The highest yield for the reaction (72%) is achieved with no halide salt added, however the enantiomeric excess (*ee*) is low (43%), a similar outcome is observed with added $[Bu_4N]OTf$. Adding $[Bu_4N]Cl$ or $[Bu_4N]Br$ produces a large improvement in *ee* (93%) at the expense of yield (52% and 59%, respectively). Adding $[Bu_4N]I$ gives a better yield (62%) with a slight reduction in *ee* (90%). The halide is thought to influence the reaction by coordinating to the Pd(II) species (formed from oxidative addition of the aryltriflate) during the enantioselective step of alkene coordination. In the absence of added halide (or with added triflate) the anion dissociates after oxidative addition and the alkene coordinates to a coordinatively unsaturated cationic Pd(II) species with reduced enantioselective bias.

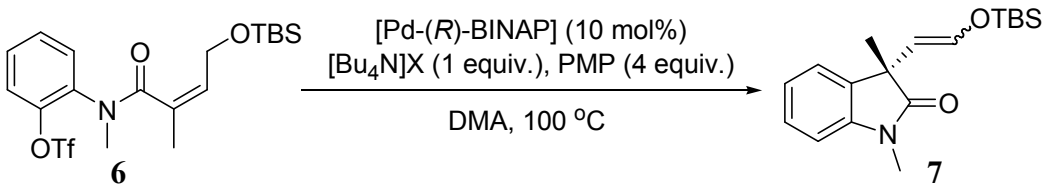

Entry	X	Yield (%)	*ee* (%)
1	None	72	43
2	OTf	70	42
3	Cl	52	93
4	Br	59	93
5	I	62	90

{(*R*)-BINAP is (*R*)-(+)-2,2′-bis(diphenylphosphino)-1,1′-binaphthyl, PMP is 1,2,2,6,6-pentamethylpiperidine, TBS is *tert*-butyldimethylsilyl}

Scheme 3. The effect of $[Bu_4N]X$ additives on the yield and enantiomeric excess of a [Pd-(R)-BINAP] catalysed asymmetric Heck reaction.

Bovens *et al.*[8] observed a similar effect of halide salt additives on the yield and enantiomeric excess of a palladium catalysed asymmetric allylic alkylation (Scheme 4). In the absence of a halide salt high yield (90%) but moderate *ee* (66%) was observed, and addition of $[NBu_4]Br$ gave similar results. Added $[NBu_4]Cl$ however reduces the yield slightly (85%) but gives much improved *ee* (83%), whereas addition of $[NBu_4]I$ poisons the catalyst resulting in only 4% yield and 51% *ee*.

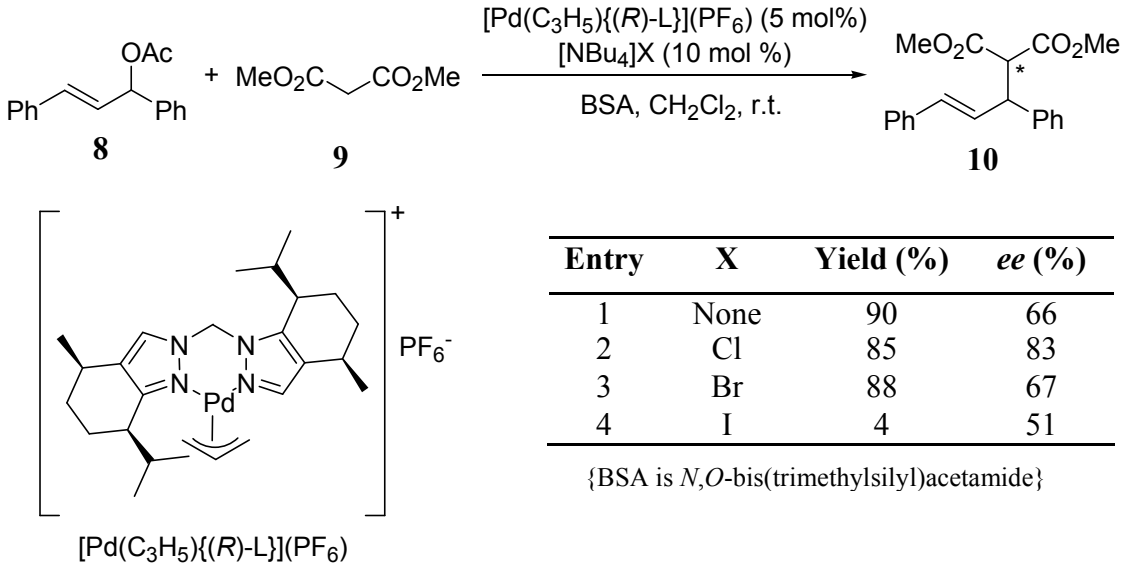

Entry	X	Yield (%)	*ee* (%)
1	None	90	66
2	Cl	85	83
3	Br	88	67
4	I	4	51

{BSA is *N*,*O*-bis(trimethylsilyl)acetamide}

Scheme 4. The effect of $[NBu_4]X$ additives on the yield and enantiomeric excess of a Pd catalysed asymmetric allylic alkylation reaction.

These examples demonstrate not only the impact anionic ligands and additives can have on all aspects of a reaction outcome but also the difficulty of predicting the effect of the nature of the ligand on the reaction. Optimising a catalyst for both yield and enantiomeric excess using the limited halide series of ligands is a significant challenge.

1.2. Imidate anions as pseudohalides

The groups of Fairlamb, Taylor and Serrano[9] found that the nature of the anionic ligand in Pd(II) catalysed Stille cross coupling reactions had a considerable impact on product yields, with imidate[10] ligands, such as succinimidate, found to be particularly effective (Table 1). For example, in the reaction of benzyl bromide (**11**) with ethyl (*Z*)-3-(tributylstannyl)propenoate (**12**) $[PdBr(N\text{-succ})(PPh_3)_2]$[11] was found to be very efficient (99% yield in 1.5 hours) relative to $Pd(PPh_3)_4$ (17% in 18 hours) and $Pd(OAc)_2/PPh_3$ (16% in 18 hours). A significant effect of the imidate ligand on reactivity was observed, $[PdBr(N\text{-succ})(PPh_3)_2]$ was shown to be more active than $[PdI(N\text{-succ})(PPh_3)_2]$ (56%, 18 hours), $[PdBr_2(PPh_3)_2]$ (23%, 18 hours), $[Pd(N\text{-succ})_2(PPh_3)_2]$ (10%, 48 hours) and $[PdBr(N\text{-ptm})(PPh_3)_2]$ (73%, 1.5 hours).

Table 1. The effect of changing anionic ligands on rate and yield in a palladium catalysed Stille cross coupling reaction.

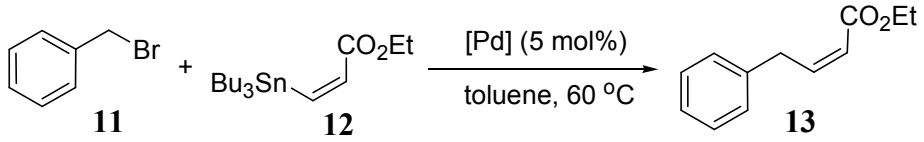

11 **12** **13**

Entry	Complex	Time (hrs)	Yield (%)
1	[PdBr(*N*-succ)(PPh_3)$_2$]	1.5	99
2	[Pd(PPh_3)$_4$]	18	17
3	Pd(OAc)$_2$/PPh_3	18	16
4	[PdI(*N*-succ)(PPh_3)$_2$]	18	56
5	[PdBr$_2$(PPh_3)$_2$]	18	23
6	[Pd(*N*-succ)$_2$(PPh_3)$_2$]	48	10
7	[PdBr(*N*-ptm)(PPh_3)$_2$]	1.5	72

The validity of succinimidate as a halide mimic (pseudohalide) was established by Adams *et al.*[12] who studied the σ and π donor properties of the succinimidate ligand using a method developed by Graham.[13] This method involves the synthesis of [MnX(CO)$_5$] complexes, where X is the anionic ligand under study, and the measurement of the carbonyl stretching frequencies of the CO ligands by infra-red spectroscopy. This data is used to calculate force constants for the bonds from which σ and π, donor and acceptor bonding parameters are calculated relative to [Mn(CH_3)(CO)$_5$] (Table 2).

Table 2. Calculated σ and π bonding parameters for anionic ligands in [MnX(CO)$_5$] complexes.

Entry	X	σ (mdyn.Å^{-1})	π (mdyn.Å^{-1})
1	CH_3	0	0
2	succinimidate	1.32	-0.65
3	Cl	1.25	-0.57
4	Br	1.03	-0.44
5	I	0.73	-0.27

Large positive σ values correspond to weak σ donor ligands (strictly as the ligands are assumed to be neutral in the model they correspond to strong σ acceptors of the electron density in the Mn-X bond) and large negative π values correspond to strong π donor

ligands. These values show that, as would be expected, chloride is a weaker σ donor but stronger π donor than bromide and iodide. Succinimidate is calculated to have comparable properties to chloride, with slightly weaker σ donor and slightly stronger π bonding parameters.

1.3. Scope of this project

This project specifically focuses on studying the effect of substituting halide for imidate pseudohalide ligands in homogeneous organometallic transition metal catalysts. The principal imidate ligands that have been employed are succinimidate (**14**), 2,3-dibromosuccinimidate (**15**), tetrafluorosuccinimidate (**16**), maleimidate (**17**), phthalimidate (**18**) and *o*-benzoic sulfimidate (**19**). The electronic properties of the imidate ligand is dependant on the substituents on the ligand backbone.[14] Succinimidate is a legitimate mimic of a chloride ligand (*vide supra*), the other imidates under study contain electron withdrawing functionality and so would be expected to be weaker σ donors and stronger π donors based on the pK_a of the parent imide (Figure 1).

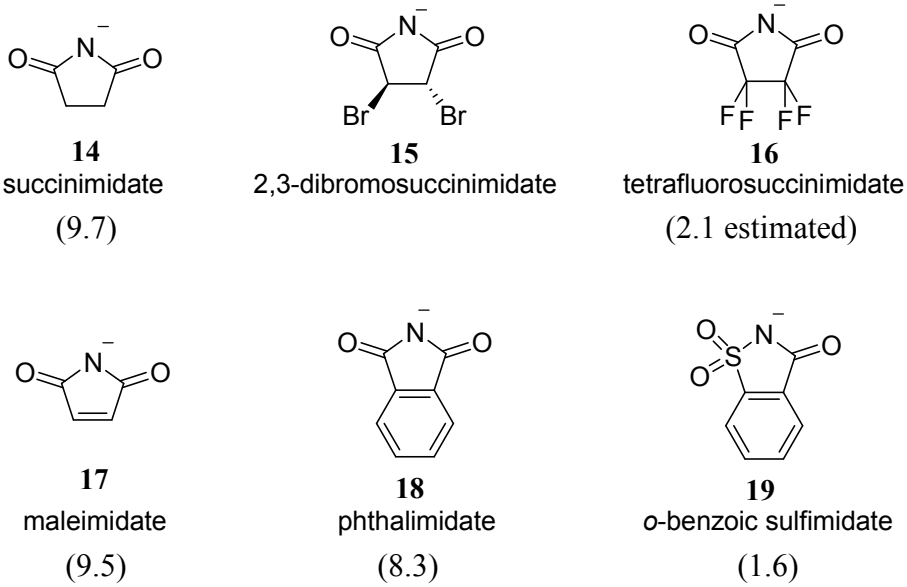

Figure 1. Imidate anions used as pseudohalide ligands in this study. The pK_a's of the parents imides in water are given where known.[15]

Imidate ligands have been reported to coordinate to metal atoms in three general ways; *N*-monodentate (I),[16] *N*,*O*-bidentate chelating (II)[17] and *N*,*O*-bidentate bridging (III)[18] (Figure 2).

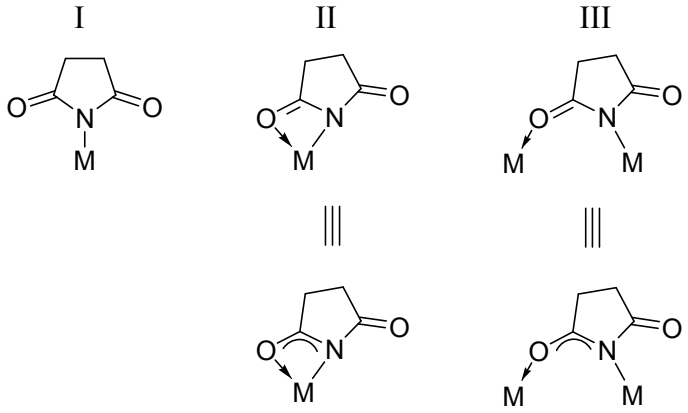

Figure 2. The three general coordination modes of imidate ligands in transition metal complexes.

This study will investigate the effect of substituting halide for imidate ligands in three topical transition metal catalysed processes studied within the Fairlamb research group, Au catalysed enyne cycloisomerisation,[19] Ru catalysed diene metathesis[20] and Pd catalysed direct arylation of arylhalides and heteroarenes.[21] A series of complexes containing the range of imidate ligands shown above will be prepared in order to study the effect of the nature of the imidate ligand on the properties and reactivity of these, relative to parent halide, complexes.

The results of this study are divided into three chapters, Chapter 2: Au complexes, Chapter 3: Ru complexes and Chapter 4: Pd complexes. A detailed introduction to these specific areas is given at the beginning of each chapter to aid and direct the reader.

1.4. References

(1) Fagnou, K.; Lautens, M. *Angew. Chem. Int., Ed.* **2002**, *41*, 26-47.

(2) Caulton, K. G. *New J. Chem.* **1994**, *18*, 25-41.

(3) Favez, R.; Roulet, R.; Pinkerton, A. A.; Schwarzenbach, D. *Inorg. Chem.* **1980**, *19*, 1356-1365.

(4) Anderson, G. K.; Cross, R. J. *J. Chem. Soc. Rev.* **1980**, *9*, 185-215.

(5) Jiang, Q.; Jiang, Y.; Xiao, D.; Cao, P.; Zhang, X. *Angew. Chem., Int. Ed.* **1998**, *37*, 1100-1103.

(6) Cooper, A. C.; Caulton, K. G. *Inorg. Chim. Acta.* **1996**, *251*, 41-51.

(7) Ashimori, A.; Bachand, B.; Calter, M. A.; Govek, S. P.; Overman, L. E.; Poon, D. J. *J. Am. Chem. Soc.* **1998**, *120*, 6488-6499.

(8) Bovens, M.; Togni, A.; Venanzi, L. M. *J. Organomet. Chem.* **1993**, *451*, C28-C31.

(9) (a) Crawforth, C. M.; Burling, S.; Fairlamb, I. J. S.; Taylor, R. J. K..; Whitwood, A. C. *Chem. Commun.* **2003**, 2194 – 2195; (b) Fairlamb, I. J. S.; Taylor, R. J. K.; Serrano, J. L.; Sanchez, G. *New J. Chem.* **2006**, *30*, 1695-1704.

(10) The name "imidate" is derived from the anions of imide-type compounds (*e.g.* succinimide, maleimide and phthalimide), which is commonly used in organometallic chemistry. Imino groups, and associated imidates, can mean something slightly different in organic chemistry {*e.g.* ROC(=NR')R" or ROC(=NHR'$^{+}$)R"}.

(11) Serrano, J. L.; Zheng, Y.; Dilworth, J. R.; Sánchez, G. *Inorg. Chem. Commun.* **1999**, *2*, 407-410.

(12) Adams, H.; Bailey, N. A.; Briggs, T. N.; Mccleverty, J. A.; Colquhoun, H. M.; Williams, D. J. *J. Chem. Soc., Dalton Trans.* **1986**, 813-819.

(13) Graham, W. A. G. *Inorg. Chem.* **1968**, *7*, 315-321.

(14) Hine, J.; Hahn, S.; Hwang, J. *J. Org. Chem*. **1988**, *53*, 884-887.

(15) (a) *o*-Benzoic sulfimide: Bell, R. P.; Higginson, W. C. E. *Proc. Roy. Soc. A* **1949**, *197*, 141-159; (b) The pK_a of tetrafluorosuccinimide was estimated by the authors by comparison of the pK_a of succinimide to pyrollidium (11.31) and 3,3,4,4-tetrafluoropyrrolidinium (4.05) ions: Hine, J.; Hahn, S.; Hwang, J. *J. Org. Chem.* **1988**, *53*, 884–887; (c) Phthalimide: Bell, R. P.; Higginson, W. C. E. *Proc. Roy. Soc. A* **1949**, *197*, 141-159; (d) Maleimide: Darnall, K. R.; Townsend, L. B.; Robins, R. K. *Proc. Nat. Ac. Sc. USA* **1967**, *57*, 548-553; (e) Succinimide: Schwarzenbach, G.; Lutz, K. *Helv. Chim. Acta.* **1940**, *23*, 1162-1190.

(16) (a) Price, S. J. B.; DiMartino, M. J.; Hill, D. T.; Kuroda, R.; Mazid, M. A.; Sadler, P. J. *Inorg. Chem.* **1985**, *24*, 3425-3434; (b) Shaver, A.; Hartgerink, J.; Lal, R. D.; Bird, P.; Ansari, N. *Organometallics* **1983**, *2*, 938-940; (c) Treichel, P. M.; Nakagaki, P. C.; Haller, K. J. *J. Organomet. Chem.* **1987**, *327*, 327-337; (d) Bukowska-Strzyzewska, M.; Tosik, A.; Wodka, D.; Zakrzewski, J. *Polyhedron* **1994**, *13*, 1689-1694.

(17) (a) Kurishima, S.; Matsuda, N.; Tamura, N.; Ito, T. *J. Chem. Soc., Dalton Trans.* **1991**, 1135-1142; (b) Bozkurt, E.; Karabulut, B.; Kartal, I. *Spectrochim. Acta, Part A* **2009**, *73*, 163-167.

(18) (a) Sahajpal, A.; Robinson, S. D.; Hursthouse, M. B.; Mazid, M. A. *J. Chem. Soc., Dalton Trans.* **1993**, 393-396; (b) Barbaris, M.; Estevan, F.; Lahuerta, P.; Perez-Prieto, J.; Sanau, M. *Inorg. Chem.* **2001**, *40*, 4226-4229; (c) Dohta, Y.; Browning, C. S.; Rekonen, P.; Kodaka, M.; Okada, T.; Okamoto,

K.-I.; Natale, R.; Yip, C.; Farrar, D.H.; Okuno, H. *Inorg. Chim. Acta* **1997**, *263*, 69-80; (d) Esteban, J.; Hirva, P.; Lahuerta, P.; Martinez, M. *Inorg. Chem.* **2006**, *45*, 8776-8784.

(19) Luzung, M. R.; Markham, J. P.; Toste, F. D. *J. Am. Chem. Soc.* **2004**, *126*, 10858-10859.

(20) Ritter, T.; Hejl, A.; Wenzel, A. G.; Funk, T. W.; Grubbs, R. H. *Organometallics* **2006**, *25*, 5740-5745.

(21) (a) Bellina, F.; Calandri, C.; Cauteruccio, S.; Rossi, R. *Tetrahedron* **2007**, *63*, 1970-1980; (b) Bellina, F.; Cauteruccio, S.; Rossi, R. *Eur. J. Org. Chem*. **2006**, 1379-1382.

Chapter 2: Au(I) and Au(III) imidate complexes; synthesis and catalytic activity

2.1. Introduction

2.1.1. Au catalysis

2.1.1.1. Au catalysts and Au catalysed transformations

In recent years there has been a surge in interest in the catalytic properties of gold in applied synthetic chemistry.[1] Au-complexes efficiently catalyze the transformation of C=C and C≡C bonds[2] in a diverse array of reactions including: nucleophilic substitution,[3] hydration,[4] cycloaddition,[5] rearrangement,[6] hydrosilylation,[7] polymerisation,[8] oxidation,[9] carbene transfer (C-H functionalisation/activation),[10] epoxidation,[11] hydroamination,[12] cycloisomerisation[13] and many tandem and domino processes.[14]

Au(I) complexes, typically of the type [AuXL], where L is a phosphine[15] or N-heterocyclic carbene (NHC)[16] ligand and X is a weakly coordinating anion (usually $^{-}$OTf or $^{-}PF_6$), have been widely used as catalysts for these reactions. First isolated by Arduengo[17] in the early 1990's, NHCs are N-stabilised Fischer carbenes based on an N-substituted imidazole unit.[18] These are stronger σ donors than phosphines, with little or no back donation, but without the drawback of sensitivity to oxygen. They are also easily electronically and sterically tuneable by changing the imidazole nature (*e.g.* saturation) and N substituents. NHCs also provide valuable information spectroscopically of the nature of *trans*-ligands and the electronic properties of the coordinated metal atom (by monitoring of the ^{13}C NMR signal of the carbene carbon).[19] Many different types have been prepared, mainly focusing on the variation in N substituents for saturated and unsaturated imidazole rings. *tert*-Butyl groups have been used to probe steric and inductive effects, but *tert*-pentyl have not. These alkyl groups are very similar electronically but the pentyl groups offer enhanced steric control and directing ability,[20] especially when combined with other asymmetric directing groups.

Inorganic Au(III) complexes and related salts, such as $AuCl_3$ and $Na[AuCl_4]$, have also been used to carry out similar transformations.[21] Generally, less attention has been directed toward the development of organometallic Au(III) catalysts and complexes.[22] Key examples include pyridine-derived iminophosphorane **20**[23] and *ortho*-carboxylate **21**[24] precatalysts (Figure 3). This is perhaps surprising, as Au(III) can promote Lewis acid-type

catalysis.[3a,25] Some examples include: hydrogenation,[26] hydrosilation,[27] addition of water and alcohols to triple bonds,[28] cycloisomerisation[24] and coupling of aldehydes, amines and terminal alkynes to produce propargyl amines.[29]

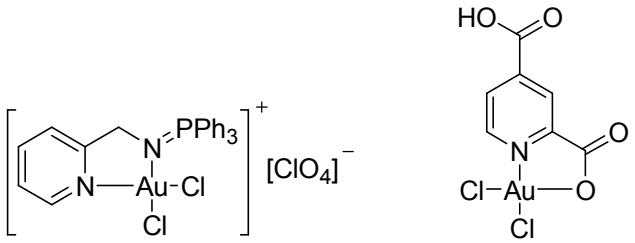

20 **21**

Figure 3. Pyridine-derived iminophosphorane (**20**) and *ortho*-carboxylate (**21**) precatalysts.

2.1.1.2. Active catalytic species in Au catalysis

Au(I) and Au(III) can display markedly different behaviour in reactions, proceeding *via* separate mechanisms to give different products and substitution patterns.[30] For example, the cycloisomerisation of 1,7-allenyne **22** in the presence of Au(I) results in *exo*- and *endo*-cyclohexenes **23** and Au(III) results in tetrahydroindene **24** (Scheme 5).[21d]

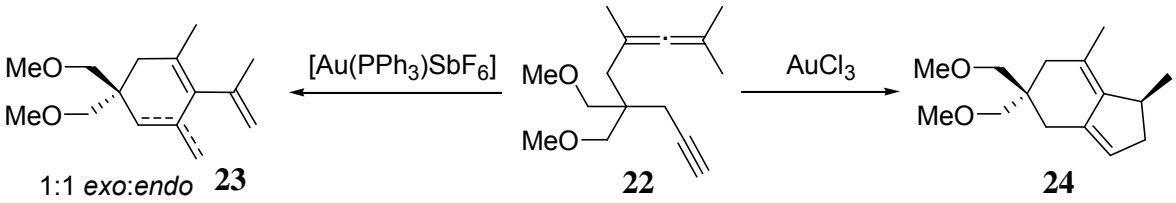

Scheme 5. Divergent cycloisomerisation of a 1,7-allenyne (**22**) in the presence of Au(I) and Au(III) catalysts (*exo*/*endo* refers to the position of the C=C bond in the product).

There is some contention about the role played by Au(III) in these reactions. It is known that Au(III) can be reduced to Au(I) during the course of reactions[31] and so Au(I) may be the catalytically active species in such processes. However, Au(I) can disproportionate into Au(0) and Au(III) photochemically,[32] thermally[33] and chemically,[34] a process used in the preparation of Au(0) nanoparticles. It is possible that both oxidation states could play a role in reactions, for example, Au(I) could be the active species where a soft π-acid is required (such as in cycloisomerisations), whereas Au(III) may be the active species where Lewis acidity is required (in neutral or cationic form).[35] Straub has carried out DFT calculations on the Au(I) and Au(III) catalysed intramolecular benzannulation of ethynyl benzaldehyde

and ethyne and found out that the overall activation barriers were essentially identical for both Au(I) and Au(III) catalysts.[36] Nolan[37] has stated that he suspects that the active catalyst in the reported hydration of alkynes and polymerisation of styrene mediated by [$AuBr_3$(NHC)] complexes and Au(III) salts is actually an Au(I) species formed by reductive elimination of the halide ligands. Au(III) is suspected to be the active species in other transformations[38] and protons may also play a role.[39] There is much spectroscopic and crystallographic evidence for the existence of $Au(I)^+$ ions in solution and the binding of alkenes and alkynes to such ions.[40] However, there has been no direct evidence of binding to $Au(III)^+$ ions and only some tentative NMR spectroscopic evidence of styrene binding to an $Au(III)^+$ ion (which has not been substantiated).[41]

2.1.1.3. Relativistic effects in Au catalysis

The unique reactivity of Au complexes stems from relativistic effects which are greatest for Au of all the elements (as the 4f and 5d orbitals are filled), although it is also large for Pt and Hg. Relativity becomes important where electrons have a velocity which is significant relative to the speed of light (about 58% for Au), when electrons are close to the heavy nucleus, increasing electron mass and causing orbital contraction of 6s and 6p and expansion of 5d orbitals. This results in increased metal-ligand bond strengths, decreased sensitivity to water and oxygen, reduced cycling between Au(I) and Au(III) oxidation states, reduced LUMO energy, and high electronegativity, ionisation energy and electron affinity. The low LUMO energy results in Lewis acidity, allowing Au to bind to alkenes and alkynes (binding is stronger to alkenes but only alkynes are reactive due to a lower LUMO). The anti-bonding orbitals are too high in energy for π back-bonding from Au and so the alkyne is efficiently activated for nucleophilic attack. Au is however able to back-bond into lower energy empty p orbitals which may be critical for the stabilisation of carbocationic intermediates in catalytic transformations.[42]

2.1.2. Au catalysis in the synthesis of biologically active molecules

As a result of these properties Au catalysts have found application in the total syntheses of natural products of biological importance.[43] An example is the total synthesis of ventricos-7(13)-ene (**25**),[44] a natural product found in liverwort (*Lophozia ventricosa*),[45] reported by Sethofer *et al*.. This synthesis utilises an Au(I) catalyst to carry out a tandem cyclisation/semipinacol rearrangement of cyclopropanol **26** to form hydrated

cyclobuta[*c*]pentalene **27**, which, following allylation and a palladium catalysed oxidative ring expansion, yields the hydrated cyclopenta[*c*]pentalene core (Scheme 6).

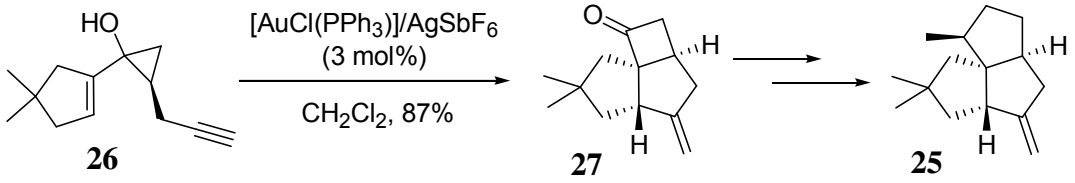

Scheme 6. Key Au-catalysed transformation in the total synthesis of ventricos-7(13)-ene (**25**).

Another example from the group of Toste is that of (+)-lycopladine A (**28**),[46] a natural product from the club moss *Lycopodium complanatum*.[47] Au-catalysed cycloisomerisation of 1,5-enyne **29** yields the bicyclo[4.3.0]nonane core (**30**) (Scheme 7).

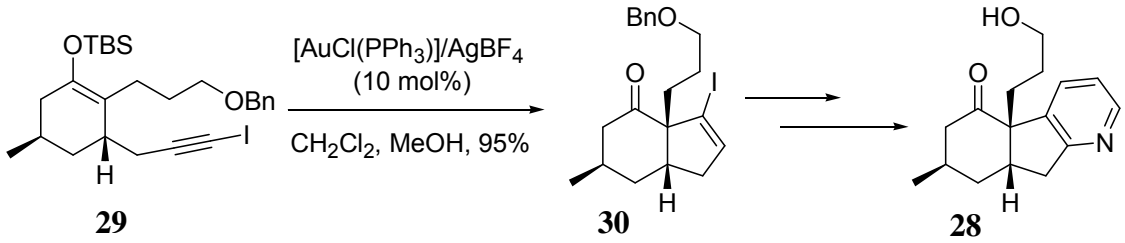

Scheme 7. Key Au-catalysed transformation in the total synthesis of (+)-lycopladine A (**28**).

2.1.3. Cycloisomerisation

2.1.3.1. 1,*n*-Enyne cycloisomerisation

The cycloisomerisation of 1,*n*-enynes, mediated by Au(I) and Au(III) salts, has received considerable attention, particularly 1,5-[15,48] and 1,6-,[49] although 1,7-[50] and 1,8-enynes[51] have also been investigated. Enyne cycloisomerisation can be catalysed by Ru,[52] Pd,[53] Pt,[54] Ir,[55] Rh,[56] Re[57], Ga[58] and In,[59] however Au(I) is usually more active and displays very high (and often different) selectivity.[60] Investigations have been carried out into the mechanisms of these reactions, as the reaction pathways are very dependant on the nature of the catalysts and substrates employed and result in a variety of cyclic alkene and diene products.[49a,49c,61] For example, 1,6-enynes (**31**) can undergo either 5-*exo-dig* or 6-*endo-dig* cyclisations to give bicyclo[3.1.0]hexane (**32**) or bicyclo[4.1.0]heptane (**33**) intermediates depending on the site of nucleophilic attack (Scheme 8).[61]

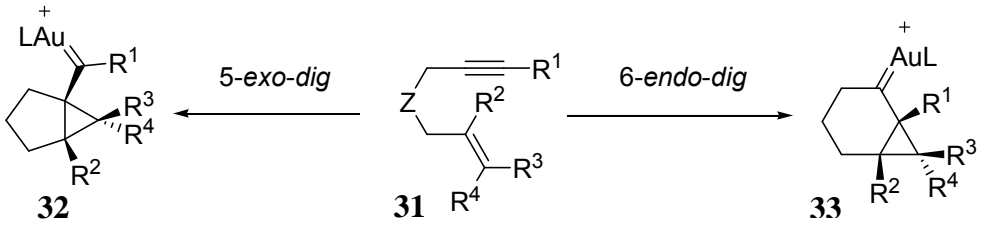

Scheme 8. 5-*Exo-dig* and 6-*endo-dig* cyclisations of 1,6-enynes.[61]

In combination with the array of possible subsequent rearrangements involving migrations and fragmentations, a number of possible cycloisomerisation products (**34**-**39**) are observed (Scheme 9).

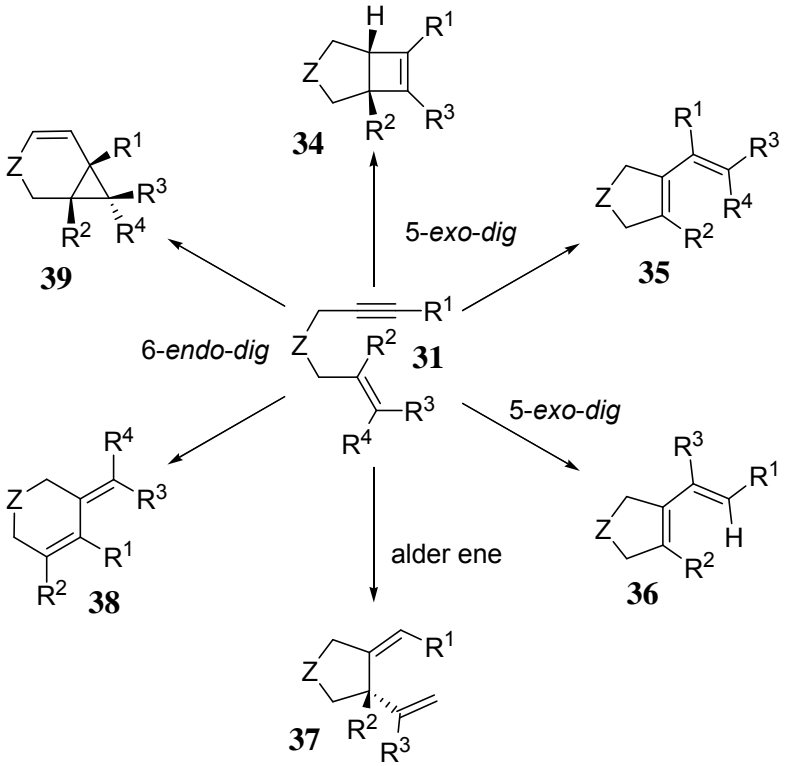

Scheme 9. Products observed in 1,6-enyne cycloisomerisation processes.

2.1.3.2. 1,5-Enyne cycloisomerisation; production of bicyclo[3.1.0]hexanes

The cycloisomerisation of 1,5-enynes is particularly facile.[15,48] For example, the group of Toste has shown that a range of alkyl and aryl substituted 1,5-enynes (**40**) undergo Au(I) and Au(III) catalysed cycloisomerisation to afford bicyclo[3.1.0]hexyl ring systems (**41**) (Scheme 10).[15]

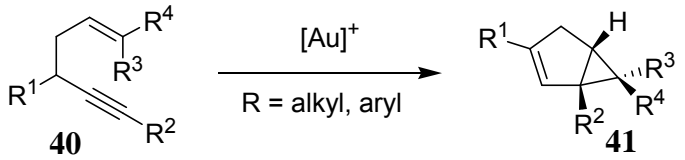

Scheme 10. The Au(I) catalysed cycloisomerisation of 1,5-enynes (**40**) to produce bicyclo[3.1.0]hex-2-enes (**41**).

There are a number of natural products containing the bicyclo[3.1.0]hexane core, for example, 4',1'a-methanocarbocyclic thymidine (**42**) (an anti herpes virus agent)[62] and prostaglandin El analogues such as **43** (key intermediates in E1 synthesis) (Figure 4).[63]

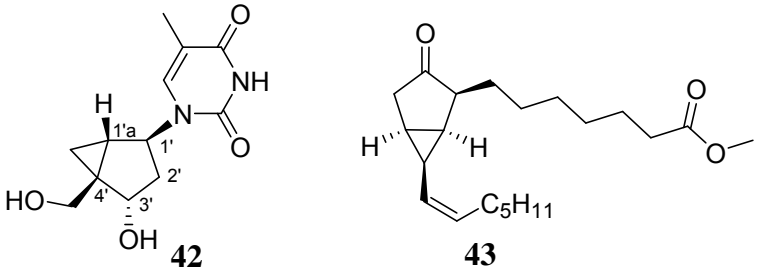

Figure 4. The structures of 4',1'a-methanocarbocyclic thymidine (**42**) and a prostaglandin El analogue (**43**).

Another example is that of ◘-cubebene (**44**) (a tricyclic sesquiterpene) isolated from commercial cubeb oil (*Piper cubeba L.*), used in flavourings and traditional medicines, which contains a tricyclo[4.4.0.0^{1,5}]decane core (Figure 5).[64] Fürstner has carried out a total synthesis of ◘-cubebene using a $PtCl_2$-catalysed tandem 1,5-enyne cycloisomerisation-allylic acetate rearrangement as the key step.[65]

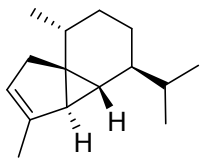

44

Figure 5. Structure of ◘-cubebene (**44**).

Fürstner has also prepared a range of sesquisabinene and sesquithujene terpenoids containing the bicyclo[3.1.0]hexane core using [$AuCl_3$(pyridine)] catalysed cycloisomerisation of 1,5-enynes. These include sesquisabinene (**45**), found in pepper

(*Piper nigrum*), and sesquithujene (**46**), a major constituent of the essential oil of ginger (*Zingiber officinale*). They have also completed a formal total synthesis of cedrine and cedrol (**48**) (from oil of cedar, used for fragrances and flavourings) by preparing key intermediate **47** (Figure 6).[66]

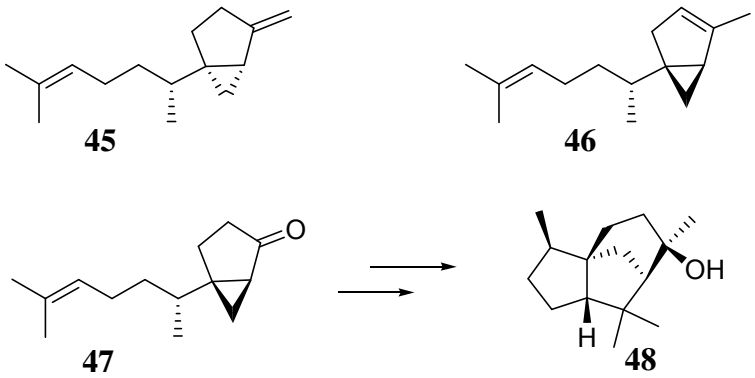

Figure 6. Structures of sesquisabinene A (**45**), sesquithujene (**46**) and cedrol (**48**).

2.1.3.3. Tandem nucleophilic substitution-cycloisomerisation

Georgy *et al.* have reported that Au(III) salts can catalyse the nucleophilic substitution of propargyl alcohols with allyltrimethylsilane to produce 1,5-enynes.[25a] A small amount (11%) of the cycloisomerisation product was produced using the Au salt, $HAuCl_4.3H_2O$ and 1-phenylhex-2-yn-1-ol. Nucleophilic substitution of propargyl alcohols has traditionally been carried out by multi-step stoichiometric reactions involving cobalt (Nicholas reaction-$[Co_2(CO)_8]$)[67] or chromium[68] and there have been several recent reports in the literature of efficient catalysts for the direct nucleophilic substitution of propargyl alcohols, including: $FeCl_3$,[69] I_2,[70] PTSA,[71] $[ReCl_3O(dppm)]$,[72] $BiCl_3$,[73] BCl_3 (with n-BuLi),[74] $[\{RuCl(Cp^*)(\mu_2\text{-SMe})\}_2]$[75] and $Cu(BF_4)_2$.[76] There have been three examples of two catalyst systems which can carry out the nucleophilic substitution of propargyl alcohols with allylsilanes using a Lewis or Brønsted acid followed by a cycloisomerisation of the resultant 1,5-enyne using an Au(I) catalyst/precatalyst. Toste[15] and co-workers reported a Re and Au catalyst combination which can catalyse the nucleophilic substitution-cycloisomerisation of 1,3-diphenylprop-2-yn-1-ol and allyltrimethylsilane. Georgy *et al.* used a combination of $AuCl_3$ followed by $[Au(OTf)(PPh_3)]$ to catalyse the reaction of 1-phenyloct-2-yn-1-ol (**49**) and allyltrimethylsilane to generate bicyclo[3.1.0]hexene **50** *via* 1,5-enyne **51** (Scheme 11).[77] Sanz *et al.* have developed a

para-toluenesulfonic acid catalysed nucleophilic substitution which is followed by a [AuCl(PPh$_3$)]/AgSbF$_6$ catalysed cycloisomerisation.[78]

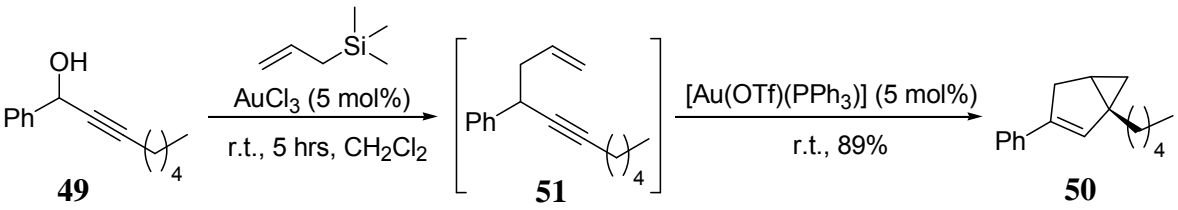

49 **51** **50**

Scheme 11. Concurrent AuCl$_3$ catalysed nucleophilic substitution and [Au(OTf)(PPh$_3$)] catalysed cycloisomerisation.

2.1.4. Au imidate and NHC complexes; therapeutic and catalytic properties

Au complexes have demonstrated activity against many biological targets including HIV[79] and bacteria.[80] The Au complex 2,3,4,6-tetra-O-acetyl-1-thio-□-D-pyranosato-S-(triethylphosphine)gold(I) (Auranofin) is used therapeutically to treat rheumatoid arthritis[81] and the investigation into Au(I) and Au(III) complexes for therapeutic applications is ongoing, particularly due to cytotoxic activity.[82] Electron-deficient biocompatible imidate anions ligate both Au(I) and Au(III),[83] an attribute that has been exploited therapeutically.[84] In the 1920's, Pope prepared a series of succinimidate (**14**) gold complexes, including H[Au(*N*-succ)$_2$], [Au(*N*-succ)$_2$(NH$_3$)$_2$]Cl, and [Au(*N*-succ)$_3$(NH$_3$)] (*N*-succ is *N*-succinimidate), citing the use of such compounds as therapeutic agents where it is desirable to administer the compounds in a form not as auric acid or ions.[83a] Further studies were carried out by Tyabji and Gibson, who claimed to have prepared K[AuX$_2$(*N*-imidate)$_2$] complexes (where X is Br, Cl and OH),[84a] and also by Kharasch and Isbell who prepared NH$_4$[Au(*N*-imidate)$_4$] and H[Au(*N*-imidate)$_4$] complexes.[84b] However, later investigations by Malik *et al.*, who synthesised a sodium bis(*N*-methylhydantoinato)gold(I) complex, suggested that these were most likely anionic gold(I) bisimidate complexes.[83b]

Kilpin *et al.* prepared a range of Au(III) complexes using the anions of phthalimide (**18**), *o*-benzoic sulfimide (saccharin) (**19**) and isatin as ligands in complexes of the type [Au(*N*-imidate)$_2$(2-bp)] and [Au(*N*-imidate)(damp)] (2-bp is 2-benzylpyridyl; damp is Me$_2$NCH$_2$C$_6$H$_4$) which exhibited anti-tumour and anti-microbial activity.[83c] The first Au complex of the type [Au(*N*-imidate)L], [Au(*N*-succ)(PPh$_3$)] (**52**), was prepared by Goodgame *et al.* in 1993,[85] and later Bonatti *et al.* prepared [Au(*N*-ptm)(PCy$_3$)] and [Au(*N*-obs)(PCy$_3$)] (*N*-ptm is *N*-phthalimidate (**18**); *N*-obs is *N*-*o*-benzoic sulfimidate (**19**)).[84c]

More recently, Berners-Price *et al.* reported a number of [Au(*N*-imidate)(PR_3)] complexes, including [Au(*N*-ptm)(PEt_3)], *trans*-[$AuBr_2$(*N*-ptm)(PEt_3)] (**53**), [Au(*N*-rib)(PEt_3)] and [Au_2(*N*-ptm)$_2$(μ-depe)] (rib is the anion of riboflavin; depe is 1,2-bis(diethylphosphino)ethane).[84d] These gold complexes exhibit anti-inflammatory activity.

Nolan and co-workers have produced the first [Au(N-imidate)(NHC)] complex, [Au(*N*-obs)(IPr)] (**54**) (IPr is bis(2,6-diisopropylphenyl)imidazol-2-ylidene), and also [Au(*S*-tgt)(IPr)] (*S*-tgt is 2,3,4,6-tetra-*O*-acetyl-1-thio-β-D-pyranosatothiolato anion).[84e] Nolan's group has previously prepared a series of Au(III) complexes of the type [$AuBr_3$(NHC)], by oxidative bromination of [AuBr(NHC)] complexes, which have been shown to catalyze the addition of water to phenyl acetylene[86] and to effectively promote styrene polymerisation.[87] More recently they have reported a series of [$AuCl_3$(NHC)] complexes[37] (only synthetic and structural studies). Ricard and Gagosz have synthesised a related series of N-heterocyclic carbene Au(I) bis(trifluoromethanesulfonyl)imidate complexes.[88] Baker *et al.* have prepared a range of [AuX(I^{t}Bu)] complexes (I^{t}Bu is *N,N'*-di-*tert*-butyl-butylimidazol-2-ylidene), where X is a range of pseudohalide ligands, and found that the σ donor capacity of the pseudohalide ligand had a direct effect on the length of the carbene-gold bond.[89]

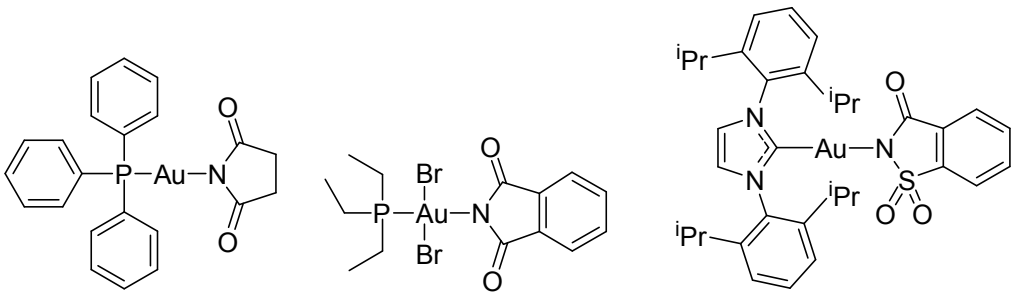

52 **53** **54**

Figure 7. Structures of reported Au(I) and Au(III) imidate complexes **52**-**54**.

Phthalimide has been used in conjunction with gold catalytically. Cui *et al.*[90] found that the addition of sulfonic acids to alkynes to give vinyl sulfonates could be catalysed by [Au(NO_3)(PPh_3)] (2 mol%) and when they added phthalimide (4 mol%) the yield increased from 58 to 74%. The authors speculated that [Au(*N*-ptm)(PPh_3)] formed and observed a 53% yield when [Au(*N*-ptm)(PPh_3)] (2 mol%) was added to the reaction. The conditions used are harsh (100 ˚C for 4 hours), which certainly results in colloidal gold formation, and so the nature of the catalytically active species is unclear.

2.1.5. Aims

The initial aim of this study was to investigate the structure and bonding of Au(I) and Au(III) complexes containing NHC and imidate ligands. The complexes would then be applied to Au(III)-catalysed processes and the effect of the nature of the imidate and NHC ligands on catalytic activity investigated. Au(III) imidate complexes are likely to act as soft π-acidic 1,5-enyne cycloisomerisation catalysts, and as Lewis acid catalysts which is advantaged by the highly electron-withdrawing imidate ligands. It was hypothesised that these properties could be combined into a single catalyst system, enabling an efficient tandem nucleophilic substitution-cycloisomerisation process. It was also intended to study the effects of new super non-coordinating anions[91] on these transformations.

2.2. Results and discussion

2.2.1. Synthesis and characterisation of Au complexes

2.2.1.1. Synthesis and characterisation of Au(I) complexes

A range of [Au(*N*-imidate)(NHC)] complexes (**55**-**57**) {*N*-imidate is *N*-succinimidate (**14**), *N*-tetrafluorosuccinimidate (**16**), *N*-maleimidate (**17**), *N*-phthalimidate (**18**) and *N*-*o*-benzoic sulfimidate (**19**); NHC is *N,N'*-di-*tert*-butyl-butylimidazol-2-ylidene (I^{t}Bu) (**58**), *N,N'*-di-*tert*-pentyl-butylimidazol-2-ylidene (I^{t}Pe) (**59**) and *N*,*N'*-bis(2,4,6-trimethylphenyl)imidazol-2-ylidene (IMes) (**60**)} were prepared in order to study the electronic properties of the imidate ligands and as precursors to [AuBr$_2$(*N*-imidate)(NHC)] complexes (Figure 8).

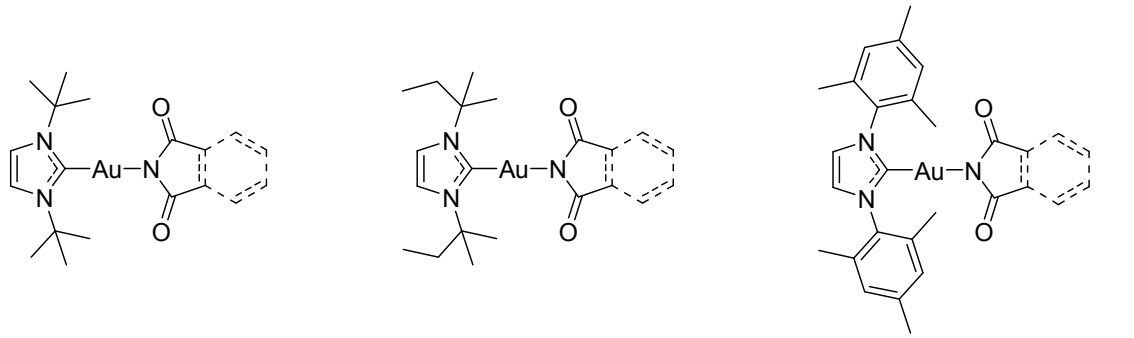

55a = *N*-succinimido (87%)
55b = *N*-tetrafluorosuccinimido (91%)
55c = *N*-maleimido (93%)
55d = *N*-phthalimido (92%)
55e = *N*-*o*-benzoic sulfimido (89%)

56a = *N*-succinimido (93%)
56b = *N*-tetrafluorosuccinimido (93%)
56c = *N*-maleimido (96%)
56d = *N*-phthalimido (96%)
56e = *N*-*o*-benzoic sulfimido (94%)

57a = *N*-succinimido (97%)
57b = *N*-tetrafluorosuccinimido (87%)
57c = *N*-maleimido (93%)
57d = *N*-phthalimido (94%)
57e = *N*-*o*-benzoic sulfimido (90%)

Figure 8. [Au(*N*-imidate)(NHC)] complexes prepared, including yields.

Preparation of [Au(*N*-imidate)(NHC)] (**55-57**) complexes was first attempted by the method described for related phosphine Au(I) complexes.[84d] The reaction of sodium imidates with [AuCl(NHC)] **(55f**-**57f)** complexes in an ethanol/water solvent system gave low yields, presumably due to the sensitivity of the carbene centre(s) to water. Use of neat ethanol gave improved yields, but virtually quantitative yields (87-96%) were achieved by treatment of the parent [AuCl(NHC)] (**55f**-**57f**) complex with the silver salt of the relevant imidate in dichloromethane (Scheme 12). In the case of the *N*-tfs (**16**) and *N*-obs (**19**) ligands the silver salts were prepared *in situ* due to the hygroscopic nature of the salts and the sensitivity of tetrafluorosuccinimide and its silver salt to water. Tetrafluorosuccinimide

is prepared from tetrafluorosuccinamide by reaction with stoichiometric neat sulphuric acid at 190 ˚C followed by isolation *via* sublimation.

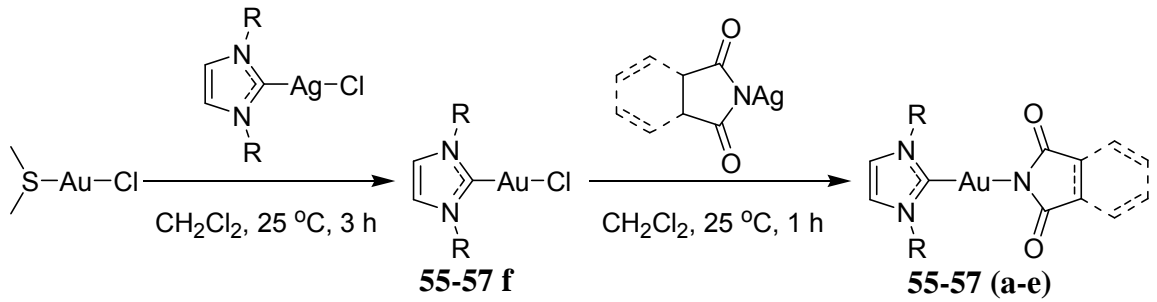

Scheme 12. Preparation of [Au(*N*-imidate)(NHC)] complexes.

The novel NHC ligand, namely *N,N'*-di-*tert*-pentyl-butylimidazol-2-ylidene (I^{t}Pe) (**59**), was synthesised from the hydrochloride salt (**61**) by a method similar to that reported (Scheme 13).[92] This allows a comparison of any subtle electronic and steric effects with the related I^{t}Bu NHC ligand (**58**) and provides steric control for intended combination with chiral imidates for asymmetric catalysis. The hydrochloride salt I^{t}Pe.HCl (**61**) could not be prepared by the method analogous to that of I^{t}Bu.HCl (**62**) due to poor reactivity (or solubility) in the first step resulting in recovery of ^{t}PeNH$_2$.HCl only.

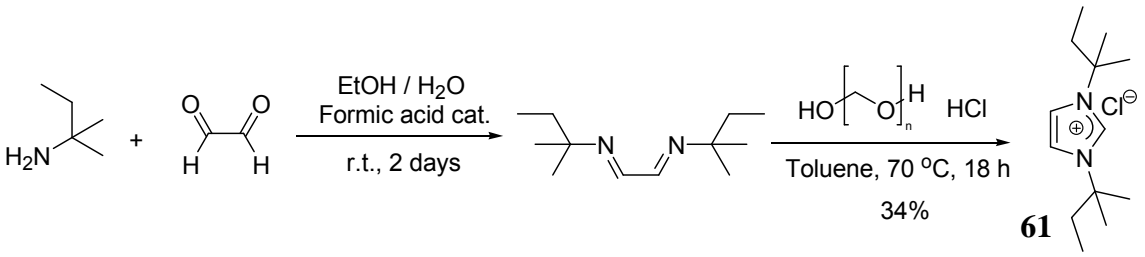

Scheme 13. Synthesis of I^{t}Pe.HCl (**61**).

The Au(I) complexes are white powders which are air stable but decompose slowly in water. Attempts were also made to synthesise an IMe analogue, however this ligand proved unstable, resulting in multiple products and decomposition, when synthesis of the [AuCl(IMe)] complex was attempted. The Au(I) complexes were fully characterised by ^{1}H, ^{19}F, ^{13}C, IR and ESI-MS studies and several by X-ray diffraction studies.

The novel I^{t}Pe ligand (**59**) shows very similar electronic properties to the I^{t}Bu ligand (**58**).[93] The NMR spectroscopic data of the compounds is consistent with greater electron donation from the ^{t}Pe compared with the ^{t}Bu group. The imidazolium protons of the I^{t}Pe group have a small upfield shift in the hydrochloride salt (**61**) (0.19 ppm) and chloride

complex (**56f**) (0.05 ppm) and the imidazole carbon signals have a small downfield shift (0.8-0.9 ppm), relative to the I^{t}Bu analogues. The imidate ligand protons are shifted upfield by up to 0.4 ppm compared to the neutral imides which is consistent with a more electron deficient environment.

The NHC ligands have a noticeable effect on the imidate proton NMR signals. The IMes ligand (**60**) shifts the proton signals upfield with respect to I^{t}Bu (**58**) and I^{t}Pe (**59**) in the order: IMes < I^{t}Pe ≤ I^{t}Bu. There is little difference (< 0.05 ppm) between I^{t}Bu (**55**) and I^{t}Pe (**56**) complexes but up to 0.25 ppm difference between the signals of IMes (**57**) and I^{t}Bu (**55**) complexes. However, there is little change in the carbon signals of the imidates (< 0.4 ppm). The phosphine Au(I) complexes reported[85] exhibit similar imidate NMR chemical shifts to the I^{t}Pe (**56**) and I^{t}Bu (**55**) complexes.

The imidate ligands have a moderate impact on the NHC ^{1}H NMR signals but a trend is revealed in the chemical shift of the NHC imidazole proton signals of:

Cl ≤ Br ≤ *N*-succ ≤ *N*-mal < *N*-ptm < *N*-obs < *N*-tfs

(with ranges of: **55 a-g** 7.09-7.15 ppm, **56 a-g** 7.04-7.11 ppm, **57 a-g** 7.09-7.17 ppm)

The *N*-succ (**55-57 a**), *N*-mal (**55-57 c**) and *N*-ptm (**55-57 d**) complexes show similar spectra to the chloride (**55-57 f**) and bromide analogues (**55-57 g**), with less than 0.03 ppm difference in the imidazole proton signals. However, the more electron-withdrawing imidate ligands, *N*-tfs and *N*-obs, shift the imidazole signal downfield by up to 0.07 and 0.06 ppm, respectively. This is in part reflected in the Au-C carbene carbon shift (Table 3) where the following trend is revealed:

N-tfs < *N*-obs < Cl < *N*-mal ≤ *N*-succ < *N*-ptm < Br

(with ranges of: **55 a-g** 167.0-172.4 ppm, **56 a-g** 167.5-172.3 ppm, **57 a-g** 171.9-176.9 ppm)

Less than 0.4 ppm difference is observed between the *N*-succ (**55-57 a**), *N*-mal (**55-57 c**) and *N*-ptm (**55-57 d**) complexes but an upfield shift of up to 3.9 ppm is observed for the *N*-tfs (**55-57 b**) and *N*-obs (**55-57 e**) complexes. The related bromide analogues (**55-57 g**) appear downfield relative to the imidates, although the chloride analogues (**55-57 f**) appear upfield. This upfield shift in the electron-deficient complexes is seen in other types of Au(I) complexes,[85,86] and is speculated to be due to the polarisation of the NHC ligand by the more electron-deficient Au(I) atom. The imidazole proton and carbene carbon signals are similar to those reported by Baker (**62** and **63**).[89] These similarities confirm the validity

of imidate anions as pseudohalide ligands, and are in keeping with other trends reported for metal imidate complexes.[94]

Table 3. The ^{13}C NMR chemical shifts of the carbene carbon of [Au(*N*-imidate)(NHC)] complexes (**55-57**).[a]

Entry	Complex	δ_C (ppm)	Entry	Complex	δ_C (ppm)
1	[Au(*N*-succ)(I^{t}Bu)] (**55a**)	170.8	13	[AuCl(I^{t}Pe)] (**56f**)	168.1
2	[Au(*N*-tfs)(I^{t}Bu)] (**55b**)	167.0	14	[AuBr(I^{t}Pe)] (**56g**)	172.3
3	[Au(*N*-mal)(I^{t}Bu)] (**55c**)	170.5	15	[Au(*N*-succ)(IMes)] (**57a**)	174.9
4	[Au(*N*-ptm)(I^{t}Bu)] (**55d**)	170.9	16	[Au(*N*-tfs)(IMes)] (**57b**)	171.9
5	[Au(*N*-obs)(I^{t}Bu)] (**55e**)	167.5	17	[Au(*N*-mal)(IMes)] (**57c**)	175.1
6	[AuCl(I^{t}Bu)][89] (**55f**)	168.2	18	[Au(*N*-ptm)(IMes)] (**57d**)	175.2
7	[AuBr(I^{t}Bu)][89] (**55g**)	172.4	19	[Au(*N*-obs)(IMes)] (**57e**)	172.9
8	[Au(*N*-succ)(I^{t}Pe)] (**56a**)	170.8	20	[AuCl(IMes)][86] (**57f**)	173.4
9	[Au(*N*-tfs)(I^{t}Pe)] (**56b**)	167.5	21	[AuBr(IMes)][86] (**57g**)	176.9
10	[Au(*N*-mal)(I^{t}Pe)] (**56c**)	170.7	22	[Au(ONO$_2$)(I^{t}Bu)][89] (**62**)	156.3
11	[Au(*N*-ptm)(I^{t}Pe)] (**56d**)	171.0	23	[Au(CH$_3$)(I^{t}Bu)][89] (**63**)	198.7
12	[Au(*N*-obs)(I^{t}Pe)] (**56e**)	167.9			

[a] In $CDCl_3$ at 400 MHz.

The stretching frequencies of the imidate ligand carbonyl bonds (Table 4) are 53-78 cm^{-1} lower than the free imides, which would suggest more electron density on the imidate nitrogen in the complexes than in the free imide.[95] This has been observed in other imidate metal complexes and there have been several explanations proposed.[96] The most convincing of these[97] is that there is a degree of ionic character associated with the metal-imidate bond resulting in the shift of electron density from the Au-N into the N-C bond and so from the carbonyl bond on to the carbonyl oxygen. The stretching frequencies reflect the NMR spectroscopic data allowing the following trend to be established:

N-succ < *N*-mal < *N*-ptm < *N*-obs < *N*-tfs

(with ranges of: **55 a-e** 1645-1704 cm^{-1}, **56 a-e** 1644-1704 cm^{-1}, **57 a-e** 1648-1705 cm^{-1})

The range is up to 60 cm^{-1} with the higher frequencies (stronger carbonyl bonds) reflecting the increased electron-withdrawing capacity of the imidates. This also largely reflects the pK_a of the parent imides:

obs (1.6)[98] < tfs (2.1 est.)[99] < ptm (8.3)[98] < mal (9.5)[100] < succ (9.7)[101]

The pK_a of tfs does not fit the pattern exactly, although this is an estimated value. The pK_a was estimated by comparison of the pK_a of succinimide to pyrollidium (11.31) and 3,3,4,4-tetrafluoropyrrolidinium (4.05) ions. The NHC ligands have little effect on the carbonyl stretching frequencies of the imidate ligands (<4 cm^{-1}). The effect on the frequency of each imidate follows the trend:

$I^tPe < I^tBu < IMes$

Table 4. The infra-red absorbance frequencies of the imidate carbonyl groups in [Au(*N*-imidate)(NHC)] complexes and free imides in CH_2Cl_2.[a]

Entry	Complex	υ_{max} (cm^{-1})	Entry	Complex	υ_{max} (cm^{-1})
1	[Au(*N*-succ)(I^tBu)] (**55a**)	1645	11	[Au(*N*-succ)(IMes)] (**57a**)	1648
2	[Au(*N*-tfs)(I^tBu)] (**55b**)	1704	12	[Au(*N*-tfs)(IMes)] (**57b**)	1705
3	[Au(*N*-mal)(I^tBu)] (**55c**)	1662	13	[Au(*N*-mal)(IMes)] (**57c**)	1662
4	[Au(*N*-ptm)(I^tBu)] (**55d**)	1667	14	[Au(*N*-ptm)(IMes)] (**57d**)	1667
5	[Au(*N*-obs)(I^tBu)] (**55e**)	1689	15	[Au(*N*-obs)(IMes)] (**57e**)	1680
6	[Au(*N*-succ)(I^tPe)] (**56a**)	1644	16	succinimide	1722
7	[Au(*N*-tfs)(I^tPe)] (**56b**)	1704	17	maleimide	1731
8	[Au(*N*-mal)(I^tPe)] (**56c**)	1660	18	phthalimide	1741
9	[Au(*N*-ptm)(I^tPe)] (**56d**)	1667	19	*o*-benzoic sulfimide	1742
10	[Au(*N*-obs)(I^tPe)] (**56e**)	1689			

[a] Carbonyl stretching frequency of tetrafluorosuccinimide not obtained due to poor solubility in CH_2Cl_2.

The complexes, [Au(*N*-succ)(I^{t}Bu)] (**55a**), [Au(*N*-ptm)(I^{t}Bu)] (**55d**) and [Au(*N*-succ)(IMes)] (**57a**), were crystallised from fluorobenzene in a solution saturated with pentane, which allowed their structures to be determined by X-ray diffraction (Figure 9). Selected bond lengths of these and related complexes are displayed in Table 5.

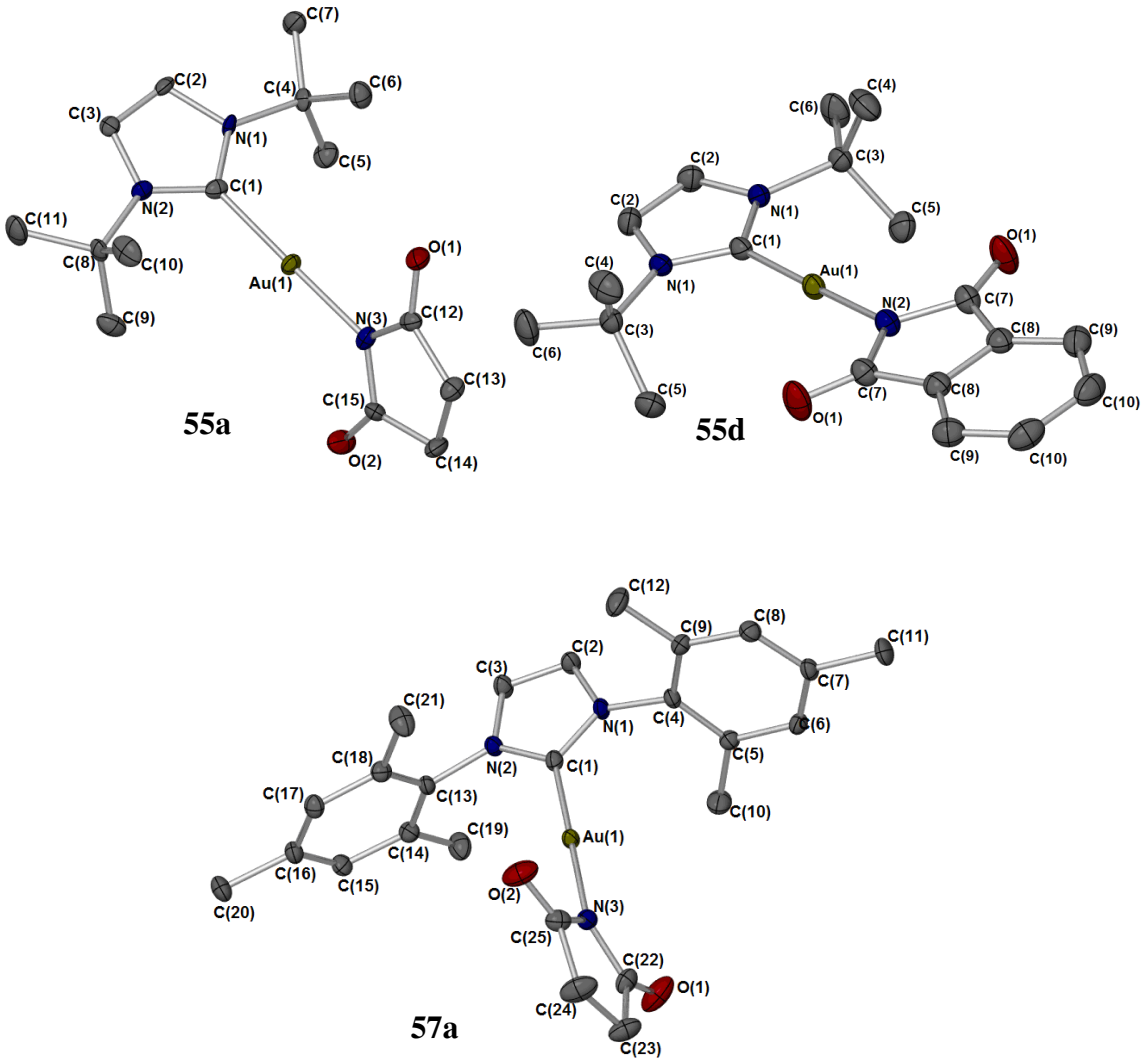

Figure 9. Molecular structures of **55a**, **55d** and **57a**. Displacement ellipsoids are shown at the 50% probability level. Hydrogen atoms have been omitted for clarity.

Table 5. The bond lengths (Å) of imidate and NHC ligands in Au(I) complexes.[a]

Entry	Complex	Imidate ligand					NHC ligand			
		Au-Anion	**N-C (1)**	**N-C (2)**	**C=O (1)**	**C=O (2)**	**Au-C**	**C-N(1)**	**C-N(2)**	**Imidazole C=C**
1	[Au(*N*-succ)(I^{t}Bu)] (**55a**)[b]	2.037(4)	1.372(8)	1.375(9)	1.232(6)	1.211(13)	2.005(4)	1.349(8)	1.354(7)	1.340(7)
		2.042(4)	1.369(8)	1.385(7)	1.227(12)	1.212(6)	2.008(4)	1.370(7)	1.359(8)	1.344(6)
2	[Au(*N*-ptm)(I^{t}Bu)] (**55d**)	2.029(3)	1.380(3)	1.380(3)	1.212(3)	1.212(3)	1.987(3)	1.361(3)	1.361(3)	1.345(4)
3	[Au(*N*-succ)(IMes)] (**57a**)	2.021(2)	1.378(3)	1.372(4)	1.212(4)	1.217(3)	1.965(3)	1.355(3)	1.361(3)	1.347(3)
4	[Au(*N*-ptm)(PPh_3)] (**64**)[85]	2.05(2)	1.39(1)	1.40(1)	1.22(1)	1.22(1)				
5	Phthalimide[102]		1.381	1.395	1.216	1.222				
6	[AuCl(I^{t}Bu)] (**55f**)[89]	2.2742(7)					2.018(3)			
7	[AuBr(I^{t}Bu)] (**55g**)[89]	2.3994(5)					1.999(4)			
8	[AuCl(IMes)] (**57f**)[103]						1.999	1.337	1.339	
9	[Au(NTf_2)(IMes)] (**65**)[88]	2.077(3)					1.976(3)	1.358(5)	1.341(5)	

[a] ESD values are given in brackets where known. [b] **55a** contains two [Au(*N*-succ)(I^{t}Bu)] conformers.

Complexes **55a** (which contains two [Au(*N*-succ)(I^{t}Bu)] conformers), **55d** and **57a** have two-coordinate linear structures with N-Au-C bond angles close to 180˚ {176.17(18)˚ and 176.98(18)˚ for **55a**, 178.30(10)˚ for **55d** and 179.65(9)˚ for **57a**}. The solid-state structure of **55d** is planar, whilst **55a** has torsion angles of 70.5˚ and 69.6˚ and **57a** a 76.1˚ torsion angle between the NHC imidazole and *N*-succ rings. The crystal structures show that there is little variation in equivalent bond lengths of the imidate ligands in complexes **55a**, **55d**, **57a** and [Au(*N*-ptm)(PPh_3)] (**64**). The imidate Au-N bond length for **55a** (2.037(4) Å and 2.042(4) Å) is slightly longer (statistically significant) by 0.016(6) and 0.021(6) Å than **57a** {2.021(2) Å}. The Au-N bond is significantly shorter in these complexes {up to 0.056(5) Å} than in [Au(NTf_2)(IMes)] (**65**)[88] due to greater electron withdrawing ability of the triflate substituents. Phthalimide has bond lengths in the range of those of the phosphine complex and **57d**, highlighting the similarity (and isolobal relationship) between the Au(I) centre and a proton.

The Au-anion bond lengths in the I^{t}Bu complexes **55a** and **55d (**2.040(4) and 2.029(3), respectively) are significantly shorter than the analogous chloride (**55f**) and bromide (**55g**) complexes (2.2742(7) and 2.3994(5) Å, respectively), however they are similar to the $^-$CN (2.009(7) and 2.043(6) Å), acetate (2.040(2) Å), and $^-ONO_2$ (2.056(3) Å) complexes reported by Baker.[89]

The bond lengths observed for the NHC ligands are also similar; complex **57a** has a shorter Au-C bond than **55a** (by 0.040(7) to 0.043(7) Å) and **55d** (by 0.022(6) Å), consistent with similar complexes;[37,86] **55a** and **55d** are not significantly different. All three complexes have similar C-N and C=C bonds lengths. Complexes **55a** and **55d** have similar bond lengths to the analogous Au(I) bromide complex **55g** and complex **57a** to the analogous NTf_2 and chloride (**57g**) complexes has a slightly longer Au-C bond by 0.034(9) Å).

The complexes are reasonably stable in air and solution (although with some susceptibility to hydrolysis) with formation of colloidal gold after several weeks at ambient temperature. Anionic ligand exchange is facile. Treatment of [Au(*N*-tfs)(I^{t}Pe)] (**56b**) with one equivalent of [(*n*Bu)$_4$N]Br results in partial exchange of tfs and Br anions, similarly with [Au(*N*-succ)(IMes)] (**57a**) and LiBr.

Interestingly, the [Au(*N*-mal)(NHC)] complexes **55d** and **56d** can undergo a dimerisation reaction by a $\pi 2_S + \pi 2_S$ cycloaddition (Scheme 14). This has been reported for neutral maleimide under the influence of UV light, but no examples involving metal complexes are

known.[104] Formation of the dimer (**55h** and **56h**) was observed in up to 33% (relative to undimerised complex) for **56d** and 7% for **55d**, depending on the age of the sample. Evidence for this transformation was provided by mass spectral and NMR analysis, with the ^{1}H NMR signal for the imidate protons shifting from 6.54 to 3.33 ppm in **56d** (6.56 to 3.34 ppm in **55d**). These NMR changes are consistent with a conversion of alkene to cyclobutane. The relative stereochemistry (*cis* or *trans*-disposed), which will be influenced by the packing of the solid state structure, was not determined. No cycloaddition was observed for **57d**. Exposure of the complexes to natural light (for 2 weeks) did not significantly increase the proportion of dimerised complex.

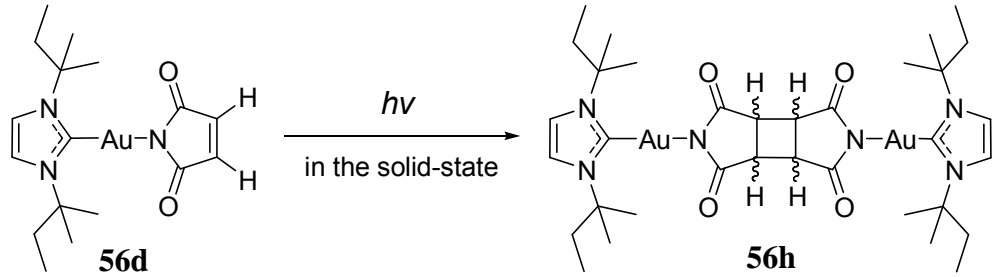

56d **56h**

Scheme 14. Photodimerisation of **56d** to **56h**.

2.2.1.2. Synthesis and characterisation of Au(III) complexes

A range of Au(III) complexes of the type [AuBr$_2$(*N*-imidate)(I^{t}Bu)] (**66**), [AuBr$_2$(*N*-imidate)(I^{t}Pe)] (**67**) and [AuBr$_2$(*N*-imidate)(IMes)] (**68**) were prepared by treatment of [Au(*N*-imidate)(NHC)] complexes (**55**-**57**) with bromine using the method of Nolan *et al.*[86] (Scheme 15, Figure 10). Complexes **66**(**a**, **c**, **e**, **f**), **67**(**a**, **c**, **e**, **f**) and **68**(**a**, **c**) were prepared by this method. The analogous IMes complexes (**68**) containing the *N*-tfs and *N*-obs ligands could not be prepared due to decomposition of the complexes on treatment with bromine.

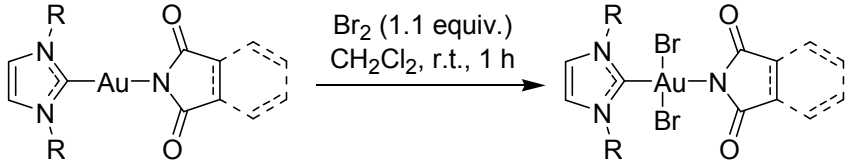

55-**57** **66**-**68**

Scheme 15. General method for the preparation of [AuBr$_2$(*N*-imidate)(NHC)] complexes (**66**-**68**).

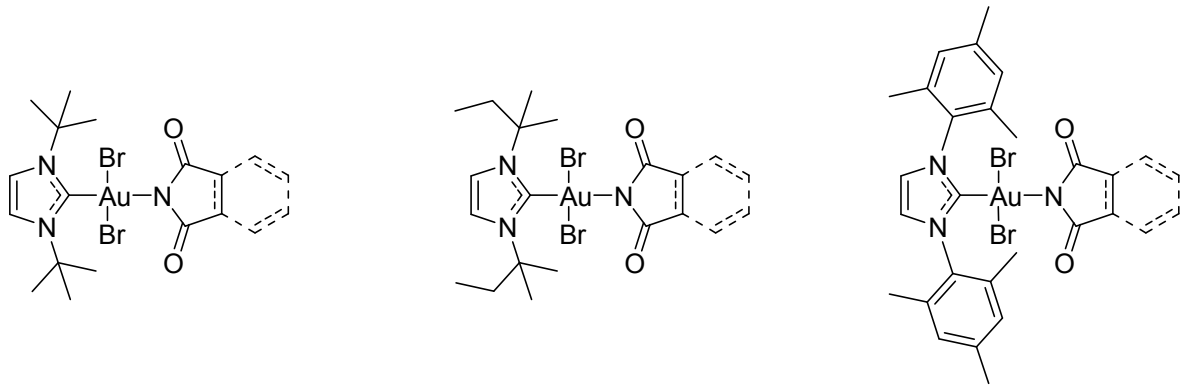

66a = *N*-succinimido (84%)
66b = *N*-2,3-dibromosuccinimido (93%)
66c = *N*-tetrafluorosuccinimido (91%)
66d = *N*-maleimido (90%)
66e = *N*-phthalimido (89%)
66f = *N*-*o*-benzoic sulfimido (92%)

67a = *N*-succinimido (98%)
67b = *N*-2,3-dibromosuccinimido (87%)
67c = *N*-tetrafluorosuccinimido (93%)
67d = *N*-maleimido (87%)
67e = *N*-phthalimido (97%)
67f = *N*-*o*-benzoic sulfimido (94%)

68a = *N*-succinimido (86%)
68b = *N*-maleimido (96%)
68c = *N*-phthalimido (95%)

Figure 10. The [$AuBr_2$(*N*-imidate)(NHC)] complexes prepared in this study, including yields.

The *N*-mal complexes **66d**, **67d** and **68b** were prepared by the same method at -78 °C with one equivalent of bromine due to competing bromination of the maleimidate double bond and Au-maleimidate bond. *N*-dbs (*N*-2,3-dibromosuccimidate) complexes **66b** and **67b** can be prepared by treatment of [Au(*N*-mal)(NHC)] complexes (**55c** and **56c**) with two equivalents of bromine or [$AuBr_2$(*N*-mal)(NHC)] complexes (**66d** and **67d**) with one equivalent of bromine at ambient temperature. The IMes complex containing a *N*-dbs ligand cannot be prepared under these conditions due to preferential addition of bromine to the Au-imidate bond even at low temperatures. This may occur *via* an Au(III) complex as seen for other Au(I) oxidative halogenation reactions.[105] Attempts to prepare the free 2,3-dibromomaleimidate anion (**15**) were unsuccessful because treatment of the neutral imide with base resulted in elimination of HBr to form 2-bromomaleimide, rather than deprotonation (Scheme 16). Preparation of silver 2,3-dibromomaleimidate directly by bromination of silver maleimidate was also unsuccessful due to AgBr formation.

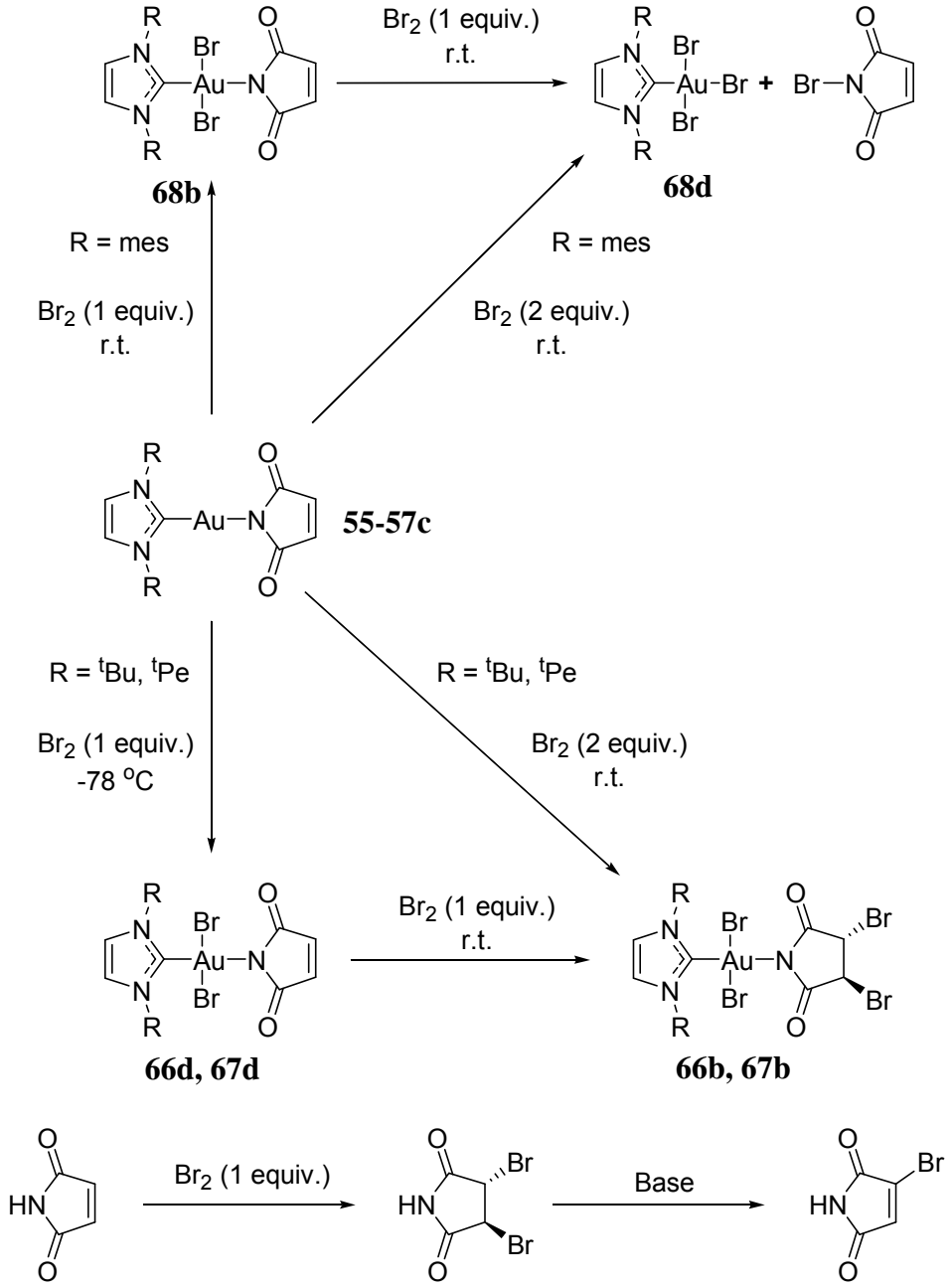

Scheme 16. Reaction of maleimide and [Au(*N*-mal)(NHC)] complexes with bromine in CH_2Cl_2.

The analogous [$AuBr_3$(NHC)] complexes (**66g**, **67g** and **68d**) were prepared by the same synthetic method.[86,89] The Au complexes were isolated in high yields (84-98%) as air stable yellow solids *via* simple purification, involving precipitation from dichloromethane/pentane and washing with pentane and cold diethyl ether. Berners-Price *et al.*[84d] reported that analogous "*trans*-$AuPR_3$" complexes underwent isomerisation to the *cis* isomeric form over a period of days. This was not observed in the NHC Au(III) complexes due to the greater steric bulk of the ligands. Ligand exchange occurs in solution, treatment

of [AuBr$_2$(*N*-tfs)(I^{t}Pe)] **67c** with [(*n*Bu)$_4$N]Br results in formation of [AuBr$_3$(I^{t}Pe)] (**67g**). However, exchange does not occur between complexes, mixing **67d** and **68a** in solution did not result in ligand exchange and so the exchange presumably occurs associatively rather than dissociatively. There was no $\pi 2_S + \pi 2_S$ cycloaddition observed for the Au(III) maleimidate complexes (**66d**, **67d** and **68b**) as was seen with Au(I) complexes **55d** and **56d**, presumably due to unfavourable crystal packing and reduced electron density in the maleimidate alkene bond. The complete library of Au(III) complexes have been fully characterised by ^{1}H, ^{13}C, IR, ESI-MS, and for selected examples, by crystallography using X-ray diffraction.

As for Au(I) the I^{t}Pe ligand **59** has similar NMR characteristics to I^{t}Bu **58**. The I^{t}Pe imidazole protons are shifted slightly more downfield (< 0.1 ppm), however, the Au-C carbene carbon is up to 1.1 ppm further downfield (Table 6). There is little difference in imidazole and carbon imidate signals for the two sets of complexes and this is consistent with Au(I) [Au(*N*-imidate)(NHC)] complexes (**55** and **56**).

Au(III) complexes containing the IMes ligand (**68**) have more upfield imidazole (up to 0.19 ppm) and imidate proton signals (up to 0.24 ppm) than the I^{t}Bu (**66**) and I^{t}Pe (**67**) containing complexes. The Au-C carbene carbon signals are up to 10.7 ppm and the imidazole signals up to 3.5 ppm more downfield, which is concurrent with other known Au(I) and Au(III) complexes.[37,86] The imidate carbon signals are similar to those of I^{t}Bu and I^{t}Pe containing Au(III) complexes (**66** and **67**).

Table 6. The Au-C carbene carbon chemical shifts of [$AuBr_2$(*N*-imidate)(NHC)] complexes.[a]

Entry	Complex	δ_C (ppm)	Entry	Complex	δ_C (ppm)
1	[$AuBr_2$(*N*-succ)(I^tBu)] (**66a**)	131.9	11	[$AuBr_2$(*N*-mal)(I^tPe)] (**67d**)	132.0
2	[$AuBr_2$(*N*-dbs)(I^tBu)] (**66b**)	128.1	12	[$AuBr_2$(*N*-ptm)(I^tPe)] (**67e**)	132.4
3	[$AuBr_2$(*N*-tfs)(I^tBu)] (**66c**)	124.9	13	[$AuBr_2$(*N*-obs)(I^tPe)] (**67f**)	126.6
4	[$AuBr_2$(*N*-mal)(I^tBu)] (**66d**)	131.3	14	[$AuBr_3$(I^tPe)] (**67g**)	135.6
5	[$AuBr_2$(*N*-ptm)(I^tBu)] (**66e**)	131.5	15	[$AuBr_2$(*N*-succ)(IMes)] (**68a**)	142.2
6	[$AuBr_2$(*N*-obs)(I^tBu)] (**66f**)	125.6	16	[$AuBr_2$(*N*-mal)(IMes)] (**68b**)	141.4
7	[$AuBr_3$(I^tBu)][86] (**66g**)	134.2	17	[$AuBr_2$(*N*-ptm)(IMes)] (**68c**)	142.2
8	[$AuBr_2$(*N*-succ)(I^tPe)] (**67a**)	132.6	18	[$AuBr_3$(IMes)][86] (**68d**)	144.4
9	[$AuBr_2$(*N*-dbs)(I^tPe)] (**67b**)	128.7	19	[$AuCl_3$(I^tBu)][37] (**69**)	135.7
10	[$AuBr_2$(*N*-tfs)(I^tPe)] (**67c**)	126.0	20	[$AuCl_3$(IMes)][37] (**70**)	144.6

[a] In $CDCl_3$ at 400 MHz.

The chemical shift of the NHC imidazole proton signal is also correlated with the electronic properties of the imidate ligands. The more electron-withdrawing imidates shift the signal downfield, with a range of 0.07-0.10 ppm, in the order:

N-succ < *N*-mal < *N*-ptm (≈ Cl_3) < *N*-dbs < Br < *N*-obs < *N*-tfs

(with ranges of: **66 a-g** 7.41-7.51 ppm, **67 a-g** 7.36-7.43 ppm, **68 a-d** 7.26-7.32 ppm)

There is a similar trend in Au-C carbene ^{13}C chemical shifts, the more electron-withdrawing imidates result in a shift upfield, in the order:

N-tfs < *N*-obs < *N*-dbs < *N*-mal < *N*-ptm < *N*-succ < Br_3 (< Cl_3)

(with ranges of: **66 a-g** 131.9-134.2 ppm, **67 a-g** 132.6-135.6 ppm, **68 a-d** 142.2-144.4 ppm)

The *N*-tfs containing Au(III) complexes (**66c** and **67c**) are shifted up to 9.6 ppm further upfield than the tribromide complexes (**66g** and **67g**) (and up to 10.8 ppm further than the trichloride complexes). The *N*-mal, *N*-succ and *N*-ptm ligands give similar values. The greater electron-withdrawing capacity of the imidate results in greater polarisation of NHC ligand resulting in a shift upfield, as seen in similar complexes.[89]

On oxidative bromination, from Au(I) to Au(III), the ^{13}C NMR signals of the NHC substituents are shifted downfield by up to 6.0 ppm and the Au-C ^{13}C carbene signals 32-42 ppm upfield. The greatest difference is seen with the more electronegative *N*-tfs ligand. This upfield chemical shift of the carbene signal on oxidation of the Au atom has been seen in other classes of Au complexes[86,105] and is postulated to be due to polarisation of the NHC ligand by the electrophilic Au(III) centre. In addition, the NHC imidazole protons are shifted up to 0.40 ppm and the imidate protons 0.25 ppm downfield on oxidation, as would be expected for ligands in a more electron poor complex. However, in I^{t}Pe containing Au(III) complexes (**66**), the ^{t}Pe group methylene signal is shifted upfield by 0.42-0.51 ppm. This could be due to a non-bonding interaction between the methylene protons and bromide ligands, although this is not evidenced in the crystal structure (*vide infra*). The imidate carbonyl ^{13}C NMR signals also move upfield by 2.0-5.5 ppm.

The imidate carbonyl stretching frequencies (Table 7) also show a trend of increasing frequency, with a range of up to 55 cm^{-1}, in the order:

N-succ < *N*-mal < *N*-ptm < *N*-dbs < *N*-obs < *N*-tfs

(with ranges of: **66 a-f** 1663-1718 cm^{-1}, **67 a-f** 1663-1716 cm^{-1}, **68 a-c** 1665-1683 cm^{-1})

This order reflects the electron-withdrawing capacity of the imidates, with decreasing C=O bond order, which is consistent with Au(I) complexes **55-57** and the observations made by NMR spectroscopy *vide supra*. There is little effect of the NHC ligand on the frequencies, with less than 2cm^{-1} variation. On oxidation, from Au(I) (**55**-**57**) to Au(III) (**66**-**68**) complexes, the frequency is increased by 14-18 cm^{-1}, reflecting the greater donation of the imidate nitrogen lone pair into the Au-N rather than the N-C bond, resulting in more C=O bond character.

Table 7. The infra-red absorbance frequencies of the imidate carbonyl groups in [$AuBr_2$(*N*-imidate)(NHC)] complexes and free imides in CH_2Cl_2.[a]

Entry	Complex	υ_{max} (cm^{-1})	Entry	Complex	υ_{max} (cm^{-1})
1	[$AuBr_2$(*N*-succ)(I^tBu)] (**66a**)	1663	11	[$AuBr_2$(*N*-ptm)(I^tPe)] (**67e**)	1682
2	[$AuBr_2$(*N*-dbs)(I^tBu)] (**66b**)	1690	12	[$AuBr_2$(*N*-obs)(I^tPe)] (**67f**)	1694
3	[$AuBr_2$(*N*-tfs)(I^tBu)] (**66c**)	1718	13	[$AuBr_2$(*N*-succ)(IMes)] (**68a**)	1665
4	[$AuBr_2$(*N*-mal)(I^tBu)] (**66d**)	1675	14	[$AuBr_2$(*N*-mal)(IMes)] (**68b**)	1677
5	[$AuBr_2$(*N*-ptm)(I^tBu)] (**66e**)	1682	15	[$AuBr_2$(*N*-ptm)(IMes)] (**68c**)	1683
6	[$AuBr_2$(*N*-obs)(I^tBu)] (**66f**)	1694	16	succinimide	1722
7	[$AuBr_2$(*N*-succ)(I^tPe)] (**67a**)	1663	17	2,3-dibromosuccinimide	1744
8	[$AuBr_2$(*N*-dbs)(I^tPe)] (**67b**)	1690	18	maleimide	1731
9	[$AuBr_2$(*N*-tfs)(I^tPe)] (**67c**)	1716	19	phthalimide	1741
10	[$AuBr_2$(*N*-mal)(I^tPe)] (**67d**)	1675	20	*o*-benzoic sulfimide	1742

[a] Carbonyl stretching frequency of tetrafluorosuccinimide not obtained due to poor solubility in CH_2Cl_2.

The carbonyl stretching frequency of the imidate ligands were compared to the ^{13}C NMR carbene carbon shift of the NHC ligands for both [Au(*N*-imidate)(NHC)] (**55-57**) and [$AuBr_2$(*N*-imidate)(NHC)] (**66-68**) complexes (Figure 11). The plot clearly shows the difference in ^{13}C NMR carbene carbon shift between the Au(I) and Au(III) complexes, and the electronic similarity of I^tBu and I^tPe ligands compared to IMes. *N*-succ, *N*-mal and *N*-ptm ligands are relatively similar in both carbonyl stretching frequency and the carbene chemical shift. *N*-Obs (for Au(I)) and particularly *N*-tfs (for Au(I) and Au(III)) are outlying in both respects due to the electron withdrawing ability of their substituents creating a more electron deficient Au atom.

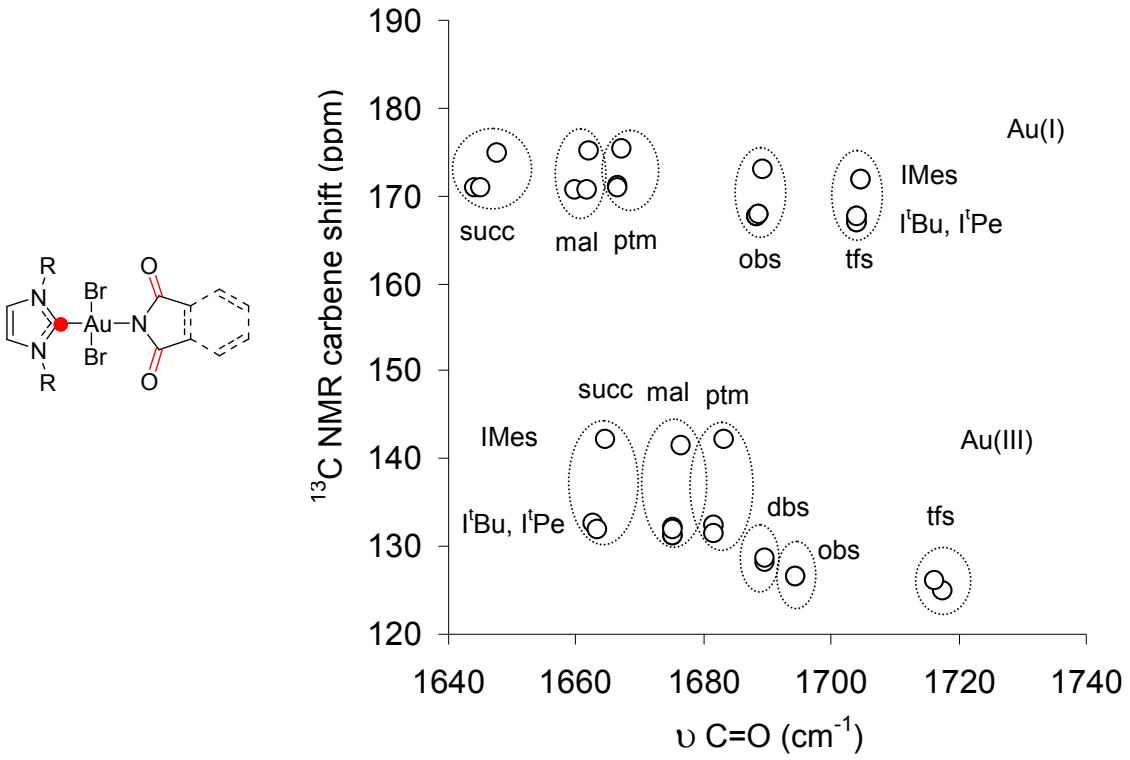

Figure 11. Comparison of the ^{13}C NMR carbene carbon shifts[a] and carbonyl C=O stretching frequencies of [Au(*N*-imidate)(NHC)] and [AuBr$_2$(*N*-imidate)(NHC)] complexes.[b]

[a] In $CDCl_3$ at 400 MHz. [b] In CH_2Cl_2.

Complexes **66a**, **66e**, **67a**, **67c** and **68c** were crystallised from fluorobenzene in a pentane saturated solution, which allowed their structures to be determined by X-ray diffraction (Figure 12). Selected bond lengths of these and related complexes are displayed in Table 8.

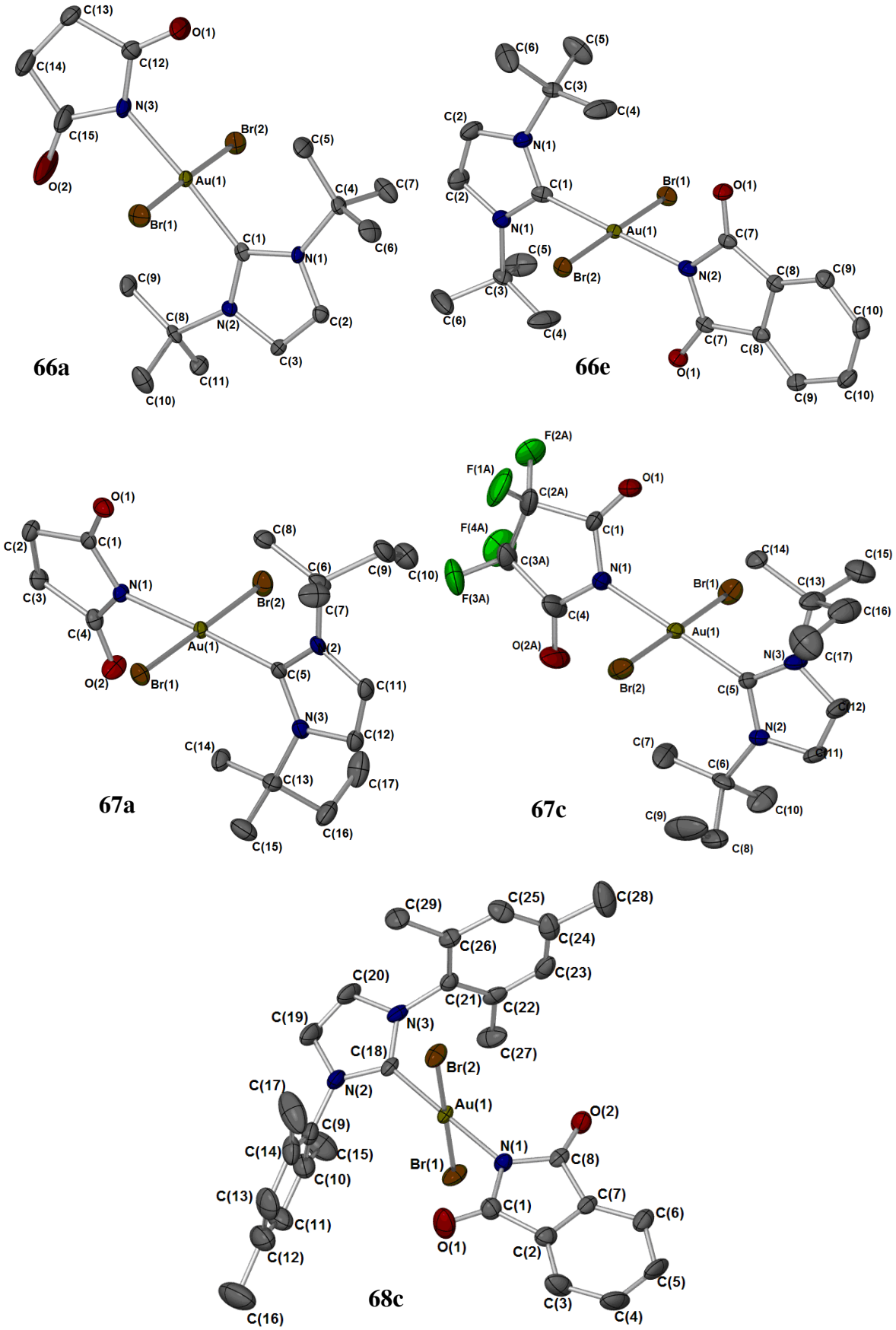

Figure 12. Molecular structures of **66a**, **66e**, **67a**, **67c** and **68c**. Displacement ellipsoids are shown at the 50% probability level. Hydrogen atoms have been omitted for clarity.

Table 8. The bond lengths (Å) of halide, imidate and NHC ligands in Au(III) complexes.[a]

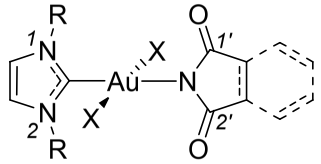

Entry	Complex	Halide			NHC				Imidate				
		Au-X(1)	Au-X(2)	Au-X(3) (*trans*)	Au-C	C-N(1)	C-N(2)	C=C	Au-N	N-C (1')	N-C (2')	C=O (1')	C=O (2')
1	[AuBr$_2$(*N*-succ)(I^{t}Bu)] (**66a**)[b]	2.4144(5)	2.4390(5)		2.006(4)	1.350(5)	1.356(5)	1.337(6)	2.054(3)	1.341(6)	1.364(6)	1.206(5)	1.204(7)
		2.4247(5)	2.4264(4)		2.016(4)	1.349(5)	1.355(5)	1.342(6)	2.040(3)	1.370(5)	1.381(5)	1.205(5)	1.214(5)
2	[AuBr$_2$(*N*-ptm)(I^{t}Bu)] (**66e**)[c]	2.4328(6)	2.4310(6)		2.001(6)	1.367(5)	–	1.333(10)	2.016(5)	1.389(5)	–	1.217(5)	–
3	[AuBr$_2$(*N*-succ)(I^{t}Pe)](**67a**)[b]	2.4264(3)	2.4304(4)		2.019(3)	1.347(3)	1.353(4)	1.332(4)	2.039(2)	1.370(4)	1.377(3)	1.218(4)	1.226(3)
		2.4273(4)	2.4308(4)		1.999(3)	1.360(4)	1.357(4)	1.324(5)	2.038(2)	1.381(3)	1.374(3)	1.225(3)	1.228(3)
4	[AuBr$_2$(*N*-tfs)(I^{t}Pe)] (**67c**)	2.4182(8)	2.4225(8)		2.001(6)	1.353(8)	1.350(8)	1.344(10)	2.048(6)	1.367(9)	1.371(10)	1.198(9)	1.11(7) 1.26(3)
5	[AuBr$_2$(*N*-ptm)(IMes)] (**68c**)	2.4174(4)	2.4183(4)		2.002(3)	1.353(4)	1.352(4)	1.328(6)	2.049(3)	1.362(4)	1.383(5)	1.216(4)	1.222(4)
6	Phthalimide[102]									1.381	1.395	1.216	1.222
7	[AuBr$_3$(I^{t}Bu)][86] (**66g**)	2.4209(6)	2.4638(6)	2.4403(6)	2.015(5)	1.351	1.389						
8	[AuBr$_3$(IMes)][86] (**68d**)	2.4156(15)	2.4123(14)	2.4224(12)	2.009(8)	1.370(7)	1.342(7)						
9	[AuCl$_3$(I^{t}Bu)][37] (**69**)	2.2864(9)	2.2872(9)	2.320(13)	2.006(4)								
10	[AuCl$_3$(IMes)][37] (**70**)	2.268(2)	2.276(2)	2.306(2)	1.977(6)								
11	[Au(*N*-ptm)$_2$(2-bp)][83c] (**71**)									1.367(14)	1.382(16)	1.212(15)	1.237(16)
										1.363(16)	1.387(17)	1.228(17)	1.235(16)

[a] The ESD values are given in brackets where known. [b] Complexes **66a** and **67a** contain two molecules in the unit cell. [c] Compound **4d** is centrosymmetric.

The structures are all four coordinate, square planar, complexes with bond angles between the ligands of 87.73(8)-92.04(7)°. The imidate and NHC imidazole rings are approximately coplanar and perpendicular to the $AuBr_2$ plane, which minimises steric interactions between the ligands. The unit cell of complex **66a** contains two [$AuBr_2$(*N*-succ)(I^{t}Bu)] conformers. One has torsion angles of 73.7(4)-107.3(4)° between the imidate ring and $AuBr_2$ plane and 86.2(3)-94.9(3)° for the imidazole ring and the second 71.5(3)-108.5(3)° and 85.0(3)-95.8(3)°, respectively. Complex **66d** has coplanar ligands with torsion angles of 89.5(4)-90.5(4)°. Complex **67a** contains two [$AuBr_2$(*N*-succ)(I^{t}Pe)] conformers and a C_6H_5F molecule, the NHC ligands are coplanar with the $AuBr_2$ plane with torsion angles of 87.7(2)-91.6(2)° and 87.8(3)-92.6(3)°, respectively, and the imidates are out of plane by 74.8(2)-106.0(2)° and 72.8(2)-106.8(2)°. Complex **67c** contains one conformer in the unit cell but it has disorder about the imidate backbone (one C=O and the C-F bond). The rings are relatively coplanar, 85.1(6)-94.3(6)° for the NHC and 80.7(6)-99.4(8)° for the imidate ligand. Complex **68c** is non-planar with torsion angles of 79.2(3)-101.7(3)° for the imidate ring and 69.3(3)-111.6(3)° for the imidazole ring.

Complex **68c** has a slightly longer Au-N bond (by 0.033(8) Å) than the analogous complex **66e,** whilst the imidate bond lengths are similar. These bond lengths are also similar to those reported for [Au(*N*-ptm)$_2$(2-bp)] (**71**) by Kilpin *et al.*,[83c] and those of the neutral imide.

The *N*-succ ligand in complex **66a** has a longer Au-N bond (0.024(8)-0.038(8) Å) and shorter N-C bonds (0.013(10)-0.037(10) Å) than the *N*-ptm ligand in analogue **66d**, suggesting transfer of electron density from the Au-N to N-C bonds. Complexes **66a** and **67a** have similar bond lengths, as do **67a** and **67c**.

Complexes **66a**, **66d** and **68c** and the analogous tribromide complexes, **66g** and **68d**, all possess similar NHC bond lengths. Complexes **66a** and **66d** also have similar bromide bond lengths to the tribromide complex **66g**. This is also observed for complex **68c** and the analogous tribromide complex **68d**. On oxidative bromination, from Au(I) to Au(III), there is little variation in bond lengths for complex **66d** (compared with **55c**), which has been reported in other Au(III) NHC complexes.[37,86]

The Au-N bonds in **66a** and **66e** are significantly shorter than the Au-Cl and Br bonds *trans* to the NHC ligand in complexes **66g** and **69**. For example, for complex **66a** the differences are 0.3933(9) Å and 0.273 (6) Å, respectively, and analogously for **68c, 66d** and **70** (0.373 (4) Å and 0.257(5) Å differences, respectively).

2.2.1.3. ^{15}N labelling of Au(I) and Au(III) *N*-succinimidate complexes

[Au(^{15}*N*-succ)(I^{t}Pe)] (**72**) and [AuBr$_2$(^{15}*N*-succ)(I^{t}Pe)] (**73**) were synthesised from ^{15}N-succinimide by the normal method and fully characterised. The ^{13}C NMR spectra in $CDCl_3$ show coupling of the labelled nitrogen to the adjacent carbonyl, the succinimide CH_2 groups and the carbene carbon through the Au atom. This coupling is observed as the expected doublet (Table 9) and is consistent with the findings of Berners-Price *et al.*.[84d]

Table 9. ^{15}N to ^{13}C coupling constants in the ^{13}C NMR spectra of [Au(^{15}*N*-succ)(I^{t}Pe)] (**72**) and [AuBr$_2$(^{15}*N*-succ)(I^{t}Pe)] (**73**).

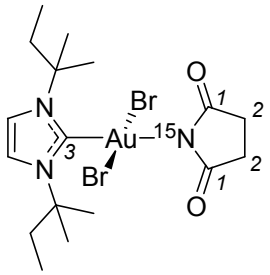

Entry	Nuclei coupled to ^{15}*N*	Coupling constant (Hz) [Au(^{15}*N*-succ)(I^{t}Pe)] (**72**)	Coupling constant (Hz) [AuBr$_2$(^{15}*N*-succ)(I^{t}Pe)] (**73**)
1	succ ^{13}C=O (1)	8	9
2	succ $^{13}CH_2$ (2)	4	5
3	carbene ^{13}C (3)	15	25

The data shows that coupling of ^{15}N to the C=O and CH_2 carbons of the succinimidate ligand is approximately the same for both complexes, increasing slightly for **73**, as the ligand's electronic structure would not alter much on oxidation of the Au atom. However, the coupling to the carbene carbon of I^{t}Pe is comparatively very strong, 15 Hz for **72** and 25 Hz for **73**. There is clearly significant communication between the two ligands *via* the Au atom. This would suggest that more electron density is present in the σ bond for **72**,[106] as the imidate would donate more electron density to the more electropositive Au atom. In the solid state-structure (for the related I^{t}Bu series, **55a** and **66a**) the bonds get slightly longer for Au(III) (although not statistically significant), also in the Au(I) crystal structure the imidate and NHC imidazole rings are perpendicular, however in the Au(III) structure they are approximately coplanar, which would alter the orbitals involved in π bonding on the metal.

The ^{15}N NMR spectrum (50 MHz, CD_2Cl_2) of **72** contains only a singlet at 209.4 ppm, and that of **73** a singlet at 179.4 ppm. The upfield signal of the Au(III) complex relative to Au(I) reflects the behaviour seen for the carbene carbon in the ^{13}C NMR spectrum, however the bonding and orbitals of the two ligands are very different. Another aspect may be the different orientations of the succinimidate ligands in the Au(I) and Au(III) complexes as described above.

It has been reported that, based upon spectroscopic evidence (particularly ^{13}C NMR), *N*-aryl substituted NHCs are actually stronger σ donors than *N*-alkyl analogues, resulting in *N*-alkyl complexes being more Lewis acidic than *N*-aryl. Likewise it is proposed that NHCs with chloride substituents on the imidazole ring decrease the Lewis acidity of a coordinated metal and methyl substituents increase the acidity relative to the unsubstituted analogue.[37,89] This is in contradiction to computational studies by Radius and Bickelhaupt who found that a *N*-isopropyl substituted NHC is a better σ donor than a *N*-phenyl substituted NHC.[107] The computational findings would appear to be more logical, based upon chemical intuition.

The spectroscopic characterisation does not give a clear indication as to whether the *N*-alkyl substituted NHCs (I^tBu and I^tPe) are better donors relative to the *N*-aryl (IMes) for the Au(I) and Au(III) imidate complexes. ^1H and ^{13}C NMR spectra of the imidate ligands suggest IMes is more donating (than I^tBu and I^tPe) as the signals are more upfield (on oxidation from Au(I) to Au(III) they shift downfield). ^{13}C NMR signals of the IMes ligand carbene carbon are shifted downfield, intuitively suggesting it is less donating, although the carbene signal moves upfield on oxidation of a coordinated metal. The infra-red carbonyl stretching frequencies suggest IMes is less donating, as the signal is at higher wavenumber (a stronger carbonyl bond indicates the nitrogen lone pair is more localised in the Au-N rather than N-C bond). X-ray diffraction data is inconclusive as the IMes Au-C bond is shorter in Au(I) complexes but longer in Au(III). Experimental evidence, such as the instability of [$AuBr_2$(*N*-imidate)(IMes)] complexes with very electron withdrawing imidates *N*-tfs, *N*-dbs and *N*-obs suggests IMes is less electron donating and so less able to stabilise the electron deficient complexes.

2.2.2. Catalysis

2.2.2.1. Cycloisomerisation of 4-phenyl-1-hexen-5-yne

The 1,5-enyne, 4-phenyl-1-hexen-5-yne (**74**), has been shown to undergo Au(I) and Au(III) catalysed cycloisomerisation to afford a bicyclo[3.1.0]hexyl ring system (Scheme 17).[15]

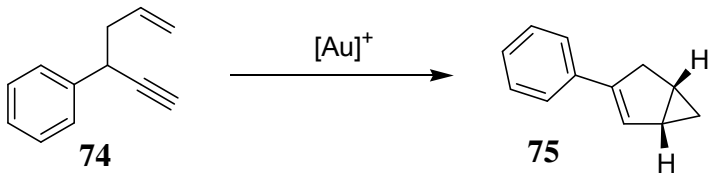

Scheme 17. The gold catalysed cycloisomerisation of 4-phenyl-1-hexen-5-yne (**74**) to produce 3-phenylbicyclo[3.1.0]hex-2-ene (**75**).

The group of Toste[15] has shown that simple Pd or Pt complexes {$[PdCl_2(MeCN)_2]$ and $PtCl_2$} achieve less than 5% conversion. However, $AuCl_3$ shows a 50% conversion after 3 hours without added salts, and quantitative conversion when 3 equivalents of $AgBF_4$ was added at 5 mol % Au loading. $[Au(PPh_3)]X$ salts (X is PF_6 or BF_4) give complete conversion at 1% Au loading in under 5 minutes.

The first step of the reaction[15] involves the binding of a gold cation (typically formed by halide abstraction from a gold complex by a silver salt) to the alkyne (Scheme 18, Step I). This withdraws electron density from the bond, due to a lack of back-bonding from gold to the alkyne antibonding orbitals,[42] making it susceptible to nucleophilic attack. The alkene acts as a nucleophile and attacks the alkyne in the Markovnikov position to form the bicyclo[3.1.0]hexane structure *via* a 5-*endo-dig*[108] cyclisation (Step II). The Au complex is thought to help stabilise the carbocation by π-backbonding to give the Au-carbon bond carbene character (the lower energy of the empty carbocation p orbital allows backbonding, *c.f.* gold alkyne bonding).[35] A hydride then migrates to form a carbocation at the adjacent position (Step III) which is quenched by elimination of Au to give the bicyclohexene **75** (Step IV). From this mechanism it would be logical to assume that a more electropositive Au cation would bind and activate the alkyne more strongly, although this may be to the detriment of stabilisation of the carbocationic intermediate. As the Au(III) imidate complexes possess *trans* geometries, the free site generated by bromide abstraction will occur *trans* to the other bromide rather than to the NHC which occurs with [AuBr(NHC)]

and [$AuBr_3$(NHC)] precatalysts. This will presumably have the effect of promoting binding and activation of the alkyne and also help stabilise the carbocation (as π-donation from bromide would be greater than from the NHC ligand). It would be reasonable to assume that the complexes with more electron withdrawing imidate ligands should be more active in reactions involving alkyne activation.

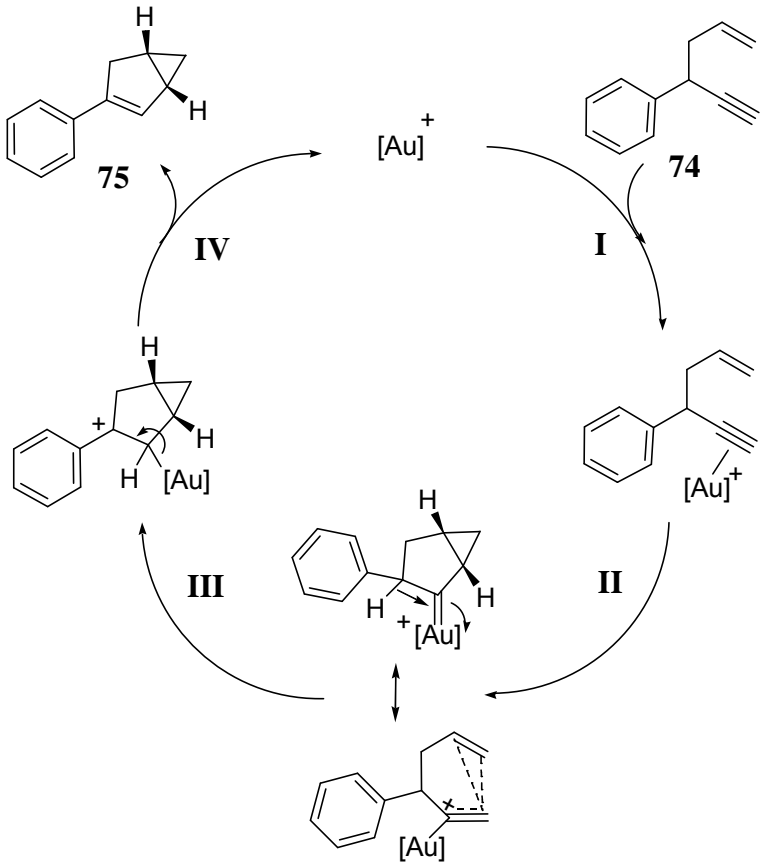

Scheme 18. The mechanism of gold catalysed 5-*endo-dig* cycloisomerisation of 4-phenyl-1-hexen-5-yne (**74**) to produce 3-phenylbicyclo[3.1.0]hex-2-ene (**75**).

Conditions for the reaction catalysed by [$AuBr_2$(*N*-imidate)(NHC)] (**66**-**68**) complexes were determined using complex **66a** and a 0.5 M solution of **74** in CH_2Cl_2 in the presence and absence of AgOTf (Table 10).

Table 10. Cycloisomerisation of 4-phenyl-1-hexen-5-yne (**74**) using **66a** and $AuCl_3$.[a]

Entry	Au catalyst	Amount (mol%)	Ag additive	Amount (mol%)	Temp (˚C)	Conv. (%)[b]
1	$AuCl_3$	1	-	-	25	60
2	-	-	AgOTf	1	25	0
3	[$AuBr_2$(*N*-succ)(I^{t}Bu)] (**66a**)	1	-	-	25	0
4	[$AuBr_2$(*N*-succ)(I^{t}Bu)] (**66a**)	1	AgOTf	1	25	32
5	[$AuBr_2$(*N*-succ)(I^{t}Bu)] (**66a**)	2	AgOTf	2	25	> 99
6	[$AuBr_2$(*N*-succ)(I^{t}Bu)] (**66a**)	1	AgOTf	1	35	95

[a] Conditions: 0.5 M 4-phenyl-1-hexen-5-yne (**74**) in CH_2Cl_2, 3 h. [b] Conversion determined by ^{1}H NMR spectroscopic analysis of the crude reaction mixture (average of two runs).

The results show that the reaction is not catalysed independently by either **66a** or AgOTf. This is consistent with previous work[15,86] and suggests that a cationic Au centre is required for effective catalytic cycloisomerisation. Consequently, when **66a** was treated with 1 equivalent of AgOTf, a 32 % conversion was achieved at 1 mol% catalyst loading, over 3 hours at 25 ˚C. If the temperature was increased to 35 ˚C, or the Au loading increased to 2 mol%, essentially the reaction reached quantitative conversion. It is interesting to note that analogous Au(I), [Au(*N*-imidate)(NHC)], complexes do not catalyse the reaction under the equivalent conditions, due to the requirement for a cationic Au centre.

Initial studies on the reaction kinetics of the 1,5-enyne cycloisomerisations revealed that there is a significant variation in the rate of bromide extraction by the silver additive (metathesis) depending on the type of imidate ligand employed. Qualitative tests revealed that there is a correlation between the electronegativity of the imidate ligand and the rate at which the bromide ligand is abstracted. In the case of the tribromide and succinimidate complexes, bromide extraction occurs immediately on mixing in solution, which is observable by the precipitation of silver(I) bromide. Complexes containing more electron-withdrawing imidates are activated more slowly, with gradual precipitation seen using phthalimidate and maleimidate, and no observable formation with tetrafluorosuccinimidate and *o*-benzoic sulfimidate complexes. This results in very low product conversions when the catalyst is added to the reaction solution without prior formation of the active catalyst for the electron-withdrawing imidates (Table 11). However, when the catalyst and silver

salt are mixed in CH_2Cl_2 and the solvent is removed *in vacuo*, redissolution in the reaction solvent results in immediate precipitation of silver(I) bromide. In order to ensure reliable results preactivation was carried out before each test.

Table 11. Effect of active catalyst preformation on the efficiency of [$AuBr_2$(*N*-imidate)(I^tPe)] complexes in the cycloisomerisation of 4-phenyl-1-hexen-5-yne (**74**).[a]

		Conversion (%)[b]	
Entry	**Complex**	**No preformation**	**Preformation**
1	[$AuBr_2$(*N*-succ)(I^tPe)] (**67a**)	29	35
2	[$AuBr_2$(*N*-tfs)(I^tPe)] (**67c**)	3	89
3	[$AuBr_2$(*N*-ptm)(I^tPe)] (**67e**)	31	66

[a] Conditions: 0.5 M solution of 4-phenyl-1-hexen-5-yne (**74**) in CH_2Cl_2, 1 mol% Au catalyst, 1 mol% AgOTf, 3 h, 25˚C. [b] Conversion determined by ^{1}H NMR spectroscopic analysis of the crude reaction mixture (average of two runs).

The remaining [$AuBr_2$(*N*-imidate)(NHC)] complexes (**66**-**68**) were tested for activity in this reaction, at 1 mol% Au and AgOTf loading, at 25 ˚C over 3 hours (Table 12).

Table 12. Comparison of [$AuBr_2$(*N*-imidate)(NHC)] (**66**-**68**) complexes using AgOTf for 4-phenyl-1-hexen-5-yne (**74**) cycloisomerisation.[a]

Entry	Complex	Conv. (%)[b]	Entry	Complex	Conv. (%)[b]
1	[$AuBr_2$(*N*-succ)(I^tBu)] (**66a**)	32	11	[$AuBr_2$(*N*-ptm)(I^tPe)] (**67e**)	66
2	[$AuBr_2$(*N*-dbs)(I^tBu)] (**66b**)	87	12	[$AuBr_2$(*N*-obs)(I^tPe)] (**67f**)	95
3	[$AuBr_2$(*N*-tfs)(I^tBu)] (**66c**)	81	13	[$AuBr_3$(I^tPe)] (**67g**)	32
4	[$AuBr_2$(*N*-mal)(I^tBu)] (**66d**)	94	14	[$AuBr_2$(*N*-succ)(IMes)] (**68a**)	51
5	[$AuBr_2$(*N*-ptm)(I^tBu)] (**66e**)	53	15	[$AuBr_2$(*N*-mal)(IMes)] (**68b**)	66
6	[$AuBr_2$(*N*-obs)(I^tBu)] (**66f**)	83	16	[$AuBr_2$(*N*-ptm)(IMes)] (**68c**)	51
7	[$AuBr_3$(I^tBu)][86] (**66g**)	34	17	[$AuBr_3$(IMes)][86] (**68d**)	3
8	[$AuBr_2$(*N*-succ)(I^tPe)] (**67a**)	35	18	[AuBr(I^tBu)][86] (**55g**)	98
9	[$AuBr_2$(*N*-dbs)(I^tPe)] (**67b**)	95	19	[AuBr(I^tPe)] (**56g**)	99
10	[$AuBr_2$(*N*-tfs)(I^tPe)] (**67c**)	89	20	[AuBr(IMes)][86] (**57g**)	68
11	[$AuBr_2$(*N*-mal)(I^tPe)] (**67d**)	99			

[a] Conditions: 0.5 M solution of 4-phenyl-1-hexen-5-yne (**74**) in CH_2Cl_2, 1 mol% Au catalyst, 1 mol% AgOTf, 3 h, 25°C. [b] Conversion determined by ^{1}H NMR spectroscopic analysis of the crude reaction mixture (average of two runs).

The results show that there is a significant effect of the nature of the imidate ligand on the catalytic activity of I^tBu and I^tPe Au(III) complexes. These sets of complexes (**66** and **67**) give very similar results due to the electronic similarities of the ligands. The succinimidate and tribromide complexes (**66a**, **66g**, **67a** and **67g)** exhibit low catalytic activity, giving approximately 30% conversion. The phthalimidate complexes (**66e** and **67e**) give higher conversion at 53 and 66%, respectively, due to the formation of more electropositive Au(III) complexes that are able to activate the alkyne more effectively. The maleimidate Au(III) complexes (**66d** and **67d**) give more than 90% conversion. This outcome is surprising considering the electronic similarity to the phthalimidate ligand.

The *N*-tfs (**66b** and **67b**), *N*-dbs (**66c** and **67c**) and *N*-obs (**66f** and **67f**) Au(III) complexes give high % conversions, of 87 and 95, 81 and 89, and 83 and 95, respectively, presumably due to the greater acidity of the activated catalysts. The Au(I) bromide

catalysts (**55g** and **56g**) show virtually quantitative conversion. The higher conversion despite the lower acidity of the active Au(I) cation could be caused by a number of factors including; reduced steric hindrance in the linear complex, better stabilisation of carbocation intermediates, less competitive binding to the cation and easier formation of the naked cation. Another explanation is that the Au(III) complexes decompose to Au(I) which could be the active catalytic species, as observed in other reactions,[31] and the conversions reflect the ease of reduction to Au(I).

The IMes substituted complexes do not follow this trend. The, *N*-succ, *N*-mal and *N*-ptm complexes (**68a**, **68b** and **68c**) all give similar conversions of 51, 66 and 51%, respectively, although **68b** is the most active as with **66d** and **67d**. The Au(I) bromide (**57g**) resulted in 68% conversion and the tribromide (**68d**) less than 5%.

A selection of the catalysts were tested using a very weakly coordinating anion derived from the silver salt, $Ag[Al(OC(CF_3)_3)_4]$ (**76**) (Table 13).[91] The results show that, as predicted, the use of this anion greatly increases the rate of reaction. For complex **67b** > 99% conversion occurs in under 30 minutes at 25 ˚C, compared with 95% after 3 hours at 25 ˚C using AgOTf. In fact 90% conversion was achieved at 0 ˚C in just 30 minutes. The weakly coordinating anion (**76**) creates a more 'naked' Au cation which is better able to coordinate the alkyne and catalyse the reaction.

A selection of the I^{t}Pe containing complexes were then tested at 0 ˚C, with a reaction time of 15 minutes. As expected the Au(I) complex [AuBr(I^{t}Pe)] (**56g**) gave the highest conversion at 95%. Under the conditions, complexes **67c** and **67f** showed the highest conversion of the imidate complexes at 90% and 87%, respectively. However, **67b** gave only 63% and **67g** 79%. The high conversion achieved for the tribromide on combination with **76** relative to AgOTf suggests that the bromide is relatively active but unstable at longer reaction times. The efficiency of catalyst activation will also have a more significant effect for short reaction times.

Table 13. Comparison of [$AuBr_2$(*N*-imidate)(I^tPe)] (**67**) complexes with $Ag[Al(OC(CF_3)_3)_4]$ (**76**) in the cycloisomerisation of 4-phenyl-1-hexen-5-yne (**74**).[a]

Entry	Au Catalyst	Time (mins)	Conversion (%)[b]
1	[$AuBr_2$(*N*-dbs)(I^tPe)] (**67b**)	30	90
2	[$AuBr_2$(*N*-dbs)(I^tPe)] (**67b**)	15	63
3	[$AuBr_2$(*N*-obs)(I^tPe)] (**67f**)	15	87
4	[$AuBr(I^tPe)$] (**56g**)	15	95
5	[$AuBr_2$(*N*-tfs)(I^tPe)] (**67c**)	15	90
6	[$AuBr_3(I^tPe)$] (**67g**)	15	79

[a] Conditions: 0.5 M solution of 4-phenyl-1-hexen-5-yne (**74**) in CH_2Cl_2, 1 mol% Au complex, 1 mol% $Ag[Al(OC(CF_3)_3)_4]$ (**76**), 0 °C. [b] Conversion determined by ^{1}H NMR spectroscopic analysis of the crude reaction mixture (average of two runs).

The silver salts AgOTf and $AgSbF_6$ were then tested under these conditions (but without preactivation) using complex **67c** (Table 14).

Table 14. Comparison of silver salts for the cycloisomerisation of 4-phenyl-1-hexen-5-yne (**74**) with **67c**.[a]

Entry	Ag co-catalyst	Time (mins)	Conversion (%)[b]
1	AgOTf	15	<1
2	$Ag[Al(OC(CF_3)_3)_4]$ (**76**)	15	90
3	$AgSbF_6$	15	>99

[a] Conditions: 0.5 M solution of 4-phenyl-1-hexen-5-yne (**74**) in CH_2Cl_2, 1 mol% Ag co-catalyst, 1 mol% **67c**, 0 °C. [b] Conversion determined by ^{1}H NMR spectroscopic analysis of the crude reaction mixture.

$Ag[Al(OC(CF_3)_3)_4]$ (**76**) is predictably superior to AgOTf under these conditions, with <1% conversion for the triflate salt. However, $AgSbF_6$ appears to be even more efficient which is very surprising given that it is more strongly coordinating than **76**. Due to the short reaction time the solubility of the Ag salts will be a significant factor and so these results may not reflect the true efficiency of the Ag co-additives.

2.2.2.2. Kinetics of 4-phenyl-1-hexen-5-yne cycloisomerisation

The kinetic profile of the Au-catalysed cycloisomerisation of enyne **74** was followed by gas chromatography. 1,2-Dichloroethane was used as solvent at a concentration of 0.2 M with a positive pressure of argon in order to reduce the effects of sampling on the reaction (1 mol% Au complex and 1 mol% AgOTf were used). Initially complex **76c** was tested to determine the order and initial rate of this reaction by plotting [enyne] and ln[enyne] against time (Figure 13 and Figure 14). As would be expected the intramolecular isomerisation reaction is to a good approximation first order (standard error is 3.4% using linear least squares regression, R^2 is 0.958) with an observed initial rate of 10.05 $x10^{-5}$ $mol.dm^{-3}.s^{-1}$.

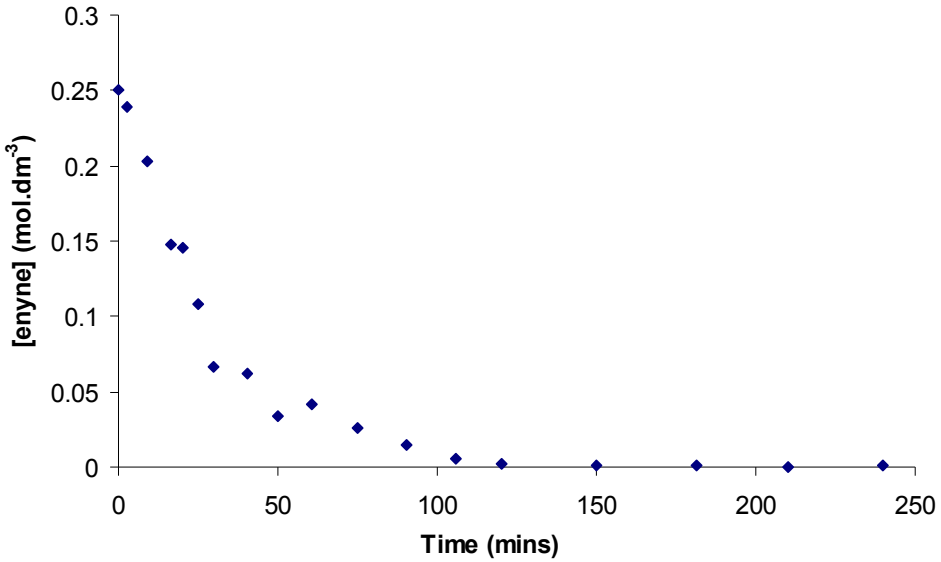

Figure 13. Plot of [enyne] against time to test for 0^{th} order kinetics.

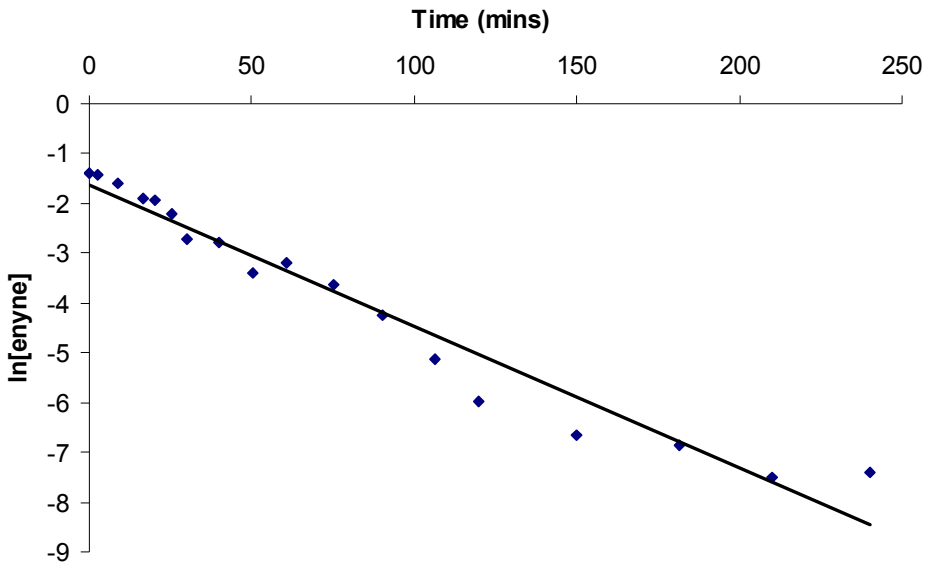

Figure 14. Plot of ln[enyne] against time to test for 1st order kinetics.

A representative sample of the complexes were analysed in this manner (Figure 15), initial rates and observed rate constants were calculated by this method (Method A) assuming 1st order kinetics. The data was further analysed using a nonlinear least-squares regression curve fitting program (Dynafit, published by Biokin)[109] which fits the experimental kinetic data to predetermined molecular mechanisms (Method B). This was used to determine the order of reaction, observed rate constants and initial rates and to fit curves to the kinetic data (Table 15, fitted curves are shown in Figure 15).

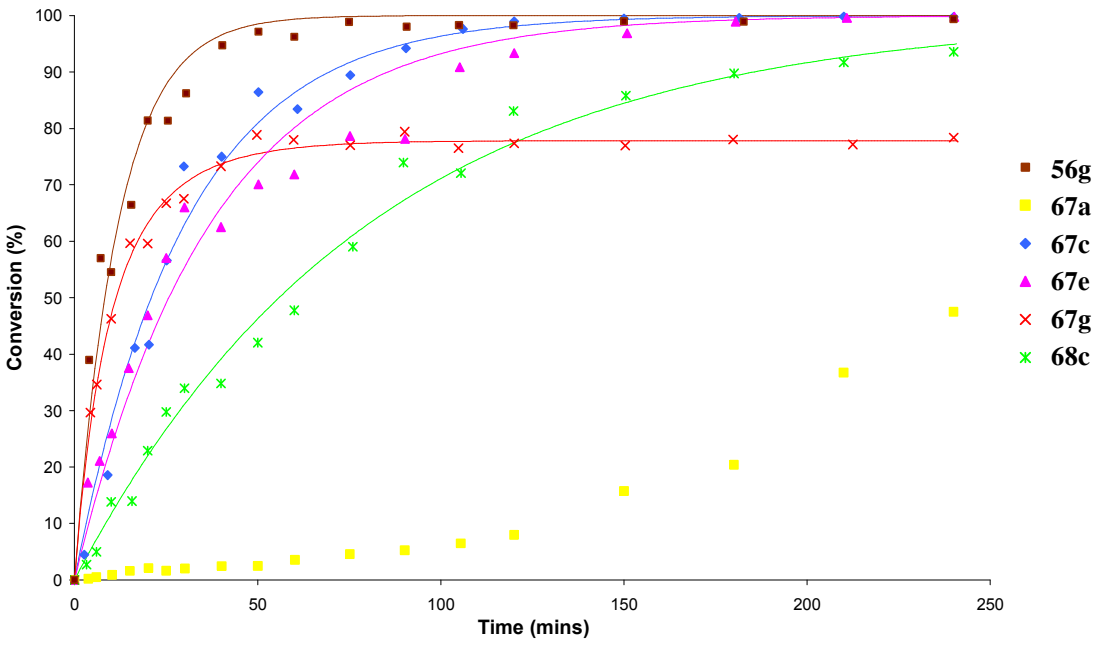

Figure 15. Kinetic profiles for Au catalysts in the cycloisomerisation of 4-phenyl-1-hexen-5-yne (**74**).[a]

[a] Conditions: 0.2 M solution of 4-phenyl-1-hexen-5-yne (**74**) in 1,2-dichloroethane, 1 mol% Au complex, 1 mol% AgOTf, 25 ˚C. Conversion determined by gas chromatographic analysis of 10 µl aliquots of the crude reaction mixture, quenched with NBu_4Br. Curves fitted using Dynafit software with standard errors < 5%.

Table 15. Observed rate constants and initial rates for Au catalysts in the cycloisomerisation of 4-phenyl-1-hexen-5-yne (**74**).

Entry	Complex	Method A (linear)				Method B (curve fitting)		
		Time period (mins)	k_{obs} x10^{-4} (s^{-1})	Rate[a]	Standard Error (%)	k_{obs} x10^{-4} (s^{-1})	Rate[a]	Standard Error (%)
1	[AuBr(I^tPe)] (**56g**)	0-50	11.90	23.84	3.1	13.98	27.96	4.2
2	[$AuBr_2$(*N*-succ)(I^tPe)] (**67a**)	0-120	0.11	0.21	2.8	0.25	0.50	8.4
		180-240	1.16	2.30	6.0			
3	[$AuBr_2$(*N*-tfs)(I^tPe)] (**67c**)	0-240	5.03	10.05	3.4	5.52	11.04	3.0
4	[$AuBr_2$(*N*-ptm)(I^tPe)] (**67e**)	0-240	4.12	8.20	3.4	4.49	8.97	4.2
5	[$AuBr_3$(I^tPe)] (**67g**)	0-50	6.11	12.24	7.5	-[b]	21.87	2.3
6	[$AuBr_2$(*N*-ptm)(IMes)] (**68c**)	0-240	2.05	4.10	2.1	2.07	4.14	2.0

[a] Rate at T_0 x10^{-5} (mol.dm^{-3}.s^{-1}). [b] Second order, k_{1obs} = 5468 x10^{-4} mol^{-1}.dm^3.s^{-1}, k_{2obs} = 9.07 x10^{-4} s^{-1} (error 3.0%).

The results show the reactions were more efficient under these conditions than in 0.5 M CH_2Cl_2 (in air). This is possibly due to reduced bimolecular decomposition under more dilute conditions, and less expeditious water and oxygen due to the argon atmosphere.

Complexes **56g**, **67c**, **67e** and **68c** show reasonable first order kinetics by both Methods A (linear regression analysis of ln[enyne] *vs* time plot) (standard error is 2.1-3.4%) and B (curve fitting using Dynafit) (error is 2.0-4.2%). The two methods of analysis gave similar rate constants where errors were low, but there were greater discrepancies where the error was higher, particularly for **56g** which has a rate constant of 11.90 x10^{-4} s^{-1} calculated by Method A and 13.98 x10^{-4} s^{-1} by B (only the initial, most linear, 50 minutes was used for the calculation by Method A, whereas all of the data was used for Method B).

Complexes **67a** and **67g** did not display 1st order kinetics. Complex **67a** has an induction period with slow conversion (rate = 0.21 x10^{-5} mol.dm^{-3}.s^{-1}, Method A) for the first 180 minutes and then more rapid conversion (rate = 2.30 x10^{-5} mol.dm^{-3}.s^{-1}, Method A). This suggests that despite the complex being preactivated (*vide supra*) an additional catalyst activation step is required for this complex. When **67a** and AgOTf are mixed the precipitation of a yellow solid immediately occurs, it is believed that activation may involve dissolution of this precipitate. An alternative explanation is that the succinimidate

complex takes longer to decompose to an active Au(I) complex as it possesses the most electron donating imidate ligand. Complex **67a** could not be fitted using Method B even if an activation rate was factored into the kinetic model.

The tribromide complex **67g** also exhibits unusual kinetics. The reaction is fast for 50 minutes (rate at T_0 = 12.24 x10^{-5} mol.dm^{-3}.s^{-1}, Method A) achieving 80% conversion, but then the complex rapidly becomes inactive. The reaction was however found to fit very well to a second order rate equation using Method B in which it was assumed that the Au catalyst decomposed over time and that the rate depended on both the concentration of enyne and catalyst. The second order rate equation is:

$$\text{Initial rate} = k_{1obs}[\text{enyne}]_0[\text{Au}]_0 = 21.87 \times 10^{-5}\ \text{mol.dm}^{-3}.\text{s}^{-1}$$

where k_{1obs} {5468 mol^{-1}.dm^3.s^{-1}} is the rate constant for the equation:

$$\text{enyne} + \text{Au} \longrightarrow \text{Au} + \text{product}$$

The rate of catalyst decomposition was:

$$\text{Initial rate of decomposition} = k_{2obs}[\text{Au}]_0 = 1.81 \times 10^{-6}\ \text{s}^{-1}$$

where k_{2obs} (9.07 x10^{-4} s^{-1}) is the rate constant for the decomposition of the Au active catalyst.

This model fitted the data well with low errors for k_{1obs} and k_{2obs} of 2.3 and 3.0%, respectively. The other complexes fitted the first order assumption with lower error than the second order model. These results clearly suggest complex **67g** is a very active catalyst, with an initial rate faster much faster than the Au(III) imidate complexes and close to that of **56g**, but decomposes rapidly, this also fits the experimental data (*vide supra*).

Taking into account the issues described above the order in initial rates is:

56g > 67g ≥ 67c > 67e > 68c > 67a

This does not entirely mirror what is seen in the % conversions (for the 3 hour, 0.5 M CH_2Cl_2 reactions):

56g > 67c > 67e > 68c > 67a > 67g

Noticeably **67g** behaves differently. In 0.5M CH_2Cl_2 this complex recorded a 32% conversion in 3 hours. This disparity also occurred when Ag[Al(OC(CF$_3$)$_3$)$_4$] (**76**) was used (0 ˚C, 15 min, CH_2Cl_2, 0.5 M). These results are explained by the kinetic analysis with the complex having high activity but low stability due to the lack of a stabilising imidate ligand {to prevent bimolecular decomposition to give colloidal Au(0)}. The complex

therefore gives relatively high conversion for fast, facile transformations but low conversions in slower more difficult processes.

It was noticed that the reaction rate was highly dependant upon the purity of the enyne (**74**). Freshly distilled enyne reacted much faster than 'aged' enyne (stored for 4 weeks), which becomes yellow in colour over time. Unfortunately this impurity has not been identified, multiple species including oxidation products (aldehydes) are observed (about 5%, relative to **74**) by ^{1}H NMR spectroscopy. A set of kinetic profiles were carried out with aged enyne to investigate the effect of impurities on the course of the reaction (Figure 16, Table 16).

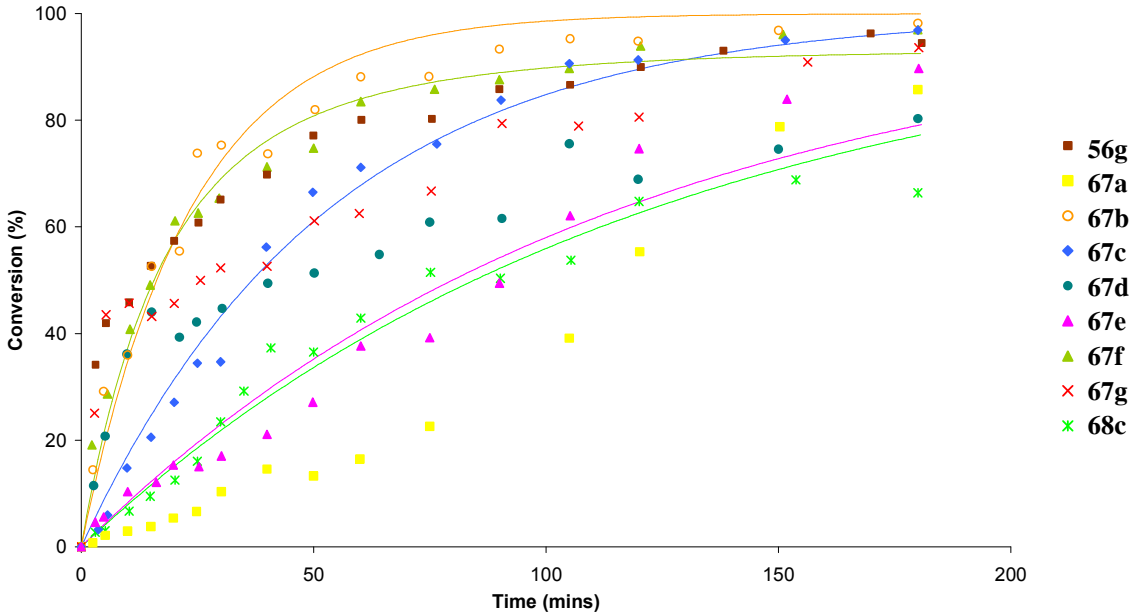

Figure 16. Kinetic profiles for Au catalysts in the cycloisomerisation of 'aged' 4-phenyl-1-hexen-5-yne (**74**).[a]

[a] Conditions: 0.2 M solution of 'aged' 4-phenyl-1-hexen-5-yne (**74**) in 1,2-dichloroethane, 1 mol% Au catalyst, 1 mol% AgOTf, 25 °C. Conversion determined by gas chromatographic analysis of 10 µl aliquots of the crude reaction mixture, quenched with NBu_4Br. Curves fitted using Dynafit software with standard errors < 5%.

Table 16. Observed rate constants and initial rates for Au catalysts in the cycloisomerisation of 'aged' 4-phenyl-1-hexen-5-yne (**74**).[a]

Entry	Complex	Method A (linear)				Method B (curve fitting)		
		Time period (mins)	k_{obs} x10^{-4} (s^{-1})	Rate[b]	Standard error (%)	k_{obs} x 10^{-4} (s^{-1})	Rate[b]	Standard error (%)
1	[AuBr(I^tPe)] (**56g**)	0-180	3.27 (2.58)	6.54 (5.17)	5.3 (6.1)	6.39 (3.70)	12.79 (7.39)	8.4 (9.3)
2	[$AuBr_2$(*N*-succ)(I^tPe)] (**67a**)	0-75 (0-90)	0.54 (0.41)	1.08 (0.82)	3.4 (3.6)	0.98 (0.67)	1.97 (1.34)	8.0 (7.8)
3	[$AuBr_2$(*N*-dbs)(I^tPe)] (**67b**)	0-180	4.32	8.63	4.9	7.12	14.24	4.2
4	[$AuBr_2$(*N*-tfs)(I^tPe)] (**67c**)	0-180	3.33 (2.87)	6.66 (5.74)	1.6 (2.1)	3.14 (2.94)	6.28 (5.87)	2.5 (1.8)
5	[$AuBr_2$(*N*-mal)(I^tPe)] (**67d**)	0-180	1.77 (1.65)	3.54 (3.29)	7.0 (4.5)	2.40 (1.87)	4.80 (3.75)	8.0 (5.3)
6	[$AuBr_2$(*N*-ptm)(I^tPe)] (**67e**)	0-180	1.78	3.57	5.2	1.45	2.89	4.2
7	[$AuBr_2$(*N*-obs)(I^tPe)] (**67f**)	0-180	3.75	7.50	4.4	-[c]	13.68	4.4
8	[$AuBr_3$(I^tPe)] (**67g**)	0-180	2.60	5.20	4.9	3.61	7.22	9.5
9	[$AuBr_2$(*N*-ptm)(IMes)] (**68c**)	0-180	1.26	2.51	4.0	1.37	2.73	2.9

[a] Repeat runs in brackets. [b] at T_0 x10^{-5} (mol.dm^{-3}.s^{-1}). [c] Second order k_{1obs} = 3420 x10^{-4} mol^{-1}.dm^3.s^{-1}, k_{2obs} = 3.19 x 10^{-4} s^{-1} (error 10%).

For the 'aged' enyne complexes **67d** (error is 7.0% for Method A and 8.0% for B) and **56g** (5.3% for A and 8.4% for B) do not give good fits to the first (or second) order models. Complex **67g** also did not fit very well to first (4.9% for A and 9.5% for B) or second order (13% for k_{1obs} for B) kinetics particularly using Method B. Complex **67f** modelled slightly better for second order (4.4% for B) than first order (4.4% for A, 5.3% for B), although the errors are similar and relatively high for both and so a clear distinction cannot be made. The rate of decomposition of the catalyst was calculated to be 6.38 x10^{-7} mol.dm^{-3}.s^{-1} (k_{2obs} = 3.19 x 10^{-4} s^{-1}, 10% error). Complexes **67c** (1.6% error for A, 2.5% error for B) and **68c** (4.0% and 2.9%) again displayed good fits to first order kinetics for both Methods A and B. Complexes **67b** (4.9% and 4.2%) and **67e** (5.2% and 4.2%) also gave acceptable first order fits using Method B. Attempts to factor in the effects of impurities into the kinetic models using the Dynafit software resulted in larger errors for the calculated rate constants.

The 'aged' enyne significantly reduces the rate of the reaction, relative to 'fresh' enyne, although the effect is not felt evenly for all the complexes. Complex **67a** has an increased rate (1.08 $x10^{-5}$ $mol.dm^{-3}.s^{-1}$ for A and 1.97 $x10^{-5}$ $mol.dm^{-3}.s^{-1}$ for B), although it is still the least active of the tested complexes. The reaction rate for **56g** is significantly reduced, from 23.84 to 6.54 $x10^{-5}$ $mol.dm^{-3}.s^{-1}$ for Method A (27.96 to 14.24 $x10^{-5}$ $mol.dm^{-3}.s^{-1}$ for B, although with 8.4% error). Similarly for **67g** with the rate reduced from (12.24) to (5.20) $x10^{-5}$ $mol.dm^{-3}.s^{-1}$ for A (21.87 to 7.22 $x10^{-5}$ $mol.dm^{-3}.s^{-1}$ for B), **67e** and **67c** are also strongly affected.

The calculated rates are generally higher using Method B than Method A except in the cases where the error is low. There are particularly large discrepancies with **56g**, **67b** and **67f**. The order of rates calculated using Method A for the complexes is:

67b > 67f > 67c ≥ 56g > 67g > 67e ≥ 67d > 68c > 67a

Using Method B a slightly different order is obtained:

67b > 67f > 56g > 67g > 67c > 67d > 67e > 68c > 67a

The difference in order may be caused by large discrepancies in the calculated rates between Methods A and B for **56g** and **67g,** which had large errors, and for **67b** and **67f,** which did not fit well to first order kinetics. Again these results do not mirror what was observed in the 0.5M CH_2Cl_2 reaction:

56g > 67d > 67b = 67f > 67c > 67e > 68c > 67a > 67g

Complexes **56g** and **67g** are noticeably lower down the order relative to fresh enyne. Complex **67d**, the most active imidate complex in 0.5M CH_2Cl_2 is also much less active than expected. It would seem that the most active catalysts are most strongly inhibited by the enyne impurities. Also as the kinetics are not modelled well by 1st or 2nd order kinetics it is not possible to determine the relative initial rates of the complexes under these conditions to a high degree of accuracy.

Repeat runs show that the kinetic profiles are reasonably reliable, although the rate for **56g** was further reduced in the repeat (from 6.54 to 5.17 $x10^{-5}$ $mol.dm^{-3}.s^{-1}$ for A, from 12.79 to 7.39 $x10^{-5}$ $mol.dm^{-3}.s^{-1}$ for B). This may be due to further decomposition of the enyne.

The effect of varying the catalyst loading using complex **67e** was investigated. Catalyst loading was tested at 0.5, 1 and 2 mol% (Figure 17, Table 17) (ratio of **67e** to AgOTf 1:1).

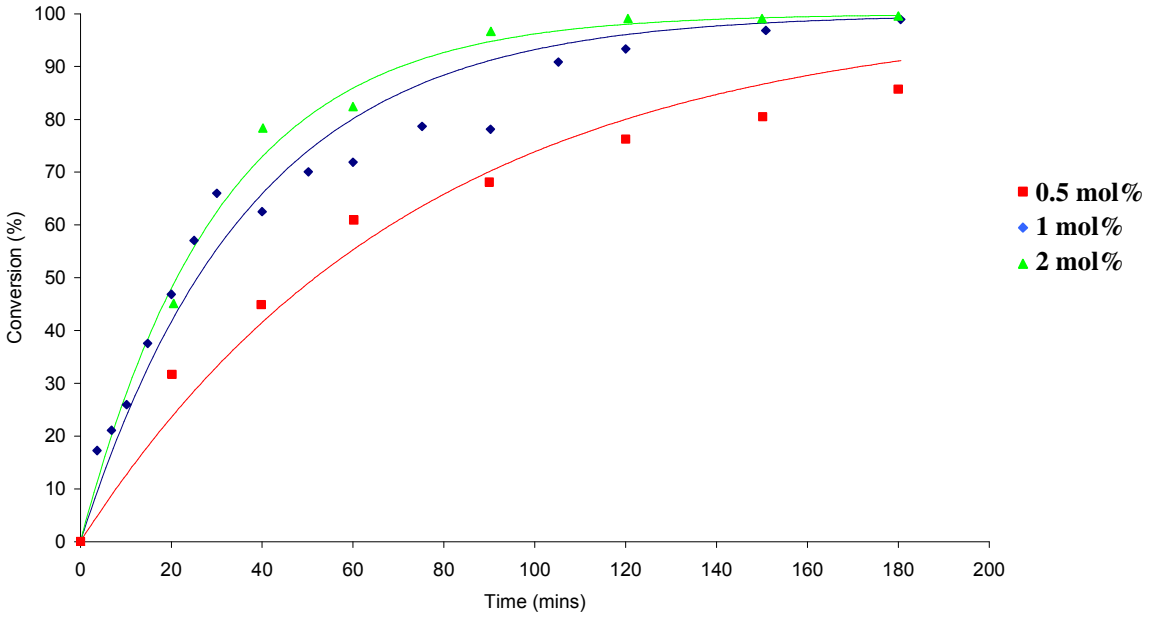

Figure 17. Effect of loading of **67e** on the kinetic profiles for the cycloisomerisation of 4-phenyl-1-hexen-5-yne (**74**).[a]

[a] Conditions: 0.2 M solution of 4-phenyl-1-hexen-5-yne (**74**) in 1,2-dichloroethane, 25 ˚C. Conversion determined by gas chromatographic analysis of 10 µl aliquots of the crude reaction mixture, quenched with NBu_4Br. Curves fitted using Dynafit software.

Table 17. Observed rate constants and initial rates for catalyst **67e** at various loadings in the cycloisomerisation of 4-phenyl-1-hexen-5-yne (**74**).

Entry	Catalyst Loading (mol%)	Method A (linear)			Method B (curve fitting)		
		k_{obs} x10^{-4} (s^{-1})	Rate [a]	Standard error (%)	k_{obs} x 10^{-4} (s^{-1})	Rate[a]	Standard error (%)
1	0.5	1.93	3.86	4.3	-[b]	4.93	3.5
2	1	4.12	8.20	3.4	4.49	8.97	4.2
3	2	5.53	11.06	4.0	5.445	10.89	3.3

[a] at T_0 x10^{-5} (mol.dm^{-3}.s^{-1}). [b] Second order k_{1obs} = 2463 x10^{-4} mol^{-1}.dm^3.s^{-1}, k_{2obs} = 1.25 x 10^{-4} s^{-1} (error 10%).

As would be expected there is a trend of increasing rate with catalyst loading. The rate is reduced significantly by reducing the loading from 1 mol% to 0.5 mol% (8.20 to 3.86 x10^{-5} mol.dm^{-3}.s^{-1} for Method A). The rate increases slightly to 11.06 x10^{-5} mol.dm^{-3}.s^{-1} when the loading is increased to 2%. Similar results were obtained using Method B, with reasonable approximation to first order for 1 and 2 mol% loadings but a better second order (3.5% error) than first order (4.5%) fit for 0.5 mol%, with a catalyst decomposition rate of 2.50

$x10^{-7}$ $mol.dm^{-3}.s^{-1}$, (k_{2obs} is 1.25 $x10^{-4}$ s^{-1}, error 10%). The error is high but the decomposition rate is low and doesn't play a major role in the kinetics.

The effect of the reaction concentration on the kinetic profile of **67e** was then investigated at 0.1, 0.2 and 0.5 M (Figure 18, Table 18).

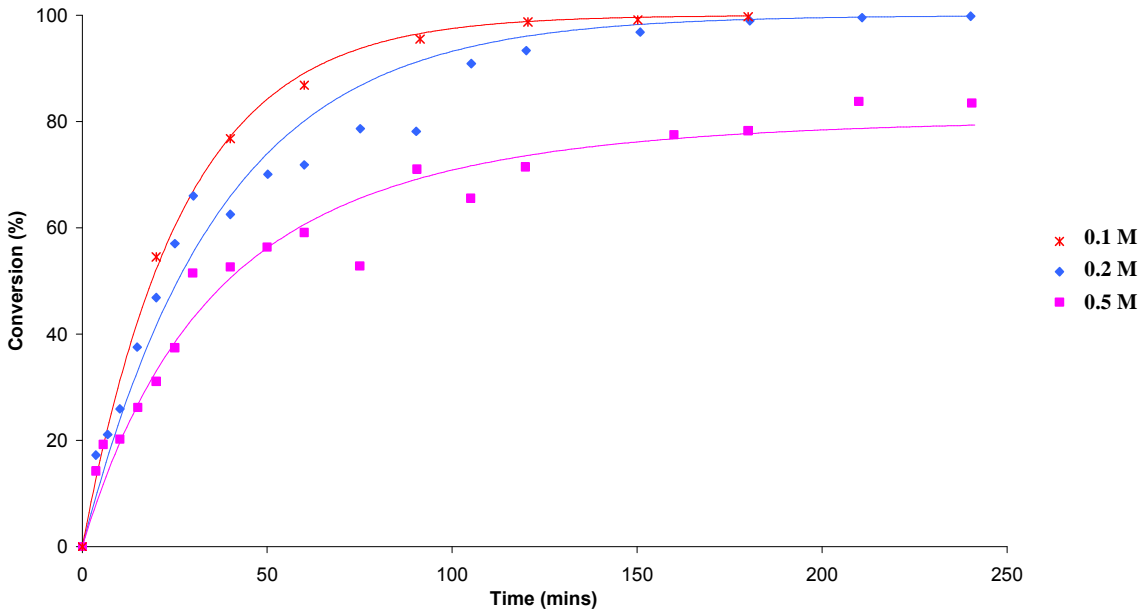

Figure 18. Effect of reaction concentration on the kinetic profile of **67e** for the cycloisomerisation of 4-phenyl-1-hexen-5-yne (**74**).[a]

[a] Conditions: 4-phenyl-1-hexen-5-yne (**74**) in 1,2-dichloroethane, 1 mol% **5e**, 1 mol% AgOTf, 25 ˚C. Conversion determined by gas chromatographic analysis of 10 µl aliquots of the crude reaction mixture, quenched with NBu_4Br. Curves fitted using Dynafit software.

Table 18. Observed rate constants and initial rates for catalyst **67e** in the cycloisomerisation of 4-phenyl-1-hexen-5-yne (**74**) at various concentrations.

		Method A (linear)			Method B (curve fitting)		
Entry	**[Enyne] ($mol.dm^{-3}$)**	**k_{obs} x 10^{-4} (s^{-1})**	**Rate[a]**	**Standard error (%)**	**k_{obs} x 10^{-4} (s^{-1})**	**Rate[a]**	**Standard error (%)**
1	0.1	5.53	5.53	2.0	6.15	6.15	1.6
2	0.2	4.12	8.20	3.4	4.49	8.97	4.2
3	0.5	1.54	7.70	6.1	-[b]	19.20	5.7

[a] at T_0 $x10^{-5}$ ($mol.dm^{-3}.s^{-1}$). [b] Second order k_{1obs} = 768 $x10^{-4}$ $mol^{-1}.dm^3.s^{-1}$, k_{2obs} = 2.36 $x10^{-4}$ s^{-1} (error 11%).

Surprisingly, the results show that increasing the concentration of the reaction reduces the rate constants (the initial rates increase with concentration as they relate to the change in enyne concentration over time).

The results show that increasing the concentration from 0.1 M to 0.2 M reduced the observed rate constant from 5.53 to 4.10 $x10^{-4}$ s^{-1} for Method A 6.15 to 4.49 $x10^{-4}$ s^{-1} for B), both concentrations fitted well to the first order model. From visual analysis of Figure 18 it is clear that the reaction is even slower at 0.5 M (k_{obs} = 1.54 $x10^{-4}$ s^{-1} for A) however the data does not fit well to the first order approximation (6.1% error for A). Using Method B the data fitted slightly better, although with high error (5.7%, 1st order 6.4%) to a 2nd order model, which results in a much higher calculated rate. The rate constant for the decomposition of the catalysts was calculated to be 2.36 $x10^{-4}$ s^{-1} with a rate of 1.18 $x10^{-6}$ $mol.dm^{-3}s^{-1}$ (11% error).

The reduction of the rate with increasing concentration could be due to reduced aggregation and bimolecular decomposition of the catalysts {to colloidal Au(0)} or substrate (enyne) induced decomposition. This would explain why complexes are more active in the kinetic profiles, than in the reactions run at 0.5 M concentration in CH_2Cl_2.

Finally, the effect of using 2 mole equivalents of AgOTf relative to **67c** in the reaction was investigated (Figure 19, Table 19).

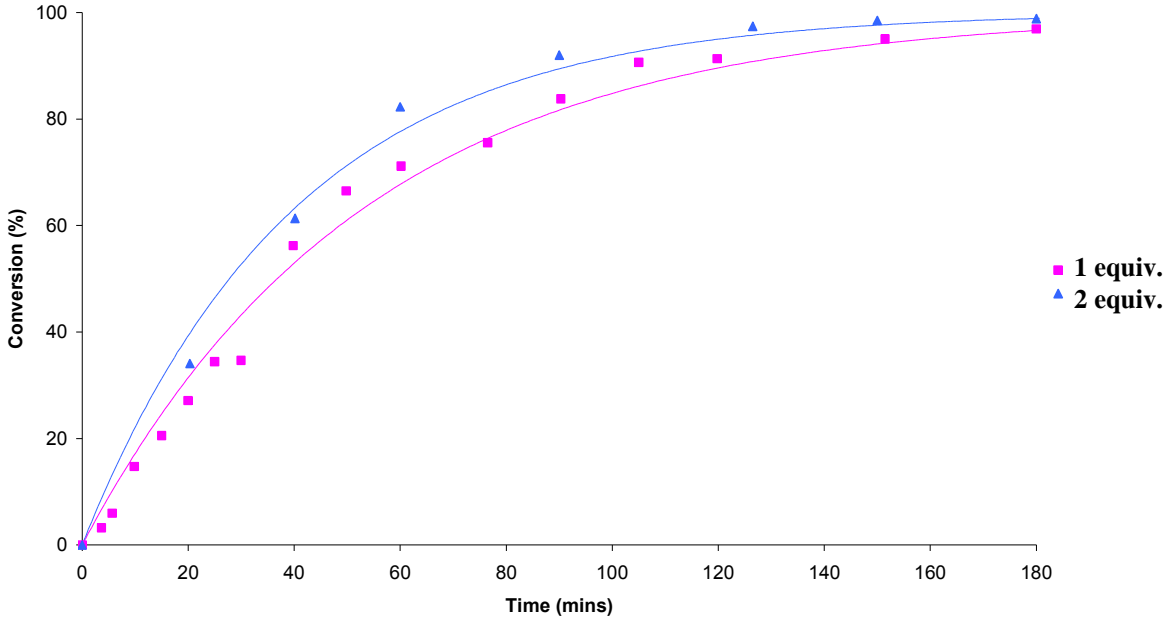

Figure 19. Effect of AgOTf loading relative to **67c** on the kinetic profile of the cycloisomerisation of 4-phenyl-1-hexen-5-yne (**74**).[a]

[a] Conditions: 4-phenyl-1-hexen-5-yne (**74**) in 1,2-dichloroethane, 1 mol% **67c** catalyst, 25 ˚C. Conversion determined by gas chromatographic analysis of 10 µl aliquots of the crude reaction mixture, quenched with NBu_4Br. Curves fitted using Dynafit software.

Table 19. Observed rate constants and initial rates for catalyst **67c** with 1 and 2 equivalents of AgOTf co-catalyst in the cycloisomerisation of 4-phenyl-1-hexen-5-yne (**74**).

		Method A (linear)			Method B (curve fitting)		
Entry	**Equiv. of Ag w.r.t. 67c**	**k_{obs} x10^{-4} (s^{-1})**	**Rate[a]**	**Standard error (%)**	**k_{obs} x 10^{-4} (s^{-1})**	**Rate[a]**	**Standard error (%)**
1	1	3.33	6.66	1.6	3.14	6.28	2.5
2	2	4.48	8.97	2.7	4.16	8.32	3.3

[a] at T_0 x10^{-5} (mol.dm^{-3}.s^{-1}).

There is a slight increase in rate of 8.20 to 8.97 x10^{-5} mol.dm^{-3}.s^{-1} (6.28 to 8.32 x10^{-5} mol.dm^{-3}.s^{-1}, Method B) when 2 equivalents of AgOTf are used. This suggests that the excess AgOTf does not react with Au to form an $Au(III)^{2+}$ ion {$Au(III)^{2+}$ complexes have however been reported to be formed by oxidation}.[110] The additional Ag^+ will presumably aid the formation of the active catalyst although the $^-$OTf counter ion will likely inhibit the reaction by competing with the enyne for coordination to the active catalyst. Analysis by Method B gave lower rates than A but both showed good fits to first order kinetics.

2.2.2.3. Cycloisomerisation of dimethyl allylpropargylmalonate

Cycloisomerisation of dimethyl allylpropargylmalonate (**77**) (2-allyl-2-prop-2-ynyl-malonic acid dimethyl ester), a 1,6-enyne prepared from allylmalonate,[111] is catalysed by a number of transition metal complexes producing three typical products, **78**-**80**, in differing ratios (Scheme 19, Table 20).

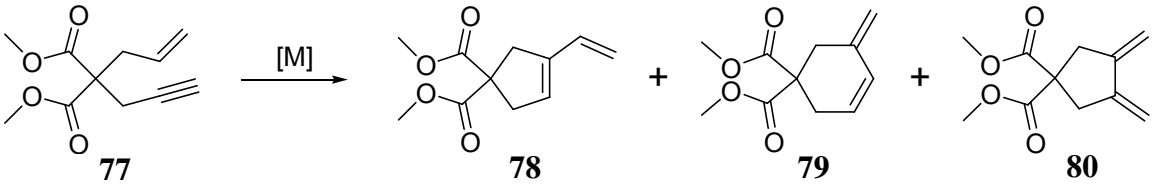

Scheme 19. Typical products from the cycloisomerisation of dimethyl allylpropargylmalonate (**77**).

Table 20. Products obtained in transition metal catalysed cycloisomerisation of dimethyl allylpropargylmalonate (**77**).

Entry	Catalyst	Solvent	Temperature (˚C) (Time)	Products
1	$[NiCl_2(Ph_3P)_2]$ + $CrCl_2$[112]	THF	r.t. (15 mins)	**79** + **80** (2.5:1)
2	$[AuCl(Ph_3P)]$ + $AgSbF_6$[49e]	CH_2Cl_2	0 (20 mins)	**78** + **79** (1:7)
3	$[RhCl(COD)]_2$ + $P(4\text{-F-Ph})_3$[113]	DMF	85 (24 h)	**79**
4	$FeCl_3$[114]	Toluene	90 (17 h)	**78**
5	[Pt][a,49c]	CH_2Cl_2	20 (2 h)	**78**

[a] cyclometallated:

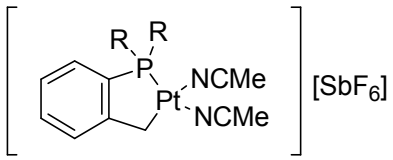

R = *o*-toluene

A combination of $[AuCl(PPh_3)]$ and $AgSbF_6$ yields products **78** and **79**, the distribution depending on the reaction conditions, with temperature having a significant effect (Table 21). At ambient temperature the product ratio is **78**:**79** 1:2; as the temperature is lowered the proportion of **78** is reduced until only **79** is produced at -45 ˚C.

Table 21. Product distributions for the Au(I) catalysed cycloisomerisation of dimethyl allylpropargylmalonate (**77**) in CH_2Cl_2.

Entry	Catalyst	Loading (mol%)	Temp. (˚C) (Time)	Product(s)	Yield (%)
1	$[AuCl(PPh_3)] + AgSbF_6$[49e]	2	0 (20 mins)	**78** + **79** (1:7)	77
2	$[AuCl(PPh_3)] + AgSbF_6$[115]	5	-45 (90 mins)	**79**	49
3	$[Au(NCMe)(PPh_3)]SbF_6$[49e]	2	23 (20 mins)	**78** + **79** (1:2)	82

A selection of the Au(III) imidate complexes were tested for activity in this transformation in combination with AgOTf and $Ag[Al(OC(CF_3)_3)_4]$ (**76**) (Table 22). The Au(III) complexes yield products **78** and **79**, with **78** as the major product, in contrast to the reported $[AuCl(PPh_3)]/AgSbF_6$ combination. The 1,6-enyne (**77**) cycloisomerisation is significantly slower than that of the 1,5-enyne (**74**) with only 13% conversion occurring with **68b** and 7% with **68d** in 3 hours at 25 ˚C (1 mol% Au and Ag loadings). The ratio **78**:**79** is approximately 6:1 in each case. Increasing the temperature to 35 ˚C only increases conversion to 17%. Increasing **68b**:AgOTf ratio to 1:2 has a significant effect, increasing the conversion to 26%, and increasing the catalysts loading from 1 to 5 mol% increases the conversion to 87% with a 7.5:1 **78**:**79** ratio, although a complex mixture of other products (oligomers and polymers) is also formed (the amount of polymer produced relative to **78** and **79** was not determined). Use of highly active catalyst **67d** with 5 mol% loading over 16 hours achieved complete conversion and a 9:1 ratio, however significant polymerisation had occurred. Complex **67b** (1 mol%) in combination with $Ag[Al(OC(CF_3)_3)_4]$ (**76**) at 0 ˚C (for 3 hours) resulted in full conversion (including polymerisation) and an A:B **78**:**79** ratio of 5:1, when this reaction was run at 25 ˚C the ratio dropped to 1.7:1.

Table 22. Conversions for the Au(III)-catalysed cycloisomerisation of dimethyl allylpropargylmalonate (**77**).[a]

Entry	Au catalyst	Loading (mol%)	Silver Salt	Time (h)	Temp (°C)	Conv.[b] (%)	Ratio A:B
1	$[AuBr_2(N\text{-mal})(IMes)]$ (**68b**)	1	AgOTf	3	25	13	5.5:1
2	$[AuBr_3(IMes)]$[86] (**68d**)	1	AgOTf	3	25	7	6:1
3	$[AuBr_2(N\text{-mal})(IMes)]$ (**68b**)	1	AgOTf	3	35	17	7.5:1
4	$[AuBr_2(N\text{-mal})(IMes)]$ (**68b**)	1	AgOTf (2 mol%)	3	25	26	5.5:1
5	$[AuBr_2(N\text{-mal})(IMes)]$ (**68b**)	5	AgOTf	3	25	87[c]	7.5:1
6	$[AuBr_2(N\text{-mal})(I^tBu)]$ (**66d**)	5	AgOTf	16	25	100[c]	9:1
7	$[AuBr_2(N\text{-dbs})(I^tBu)]$ (**66b**)	1	$Ag[Al(OC(CF_3)_3)_4]$ (**76**)	3	25	100[c]	1.7:1
8	$[AuBr_2(N\text{-dbs})(I^tBu)]$ (**66b**)	1	$Ag[Al(OC(CF_3)_3)_4]$ (**76**)	3	0	100[c]	5:1

[a] Conditions: 0.5 M dimethyl allylpropargylmalonate (**77**) in CH_2Cl_2. Conversion determined by ^1H NMR spectroscopic analysis of the crude reaction mixture. [b] Conversion of starting material. [c] Significant polymerisation and formation of multiple products (the amount of polymer produced relative to **78** and **79** was not determined).

2.2.2.4. 1,5- and 1,6-enyne cycloisomerisation kinetics

Kinetic profiles (by gas chromatographic analysis) were obtained for the cycloisomerisation of 1,5- and 1,6-enynes (**74** and **77**) to study the effect of Au(III) on the product distribution and to try to determine if $Au(I)^+$ or $Au(III)^+$ is the catalytically active species in the Au(III) imidate mediated reactions. Initially both 1,5- and 1,6-enynes (**74** and **77**) were added to the same reaction and the kinetics monitored. Complexes **56g**, **67c** and **67e** were tested in this way (Figure 20, Table 23).

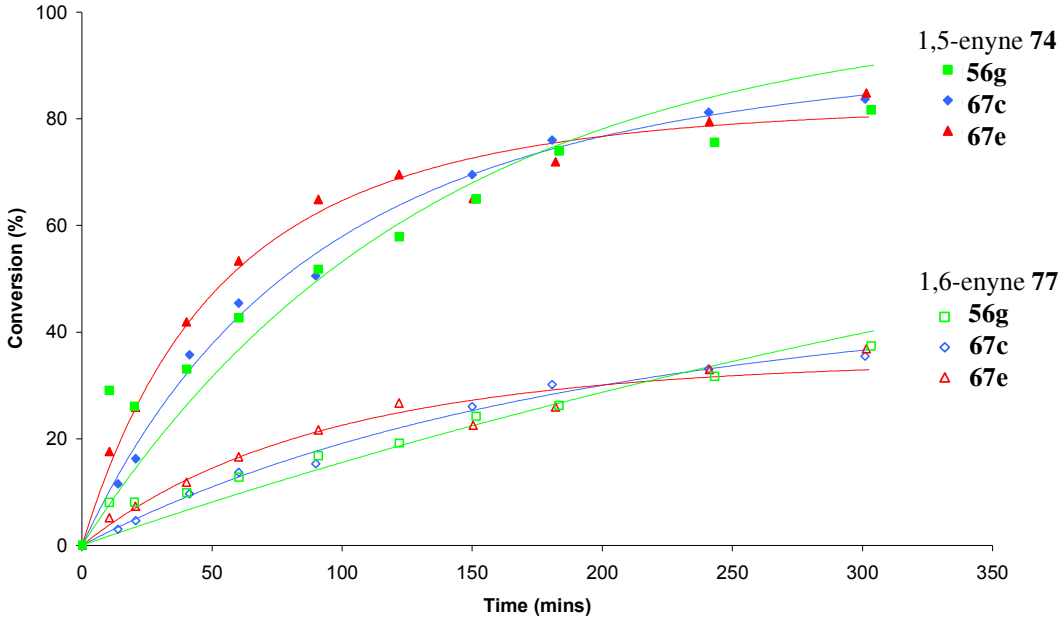

Figure 20. Kinetic profile for the concurrent cycloisomerisation of 4-phenyl-1-hexen-5-yne (**74**) and dimethyl allylpropargylmalonate (**77**) using complexes **56g**, **67c** and **67e**.[a]

[a] Conditions: 0.2 M 4-phenyl-1-hexen-5-yne (**74**), 0.2 M dimethyl allylpropargylmalonate (**77**) in 1,2-dichloroethane, 1 mol% Au, 1 mol% AgOTf, 25 ˚C. Conversion determined by gas chromatographic analysis of 10 µl aliquots of the crude reaction mixture, quenched with Bu_4NCl. Curves fitted using Dynafit software.

The kinetic profiles show that the cycloisomerisation of the 1,6-enyne **76** with rates of 0.51-0.56 x10^{-5} mol.dm^{-3}.s^{-1} using Method A (0.56-1.30 x10^{-5} mol.dm^{-3}.s^{-1} for Method B) is significantly slower than that of the 1,5-enyne **74** with rates of 2.10-2.36 x10^{-5} mol.dm^{-3}.s^{-1} (2.53-5.28 x10^{-5} mol.dm^{-3}.s^{-1} for B) and the addition of the **76** predictably reduces the rate of the cycloisomerisation of **74**.

Complex **56g** fitted better to 1st than 2nd order approximations but with high error, errors of 5.6% and 4.5% were calculated for the reactions of **74** and **76**, respectively (5.3 and 8.4% errors using Method B). Complex **67c** shows slightly better adherence to a first order approximation for the transformations of both **74** and **76** (errors are 4.6% and 4.9% for Method A, respectively, and 3.2 and 4.7% errors for Method B) but was found to fit better to a second order approximation (errors of 2.6 and 3.8%, respectively). The initial rate of decomposition of the catalyst was calculated to be 2.55 x10^{-7} mol.dm^{-3}.s^{-1} (9.2% error). Complex **67e** also fitted slightly better to second order (4.2 and 5.6% error, respectively) than first (5.7 and 8.4%), with an initial catalyst decomposition rate 6.08 x 10^{-7} mol.dm^{-3}.s^{-1} (8.0% error).

Using Method A for analysis, **56g**, **67c** and **67e** show very similar rates for both transformations. Analysis using Method B, however, calculates **67e** to be the most efficient catalyst with rates of 5.28 $x10^{-5}$ $mol.dm^{-3}.s^{-1}$ for the reaction of **74** and 1.30 $x10^{-5}$ $mol.dm^{-3}.s^{-1}$ for **77**, followed by **67c** (3.47 and 0.85 $x10^{-5}$ $mol.dm^{-3}.s^{-1}$) and **56g** the slowest (2.53 and 0.56 $x10^{-5}$ $mol.dm^{-3}.s^{-1}$). This is opposite to the order of activity that would be expected, although the differences in activity are relatively small. This may be due to the 1,6-enyne {or impurities produced by decomposition (aging) of the enynes} inhibiting the more active catalysts, such as **56g**, more significantly than the less active analogues, such as **67e**, as was observed in the reaction of the 'aged' 1,5-enyne (*vide supra*).

Table 23. Observed rate constants and initial rates for the concurrent cycloisomerisation of 4-phenyl-1-hexen-5-yne (**74**) and dimethyl allylpropargylmalonate (**77**) using complexes **56g**, **67c** and **67e**.

Entry	Complex	Method A (linear)			Method B (curve fitting)			Ratio 78:79[b]
		k_{obs} $x10^{-4}$ (s-1)	Rate[a]	R^2	k_{obs} $x10^{-4}$ (s-1)	Rate[a]	Error (%)	
	1,5-enyne 74							
1	[AuBr(I^tPe)] (**56g**)	1.05	2.10	5.6	1.27	2.53	5.3	-
2	[$AuBr_2$(*N*-tfs)(I^tPe)] (**67c**)	1.15	2.31	4.6	-[c,d]	3.47	2.6	-
3	[$AuBr_2$(*N*-ptm)(I^tPe)] (**67e**)	1.18	2.36	6.9	-[e,f]	5.28	4.2	-
	1,6-enyne 76							
4	[AuBr(I^tPe)] (**56g**)	0.28	0.51	4.5	0.28	0.56	8.4	0.28
5	[AuBr(I^tPe)] (**56g**) **1,6 only**	1.02	2.03	2.1	1.08	2.15	2.2	0.30
6	[$AuBr_2$(*N*-tfs)(I^tPe)] (**67c**)	0.28	0.56	4.9	-[d,g]	0.85	3.8	0.45
7	[$AuBr_2$(*N*-ptm)(I^tPe)] (**67e**)	0.29	0.53	6.9	-[f,h]	1.30	5.6	0.36

[a] Rate at T_0 $x10^{-5}$ ($mol.dm^{-3}.s^{-1}$). [b] After 300 minutes. [c] Second order k_{1obs} = 868.5 $x10^{-4}$ $mol^{-1}.dm^3.s^{-1}$. [d] k_{2obs} = 6.38 $x10^{-5}$ s^{-1} (error 9.2%). [e] Second order k_{1obs} = 1321 $x10^{-4}$ $mol^{-1}.dm^3.s^{-1}$. [f] k_{2obs} = 1.52 x 10^{-4} s^{-1} (error 8.0%). [g] Second order k_{1obs} = 212.8 $x10^{-4}$ $mol^{-1}.dm^3.s^{-1}$. [h] Second order k_{1obs} = 324.2 $x10^{-4}$ $mol^{-1}.dm^3.s^{-1}$.

Under these conditions **79** is the major product, from the cycloisomerisation of **77,** in contrast to the ratio observed for reactions carried out on **77** in isolation in CH_2Cl_2 (*vide supra*). The differences between these reactions are the solvent (CH_2Cl_2 compared to 1,2-dichloroethane), concentration (0.2 M compared to 0.5 M), the presence and competition of

74 in the reaction mixture and the exact nature of the complexes used. Given the sensitivity of the ratio to the reaction conditions it is possible that any of these conditions could have caused the change in selectivity.

The product ratio profiles (Figure 21) show that the ratio of the two 1,6-enyne cycloisomerisation products drops (increased amount of **79** relative to **78**) as the reaction proceeds but then levels off after 60-120 minutes, presumably the changing concentrations of the reactants and products affects the selectivity. The ratio for the three Au complexes is significantly different. Complex **67c** gives the highest ratio (0.450 after 300 minutes), followed by **67e** (0.357) and **56g** (0.279) with the highest selectivity for **79**. A repeat of the profile for **56g** showed good reproducibility. These results suggest that either the nature of the active catalyst is different in each case {i.e. $Au(III)^{+}$ *versus* $Au(I)^{+}$} or that reduction of Au(III) to Au(I) occurs, which carries out the catalysis, and that the resultant decomposition species (*e.g.* tetrafluorosuccinimide, *N*-bromo tetrafluorosuccinimide or bromine) in solution are able to influence the selectivity.

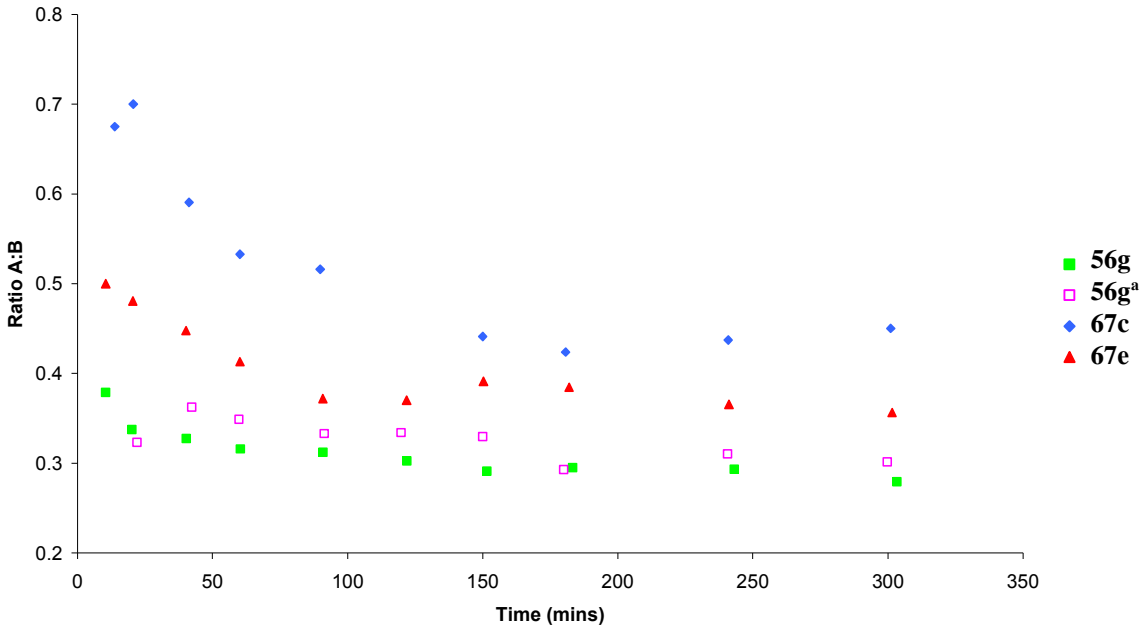

Figure 21. Product ratio profile for the cycloisomerisation of dimethyl allylpropargylmalonate (**77**) using complexes **56g**, **5c** and **5e**.[b]

[a] No 4-phenyl-1-hexen-5-yne (**74**) added. [b] Conditions: 0.2 M 4-phenyl-1-hexen-5-yne (**74**) and 0.2 M dimethyl allylpropargylmalonate (**77**) in 1,2-dichloroethane, 1 mol% Au, 1 mol% AgOTf at 25 ˚C. Conversion determined by gas chromatographic analysis of 10 µl aliquots of the crude reaction mixture.

The cycloisomerisation of **77** was also run in isolation using complex **56g**. It was found that the reaction proceeded much faster without competition from 1,5-enyne **74** with an initial rate of 2.03 $x10^{-5}$ $mol.dm^{-3}.s^{-1}$ using Method A (2.15 $x10^{-5}$ $mol.dm^{-3}.s^{-1}$ using B) and a much better adherence to a 1st order model (error is 2.1% for A and 2.2% for B). The ratio of **78**:**79** however remained similar at 0.301, although without a defined initial drop. As the ratio does not change the presence of the 1,5-enyne **74** clearly does not cause the switch in selectivity with respect to the reactions carried out in CH_2Cl_2.

Subsequently, $Ag[Al(OC(CF_3)_3)_4]$ (**76**) was tested in place of AgOTf as the silver additive, using complexes **56g** and **67c** (Figure 22, Table 24). No preactivation was carried out in order to determine if this effects the ratio of products (and also to reduce the rate of the reaction). Under these conditions **56g** carried out the cycloisomerisation extremely quickly achieving quantitative conversion of **74** in under 20 minutes (too quickly to measure the kinetics accurately) and **77** in under 60 minutes (with a rate of 31.07 $x10^{-5}$ $mol.dm^{-3}.s^{-1}$ using Method A and 33.04 using B). The reaction of **77** showed a very good fit to 1st order kinetics (2.5% error for Method A and 1.9% for B). This mirrors the increased activity of this Au/Ag combination (**56g/76**) seen with enyne **74** in isolation (*vide supra*). Complex **67c** however is inactive in both transformations for 180 minutes. This underlines the difficulty in activating the Au(III) complexes relative to Au(I). Even after 180 minutes the conversion is relatively slow (although faster than with AgOTf). The reaction was further analysed after 20 hours and it was determined to have gone to completion.

For both complexes, **78** was now found to be the major product from the cycloisomerisation of **77**, with a **78**:**79** ratio of 2.20 for **56g** and 2.16 for **67c** (after 240 minutes). Clearly the product distribution observed is dependant on the silver salt employed. After 20 hours, the ratios had changed to 1.78 for **56g** and 0.003 for **67c**. It appears by ^1H NMR spectroscopic analysis that significant polymerisation of **78** occurs in the presence of **67c**; virtually all of **78** had been consumed in this time frame. This could explain the lower **78**:**79** ratios seen for the Au(III) reactions, relative to Au(I).

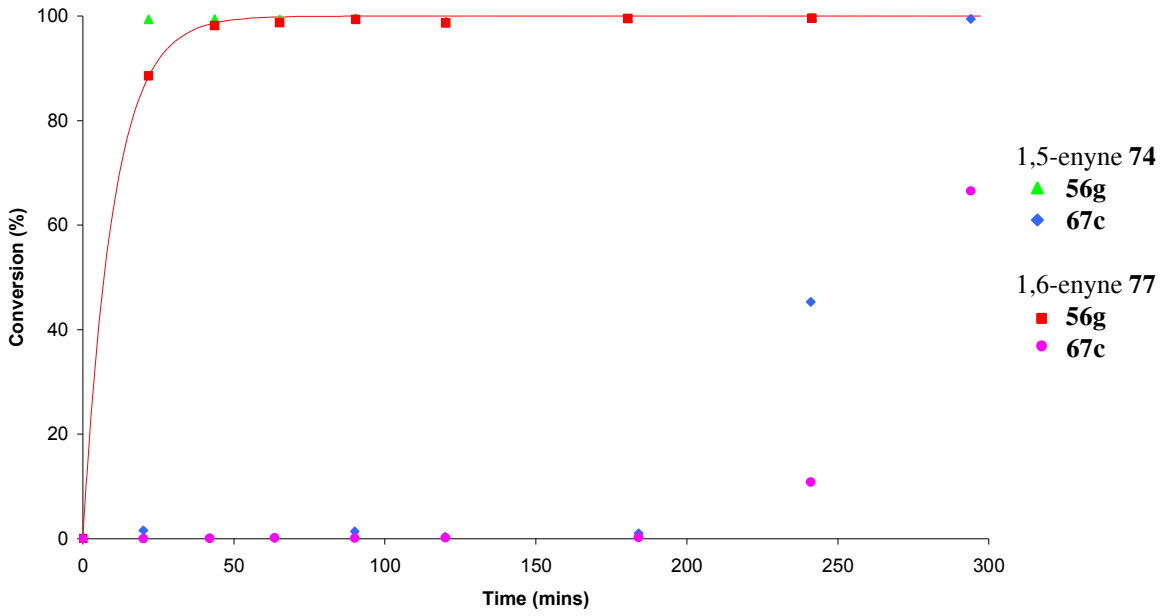

Figure 22. Kinetic profile for the concurrent cycloisomerisation of 4-phenyl-1-hexen-5-yne (**74**) and dimethyl allylpropargylmalonate (**77**) using complexes **56g** and **67c** with $Ag[Al(OC(CF_3)_3)_4]$ (**76**).

[a] Conditions: 0.2 M 4-phenyl-1-hexen-5-yne (**74**) and 0.2 M dimethyl allylpropargylmalonate (**77**) in 1,2-dichloroethane, 1 mol% Au, 1 mol% $Ag[Al(OC(CF_3)_3)_4]$ (**74**) at 25 ˚C. Conversion determined by gas chromatographic analysis of 10 µl aliquots of the crude reaction mixture, quenched with Bu_4NCl. Curve fitted using Dynafit software.

Table 24. Observed rate constants and initial rates for the concurrent cycloisomerisation of 4-phenyl-1-hexen-5-yne (**74**) and dimethyl allylpropargylmalonate (**77**) using complexes **56g** and **67c** with $Ag[Al(OC(CF_3)_3)_4]$ (**76**).

Entry	Complex	Method A (linear)			Method B (curve fitting)			Ratio A:B[b]
		k_{obs} x10^{-4} (s^{-1})	Rate[a]	R^2	k_{obs} x10^{-4} (s^{-1})	Rate[a]	Error (%)	
	1,6-enyne 77[c]							
1	[AuBr(I^tPe)] (**56g**)	15.54	31.07	2.5	16.52	33.04	1.9	2.20
2	[$AuBr_2$(*N*-tfs)(I^tPe)] (**67c**)	too slow						2.16

[a] Rate at T_0 x10^{-5} ($mol.dm^{-3}.s^{-1}$). [b] After 240 minutes. [c] The reaction of **74** was too fast for **56g** and too slow for **67c** for kinetic data to be determined accurately.

2.2.2.5. Cycloisomerisation of 1,1'-(1*E*)-hex-1-en-5-yne-1,4-diyldibenzene

The 1,5-enyne 1,1'-(1*E*)-hex-1-en-5-yne-1,4-diyldibenzene (**81**) can be prepared by treating *trans*-cinnamyl chloride (**82**) with LDA according to the method of Florio and Troisi (Scheme 20).[116]

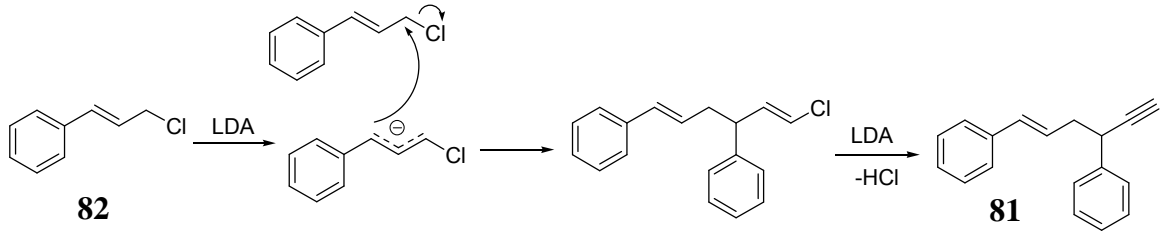

Scheme 20. The synthesis of 1,1'-(1*E*)-hex-1-en-5-yne-1,4-diyldibenzene (**81**) from *trans*-cinnamyl chloride (**82**).

In order to investigate the anomalous activity of the IMes series of catalysts (**68**) further, they were tested against the bromide analogue (**68d**) in the cycloisomerisation of 1,1'-(1*E*)-hex-1-en-5-yne-1,4-diyldibenzene (**81**) to 3,6-diphenylbicyclo[3.1.0]hex-2-ene (**83**) (Scheme 21, Table 25).

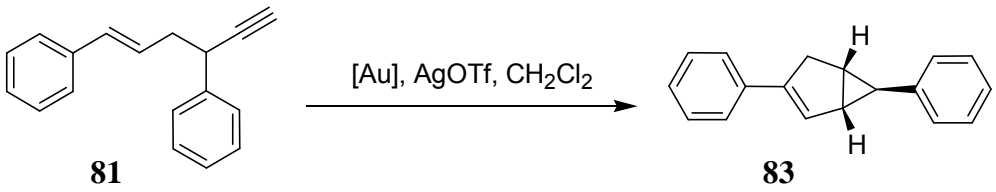

Scheme 21. The Au(III) catalysed cycloisomerisation of 1,1'-(1*E*)-hex-1-en-5-yne-1,4-diyldibenzene (**81)** to 3,6-diphenylbicyclo[3.1.0]hex-2-ene (**83**).

Table 25. Comparison of [$AuBr_2$(*N*-imidate)(IMes)] complexes (**68 a-d**) in the cycloisomerisation of 1,1'-(1*E*)-hex-1-en-5-yne-1,4-diyldibenzene (**81**).[a]

Entry	Au catalyst	Time (mins)	Conversion (%)[b]
1	[$AuBr_2$(*N*-succ)(IMes)] (**68a**)	30	22
2	[$AuBr_2$(*N*-mal)(IMes)] (**68b**)	30	67
3	[$AuBr_2$(*N*-mal)(IMes)] (**68b**)	180	>99
4	[$AuBr_2$(*N*-ptm)(IMes)] (**68c**)	30	37
5	[$AuBr_3$(IMes)] (**68d**)	30	15
6	[$AuBr_3$(IMes)] (**68d**)	180	43

[a] Conditions: 0.5 M solution of 1,1'-(1*E*)-hex-1-en-5-yne-1,4-diyldibenzene (**81**) in CH_2Cl_2, 1 mol% Au catalyst, 1 mol% AgOTf, 25˚C. [b] Conversion determined by ^{1}H NMR spectroscopic analysis of the crude reaction mixture (average of two runs).

The results show that 1,1'-(1*E*)-hex-1-en-5-yne-1,4-diyldibenzene (**81**) undergoes cycloisomerisation much more rapidly than 4-phenyl-1-hexen-5-yne (**74**), due to the phenyl activated alkene, with complete conversion occurring in under 3 hours at 25 ˚C using complex **68b**. For this enyne there is a significant imidate effect, following the trend observed for 4-phenyl-1-hexen-5-yne (**74**) with the I^{t}Bu (**66**) and I^{t}Pe (**67**) analogues. Complex **68a** gives just 22% conversion, **68b** 67% and **68c** 37%, over 30 minutes. The bromide analogue (**68d**) gives just 15% conversion over 30 minutes and only 43% after 3 hours.

2.2.2.6. Cycloisomerisation of dimethyl diallylmalonate

The cycloisomerisation of dimethyl diallylmalonate (**84**), a 1,6-diene, was attempted (Table 26). This was a test to observe if the Au(III) complexes could activate the alkene to intramolecular nucleophilic attack by the tethered alkene. However, under a variety of conditions, including high temperature, there was no reaction. Although Au can bind alkenes even more efficiently than alkynes it does not lower the LUMO sufficiently to allow nucleophilic attack by another alkene.[42]

Table 26. Comparison of Au(III) complexes and reaction conditions for the attempted cycloisomerisation of dimethyl diallylmalonate (**84**).[a]

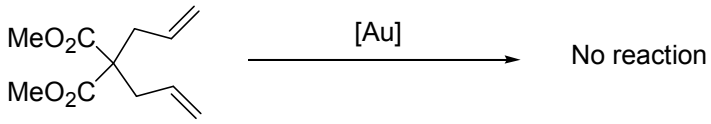

84

Entry	Complex	Silver salt	Time (h)	Temp. (°C)	Conv.[b] (%)
1	$AuCl_3$	-	20	25	0
2	$AuCl_3$	-	1	95[c]	0
3	[$AuBr_2$(*N*-succ)(I^tPe)] (**67a**)	AgOTf	1	90[c]	0
4	[$AuBr_2$(*N*-dbs)(I^tBu)] (**66b**)	Ag[Al(OC(CF_3)$_3$)$_4$] (**76**)	3	25	0

[a] Conditions: 0.5 M dimethyl diallylmalonate in CH_2Cl_2, 1 mol% Au catalyst, 1 mol% silver salt. [b] Conversion of **84** determined by ^{1}H NMR spectroscopic analysis of the crude reaction mixture. [c] Microwave heating.

2.2.2.7. Cycloisomerisation of ethyl 4-phenyl-1-hepten-5-yn-7-oate

The ability of Au(III) to activate carbon-carbon unsaturated bonds was further tested using the 1,5-enyne ethyl 4-phenyl-1-hepten-5-yn-6-oate (**85**). This was easily prepared from 4-phenyl-1-hexen-5-yne (**74**) using ethyl chloroformate.[117] No reaction was observed with complex **68b** or **68d** (Scheme 22, Table 27). The ester group will withdraw electron density from the alkyne increasing its nucleophilicity (by lowering energy of the LUMO), however it is the 5- rather than 6- position that would be activated, which does not favour bicyclo[3.1.0]hexane formation by 5-*endo-dig* cycloisomerisation. Additionally, the electron-deficient alkyne would make Au(III) binding less favourable, with the carbonyl oxygen providing a better binding site for the $Au(III)^+$ ion.

Scheme 22. The attempted Au(III) catalysed cycloisomerisation of ethyl 4-phenyl-1-hepten-5-yn-6-oate (**85**) to bicyclo[3.1.0]hexene **86**.

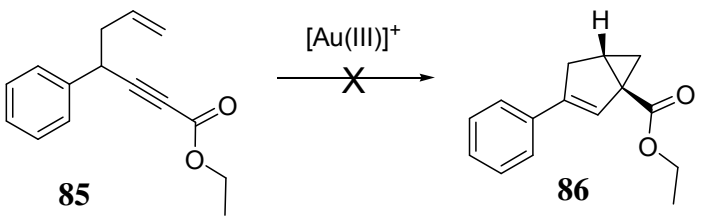

85 **86**

Table 27. Comparison of Au(III) complexes and reaction conditions for the attempted conversion of ethyl 4-phenyl-1-hepten-5-yn-6-oate (**85**).

Entry	Complex	Temperature (˚C)	Conversion (%)
1	[$AuBr_2$(*N*-mal)(IMes)] (**68b**)	25	0
2	[$AuBr_3$(IMes)] (**68d**)	25	0
3	[$AuBr_2$(*N*-mal)(IMes)] (**68b**)	35	0

Conditions: 0.5 M ethyl 4-phenyl-1-hepten-5-yn-6-oate (**85**) in CH_2Cl_2, 1 mol% Au, 1 mol% AgOTf, 3 h.

2.2.2.8. Attempted synthesis of 2,4-dimethyl-2-(2-phenyl-1-ethynyl)-4-penten-1-ol

The cycloisomerisation of racemic 2,4-dimethyl-2-(2-phenyl-1-ethynyl)-4-penten-1-ol (**87**) to furnish 1,5-dimethyl-3-phenyl-6-oxabicyclo[3.2.1]oct-2-ene (**88**) has been reported by Kosmin (Scheme 23).[118] It was found that $AuCl_3$ and [$AuCl(PPh_3)$] in combination with $AgClO_4$ were effective catalysts. Attempts were made to prepare this enyne in order to investigate the effects of the imidate complexes on the synthesis of this heterocyclic structure.

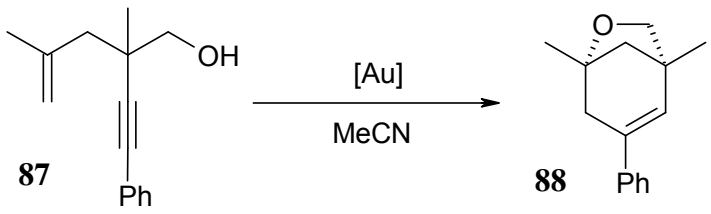

Scheme 23. The Au catalysed cycloisomerisation of 2,4-dimethyl-2-(2-phenyl-1-ethynyl)-4-penten-1-ol (**87**) to produce 1,5-dimethyl-3-phenyl-6-oxabicyclo[3.2.1]oct-2-ene (**88**).

The enyne is prepared in a three step procedure from ethyl-2-methylacetoacetate (**89**) (Scheme 24).[119]

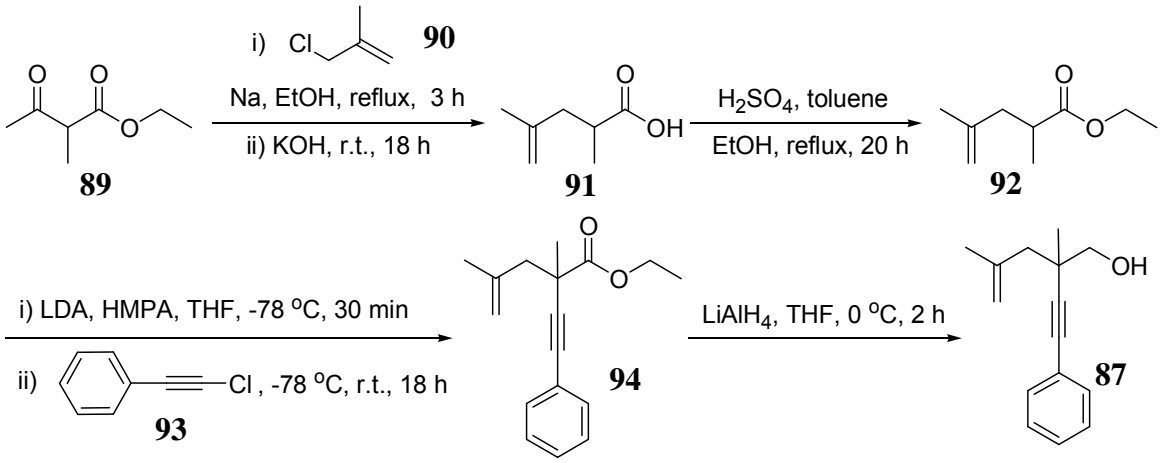

Scheme 24. Synthesis of 2,4-dimethyl-2-(2-phenyl-1-ethynyl)-4-penten-1-ol (**87**) from ethyl-2-methylacetoacetate (**89**).

A key step in the synthesis is the alkynylation of enoate **92** to produce enyne **94**. However, under the reported conditions a complex mixture of products was obtained with only 20% conversion to enyne **94**, which could not be isolated. Subsequently this method was abandoned and a more efficient route to the synthesis of enynes considered.

2.2.2.9. Synthesis of FLEXIphosO analogues

In order to utilise the bicyclo[3.1.0]hexene framework created in the cycloisomerisation of 1,5-enynes, the synthesis of an analogue of the reported FLEXIphosO ligand, (+/-)-bicyclo[3.2.0]heptane-3,6-diyl bis[diphenyl(phosphinite)] (**95**), was considered.[120] This ligand has been shown to possess conformational flexibility, forming an *exo*-envelope conformation in the solid-state and in some Pd(0) complexes, such as [Pd_2(FLEXIphosO)$_3$], but an *endo*-envelope conformation in solution and other Pd(0) and Pd(II) complexes, such as [Pd(FLEXIphosO)$_2$] and [$PdCl_2$(FLEXIphosO)] (in solution and the solid-phase) (Figure 23). This conformational flexibility allows the ligand to alter its bite angle on a metal by 'flipping' from *endo* (*cis*-square planar) to *exo* (*pseudo*-tetrahedral) conformation.

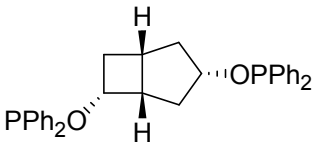

95

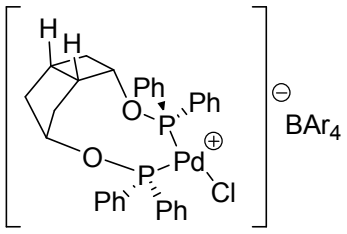

Ar = bis-3,5-trifluoromethylphenyl

96

Figure 23. The structures of (+/-)-bicyclo[3.2.0]heptane-3,6-diyl bis[diphenyl(phosphinite)] (FLEXIphosO) (**95**) and [PdCl(FLEXIphosO)]BAr_4 (**96**).

The complex [PdCl(FLEXIphosO)]BAr_4 (**96**) is an efficient catalyst for the cycloisomerisation of 1,6-dienes such as diethyl diallylmalonate, in which other bidentate bisphospinite ligands are inefficient. This is because the 'flipping' to *exo*-conformation allows the formation of a catalytically active hydride species which the more stable *endo*-form does not (Figure 24).

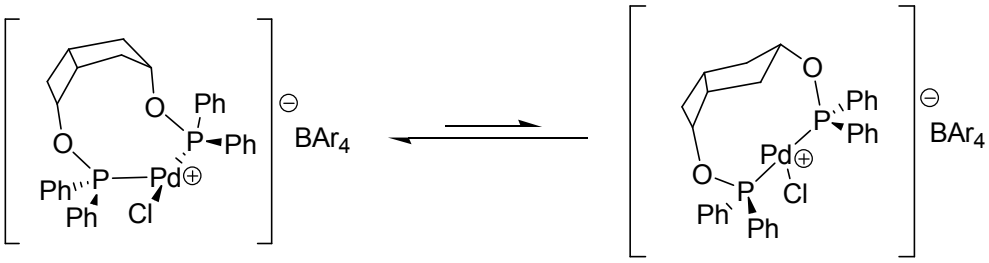

Figure 24. *Endo*/*exo* envelope conformational 'flip' of [PdCl(FLEXIphosO)]BAr_4 (**96**).

It was envisaged that the bicyclo[3.1.0]hexane structure might behave in a similar manner. Unsubstituted bicyclo[3.1.0]hexane (**97**) adopts a boat conformation,[121] but with 3,6-disubstituted bicyclo[3.1.0]hexanes {such as dimorpholino (**98** and **98'**)} both boat (in the case of an *endo*cyclic substituent at the 3- position) and chair (in the case of *exo*cyclic) are possible (Figure 25).[122]

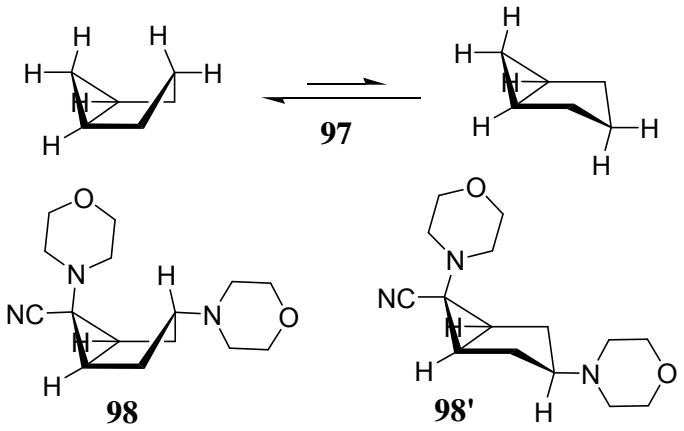

Figure 25. Conformational equilibrium in bicyclo[3.1.0]hexane (**97**) and conformations of 6□-3,6-dimorpholinobicyclo[3.1.0]hexanecarbonitriles (**98** and **98'**).[123]

The enyne precursor for the Au-catalysed synthesis of the bicyclo[3.1.0]hexane ring system can be prepared by the method of Florio and Troisi.[116] This method is simple and expedient, however it places some constraints on the ligand design; the substituent's would have a 3,6-substitution pattern (which is desired) and be identical (also desirable) and the phosphinite group would have to be linked to the bicyclo[3.1.0]hexane core by at least one carbon atom (otherwise the starting allyl chloride would be an enol). This methodology also allows easy control of the stereochemistry of the cyclopropane ring substituent, an *E*-alkene (*E*-**100**) will give an *exo* substituent (*exo*-**101**) and a *Z*-alkene (*Z*-**100**) an *endo* substituent (*endo*-**101**) (Scheme 25).[15] This will allow control over the favoured conformation of the target ligand.

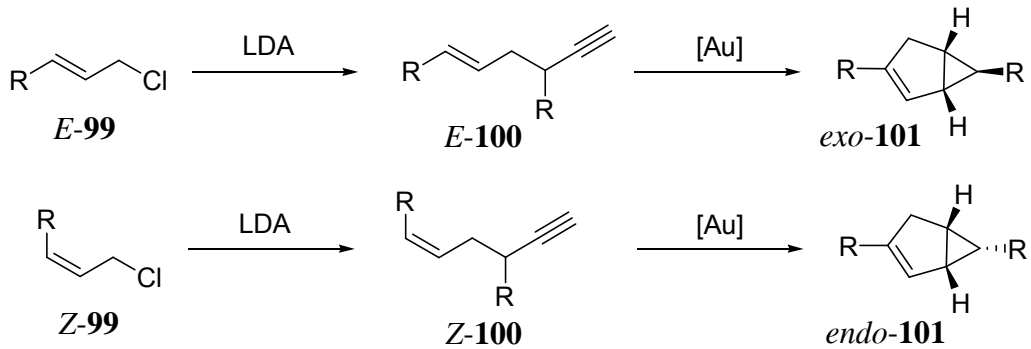

Scheme 25. Proposed preparation of 6-*exo* and 6-*endo* substituted bicyclo[3.1.0]hexenes.

The preparation of the 6-*exo* {(+/-)-**101**} and 6-*endo* {(+/-)-**102**} substituted isomers of (+/-)-3-*endo*-bicyclo[3.1.0]hexane-3,6-diylbis(methylene) bis(diphenylphosphinite) (Figure 26) and the investigation of their properties as ligands in organometallic complexes, and activity in 1,6-diene cycloisomerisation reactions in comparison with FLEXIphosO was proposed.

Figure 26. Structures of 6-*exo* {(+/-)-**101**} and 6-*endo* {(+/-)-**102**} isomers of (+/-)-3-*endo*-bicyclo[3.1.0]hexane-3,6-diylbis(methylene) bis(diphenylphosphinite), potential FLEXIphosO analogues.

The proposed synthesis of (+/-)-3-*endo*-6-*exo*-bicyclo[3.1.0]hexane-3,6-diylbis(methylene) bis(phosphinite) {(+/-)-**101**} involves the reaction of commercially available isobutyl but-3-enoate (**103**) with *N*-chlorosuccinimide and phenylselenyl chloride to produce the allyl chloride, isobutyl (2*E*)-4-chlorobut-2-enoate (**104**). Treatment of this with LDA should furnish diisobutyl(E)-5-(1-ethynyl)-2-hexenedioate (**105**) by Florio and Troisi's method. Au-catalysed cycloisomerisation should give access to the bicyclo[3.1.0]hexene core-structure (**106**), followed by reduction of the esters by $LiAlH_4$ to give the diol (**107**). Addition of H_2 to the *exo*cyclic face of the alkene using hydrogen and catalytic palladium, followed by phosphorylation with Ph_2PCl, is intended to yield the desired target ligand {(+/-)-**101**} with the desired stereochemistry (Scheme 26).

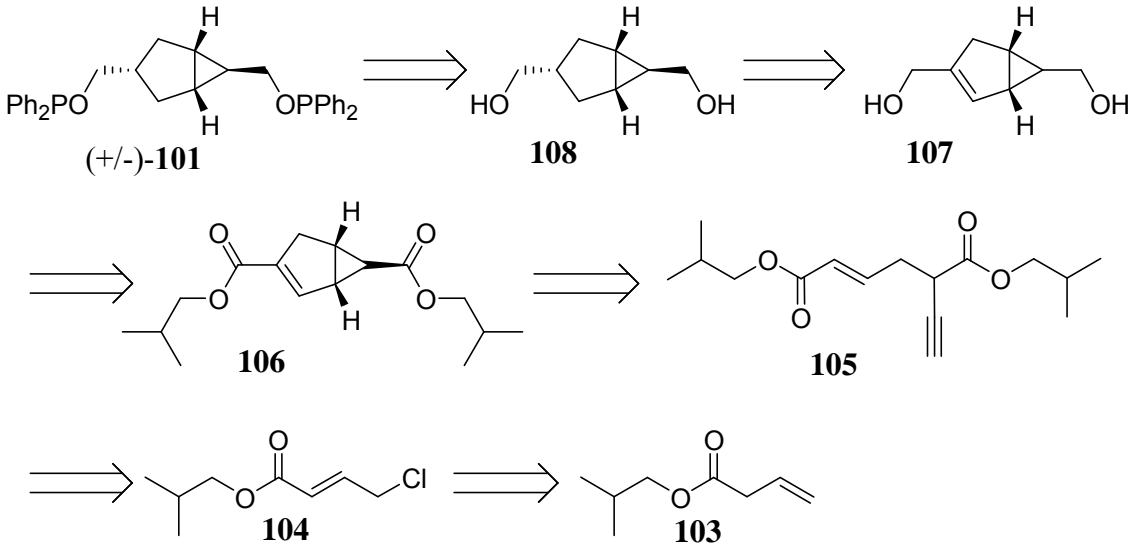

Scheme 26. Proposed retrosynthesis of (+/-)-3-*endo*-6-*exo*-bicyclo[3.1.0]hexane-3,6-diylbis(methylene) bis(phosphinite) {(+/-)-**101**}.

The synthesis of **104** by treatment of **103** with phenylselenylchloride and *N*-chlorosuccinimide proceeded as expected, although only in an unoptimised 19% yield after distillation (Scheme 27).[124]

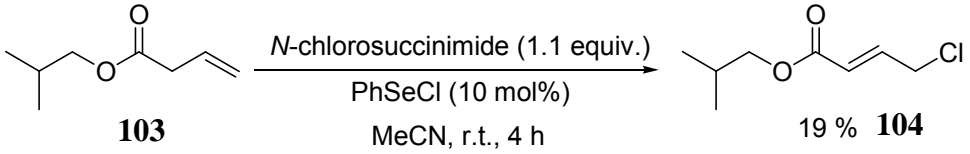

Scheme 27. The synthesis of isobutyl (2*E*)-4-chlorobut-2-enoate (**104**).

The second step however was not successful. This involved treatment of **104** with lithium diisopropylamide (LDA) in tetrahydrofuran (THF) at -78 ˚C and resulted in multiple alkene and ester products being formed in addition to isomerised (*cis*) starting material (Scheme 28).

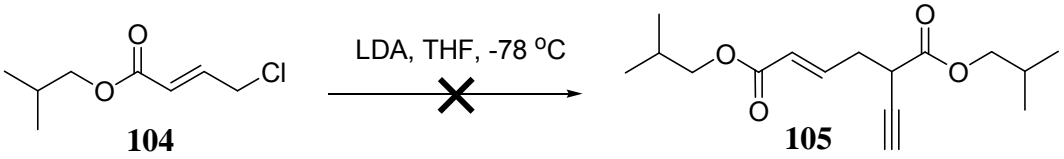

Scheme 28. The proposed synthesis diisobutyl(*E*)-5-(1-ethynyl)-2-hexenedioate (**105**).

The failure of this reaction to produce the desired product may be due to the effects of the ester group which will be reactive to nucleophilic attack by carbanions generated by LDA (by direct attack at the carbonyl and by Michael addition) but will also stabilise the carbanions - reducing their reactivity (resulting in the observed *cis*/*trans* isomerisation). As a result an alternative protecting group for the diol, which is stable to nucleophilic attack and does not reduce the carbanion reactivity, is required, and so it was envisaged that a benzyl group would be more successful. The synthesis could then proceed in a similar manner to above with a debenzylation rather than an ester reduction deprotection step.

This required a new retrosynthesis (Scheme 29) starting from *cis*-1,4-but-2enediol (**109**), (*cis* was used initially due to the availability of the starting material). One alcohol would be benzylated using benzyl bromide (**110**) and the other substituted for chlorine using mesyl chloride and triethylamine followed by lithium chloride (**111**). Formation of the enyne (**112**) could then be carried out using LDA, followed by the gold catalysed cycloisomerisation (the *cis* alkene would result in 6-*endo* stereochemistry) to give the bicyclohexene (**113**). Reductive hydrogenation catalysed by palladium should hopefully reduce the alkene and remove the benzyl protecting groups to yield the diol (**114**) which could be phosphorylated by Ph_2PCl to give the target (+/-)-3-*endo*-6-*endo*-bicyclo[3.1.0]hexane-3,6-diylbis(methylene) bis(diphenylphosphinite) {(+/-)-**115**}.

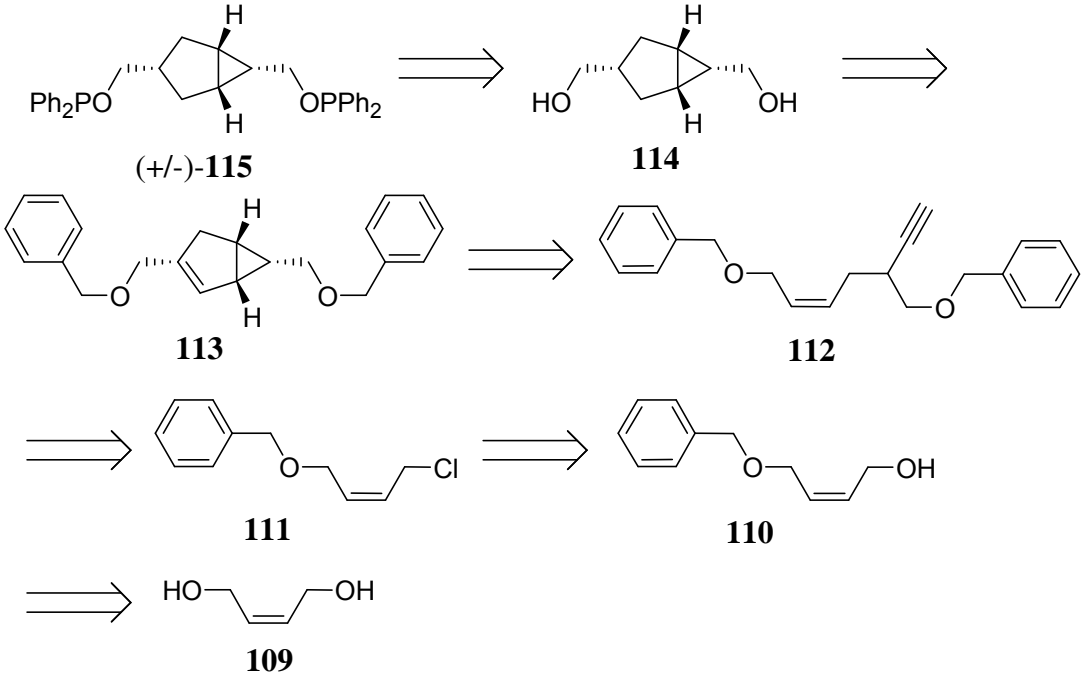

Scheme 29. Proposed retrosynthesis of (+/-)-3-*endo*-6-*endo*-bicyclo[3.1.0]hexane-3,6-diylbis(methylene) bis(diphenylphosphinite) {(+/-)-**115**}.

Synthesis of 1-chloro-4-benzyloxybut-2-ene (**111**) proceeded well in 63% over 2 steps. 1-Chloro-4-benzyloxy-(*Z*)-but-2-ene (**110**) was prepared by treatment of (*Z*)-1,4-but-2-enediol (**109**) with sodium hydride, followed by benzyl bromide, in 80% yield.[125] Substitution of the second alcohol by chlorine was carried out by mesylation of the alcohol with triethylamine and methanesulfonyl chloride followed by substitution using lithium chloride in 79% yield (Scheme 30).[126]

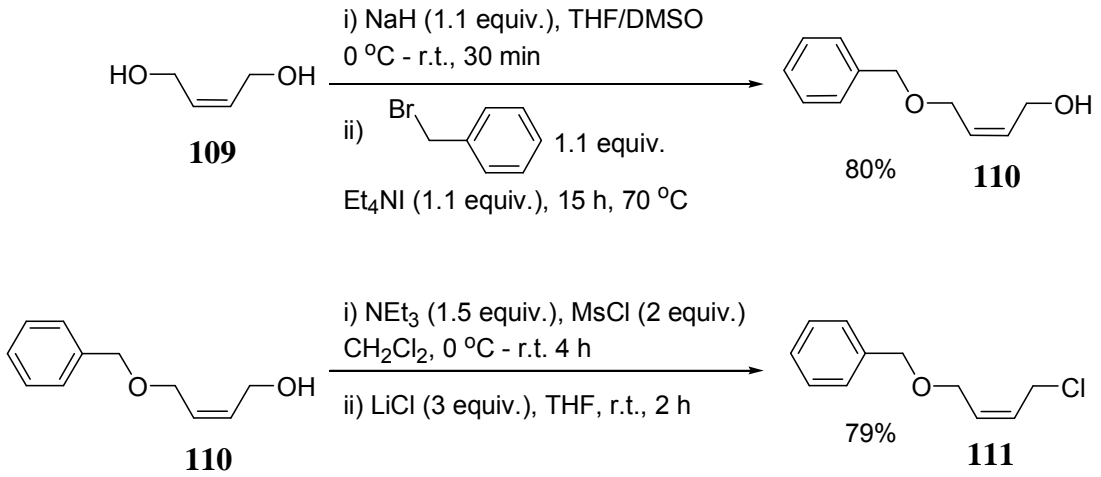

109 **110** **111**

Scheme 30. Synthesis of 1-chloro-4-benzyloxy-(Z)-but-2-ene (**111**).

Unfortunately, preparation of the enyne **112** by treatment of the allyl chloride **111** with LDA did not produce the desired product (Scheme 31), giving instead a mixture of unidentified products formed from reaction of the benzyl and vinyl CH_2 groups, including a significant amount of benzyl alcohol.

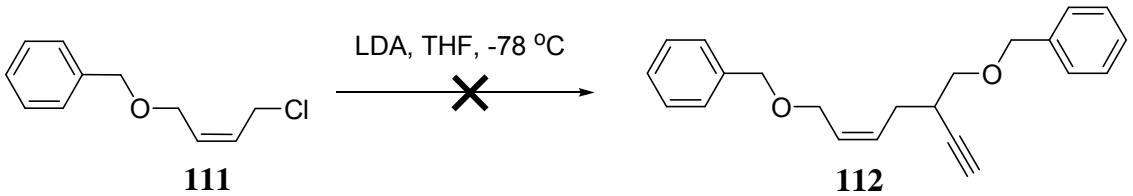

111 **112**

Scheme 31. Attempted synthesis of 1,6-dibenzyloxy-(*Z*)-5-(1-ethynyl)-2-hexene (**112**) from 1-chloro-4-benzyloxy-(Z)-but-2-ene (**111**).

The presence of protic benzyl and vinyl groups clearly led to the failure of the reaction to yield the desired enyne and so another new retrosynthesis was required to design an allyl chloride with no protic positions other than the allyl chloride methylene group. This could be achieved by the use of protected phenol substituents in both the 3- and 6- positions,

although this would not then be an exact analogue of the FLEXIphosO ligand, the use of the phenol groups would allow extra control over the ligand bite angle by having *ortho*, *meta* or *para* hydroxyl groups. Initially it was proposed to prepare *ortho*-phenol substituted bicyclo[3.1.0]hexanes {(+/-)-**116** and (+/-)-**117**} as this would potentially be closest to the bite angle displayed by the FLEXIphosO ligand (Figure 27).

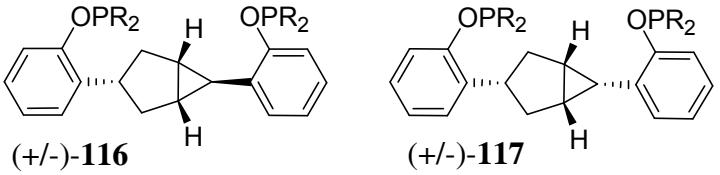

(+/-)-**116** (+/-)-**117**

Figure 27. Proposed 6-*exo* {(+/-)-**116**} and 6-*endo* {(+/-)-**117**} stereoisomers of (+/-)-3-*endo*-bicyclo[3.1.0]hexane-3,6-diyldi-2,1-phenylene bis(diphenylphosphinite) isomers as FLEXIphosO analogues.

Synthesis of the 6-*endo* stereoisomer {(+/-)-**117**} was attempted first, as a retrosynthesis was envisaged starting from commercially available coumarin (**118**) (Scheme 32). This can be reduced to 2-[(1*Z*)-3-hydroxyprop-1-en-1-yl]phenol (**119**). The phenol could then be protected with a methoxy group (**120**) and the allyl alcohol substituted with chlorine to give 1-[(1Z)-3-chloroprop-1-en-1-yl]-2-methoxybenzene (**121**). This contains no protic groups other than the methylene protons and so treatment with LDA should hopefully then lead to the enyne (**122**). Gold-catalysed cycloisomerisation followed by reduction of the alkene and deprotection of the hydroxyl groups should yield the diol (**125**), which can then be phosphorylated to give the target (+/-)-3-*endo*-6-*endo*-bicyclo[3.1.0]hexane-3,6-diyldi-2,1-phenylene bis(diphenylphosphinite) {(+/-)-**117**}.

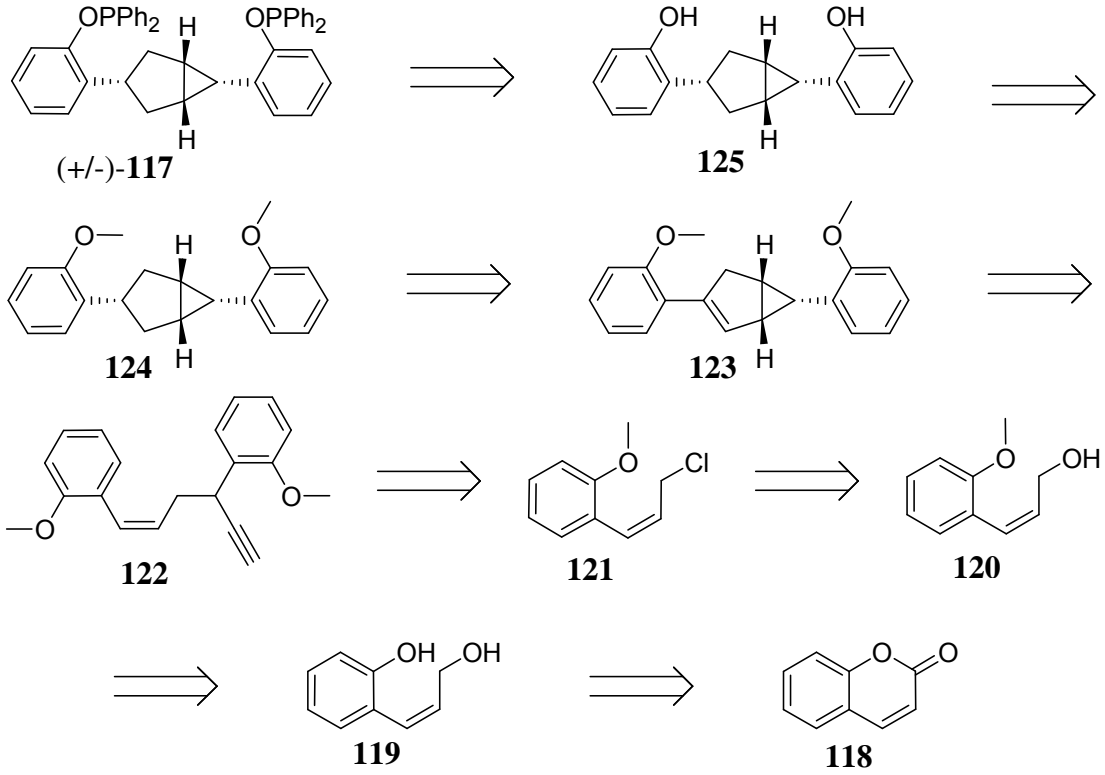

Scheme 32. Proposed retro synthesis of (+/-)-3-*endo*-6-*endo*-bicyclo[3.1.0]hexane-3,6-diyldi-2,1-phenylene bis(diphenylphosphinite) ((+/-)-**117**).

The first step, reduction of coumarin (**118**) using $LiAlH_4$, was precedented[127] and proceeded as expected to give **119** in 34% yield (Scheme 33). The yield is limited as the reaction has to be stopped before completion to prevent reduction of the alkene. The protection of the phenol alcohol using MeI to give **120** was also facile[128] and was achieved in 60% yield, as was substitution of the allyl alcohol with chloride to give **121** (83% yield).[126] The key enyne synthesis step, treatment of **121** with lithium diisopropylamide at -78 ˚C, fortunately produced the desired enyne **122** in 47% yield. The yield is low due to the difficulty in purifying the non-polar product.

A combination of 1 mol% of $[AuBr_2(N\text{-dbs})(I^tBu)]$ (**66b**) and 1 mol% $Ag[Al(OC(CF_3)_3)_4]$ (**76**) was used for the cycloisomerisation of enyne **122** giving the bicyclo[3.1.0]hexene product **123** in 71% impure yield. It was not possible to entirely purify this by column chromatography on silica-gel due to the non-polar nature of the product, starting material and side products. It was decided to take this impure material through to the next stage to determine the efficiency of the alkene reduction step. However, this resulted in a mixture of more than four inseparable products all of which were fully reduced. Due to this and the difficulty of obtaining pure material it was decided not to

further pursue this synthesis, although the limitations of Florio and Troisi's method for the synthesis of enynes has been exposed.

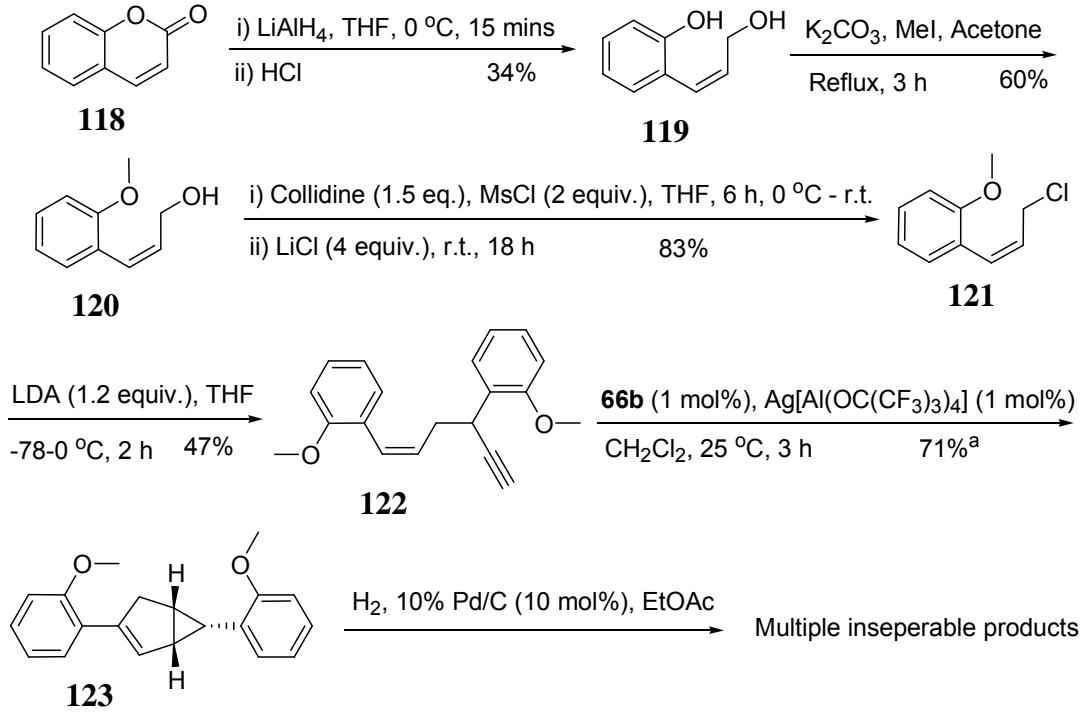

Scheme 33. Attempted synthesis of (+/-)-3-*endo*-6-*endo*-bicyclo[3.1.0]hexane-3,6-diyldi-2,1-phenylene bis(diphenylphosphinite) {(+/-)-**117**}.

[a] Impure yield.

2.2.2.10. Tandem nucleophilic substitution-cycloisomerisation

Having demonstrated the efficiency of the Au(III) imidate complexes (**66-68**) in conjunction with $Ag[Al(OC(CF_3)_3)_4]$ (**76**) as catalyst systems for 1,5- and 1,6-enyne cycloisomerisations, attention was turned to probing the Lewis acid properties of the Au(III) complexes. In order to exploit the activity of the complexes in cycloisomerisation reactions as well as probing the Lewis acidity, a two step tandem reaction requiring these two properties was required. This would necessiate the synthesis of an enyne, as a cycloisomerisation precursor, in the first step by a Lewis acid mediated reaction. As the Au(III)-catalysed nucleophilic-subsitution of propargyl alcohols with allylsilanes has been reported,[25a] this was selected to study, as a tandem nucleophilic substitution-cycloisomerisation.

The reaction of 1-phenyl-prop-2-yn-1-ol (**126**) and allyltrimethylsilane (**127a**), producing 3-phenylbicyclo[3.1.0]hex-2-ene (**75**), *via* 3-phenylhex-1-en-5-yne (**74**), was chosen for initial screening due to the proven efficiency of the Au(III) imidate complexes in the cycloisomerisation step (Scheme 34).

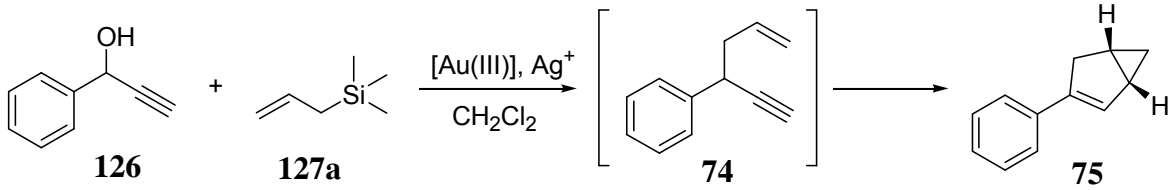

126 **127a** **74** **75**

Scheme 34. Tandem nucleophilic substitution-cycloisomerisation of 1-phenylprop-2-yn-1-ol (**126**).

Complex **67c** was selected for use in screening reaction conditions for the transformation, as it has high activity in the cycloisomerisation reactions but also is likely to be the most Lewis acidic complex due to the electron withdrawing ability of the tetrafluorosuccinimidate ligand (as shown by spectroscopic analysis). The reaction was first attempted using 2 mol% **67c**, 2 mol% $Ag[Al(OC(CF_3)_3)_4]$ (**76**) and a 0.2 M solution of 1-phenylprop-2-yn-1-ol (**126**) in CH_2Cl_2 (this concentration was used on the basis of the results of Georgy *et al.*[25a] and kinetic data on the cycloisomerisation of 3-phenylhex-1-en-5-yne (**74**)). Initially the reaction was run at ambient temperature for 18 hours which gave an unsatisfactory 20% conversion to 3-phenylbicyclo[3.1.0]hex-2-ene (**75**), with the remaining material oligomeric or polymeric in nature (Table 28). The temperature was then lowered to -40 ˚C in order to try to reduce the polymerisation, however only 8% conversion was achieved after 6 hours, with 27% of the starting material (**126**) remaining, 27% 3-phenylhex-1-en-5-yne (**74**) and 11% of symmetric ether (formed by condensation of two 1-phenylprop-2-yn-1-ol (**126**) molecules). Allowing the reaction to run to completion at this temperature was impractical and so the reaction was run at 0 ˚C and allowed to warm to ambient temperature over 18 hours. This gave a more satisfactory 38% conversion with 8% symmetric ether and the remaining material polymeric.

Table 28. Effect of reaction temperature on the tandem nucleophilic substitution-cycloisomerisation of 1-phenylprop-2-yn-1-ol (**126**) and allyltrimethylsilane (**127a**).[a]

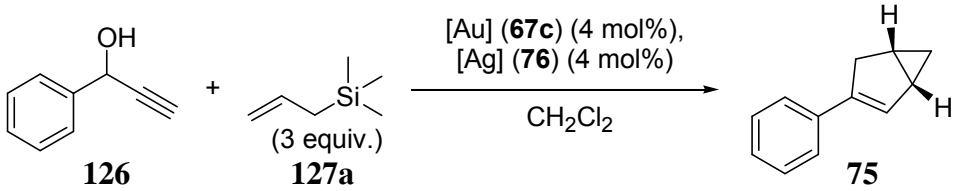

126 **127a** **75**

Entry	Time (h)	Temperature (°C)	Conversion (%)
1	18	r.t.	20
2	6	-40	8
3	18	0 - r.t.	38

[a] Conditions: 2 mol% **67c**, 2 mol% $Ag[Al(OC(CF_3)_3)_4]$ (**76**), 0.2 M 1-phenylprop-2-yn-1-ol (**126**) in CH_2Cl_2.

Having identified a practical reaction temperature, the effect of catalyst loading and the concentration of allyltrimethylsilane (**127a**) was explored (Table 29). It was found that increasing the number of equivalents of **127a** relative to **126** from 1.5 to 3 had a negative impact on the conversion to product with just 17% recorded, the remainder being uncharacterised polymeric material. It was then decided to attempt the reaction with an increased catalyst loading of 4 mol%. With 1 equivalent of **127a** there was no product observed, and with 1.5 equivalents only 1%, however with 3 equivalents the conversion improved to 46% (the remainder being polymeric). Further increasing the loading to 6 equivalents reduced the product to 19%, and increasing catalyst loading to 10 mol% allowed no conversion to product. It appears that there is a significant impact of the catalyst to allyltrimethylsilane (**127a**) loading ratio on the reaction, with 4 mol% and 3 equivalents being optimal, lowering or raising this ratio reduces conversion, due to polymerisation. To try and improve on the 46% conversion the reaction was tried with 8 mol% of $Ag[Al(OC(CF_3)_3)_4]$ (**76**) (4 mol% **67c**), however this also reduced the conversion (23%). Finally, preactivation of the complex prior to the reaction was carried out but this gave only 14% product, presumably as slow activation of the catalyst is required to reduce polymerisation.

Table 29. Effect of catalyst loading and equivalents of allyltrimethylsilane (**127a**) on the tandem nucleophilic substitution-cycloisomerisation of 1-phenylprop-2-yn-1-ol (**126**) and **127a**.[a]

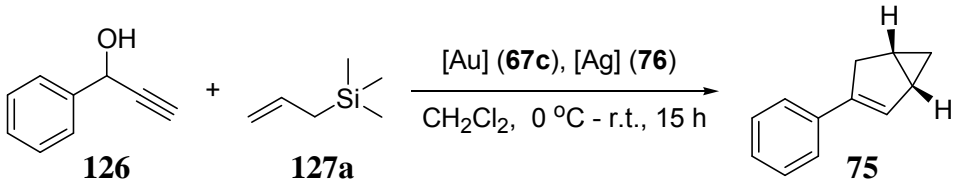

126 **127a** **75**

Entry	Loading (mol%)	Equivalents of allyltrimethylsilane (127a)	Conversion (%)
1	2	1.5	38
2	2	3	17
3	4	1	0
4	4	1.5	1
5	4	3	46
6	4	6	19
7	4 (8 mol% Ag)	3	23
8	10	3	0
9	4[b]	3	14

[a] Conditions: 0.2 M 1-phenylprop-2-yn-1-ol (**126**) in CH_2Cl_2, **67c**:**76** 1:1 (unless otherwise stated), 0 °C – r.t., 15 hours. [b] Catalyst preactivated.

Screening of the reaction solvent showed dichloromethane to be the most effective; coordinating solvents such as tetrahydrofuran and acetonitrile gave no conversion to product (only ethers), 1,2-dichloroethane gave 23% and carbon tetrachloride 15% (Table 30).

Table 30. Effect of reaction solvent on the tandem nucleophilic substitution-cycloisomerisation of **126** and **127a**.[a]

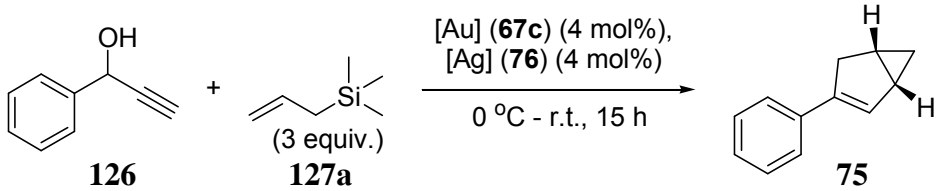

126 **127a** **75**

Entry	Solvent	Conversion (%)
1	Acetonitrile[b]	0
2	Tetrahydrofuran	0
3	Carbon tetrachloride	15
4	1,2-Dichloroethane	23
5	Dichloromethane	46

[a] Conditions: 4 mol% **67c** and $Ag[Al(OC(CF_3)_3)_4]$ (**76**), 0.2 M, 0 ˚C - r.t., 15 hours, 3 equivalents of allyltrimethylsilane (**127a**). [b] Ambient temperature and 70 ˚C gave no conversion to product.

The effect of the silver salt follows the coordinating ability of the anion with $Ag[Al(OC(CF_3)_3)_4]$ (**76**) being the most efficient and AgOTf the least (Table 31), in fact AgOTf is very inefficient, with trace product, only 3% of 3-phenylhex-1-en-5-yne (**75**) and 77% starting material. In the absence of an added silver salt the reaction did not proceed at all, with only starting material observed.

Table 31. The effect of different silver salt additives on the tandem nucleophilic substitution-cycloisomerisation of **126** and **127a**.[a]

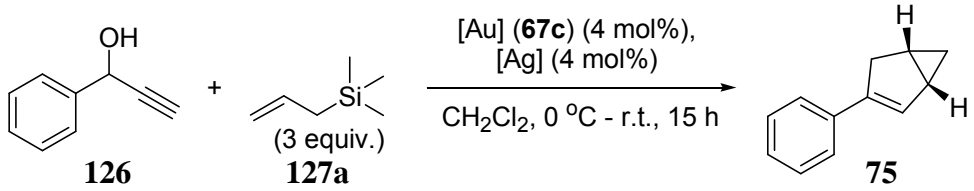

126 **127a** **75**

Entry	Silver salt additive	Conversion (%)
1	AgOTf	<1
2	$Ag[Al(OC(CF_3)_3)_4]$ (**76**)	46
3	$AgSbF_6$	14
4	-	0

[a] Conditions: 4 mol% **67c** and silver additive, 0.2 M 1-phenylprop-2-yn-1-ol (**126**) in CH_2Cl_2, 0 ˚C - r.t., 15 hours, 3 equivalents of allyltrimethylsilane (**127a**).

In order to determine the sensitivity of the reaction to possible contaminants the reaction was run with the addition of 0.1 equivalents of water and also with 0.1 equivalents of 1,3-diphenylprop-2-yn-1-one (**128**) (the oxidation product of 1,3-diphenylprop-2-yn-1-ol, used for ease of synthesis) (Table 32). The results show that adding water has a moderate effect, reducing conversion to product from 46% to 24% (with 17% starting material). Clearly, the catalysts can tolerate small amounts of water in solution and so rigorously dry conditions are not necessary (although they are ideal). The propynone **128** however has a more pronounced effect, reducing conversion to just 8% (33% starting material), presumably due to competing but unproductive coordination to the catalyst. The propynone forms slowly from the propynol at room temperature and so must be freshly distilled and stored at -20 ˚C (although 1-phenylprop-2-yn-1-ol (**126**) oxidises very slowly, with more substituted propargyl alcohols oxidation can be relatively rapid).

Table 32. The effect of additives on the tandem nucleophilic substitution-cycloisomerisation of 1-phenylprop-2-yn-1-ol (**126**) and allyltrimethylsilane (**127a**).[a]

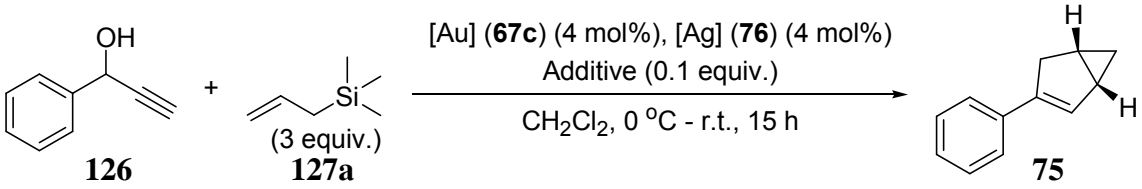

126 **127a** **75**

Entry	Additive	Conversion (%)
1	Water	24
2	1,3-diphenylprop-2-yn-1-one (**128**)	8

[a] Conditions: 4 mol% **67c** and $Ag[Al(OC(CF_3)_3)_4]$ (**76**), 0.2 M 1-phenylprop-2-yn-1-ol (**126**) in CH_2Cl_2, 0 °C - r.t., 15 hours, 3 equivalents of allyltrimethylsilane (**127a**), 0.1 equivalents of additive.

A range of allyl and vinyl nucleophiles were tested under the reaction conditions, however only allyltrimethylsilane (**127a**) was effective (Table 33, Figure 28). Allyltriphenylsilane (**127b**) gave the only other observable formation of product (4%) (the reaction was run with just one equivalent of silane due to the high molecular weight). Allyltrimethoxysilane (**127c**) and allyltributyltin (**127d**) gave no product.

Table 33. Effect of various allyl and vinyl nucleophiles in the tandem nucleophilic substitution-cycloisomerisation of 1-phenylprop-2-yn-1-ol (**126**).[a]

Entry	Nucleophile	Conversion to product (%)	Other products
1	allyltrimethylsilane (**127a**)	46	
2	allyltriphenylsilane[b] (**127b**)	<4	
3	allyltrimethoxysilane (**127c**)	0	8% cinnamaldehyde (**131**)
4	allyltributyltin (**127d**)	0	
5	vinyloxytrimethylsilane (**127e**)	0	4% 4-yn-1-one (**129a**)
6	vinyloxytrimethylsilane[c] (**127e**)	0	38% 4-yn-1-one (**129a**)
7	1-phenyl-1-trimethylsiloxy ethylene[c] (**127f**)	0	
8	allyl alcohol (**127g**)	0	36% cinnamaldehyde (**131**)
9	*N*-methyl-*N*-allylamine (**127h**)	0	
10	*N*,*O*-bistrimethylsilyl acetamide[c] (**127i**)	0	

[a] Conditions: 4 mol% **67c** and Ag[Al(OC(CF$_3$)$_3$)$_4$] (**76**), 0.2 M 1-phenylprop-2-yn-1-ol (**126**) in CH_2Cl_2, 0 °C - r.t., 15 hours, 3 equivalents of silane, alcohol, or stanane. [b] 1 Equivalent of allyltriphenylsilane (**127b**). [c] 1-(4-Chlorophenyl)-3-phenylprop-2-yn-1-ol (**133g**) was used in place of **126**.

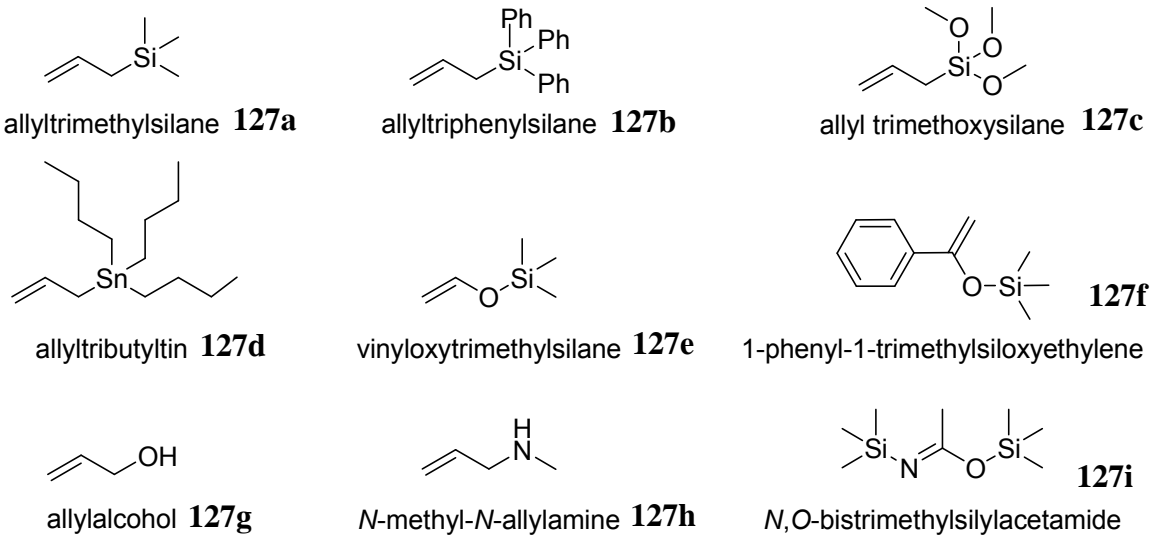

Figure 28. Allyl and vinyl compounds tested in the tandem nucleophilic substitution-cycloisomerisation of 1-phenylprop-2-yn-1-ol (**126**).

Vinyloxytrimethylsilane (**127e**) and 1-phenyl-1-trimethylsiloxyethylene (**127f**) were also tested. These would be expected to form alk-4-yn-1-ones (**129**), which has been observed with $[\{RuCl(\eta^5\text{-}C_5Me_5)(\eta^2\text{-}SMe)\}_2]$[129] and $[ReBr(CO)_3(THF)]_2$[130] catalysts (Scheme 35).

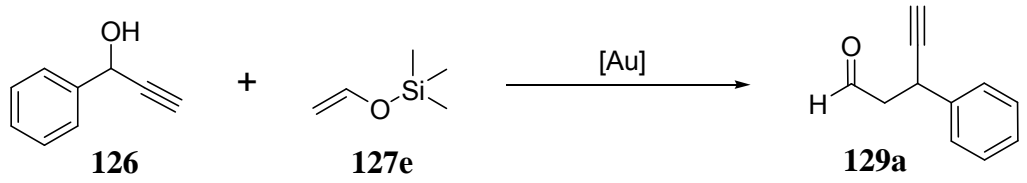

126 **127e** **129a**

Scheme 35. Proposed Au catalysed nucleophilic substitution of 1-phenylprop-2-yn-1-ol (**126**) with trimethylsiloxyethylene (**127e**) to give 3-phenylpent-4-yn-1-one (**129a**).

Alkynones have been shown to undergo gold-catalysed cycloisomerisation to give highly substituted furans (Scheme 36).[131]

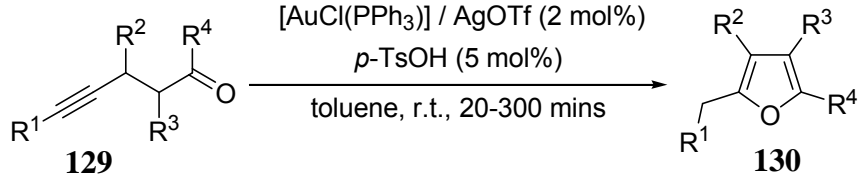

129 **130**

Scheme 36. Au(I) catalysed cycloisomerisation of alk-4-yn-1-ones (**129**) to form substituted furans (**130**).

It was anticipated that **126** would react with **127e** to produce 2-methyl-3-phenylfuran (**130a**) *via* 3-phenylpent-4-ynal (**129a**) (Scheme 37) in a tandem nucleophilic substitution-cycloisomerisation reaction.

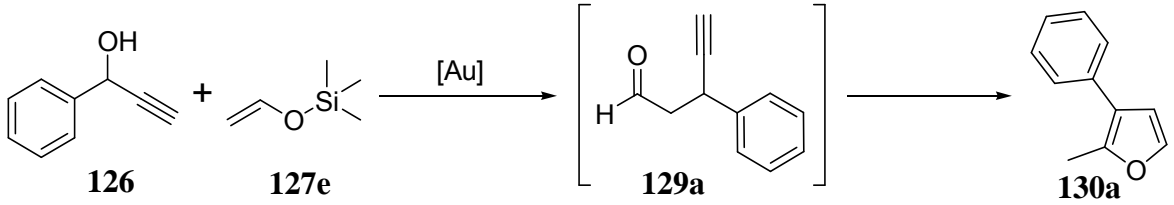

126 **127e** **129a** **130a**

Scheme 37. Proposed tandem Au catalysed nucleophilic substitution-cycloisomerisation of 1-phenylprop-2-yn-1-ol (**126**) and trimethylsiloxyethylene (**127e**) to give 2-methyl-3-phenylfuran (**130a**) *via* 3-phenylpent-4-ynal (**129a**).

Unfortunately the reaction yielded none of the cycloisomerisation product **130a**; only 4% of the aldehyde **129a** was observed (along with 8% cinnamaldehyde (**131**) and 7% starting material). The reaction was retried using 1-(4-chlorophenyl)-3-phenylprop-2-yn-1-ol (**133g**) as the propargyl alcohol in the hope that the phenyl group would help stabilize the cationic intermediates. In this case 38% of the aldehyde, 3-(4-chlorophenyl)-5-phenylpent-4-ynal (**129b**), was formed but again none of the furan, 2-benzyl-3-(4-chlorophenyl)furan (**130b**), the mass balance being polymeric material. The reaction was also tried with 1-(4-chlorophenyl)-3-phenylprop-2-yn-1-ol (**133g**) and 1-phenyl-1-trimethylsiloxyethylene (**127f**). However, no ketone, 3-(4-chlorophenyl)-1,5-diphenylpent-4-yn-1-one, (**129c**) or furan, 2-benzyl-3-(4-chlorophenyl)-5-phenylfuran (**130c**), were formed.

Allyl alcohol (**127g**) predictably slowed down the reaction {as it is likely to coordinate to the Au cation, as with coordinating solvents (*vide supra*)} and 24% starting material was observed, there was also 36% of cinnamaldehyde (**131**) from the Meyer-Schuster rearrangement. This reaction (previously reported to be catalysed by Au(I) complexes by Nolan and co-workers)[132] is promoted by alcohols but also requires the presence of a catalytic amount of water (it does not proceed under anhydrous conditions) (Scheme 38). *N*-Methyl-*N*-allylamine (**127h**) did not react (presumably as it will coordinate to Au cations) and neither did *N*,*O*-bistrimethylsilylacetamide (**127i**).

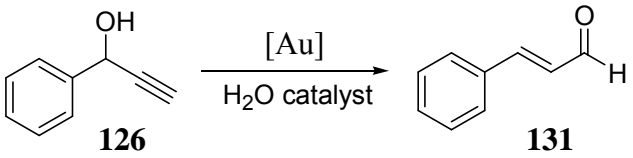

Scheme 38. The Meyer-Schuster rearrangement of 1-phenylprop-2-yn-1-ol (**126**) to produce cinnamaldehyde (**131**).

Using these optimised conditions (0.2 M solution of 1-phenylprop-2-yn-1-ol (**126**) in CH_2Cl_2, 3 equivalents of allyltrimethylsilane (**127a**), 4 mol% **67c**, 4 mol% $Ag[Al(OC(CF_3)_3)_4]$ (**76**), 0 ˚C – r.t., 15 hours) a selection of Au(I) and Au(III) complexes and salts were screened for activity in the tandem nucleophilic substitution-cycloisomerisation of **126** and **127a** (Table 34).

Table 34. Comparison of Au precatalysts for the tandem nucleophilic substitution-cycloisomerisation of 1-phenylprop-2-yn-1-ol (**126**) and allyltrimethylsilane (**127a**).[a]

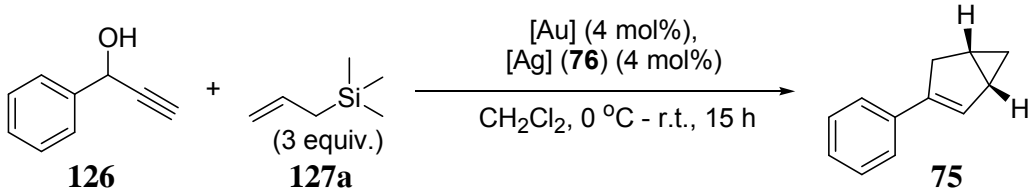

126 **127a** **75**

Entry	Au source	Conversion (%)[b]
1	[$AuBr_2$(*N*-succ)(I^tPe)] (**67a**)	2
2	[$AuBr_2$(*N*-dbs)(I^tPe)] (**67b**)	15
3	[$AuBr_2$(*N*-tfs)(I^tPe)] (**67c**)	46
4	[$AuBr_2$(*N*-mal)(I^tPe)] (**67d**)	11
5	[$AuBr_2$(*N*-ptm)(I^tPe)] (**67e**)	7
6	[$AuBr_3$(I^tPe)] (**67g**)	9
7	[AuBr(I^tPe)] (**56g**)	<1
8	$AuCl_3$[c]	<1
9	$Na[AuCl_4]$[c]	<1
10	[$AuBr_2$(*N*-ptm)(IMes)] (**68c**)	10
11	-	0

[a] Conditions: [Au] (4 mol%), $Ag[Al(OC(CF_3)_3)_4]$ (**76**) (4 mol%), 0.2 M, **127a** (3 equiv), in CH_2Cl_2, 0 °C - r.t., 15 hours. [b] Conversion by ^{1}H NMR spectroscopic analysis of the crude product(s). [c] No $Ag[Al(OC(CF_3)_3)_4]$ (**76**) added.

The results revealed that as anticipated **67c** was the most efficient precatalyst for the reaction. Of the Au(III) imidate complexes **67a**, **67b**, **67d** and **67e** gave only 2, 15, 11 and 7% conversions, respectively. Given the higher conversions achieved by **67b** and **67d** in the cycloisomerisation of 3-phenylhex-1-en-5-yne (**74**) relative to **67c** it appears that the higher Lewis acidity of **67c** is key to the initial nucleophilic substitution step, in fact the conversions achieved appear to follow the expected Lewis acidity of the complexes. Complex **68c** gave 10% conversion, slightly higher than analogue **67e**.

Bromide **67g** gave only 9% conversion, unsurprising considering its lower relative Lewis acidity and activity in the cycloisomerisation step. Simple Au(III) complexes and salts, $AuCl_3$ and $Na[AuCl_4]$ gave only trace product (<1%) under these conditions, as did the Au(I) complex **56g** – cinnamaldehyde (**131**) was the only identifiable product (24%). Given

the high activity of Au(I) sources in 1,5-enyne cycloisomerisation it was evident that Au(I) sources do not mediate an efficient nucleophilic substitution step, having less Lewis acidic character than the Au(III) complexes. In a control test, the reaction did not proceed in the absence of a gold complex (with only starting material observed).

Georgy *et al.*[77] reported that the $Na[AuCl_4]$ (5 mol% with 1.2 equivalents of **127a** in CH_2Cl_2, 4 hours at ambient temperature) catalysed nucleophilic substitution resulted in only 9% yield of **74**, claiming that the low yield was "mainly due to the instability of the compound, which rapidly decomposes at room temperature." However, our tests have shown the product and starting material to be fairly stable under ambient conditions and the low yield is likely to be due to polymerisation. The low yield highlights the difficulty associated with the nucleophilic substitution step.

Using the optimum conditions a library of propargyl alcohols were evaluated (Table 35).

Table 35. Conversions of propargyl alcohols to bicyclo[3.1.0]hexenes using complex **67c**.[a]

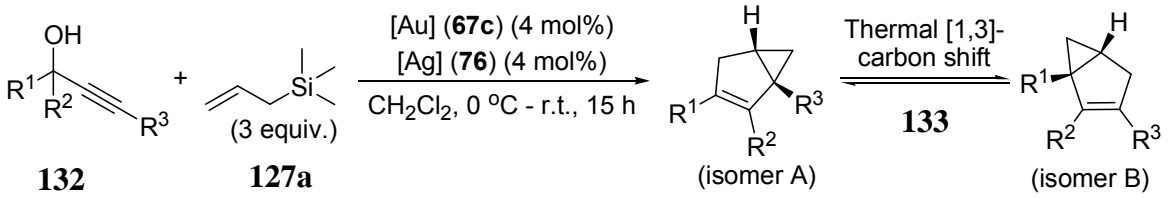

132 **127a**

Entry	Starting alcohol	R^1	R^3	Product	Conv. (%)[b]	Yield (%)	Ratio of isomers[g]
1	**126**	Phenyl	H	**75**	46	-	-
2	**132a**	Phenyl	Methyl	**133a**	30	-	-
3	**132b**	Phenyl	^{n}Butyl	**133b**	81	76	94:6
4	**132c**	Phenyl	TMS	**133c**	>99[c]	75[d]	-
5	**132d**	Phenyl	Phenyl	**133d**	>99	91	-
6	**132e**	2-Napthyl	Phenyl	**133e**	>99	68[e]	56:44
7	**132f**	Mesityl	Phenyl	**133f**	>99	72[e]	35:65
8	**132g**	4-Cl-Phenyl	Phenyl	**133g**	>99	90	59:41
9	**132h**	4-CF_3-Phenyl	Phenyl	**133h**	75	62	50:50
10	**132i**	3-Methoxyphenyl	Phenyl	**133i**	67	53	49:51
11	**132j**	3,5-Dimethoxy phenyl	Phenyl	**133j**	15	-	-
12	**132k**	Ethyl	Methyl	**133k**	0	-	-
13	**132l**	Ethyl	Phenyl	**133l**	0	-	-
14	**132m**	Phenyl[f]	Phenyl	**133m**	0	-	-
15	**132n**	Phenyl[f]	H	**133n**	0	-	-
16	**132o**	Cyclohexyl[h]	Phenyl	**135a**	33[i]	-	-
17	**132p**	Methyl[j]	Phenyl	**135b**	14[i]	-	-
18	**132q**	Cyclohexyl	Dimer[k]	**133q**	0	-	-
19	**132r**	Phenyl	Dimer[l]	**133r**	<5	-	-

[a] Conditions: **67c** (4 mol%), $Ag[Al(OC(CF_3)_3)_4]$ (**76**) (4 mol%), 0.2 M (0.38 mmol), **126 or 132** (1 equiv.), **127a** (3 equiv.), in CH_2Cl_2, 0 ˚C – r.t., 15 hours, R^2 = H unless otherwise specified. [b] Conversion by ^{1}H NMR spectroscopic analysis of the crude product(s). [c] 99% enyne, 1% **133c** after 15 h, >99 % **133c** after 10 days. [d] 68:32 silylated:desilylated product observed (R^3 = H). [e] Reaction run on 0.19 mmol scale. [f] R^2 = Ph. [g] Ratio of isomer A:isomer B by ^{1}H NMR. [h] R^1 and R^2 form a cyclohexyl ring. [i] 1,3-Cyclohexadiene product. [j] R^2 = methyl. [k] 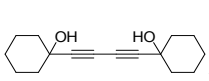 . [l] 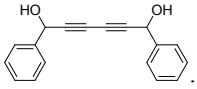 .

The results show that a methyl group at R^3 (**132a**) is not tolerated well (30% conversion to **133a**). However, the butyl derivative **132b** gives 81% conversion to **133b**, which likely stabilizes the carbocation intermediate (or affects the relative rate of cycloisomerisation *versus* polymerisation). This is supported by the work of Georgy *et al.*[77] who showed that butyl and pentyl derivatives gave good yields of the nucleophilic subsitution product with $Na[AuCl_4]$ (they did not report any methyl derivatives).

A trimethylsilyl (TMS) group at R^3 (**132c**) greatly reduced the cycloisomerisation rate, with 99% conversion to the 1,5-enyne (**134**) after 15 hours, but less than 1% of **133c**. Following prolonged reaction (10 days), the reaction had gone to completion (32% desilylated product, **75**, was present). The cycloisomerisation step of this reaction was investigated using 1-trimethylsilyl-3-phenylhex-5-en-1-yne (**134**) (Table 36). It was found that at ambient temperature the cyclosiomerisation proceeded very slowly (15% of **133c** and **75** after 15 hours) allowing significant desilylation of the product **133c** (87%) to form **75** and polymer formation (15%). At 60 ˚C (in 1,2-dichloroethane) the reaction was accelerated with 51% product (**133c** and **75**) of which only 25% was desilylated - the mass balance being uncharacterised polymer. The Au(I) complex **56g** gave only 9% cycloisomerisation product at ambient temperature (11% desilylated) with no polymerisation, however at 60 ˚C 72% product (**133c** and **75**) (14% desilylated) and 26% polymer was observed. It would appear from these results that Au(III) promotes the desilyation of the enyne (and possibly the product as well) as suggested by the higher conversion than Au(I) at ambient temperature, it also promotes polymerisation of the enyne (presumably this competes with cycloisomerisation so that at low cycloisomerisation rates the polymerisation is more pronounced).

Table 36. Effect of temperature on the Au catalysed cycloisomerisation of 1-trimethylsilyl-3-phenylhex-5-en-1-yne (**134**).[a]

Entry	Complex	Temp (˚C)	Conversion (%)		
			Silylated (133c)	Desilylated (75)	Polymer[b]
1	$[AuBr_2(N\text{-tfs})(I^tPe)]$ (**67c**)	r.t.	2	13	15
2	$[AuBr_2(N\text{-tfs})(I^tPe)]$ (**67c**)	60[c]	38	13	49
3	$[AuBr(I^tPe)]$ (**56g**)	r.t.	8	1	-
4	$[AuBr(I^tPe)]$ (**56g**)	60[c]	62	10	26

[a] Conditions: : [Au] (4 mol%), $Ag[Al(OC(CF_3)_3)_4]$ (**76**) (4 mol%), 0.2 M 1-trimethylsilyl-3-phenylhex-5-en-1-yne (**134**) in CH_2Cl_2, 15 hours. [b] Not characterised. [c] 1,2-dichloroethane solvent.

Encouragingly a phenyl group at R^3 (**132d**) showed quantitative conversion, giving **133d** in 91% yield. A variety of aromatic groups are tolerated under the optimised conditions. Quantitative conversions were noted for propargylic substrates possessing 2-napthyl (**132e**), mesityl (**132f**) and 4-chlorophenyl (**132g**) moieties. Catalyst loadings for **132g** can also be reduced to 1 mol% with 1.1 equivalents of allyltrimethylsilane (**127a**), whilst still allowing quantitative conversion to be attained.

The 4-CF_3 derivative (**132h**) was found to proceed only to 75% product conversion (mass balance being polymer), this may be due to the electron withdrawing group making carbocation formation less favourable. Methoxy substitution was also less successful with 3-methoxyphenyl (**132i**) giving 67% conversion and 3,5-dimethoxyphenyl (**132j**) only 15% with a complex mixture of products. This may be due to aromatic propargylation of the dimethoxy-aryl group by the carbocation, generated by abstraction of the hydroxyl group, which has been reported in the literature as an effective nucleophile for propargylic substitution.[25a,69-71,73]

Alkyl substitution at R^1 is not tolerated with either methyl (**132k**) or phenyl (**132l**) at R^3, resulting in polymeric/oligomeric product formation. This is due to the nucleophilic substitution step not proceeding efficiently, which has been demonstrated by Georgy *et al.*[77] who observed no reaction when treating alkyl (R^1) substituted propargyl alcohols with allyltrimethylsilane (**127a**) and $Na[AuCl_4]$.

1,1-Diphenyl substituted propargyl alcohols (**132m** and **132n**) did not undergo cycloisomerisation and the nucleophilic substitution is also difavoured (Georgy *et al.*[77] reported lower yields with 1,1-disubstituted propargyl alcohols). Where R^3 was also phenyl (**132n**) only 30% of the enyne was detected and where R^3 was H (**132m**) only polymerisation was observed.

1,1-Dialkyl-substituted propargyl alcohols (**132o** and **132p**) also gave disappointing results due to the reduced efficiency of the nucleophilic substitution. Although conversions to cycloisomerisation products of 33% in the cyclohexyl (**132o**) case and 14% in the methyl case (**132p**) were achieved, these were not to the expected products. These cycloisomerisation products were identified as 3-phenylspiro[5.5]undeca-1,3-diene (**135a**) (Scheme 39) and (4,4-dimethylcyclohexa-1,5-dien-1-yl)benzene (**135b**), respectively.

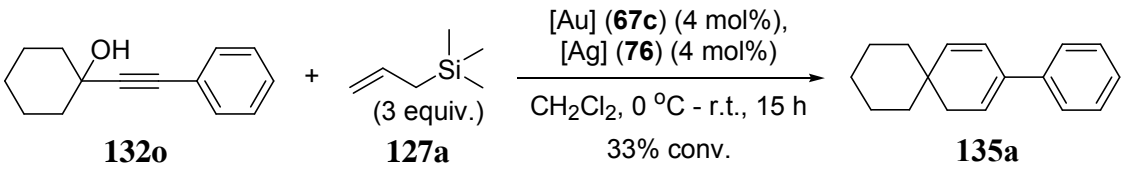

132o **127a** **135a**

Scheme 39. Gold catalysed tandem nucleophilic substitution-cycloisomerisation of 1-(phenylethynyl)cyclohexanol (**132o**) and allyltrimethylsilane (**127a**) to yield (4,4-dimethylcyclohexa-1,5-dien-1-yl)benzene (**135a**).

The cycloisomerisation step of this transformation was further investigated by preparation of the intermediate enyne (**136**) {by $FeCl_3$ catalysed nucleophilic substitution of the alcohol (**132o**) with allyltrimethylsilane (**127a**)}. Complexes **67c** and **56g** were then tested (4 mol%, with 4 mol% **76**, 0.2 M in CH_2Cl_2 at 0 ˚C to ambient temperature for 15 hours). The reaction proceeded very well with 60% conversion to the product (**135a**) for **67c** and 93% for **56g**, the remaining material was a complex mixture of products. It was found that the product was relatively unstable, with almost complete decomposition to a mixture of products (including the aromatised oxidation product) over 96 hours in solution, thus the lower conversion obtained for **67c** is likely due to more rapid decomposition of the product by Au(III) (as a more efficient polymerisation catalyst).

This usual transformation has been previously reported for a range of similar substrates by the group of Kosmin. For example, 2,4-dimethyl-2-(phenylethynyl)pent-4-en-1-yl tertbutyldimethlysiloxane (**137**) was found to undergo cycloisomerisation to yield (1,5-dimethyl-4-phenylcyclohexa-2,4-dien-1-yl)methyl *tert*-butyldimethlysiloxane (**138**) (Scheme 40).[133]

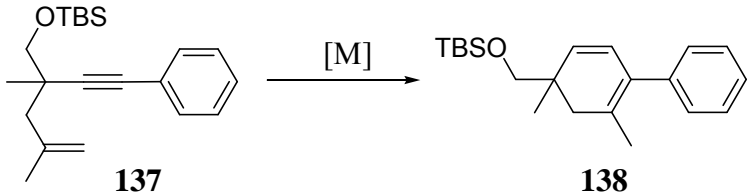

137 **138**

Scheme 40. The cycloisomerisation of 2,4-dimethyl-2-(phenylethynyl)pent-4-en-1-yl tertbutyldimethlysiloxane (**137**) to afford (1,5-dimethyl-4-phenylcyclohexa-2,4-dien-1-yl)methyl *tert*-butyldimethlysiloxane (**138**).

Kosmin and co-workers found that the reaction did not proceed well at 20 ˚C in CH_2Cl_2; $AuCl_3$ (5 mol%) achieving 22% yield, AuCl 16% and surprisingly $[Au(PPh_3)SBF_4]$ (as reported, this may be SbF_6 or BF_4) less than 5%. However, the authors did find that $PtCl_2$ in toluene (with one equivalent of MeCN) at 80 ˚C gave a 66% yield (<5% at 20 ˚C with 15 mol%), the reaction with Au sources at higher temperatures resulted in multiple unidentified products. They showed that this transformation occurred for a range of substrates with disubstitution at the propargyl position, including where the propargyl position forms part of a cyclohexane ring, however other ring sizes were not investigated. Other groups have also shown similar results with $PtCl_2$[134] and $[\{RuCl(Cp^*)(\mu_2\text{-}SMe)\}_2]$ which gives a 1,3-cyclohexadiene even with monosubstitution at the propargyl position (the mechanism in this case is believed to proceed *via* a ruthenium vinylidene complex).[135]

The mechanism for this reaction has been proposed by Kosmin *et al.* (Scheme 41, Route A).[133] Nucleophilic attack by the alkene upon the Au-activated alkyne (**139c**) (Step I) to produce a bicyclo[3.1.0]hexane is believed to occur first as in the usual mechanism. Then, rather than migration of one of the carbon atoms forming the cyclohexyl ring, migration of the adjacent cyclopropyl carbon (Step II) occurs to form a bicyclo[2.1.1]hexane. A carbocation at R^2 results in a further migration (Step III) to reform a bicyclo[3.1.0]hexane, then the metal aids the fragmentation of the bridging C-C bond (Step IV) to form a cyclohexene ring followed by elimination (Step V) to give the final 1,3-cyclohexadiene (**140**).

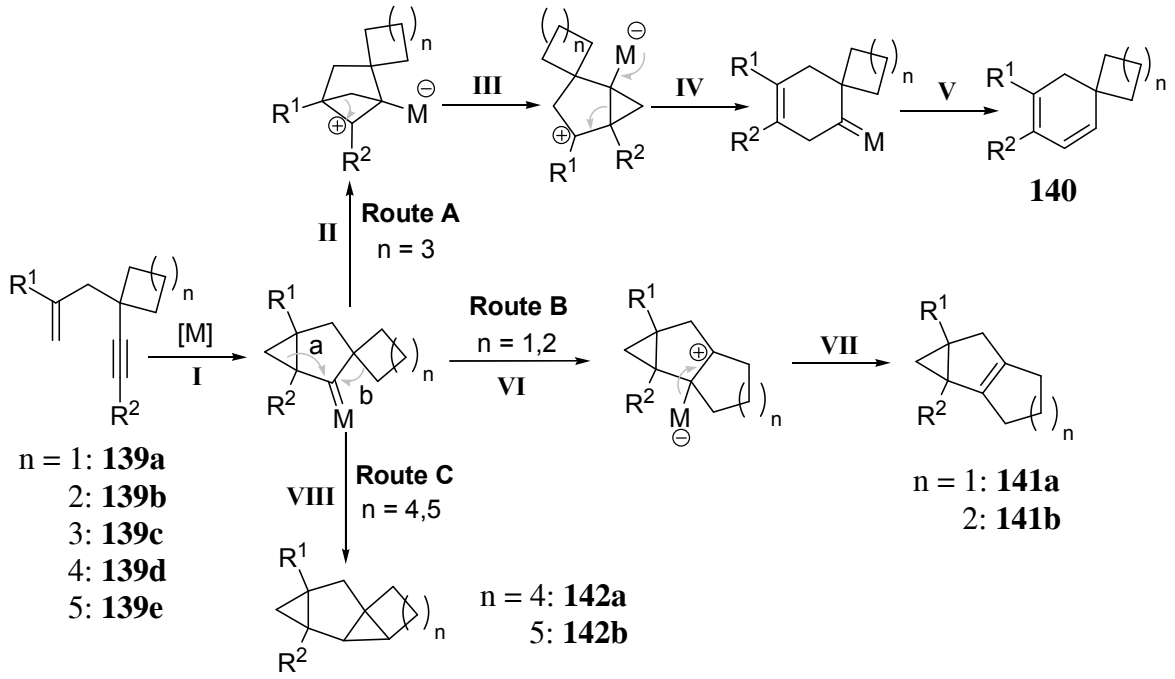

Scheme 41. Mechanism of cycloisomerisation of dipropargyl substituted 1,5-enynes (**139**) to form: a) 1,3-cyclohexadienes (**140**), b) bicyclo[3.1.0]hexenes (**141**) and c) tricyclo[4.1.0.$0^{2,4}$]heptanes (**142**).

The group of Toste has reported that where the propargyl position forms a cyclobutane (**139a**) or cyclopentane ring (**139b**) (Scheme 41, Route B) the typical mechanism of migration of one the groups at the propargyl position (Step VI) occurs resulting in a ring expanded hexahydro-1*H*-cyclopropa[*a*]pentalene (**141a**) or octahydrocyclopropa[*a*]indene (**141b**) structure, respectively (Step VII).[15] Later Toste reported that cycloheptane (**139d**) and cyclooctane (**139e**) rings at the propargyl position result in C-H insertion at the ◘-CH_2 position of the ring to give products **142a** and **142b**, respectively. This mechanism is similar to the usual mechanism except C-H insertion (Step VIII) rather than migration occurs. The reaction of a cyclohexyl substituted enyne was not reported despite hypothesising that it would undergo C-H insertion.[136] Specific examples reported by Toste using Au(I) phosphine catalysts are shown in Scheme 42.

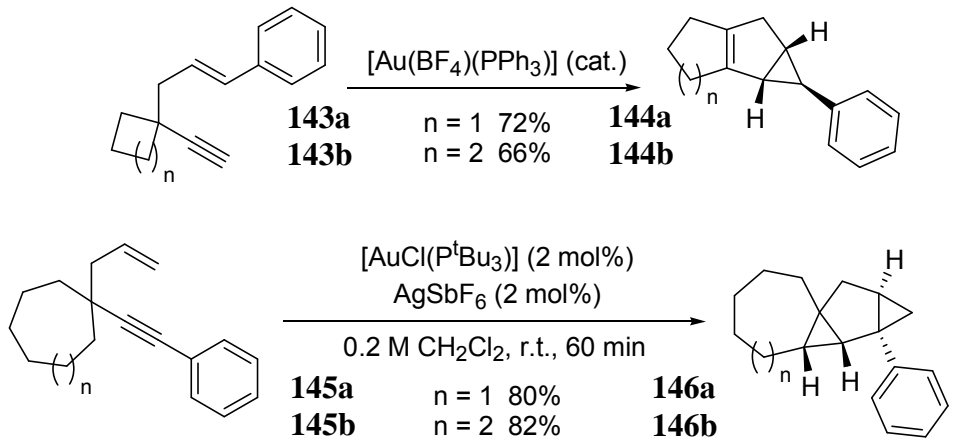

Scheme 42. Au(I) catalysed cycloisomerisations of 1-allyl-1-ethynyl cycloalkanes reported by Toste.

Toste also found that the cycloisomerisation of 1-phenyl-3,3-dimethyl-hex-5-en-1-yne (**147**) in methanol catalysed by [Au(SbF6)(PPh3)] gave 1-phenyl-3,3-dimethyl-5-methoxycyclohex-1-ene (**148**) formed by nucleophilic trapping of a carbocationic intermediate by methanol (**135b**, formed from **132p** *via* **147**, was found to have a 1,4 and not 1,3-relationship between the phenyl and dimethyl positions), however curiously the outcome of the reaction in CH_2Cl_2 was not reported (Scheme 43).[15]

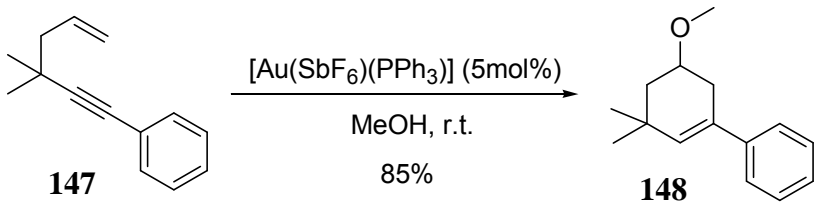

Scheme 43. Au(I) catalysed cycloisomerisation of (3,3-dimethylhex-5-en-1-yn-1-yl)benzene (**147**) in methanol reported by Toste.

The production of 1,3-cyclohexdienes (**150**) (as a minor product with 1,4-cyclohexadienes (**151**) as the major product) has also been observed for 1,5-enynes with mono-substitution at the propargyl position that contain a heteroatom bound to the enyne (**149**). The heteroatom aids the transformation *via* a ketene intermediate (in the case of disubstitution at the propargyl position only the 1,3-diene was formed, with no heteroatom the bicyclo[3.1.0]hexene was formed) (Scheme 44).[118,133,137]

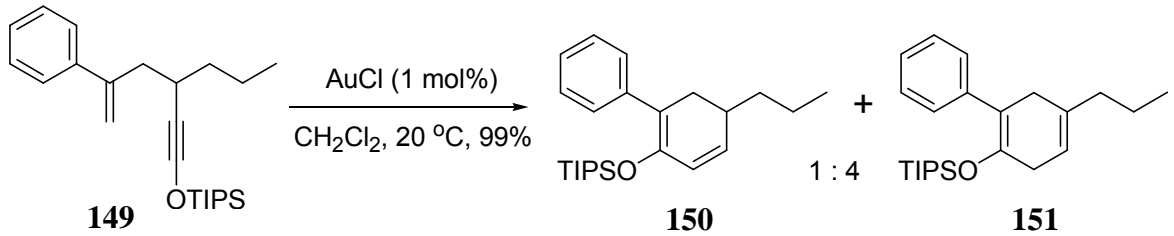

Scheme 44. Au-catalysed cycloisomerisation of 1,5-enynol **149** to give 1,3- (**150**) and 1,4- (**151**) cyclohexadienes reported by Kosmin.[137b]

Finally, the tandem nucleophilic substitution-cycloisomerisation was attempted with two diynes, 1,1'-buta-1,3-diyne-1,4-diyldicyclohexanol (**132q**) and 1,6-diphenylhexa-2,4-diyne-1,6-diol (**132r**). The cyclohexyl analogue did not yield any product, only 45% of the dienyne. With the phenyl analogue mostly starting material was observed with less than 5% of product **133r**. This lack of reactivity is mainly attributable to very low solubility of the propargyl alcohol in CH_2Cl_2.

The 1,3-diaryl (**133d**-**133i**) {and to a small extent the 1-phenyl-3-butyl (**133b**)} cycloisomerisation products showed significant isomerisation by a 1,3-carbon shift, which essentially switches the aryl group positions (Table 37). This phenomenon has been reported for other bicyclo[3.1.0]hexenes at elevated temperatures,[138] but not for 1,3-diaryl derivatives for which this process appears surprisingly facile, with the aryl substitution apparently aiding the isomerisation.

Tests to determine the cause of the isomerisation showed that it was most likely a thermal process and it was not promoted by silica-gel (it occurred equally in the absence of silica-gel). It was found that once the isomerisation had reached equilibrium further heating did not affect the ratio of isomers. The isomerisation does not occur to any appreciable extent with alkyl substituted variants and is not observed with the 1,3-diphenyl analogue **133d** as the 1,3-carbon shift isomers are identical. It would appear that more electron-donating aryl substituents in the R^1 position aid the isomerisation with the equilibrium lying to the right with more of the carbon shift isomer, although they do not fit well to the Hammett equation.[139]

Table 37. Ratio of isomers of bicyclo[3.1.0]hexene cycloisomerisation products.[a]

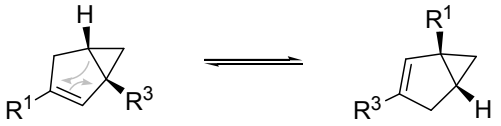

Isomer A (cylcoisomerisation product) Isomer B (Rearranged product)

Entry	R^1	R^3		A:B crude	A:B purified
1	Phenyl	Butyl	**133b**	96:4	94:6
2	Phenyl	Phenyl	**133d**	-	-
3	2-Napthyl	Phenyl	**133e**	83:17	56:44
4	Mesityl	Phenyl	**133f**	97:3	35:65
5	4-Cl-phenyl	Phenyl	**133g**	88:12	59:41[b]
6	4-CF_3-phenyl	Phenyl	**133h**	91:9	50:50[c]
7	3-Methoxyphenyl	Phenyl	**133i**	73:27	49:51

[a] R^2 = H. [b] Heating at 60 ˚C for 3 days did not affect the ratio. [c] Stirring with silica-gel overnight did not effect the ratio of products.

Doering *et al.*[140] have studied the kinetics of the thermal isomerisations of an □[2]-thujene system (**152**) containing a bicyclo[3.1.0]hexene ring system at 207 and 237 ˚C. They found that, as with other similar systems,[141] there were three significant isomerisation processes, 1,3-carbon shifts with *sr* (*suprafacial* with retention) and *ai* (*antarafacial* with inversion) stereochemistry (k_{sr} and k_{ai}) and ring flipping (inversion of chirality, $k_{ring\text{-}flip}$) (Scheme 45). These symmetry forbidden isomerisations are thought to occur *via* a diradical intermediate (153). The relative importance of these processes are k_{sr}:$k_{(ring\text{-}flip)}$:k_{ai} - 56:24:20, with a calculated activation energy of 182 kJ.mol^{-1} (in the gas phase). Doering and co-workers found that the relative importance of each process depended on the substituents on the bicyclo[3.1.0]hexene ring system but not on temperature, which only affected the rate of isomerisation.[142]

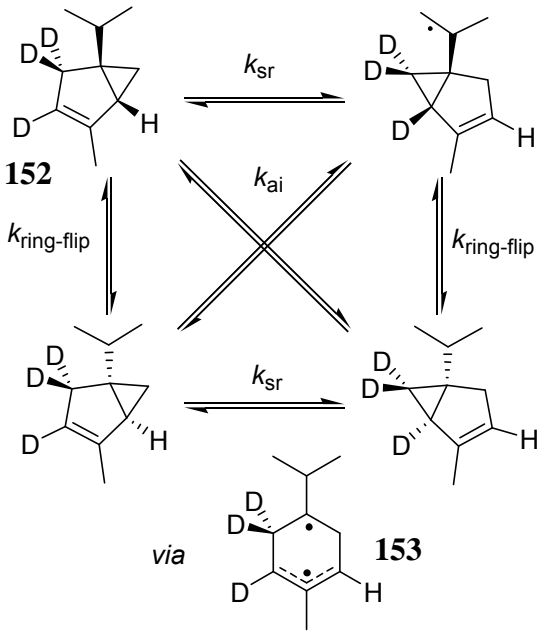

Scheme 45. Thermal isomerisation pathways of a □[2]-thujene (**152**) *via* a diradical intermediate (**153**) reported by Doering *et al.*.

These processes for the 1,3-diarylbicyclo[3.1.0]hexene cycloisomerisation products (**133d-i**) result in two observed species by NMR spectroscopy, the starting 1,3-diaryl (isomer A) and the observed 1,3-diaryl isomerisation product (isomer B). Both enantiomers of the starting and product species would be interconverted but this could not be monitored by NMR spectroscopy as the starting material was racemic (Scheme 46).

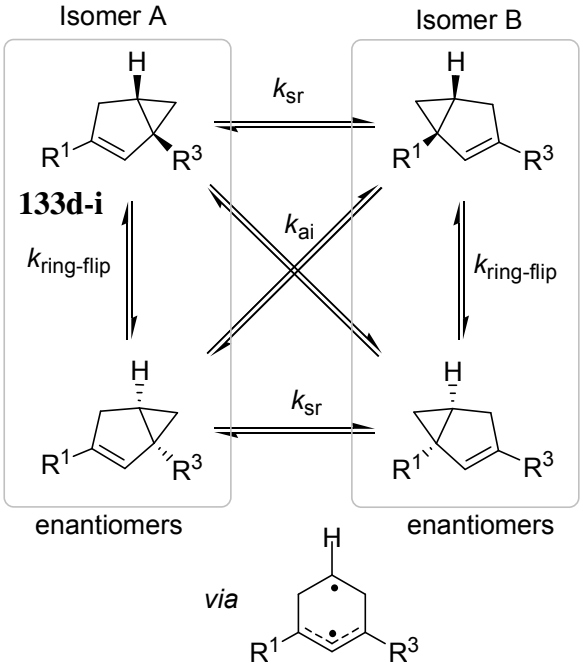

Scheme 46. Proposed thermal isomerisation pathways of 1,3-diarylbicyclo[3.1.0]hexenes (**133d-i**).

Interestingly, Sanz *et al.*[78] have also reported the tandem nucleophilic substitution-cycloisomerisation of allyltrimethylsilane (**127a**) and 1-(3-methoxyphenyl)-3-phenylpropynol (**133i**) using *p*-toluenesulfonic acid followed by [AuCl(PPh$_3$)]/AgSbF$_6$ as a catalytic system. They reported a 61% yield but did not report any isomerisation and the characterisation data quoted corresponds to isomer A. This is an intriguing result and it is not immediately obvious why the results are different to those in this study.

In order to determine if the nucleophilic substitution was actually catalysed by degradation products of the Au(III) complex rather than the metal itself, the reaction was tested in the presence of bromine and *N*-bromosuccinimide. It was found that the nucleophilic substitution of 1-(4-chlorophenyl)-3-phenylprop-2-yn-1-ol (**132g**) is catalysed by bromine although a 4% loading gave only a 67% conversion to the enyne nucleophilic substitution product after 2 days at ambient temperature (with the mass balance being 6% oligomerisation and 27% starting material). This suggests the bromine may aid nucleophilic substitution but it is not the principal agent. *N*-bromosuccinimide alone did not catalyse the reaction under these conditions.

The catalytic properties of the complexes indicate that the IMes ligand is less electron donating than the alkyl analogues. The poor cycloisomerisation ability of the IMes series with 4-phenyl-1-hexen-5-yne (**74**) but higher conversions with the more reactive 1,1'-(1*E*)-hex-1-en-5-yne-1,4-diyldibenzene (**81**), suggest the complexes have reasonable activity but poor stability, presumably due to an electron deficient Au atom. The relatively high 10% conversion in the tandem nucleophilic substitution-cycloisomerisation reaction suggests relatively high Lewis acidity despite poor cycloisomerisation ability.

Studies to try and determine the catalytically active species involved in these reactions are detailed in Appendix 1.

2.3. Conclusion

A general method for the preparation of a library of [Au(*N*-imidate)(NHC)] (**55**-**57**) and [$AuBr_2$(*N*-imidate)(NHC)] (**66**-**68**) complexes in high yield has been developed. A comprehensive analysis shows that the spectroscopic characteristics of the gold complexes are determined by the electronic properties of the NHC and imidate ligands. The Au(III) complexes (**66**-**68**) exhibit good catalytic activity in the cycloisomerisation of 4-phenyl-1-hexen-5-yne (**74**) and 1,1'-(1*E*)-hex-1-en-5-yne-1,4-diyldibenzene (**81**). In the case of [$AuBr_2$(*N*-tfs)(I^tPe)] (**67c**) an efficient and unique tandem nucleophilic substitution-cycloisomerisation reaction of propargyl alcohols (**132**) and allylsilanes (**127**) to give bicyclo[3.1.0]hexenes (**133**) was made possible. The use of $Ag[Al(OC(CF_3)_3)_4]$ (**76**) in comparison to AgOTf as an additive greatly increased the rate of reactions. It is anticipated that the gold catalysis field could benefit from the use of this non-coordinating anion for highly active Au-catalysis. The I^tBu and I^tPe complexes exhibit similar spectroscopic properties and catalytic activity, whereas IMes complexes exhibited poor stability and low catalytic activity. A significant effect of the structure of the imidate ligand on catalytic activity was observed, with more electronegative imidates resulting in higher conversions. An exception was the maleimidate Au complexes which possess high activity despite a relatively low electronegativity.

Kinetic analysis of the cycloisomerisation of **74** showed that [AuBr(I^tPe)] (**56g**) and [$AuBr_2$(*N*-ptm)(ItPe)] (**67e**), and particularly [$AuBr_2$(*N*-tfs)(I^tPe)] (**67c**) and [$AuBr_2$(*N*-ptm)(IMes)] (**68c**) complexes observed first order kinetics, suggesting stable active catalytic species. [$AuBr_3$(I^tPe)] (**67g**) fitted well to second order kinetics, indicating relatively rapid decomposition of the active catalyst during the reaction. [$AuBr_2$(*N*-tfs)(I^tPe)] (**67a**) did not fit to first or second order kinetics due to a long initiation period. Kinetic analysis of the complexes using 'aged enyne' resulted in reduced reaction rates, the impurity clearly playing a role in the kinetics. These results show that the use of pseudohalide ligands, as mimics for bromide, significantly increases the stability of NHC Au(III) catalysts. The product distribution from the cycloisomerisation of dimethyl allylpropargylmalonate (**77**) was found to be dependant on the nature of the silver additive used, the oxidation state of the Au precatalyst and the reaction conditions employed.

The identity of the catalytically active species in these reactions remains unclear and the involvement of $Au(I)^+$ species cannot be ruled out, the binding of Ag^+ by alkenes solubilises the silver salt which is likely to play a role in catalyst activation and possibly the cycloisomerisation mechanism.

2.4. Future Work

In order to increase the efficiency of [$AuBr_2$(*N*-imidate)(NHC)] precatalysts the rate of formation, solubility (in CH_2Cl_2) and stability (to reduction) of the Au(III) cation generated by halide abstraction must be improved. Solubility could be improved by incorporating additional hydrocarbon groups onto the imidate or NHC ligands. To improve stability reductive elimination of bromine and *N*-bromoimides from the Au complex must be prevented which could be achieved by tethering the NHC and anionic ligands (as polydentate ligands) (Figure 29).

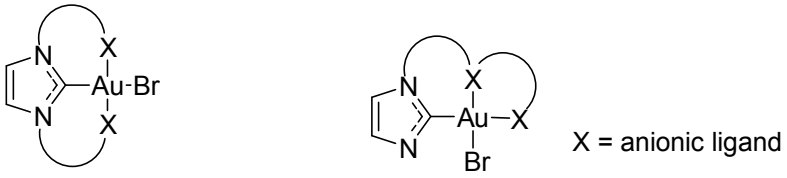

Figure 29. Depiction of Au(III) complexes bearing tethered NHC and anionic ligands.

Further investigation of the mechanism and active catalytic species formed from [$AuBr_2$(*N*-imidate)(NHC)] complexes (and other Au(III) complexes) is required to determine if Au(III) complexes are precursors to Au(III) or Au(I) cations as the active catalytic species.

The development of the unique single catalyst nucleophilic substitution-cycloisomerisation process should lead to the use of Au(III) imidate and other catalysts in further tandem processes where Lewis acidity as well as alkyne activation is required.

The demonstration of the benefits of pseudohalide ligands in this study should prompt the investigation of other electron-withdrawing pseudohalides as ligands in Au(III) complexes for catalytic applications, for example perfluoro-carboxylates (Figure 30).

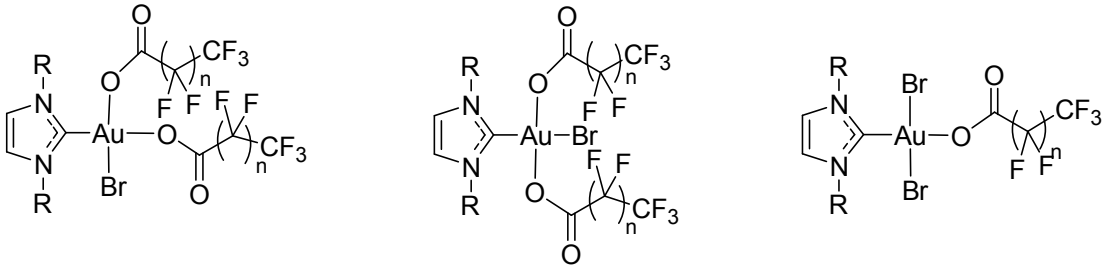

Figure 30. Depiction of Au(III) complexes bearing perfluorocarboxylate ligands.

The efficiency of highly electron-withdrawing imidate ligands, particularly tetrafluorosuccinimidate, should lead to their implementation in other catalytic systems involving transition metal (*pseudo*)halide catalysts, especially where reduced electron density on the metal will increase activity.

The Au(I) and Au(III) imidate complexes should also be tested for biological activity, as gold complexes have shown activity against cancer,[82] HIV[79] and bacteria,[80] as well as being used to treat rheumatoid arthritis.[81]

2.5. Experimental

2.5.1. General Details

All reactions involving silver salts were carried out in the absence of light. Dichloromethane, acetonitrile and diethyl ether were dried by passing through a column of activated alumina, tetrahydrofuran was distilled from sodium benzophenone ketyl, ethanol was distilled from sodium ethoxide, acetone was distilled from calcium chloride and dimethyl sulphoxide was distilled from calcium hydride. Infra-red spectra were recorded on a Unicam Research Series FT-IR spectrometer. Mass spectrometry was carried out using a Bruker Daltronics micrOTOF instrument. ^{1}H, ^{13}C and ^{19}F NMR spectra were collected on a JEOL ECX400 spectrometer operating at 400, 101 and 376 MHz, respectively, and referenced to residual solvent signals. ^{13}C NMR signals are singlets unless otherwise stated. ^{15}N NMR spectra were collected on a Bruker AMX500 spectrometer operating at 50 MHz. All column chromatography was performed using silica-gel (mesh 220-440) purchased from Fluka Chemicals with the solvent systems specified within the text. TLC analysis was performed using Merck 5554 aluminium backed silica plates, compounds were visualised using UV light (254 nm) and a basic aqueous solution of potassium permanganate. Melting points were measured in open capillary tubes using a Stuart SMP3 Digital Melting Point Apparatus and are uncorrected. 1-Phenyl-2-propyn-1-ol, allyltrimethylsilane and silver(I)triflate were purchased from Alfa Aesar. Tetrafluorosuccinamide was purchased from Fluorochem. All other chemicals were purchased from Sigma Aldrich Inc. and used without further purification unless otherwise stated.

2.5.2. Gas chromatography

Gas chromatography was carried out on a Varian 430 instrument with a Factor Four Capillary column (VF-1ms, 15 m, 0.25 mm) and a flame ionisation detector. Samples of 10 □l were taken *via* syringe from the reaction mixtures at the specified time points. The samples were immediately quenched by addition of the aliquots to a solution of tetra-*n*-butylammonium chloride (8 mM, 20 □l) in CH_2Cl_2. Conversion was determined *via* gas chromatography using a 1 □l sample injected directly into the instrument *via* syringe. Further sampling was carried out on selected aliquots over a period of time to ensure no further conversion occurred after quenching. The instrument settings and retention times for specific species are specified within the text.

Values for the integrated areas of the GC signals corresponding to starting materials and products were inputted into Microsoft Excel spreadsheet software. This software was used to calculate percent conversions by comparison of starting material and product signal areas. The concentration of the species in solution was determined from the percent conversions and the initial starting material concentration. Selected aliquots were analysed by ^{1}H NMR spectroscopy to ensure consistency with conversions measured by GC. The reaction kinetics were calculated assuming a first order kinetic model by plotting ln[enyne] against time. Linear least-squares regression was used to calculate observed rate constants, initial rates and standard errors. The calculated concentrations of starting materials and products during the course of the reactions were also inputted into Dynafit software (published by Biokin).[109] Nonlinear least-squares regression was used to fit the experimental kinetic data to predetermined molecular mechanisms as described in the text. This was used to determine the order of reaction, observed rate constants, initial rates and standard errors and to fit curves to the kinetic data.

2.5.3. X-Ray crystallography

Diffraction data were collected at 110 K on a Bruker Smart Apex diffractometer with Mo-K_α radiation (λ = 0.71073 Å) using a SMART CCD camera. Diffractometer control, data collection and initial unit cell determination was performed using "SMART" (v5.625 Bruker-AXS). Frame integration and unit-cell refinement software was carried out with "SAINT+" (v6.22, Bruker AXS). Absorption corrections were applied by SADABS (v2.03, Sheldrick). Structures were solved by direct methods using SHELXS-97 (Sheldrick, 1990) and refined by full-matrix least squares using SHELXL-97 (Sheldrick, 1997). All non-hydrogen atoms were refined anisotropically. Hydrogen atoms were placed using a "riding model" and included in the refinement at calculated positions.

2.5.4. Compounds

I^{t}Bu.HCl (62)

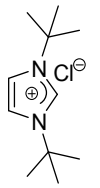

Prepared by a protocol reported by Herrmann *et al.*.[143] Paraformaldehyde (0.901 g, 30.0 mmol, 1 equiv.) was dissolved in toluene (30ml, dry) and ^{t}butyl amine (3.20 ml, 2.23 g, 30.0 mmol, 1 equiv.) was added dropwise. The suspension was stirred at 50 ˚C until a clear solution formed (20 min). It was cooled to 0 ˚C and ^{t}butyl amine (3.20 ml, 2.23 g, 30.0 mmol, 1 equiv.) was added dropwise. HCl (3 M aq., 10 ml, 30.0 mmol) was added dropwise to give a clear solution. Glyoxal (40% aq., 3.4 ml, 30.0 mmol) was added dropwise and the solution was stirred at 40 ˚C for 15 hours. The solution was diluted (50 ml saturated aq. $NaHCO_3$), washed with diethyl ether (3 x 6 ml) and reduced to dryness *in vacuo*. The crude solid was extracted with dichloromethane (3 x 15 ml) and reduced to dryness *in vacuo* to give a brown solid. This was purified by washing with a minimum amount of cold acetone (this differs from the literature preparation) to give the product as a white powder (2.68g, 12.4 mmol, 41%). ^{1}H NMR (400 MHz, $CDCl_3$) δ 10.26 (t, *J* = 1.7 Hz, 1H, N_2CH), 7.59 (d, *J* = 1.7 Hz, 2H, imidazole C*H*), 1.72 (s, 18H, ^{t}Bu CH_3). ^{13}C NMR (400 MHz, $CDCl_3$) δ 134.5 (N_2CH), 119.5 (imidazole *C*H), 60.5 (^{t}Bu quaternary *C*), 30.1 (^{t}Bu CH_3). IR (CH_2Cl_2, cm^{-1}) υ_{max} 3655 (w), 3316 (w), 3164 (m), 3070 (m), 3038 (m), 2955 (s), 2813 (w), 2548 (w), 2324 (w), 1624 (w), 1556 (m), 1537 (m), 1469 (m), 1407 (w), 1384 (m), 1281 (m), 1237 (w), 1201 (s), 1127 (m). ESI$^+$-MS *m/z* 181.2 (100%, $[M\text{-}Cl]^+$). ESI$^+$-HRMS calcd. for $C_{11}ClH_{22}N_2$ ($[MH]^+$) 181.1699; found 181.1697. Data in accordance with the literature.[143]

[AuCl(I^{t}Bu)] (55f)

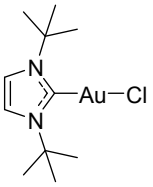

Prepared by a protocol reported by Baker *et al.*.[89] I^{t}Bu.HCl (**62**) (0.330 g, 1.53 mmol, 1.85 equiv.) and silver(I) oxide (0.208 g, 0.897 mmol, 1.1 equiv.) in dichloromethane (60 ml) were stirred at room temperature for 15 hours under a N_2 atmosphere. The solution was added *via* cannula filtration to [$AuCl(SMe_2)$] (0.414 g, 1.40 mmol, 1 equiv.) and stirred at

room temperature (18 hours). The solution was filtered through Celite™, concentrated to 2 ml and pentane (20 ml) added. The resulting white precipitate was separated by filtration, washed (pentane, diethyl ether) and dried *in vacuo* to yield the title compound as a white powder (0.598 g, 1.45 mmol, 95%). ^{1}H NMR (400 MHz, $CDCl_3$) δ 7.09 (s, 2H, imidazole C*H*), 1.86 (s, 18H, ^{t}Bu C*H*$_3$). ^{13}C NMR (100 MHz, $CDCl_3$) δ 167.7 (carbene Au-*C*), 116.4 (imidazole *C*H), 58.8 (^{t}Bu *C*$(CH_3)_3$), 31.7 (^{t}Bu C(*C*$H_3)_3$). IR (CH_2Cl_2, cm^{-1}) υ_{max} 3735 (w), 3172 (w), 3045 (w), 2975.19 (m), 2359 (w), 1670 (w), 1568 (w), 1541 (w), 1476 (w), 1407 (m), 1378 (m), 1369 (m), 1304 (w), 1233 (w), 1213 (m), 1189 (m), 1158 (w). ESI$^+$-MS *m/z* 418.2 (100%, $[MH]^+$), 349.1 (1%), 293.0 (3%). ESI$^+$-HRMS calcd. for $C_{13}H_{23}AuN_3$ ($[MH]^+$) 418.1552; found 418.1554. Data in accordance with the literature.[89]

[Au(*N*-succ)(I^{t}Bu)] (55a)

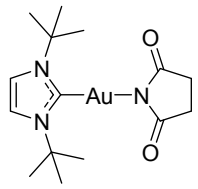

[AuCl(I^{t}Bu)] (**55f**) (121 mg, 294 μmol, 1 equiv.) and silver succinimidate (60.3 mg, 294 μmol, 1 equiv.) were dissolved in dichloromethane (10 ml) and stirred at room temperature for 1 hour. The suspension was filtered through Celite™ and the filtrate reduced to dryness *in vacuo*. The resulting white powder was precipitated from dichloromethane/pentane and washed with diethyl ether to give the title compound as a white powder (122 mg, 256 μmol, 87%). ^{1}H NMR (400 MHz, $CDCl_3$) δ 7.08 (s, 2H, imidazole C*H*), 2.64 (s, 4H, succ C*H*$_2$), 1.89 (s, 18H, ^{t}Bu C(C*H*$_3)_3$). ^{13}C NMR (400 MHz, $CDCl_3$) δ 188.8 (succ *C*=O), 170.8 (carbene Au-*C*), 116.4 (imidazole *C*H), 59.1 (^{t}Bu *C*$(CH_3)_3$), 31.8 (^{t}Bu C(*C*$H_3)_3$), 31.6 (succ *C*H$_2$). IR (CH_2Cl_2, cm^{-1}) υ_{max} 3684 (w), 3172 (w), 3045 (w), 2972 (m), 2932 (m), 1712 (w), 1645 (s), 1458 (w), 1434 (w), 1408 (w), 1380 (w), 1352 (m), 1285 (m), 1230 (m), 1158 (w). ESI$^+$-MS *m/z* 498.1 (9%, $[MNa]^+$), 476.2 (100%, $[MH]^+$), 420.1 (4%, $[M-^{t}Bu+2H]^+$), 405.1 (31%), 349.1 (8%), 293.0 (3%). ESI$^+$-HRMS calcd. for $C_{15}H_{25}AuN_3O_2$ ($[MH]^+$) 476.1607; found 476.1596. Melting point 230 °C decomposes.

Tetrafluorosuccinimide

Prepared using a protocol similar to that of Henne and Zimmer.[144] Tetrafluorosuccinamide (1.00 g, 5.31 mmol, 1 equiv.) was placed in a dry Schlenk tube under an atmosphere of N_2 and conc. sulphuric acid (0.29 ml, 5.44 mmol, 1.03 equiv.) was added *via* syringe. The mixture was stirred under a static vacuum (0.7 mm Hg, 10 mins), placed under an atmosphere of N_2 and a cold finger (-196 ˚C) added. The apparatus was placed under a static vacuum (0.7 mm Hg) and heated to 120 ˚C over 1 hour. The product was collected as a white solid on the cold finger and resublimed (taking care not to expose it to moisture) (0.7 mmHg, 60 ˚C) to give the title compound as a white crystalline powder (0.793 g, 4.64 mmol, 87%). ^{1}H NMR (400 MHz, $CDCl_3$) δ 9.12 (br s, N*H*). ^{1}H NMR {400 MHz, $(CD_3)_2CO$} δ 11.5 (br. s, N*H*). ^{19}F NMR (376 MHz, $CDCl_3$) δ -127.4 (s, C*F*$_2$). ^{19}F NMR {376 MHz, $(CD_3)_2CO$} δ -128.1 (s, C*F*$_2$). ^{13}C NMR (100 MHz, $CDCl_3$) δ 159.8 (t, *J* = 33 Hz, *C*=O), 105.8 (tt, *J* = 269 and 23 Hz, *C*F$_2$). ^{13}C NMR {100 MHz, $(CD_3)_2CO$} δ 162.2 (t, *J* = 32 Hz, *C*=O), 107.0 (tt, *J* = 267 and 22 Hz, *C*F$_2$). IR (solid, cm^{-1}) υ_{max} 3232 (m br), 3145 (m), 2161 (w), 2022(w), 1751 (s), 1685 (w), 1390 (m), 1334 (w), 1300 (s), 1173 (m), 1131 (s), 1060 (s) 984 (m), 774 (s), 695 (m). ESI$^-$-MS *m/z* 188.0, (10%, [M+OH]$^-$), 170.0 (100%, [M-H]$^-$). ESI$^-$-HRMS: calcd. for $C_4F_4NO_2$ ([M-H]$^-$) 169.9871; found 169.9888. Melting point 64-66 ˚C (Lit. 66-68 ˚C). Data in accordance with the literature.[144]

[Au(*N*-tfs)(I^{t}Bu)] (55b)

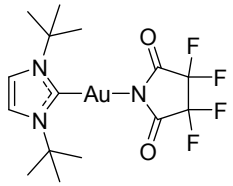

[AuCl(I^{t}Bu)] (**55f**) (70.9 mg, 172 μmol, 1 equiv.), silver(I) oxide (24.0 mg, 103 μmol, 0.6 equiv.) and tetrafluorosuccinimide (32.5 mg, 190 μmol, 1.1 equiv.) were mixed in dichloromethane (5 ml) under an atmosphere of N_2 and stirred at room temperature for 2 hours. The suspension was filtered through Celite™ and the filtrate reduced to dryness *in vacuo*. The resulting white powder was precipitated from dichloromethane/pentane, washed with diethyl ether and dried *in vacuo* to give the title compound as a white powder (85.6 mg, 157 μmol, 91%). ^{1}H NMR (400 MHz, $CDCl_3$) δ 7.15 (s, 2H, imidazole C*H*), 1.88

(s, 18H, ^{t}Bu C(CH_3)$_3$). ^{19}F NMR (376 MHz, $CDCl_3$) δ -127.5 (s, tfs CF_2). ^{13}C NMR (101 MHz, $CDCl_3$) δ 170.4 (m, tfs *C*=O),[145] 167.0 (carbene Au-*C*), 116.9 (imidazole *C*H), 107.4 (tt, *J* = 267, 22 Hz, tfs *C*F$_2$), 59.2 (^{t}Bu *C*(CH$_3$)$_3$), 31.8 (^{t}Bu C(*C*H$_3$)$_3$). IR (CH_2Cl_2, cm^{-1}) υ_{max} 3471 (w), 3196 (w), 3172 (w), 3061 (w), 2974 (m), 2360 (m), 2341 (m), 1704 (s), 1408 (m), 1400 (m), 1381 (m), 1371 (m), 1305 (s), 1269 (s), 1192 (s), 1150 (s), 1067 (m), 1016 (m). ESI$^+$-MS *m/z* 611.1 (16%, [MNa+MeCN]$^+$), 570.1 (100%, [MNa]$^+$), 548.1 (1%), 445.1 (2%), 418.2 (13%). ESI$^+$-HRMS calcd. for ([MNa]$^+$) $C_{15}H_{20}AuF_4N_3NaO_2$ 570.1055; found 570.1047. Melting point 166-168 °C.

[Au(*N*-mal)(I^{t}Bu)] (55c)

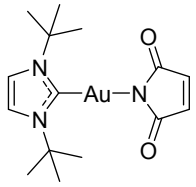

A protocol similar to that used for **55a** gave the title compound as a white solid {from 120 mg, 291 μmol, of [AuCl(I^{t}Bu)] (**55f**)} (128.7 mg, 272 μmol, 93%). ^{1}H NMR (400 MHz, $CDCl_3$) δ 7.09 (s, 2H, imidazole C*H*), 6.56 (s, 2H, mal C*H*), 1.88 (s, 18H, ^{t}Bu C(C*H*$_3$)$_3$). ^{13}C NMR (400 MHz, $CDCl_3$) δ 182.4 (mal *C*=O), 170.5 (carbene Au-*C*), 136.0 (mal *C*H), 116.3 (imidazole *C*H), 59.0 (^{t}Bu *C*(CH$_3$)$_3$), 31.8 (^{t}Bu C(*C*H$_3$)$_3$). IR (CH_2Cl_2, cm^{-1}) υ_{max} 3171 (w), 3053 (m), 2973 (m), 1662 (s), 1641 (m), 1608 (w), 1567 (w), 1475 (w), 1408 (m), 1380 (m), 1370 (m), 1347 (s), 1304 (w), 1281 (w), 1234 (w), 1213 (m), 1178 (m), 1158 (w). ESI$^+$-MS *m/z* 474.1 (100%, [MH]$^+$), 418.2 (8%), 181.2 (1%, [I^{t}BuH]$^+$). ESI$^+$-HRMS calcd. for $C_{15}H_{23}AuN_3O_2$ ([MH]$^+$) 474.1450; found 474.1439. Melting point 190 °C decomposes.

[Au(*N*-ptm)(I^{t}Bu)] (55d)

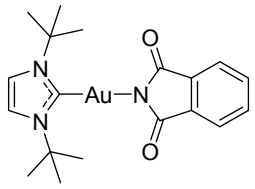

A protocol similar to that used for **55a** gave the title compound as a white solid {from 121.4 mg, 295 μmol of [AuCl(I^{t}Bu)] (**55f**)} (142 mg, 271 μmol, 92%). ^{1}H NMR (400 MHz, $CDCl_3$) δ 7.70 (dd, *J* = 5.4 Hz and 3.0 Hz, 2H, ptm aromatic C*H*), 7.55 (dd, *J* = 5.4 Hz and 3.0 Hz, 2H, ptm aromatic C*H*), 7.11 (s, 2H, imidazole C*H*), 1.92 {s, 18H, ^{t}Bu

C(C*H*$_3$)$_3$}. ^{13}C NMR (400 MHz, $CDCl_3$) δ 178.9 (ptm *C*=O), 170.9 (carbene Au-*C*), 136.4 (ptm *ortho* aromatic *C*), 132.1 (ptm *meta* aromatic *C*H), 121.6 (ptm *para* aromatic *C*H), 116.4 (imidazole *C*H), 59.1 {^{t}Bu *C*(CH$_3$)}, 31.8 {^{t}Bu C(*C*H$_3$)$_3$}. IR (CH_2Cl_2, cm^{-1}) υ_{max} 3677 (w), 3171 (w), 3058 (w), 2973 (m), 2364 (w), 1736 (m), 1667 (s), 1639 (s), 1606 (m), 1568 (w), 1540 (w), 1464 (m), 1422 (w), 1407 (m), 1374 (s), 1352 (m), 1309 (s), 1214 (m), 1190 (m), 1176 (m), 1158 (w), 1124 (m). ESI$^+$-MS *m/z* 524.2 (100%, [MH]$^+$), 418.2 (3%), 181.2 (61%, [I^{t}BuH]$^+$). ESI$^+$-HRMS calcd. for $C_{19}H_{25}AuN_3O_2$ ([MH]$^+$) 524.1607; found 524.1588. Melting point 160 °C decomposes.

[Au(*N*-obs)(I^{t}Bu)] (55e)

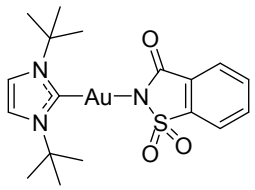

[AuCl(I^{t}Bu)] (**55f**) (70.9 mg, 172 μmol, 1 equiv.), silver(I) oxide (24.0 mg, 103 μmol, 0.6 equiv.), and *o*-benzoic sulfimide (34.7 mg, 190 μmol, 1.1 equiv.) were mixed in dichloromethane (5 ml) under an inert atmosphere and stirred at room temperature for 2 hours. The suspension was filtered through Celite™ and the filtrate reduced to dryness *in vacuo*. The resulting white powder was precipitated from dichloromethane/pentane, washed with diethyl ether and dried *in vacuo* to give the title compound as a white powder (85.0 mg, 152 μmol, 89%). ^{1}H NMR (400 MHz, $CDCl_3$) δ 7.94-7.90 (m, 1H, obs aromatic C*H*), 7.85-7.81 (m, 1H, obs aromatic C*H*), 7.72-7.64 (m, 2H, obs aromatic C*H*), 7.12 (s, 2H, imidazole C*H*), 1.91 (s, 18H, ^{t}Bu C(C*H*$_3$)$_3$). ^{13}C NMR (101 MHz, $CDCl_3$) δ 167.5 (carbene Au-*C*), 166.1 (obs *C*=O), 141.7 (obs aromatic *C*), 132.9 (obs aromatic *C*H), 132.8 (obs aromatic *C*H), 131.8 (obs aromatic *C*), 124.1 (obs aromatic *C*H), 120.3 (obs aromatic *C*H), 116.7 (imidazole *C*H), 59.1 {^{t}Bu *C*(CH$_3$)$_3$}, 31.8 {^{t}Bu C(*C*H$_3$)$_3$}. IR (CH_2Cl_2, cm^{-1}) υ_{max} 3364 (m), 3172 (w), 3061 (m), 2973 (m), 1742 (m), 1689 (s) 1559 (w), 1540 (w), 1521 (w), 1459 (m), 1400 (m), 1382 (m), 1371 (m), 1338 (m), 1303 (s), 1266 (s), 1249 (s), 1212 (m), 1173 (s), 1157 (s), 1122 (m), 1057 (w). ESI$^+$-MS *m/z* 714.5 (3%), 675.2 (3%), 582.1 (100%, [MNa]$^+$), 528.2 (2%), 435.1 (41%, [MNa-obs+Cl]$^+$), 394.2 (13%, [M-obs+NH$_3$]$^+$), 360.3 (2%), 274.3 (1%), 172.1 (7%). ESI$^+$-HRMS calcd. for $C_{18}H_{24}AuN_3NaO_3S$ ([MNa]$^+$) 582.1096; found 582.1083. Melting point 150 °C decomposes.

[AuBr(I^{t}Bu)] (55g)

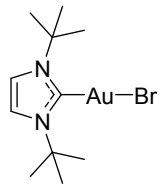

A protocol reported by de Frémont *et al.* was used.[86] [AuCl(I^{t}Bu)] (**55f**) (105 mg, 255 □mol, 1 equiv.) and LiBr (186 mg, 2.13 mmol, 8.4 equiv.) were mixed in acetone (4 ml) at room temperature for 24 hours. The resulting solution was reduced to dryness *in vacuo* and redissolved in dichloromethane, dried ($MgSO_4$) and filtered through a plug of silica-gel. The volume was reduced to <0.5 ml and pentane was added resulting in a white precipitate. This was separated by filtration, washed with cold pentane and dried *in vacuo* to give the title compound as a white powder (99.2 mg, 217 □mol, 85%). ^{1}H NMR (400 MHz, $CDCl_3$) δ 7.09 (s, 2H, imidazole C*H*), 1.87 (s, 18H, ^{t}Bu CH_3). ^{13}C NMR (100 MHz, $CDCl_3$) δ 172.5 (carbene Au-*C*), 116.3 (imidazole *C*H), 59.1 (^{t}Bu quaternary *C*), 31.8 (^{t}Bu CH_3). ESI$^+$-MS *m/z* 479.0 (2%, [MNa]$^+$), 405.1 (9%, [M-Br+CO]$^+$), 349.1 (21%, [M-Br-^{t}Bu+H+CO]$^+$), 293.0 (100%, [M-Br-2^{t}Bu+2H+CO]$^+$), 266.0 (3%). ESI$^+$-HRMS calcd. for $C_{11}H_{20}AuBrN_2Na$ ([MNa]$^+$) 479.0368; found 479.0359. Data in accordance with the literature.[86]

I^{t}Pe.HCl (61)

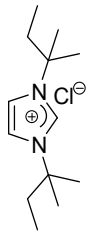

A protocol similar to that reported by Jafarpour *et al.*. was used.[92] *tert*-Pentylamine (5.18 g, 59.4 mmol, 2 equiv.) and glyoxal (3.35 ml, 29.8 mmol, 1 equiv., 40% in water) were dissolved in ethanol (50 ml). Formic acid (4 drops) was added and the solution was stirred at room temperature for 2 days. The resulting yellow solution was reduced *in vacuo* to give a yellow oil and redissolved in toluene (60 ml). Paraformaldehyde (0.612 g, 20.4 μmol, 0.7 equiv.) was added and the suspension stirred at 100 °C until a clear solution formed. HCl (5.10 ml, 20.4 μmol, 0.7 equiv., 4 M in dioxane) was added at 40 °C and the solution was then stirred at 70 °C overnight. The resulting white precipitate was separated by filtration and washed with acetone to give the title product as a white powder (2.50 g, 10.2 mmol, 34%). ^{1}H NMR (400 MHz, $CDCl_3$) δ 10.45 (t, *J* = 2 Hz, 1H, N_2C*H*), 7.48 (d, *J* = 2 Hz, 2H,

imidazole C*H*), 2.04 (q, *J* = 7.5 Hz, 4H, ^{t}Pe C*H*$_2$CH$_3$), 1.75 (s, 12H, ^{t}Pe C(C*H*$_3$)$_2$), 0.75 (t, *J* = 7.5 Hz, 6H, ^{t}Pe CH$_2$C*H*$_3$). ^{13}C NMR (101 MHz, CDCl$_3$) δ 135.3 (N$_2$*C*H), 119.7 (imidazole *C*H), 63.5 (^{t}Pe quaternary *C*), 35.3 (^{t}Pe *C*H$_2$CH$_3$), 27.4 {C(*C*H$_3$)$_2$}, 8.1 (^{t}Pe CH$_2$*C*H$_3$). IR (CH$_2$Cl$_2$, cm^{-1}) υ_{max} 3657 (w), 3338 (w), 3165 (w), 3041 (w), 2972 (s), 2358 (w), 1534 (w), 1463 (m), 1386 (m), 1274 (m), 1184 (m), 1126 (m). ESI$^+$-MS *m/z* 209.2 (100%, [MH]$^+$), 139.1 (4%). ESI$^+$-HRMS calcd. for C$_{13}$H$_{26}$ClN$_2$ ([MH]$^+$) 209.2012; found 209.2014. Melting point 228-230 °C.

[AuCl(I^{t}Pe)] (56f)

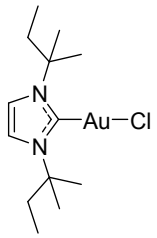

A protocol similar to that used for [AuCl(I^{t}Bu)] (**55f**) gave the title compound as a white solid (from 390 mg, 1.60 mmol of I^{t}Pe.HCl) (0.642 g, 1.46 mmol, 99%). ^{1}H NMR (400 MHz, CDCl$_3$) δ 7.04 (s, 2H, imidazole C*H*), 2.48 (q, *J* = 7.5 Hz, 4H, ^{t}Pe C*H*$_2$CH$_3$), 1.79 (s, 12H, ^{t}Pe C*H*$_3$), 0.64 (t, *J* = 7.5 Hz, 6H, ^{t}Pe CH$_2$C*H*$_3$). ^{13}C NMR (400 MHz, CDCl$_3$) δ 168.1 (carbene Au-*C*), 117.3 (imidazole *C*), 61.7 (^{t}Pe quaternary *C*), 36.3 (^{t}Pe *C*H$_2$CH$_3$), 29.3 (^{t}Pe CH$_2$*C*H$_3$), 7.8 {^{t}Pe C(*C*H$_3$)$_2$}. IR (CH$_2$Cl$_2$, cm^{-1}) υ_{max} 3680 (w), 3196 (w), 3172 (w), 3046 (m), 2972 (s), 2929 (m), 2880 (m), 2360 (w), 1604 (w), 1567 (w), 1460 (m), 1407 (m), 1393 (s), 1377 (s), 1339 (w), 1309 (m), 1228 (m), 1190 (s), 1152 (w). ESI$^+$-MS *m/z* 463.1 (100%, [MNa]$^+$), 226.9 (5%). ESI$^+$-HRMS calcd. for C$_{13}$H$_{24}$AuClN$_2$Na ([MNa]$^+$) 463.1186; found 463.1186. Melting point 157-158 °C.

[Au(*N*-succ)(I^{t}Pe)] (56a)

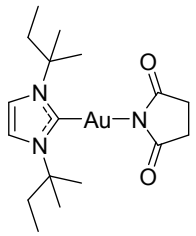

A protocol similar to that used for **55a** gave the title compound as a white solid {from 120 mg, 269 μmol, of [AuCl(I^{t}Pe)] (**56f**)} (126 mg, 251 μmol, 93%). ^{1}H NMR (400 MHz, CDCl$_3$) δ 7.05 (s, 2H, imidazole C*H*), 2.62 (s, 4H, succ C*H*$_2$), 2.48 (q, *J* = 7.5 Hz, 4H, ^{t}Pe C*H*$_2$), 1.82 {s, 12H, ^{t}Pe C(C*H*$_3$)$_2$}, 0.66 (t, *J* = 7.5 Hz, 6H, ^{t}Pe CH$_2$C*H*$_3$). ^{13}C NMR (400

MHz, $CDCl_3$) δ 188.7 (succ *C*=O), 170.8 (carbene Au-*C*), 117.3 (imidazole *C*H), 61.9 (^{t}Pe quaternary *C*), 36.3 (^{t}Pe *C*$H_2$$CH_3$), 31.6 (succ *C*$H_2$), 29.3 {^{t}Pe C(*C*$H_3$)$_2$}, 7.9 (^{t}Pe CH_2*C*H_3). IR (solid, cm^{-1}) υ_{max} 2963 (w), 2160 (m), 2028 (m), 1631 (s), 1561 (w), 1460 (w), 1395 (w), 1378 (w), 1353 (s), 1284 (w), 1260 (w), 1227 (s), 1140 (w), 1009 (m), 817 (m), 739 (m), 703 (m), 656 (m), 621 (m). IR (CH_2Cl_2, cm^{-1}) υ_{max} 3670 (w), 3172 (w), 3052 (m), 2970 (m), 2936 (m), 2880 (m), 2360 (w), 1644 (s), 1461 (m), 1435 (w), 1407 (m), 1393 (m), 1379 (m), 1352 (s), 1310 (w), 1285 (m), 1230 (s), 1191 (m). ESI$^+$-MS *m/z* 504.2 (100%, $[MH]^+$), 433.2 (21%), 363.1 (6%), 292.0 (4%), 209.2 (4%). ESI$^+$-HRMS calcd. for $C_{17}H_{29}AuN_3O_2$ ($[MH]^+$) 504.1920; found 504.1916. Melting point 140-142 °C.

[Au(*N*-tfs)(I^{t}Pe)] (56b)

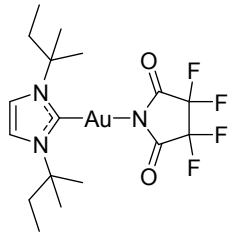

A protocol similar to that used for **55b** gave the title compound as a white solid {from 100 mg, 228 μmol, of [AuCl(I^{t}Pe)] (**56f**)} (122 mg, 212 μmol, 93%). ^{1}H NMR (400 MHz, $CDCl_3$) δ 7.11 (s, 2H, imidazole C*H*), 2.48 (q, *J* = 7.5 Hz, 4H, ^{t}Pe C*H*$_2$$CH_3$), 1.83 {s, 12H, ^{t}Pe C(*C*H_3)$_2$}, 0.69 (t, *J* = 7.5 Hz, 6H, ^{t}Pe CH_2C*H*$_3$). ^{19}F NMR (376 MHz, $CDCl_3$) δ -127.5 (s, C*F*$_2$). ^{13}C NMR (101 MHz, $CDCl_3$) δ 170.4 (m, *C*=O),[145] 167.5 (carbene Au-*C*), 117.8 (imidazole *C*H), 107.4 (tt, *J* = 267 and 22 Hz, tfs *C*F_2), 62.1 (^{t}Pe quaternary *C*), 36.6 (^{t}Pe *C*$H_2$$CH_3$), 29.4 {^{t}Pe C(*C*$H_3$)$_2$}, 7.9 (^{t}Pe CH_2*C*H_3). IR (CH_2Cl_2, cm^{-1}) υ_{max} 3173 (w), 2971 (s), 2930 (m), 2880 (m), 1784 (w), 1704 (s), 1559 (w), 1540 (w), 1461 (m), 1394 (m), 1380 (m), 1305 (s), 1271 (s), 1260 (s), 1193 (s), 1150 (s), 1067 (s), 1016 (s). ESI$^+$-MS *m/z* 598.1 (95%, $[MNa]^+$), 463.1 (23%), 422.2 (100%), 239.2 (6%). ESI$^+$-HRMS calcd. for $C_{17}H_{24}AuF_4N_3NaO_2$ ($[MNa]^+$) 598.1362; found 598.1380. Melting point 145-147 °C.

[Au(*N*-mal)(I^{t}Pe)] (56c)

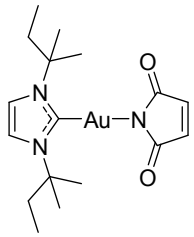

A protocol similar to that used for **55a** gave the title compound as a white solid {from 117 mg, 267 μmol, of [AuCl(I^{t}Pe)] (**56f**)} (128 mg, 256 μmol, 96%). ^{1}H NMR (400 MHz, $CDCl_3$) δ 7.05 (s, 2H, imidazole C*H*), 6.54 (s, 2H, mal C*H*), 2.50 (q, *J* = 7.5 Hz, 4H, ^{t}Pe C*H*$_2$CH$_3$), 1.82 {s, 12H, ^{t}Pe C(C*H*$_3$)$_2$}, 0.67 (t, *J* = 7.5 Hz, 6H, ^{t}Pe CH$_2$C*H*$_3$). ^{13}C NMR (400 MHz, $CDCl_3$) δ 182.3 (mal *C*=O), 170.7 (carbene Au-*C*), 135.9 (mal *C*H), 117.3 (imidazole *C*H), 61.8 (^{t}Pe quaternary *C*), 36.3 (^{t}Pe *C*H$_2$CH$_3$), 29.3 (^{t}Pe C(*C*H$_3$)$_2$), 7.9 (^{t}Pe CH$_2$*C*H$_3$). IR (CH_2Cl_2, cm^{-1}) υ_{max} 3680 (w), 3195 (w), 3172 (w), 3062 (w), 2971 (s), 2933 (m), 2880 (w), 1660 (s), 1608 (w), 1567 (w), 1460 (m), 1407 (w), 1393 (m), 1380 (m), 1347 (s), 1310 (w), 1228 (m), 1179 (m). ESI$^+$-MS *m/z* 524.2 (3%, [MNa]$^+$), 502.2 (100%, [MH]$^+$), 433.2 (46%), 363.1 (16%), 293.0 (8%), 272.8 (2%). ESI$^+$-HRMS calcd. for $C_{17}H_{27}AuN_3O_2$ ([MH]$^+$) 502.1763; found 502.1760. Melting point 135-137 ˚C.

[Au(*N*-ptm)(I^{t}Pe)] (56d)

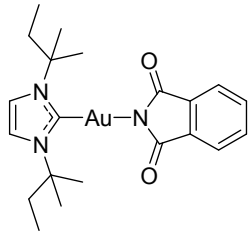

A protocol similar to that used for **55a** gave the title compound as a white solid {from 127 mg, 288 μmol, of [AuCl(I^{t}Pe)] (**56f**)} (152 mg, 277 μmol, 96%). ^{1}H NMR (400 MHz, $CDCl_3$) δ 7.69 (dd, *J* = 5.4 and 3.0 Hz, 2H, ptm aromatic C*H*), 7.54 (dd, *J* = 5.4 and 3.0 Hz, 2H, ptm aromatic C*H*), 7.06 (s, 2H, imidazole C*H*), 2.56 (q, *J* = 7.4 Hz, 4H, ^{t}Pe C*H*$_2$CH$_3$), 1.85 (s, 12H, ^{t}Pe C(C*H*$_3$)$_2$), 0.68 (t, *J* = 7.4 Hz, 6H, ^{t}Pe CH$_2$C*H*$_3$). ^{13}C NMR (400 MHz, $CDCl_3$) δ 178.8 (ptm *C*=O), 171.0 (carbene *C*), 136.4 (ptm *ortho* aromatic *C*), 132.1 (ptm *meta* aromatic *C*H), 121.5 (ptm *para* aromatic *C*H), 117.3 (imidazole *C*H), 61.9 (^{t}Pe quaternary *C*), 36.3 (^{t}Pe *C*H$_2$CH$_3$), 29.3 (^{t}Pe C(*C*H$_3$)$_2$), 7.9 (^{t}Pe CH$_2$*C*H$_3$). IR (CH_2Cl_2, cm^{-1}) υ_{max} 3674 (w), 3172 (w), 3056 (m), 2970 (m), 2933 (w), 2879 (w), 2360 (w), 1736 (w), 1667 (s), 1638 (m), 1606 (m), 1539 (w), 1462 (m), 1393 (m), 1373 (s), 1352 (m), 1309 (s), 1227 (w), 1191 (m), 1176 (m). ESI$^+$-MS *m/z* 552.2 (100%, [MH]$^+$), 482.1 (6%), 433.2

(5%), 363.1 (2%), 272.8 (5%). ESI$^+$-HRMS calcd. for $C_{21}H_{29}AuN_3O_2$ ([MH]$^+$) 552.1920; found 552.1927. Melting point 140 ˚C decomposes.

[Au(*N*-obs)(I^{t}Pe)] (56e)

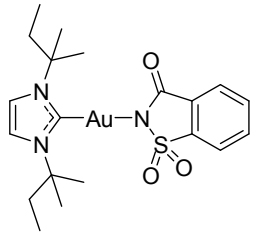

A protocol similar to that used for **55e** gave the title compound as a white solid {from 90.3 mg, 205 μmol, of [AuCl(I^{t}Pe)] (**56f**)} (113 mg, 193 μmol, 94%). ^{1}H NMR (400 MHz, $CDCl_3$) 7.92-7.88 (m, 1H, obs aromatic C*H*), 7.83-7.80 (m, 1H, obs aromatic C*H*), 7.73-7.64 (m, 2H, obs aromatic C*H*), 7.10 (s, 2H, imidazole C*H*), 2.52 (q, *J* = 7.4 Hz, 4H, ^{t}Pe C*H*$_2$CH$_3$), 1.85 (s, 12H, C*H*$_3$), 0.70 (t, *J* = 7.4 Hz, 6H, ^{t}Pe CH$_2$C*H*$_3$). ^{13}C NMR (101 MHz, $CDCl_3$) δ 167.9 (carbene Au-*C*), 166.0 (obs *C*=O), 141.8 (obs aromatic *C*), 132.9 (obs aromatic *C*H), 132.8 (obs aromatic *C*H), 131.8 (obs aromatic *C*), 124.0 (obs aromatic *C*H), 120.3 (obs aromatic *C*H), 117.6 (imidazole *C*H), 62.0 (^{t}Pe quaternary *C*), 36.4 (^{t}Pe *C*H$_2$CH$_3$), 29.4 {^{t}Pe (C(*C*H$_3$)$_2$}, 7.9 (^{t}Pe CH$_2$*C*H$_3$). IR (CH_2Cl_2, cm^{-1}) υ_{max} 3362 (w), 3172 (w), 3061 (m), 2971 (s), 2931 (m), 2880 (w), 1741 (m), 1689 (s), 1596 (m), 1461 (m), 1380 (m), 1303 (s), 1260 (s), 1249 (s), 1173 (s), 1157 (s), 1123 (m), 1057 (m). ESI$^+$-MS *m/z* 678.1 (4%), 610.1 (90%, [MNa]$^+$), 556.2 (3%), 504.1 (11%), 463.1 (100%, [MNa-obs+Cl]$^+$), 422.2 (3%), 157.1 (5%). ESI$^+$-HRMS calcd. for $C_{20}H_{28}AuN_3NaO_3S$ ([MNa]$^+$) 610.1409; found 610.1408. Melting point 150 ˚C decomposes.

[AuBr(I^{t}Pe)] (56g)

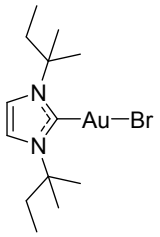

A protocol similar to that used for [AuBr(I^{t}Bu)] (**55g**) gave the title compound as a white solid {from 83.6 mg, 190 μmol of [AuCl(I^{t}Pe)] (**56f**)} (87.9 mg, 180 μmol, 95%). ^{1}H NMR (400 MHz, $CDCl_3$) δ 7.05 (s, 2H, imidazole C*H*), 2.48 (q, *J* = 7.5 Hz, 4H, ^{t}Pe C*H*$_2$CH$_3$), 1.81 {s, 12H, ^{t}Pe C(C*H*$_3$)$_2$}, 0.65 (t, *J* = 7.5 Hz, 6H, ^{t}Pe CH$_2$C*H*$_3$). ^{13}C NMR (400 MHz, $CDCl_3$) δ 172.3 (carbene Au-*C*), 117.2 (imidazole *C*H), 61.8 (^{t}Pe quaternary *C*), 36.3 (^{t}Pe

*C*H$_2$CH$_3$), 29.3 {^{t}Pe C(*C*H$_3$)$_2$}, 7.9 (^{t}Pe CH$_2$*C*H$_3$). IR (CH$_2$Cl$_2$, cm^{-1}) υ_{max} 3196 (w), 3172 (w), 3047 (m), 2972 (s), 2930 (m), 2880 (w), 1704 (w), 1566 (w), 1558 (w), 1461 (m), 1406 (w), 1266 (m), 1260 (m), 1229 (m), 1271 (s), 1227 (m), 1191 (s), 1064 (w), 1037 (w), 1005 (w). ESI$^+$-MS *m/z* 507.1 (6%, [MNa]$^+$), 433.2 (15%), 413.3 (2%), 363.1 (19%), 293.0 (100%), 266.0 (2%). ESI$^+$-HRMS calcd. for C$_{13}$H$_{24}$AuBrN$_2$Na ([MNa]$^+$) 507.0681; found. 507.0675. Melting point 149-151 ˚C.

[{Au(*N*-mal)(I^{t}Pe)}$_2$] (56h)

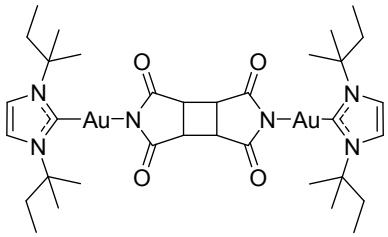

Not isolated {[Au(*N*-mal)(I^{t}Pe)] (**56c**):[{Au(*N*-mal)(I^{t}Pe)}$_2$] (**56h**) 76:24}. ^{1}H NMR (400 MHz, CDCl$_3$) selected peaks δ 7.05 (s, 2H, imidazole C*H*), 3.33 (s, 2H, imidate CH), 2.50 (q, *J* = 7.5 Hz, 4H, ^{t}Pe C*H*$_2$CH$_3$), 1.82 (s, 12H, ^{t}Pe C(C*H*$_3$)$_2$), 0.67 (t, *J* = 7.5 Hz, 6H, ^{t}Pe CH$_2$C*H*$_3$). ESI$^+$-MS *m/z* 1025.3 (100%, [MNa]$^+$), 1003.3 (84%, [MH]$^+$), 906.3 (99%, [(ItPe)$_2$Au$_2$(mal)]$^+$). ESI$^+$-HRMS calcd. for C$_{34}$H$_{52}$Au$_2$N$_6$NaO$_4$ ([MNa]$^+$) 1025.3273; found 1025.3279.

[AuCl(IMes)] (57f)

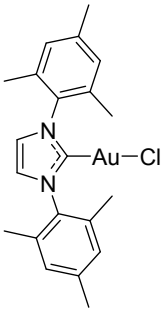

A protocol similar to that used for [AuCl(I^{t}Bu)] (**55f**) gave the title compound as a white powder (from 0.604 g, 1.78 mmol of IMes.HCl) (0.572 g, 1.07 mmol, 98%). ^{1}H NMR (400 MHz, CDCl$_3$) δ 7.09 (s, 2H, imidazole C*H*), 6.99 (s, 4H, Mes aromatic C*H*), 2.34 (s, 6H, Mes *para* C*H*$_3$), 2.10 (s, 12H, Mes *ortho* C*H*$_3$). ^{13}C NMR (100 MHz, CDCl$_3$) δ 173.4 (carbene Au-*C*), 139.8 (Mes aromatic *C*), 134.7 (Mes aromatic *C*), 129.5 (Mes aromatic *C*), 122.2 (imidazole *C*H), 21.2 (Mes *para* *C*H$_3$), 17.8 (Mes *ortho* *C*H$_3$). ESI$^+$-MS *m/z* 559.1 (27%, [MNa]$^+$), 542.2 (100%, [M-Cl+MeCN]$^+$), 529.2 (8%), 518.2 (4%). ESI$^+$-HRMS

calcd. for $C_{21}H_{24}AuClN_2Na$ 559.1186; found 559.1186. Data in accordance with the literature.[86]

[Au(*N*-succ)(IMes)] (57a)

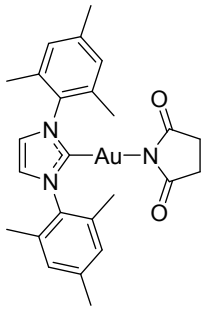

A protocol similar to that used for **55a** gave the title compound as a white solid {from 38.2 mg, 71.3 μmol, of [AuCl(IMes)] (**57f**)} (41.6 mg, 69.4 μmol, 97%). ^{1}H NMR (400 MHz, $CDCl_3$) δ 7.10 (s, 2H, imidazole C*H*), 7.01 (s, 4H, Mes aromatic C*H*), 2.40 (s, 4H, succ CH_2), 2.34 (s, 6H, Mes *para* CH_3), 2.16 (s, 12H, Mes *ortho* CH_3). ^{13}C NMR (101 MHz, $CDCl_3$) δ 188.5 (succ *C*=O), 174.9 (carbene Au-C), 139.4 (Mes aromatic *C*), 134.7 (Mes aromatic *C*), 134.6 (Mes aromatic *C*), 129.4 (Mes aromatic *C*), 122.3 (imidazole *C*H), 31.4 (succ *C*H$_2$), 21.1 (Mes *para* *C*H$_3$), 17.9 (Mes *ortho* *C*H$_3$). IR (CH_2Cl_2, cm^{-1}) υ_{max} 3670 (w), 3141 (m), 3052 (m), 2981 (m), 2359 (w), 1648 (s), 1540 (w), 1488 (m), 1435 (w), 1415 (w), 1351 (m), 1285 (m), 1230 (m). ESI$^+$-MS *m/z* 622.2 (15%, [MNa]$^+$), 600.2 (100%, [MH]$^+$), 528.2 (49%). ESI$^+$-HRMS calcd. for $C_{25}H_{29}AuN_3O_2$ ([MH]$^+$) 600.1925; found 600.1924. Melting point 170 ˚C decomposes.

[Au(*N*-tfs)(IMes)] (57b)

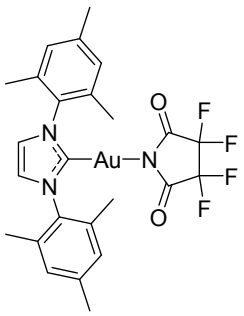

A protocol similar to that used for **55b** gave the title compound as a white solid {from 101 mg, 188 μmol, of [AuCl(IMes)] (**57f**)} (109 mg, 163 μmol, 87%). ^{1}H NMR (400 MHz, $CDCl_3$) δ 7.17 (s, 2H, imidazole C*H*), 7.04 (s, 4H, Mes aromatic C*H*), 2.36 (s, 6H, Mes *para* CH_3), 2.16 (s, 12H, Mes *ortho* CH_3). ^{19}F NMR (376 MHz, $CDCl_3$) δ -127.6 (s, tfs CF_2). ^{13}C NMR (101 MHz, $CDCl_3$) δ 171.9 (carbene Au-*C*), 170.0 (m, tfs *C*=O),[145] 140.0

(Mes aromatic *C*), 134.6 (Mes aromatic *C*), 134.2 (Mes aromatic *C*), 129.6 (Mes aromatic *C*H), 122.8 (imidazole *C*H), 107.1 (tt, *J* = 267 and 22 Hz, tfs *C*F_2), 21.1 (Mes *para* *C*H_3), 17.8 (Mes *ortho* *C*H_3). IR (CH_2Cl_2, cm^{-1}) υ_{max} 3167 (w), 3141 (w), 3055 (m), 2923 (w), 1784 (w), 1772 (w), 1705 (s), 1670 (w), 1609 (w), 1559 (w), 1540 (w), 1487 (m), 1420 (m), 1381 (w), 1324 (w), 1305 (m), 1235 (w), 1192 (s), 1150 (m), 1067 (m), 1016 (m). ESI^+-MS *m/z* 694.1 (100%, $[MNa]^+$), 542.2 (55%, $[M\text{-tfs+MeCN}]^+$), 413.3 (3%), 358.1 (5%), 336.1 (5%). ESI^+-HRMS calcd. for $C_{25}H_{24}AuF_4N_3NaO_2$ ($[MNa]^+$) 694.1362; found 694.1355. Melting point 200 ˚C decomposes.

[Au(*N*-mal)(IMes)] (57c)

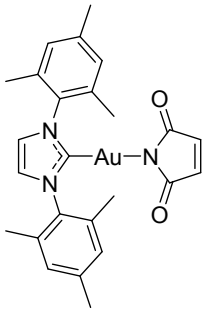

A protocol similar to that used for **55a** gave the title compound as a white solid {from 151 mg, 282 μmol, of [AuCl(IMes)] (**57f**)} (157 mg, 263 μmol, 93%). ^1H NMR (400 MHz, $CDCl_3$) δ 7.10 (s, 2H, imidazole C*H*), 7.00 (s, 4H, Mes aromatic C*H*), 6.31 (s, 2H, mal C*H*), 2.33 (s, 6H, Mes *para* CH_3), 2.16 (s, 12H, Mes *ortho* CH_3). ^{13}C NMR (101 MHz, CDCl3) δ 182.1 (mal *C*=O), 175.1 (carbene Au-*C*), 139.5 (Mes aromatic *C*), 135.7 (mal *C*H), 134.7 (Mes aromatic *C*), 134.6 (Mes aromatic *C*), 129.4 (Mes aromatic *C*), 122.3 (imidazole *C*H), 21.1 (Mes *para* *C*H_3), 18.0 (Mes *ortho* *C*H_3). IR (CH_2Cl_2, cm^{-1}) υ_{max} 3677 (w), 3167 (w), 3141 (w), 3063 (w), 2922 (m), 1730 (m), 1662 (s), 1640 (m), 1608 (m), 1488 (m), 1415 (m), 1380 (m), 1345 (s), 1235 (m), 1177 (m). ESI^+-MS *m/z* 598.2 (11%, $[MH]^+$), 528.2 (92%), 305.2 (100%, $[IMesH]^+$). ESI^+-HRMS calcd. for $C_{25}H_{27}AuN_3O_2$ ($[MH]^+$) 598.1763; found 598.1737. Melting point 200 ˚C decomposes.

[Au(*N*-ptm)(IMes)] (57d)

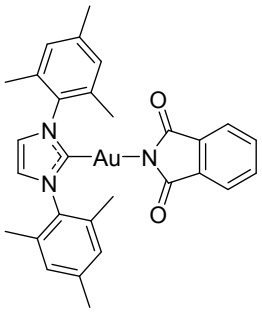

A protocol similar to that used for **55a** gave the title compound as a white solid {from 71.1 mg, 132 μmol of [AuCl(IMes)] (**57f**)} (80.3 mg, 124 μmol, 94%). ^{1}H NMR (400 MHz, $CDCl_3$) δ 7.54 (dd, *J* = 5.4 and 3.0, 2H, ptm aromatic C*H*), 7.44 (dd, *J* = 5.4 and 3.0 Hz, 2H, ptm aromatic C*H*), 7.12 (s, 2H, imidazole C*H*), 7.02 (s, 4H, Mes aromatic C*H*), 2.33 (s, 6H, Mes *para* CH_3), 2.20 (s, 12H, Mes *ortho* CH_3). ^{13}C NMR (101 MHz, $CDCl_3$) δ 178.6 (ptm *C*=O), 175.2 (carbene Au-*C*), 139.5 (Mes aromatic *C*), 136.2 (ptm aromatic *C*), 134.7 (Mes aromatic *C*), 134.6 (Mes aromatic *C*), 131.8 (ptm aromatic *C*H), 129.4 (Mes aromatic *C*H), 122.3 (imidazole *C*H), 121.3 (ptm aromatic *C*H), 21.1 (Mes *para* *C*H_3), 18.0 (Mes *ortho* *C*H_3). IR (CH_2Cl_2, cm^{-1}) υ_{max} 3674 (w), 3458 (w), 3140 (w), 3063 (w), 3045 (m), 2983 (m), 2921 (m), 2324 (w), 1737 (m), 1667 (s), 1639 (m), 1607 (m), 1540 (w), 1488 (m), 1414 (m), 1372 (m), 1351 (m), 1308 (m), 1236 (m), 1176 (m), 1124 (m). ESI$^+$-MS *m/z* 648.2 (2%, $[MH]^+$), 528.2 (50%), 305.2 (100%, $[IMesH]^+$), 267.2 (4%), 136.1 (3%). ESI$^+$-HRMS calcd. for $C_{29}H_{29}AuN_3O_2$ ($[MH]^+$) 648.1920; found 648.1908. Melting point 150 ˚C decomposes.

[Au(*N*-obs)(IMes)] (57e)

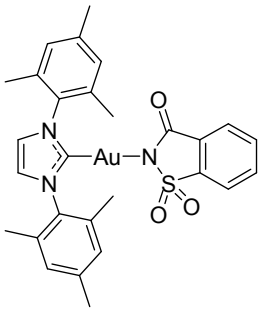

A protocol similar to that used for **55e** gave the title compound as a white solid {from 99.9 mg, 186 μmol, of [AuCl(IMes)] (**57f**)} (115 mg, 168 μmol, 90%). ^{1}H NMR (400 MHz, $CDCl_3$) δ 7.78-7.76 (m, 1H, obs aromatic C*H*), 7.72-7.70 (m, 1H, obs aromatic C*H*), 7.62-7.55 (m, 2H, obs aromatic C*H*), 7.16 (s, 2H, imidazole C*H*), 7.04 (s, 4H, Mes

aromatic C*H*), 2.35 (s, 6H, Mes *para* C*H*$_3$), 2.19 (s, 12H, Mes *ortho* C*H*$_3$). ^{13}C NMR (101 MHz, $CDCl_3$) δ 172.9 (carbene Au-*C*), 165.8 (obs *C*=O), 141.6 (obs aromatic *C*), 139.8 (Mes aromatic *C*), 134.6 (Mes aromatic *C*), 134.4 (Mes aromatic *C*), 132.7 (obs aromatic *C*H), 132.6 (obs aromatic *C*H), 131.7 (obs aromatic *C*), 129.5 (Mes aromatic *C*H), 123.9 (obs aromatic *C*H), 122.5 (imidazole *C*H), 120.1 (obs aromatic *C*H), 21.2 (Mes *para* *C*H$_3$), 17.9 (Mes *ortho* *C*H$_3$). IR (CH_2Cl_2, cm^{-1}) υ_{max} 3167 (w), 3141 (w), 3054 (m), 2982 (w), 2952 (w), 2922 (m), 2861 (w), 1689 (s), 1608 (w), 1599 (w), 1559 (w), 1540 (w), 1487 (m), 1459 (w), 1419 (m), 1380 (m), 1337 (w), 1303 (s), 1248 (m), 1173 (s), 1157 (s), 1123 (w). ESI$^+$-MS *m/z* 706.1 (13%, [MNa]$^+$), 542.2 (100%, [M-obs+MeCN]$^+$), 413.3 (2%), 235.1 (2%). ESI$^+$-HRMS calcd. for $C_{28}H_{28}AuN_3NaO_3S$ ([MNa]$^+$) 706.1409; found 706.1415. Melting point 160 ˚C decomposes.

[AuBr(IMes)] (57g)

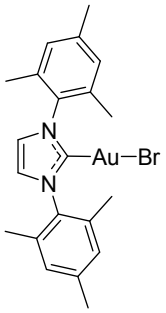

A protocol similar to that used for [AuBr(I^{t}Bu)] (**55g**) gave the title compound as a white solid {from 101 mg, 188 μmol of [AuCl(IMes)] (**57f**)} (94.0 mg, 162 □mol, 86%). ^{1}H NMR (400 MHz, $CDCl_3$) δ 7.09 (s, 2H, imidazole C*H*), 6.99 (s, 4H, aromatic C*H*), 2.34 (s, 6H, Mes *para* C*H*$_3$), 2.11 (s, 12H, Mes *ortho* C*H*$_3$). ^{13}C NMR (100 MHz, $CDCl_3$) δ 176.9 (carbene Au-C), 139.7 (Mes aromatic *C*), 134.6 (Mes aromatic *C*), 134.6 (Mes aromatic *C*), 129.5 (Mes aromatic *C*), 122.1 (imidazole *C*H), 21.1 (Mes *para* *C*H$_3$), 17.7 (Mes *ortho* *C*H$_3$). ESI$^+$-MS *m/z* 603.1 (9%, [MNa]$^+$), 542.2 (100%, [M-Br+MeCN]$^+$), 529.2 (6%, [M-Br+CO]$^+$). ESI$^+$-HRMS calcd. for $C_{21}H_{24}AuB[rN_2Na$ ([MNa]$^+$) 603.0681; found 603.0668. Data in accordance with the literature.[86]

[AuBr$_2$(*N*-succ)(I^{t}Bu)] (66a)

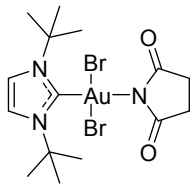

[Au(*N*-succ)(I^{t}Bu)] (**55a**) (28.5 mg, 59.9 μmol, 1 equiv.) was dissolved in dichloromethane (1 ml), bromine (10.5 mg, 65.9 μmol, 1.1 equiv.) was added and the brown solution stirred for 1 hour at room temperature. The solution was reduced *in vacuo* to <0.5 ml and pentane (5 ml) added producing a yellow precipitate. This was separated by filtration, washed (pentane/diethyl ether) and dried *in vacuo* to give the title compound as a yellow powder (32.2 mg, 50.6 μmol, 84%). ^{1}H NMR (400 MHz, $CDCl_3$) δ 7.41 (s, 2H, imidazole C*H*), 2.72 (s, 4H, succ CH_2), 1.96 {s, 18H, ^{t}Bu C(CH_3)$_3$}. ^{13}C NMR (400 MHz, $CDCl_3$) δ 183.8 (succ *C*=O), 131.9 (carbene Au-*C*), 122.1 (imidazole *C*H), 62.4 (^{t}Bu *C*(CH$_3$)$_3$), 32.1 (^{t}Bu C(*C*H$_3$)$_3$), 31.4 (succ *C*H$_2$). IR (CH_2Cl_2, cm^{-1}) υ_{max} 3168 (w), 3063 (w), 2988 (m), 2360 (w), 1663 (s), 1576.1 (m), 1480 (w), 1415 (w), 1375 (m), 1352 (m), 1284 (w), 1230 (m), 1196 (w), 1182 (m), 1156 (w). ESI$^+$-MS *m/z* 636.0 (81%, [MH]$^+$), 418.2 (66%), 259.1 (15%, [I^{t}BuBr]$^+$), 181.2 (100%, [I^{t}BuH]$^+$). ESI$^+$-HRMS calcd. for $C_{15}H_{23}AuBr_2N_3O_2$ ([MH]$^+$) 633.9949; found 633.9974. Melting point 160 ˚C decomposes.

[AuBr$_2$(*N*-dbs)(I^{t}Bu)] (66b)

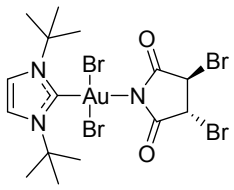

[Au(*N*-mal)(I^{t}Bu)] (**55c**) (30.1 mg, 63.6 μmol, 1 equiv.) was dissolved in dichloromethane (1 ml), bromine (20.4 mg, 128 μmol, 2 equiv.) was added and the yellow solution stirred for 1 hour at room temperature. The solution was reduced *in vacuo* to <0.5 ml and hexane (5 ml) added producing a yellow precipitate. This was separated by filtration, washed (pentane, diethyl ether) and dried *in vacuo* to give the title compound as a yellow powder (37.5 mg, 59.2 μmol, 93%). ^{1}H NMR (400 MHz, $CDCl_3$) δ 7.47 (s, 2H, imidazole C*H*), 4.82 (s, 2H, dbs C*H*), 1.99 {s, 18H, ^{t}Bu C(CH_3)$_3$}. ^{13}C NMR (400 MHz, $CDCl_3$) δ 175.7 (dbs *C*=O), 128.1 (carbene Au-*C*), 122.4 (imidazole *C*H), 62.6 (^{t}Bu *C*(CH$_3$)$_3$), 46.6 (dbs *C*H), 32.1 {^{t}Bu C(*C*H$_3$)$_3$}. IR (CH_2Cl_2, cm^{-1}) υ_{max} 3054 (m), 2986 (m), 2360 (m), 2341 (m), 1733 (m), 1690 (s), 1653 (m), 1636 (m), 1559 (m), 1540 (m), 1521

(m), 1507 (m), 1497 (m), 1473 (m), 1457 (m), 1437 (m), 1420 (m), 1376 (m), 1338 (m), 1271 (s), 1230 (m), 1179 (m). ESI$^+$-MS *m/z* 815.8 (100%, [MNa]$^+$), 733.9 (3%, [MNa–HBr]$^+$), 664.9 (4%), 596.9 (4%), 528.9 (4%). ESI$^+$-HRMS calcd. for $C_{15}H_{22}AuBr_4N_3NaO_2$ ([MNa]$^+$) 815.7963; found 815.7958. Melting point 160 ˚C decomposes.

[AuBr$_2$(*N*-tfs)(I^{t}Bu)] (66c)

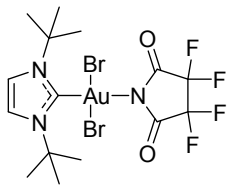

A protocol similar to that used for **66a** gave the title compound as a yellow powder {from 57.0 mg, 104 μmol, of [Au(*N*-tfs)(I^{t}Bu)] (**55b**)} (67.2 mg, 95.0 μmol, 91%). ^{1}H NMR (400 MHz, $CDCl_3$) δ 7.51 (s, 2H, imidazole C*H*), 1.98 {s, 18H, ^{t}Bu C(C*H*$_3$)$_3$}. ^{19}F NMR (376 MHz, $CDCl_3$) δ -127.1 (s, tfs C*F*$_2$). ^{13}C NMR (100 MHz, $CDCl_3$) δ 167.1 (m, tfs *C*=O),[145] 124.9 (carbene Au-*C*), 122.8 (imidazole *C*H), 106.8 (tt, *J* = 269 and 23 Hz, tfs *C*F$_2$), 62.8 {^{t}Bu *C*(CH$_3$)$_3$}, 32.0 {^{t}Bu C(*C*H$_3$)$_3$}. IR (CH_2Cl_2, cm^{-1}) υ_{max} 3491 (w), 3200 (w), 3168 (w), 3056 (w), 2987 (m), 1789 (w), 1718 (s), 1584 (w), 1479 (m), 1418 (m), 1386 (m), 1376 (m), 1322 (m), 1305 (s), 1197 (s), 1156 (s), 1065 (m), 1017 (m). ESI$^+$-MS *m/z* 797.9 (3%), 729.9 (100%, [MNa]$^+$), 498.9 (2%), 259.1 (6%, [I^{t}Bu+HBr]$^+$), 227.0 (3%), 191.1 (1%), 107.2 (2%). ESI$^+$-HRMS calcd. for $C_{15}H_{20}AuBr_2F_4N_3NaO_2$ ([MNa]$^+$) 729.9396; found 729.9390. Melting point 160˚C decomposes.

[AuBr$_2$(*N*-mal)(I^{t}Bu)] (66d)

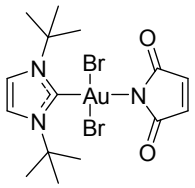

[Au(*N*-mal)(I^{t}Bu)] (**55c**) (51.2 mg, 108 μmol, 1 equiv.) was dissolved in dichloromethane (1 ml), bromine (17.3 mg, 108 μmol, 1 equiv.) was added and the brown solution stirred for 1 hour at -78˚C. The solution was reduced under vacuum to <0.5 ml and pentane (5 ml) added producing a yellow precipitate. This was separated by filtration, washed (pentane, diethyl ether) and dried *in vacuo* to give the title compound as a yellow powder (61.3 mg, 96.8 μmol, 90%). ^{1}H NMR (400 MHz, $CDCl_3$) δ 7.44 (s, 2H, imidazole C*H*), 6.64 (s, 2H, mal C*H*), 2.01 {s, 18H, ^{t}Bu C(C*H*$_3$)$_3$}. ^{13}C NMR (100 MHz, $CDCl_3$) δ 177.3 (mal *C*=O),

136.8 (mal *C*H), 131.2 (carbene Au-*C*), 122.2 (imidazole *C*H), 62.4 {^{t}Bu *C*(CH$_3$)$_3$}, 32.1 {^{t}Bu C(*C*H$_3$)$_3$}. IR (CH$_2$Cl$_2$, cm^{-1}) υ_{max} 3200 (w), 3169 (w), 3055 (m), 2985 (m), 1733 (m), 1676 (s), 1653 (w), 1589 (w), 1540 (w), 1506 (w), 1417 (m), 1376 (m), 1346 (s), 1321 (w), 1271 (s), 1233 (m), 1181 (s), 1155 (m), 1063 (w). ESI$^+$-MS *m/z* 656.0 (100%, [MNa]$^+$), 498.9 (4%, [MNa-2Br]$^+$), 430.9 (4%), 289.2 (10%). ESI$^+$-HRMS calcd. for C$_{15}$H$_{22}$AuBr$_2$N$_3$NaO$_2$ ([MNa]$^+$) 655.9617; found 655.9649. Melting point 190 ˚C decomposes.

[AuBr$_2$(*N*-ptm)(I^{t}Bu)] (66e)

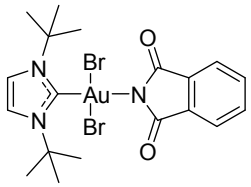

A protocol similar to that used for **55a** gave the title compound as a yellow powder {from 99.1 mg, 189 μmol, of [Au(*N*-ptm)(I^{t}Bu)] (**55d**)} (115 mg, 168 μmol, 89%). ^{1}H NMR (400 MHz, CDCl$_3$) δ 7.71 (dd, *J* = 5.4 and 3.0 Hz, 2H, ptm *meta* aromatic C*H*), 7.57 (dd, *J* = 5.4 and 3.0 Hz, 2H, ptm *para* aromatic C*H*), 7.45 (s, 2H, imidazole C*H*), 2.04 {s, 18H, ^{t}Bu C(C*H*$_3$)$_3$}. ^{13}C NMR (101 MHz, CDCl$_3$) δ 174.4 (ptm *C*=O), 136.4 (ptm aromatic *C*), 132.2 (ptm aromatic *C*H), 131.5 (carbene Au-*C*), 122.1 (imidazole *C*H), 121.9 (ptm aromatic *C*H), 62.5 {^{t}Bu *C*(CH$_3$)$_3$}, 32.2 {^{t}Bu C(*C*H$_3$)$_3$}. IR (CH$_2$Cl$_2$, cm^{-1}) υ_{max} 3053 (m), 2987 (m), 2359 (w), 1682 (s), 1646 (m), 1609 (w), 1540 (w), 1465 (m), 1417 (m), 1374 (m), 1352 (m), 1312 (s), 1178 (m), 1157 (w), 1128 (m). ESI$^+$-MS *m/z* 684.0 (51%, [MH]$^+$), 418.2 (51%), 338.3 (18%), 259.1 (36%, [I^{t}BuBr]$^+$), 181.2 (100%, [ItBuH]$^+$). ESI$^+$-HRMS calcd. for C$_{19}$H$_{25}$AuBr$_2$N$_3$O$_2$ ([MH]$^+$) 681.9974; found 681.9988. Melting point 210 ˚C decomposes.

[AuBr$_2$(*N*-obs)(I^{t}Bu)] (66f)

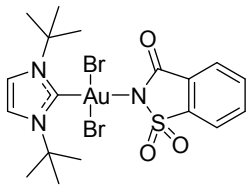

A protocol similar to that used for **66a** gave the title compound as a yellow powder {from 38.4 mg, 68.7 μmol, of [Au(*N*-obs)(I^{t}Bu)] (**55e**)} (45.4 mg, 63.1 μmol, 92%). ^{1}H NMR (400 MHz, CDCl$_3$) δ 7.93-7.84 (m, 2H, aromatic C*H*), 7.72-7.66 (m, 2H, aromatic C*H*), 7.50 (s, 2H, imidazole C*H*), 2.03 {s, 18H, ^{t}Bu C(C*H*$_3$)$_3$}. ^{13}C NMR (100 MHz,

$CDCl_3$) δ 164.0 (obs *C*=O), 142.3 (obs aromatic *C*), 133.0 (obs aromatic *C*H), 131.3 (obs aromatic *C*), 125.6 (carbene Au-*C*), 124.1 (obs aromatic *C*H), 122.7 (imidazole *C*H), 120.5 (obs aromatic *C*H), 62.7 {^{t}Bu *C*(CH_3)$_3$}, 32.0 {^{t}Bu C(*C*H_3)$_3$)}. IR (CH_2Cl_2, cm^{-1}) υ_{max} 3676 (w), 3062 (w), 2986 (m), 2929 (m), 1734 (w), 1694 (s), 1653 (w), 1597 (w), 1559 (w), 1460 (m), 1417 (m), 1376 (m), 1336 (w), 1315 (s), 1287 (m), 1247 (m), 1192 (w), 1176 (s), 1158 (m), 1124 (w), 1014 (w), 979 (m), 971 (m). ESI$^+$-MS *m/z* 741.9 (100%, [MNa]$^+$), 698.0 (2%), 640.9 (1%), 582.1 (2%), 481.0 (7%), 435.1 (6%), 336.1 (1%), 259.1 (15%), 215.1 (2%), 181.2 (4%), 147.0 (2%). ESI$^+$-HRMS calcd. for $C_{18}H_{24}AuBr_2N_3NaO_3S$ ([MNa]$^+$) 741.9448; found 741.9442. Melting point 150 ˚C decomposes.

[$AuBr_3$(I^tBu)] (66g)

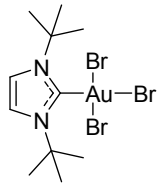

Prepared by a protocol reported by de Frémont *et al.*.[86] [AuBr(I^tBu)] (**55g**) (40.7 mg, 89.1 μmol, 1 equiv.) was dissolved in dichloromethane (2 ml) and bromine (0.80 ml, 98 μmol, 1.1 equiv.) was added. The orange solution was stirred at room temperature for 1 hour. The volume was reduced *in vacuo* to <0.5 ml and hexane added to give an orange precipitate. This was separated by filtration, washed (hexane) and dried *in vacuo* to give the title compound as an orange powder (53.1 mg, 86.1 μmol, 97%). ^{1}H NMR (400 MHz, $CDCl_3$) δ 7.45 (s, 2H, imidazole C*H*), 1.94 (s, 18H, ^{t}Bu C*H*$_3$). ^{13}C NMR (100 MHz, $CDCl_3$) δ 134.8 (carbene Au-*C*), 122.2 (imidazole C*H*), 62.4 (^{t}Bu quaternary *C*), 32.0 (^{t}Bu C*H*3). ESI$^+$-MS *m/z* 656.8 (61%, [MK]$^+$), 640.9 (100%, [MNa]$^+$), 633.9 (30%), 582.8 (12%), 526.7 (8%), 481.0 (7%, [MNa-2Br]$^+$), 429.4 (16%), 413.3 (58%), 369.3 (36%), 349.1 (24%), 293.0 (70%), 259.1 (77%). ESI$^+$-HRMS calcd. for $C_{11}H_{20}N_2AuBr_3Na$ 640.8694 ([MNa]$^+$); found 640.8677. Data in accordance with the literature.[86]

[AuBr$_2$(*N*-succ)(I^{t}Pe)] (67a)

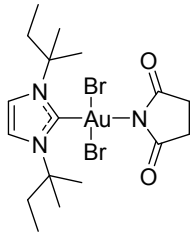

A protocol similar to that used for **66a** gave the title compound as a yellow powder {from 98.8 mg, 196 μmol, of [Au(*N*-succ)(I^{t}Pe)] (**56a**)} (127 mg, 192 μmol, 98%). ^{1}H NMR (400 MHz, $CDCl_3$) δ 7.36 (s, 2H, imidazole C*H*), 2.74 (s, 4H, succ CH_2), 2.04 (s, 12H, ^{t}Pe C(CH_3)$_2$), 2.03 (q, *J* = 7.5 Hz, 4H, ^{t}Pe CH_2CH$_3$), 0.84 (t, *J* = 7.5 Hz, 6H, ^{t}Pe CH$_2$CH_3). ^{13}C NMR (101 MHz, $CDCl_3$) δ 183.9 (succ *C*=O), 132.6 (carbene Au-*C*), 122.1 (imidazole *C*H), 65.4 (^{t}Pe quaternary *C*), 36.8 (^{t}Pe *C*H$_2$CH$_3$), 31.4 (succ *C*H$_2$), 29.8 {^{t}Pe C(*C*H$_3$)$_2$}, 8.5 (^{t}Pe CH$_2$*C*H$_3$). IR (solid, cm^{-1}) υ_{max} 2967 (w), 1665 (s), 1461 (w), 1414 (w), 1224 (s), 1003 (s), 798 (s), 683 (m). IR (CH_2Cl_2, cm^{-1}) υ_{max} 3686 (w), 3052 (m), 2979 (m), 2940 (w), 2882 (w), 1663 (s), 1540 (w), 1465 (m), 1434 (w), 1414 (w), 1387 (m), 1352 (m), 1284 (m), 1230 (m), 1176 (w). ESI$^+$-MS *m/z* 664.0 (100%, [MH]$^+$), 593.9 (72%), 523.9 (86%), 472.9 (21%), 433.2 (34%), 414.3 (93%), 391.3 (99%), 289.1 (58%), 217.0 (42%), 149.0 (58%), 127.3 (23%). ESI$^+$-HRMS calcd. for $C_{17}H_{29}AuBr_2N_3O_2$ ([MH]$^+$) 662.0287; found 662.0313. Melting point 190 ˚C decomposes.

[AuBr$_2$(*N*-dbs)(I^{t}Pe)] (67b)

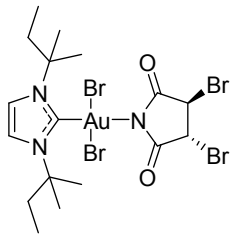

A protocol similar to that used for **66b** gave the title compound as a yellow powder {from 31.4 mg, 62.7 μmol, of [Au(*N*-mal)(I^{t}Pe)] (**56c**)} (36.2 mg, 54.8 μmol, 87%). ^{1}H NMR (400 MHz, $CDCl_3$) δ 7.39 (s, 2H, imidazole C*H*), 4.81 (s, 2H, dbs C*H*), 2.03 {m, 16H, ^{t}Pe CH_2CH$_3$ and ^{t}Pe C(CH_3)$_2$}, 0.85 (t, *J* = 7.4 Hz, 6H, tPe CH$_2$CH_3). ^{13}C NMR (100 MHz, $CDCl_3$) δ 175.7 (dbs *C*=O), 128.7 (carbene Au-*C*), 122.4 (imidazole *C*H), 65.6 (^{t}Pe quaternary *C*), 46.6 (dbs *C*-H), 36.8 (^{t}Pe *C*H$_2$CH$_3$), 29.7 {^{t}Pe C(*C*H$_3$)$_2$}, 8.5 (^{t}Pe CH$_2$*C*H$_3$). IR (CH_2Cl_2, cm^{-1}) υ_{max} 3421 (w), 3200 (w), 2976 (w), 2976 (m), 2930 (w), 2360 (m), 2341 (m), 1741 (m), 1690 (s), 1465 (m), 1419 (m), 1387 (m), 1337 (s), 1269 (s), 1227 (m), 1198 (w), 1174 (w). ESI$^+$-MS *m/z* 843.8 (100%, [MNa]$^+$). ESI$^+$-HRMS calcd. for

$C_{17}H_{26}AuBr_4N_3NaO_2$ ([MNa]$^+$) 843.8277; found 843.8288. Melting point 170 ˚C decomposes.

[AuBr$_2$(*N*-tfs)(I^{t}Pe)] (67c)

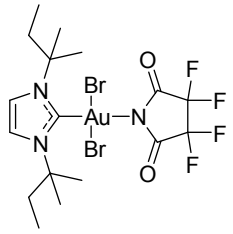

A protocol similar to that used for **66a** gave the title compound as a yellow powder {from 50.5 mg, 87.8 μmol, of [Au(*N*-tfs)(I^{t}Pe)] (**56b**)} (60.0 mg, 81.6 μmol, 93%). ^{1}H NMR (400 MHz, $CDCl_3$) δ 7.43 (s, 2H, imidazole C*H*), 2.05 {s, 12H, ^{t}Pe C(C*H*$_3$)$_2$}, 2.04 (q, *J* = 7.5 Hz, 4H, ^{t}Pe C*H*$_2$CH$_3$), 0.86 (t, *J* = 7.5 Hz, 6H, ^{t}Pe CH$_2$C*H*$_3$). ^{19}F NMR (376 MHz, $CDCl_3$) δ -127.1 (s, C*F*$_2$). ^{13}C NMR (101 MHz, $CDCl_3$) δ 167.0 (m,[145] *C*=O), 126.0 (carbene Au-*C*), 122.8 (imidazole *C*H), 107.0 (tt, *J* = 269 and 23 Hz, C*F*$_2$), 65.8 (^{t}Pe quaternary *C*), 36.8 (^{t}Pe *C*H$_2$CH$_3$), 29.7 (^{t}Pe C(*C*H$_3$)$_2$), 8.5 (^{t}Pe *C*H$_2$*C*H$_3$). IR (CH_2Cl_2, cm^{-1}) υ_{max} 3490 (w), 3200 (w), 3166 (w), 2979 (m), 2941 (w), 2884 (w), 1819 (w), 1789 (w), 1720 (m), 1716 (s), 1586 (w), 1480 (w), 1465 (w), 1417 (w), 1387 (m), 1322 (m), 1305 (m), 1195 (s), 1156 (m), 1065 (m), 1017 (m). ESI$^+$-MS *m/z* 799.0 (6%, [MNa+MeCN]$^+$), 758.0 (100%, [MNa]$^+$), 598.1 (3%), 463.1 (4%). ESI$^+$-HRMS calcd. for $C_{17}H_{24}AuBr_2F_4N_3NaO_2$ ([MNa]$^+$) 757.9714; found 757.9703. Melting point 150 ˚C decomposes.

[AuBr$_2$(*N*-mal)(I^{t}Pe)] (67d)

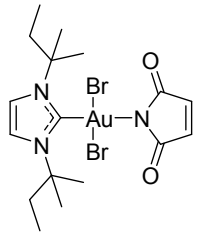

A protocol similar to that used for **66d** gave the title compound as a yellow powder {from 30.1 mg, 60.1 μmol, of [Au(*N*-mal)(I^{t}Pe)] (**56c**)} (34.7 mg, 52.5 μmol, 87%). ^{1}H NMR (400 MHz, $CDCl_3$) δ 7.38 (s, 2H, imidazole C*H*), 6.64 (s, 2H, mal C*H*), 2.07 {s, 12H, ^{t}Pe C(C*H*$_3$)$_2$}, 2.03 (q, *J* = 7.5 Hz, 4H, ^{t}Pe C*H*$_2$CH$_3$), 0.86 (t, *J* = 7.5 Hz, 6H, ^{t}Pe CH$_2$C*H*$_3$). ^{13}C NMR (101 MHz, $CDCl_3$) δ 177.3 (mal *C*=O), 136.8 (mal *C*H), 132.0 (carbene Au-*C*), 122.2 (imidazole *C*H), 65.4 (^{t}Pe quaternary *C*), 36.9 (^{t}Pe *C*H$_2$CH$_3$), 29.8

{^{t}Pe C(CH_3)$_2$}, 8.6 (^{t}Pe CH_2CH_3). IR (CH_2Cl_2, cm^{-1}) υ_{max} 3054 (m), 2979 (m), 2940 (w), 2883 (w), 2360 (m), 2342 (m), 1734 (m), 1676 (s), 1437 (m), 1419 (m), 1348 (s), 1269 (s), 1180 (m). ESI$^+$-MS *m/z* 684.0 (100%, [MNa]$^+$), 649.2 (33%), 619.0 (9%), 524.2 (12%). ESI$^+$-HRMS calcd. for $C_{17}H_{26}AuBr_2N_3NaO_2$ 683.9935; found 683.9901. Melting point 160 ˚C decomposes.

[AuBr$_2$(*N*-ptm)(I^{t}Pe)] (67e)

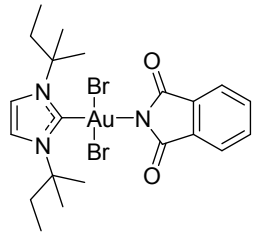

A protocol similar to that used for **66a** gave the title compound as a yellow powder {98.5 mg, 179 μmol, of [Au(*N*-ptm)(I^{t}Pe)] (**56d**)} (123 mg, 173 μmol, 97%). ^{1}H NMR (400 MHz, $CDCl_3$) δ 7.70 (dd, *J* = 5.4 and 3.0 Hz, 2H, ptm aromatic C*H*), 7.56 (dd, *J* = 5.4 and 3.0 Hz, 2H, ptm aromatic C*H*), 7.39 (s, 2H, imidazole C*H*), 2.10 {s, 12H, ^{t}Pe C(CH_3)$_2$}, 2.05 (q, *J* = 7.4 Hz, 4H, ^{t}Pe CH_2CH$_3$), 0.86 (t, *J* = 7.4 Hz, 6H, ^{t}Pe CH$_2$CH_3). ^{13}C NMR (101 MHz, $CDCl_3$) δ 174.3 (ptm *C*=O), 136.2 (ptm *ortho* aromatic *C*), 132.4 (carbene Au-*C*), 132.3 (ptm *meta* aromatic *C*), 122.3 (ptm *para* aromatic *C*), 121.8 (imidazole *C*H), 65.3 (^{t}Pe quaternary *C*), 36.8 (^{t}Pe *C*H$_2$CH$_3$), 29.8 {^{t}Pe C(*C*H$_3$)$_2$}, 8.5 (^{t}Pe CH$_2$*C*H$_3$). IR (CH_2Cl_2, cm^{-1}) υ_{max} 3199 (w), 3057 (w), 2979 (m), 2940 (w), 2882 (w), 1742 (w), 1682 (s), 1646 (m), 1609 (w), 1540 (w), 1465 (m), 1416 (m), 1373 (m), 1352 (m), 1311 (s), 1284 (m), 1214 (w), 1175 (m), 1128 (m). ESI$^+$-MS *m/z* 712.0 (100%, [MH]$^+$), 642.0 (41%, [MH-^{t}Pe]$^+$), 571.9 (35%, [MH$_2$-2^{t}Pe]$^+$), 472.9 (6%), 391.3 (68%), 363.1 (3%), 289.1 (16%, [I^{t}PeBr]$^+$), 272.7 (18%), 217.0 (14%, [I^{t}PeBrH-^{t}Pe]$^+$), 149.0 (24%), 127.3 (5%). ESI$^+$-HRMS calcd. for $C_{21}H_{29}AuBr_2N_3O_2$ ([MH]$^+$) 710.0287; found 710.0309. Melting point 220 ˚C decomposes.

[AuBr$_2$(*N*-obs)(I^{t}Pe)] (67f)

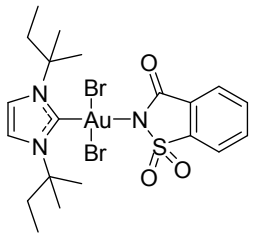

A protocol similar to that used for **66a** gave the title compound as a yellow powder {from 40.6 mg, 69.2 μmol, of [Au(*N*-obs)(I^{t}Pe)] (**56e**)} (48.6 mg, 65.1 μmol, 94%). ^{1}H NMR (400 MHz, $CDCl_3$) δ 7.97-7.93 (m, 1H, obs aromatic C*H*), 7.90-7.87 (m, 1H, obs aromatic C*H*), 7.72-7.66 (m, 2H, obs aromatic C*H*), 7.43 (s, 2H, imidazole C*H*), 2.12 {s, 12H, ^{t}Pe C(CH_3)$_2$}, 2.05 (q, *J* = 7.4 Hz, 4H, ^{t}Pe CH_2CH$_3$), 0.88 (t, *J* = 7.4 Hz, 6H, ^{t}Pe CH$_2$CH_3). ^{13}C NMR (100 MHz, $CDCl_3$) δ 164.0 (obs *C*=O), 142.3 (obs aromatic *C*), 133.0 (obs aromatic 2*C*H), 131.3 (obs aromatic *C*), 126.6 (carbene Au-*C*), 124.1 (obs aromatic *C*H), 122.7 (imidazole *C*H), 120.4 (obs aromatic *C*H), 65.8 (^{t}Pe quaternary *C*), 36.9 (^{t}Pe *C*H$_2$CH$_3$), 29.7 {s, ^{t}Pe C(*C*H$_3$)$_2$}, 8.6 (s, ^{t}Pe CH$_2$*C*H$_3$). IR (CH_2Cl_2, cm^{-1}) υ_{max} 3675 (w), 3199 (w), 3063 (w), 2979 (m), 2940 (m), 2883 (m), 1694 (s), 1653 (w), 1596 (m), 1506 (w), 1461 (m), 1417 (m), 1388 (m), 1337 (w), 1315 (s), 1287 (s), 1248 (s), 1192 (w), 1176 (s), 1160 (m), 1124 (w), 1059 (w). ESI$^+$-MS *m/z* 838.0 (4%), 770.0 (100%, [MNa]$^+$), 633.0 (12%), 446.2 (11%). ESI$^+$-HRMS calcd. for $C_{20}H_{28}AuBr_2N_3NaO_3S$ ([MNa]$^+$) 769.9761; found 769.9764. Melting point 180 ˚C decomposes.

[AuBr$_3$(I^{t}Pe)] (67g)

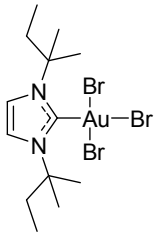

A protocol similar to that used for **66g** gave the title compound as an orange solid {from 40.7 mg, 89.1 μmol, of [AuBr(I^{t}Pe)] (**56g**)} (53.1 mg, 86.1 μmol, 97%). ^{1}H NMR (400 MHz, $CDCl_3$) δ 7.39 (s, 2H, imidazole C*H*), 2.02 (q, *J* = 7.5 Hz, 4H, ^{t}Pe CH_2CH$_3$), 2.01 {s, 12H, ^{t}Pe C(CH_3)$_2$}, 0.86 (t, *J* = 7.5 Hz, 6H, ^{t}Pe CH$_2$CH_3). ^{13}C NMR (101 MHz, $CDCl_3$) δ 135.6 (carbene Au-*C*), 122.2 (imidazole *C*H), 65.5 (^{t}Pe quaternary *C*), 36.7 (^{t}Pe *C*H$_2$CH$_3$), 29.6 {^{t}Pe C(*C*H$_3$)$_2$}, 8.6 (^{t}Pe CH$_2$*C*H$_3$). IR (CH_2Cl_2, cm^{-1}) υ_{max} 3200 (m), 3165 (m), 3050 (m), 2979 (s), 2941 (m), 2883 (m), 1585 (w), 1465 (m), 1413 (m), 1382 (m), 1281 (w), 1260 (s), 1199 (m), 1175 (s), 1161 (m), 1067 (w), 1033 (w), 1006 (w). ESI$^+$-MS *m/z* 666.9

(100%, $[MNa]^+$), 507.1 (54%), 463.1 (8%), 289 (37%). ESI^+-HRMS calcd. for $C_{13}H_{24}AuBr_3N_2Na$ ($[MNa]^+$) 666.9027; found 666.9066. Melting point 170 ˚C decomposes.

[$AuBr_2$(*N*-succ)(IMes)] (68a)

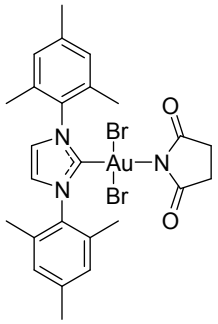

A protocol similar to that used for **66a** gave the title compound as a yellow powder {57.9 mg, 96.7 μmol, of [Au(*N*-succ)(IMes)] (**57a**)} (63.3 mg, 83.4 μmol, 86%). ^1H NMR (400 MHz, $CDCl_3$) δ 7.26 (s, 2H, imidazole C*H*), 7.06 (s, 4H, Mes aromatic C*H*), 2.52 (s, 4H, succ CH_2), 2.37 (s, 6H, Mes *para* CH_3), 2.33 (s, 12H, Mes *ortho* CH_3). ^{13}C NMR (100 MHz, $CDCl_3$) δ 183.1 (succ *C*=O), 142.2 (carbene Au-*C*), 140.6 (Mes aromatic *C*), 135.0 (Mes aromatic *C*), 133.0 (Mes aromatic *C*), 129.9 (Mes aromatic *C*H), 125.5 (imidazole *C*H), 31.3 (succ *C*H_2), 21.2 {Mes *para* C(*C*H_3)}, 19.5 {Mes *ortho* C(*C*H_3)}. IR (CH_2Cl_2, cm^{-1}) υ_{max} 3677 (w), 3144 (w), 3055 (m), 2979 (w), 2924 (w), 2363 (w), 1723 (w), 1665 (s), 1608 (w), 1540 (w), 1482 (m), 1434 (m), 1381 (w), 1351 (m), 1281 (m), 1232 (m), 1168 (w). ESI^+-MS *m/z* 782.0 (10%, $[MNa]^+$), 760.0 (100%, $[MH]^+$), 542.2 (5%). ESI^+-HRMS calcd. for $C_{25}H_{29}AuBr_2N_3O_2$ ($[MH]^+$) 758.0287; found 758.0282. Melting point 180 ˚C decomposes.

[AuBr$_2$(*N*-mal)(IMes)] (68b)

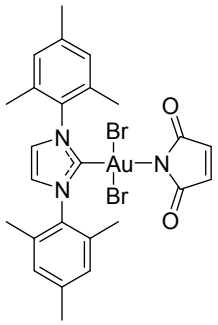

A protocol similar to that used for **66d** gave the title compound as a yellow powder {105 mg, 176 μmol, of [Au(*N*-mal)(IMes)] (**57c**)} (129 mg, 170 μmol, 96%). ^{1}H NMR (400 MHz, $CDCl_3$) δ 7.27 (s, 2H, C*H* imidazole), 7.07 (s, 4H, Mes aromatic C*H*), 6.39 (s, 2H, mal C*H*), 2.33 (m, 18 H, Mes C*H*$_3$). ^{13}C NMR (101 MHz, $CDCl_3$) δ 176.6 (mal *C*=O), 141.4 (carbene Au-*C*), 140.7 (Mes aromatic *C*), 136.7 (mal *C*H), 135.0 (Mes aromatic *C*), 133.0 (Mes aromatic *C*), 129.9 (Mes aromatic *C*H), 125.6 (imidazole *C*H), 21.2 (Mes *para* C*C*H$_3$), 19.5 (Mes *ortho* C*C*H$_3$). IR (CH_2Cl_2, cm^{-1}) υ_{max} 3686 (w), 3143 (w), 2984 (w), 2352 (w), 1677 (s), 1608 (m), 1540 w), 1484 (m), 1432 (w), 1380 (w), 1349 (m), 1284 (w), 1229 (m), 1181 (m), 1128 (w). ESI$^+$-MS *m/z* 758.0 (1%, [MH]$^+$), 620.2 (12%, [MNa-2Br]$^+$), 598.2 (88%, [MH-2Br]$^+$), 550.2 (4%), 529.2 (64 %), 385.1 (31%, [IMesBr]$^+$), 335.2 (2%), 305.2 (100%, [IMesH]$^+$), 267.2 (2%). ESI$^+$-HRMS calcd. for $C_{25}H_{27}AuBr_2N_3O_2$ ([MH]$^+$) 758.0115; found 758.0185. Melting point 190 ˚C decomposes.

[AuBr$_2$(*N*-ptm)(IMes)] (68c)

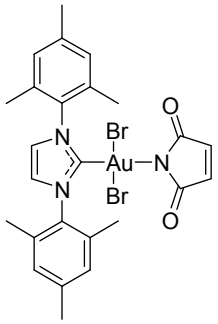

A protocol similar to that used for **66a** gave the title compound as a yellow powder {40.3 mg, 62.3 μmol, of [Au(*N*-ptm)(IMes)] (**57d**)} (48.0 mg, 59.4 μmol, 95%). ^{1}H NMR (400 MHz, $CDCl_3$) δ 7.56 (dd, *J* = 5.4 and 3.0 Hz, 2H, ptm aromatic C*H*), 7.44 (dd, *J* = 5.4 and 3.0 Hz, 2H, ptm aromatic C*H*), 7.29 (s, 2H, imidazole C*H*), 7.09 (s, 4H, Mes aromatic C*H*), 2.38 (s, 6H, Mes *para* C*C*H$_3$), 2.34 (s, 12H, Mes *ortho* C*C*H$_3$). ^{13}C NMR (400 MHz, $CDCl_3$) δ 173.7 (ptm *C*=O), 142.2 (carbene Au-*C*), 140.6 (Mes aromatic *C*), 136.3 (ptm

ortho aromatic *C*), 135.0 (Mes aromatic *C*), 133.1 (Mes aromatic *C*), 132.0 (ptm *meta* aromatic *C*H), 129.9 (Mes aromatic *C*H), 125.6 (imidazole *C*H), 121.7 (ptm *para* aromatic *C*H), 21.2 {Mes *para* C(*C*H$_3$)}, 19.5 {Mes *ortho* C(*C*H$_3$)}. IR (CH_2Cl_2, cm^{-1}) υ_{max} 3686 (w), 3421 (w), 3170 (w), 3143 (w), 2925 (w), 2360 (w), 1777 (w), 1741 (m), 1683 (s), 1646 (m), 1609 (m), 1540 (w), 1484 (m), 1418 (w), 1372 (m), 1351 (m), 1310 (m), 1230 (m), 1172 (m), 1129 (m). ESI$^+$-MS *m/z* 808.0 (100%, $[MH]^+$), 728.1 (2%, $[M-Br]^+$), 648.2 (48%, $[MH-2Br]^+$), 622.1 (4%), 542.2 (84%). ESI$^+$-HRMS calcd. for $C_{29}H_{29}AuBr_2N_3O_2$ ($[MH]^+$) 808.0268; found 808.0283. Melting point 125-127 ˚C.

[AuBr$_3$(IMes)] (68d)

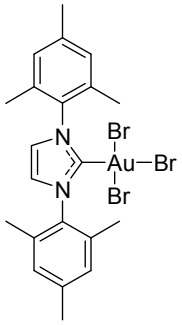

A protocol similar to that used for **66g** gave the title compound as an orange solid {from 65.8 mg, 113 μmol, of [AuBr(IMes)] (**57g**)} (55.6 mg, 75.1 □mol, 66%). ^{1}H NMR (400 MHz, $CDCl_3$) δ 7.27 (s, 2H, imidazole C*H*), 7.01 (s, 4H, aromatic C*H*), 2.36 (s, 6H, Mes *para* C*H*$_3$), 2.30 (s, 12H, Mes *ortho* C*H*$_3$). ^{13}C NMR (100 MHz, $CDCl_3$) δ 144.2 (carbene Au-C), 140.8 (Mes aromatic *C*), 135.1 (Mes aromatic *C*), 132.7 (Mes aromatic *C*), 129.9 (Mes aromatic *C*), 125.6 (imidazole *C*H), 21.1 (Mes *para* *C*H$_3$), 19.5 (Mes *ortho* *C*H$_3$). ESI$^+$-MS *m/z* 1081.2 (4%, $[\{(IMes)Au\}_2Br]^+$), 965.2 (17%, $[(IMes)_2AuBr_2]^+$), 762.9 (4%, $[MNa]^+$), 693.0 (8%, $[M-Br+MeOH]^+$), 661.0 (7%, $[M-Br]^+$), 605.1 (5%, $[MNa-2Br]^+$), 542.2 (6%, $[(IMes)Au+MeCN]^+$), 385.1 (29%, $[IMesBr]^+$), 305.3 (100%, $[IMesH]^+$). ESI$^+$-HRMS calcd. for $C_{21}H_{24}AuBr_3N_2Na$ ($[MNa]^+$) 762.9032; found 762.9020. Data in accordance with the literature.[86]

2,3-Dibromosuccinimide

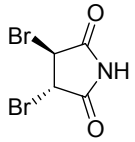

A protocol based on that reported by Davis was used.[146] Maleimide (100 mg, 1.04 mmol, 1 equiv.) was dissolved in dichloromethane (5ml) and a solution of bromine (173 mg, 1.08

mmol, 1.04 equiv.) in dichloromethane (1 ml) was added dropwise. The solution was stirred (r.t., 3 days) to give an orange solution and reduced *in vacuo* to a white powder. The product was precipitated from dichloromethane/hexane, filtered and purified by recrystallisation (diethyl ether/ hexane) to give the title compound as a white powder (101 mg, 0.393 mmol, 38%). ^{1}H NMR (400 MHz, CD_3OD) δ 5.07 (s). ^{13}C NMR (100 MHz, CD_3OD) δ 173.1, 45.8. IR (CH_2Cl_2, cm^{-1}) υ_{max} 3374 (br, m), 3056 (m), 2927 (w), 2360 (m), 2341 (m), 2305 (w), 1801 (w), 1783 (w), 1744 (s), 1653 (w), 1605 (m), 1559 (w), 1540 (w), 1506 (w), 1421 (m), 1337 (br m), 1271 (s), 1170 (s), 1136 (w), 921 (w). ESI$^+$-MS *m/z* 317.2 (14%), 301.1 (100%), 257.9 (18%, $[MH]^+$), 245.1 (27%), 239.2 (9%), 227.1 (26%), 143.1 (41%), 124.9 (21%), 100.1 (13%, $[succH]^+$). ESI$^+$-HRMS calcd. for $C_4H_4Br_2NO_2$ ($[MH]^+$) 255.8603; found 255.8612. Data in accordance with the literature.[146]

2-Bromomaleimide

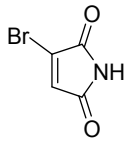

2,3-Dibromosuccinimide (53.5 mg, 202 □mol, 1 equiv.) and sodium hydroxide (9.2 mg, 230 □mol, 1.1 equiv.) were mixed in water (10 ml) (r.t., 18 hours). The solution was reduced *in vacuo* and the residue redissolved in dichloromethane, filtered and reduced *in vacuo* to give the title compound as a white powder (24.6 mg, 140 □mol, 67%). ^{1}H NMR (400 MHz, CD_3OD) δ 7.02 (s). ^{13}C NMR (100 MHz, $CDCl_3$) δ 171.1, 167.9, 166.1, 134.3, 132.5. IR (solid, cm^{-1}) υ_{max} 3235 (s), 3152 (w), 3102 (m), 2923 (m), 2852 (w), 2682 (w), 2447 (m), 2384 (m), 2161 (m), 2032 (m), 1977 (w), 1780 (m), 1763 (m), 1707 (br s), 1577 (s), 1330 (s), 1231 (m), 1207 (m), 1125 (m), 996 (m), 961 (w), 910 (w), 870 (m), 844 (w), 767 (w), 716 (w), 673 (m), 657 (m). EI$^+$-MS *m/z* 175 (73%, $[M]^+$), 132 (100%, $[M-CONH]^+$), 106 (54%, $[C_2HBr]^+$), 79 (6%, Br^+), 53 (31%). EI$^+$-HRMS calcd. for. $C_4H_2NO_2Br$ ($[M]^+$) 174.9269; found 174.9264. Data in accordance with the literature.[147]

[Au(*N*^{15}-succ)(I^{t}Pe)] (72)

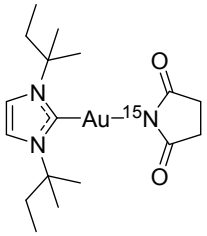

^{15}N-Succinimide (15.8 mg, 15.8 μmol, 1.1 equiv.), silver(I) oxide (20.0 mg, 86.2 μmol, 0.6 equiv.) and [AuCl(I^{t}Pe)] (**56f**) (63.2 mg, 144 μmol, 1 equiv.) were mixed in dichloromethane (2 ml) in the absence of light for 18 hours. The suspension was filtered through Celite^{TM}, reduced to <0.5 ml and pentane added, resulting in a white precipitate. This was washed (cold pentane and diethyl ether) and dried *in vacuo* to give the title compound as a white powder (65.2 mg, 130 μmol, 90%). ^{1}H NMR (400 MHz, $CDCl_3$) δ 7.04 (s, 2H, imidazole C*H*), 2.61 (s, 4H, succ CH_2), 2.48 (q, *J* = 7.5 Hz, 4H, ^{t}Pe CH_2), 1.81 {s, 12H, ^{t}Pe C(CH_3)$_2$}, 0.65 (t, *J* = 7.5 Hz, 6H, ^{t}Pe CH_2CH_3). ^{13}C NMR (100 MHz, $CDCl_3$) δ 188.7 (d, *J* = 8 Hz, succ *C*=O), 170.8 (d, *J* = 15 Hz, carbene Au-*C*), 117.3 (imidazole *C*H), 61.8 (^{t}Pe quaternary *C*), 36.3 (^{t}Pe *C*$H_2$$CH_3$), 31.6 (d, *J* = 4 Hz, succ *C*H_2), 29.3 (^{t}Pe C(*C*H_3)$_2$), 7.9 (^{t}Pe CH_2*C*H_3). ^{15}N NMR (50 MHz, CD_2Cl_2) δ 209.4 (s). IR (solid, cm^{-1}) υ_{max} 2964 (m), 2933 (w), 2533 (w), 2160 (m), 2028 (m), 1978 (m), 1646 (s), 1561 (w), 1459 (w), 1396 (w), 1378 (w), 1333 (s), 1279 (m), 1212 (s), 1152 (w), 1067 (w), 1039 (w), 1006 (w), 972 (w), 919 (w), 816 (m), 759 (m), 759 (w), 732 (m), 701 (m), 653 (m), 620 (m). IR (CH_2Cl_2, cm^{-1}) υ_{max} 3020 (m), 2971 (m), 2937 (w), 2880 (w), 2005 (w), 2360 (w), 2342 (w), 1646, 1559 (w), 1522 (w), 1461 (w), 1436 (w), 1406 (w), 1393 (w), 1379 (m), 1336 (m), 1310 (w), 1284 (m), 1269 (s), 1217 (s), 1005 (w), 917 (w), 896 (m). ESI $^{+}$-MS *m/z* 527.2 (12%, [MNa]$^{+}$), 505.2 (100%, [MH]$^{+}$), 433.2 (1%), 209.2 (3%, [I^{t}PeH]$^{+}$). ESI^{+}-HRMS calcd. for $C_{17}H_{29}Au^{14}N_2{}^{15}NO_2$ ([MH]$^{+}$) 505.1896; found 505.1891.

[AuBr$_2$(*N*^{15}-succ)(I^{t}Pe)] (73)

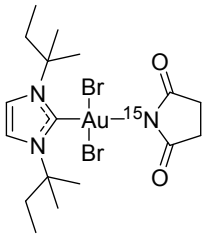

[Au(*N*^{15}-Succ)(I^{t}Pe)] (**72**) (41.3 mg, 81.9 μmol, 1 equiv.) was dissolved in dichloromethane (2 ml) and bromine (14.4 mg, 90.0 μmol, 1.1 equiv.) was added dropwise. The yellow solution was stirred at room temperature for 1 hour. The volume was reduced

to <0.5 ml *in vacuo* and hexane added resulting in a yellow precipitate. This was separated by filtration, washed (cold hexane and diethyl ether) and dried *in vacuo* to give the title compound as a yellow powder (51.1 mg, 70.0 ◘mol, 94%). ^{1}H NMR (400 MHz, $CDCl_3$) δ 7.36 (s, 2H, imidazole C*H*), 2.73 (s, 4H, succ CH_2), 2.06 {s, 12H, ^{t}Pe C(CH_3)$_2$}, 2.04 (q, *J* = 7.5 Hz, 4H, ^{t}Pe CH_2CH$_3$), 0.84 (t, *J* = 7.5 Hz, 6H, ^{t}Pe CH$_2$CH_3). ^{13}C NMR (101 MHz, $CDCl_3$) δ 183.9 (d, *J* = 9 Hz, succ *C*=O), 132.8 (d, *J* = 25 Hz, carbene Au-*C*), 122.3 (imidazole *C*H), 65.6 (^{t}Pe quaternary *C*), 37.0 (^{t}Pe *C*H$_2$CH$_3$), 31.5 (d, *J* = 5 Hz, succ *C*H$_2$), 29.9 {^{t}Pe C(*C*H$_3$)$_2$}, 8.7 (^{t}Pe CH$_2$*C*H$_3$). ^{15}N NMR (50 MHz, CD_2Cl_2) δ 179.4 (s). IR (solid, cm^{-1}) υ_{max} 2976 (s), 2165 (m), 2037 (m), 1662 (s), 1461 (m), 1419 (w), 1392 (w), 1331 (s), 1280 (m), 1211 (s), 1164 (m), 1065 (w), 1002 (w), 809 (m). IR (CH_2Cl_2, cm^{-1}) υ_{max} 2978 (m), 2941 (w), 2881 (w), 1744 (w), 1702 (w), 1662 (s), 1583 (w), 1481 (w), 1464 (w), 1413 (w), 1385 (w), 1337 (m), 1283 (w), 1216 (m), 1176 (w), 1163 (w), 1151 (w), 1066 (w), 1035 (w), 1003 (w). ESI^{+}-MS *m/z* 728.0 (2%, [MNa+MeCN]$^{+}$), 687.0 (5%, [MNa]$^{+}$), 665.0 (100%, [MH]$^{+}$), 610.2 (1%), 591.3 (3%), 536.2 (3%), 505.2 (2%, [MH-2Br]$^{+}$), 401.0 (5%), 287.1 (38%, [I^{t}PeBr]$^{+}$), 209.2 (51%, [I^{t}PeH]$^{+}$), 176.4 (3%). ESI^{+}-HRMS calcd. for $C_{17}H_{29}AuBr_2{}^{14}N_2{}^{15}NO_2$ ([MH]$^{+}$) 665.0242; found 665.0232.

General procedure for the cycloisomerisation of 4-phenyl-1-hexen-5-yne (74)

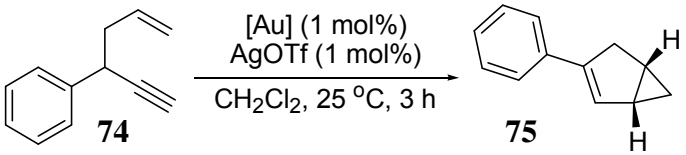

To a solution of 4-phenyl-1-hexen-5-yne (**74**) (50.0 mg, 321 μmol, 1 equiv.) in dichloromethane (0.64 mL, 0.50 M), AgOTf (0.8 mg, 3.1 μmol, 0.01 equiv.) and gold complex (3.2 μmol, 0.01 equiv.) were added. The solution was stirred at 25 ˚C for 3 hours and filtered through a plug of silica-gel which was washed with dichloromethane (2 ml). The solution was reduced *in vacuo* and conversion was determined by ^{1}H NMR spectroscopy. For characterisation purposes the product can be purified by column chromatography on silica-gel using petroleum ether (40-60) as eluent (R.F. 0.76). Fractions containing the product were combined and reduced *in vacuo* to give the title compound as a white powder.

General procedure for the kinetic evaluation of the gold catalysed cycloisomerisation of 4-phenyl-1-hexen-5-yne (74) by gas chromatography.

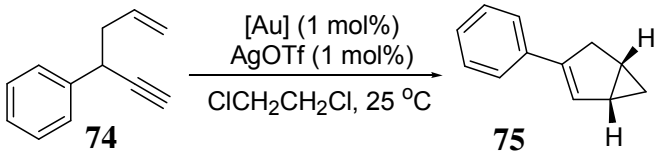

Au complex (3.2 μmol, 0.01 equiv.) and AgOTf (0.8 mg, 3.2 μmol, 0.01 equiv.) were mixed in dichloromethane in a screw cap vial (1 min) and the solvent removed *in vacuo*. A solution of 4-phenyl-1-hexen-5-yne (**74**) (50.0 mg, 321 μmol, 1 equiv.) in 1,2-dichloroethane (1.60 ml, 0.20 M) was added, the vial sealed with a rubber septum and a positive pressure of argon applied *via* an argon balloon. The mixture was stirred at 25 ˚C in the absence of light. Samples of 10 μl were taken *via* syringe and added immediately to a solution of tetra-*n*-butylammonium chloride (8 mM, 20 μl) in CH_2Cl_2. Conversion was determined *via* gas chromatography using a 1 μl sample. The chromatogram was run with an injector temperature of 250 ˚C and an initial oven temperature of 80 ˚C (0.5 mins), heated to 160 ˚C, at a rate of 20 ˚C.min^{-1}, and maintained at 160 ˚C (1 minute). The retention times were: 2.58 minutes for 4-phenyl-1-hexen-5-yne (**74**) and 3.89 minutes for 3-phenylbicyclo[3.1.0]hex-2-ene (**75**).

1-Phenylprop-2-yn-1-yl chloroacetate

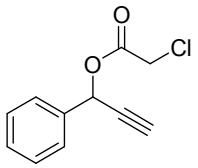

Prepared by a protocol reported by Schwier *et al.*.[148] 1-Phenyl-prop-2-yn-1-ol (**126**) (1.85 g, 14.0 mmol, 1 equiv.), pyridine (1.58 ml, 19.6 mmol, 1.4 equiv.) and dimethyl aminopyridine (5 mg, 40 □mol, 0.003 equiv.) were dissolved in dichloromethane (15 ml, dry) under an atmosphere of N_2. The solution was cooled to 0 ˚C and chloroacetyl chloride (1.35 ml, 16.8 mmol, 1.2 equiv.) was added dropwise. The resulting solution was stirred overnight (r.t.). The reaction was quenched with HCl (2 M aq., 20 ml), extracted (3 x 10ml diethyl ether), washed (sat. aq. $NaHCO_3$ 10ml, brine 10ml), dried ($MgSO_4$), filtered and reduced *in vacuo*. The resulting brown oil was purified by column chromatography on silica-gel, eluting with petroleum ether (40-60):ethyl acetate 100:0 to 95:5, to give the title compound as a colourless oil (2.41 g, 11.6 mmol, 83%).^{1}H NMR (400 MHz, $CDCl_3$) δ 7.57-7.53 (m, 2H), 7.43-7.39 (m, 3H), 6.52 (app. d, *J* = 2.3 Hz, 1H), 4.10 (m, 2H), 2.72 (d, *J* = 2.3 Hz, 1H). ^{13}C NMR (100 MHz, $CDCl_3$) δ 166.1, 135.5, 129.4, 128.8, 127.8, 79.2,

76.4, 67.1, 40.8. ESI$^+$-MS *m/z* 242.3 (1%), 231.0 (100%, [MNa]$^+$), 191.1 (15%), 180.1 (1%), 116.1 (3%), 107.0 (11%). ESI$^+$-HRMS calcd. for. $C_{11}H_9ClNaO_2$ ([MNa]$^+$) 231.0183; found 231.0179. Data in accordance with the literature.[148]

4-Phenyl-1-hexen-5-yne (74)

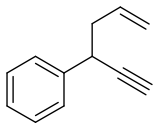

Synthesis was achieved by two methods.

Method 1:[148] 1-Phenylprop-2-yn-1-yl chloroacetate (3.17 g, 15.2 mmol, 1 equiv.) and allyltrimethylsilane (**127a**) (2.57 g, 22.5 mmol, 1.5 equiv.) were mixed in dichloromethane (15 ml, dry) and a solution of $B(C_6F_5)_3$ (202 mg, 0.395 mmol, 0.026 equiv.) in 15 ml dichloromethane was added. The mixture was stirred (r.t., 18 hours) to give a brown solution. This was filtered through a plug of silica-gel and concentrated *in vacuo*. Purification was achieved by column chromatography, eluting with 100% petroleum ether (40-60), followed by distillation (Kugelohr) (1 mm Hg, 50 ˚C) to give the title compound as a colourless oil (1.53 g, 9.80 mmol, 65%).

Method 2:[69] 1-Phenyl-prop-2-yn-1-ol (**126**) (2.53 ml, 20.4 mmol, 1 equiv.) and allyltrimethylsilane (9.78 ml, 61.4 mmol, 3 equiv.) were mixed in acetonitrile (40 ml, dry). $FeCl_3$ (anhydrous, 166 mg, 1.02 mmol, 0.05 equiv.) in acetonitrile (5 ml, dry) was added dropwise. The reaction was stirred (2 hours, r.t.). $FeCl_3$ (anhydrous, 166 mg, 1.02 mmol, 0.05 equiv.) in acetonitrile (5 ml dry) was added dropwise and the reaction stirred (1 hour, r.t.). The solution was reduced *in vacuo* and the product was purified by column chromatography, eluting with 100% petroleum ether (40-60), to give the title compound as a colourless oil (2.70 g, 17.3 mmol, 85%). ^{1}H NMR (400 MHz, $CDCl_3$) δ 7.41-7.32 (m, 4H), 7.29-7.24 (m, 1H), 5.87 (ddtd, *J* = 17.1, 10.2, 7.0 and 1.3 Hz, 1H), 5.13-5.06 (m, 2H), 3.72 (td, *J* = 7.2 and 2.4 Hz, 1H), 2.54 (t, *J* = 7.2 Hz, 2H), 2.32 (app. d, *J* = 2.4 Hz, 1H). ^{13}C NMR (100 MHz, $CDCl_3$) δ 140.7, 135.1, 128.5, 127.4, 126.9, 117.1, 85.3, 71.4, 42.4, 37.6. EI$^+$-MS *m/z* 156 (4%, [M]$^+$), 155 (7%), 141 (8%, [M-CH_3]$^+$), 128 (6%, [M-C_2H_4]$^+$), 115 (100%, [M-allyl]$^+$), 91 (6%), 89 (8%), 65 (3%), 63 (5%). EI$^+$-HRMS calcd. for. $C_{12}H_{12}$ ([M]$^+$) 156.0939; found 156.0943. Data in accordance with the literature.[148]

3-Phenylbicyclo[3.1.0]hex-2-ene (75)

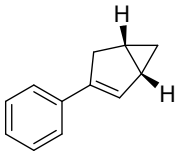

^{1}H NMR (400 MHz, $CDCl_3$) δ 7.45-7.42 (m, 2H), 7.38-7.33 (m, 2H), 7.26 (m, 1H), 6.48 (q, *J* = 2 Hz, 1H), 3.08 (ddd, *J* = 17, 7.5 and 2 Hz, 1H), 2.80 (app. d, *J* = 17 Hz, 1H), 2.01 (m, 1H), 1.79 (m, 1H), 1.00 (td, *J* = 7.5 and 4 Hz, 1H), 0.17 (dd, *J* = 7 and 4 Hz, 1H). ^{13}C NMR (101 MHz, $CDCl_3$) δ 139.7, 136.6, 129.6, 128.2, 126.7, 125.1, 36.3, 23.8, 17.6, 15.4. EI^+-MS 156 (100%, $[M]^+$), 141 (56%), 128 (39%), 115 (43%), 102 (7%), 91 (18%), 77 (12%), 63 (5%), 51 (6%). EI^+-HRMS calcd. for $C_{12}H_{12}$ ($[M]^+$) 156.0939; found 156.0934. Data in accordance with the literature.[15]

General procedure for the kinetic evaluation of the gold catalysed concurrent cycloisomerisation of 4-phenyl-1-hexen-5-yne (74) and dimethyl allylpropargylmalonate (77) by gas chromatography.

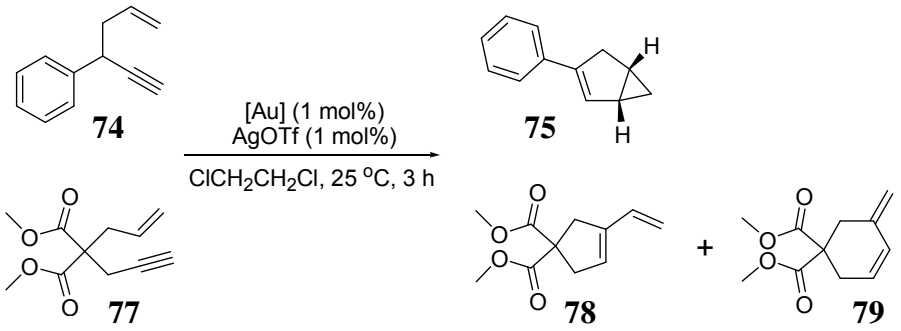

Au complex (3.2 μmol, 0.01 equiv.) and AgOTf (0.8 mg, 3.2 μmol, 0.01 equiv.) were mixed in dichloromethane in a screw cap vial (1 min) and the solvent removed *in vacuo*. A solution of 4-phenyl-1-hexen-5-yne (**74**) (50.0 mg, 321 μmol, 1 equiv.) and dimethyl allylpropargylmalonate (**77**) (67.4 mg, 321 μmol, 1 equiv.) in 1,2-dichloroethane (1.60 ml, 0.20 M) was added, the vial sealed with a rubber septum and a positive pressure of argon applied *via* an argon balloon. The mixture was stirred at 25 ˚C in the absence of light. Samples of 10 μl were taken *via* syringe and added immediately to a solution of tetra-*n*-butylammonium chloride (8 mM, 20 μl) in CH_2Cl_2. Conversion was determined *via* gas chromatography using a 1 μl sample. The chromatogram was run with an injector temperature of 250 ˚C and an initial oven temperature of 80 ˚C (0.5 mins), heated to 160 ˚C, at a rate of 10 ˚C.min^{-1}, and maintained at 160 ˚C (1 minute). The retention times were: 4.04 minutes for 4-phenyl-1-hexen-5-yne (**74**), 7.94 minutes for 3-phenylbicyclo[3.1.0]hex-

2-ene (**75**), 5.53 minutes for dimethyl allylpropargylmalonate (**77**), 7.73 minutes for **78** and 8.15 minutes for **79**.

Dimethyl allylpropargylmalonate (77)

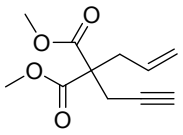

A protocol based on that reported by Ojima *et al.* was used.[111] Sodium methoxide (1.63 g, 30.2 mmol, 1.3 equiv.) was dissolved in methanol (10 ml, dry) and a solution of dimethyl allylmalonate (3.75 ml, 23.3 mmol, 1 equiv.) in methanol (6 ml) was added dropwise under an atmosphere of N_2 and the solution stirred (30 min, r.t.). Propargyl bromide (80% w/v in toluene, 3.10 ml, 27.8 mmol, 1.2 equiv.) was added in a slow stream and the solution stirred at 45 ˚C for 2 hours. The solution was cooled to 0 ˚C, quenched with water (10ml), extracted with diethyl ether, dried ($MgSO_4$), filtered and reduced *in vacuo*. The crude oil was purified by Kugelrohr distillation (0.7 mm Hg, 90 ˚C) to give the title compound as a colourless oil (3.61 g, 17.2 mmol, 74%). ^{1}H NMR (400 MHz, $CDCl_3$) 5.60 (m, 1H), 5.20-5.10 (m, 2H), 3.73 (s, 6H), 2.79, (dt, J = 7.5 and 1.0 Hz, 2H) and 2.78 (d, J = 2.6 Hz, 2H), 2.01 (t, J = 2.6 Hz, 1H). ^{13}C NMR (100 MHz, $CDCl_3$) δ 170.0, 131.5, 119.8, 78.5, 71.4, 56.7, 52.5, 36.3, 22.5. ESI$^+$-MS *m/z* 233.1 (85%, $[MNa]^+$), 211.1 (100%, $[MH]^+$), 179.1 (27%, $[M\text{-}MeO]^+$), 151.1 (35%), 137.1 (10%), 119.1 (13%), 91.1 (11%). ESI$^+$-HRMS calcd. for.$C_{11}H_{15}O_4$ ($[MH]^+$) 211.0965; found 211.0969. Data in accordance with the literature.[111]

General procedure for the Au catalysed cycloisomerisation of 1,1'-(1*E*)-hex-1-en-5-yne-1,4-diyldibenzene (81).

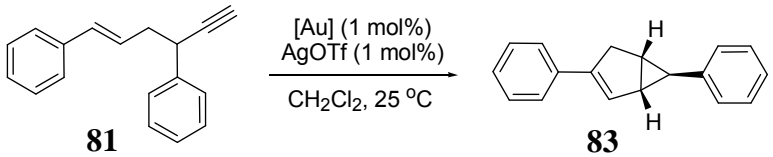

81 **83**

To a solution of 1,1'-(1*E*)-hex-1-en-5-yne-1,4-diyldibenzene (**81**) (50.0 mg, 216 μmol, 1 equiv.) in CH_2Cl_2 (0.5 M), AgOTf (0.6 mg, 2.1 μmol, 0.01 equiv.) and Au complex (2.1 μmol, 0.01 equiv.) were added. The solution was stirred at 25 ˚C for 30 minutes and filtered through a plug of silica-gel which was washed with dichloromethane (2 ml). The solution was reduced *in vacuo* and conversion was analysed by ^{1}H NMR spectroscopy. For characterisation purposes the product can be purified by column chromatography using

petroleum ether (40-60) as eluent. Fractions containing the product were combined and reduced *in vacuo* to give the title compound as a white powder.

1,1'-(1*E*)-Hex-1-en-5-yne-1,4-diyldibenzene (81)

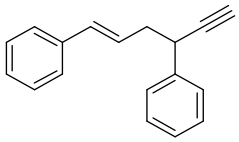

Prepared by a protocol reported by Florio and Troisi.[116] Diisopropyl amine (4.83 ml, 34.6 mmol, 1.2 equiv.) was dissolved in tetrahydrofuran (20 ml, dry) under an atmosphere of N_2 and cooled to -78 ˚C. *n*-Butyl lithium (2 M in hexanes, 13.8 ml, 34.6 mmol, 1.2 equiv.) was added dropwise and the solution warmed slowly to 0 ˚C and then cooled to -78 ˚C. *trans*-Cinnamyl chloride (**82**) (4.4 ml, 29 mmol, 1 equiv.) was added dropwise, stirred (-78 ˚C, 30 minutes) and warmed to ambient temperature. The reaction was quenched (saturated aq. NH_4Cl) and extracted with diethyl ether, washed (water, brine), dried ($MgSO_4$), filtered and reduced *in vacuo*. Purification was achieved by Kugelrohr distillation (2 mmHg, 150 ˚C) to give the title compound as a colourless oil (1.46 g, 6.29 mmol, 44%). ^{1}H NMR (400 MHz, $CDCl_3$) δ 7.50-7.26 (m, 10H), 6.50 (app. d, *J* = 15.8 Hz, 1H), 6.34 (app. dt, *J* = 15.8 and 7.3 Hz, 1H), 3.86 (m, 1H), 2.74 (m, 2H), 2.39 (m, 1H). ^{13}C NMR (100 MHz, $CDCl_3$) δ 140.6, 137.3, 132.3, 128.5, 128.4, 127.4, 127.1, 126.9, 126.8, 126.1, 85.3, 71.7, 41.6, 38.0. EI$^+$-MS *m/z* 232.1 (10%, $[M]^+$), 217.1 (4%), 204.1 (1%), 191.1 (1%), 154.1 (1%), 117.1 (100%, $[PhC_3H_4]^+$), 115.1 (46%), 91.1 (12%). EI$^+$-HRMS calcd. for. $C_{18}H_{16}$ ($[M^+]$) 232.1252; found 232.1244. Data in accordance with the literature.[116]

3,6-Diphenylbicyclo[3.1.0]hex-2-ene (83)

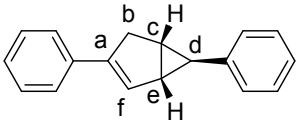

Preparation by the general procedure gave the title compound as a white solid (from 100 mg, 431 μmol, of 1,1'-(1*E*)-hex-1-en-5-yne-1,4-diyldibenzene (**81**) and 3.2 mg, 4.2 μmol, of **68b**) (88.9 mg, 383 μmol, 90%). ^{1}H NMR (400 MHz, $CDCl_3$) δ 7.49 (m, 2H, aromatic C*H*), 7.40-7.21 (m, 6H, aromatic C*H*), 7.11-7.08 (m, 2H, aromatic C*H*), 6.55 (dd, *J* = 3.9 and 1.9 Hz, 1H, f C*H*), 3.24 (ddd, *J* = 17.3, 7.0 and 1.9 Hz, 1H, b CH_2), 3.02 (d, *J* = 17.3 Hz, 1H, b CH_2), 2.33 (m, 1H, e C*H*), 2.15 (m, 1H, c C*H*), 1.61 (app. t, *J* = 3.0 Hz, 1H, d C*H*) . ^{13}C NMR (101 MHz, $CDCl_3$) δ 142.7 (a *C*), 141.3 (aromatic *C*), 136.2 (aromatic *C*), 128.4 (f *C*H), 128.3 (aromatic *C*H), 128.3 (aromatic *C*H), 127.0 (aromatic *C*H), 125.3

(aromatic *C*H), 125.2 (aromatic *C*H), 125.2 (aromatic *C*H), 37.3 (b *C*H$_2$), 36.8 (e *C*H), 35.4 (d *C*H), 27.5 (c *C*H). IR (CH_2Cl_2, cm^{-1}) υ_{max} 3303 (w), 3064 (m), 3033 (s), 2903 (m), 2837 (m), 2359 (m), 2342 (m), 1947 (w), 1876 (w), 1804 (w), 1701 (w), 1606 (s), 1958 (s), 1493 (s), 1453 (m), 1446 (m), 1325 (m), 1304 (m), 1210 (m), 1173 (m), 1154 (m), 1075 (m), 1058 (m). EI$^+$-MS *m/z* 232 (100%, $[M]^+$), 215 (26%), 202 (14%), 154 (14%, $[M\text{-}Ph]^+$), 141 (50%), 128 (20%), 115 (24%), 91 (64%). EI$^+$-HRMS calcd. for $C_{18}H_{16}$ ($[M]^+$) 232.1252; found 232.1255.

Dimethyl diallylmalonate (84)

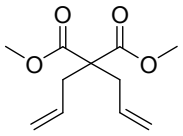

Prepared by a protocol reported by Harrowven *et al.*.[149] Sodium hydride (60% in mineral oil, 3.67 g, 91.7 mmol, 3.5 equiv.) was suspended in dry tetrahydrofuran (50 ml) under an inert atmosphere and cooled to 0 ˚C. A solution of dimethyl malonate (2.94 ml, 25.7 mmol, 1 equiv.) in dry tetrahydrofuran (20 ml) was added dropwise and the solution stirred (r.t., 2 h). The solution was cooled to 0 ˚C and allyl bromide (5.58 ml, 64.5 mmol, 2.5 equiv.) was added dropwise and the mixture stirred (r.t., 16 h). The solution was filtered through a pad of Celite™ and eluted with hexane. The filtrate was concentrated to a yellow oil *in vacuo* and purified by column chromatography, eluting with petroleum ether (40-60):ethyl acetate 95:5, to give the title compound as a colourless oil (3.31 g, 19.3 mmol, 75%). ^{1}H NMR (400 MHz, $CDCl_3$) δ 5.60 (m, 2H), 5.07-5.01 (m, 4H), 3.65 (s, 6H), 2.57 (d, *J* = 7.5 Hz, 4H). ^{13}C NMR (100 MHz, $CDCl_3$) δ 171.0, 132.1, 119.1, 57.5, 52.2, 36.8. ESI$^+$-MS *m/z* 235.1 (100%, $[MNa]^+$), 213.1 (5%), 181.1 (4%), 149.1 (5%), 121.1 (4%). ESI$^+$-HRMS calcd. for $C_{11}H_{16}NaO_4$ ($[MNa]^+$) 235.0941; found 235.0942. Data in accordance with the literature.[149]

Ethyl 4-phenyl-1-hepten-5-yn-7-oate (85)

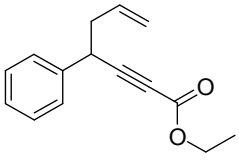

A protocol based on that reported by Cai *et al.* was used.[117] 4-Phenyl-1-hexen-5-yne (396 mg, 2.54 mmol, 1 equiv.) was dissolved in tetrahydrofuran and cooled to -78 ˚C. *n*-Butyl lithium (1.84 M, 1.38 ml, 2.55 mmol, 1 equiv.) was added dropwise and stirred at -78 ˚C

for 30 minutes. Ethyl chloroformate (0.360 ml, 3.79 mmol, 1.5 equiv.) was added dropwise and stirred at -78 ˚C for 30 minutes. The orange solution was warmed to ambient temperature resulting in a white precipitate. The reaction was quenched (saturated aq. NH_4Cl) and the product was extracted with diethyl ether, washed (brine, water), dried ($MgSO_4$), filtered and reduced *in vacuo* to give an orange oil. The crude product was purified by column chromatography on silica-gel, eluting with petroleum ether (40-60):ethyl acetate 100:0 to 95:5, followed by Kugelrohr distillation (0.7 mm Hg, 120 ˚C), to give the title compound as a colourless oil (0.373 g, 1.63 mmol, 64%). ^{1}H NMR (400 MHz, $CDCl_3$) 7.38-7.30 (m, 4H), 7.30-7.23 (m, 1H), 5.80 (ddt, *J* = 16.9, 10.4 and 7.0 Hz, 1H), 5.10 (dq, *J* = 8.0 and 1.5 Hz, 1H), 5.07 (t, *J* = 1.3 Hz, 1H), 4.22 (q, *J* = 7.1 Hz, 2H), 3.81 (dd, *J* = 7.9 and 6.5 Hz, 1H), 2.57 (m, 2H), 1.30 (t, *J* = 7.1 Hz, 3H). ^{13}C NMR (100 MHz, $CDCl_3$) δ 153.7, 138.8, 134.1, 128.6, 127.4, 127.2, 117.8, 89.0, 75.6, 61.8, 41.4, 37.7, 13.9. IR (Neat, cm^{-1}) υ_{max} 3648 (w), 3469 (br, m), 3064 (w), 2981 (w), 2371 (w), 2233 (s), 2161 (w), 2031 (m), 1977 (m), 1737 (w), 1707 (s), 1674 (m), 1619 (w), 1597 (m), 1494 (w), 1449 (m), 1394 (w), 1367 (m), 1301 (w), 1247 (s), 1184 (m), 1095 (s), 1017 (m), 920 (m), 858 (m), 752 (m), 698 (m). ESI$^+$-MS *m/z* 385.1 (15%), 346.2 (27%), 318.2 (16%), 299.1 (13%), 283.1 (22%), 267.1 (12%, $[MK]^+$), 251.1 (100%, $[MNa]^+$), 229.1 (54%, $[MH]^+$), 217.1 (11%), 187.1 (22%), 155.1 (12%), 142.0 (28%), 123.0 (20%), 97.0 (22%), 83.0 (73%), 67.0 (10%). ESI$^+$-HRMS calcd. for. $C_{15}H_{16}NaO_2$ ($[MNa]^+$) 251.1043; found 251.1037.

Ethyl-2,4-dimethyl-4-pentenoate (92)

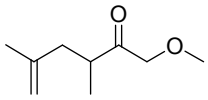

Prepared by a protocol reported by Wollowitz and Halpern.[119] Sodium metal (0.582 g, 25.3 mmol, 1.2 equiv.) was dissolved in ethanol (45 ml, dry) and the solution cooled to ambient temperature. Ethyl-2-methylacetoacetate (**89**) (3.00 ml, 21.3 mmol, 1 equiv.) and 3-chloro-2-methyl propene (2.80 ml, 28.5 mmol, 1.35 equiv.) were added and the solution refluxed (3 hours). After cooling to ambient temperature, KOH (5.00 g, 89.3 mmol, 4.2 equiv.) was added and stirred (r.t., 18 hours). The solution was reduced to dryness *in vacuo*, dissolved in water (50 ml), washed with diethyl ether (15 ml) and acidified (conc. HCl). The product was extracted with diethyl ether (3 x 25 ml), dried ($MgSO_4$), filtered and reduced *in vacuo* to give a yellow oil. The crude oil was dissolved in a mixture of toluene (20 ml), ethanol (10 ml) and sulphuric acid (conc., 3 drops) and refluxed in Dean Stark

apparatus for 20 hours. The volume was reduced to half *in vacuo* and diethyl ether (15 ml) added. The solution was washed with water (1 x 15 ml), saturated aq. $NaHCO_3$ (2 x 15 ml), water (1 x 15 ml) and brine (1 x 10ml), dried (K_2CO_3), filtered and reduced *in vacuo* to give a yellow oil. Purification was achieved by Kugelrohr distillation (1 mmHg, 30 ˚C) to give the title compound as a colourless oil (2.54 g, 16.3 mmol, 76%). ^{1}H NMR (400 MHz, $CDCl_3$) δ 4.73 (m, 1H), 4.67 (m, 1H), 4.09 (app. q, *J* = 7.0 Hz, 2H), 2.60 (m, 1H), 2.38 (dd, *J* = 14.1 and 7.5 Hz, 1H), 2.05 (dd, *J* = 14.1 and 7.5, 1H), 1.68 (s, 3H), 1.21 (t, *J* = 7.1 Hz, 3H), 1.10 (d, *J* = 7.1 Hz, 3H). ^{13}C NMR (100 MHz, $CDCl_3$) δ 176.3, 128.1, 112.1, 60.1, 41.8, 37.7, 26.8, 22.0, 16.7. EI$^+$-MS *m/z* 156 (4%, $[M]^+$), 141 (3%, $[M\text{-}Me]^+$), 111 (8%, $[M\text{-}OEt]^+$), 95 (2%, $[M\text{-}O_2Et]^+$), 83 (100%, $[M\text{-}CO_2Et]^+$), 67 (15%), 55 (51%), 41 (26%). Data in accordance with the literature.[119]

1-Chloro-2-phenylacetylene (93)

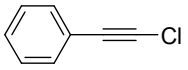

Prepared by a protocol reported by Barluenga *et al.*.[150] Phenyl acetylene (7.65 ml, 69.7 mmol, 1 equiv.) was dissolved in tetrahydrofuran (300 ml) under an atmosphere of N_2. Lithium aluminium hydride (95%, 0.90 g, 23.7 mmol, 0.33 equiv.) was added and the mixture was stirred (r.t., 1 hour) resulting in effervescence. *N*-Chlorosuccinimide (9.27 g, 69.7 mmol, 1 equiv.) was added and the solution stirred (r.t., 30 mins). Water (500 ml) was added and the solution extracted with dichloromethane (3 x 500 ml), dried ($MgSO_4$), filtered and reduced *in vacuo*. Purification was achieved by Kugelrohr distillation (3 mmHg, 50 ˚C) to give the title compound as a colourless oil (3.13 g, 22.9 mmol, 33%). ^{1}H NMR (400 MHz, $CDCl_3$) δ 7.67-7.27 (m, 5H). ^{13}C NMR (100 MHz, $CDCl_3$) δ 133.0, 128.6, 128.4, 122.0, 69.3, 67.2. EI$^+$-MS *m/z* 136 (44%, $[M]^+$), 102 (100%, $[MH\text{-}Cl]^+$), 76 (17%), 50 (6%). Data in accordance with the literature.[150]

Isobutyl (2*E*)-4-chlorobut-2-enoate (104)

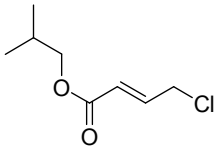

Prepared by a protocol similar to that reported by Mellegaard-Waetzig *et al.*.[124b] Phenylselenyl chloride (408 mg, 2.13 mmol, 0.1 equiv.) was dissolved in acetonitrile (dry, 50 ml) under an atmosphere of N_2. Molecular sieves (4 Å, a few) and isobutyl vinyl acetate (**103**) (3.37 ml, 21.1 mmol, 1 equiv.) were added, followed by dropwise addition of *N*-

chlorosuccinimide (3.09 g, 23.2 mmol, 1.1 equiv.) in acetonitrile (50 ml). The solution was stirred (r.t., 18 hours) and reduced to 10 ml *in vacuo*. Diethyl ether was added and the mixture filtered, washed (water), dried ($MgSO_4$), filtered and reduced *in vacuo*. The crude oil was purified by distillation (80 ˚C, 0.7 mm Hg) to give the title compound as a colourless oil (719 mg, 4.07 mmol, 19%). ^{1}H NMR (400 MHz, $CDCl_3$) δ 6.92 (dt, *J* = 15.4 and 6.1 Hz, 1H), 6.07 (dt, *J* = 15.4 and 1.5 Hz, 1H), 4.12 (dd, *J* = 6.1 and 1.5 Hz, 2H), 3.89 (d, *J* = 6.7 Hz, 2H), 1.91 (app. nonet, *J* = 6.5 Hz, 1H), 0.89 (d, *J* = 6.7 Hz, 6H). ^{13}C NMR (100 MHz, $CDCl_3$) δ 165.5, 141.5, 123.9, 70.6, 42.4, 27.6, 18.9. ESI$^+$-MS *m/z* 213.1 (1%), 199.1 (3%, $[MNa]^+$), 177.1 (21%, $[MH]^+$), 146.1 (1%), 121.0 (100%, $[M\text{-}C_4H_7]^+$), 101.0 (3%). ESI$^+$-HRMS calcd. for. $C_8H_{14}ClO_2$ ($[MH]^+$) 177.0677; found 177.0676. Data in accordance with the literature.[124b]

(2*Z*)-4-(Benzyloxy)but-2-en-1-ol (110)

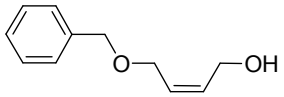

Prepared by a protocol reported by Schomaker *et al.*.[125] Sodium hydride (95%, 1.32 g, 55.0 mmol, 1.1 equiv.) was dissolved in tetrahydrofuran/dimethyl sulphoxide 4:1 (dry, 250 ml) and *cis*-butene-1,4-diol (**109**) (4.10 ml, 49.9 mmol, 1 equiv.) in tetrahydrofuran (120 ml) was added dropwise at 0 ˚C. The mixture was stirred (r.t., 30 min) and benzyl bromide (6.61 ml, 55.6 mmol, 1.1 equiv.) in tetrahydrofuran (120 ml) was added dropwise at room temperature. Tetraethyl ammonium iodide (9.25 g, 36.0 mmol, 0.72 equiv.) was added, the mixture stirred (70 ˚C, 15 hours) and water (500 ml) added. The product was extracted with diethyl ether, washed (brine), dried (Na_2SO_4), filtered and reduced *in vacuo* to give an orange oil. Purification was achieved by Kugelrohr distillation (130-140 ˚C, 1 mmHg) to give the title compound as a colourless oil (7.13g, 40.1 mmol, 80%). ^{1}H NMR (400 MHz, $CDCl_3$) δ 7.43-7.27 (m, 5H, aromatic C*H*), 5.77 (m, 2H, alkene C*H*), 4.53 (s, 2H, benzyl CH_2), 4.14 (d, *J* = 5.9 Hz, 2H, vinyl CH_2), 4.09 (d, *J* = 5.7 Hz, 2H, vinyl CH_2), 2.75-2.50 (br s, 1H, O*H*). ^{13}C NMR (100 MHz, $CDCl_3$) δ 137.7, 132.4, 128.4, 127.9, 127.8, 127.7, 72.3, 65.5, 58.4. ESI$^+$-MS *m/z* 393.2 (68%), 375.2 (46%), 349.1 (10%), 323.1 (11%), 305.1 (40%), 291.1 (15%, $[M + Bn\text{-}H]^+$), 229.1 (11%), 201.1 (60%, $[MNa]^+$), 181.1 (13%), 161.1 (13%, $[M\text{-}OH]^+$), 143.1 (18%), 131.1 (11%), 117.1 (4%), 91.1 (100%, $[Bn]^+$). EI$^+$-MS *m/z* 160 (1%), 131 (1%), 107 (9%), 105 (18%), 91 (100%), 79 (8%), 77 (9%), 65 (9%). ESI$^+$-HRMS calcd. for. $C_{11}H_{14}NaO_2$ ($[MNa]^+$) 201.0886; found 201.0888. Data in accordance with the literature.[125]

Benzyl (2Z)-4-chlorobut-2-en-1-yl ether (111)

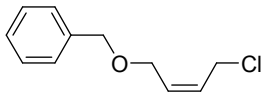

A protocol based on that reported by Gansäuer *et al.* was used.[126] (2*Z*)-4-(Benzyloxy)but-2-en-1-ol (**110**) (1.99 g, 11.2 mmol, 1 equiv.) and triethylamine (2.33 ml, 16.8 mmol, 1.5 equiv.) were dissolved in dichloromethane (22 ml) under an atmosphere of N_2 and mesyl chloride (1.74 ml, 22.4 mmol, 2 equiv.) was added dropwise at 0 ˚C and stirred (4 h, 0 ˚C-r.t.). The solution was reduced *in vacuo* and tetrahydrofuran (30 ml) and lithium chloride (1.41 g, 33.6 mmol, 3 equiv.) added and stirred (r.t., 2 hours). Cold water (20 ml) was added and the organic phase was washed (saturated aq. $NaHCO_3$, water and brine), dried ($MgSO_4$), filtered and reduced *in vacuo*. The crude oil was dissolved in hexane (20 ml) washed with water, dried ($MgSO_4$), filtered and reduced *in vacuo*. The crude oil was purified by Kugelrohr distillation (110 ˚C, 0.7 mm Hg) to give the title compound as a colourless oil (1.74 g, 8.85 mmol, 79%). ^{1}H NMR (400 MHz, $CDCl_3$) δ 7.38-7.29 (m, 5H), 5.87-5.78 (m, 2H), 4.54 (s, 2H), 4.16-4.14 (m, 2H), 4.12-4.10 (m, 2H). ^{13}C NMR (100 MHz, $CDCl_3$) δ 137.8, 130.7, 128.4, 128.4, 127.7, 127.7, 72.3, 65.0, 39.1 EI$^+$-MS *m/z* 161 (2%, $[M\text{-}Cl]^+$), 131 (5%), 126 (5%), 107 (4%), 105 (5%, $[M\text{-}PhCH_2]^+$), 91 (100%, $[PhCH_2]^+$), 79 (14%), 77 (14%), 65 (15%). ESI$^+$-MS *m/z* 311.0 (9%), 291.1 (100%, $[MNa\text{-}Cl+OBn]^+$), 281.1 (11%), 271.1 (51%), 233.1 (4%), 219.0 (17%, $[MNa]^+$), 202.1 (3%), 179.1 (29%, $[M\text{-}Cl+OH_2]^+$), 161.1 [16%, $[M\text{-}Cl]^+$), 143.1 (33%), 131.1 (5%), 117.1 (9%), 91.1 (69%, $[PhCH_2]^+$). ESI$^+$-HRMS calcd. for. $C_{11}H_{13}ClNaO$ ($[MNa]^+$) 219.0547; found 219.0548. Data in accordance with the literature.[151]

2-[(Z)-3-Hydroxy-1-propenyl] phenol (119)

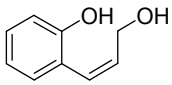

Prepared by a protocol reported by Wang *et al.*.[127] Coumarin (**118**) (2.51 g, 17.2 mmol, 1 equiv.) was dissolved in diethyl ether (dry, 60 ml) under an atmosphere of N_2 and cooled to 0 ˚C. Lithium aluminium hydride (1.30 g, 34.3 mmol, 2 equiv.) in diethyl ether (30 ml) was added *via* cannula and the mixture stirred (0 ˚C, 15 min) followed by dropwise addition of HCl (1 M aq., 120 ml) to give an orange solution/suspension. The product was extracted with diethyl ether, dried ($MgSO_4$), filtered and reduced *in vacuo*. Purification by recrystallisation (dichloromethane/ethyl acetate) yielded the title compound as a white powder (0.872 g, 5.81 mmol, 34%). ^{1}H NMR {400 MHz, $(CD_3)_2CO$} δ 8.37 (br s, 1H, Ar-

O*H*), 7.08 (m, 2H, aromatic C*H*), 6.88 (app. d, *J* = 7.4 Hz, 1H, aromatic C*H*), 6.79 (tdd, *J* = 7.9, 1.2 and 0.5 Hz, 1H, aromatic C*H*), 6.61 (dq, *J* = 11.8 and 0.4 Hz, 1H, benzylic C*H*), 5.83 (dt, *J* = 11.8 and 6.4 Hz, 1H, alkene C*H*), 4.29 (dd, *J* = 6.4 and 1.7 Hz, 2H, CH_2), 4.02 (br s, 1H, CH_2O*H*). ^{13}C NMR {100 MHz, $(CD_3)_2CO$} δ 155.6, 132.7, 131.0, 129.3, 125.9, 124.7, 119.9, 116.1, 59.7. EI$^+$-MS *m/z* 284 (35%), 266 (5%), 237 (4%), 177 (4%), 159 (32%), 151 (5%), 145 (7%), 133 (75%, [M-OH]$^+$), 131 (51%), 121 (45%), 107 (100%, [M-$HOCH_2C$]$^+$), 91 (36%), 77 (64%), 65 (6%). Data in accordance with the literature.[127]

(2*Z*)-3-(2-Methoxyphenyl)prop-2-en-1-ol (120)

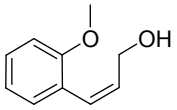

Prepared by a protocol similar to that reported by Huang *et al.*.[128] Potassium carbonate (231 mg, 1.67 mmol, 1 equiv.) and iodomethane (237 mg, 1.67 mmol, 1 equiv.) were suspended in acetone (dry, 4 ml). 2-[(Z)-3-Hydroxy-1-propenyl] phenol (**119**) (250 mg, 1.67 mmol, 1 equiv.) was added and the mixture refluxed (3 hours). The solution was cooled to ambient temperature, filtered, reduced *in vacuo* and purified by column chromatography, eluting with dichloromethane:methanol 92:2, to give the title compound as a yellow oil (165 mg, 1.01 mmol, 60%). ^{1}H NMR (400 MHz, $CDCl_3$) δ 7.27 (td, *J* = 8.0 and 1.8 Hz, 1H, aromatic C*H*), 7.11 (dd, *J* = 7.5 and 1.7 Hz, 1H, aromatic C*H*), 6.89 (dd, *J* = 15.6 and 7.9 Hz, 2H, aromatic C*H*), 6.69 (d, *J* = 11.6 Hz, 1H, benzylic C*H*), 5.93 (dt, *J* = 11.6 and 6.7 Hz, 1H alkene C*H*), 4.32 (dd, *J* = 6.7 and 1.3 Hz, 2H, CH_2), 3.85 (s, 3H, OCH_3), 1.67 (br s, 1H, CH_2O*H*). ^{13}C NMR (100 MHz, $CDCl_3$) δ 156.8, 130.9, 130.2, 128.8, 126.7, 125.3, 120.1, 110.4, 59.7, 55.4. ESI$^+$-MS *m/z* 187.1 (100%, [MNa]$^+$), 172.1 (8%). ESI$^+$-HRMS calcd. for. $C_{10}H_{12}NaO_2$ ([MNa]$^+$) 187.0730; found 187.0729. Data in accordance with the literature.[152]

1-[(1*Z*)-3-Chloroprop-1-en-1-yl]-2-methoxybenzene (121)

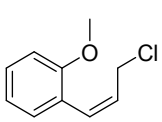

Prepared by a protocol based on that of Gansäuer *et al.*.[126] (2*Z*)-3-(2-Methoxyphenyl)prop-2-en-1-ol (**120**) (1.74 g, 10.6 mmol, 1 equiv.) and collidine (2.11 ml, 16.0 mmol, 1.5 equiv.) were dissolved in dry tetrahydrofuran (30 ml) under N_2 and cooled to 0 ˚C. Mesyl chloride (1.65ml, 21.2 mmol, 2 equiv.) was added and stirred (6 hours, 0 ˚C - r.t.). Lithium chloride (1.78g, 42.4 mmol, 4 equiv.) was added and the mixture stirred

(r.t., 15 hours). Cold water (20 ml) was added, the product extracted with diethyl ether, washed (20ml 2 M aq. HCl, saturated aq. $NaHCO_3$, water and brine), dried ($MgSO_4$), filtered and reduced *in vacuo*. The crude product was dissolved in hexane, washed (water), dried ($MgSO_4$), filtered, reduced *in vacuo* and purified by column chromatography, eluting with hexane:ethyl acetate 6:1, to give the title compound as a colourless oil (1.59 g, 8.76 mmol, 83%). ^{1}H NMR (400 MHz, $CDCl_3$) δ 7.31 (m, 2H, aromatic C*H*), 6.98 (dt, *J* = 7.5 and 0.8 Hz, 1H, aromatic C*H*), 6.91 (dd, *J* = 8.6 and 0.8 Hz, 1H, aromatic C*H*), 6.76 (d, *J* = 11.3 Hz, 1H, benzylic C*H*), 5.93 (dt, *J* = 11.3 and 8.0 Hz, 1H, alkene C*H*), 4.23 (dd, *J* = 8.0 and 1.0 Hz, 2H, CH_2), 3.85 (s, 3H, OCH_3). ^{13}C NMR (100 MHz, $CDCl_3$) δ 157.0 (aromatic *C*), 129.9 (aromatic *C*H), 129.3 (aromatic *C*H), 129.1 (aromatic *C*H), 126.8 (aromatic *C*H), 124.4 (aromatic *C*), 120.3 (alkene benzyl *C*H), 110.8 (alkene *C*H), 55.4 (O*C*H_3), 41.3 (*C*H_2). EI$^+$-MS *m/z* 182 (10%, [M]$^+$), 163 (2%), 155 (6%), 147 (100%, [M-Cl]$^+$), 131 (46%), 121 (20%), 115 (34%, [M-Cl-OMe]$^+$), 103 (28%), 91 (73%), 77 (38%), 63 (12%), 51 (19%). EI$^+$-HRMS calcd. for. $C_{10}H_{11}OCl$ ([M]$^+$) 182.0498; found 182.0502.

1,1'-(1*Z*)-Hex-1-en-5-yne-1,4-diylbis(2-methoxybenzene) (122)

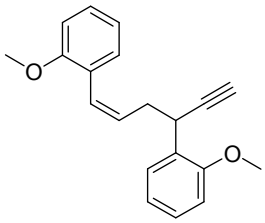

A protocol based on that of Florio and Troisi was used.[116] 1-[(1*Z*)-3-Chloroprop-1-en-1-yl]-2-methoxybenzene (**121**) (0.647 g, 3.55 mmol, 1 equiv.) was dissolved in tetrahydrofuran (10 ml) and cooled to -78 ˚C. Lithium diisopropylamide (1.3 M in hexanes, 3.28 ml, 4.26 mmol, 1.2 equiv.) was added dropwise and the solution stirred (-78 - 0 ˚C, 2 hours). Saturated aq. NH_4Cl was added and the product extracted with diethyl ether, washed (water, brine), dried ($MgSO_4$), filtered and reduced *in vacuo*. The crude product was purified by column chromatography, eluting with hexane, to give the title compound as a colourless oil (0.241 g, 0.826 mmol, 47%). ^{1}H NMR (400 MHz, $CDCl_3$) δ 7.57 (dd, *J* = 7.6 and 1.7 Hz, 1H, aromatic CH), 7.26-7.18 (m, 3H, aromatic CH), 6.96 (m, 1H, aromatic CH), 6.91-6.82 (m, 3H), 6.63 (d, *J* = 11.7 Hz, 1H, PhC*H*=CH), 5.94 (dt, *J* = 11.7 and 7.4 Hz, 1H, PhCH=C*H*), 4.28-4.23 (m, 1H, PhC*H*), 3.82 (s, 3H, OCH_3), 3.78 (s, 3H, OCH_3), 2.81-2.73 (m, 1H, CH_2), 2.65-2.57 (m, 1H, CH_2), 2.29 (d, *J* = 2.5 Hz, 1H, alkyne C*H*). ^{13}C NMR (100 MHz, $CDCl_3$) δ 157.0 (*C*), 156.1 (*C*), 130.0 (*C*H), 129.4 (*C*H), 129.0 (*C*), 128.4 (*C*H), 128.0 (*C*H), 127.9 (*C*H), 126.3 (*C*), 126.0 (*C*H), 120.6 (*C*H), 119.9 (*C*H),

110.3 (*C*H), 110.3 (*C*H), 85.8 (*C*), 70.7 (*C*H), 55.4 (CH_3), 55.2 (CH_3), 34.9 (CH_2), 31.2 (*C*H). Assignments from DEPT 135. IR (neat, cm^{-1}) υ_{max} 3295 (w), 3061 (w), 3025 (w), 2932 (m), 2372 (w), 2161 (s), 2031 (m), 1977 (m), 1671 (w), 1598 (s), 1489 (s), 1463 (s), 1437 (m), 1397 (w), 1374 (w), 1289 (m), 1241 (s), 1177 (w), 1162 (w), 1108 (m), 1051 (w), 1028 (m), 750 (s), 699 (m), 636 (w). ESI^+-MS *m/z* 343.3 (9%), 311.3 (3%), 293.2 (100%, $[MH]^+$), 265.1 (4%), 221.1 (3%), 185.1 (5%), 159.1 (6%), 121.1 (9%). ESI^+-HRMS calcd. for $C_{20}H_{21}O_2$ ($[MH]^+$) 293.1536; found 293.1525.

3,6-Bis(2-methoxyphenyl)bicyclo[3.1.0]hex-2-ene (123)

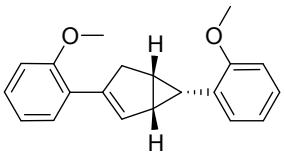

1,1'-(1*Z*)-Hex-1-en-5-yne-1,4-diylbis(2-methoxybenzene) (**122**) (0.241 g, 826 μmol, 1 equiv.) was dissolved in dichloromethane (1.5 ml), [$AuBr_2$(*N*-dbs)(I^tPe)] (**67b**) (6.5 mg, 8.2 μmol, 0.01 equiv.) and $Ag[Al(OC(CF_3)_3)_4]$ (**76**) (8.9 mg, 8.3 μmol, 0.01 equiv.) were added and the mixture stirred in the absence of light (r.t., 3 hours). The reaction mixture was filtered through a plug of silica-gel, eluting with dichloromethane, and reduced *in vacuo*. Partial purification was achieved by column chromatography, eluting with hexane, to give the title compound as a white solid {172 mg, 588 μmol, 71% (impure)}. ^1H NMR (400 MHz, $CDCl_3$) δ 7.27-7.24 (dd, *J* = 7.5, 1.7 Hz, 1H), 7.21-7.17 (app. dt, *J* = 7.7 and 1.7 Hz, 1H), 7.14-7.10 (app. dt, *J* = 7.8 and 1.7 Hz, 1H), 6.94-6.78 (m, 6H), 3.88 (s, 3H), 3.82 (s, 3H), 3.24 (dd, *J* = 17.2 and 7.0 Hz, 1H), 3.00 (app. d, *J* = 17.2 Hz, 1H), 2.28 (dq, *J* = 6.2 and 2.6 Hz, 1H)), 2.02 (td, *J* = 6.5 and 3.7 Hz, 1H), 1.93 (dd, *J* = 3.3 and 2.6 Hz, 1H). ^{13}C NMR (100 MHz, $CDCl_3$) δ 157.8, 151.4, 141.6, 141.1, 137.9, 133.3, 128.5, 127.6, 125.9, 124.1, 1205, 120.4, 110.8, 110.2, 55.5, 55.2, 39.2, 36.7, 28.6, 26.2. EI^+-MS *m/z* 292 (84%, $[M]^+$), 280 (6%), 515 (5%), 186 (14%), 171 (8%), 167 (10%), 149 (39%), 131 (9%), 121 (100%, $[PhOMeCH_2]^+$), 115 (7%), 91 (59%). EI^+-HRMS calcd. for $C_{20}H_{20}O_2$ ($[M]^+$) 292.1263; found 292.1471.

1,3-Diphenylprop-2-yn-1-one (128)

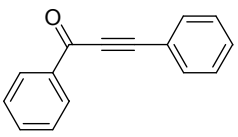

Prepared by a protocol reported by Cox *et al.*.[153] Benzoyl chloride (0.500 g, 413 μl, 3.56 mmol, 1.5 equiv.) and phenyl acetylene (242 mg, 260 μl, 2.37 mmol, 1 equiv.) were

dissolved in dry tetrahydrofuran (5 ml) under an atmosphere of N_2. $[PdCl_2(PPh_3)_2]$ (15.0 mg, 0.021 mmol, 0.009 equiv.) was added followed by copper(I) iodide (13.5 mg, 0.071 mmol, 0.03 equiv.) and the solution stirred (1 min). Triethylamine (300mg, 413 µl, 2.96 mmol, 1.25 equiv.) was added and the solution stirred (r.t., 2 hours). The mixture was diluted with diethyl ether, extracted with dichloromethane and washed with water. The organic fraction was dried ($MgSO_4$), filtered, reduced *in vacuo* and purified by column chromatography, eluting with petroleum ether (40-60):ethyl acetate 95:5, to give the title compound as a yellow oil (441 mg, 2.14 mmol, 90%). ^{1}H NMR (400 MHz, $CDCl_3$) δ 8.35-8.22 (m, 2H), 7.71-7.67 (m, 2H), 7.65-7.61 (m, 1H), 7.55-7.46 (m, 3H), 7.45-7.40 (m, 2H). ^{13}C NMR (101 MHz, $CDCl_3$) δ 178.1, 137.0, 134.2, 133.2, 130.9, 129.7, 128.8, 128.7, 120.2, 93.2, 87.0. EI$^+$-MS 206 (58 %, $[M]^+$), 178 (100%), 152 (8 %), 129 (58%), 101 (8%), 77 (7%), 75 (9%), 51 (6%). EI$^+$-HRMS calcd. for $C_{15}H_{10}O$ ($[M]^+$) 206.0732; found 206.0731. Data in accordance with the literature.[154]

General procedure for the tandem nucleophilic substitution-cycloisomerisation of propargyl alcohols

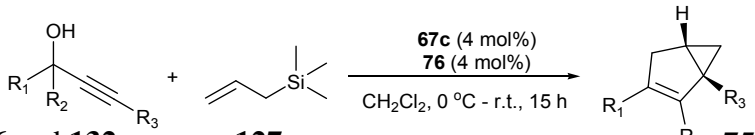

126 and **132** **127a** **75** and **133**

Propargyl alcohol (**126** and **132**) (378 µmol, 1 equiv.) was dissolved in dichloromethane (2 ml, 0.2 M) and allyltrimethylsilane (**127a**) (180 µl, 1.13 mmol, 3 equiv.) was added, followed by $Ag[Al(OC(CF_3)_3)_4]$ (**76**) (16 mg, 15 µmol, 0.04 equiv.) and $[AuBr_2(N\text{-tfs})(I^tPe)]$ (**67c**) (11 mg, 15 µmol, 0.04 equiv.). The solution was stirred in the dark at 0 °C and allowed to warm to ambient temperature over 15 hours. The solution was filtered through a plug of silica-gel which was washed with dichloromethane (2 ml). The solution was reduced *in vacuo* and conversion analysed by ^{1}H NMR spectroscopy. For characterisation purposes the products can be purified by column chromatography on silica-gel using petroleum ether (40-60) as eluent. Fractions containing the products were combined and reduced *in vacuo* to give the title compounds.

1-Phenyl-2-heptyn-1-ol (132b)

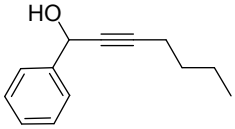

1-Hexyne (0.465 g, 0.650 ml, 5.66 mmol, 1.2 equiv.) was dissolved in tetrahydrofuran (15 ml) under an atmosphere of N_2 and cooled to -40 ˚C. *n*-Butyl lithium (2.5 M, 2.0 ml, 4.95 mmol, 1.05 equiv.) was added dropwise and the solution stirred (-50 ˚C, 30 mins). Benzaldehyde (0.500 g, 0.48 ml, 4.70 mmol, 1 equiv.) was added and the mixture was stirred and allowed to warm to ambient temperature overnight. The reaction was quenched with water, poured into saturated brine and extracted with diethyl ether. The solution was reduced *in vacuo* and purified by column chromatography, eluting with petroleum ether (40-60):ethyl acetate 9:1, to give the title compound as a colourless oil (0.709 g, 3.77 mmol, 80%). ^{1}H NMR (400 MHz, $CDCl_3$) δ 7.57-7.54 (m, 2H), 7.41-7.31 (m, 3H), 5.45 (t, *J* = 2.2 Hz, 1H), 2.45 (br s, 1H), 2.29 (td, *J* = 7.1, 2.1 Hz, 2H), 1.59-1.51 (m, 2H), 1.49-1.39 (m, 2H), 0.94 (t, *J* = 7.3 Hz, 3H). ^{13}C NMR (101 MHz, $CDCl_3$) δ 141.2, 128.4, 128.1, 126.6, 87.5, 79.9, 64.7, 30.6, 21.9, 18.4, 13.5. EI$^+$-MS 188 (62%, $[M]^+$), 170 (6%), 145 (47%), 131 (31%), 128 (41%), 117 (26%), 115 (46%), 106 (72%), 105 (100%), 91 (21%), 77 (96%), 67 (36%). EI$^+$-HRMS calcd. for $C_{13}H_{16}O$ ($[M]^+$) 188.1201; found 188.1194. Data in accordance with the literature.[155]

1-Phenyl-3-trimethylsilyl-2-propyn-1-ol (132c)

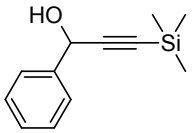

A protocol similar to that used for **132b** gave the title compound as a colourless oil (from 0.388 ml, 2.75 mmol, 1.1 equiv. of trimethylsilyl acetylene and 0.265 g, 2.50 mmol, 1 equiv. of benzaldehyde) (0.190 g, 0.931 mmol, 37%).^{1}H NMR (400 MHz, $CDCl_3$) δ 7.55 (d, *J* = 7.3 Hz, 2H, Ar*H*), 7.41-7.31 (m, 3H Ar*H*), 5.45 (d, *J* = 5.5 Hz, 1H, C*H*OH), 2.42 (d, *J* = 5.5 Hz, 1H, O*H*), 0.22 {s, 9H, Si(CH_3)$_3$}. ^{13}C NMR (101 MHz, $CDCl_3$) δ 140.3, 128.5, 128.3, 126.7, 104.9, 91.5, 64.9, -0.2. EI$^+$-MS 204 (50%, $[M]^+$), 187 (10%, $[M\text{-}OH]^+$), 173 (6%), 161 (100%, $[M\text{-}C_3H_9]^+$), 145 (6%), 128 (12%), 114 (81%), 105 (13%), 83 (13%), 77 (33%), 73 (57%). EI$^+$-HRMS calcd. for $C_{12}H_{16}OSi$ ($[M]^+$) 204.0970; found 204.0963. Data in accordance with the literature.[155]

1,3-Diphenyl-2-propyn-1-ol (132d)

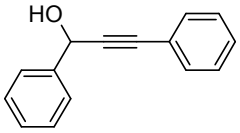

A protocol similar to that used for **132b** gave the title compound as a colourless oil (from 1.30 ml, 11 mmol, 1.1 equiv. of phenyl acetylene and 1.06 g, 10.0 mmol, 1 equiv. of benzaldehyde) (1.79 g, 8.61 mmol, 86%). ^{1}H NMR (400 MHz, $CDCl_3$) δ 7.67-7.63 (app. d, *J* = 7.2 Hz, 2H, Ar H), 7.53-7.50 (m, 2H, Ar H), 7.46-7.33 (m, 6H, Ar H), 5.72 (s, 1H, C*H*OH), 2.81 (br s, 1H, O*H*). ^{13}C NMR (101 MHz, $CDCl_3$) δ 140.6 (Ar *C*), 131.7 (Ar *C*H), 128.6 (Ar *C*H), 128.5 (Ar *C*H), 128.3 (Ar *C*H), 128.2 (Ar *C*H), 126.7 (Ar *C*H), 122.3 (Ar *C*), 88.7 (alkyne *C*), 86.5 (alkyne *C*), 64.9 (*C*HOH). EI$^+$-MS 208 (68%, $[M]^+$), 207 (100%), 191 (46%), 189 (32%), 178 (86%), 165 (29%), 129 (58%), 105 (33%), 102 (60%), 77 (42%), 51 (9%). EI$^+$-HRMS calcd. for $C_{15}H_{12}O$ ($[M]^+$) 208.0888; found 208.0883. Data in accordance with the literature.[155]

1-(2-Napthyl)-3-phenyl-2-propyn-1-ol (132e)

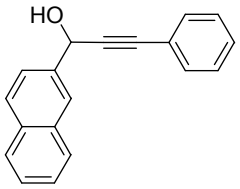

A protocol similar to that used for **132b** gave the title compound as a colourless oil (from 0.300 ml, 2.73 mmol, 1.1 equiv. of phenyl acetylene and 0.390 g, 2.50 mmol, 1 equiv. of 2-napthaldehyde) (0.608 g, 2.36 mmol, 94%). ^{1}H NMR (400 MHz, $CDCl_3$) δ 8.07 (s, 1H), 7.93-7.85 (m, 3H), 7.75 (dd, *J* = 8.6 and 1. 7 Hz, 1 H), 7.55-7.48 (m, 4H), 7.37-7.31 (m, 3H), 5.87 (d, *J* = 5.6 Hz, 1H), 2.42 (d, *J* = 6.0 Hz, 1H). ^{13}C NMR (101 MHz, $CDCl_3$) δ 137.9, 133.2, 133.1, 131.7, 128.6, 128.6, 128.3, 128.2, 127.7, 126.3, 126.3, 125.5, 124.6, 122.3, 88.7, 86.9, 65.2. EI$^+$-MS 258 (78% $[M]^+$), 241 (100%, $[M\text{-}OH]^+$), 239 (58%), 229 (43%), 215 (14%), 202 (6%), 181 (8%), 165 (8%), 155 (70%), 152 (16%), 127 (91%), 102 (76%), 77 (14%), 63 (7%), 51 (8%). EI$^+$-HRMS calcd. for $C_{19}H_{14}O$ ($[M]^+$) 258.1045; found 258.1043. Data in accordance with the literature.[155]

1-Mesityl-3-phenyl-2-propyn-1-ol (132f)

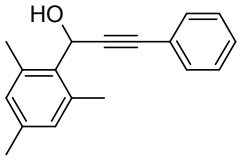

A protocol similar to that used for **132b** gave the title compound as a colourless oil (from 0.300 ml, 2.73 mmol, 1.1 equiv. of phenyl acetylene and 0.370 g, 2.50 mmol, 1 equiv. of 2,4,6-trimethylbenzaldehyde) (0.525 g, 2.10 mmol, 84 %). ^{1}H NMR (400 MHz, $CDCl_3$) δ 7.47-7.40 (m, 2H, Ar*H*), 7.34-7.28 (m, 3H, Ar*H*), 6.89 (s, 2H, Mes Ar*H*), 6.13 (d, *J* = 3.5 Hz, 1H, C*H*OH), 2.57 (s, 6H, *o*-CH_3), 2.29 (s, 3H, *p*-CH_3), 2.12 (d, *J* = 3.7 Hz, 1H, O*H*). ^{13}C NMR (101 MHz, $CDCl_3$) δ 137.8, 136.5, 133.5, 131.6, 130.0, 128.3, 128.2, 122.8, 88.8, 85.6, 60.7, 20.8, 20.3. EI$^+$-MS 250 (5%, $[M]^+$), 235 (100%), 219 (13%), 202 (14%), 192 (9%), 159 (8%), 147 (19%), 129 (8%), 119 (12%), 115 (10%), 105 (10%), 102 (15%), 91 (9%), 77 (8%). EI$^+$-HRMS calcd. for $C_{18}H_{18}O$ ($[M]^+$) 250.1358; found 250.1353.

1-(4-Chlorophenyl)-3-phenyl-2-propyn-1-ol (132g)

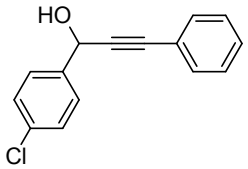

A protocol similar to that used for **132b** gave the title compound as a colourless oil (from 0.300 ml, 2.73 mmol, 1.1 equiv. of phenyl acetylene and 0.352 g, 2.50 mmol, 1 equiv. of 4-chlorobenzaldehyde) (0.433g, 1.78 mmol, 71%). ^{1}H NMR (400 MHz, $CDCl_3$) δ 7.58-7.55 (app. d, *J* = 8.5 Hz, 2H, Ar*H*), 7.49-7.46 (m, 2H, Ar*H*), 7.40-7.31 (m, 5H, Ar*H*), 5.68 (d, *J* = 2.7 Hz, 1H, C*H*OH), 2.39 (d, *J* = 3.9 Hz, 1H, O*H*). ^{13}C NMR (101 MHz, $CDCl_3$) δ 139.1 (Ar *C*), 134.2 (Ar *C*), 131.7 (Ar *C*H), 128.8 (Ar *C*H), 128.4 (Ar *C*H), 128.1 (Ar *C*H), 122.1 (Ar *C*), 88.2 (alkyne *C*), 87.0 (alkyne *C*), 64.4 (*C*HOH). EI$^+$-MS 242 (19% $[M]^+$), 241 (27%), 225 (12%), 207 (100%), 189 (17%), 178 (57%), 139 (15%), 129 (25%), 111 (14%), 102 (20%), 77 (15%), 75 (15%). EI$^+$-HRMS calcd. for $C_{15}H_{11}ClO$ ($[M]^+$) 241.0420; found 241.0429. Data in accordance with the literature.[155]

3-Phenyl-1-[4-(trifluoromethyl)phenyl]-2-propyn-1-ol (132h)

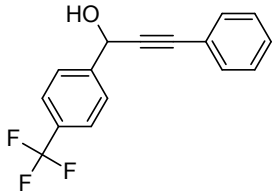

A protocol similar to that used for **132b** gave the title compound as a colourless oil (from 0.300 ml, 2.73 mmol, 1.1 equiv. of phenyl acetylene and 0.435 g, 0.341 ml, 2.50 mmol, 1 equiv. of 4-trifluoromethylbenzaldehyde) (0.671 g, 2.43 mmol, 97%). ^{1}H NMR (400 MHz, $CDCl_3$) δ 7.74 (d, *J* = 8.2 Hz, 2H, CF_3Ar*H*), 7.65 (d, *J* = 8.2 Hz, 2H, CF_3Ar*H*), 7.48-7.44 (m, 2H, Ph*H*), 7.38-7.29 (m, 3H, Ph*H*), 5.75 (s, 1H, C*H*OH), 3.19 (br s, 1H, O*H*). ^{13}C NMR (101 MHz, $CDCl_3$) δ 144.5, 131.7, 130.3 (q, *J* = 32 Hz), 128.8, 128.3, 126.9, 125.5 (q, *J* = 4 Hz), 124.0 (q, *J* = 272 Hz), 122.0, 88.0, 87.0, 64.2. ^{19}F (376 MHz, $CDCl_3$) δ -62.5 (s). EI$^+$-MS 276 (100%, $[M]^+$), 275 (99%), 259 (21%), 207 (76%), 178 (46%), 145 (22%), 131 (13%), 129 (28%), 103 (10%), 77 (14%). EI$^+$-HRMS calcd. for $C_{16}H_{11}F_3O$ ($[M]^+$) 276.0762; found 276.0767. Data in accordance with the literature.[156]

1-(3-Methoxyphenyl)-3-phenyl-2-propyn-1-ol (132i)

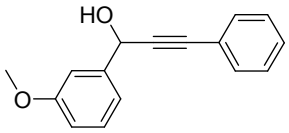

A protocol similar to that used for **132b** gave the title compound as a colourless oil (from 0.604 ml, 5.51 mmol, 1.1 equiv. of phenyl acetylene and 0.609 ml, 5.01 mmol, 1 equiv. of 3-methoxybenzaldehyde) (0.945 g, 3.97 mmol, 79%). ^{1}H NMR (400 MHz, $CDCl_3$) δ 7.50-7.47 (m, 2H), 7.35-7.29 (m, 4H), 7.23-7.19 (m, 2H), 6.90 (ddd, *J* = 8.2, 2.5 and 1.0 Hz, 1H), 5.67 (s, 1H), 3.82 (s, 3H), 2.97 (br s, 1H). ^{13}C NMR (100 MHz, $CDCl_3$) δ 159.7, 142.2, 131.6, 129.6, 128.5, 128.2, 122.3, 118.9, 114.0, 112.1, 88.7, 86.4, 64.8, 55.2. EI$^+$-MS *m/z* 238 (100%, $[M]^+$), 223 (28%, $[M\text{-}Me]^+$), 207 (41%, $[M\text{-}OMe]^+$), 194 (43%), 189 (10%), 178 (52%), 165 (39%), 160 (9%), 152 (23%), 135 (9%), 129 (43%), 109 (14%), 102 (13%), 92 (8%), 77 (26%, $[Ph]^+$). EI$^+$-HRMS calcd. for. $C_{16}H_{14}O_2$ ($[M]^+$) 238.0994; found 238.0998. Data in accordance with the literature.[155]

1-(3,5-Dimethoxyphenyl)-3-phenyl-2-propyn-1-ol (132j)

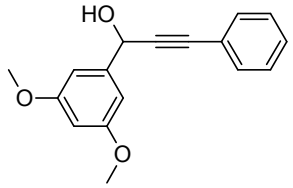

A protocol similar to that used for **132b** gave the title compound as a colourless oil (from 0.300 ml, 2.73 mmol, 1.1 equiv. of phenyl acetylene and 0.415 g, 2.50 mmol, 1 equiv. of 3,5-dimethoxybenzaldehyde) (0.664 g, 2.48 mmol, 99%). ^{1}H NMR (400 MHz, $CDCl_3$) δ 7.50-7.45 (m, 2H, phenyl Ar*H*), 7.35-7.29 (m, 3H, phenyl Ar*H*), 6.80 (d, *J* = 2.3 Hz, 2H, dimethoxyphenyl *ortho* Ar*H*), 6.45 (t, *J* = 2.3 Hz, 1H, *para* dimethoxyphenyl Ar*H*), 5.63 (d, *J* = 5.6 Hz, 1H, C*H*OH), 3.82 (s, 6H, OCH_3), 2.60 (br s, 1H, O*H*). ^{13}C NMR (101 MHz, $CDCl_3$) δ 160.9, 143.0, 131.7, 128.6, 128.3, 122.3, 104.6, 100.4, 88.5, 86.4, 65.0, 55.4. ESI$^+$-MS 307.1 (1%, $[MK]^+$), 291.1 (45%, $[MNa]^+$), 269.1 (2%, $[MH]^+$), 251.1 (100%), 213.1 (1%). ESI$^+$-HRMS calcd. for $C_{17}H_{16}NaO_3$ ($[M]^+$) 291.0992; found 291.0998.

1-Phenyl-2-pentyn-3-ol (132l)

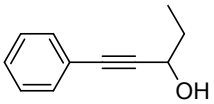

A protocol similar to that used for **132b** gave the title compound as a colourless oil (from 1.30 ml, 11.0 mmol, 1.2 equiv. of phenyl acetylene and 0.532 g, 9.16 mmol, 1 equiv. of propionaldehyde) (1.08 g, 6.73 mmol, 73%). ^{1}H NMR (400 MHz, $CDCl_3$) δ 4.46-7.41 (m, 2H, Ar*H*), 7.32-7.26 (m, 3H, Ar*H*), 4.56 (dd, *J* = 12.0 and 6.1 Hz, 1H, C*H*OH), 2.82-2.36 (br s, 1H, O*H*), 1.91-1.76 (m, 2H, CH_2), 1.08 (t, *J* = 7.4 Hz, 3H, CH_3). ^{13}C NMR (101 MHz, $CDCl_3$) δ 131.6, 128.2, 128.2, 122.6, 90.0, 84.8, 64.0, 30.9, 9.5. EI$^+$-MS 160 (9%, $[MH]^+$), 159 (7%, $[M]^+$), 131 (100%, $[M\text{-}Et]^+$), 129 (11%), 115 (9%, $[M\text{-}OEt]^+$), 103 (34%, $[M\text{-}COEt]^+$), 77 (23%, $[Ph]^+$), 51 (6%). EI$^+$-HRMS calcd. for $C_{11}H_{11}O$ ($[M]^+$) 159.0810; found 159.0812. Data in accordance with the literature.[157]

1,1-Dimethyl-3-phenyl-2-propyn-1-ol (132p)

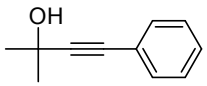

A protocol similar to that used for **132b** gave the title compound as a colourless oil (from 0.300 ml, 2.73 mmol, 1 equiv. of phenyl acetylene and 0.174 g, 3.00 mmol, 1.1 equiv. of acetone) (172 mg, 1.08 mmol, 40%). ^{1}H NMR (400 MHz, $CDCl_3$) δ 7.46-7.40 (m, 2H,

Ar*H*), 7.33-7.29 (m, 3H, Ar*H*), 2.23-2.16 (br s, 1H, O*H*), 1.63 (s, 6H, C*H*$_3$). ^{13}C NMR (101 MHz, $CDCl_3$) δ 131.6, 128.2, 122.7 , 93.7, 82.1, 65.6, 31.5. EI$^+$-MS 160 (19%, $[M]^+$), 145 (100%, $[M\text{-}CH_3]^+$), 141 (8%), 129 (7%), 117 (14%), 115 (19%), 102 (23%), 77 (6%), 43 (15%). EI$^+$-HRMS calcd. for $C_{11}H_{12}O$ ($[M]^+$) 160.0888; found 160.0894. Data in accordance with the literature.[158]

1,6-Diphenylhexa-2,4-diyne-1,6-diol (132r)

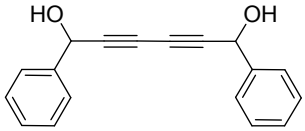

Prepared by a protocol similar to that reported by Smith *et al.*.[159] 1-Phenylprop-2-yn-1-ol (**126**) (1.50 g, 11.4 mmol, 1 equiv.), tetramethylethylenediamine (1.71 ml, 11.4 mmol, 1 equiv.) and copper(I) chloride (1.13 g, 11.4 mmol, 1 equiv.) were mixed in acetone (25 ml) under a positive pressure of air (*via* balloon) and stirred (r.t., 15 hours). The reaction mixture was filtered, reduced *in vacuo* and purified by column chromatography, eluting with petroleum ether (40-60):ethyl acetate 100:0 to 60:40, to give the title compound as a yellow powder (1.20 g, 4.59 mmol, 80%). ^{1}H NMR {400 MHz, $(CD_3)_2CO$} δ 7.54-7.51 (m, 4H), 7.41-7.36 (m, 4H), 7.34-7.30 (m, 2H), 5.60 (d, *J* = 5.8 Hz, 2H, O*H*), 5.31 (d, *J* = 5.8 Hz, 2H). ^{13}C NMR {100 MHz, $(CD_3)_2CO$} δ 141.8, 129.2, 128.8, 127.2, 81.7, 69.8, 64.6. ESI$^+$-MS *m/z* 301.1 (5%, $[MK]^+$), 285.1 (24%, $[MNa]^+$), 245.1 (100%, $[M\text{-}OH]^+$), 217.1 (27%), 202.1 (1%), 139.1 (3%). ESI$^+$-HRMS calcd. for. $C_{18}H_{14}NaO_2$ ($[MNa]^+$) 285.0886; found 285.0883. Data in accordance with the literature.[160]

1-Butyl-3-phenylbicyclo[3.1.0]hex-2-ene (133b)

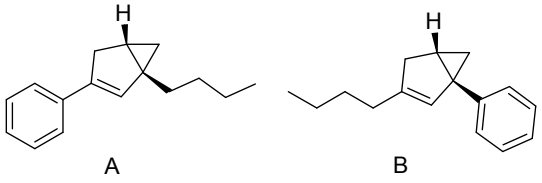

Ratio of isomers A:B 94:6 (By ^{1}H NMR)

Preparation by the general procedure gave the title compound as a colourless oil {from 71.1 mg, 378 μmol, of 1-phenyl-2-heptyn-1-ol (**132b**)} (61.1 mg, 288 μmol, 76%). **Isomer A (94%):** ^{1}H NMR (400 MHz, $CDCl_3$) δ 7.42-7.36 (m, 2H), 7.34-7.28 (at, *J* = 7.5 Hz, 2H), 7.21 (m, 1H), 6.35 (br s, 1H), 3.07 (ddd, *J* = 17, 7 and 2 Hz, 1H), 2.72 (d, *J* = 17 Hz, 1H), 1.74 (m, 1H), 1.56-1.33 (m, 6H), 0.97-0.91 (m, 3H), 0.84 (m, 1H), 0.28 (m, 1H). ^{13}C NMR (101 MHz, $CDCl_3$) δ 138.6, 137.7, 132.2, 128.2, 126.6, 125.1, 36.8, 36.5, 33.1, 30.8, 23.2,

22.8, 21.3, 14.2. EI^+-MS 212 (19%, $[M]^+$), 170 (53%), 155 (100%), 141 (21%), 128 (14%), 115 (14%), 91 (12%), 77 (6%). EI^+-HRMS calcd. for $C_{16}H_{20}$ ($[M]^+$) 212.1561; found 212.1565. {**Isomer B (6%):** Selected Peaks, ^1H NMR (400 MHz, $CDCl_3$) δ 5.81 (s, 1H), 2.77 (dd, *J* = 17 and 6.5 Hz, 1H), 2.32 (d, *J* = 17 Hz, 1H), 2.09 (app. t, *J* = 7.5 Hz, 2H), 0.63 (m, 1H), 0.12 (m, 1H) (other peaks overlapping with isomer A). ^{13}C NMR (101 MHz, $CDCl_3$) δ (selected peaks) 143.0, 128.5, 128.2, 125.9, 125.2, 38.8, 38.6, 30.5, 30.3, 26.7, 25.1, 22.4, 14.0.} Data in accordance with the literature (Isomer A).[78]

1-Trimethylsilyl-3-phenylbicyclo[3.1.0]hex-2-ene (133c)

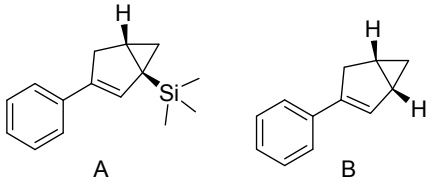

Ratio A:B 68:32 (By ^1H NMR)

Preparation by the general procedure gave the title compound as a colourless oil {from 76.9 mg, 377 μmol, of 1-phenyl-3-trimethylsilyl-2-propyn-1-ol (**132c**)} (57.6 mg, 281 μmol, 75%). ^1H NMR (400 MHz, $CDCl_3$) δ 7.40-7.36 (m, 2H, A and B), 7.33-7.27 (m, 2H, A and B), 7.24-7.18 (m, 1H, A and B), 6.42 (q, *J* = 2 Hz, 1H, B), 6.34 (t, *J* = 2 Hz, 1H, A), 3.02 (app. ddd, *J* = 17, 7 and 1.5 Hz, 1H, A and B), 2.89 (app. ddd, *J* = 17, 2 and 1 Hz, 1H, A), 2.75 (app. ddd, *J* = 17, 3.5 and 1.5 Hz, 1H, B), 1.96 (m, 1 H, B), 1.75 (m, 1H, b), 1.69 (tdd, *J* = 7, 4 and 1 Hz, 1H, A), 0.98-0.93 (m, 1H, A and B), 0.28 (dd, *J* = 4 and 3.5 Hz, 1H, A), 0.11 (q, *J* = 4 Hz, 1H, B), 0.05 (s, 9H, A). ^{13}C NMR (101 MHz, $CDCl_3$) δ 139.8 (A), 139.7 (B), 136.7 (A), 136.6 (B), 132.4 (A), 129.6 (B), 128.2 (A and B), 126.7 (B), 126.5 (A), 125.1 (B), 125.0 (A), 36.7 (A), 36.3 (B), 24.1 (A), 23.8 (B), 21.9 (A), 20.5 (A), 17.6 (B), 15.4 (B), -2.4(A). EI^+-MS 228 (30%, $[M(A)]^+$), 213 (10%), 154 (100%), 135 (19%), 128 (8%), 115 (10%), 73 (48%), 59 (15%), 45 (11%). EI^+-HRMS calcd. for $C_{15}H_{20}Si$ 228.1334 ($[M(A)]^+$) ; found 228.1325.

1,3-Diphenylbicyclo[3.1.0]hex-2-ene (133d)

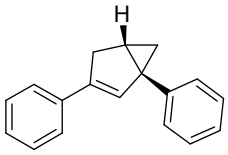

Preparation by the general procedure gave the title compound as a white powder {from 78.6 mg, 378 μmol, of 1,3-diphenyl-2-propyn-1-ol (**132d**)} (80.2 mg, 346 μmol, 91%). ^{1}H NMR (400 MHz, $CDCl_3$) δ 7.48 (d, *J* = 8 Hz, 2H), 7.40-7.22 (m, 8H), 6.67 (s, 1H), 3.27 (dd, *J* = 17 and 7 Hz, 1H), 2.88 (d, *J* = 17 Hz, 1H), 2.00 (m, 1H), 1.68 (dd, *J* = 8 and 4 Hz, 1H), 0.82 (app. t, *J* = 4 Hz, 1H). ^{13}C NMR (101 MHz, $CDCl_3$) δ 142.4, 139.7, 136.3, 130.9, 128.4, 128.3, 127.1, 126.3, 125.7, 125.3, 39.7, 37.0, 26.7, 25.1. EI$^+$-MS *m/z* 232 (100%, $[M]^+$), 217 (44%), 202 (22%), 191 (6%), 153 (13%), 141 (13%), 128 (11%), 115 (14%), 91 (12%), 69 (6%). EI$^+$-HRMS calcd. for $C_{18}H_{16}$ ($[M]^+$) 232.1252; found 232.1243. Data in accordance with the literature.[15]

3-(2-Napthyl)-1-phenylbicyclo[3.1.0]hex-2-ene (133e)

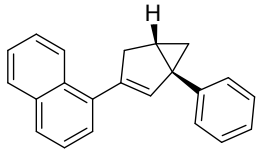

A

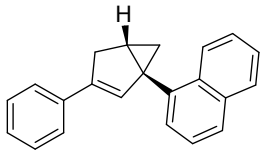

B

Ratio of isomers A:B 56:44 (Crude 83:17) (By ^{1}H NMR)

Preparation by the general procedure gave the title compound as a white powder {from 48.7 mg, 189 μmol, of 1-(2-napthyl)-3-phenyl-2-propyn-1-ol (**132e**)} (36.2 mg, 128 μmol, 68%). ^{1}H NMR (400 MHz, $CDCl_3$) δ 7.85-7.68 (m, 5H, A and B), 7.52-7.21 (m, 7H, A and B), 6.77 (s, 1H, A), 6.73 (s, 1H, B), 3.40-3.26 (m, 1H, A and B), 2.99 (d, *J* = 17 Hz, 1H, A), 2.89 (d, *J* = 17 Hz, 1H, B), 2.09-2.00 (m, 1H, A and B), 1.78 (dd, *J* = 8 and 4 Hz, 1H, B), 1.69 (dd, *J* = 8 and 4 Hz, 1H, A), 0.89-0.83 (m, 1H, A and B). ^{13}C NMR (101 MHz, $CDCl_3$) (Mixture of isomers A and B, all data quoted) δ 142.4, 140.0, 139.9, 139.8, 136.3, 133.7, 133.5, 133.5, 132.6, 131.9, 131.7, 130.9, 128.4, 128.3, 128.0, 127.9, 127.8, 127.6, 127.6, 127.4, 127.1, 126.4, 126.2, 126.1, 125.7, 125.6, 125.3, 125.2, 125.2, 124.5, 123.9, 123.8, 40.0, 39.9, 37.0 (2 peaks), 26.9, 26.8, 25.5, 25.1. EI$^+$-MS 282 (100%, $[M]^+$), 267 (39%), 265 (29%), 252 (19%), 239 (5%), 203 (5%), 191 (16%), 178 (6%), 165 (6%), 141 (25%). EI$^+$-HRMS calcd. for $C_{22}H_{18}$ ($[M]^+$) 282.1409; found 282.1418. {**Isomer A from analysis of crude product**: ^{1}H NMR (400 MHz, $CDCl_3$) δ 7.85-7.76 (m, 3H), 7.74-7.68 (m, 2H), 7.52-7.43 (m, 2H), 7.39-7.32 (m, 4H), 7.25 (m, 1H), 6.77 (t, *J* = 2 Hz, 1H), 3.36

(ddd, *J* = 17, 7 and 2 Hz, 1H), 2.99 (d, *J* = 17 Hz, 1H), 2.05 (m, 1H), 1.69 (dd, *J* = 8 and 4 Hz, 1H), 0.86 (t, *J* = 4 Hz, 1H).}

3-Mesityl-1-phenylbicyclo[3.1.0]hex-2-ene (133f)

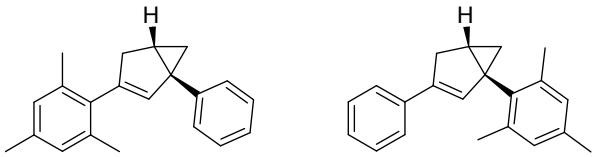

A B

Ratio of isomers A:B 35:65 (Crude 97:3) (By ^{1}H NMR)

Preparation by the general procedure gave the title compound as a white powder {from 47.3 mg, 189 μmol, of 1-mesityl-3-phenyl-2-propyn-1-ol (**132f**)} (37.5 mg, 137 μmol, 72%). ^{1}H NMR (400 MHz, $CDCl_3$) δ 7.45-7.21 (m, 5H, A and B), 6.97-6.85 (m, 2H, A and B), 6.31 (t, *J* = 1.5 Hz, 1H, B), 5.95 (t, *J* = 2 Hz, 1H, A), 3.25 (ddd, *J* = 17, 7 and 1.5 Hz, 1H, B), 3.03 (ddd, *J* = 17.5, 7 and 2 Hz, 1H, A), 2.96 (dd, *J* = 17 and 1 Hz, 1H, B), 2.59 (d, *J* = 17.5 Hz, 1H, A), 2.52 (br s, 3H, B), 2.30 (m, 9H A and 6H B), 2.02-1.92 (m, 1H, A and B), 1.68 (dd, *J* = 8.5 and 4 Hz, 1H, A), 1.24 (dd, *J* = 8.5 and 4 Hz, 1H, B), 0.96 (t, *J* = 4 Hz, 1H, A), 0.87 (t, *J* = 4 Hz, 1H, B). ^{13}C NMR (101 MHz, $CDCl_3$) (Mixture of isomers A and B, all data quoted) δ 142.8, 140.6, 138.6, 136.4, 136.3, 136.3, 135.9, 134.6, 134.5, 133.5, 131.7, 128.8, 128.3, 128.0, 126.9, 126.1, 15.5, 125.2, 40.0, 39.7, 37.0, 36.2, 27.4, 26.2, 24.5, 24.0, 20.9, 20.9, 20.1. EI^{+}-MS *m/z* 274 (100%, $[M]^{+}$), 259 (73%), 244 (27%), 229 (30%), 215 (15%), 202 (11%), 197 (7%), 183 (11 %), 170 (21%), 157 (17%), 141 (9%), 133 (15%), 128 (12%), 115 (12%), 103 (5%), 91 (8%), 77 (6%). EI^{+}-HRMS calcd. for $C_{21}H_{22}$ ($[M]^{+}$) 274.1722; found 274.1725. {**Isomer A from analysis of crude product:** ^{1}H NMR (400 MHz, $CDCl_3$) δ 7.45-7.22 (m, 5H), 6.94 (s, 2H), 5.95 (t, *J* = 2 Hz, 1H), 3.03 (ddd, *J* = 17.5, 7 and 2 Hz, 1H), 2.59 (d, *J* = 17.5 Hz, 1H), 2.32 (s, 3H), 2.29 (s, 6H), 1.97 (m, 1 H), 1.68 (dd, *J* = 8.5 and 4 Hz, 1H), 0.96 (t, *J* = 4 Hz, 1H).}

3-(4-Chlorophenyl)-1-phenylbicyclo[3.1.0]hex-2-ene (133g)

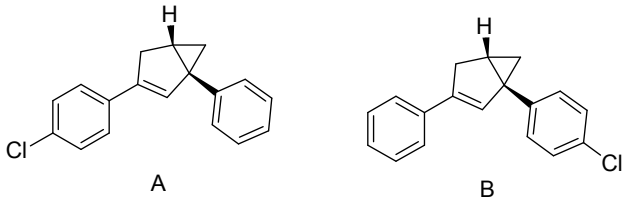

Ratio of isomers A:B 59:41 (Crude 88:12) (By ^{1}H NMR)

Preparation by the general procedure gave the title compound as a white powder {from 91.7 mg, 378 μmol, of 1-(4-chlorophenyl)-3-phenyl-2-propyn-1-ol (**132g**)} (90.6 mg, 340 μmol, 90%). ^{1}H NMR (400 MHz, $CDCl_3$) δ 7.45 (m, 1H, B), 7.39-7.19 (m, 9H A and 8H B), 6.62 (t, *J* = 1.5 Hz, 1H, A), 6.56 (t, *J* = 1.5 Hz, 1H, B), 3.28-3.16 (m, 1H, A and B), 2.87-2.77 (m, 1H, A and B), 2.02-1.91 (m, 1H, A and B), 1.67-1.58 (m, 1H, A and B), 0.82-0.77 (m, 1H, A and B). ^{13}C NMR (101 MHz, $CDCl_3$) (Mixture of isomers A and B, all data quoted) δ 142.1, 141.0, 140.2, 138.6, 136.1, 134.8, 132.6, 131.6, 131.3, 130.3, 128.5, 128.4, 128.3, 127.8, 127.2, 126.5, 126.3, 125.8, 123.3, 39.8, 39.3, 37.0, 36.9, 26.9, 26.7, 25.2, 25.1. EI^{+}-MS 266 (100%, ^{35}Cl[M]$^{+}$), 251 (18%), 231 (35%), 229 (11%), 215 (49%), 202 (7%), 189 (6%), 153 (11%), 141 (10%), 125 (10%), 115 (8%), 101 (6%), 91 (14%). EI^{+}-HRMS calcd. for $C_{18}H_{15}Cl$ ([M]$^{+}$) 266.0862; found 266.0865. {**Isomer A from analysis of crude product:** ^{1}H NMR (400 MHz, $CDCl_3$) δ 7.39-7.19 (m, 9H, ArH), 6.62 (t, *J* = 1.5 Hz, 1H), 3.21 (ddd, *J* = 17, 7 and 2 Hz, 1H), 2.81 (dd, *J* = 17 and 1 Hz, 1H), 1.99 (m, 1H), 1.65 (dd, *J* = 8 and 4 Hz, 1H), 0.79 (t, *J* = 4 Hz, 1H).}

3-(4-CF_3-phenyl)-1-phenylbicyclo[3.1.0]hex-2-ene (133h)

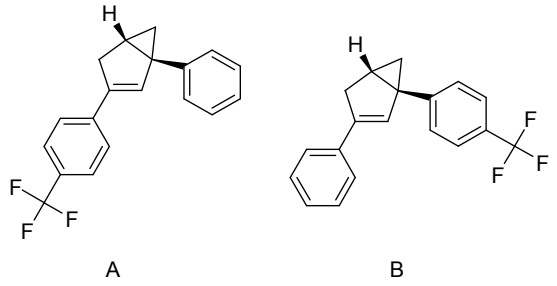

Ratio of isomers A:B 50:50 (Crude 91:9) (By ^{1}H NMR)

Preparation by the general procedure gave the title compound as a white powder {from 51.6 mg, 187 □mol, of 1-(4-CF_3-phenyl)-3-phenyl-2-propyn-1-ol (**132h**)} (32.2 mg, 117 μmol, 62%). ^{1}H NMR (400 MHz, $CDCl_3$) δ 7.60-7.50 (m, 4H A and 2H B), 7.48-7.44 (m, 2H, B), 7.39-7.21 (m, 5H, A and B), 6.74 (app. t, *J* = 1.7 Hz, 1H, A), 6.62 (dd, *J* = 1.9 and 1.3 Hz, 1H, B), 3.30-3.20 {m, (overlapping ddd's), 1H, A and B}, 2.87 (d, *J* = 17.0 Hz, 1H,

B), 2.86 (d, *J* = 16.9 Hz, 1H, A), 2.06-1.99 (m, 1H, A and B), 1.70 (dd, *J* = 7.8 and 4.2 Hz, 1H, B), 1.68 (dd, *J* = 7.8 and 4.2 Hz, 1H, A), 0.89 (app. t, *J* = 4.5 Hz, 1H, B), 0.81 (app. t, *J* = 4.5 Hz, 1H, A). ^{19}F (376 MHz, $CDCl_3$) δ -62.1 (s, B), -62.3 (s, A). ^{13}C NMR (101 MHz, $CDCl_3$) (Mixture of isomers A and B, all data quoted) δ 146.8, 141.8, 140.6, 139.7 (q, *J* = 2 Hz), 138.5, 136.0, 133.8, 129.5, 128.8 (q, *J* = 32 Hz), 128.4, 128.4, 127.8 (q, *J* = 32 Hz), 127.4, 126.4, 126.3, 125.9, 125.4, 125.3, 125.3 (q, *J* = 4 Hz), 125.2 (q, *J* = 4 Hz), 124.3 (q, *J* = 272 Hz), 124.2 (q, *J* = 272 Hz), 40.0, 39.5, 36.9, 36.9, 27.7, 26.7, 25.8, 25.2. EI$^+$-MS 300 (100%, $[M]^+$), 285 (26%), 259 (11%), 231 (10%), 215 (21%), 202 (5%), 153 (8%), 141 (11%), 128 (6%), 115 (7%), 91 (11%). EI$^+$-HRMS calcd. for $C_{19}H_{15}F_3$ ($[M]^+$) 300.1126; found 300.1129. {**Isomer A from analysis of crude product:** ^{1}H NMR (400 MHz, $CDCl_3$) δ 7.56 (app. dd, *J* = 23.0 and 8.3 Hz, 4H), 7.38-7.32 (m, 2H), 7.32-7.28 (m, 2H), 7.27-7.22 (m, 1H), 6.76 (t, *J* = 1.9 Hz, 1H), 3.25 (ddd, *J* = 17.1, 6.9 and 1.8 Hz, 1H), 2.86 (d, *J* = 17.1 Hz, 1H), 2.07-2.00 (m, 1H), 1.69 (dd, *J* = 8.2 and 4.2 Hz, 1H), 0.82 (app. t, *J* = 4.5 Hz, 1H).}

3-(3-Methoxyphenyl)-1-phenylbicyclo[3.1.0]hex-2-ene (133i)

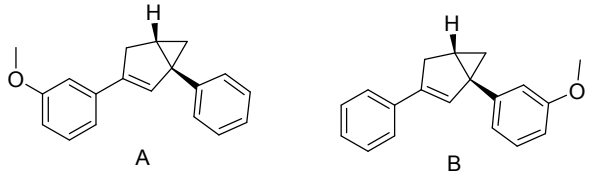

Ratio of isomers A:B 51:49 (Crude 74:26) (By ^{1}H NMR)

Preparation by the general procedure gave the title compound as a white powder {from 89.7 mg, 377 □mol of 1-(3-methoxyphenyl)-3-phenyl-2-propyn-1-ol (**132i**)} (52.4 mg, 200 □mol, 53%). ^{1}H NMR (400 MHz, $CDCl_3$) δ 7.45 (m, 1H, B), 7.37-7.30 (m, 6H A and 5H B), 7.30-7.20 (m, 5H, A and B), 7.06 (dt, *J* = 7.6 and 1.2 Hz, 1H, A), 6.99 (t, *J* = 2.0 Hz, 1H, A), 6.89 (dd, *J* = 7.7 and 0.89 Hz, 1H, B), 6.85 (t, *J* = 2.0 Hz, 1H, B), 6.81 (ddd, *J* = 8.0, 2.6 and 0.7 Hz, 1H, A), 6.77 (ddd, *J* = 8.1, 2.5 and 0.8 Hz, 1H, B), 6.64 (t, *J* = 1.8 Hz, 1H, A), 6.62 (t, *J* = 1.8 Hz, 1H, B), 3.85 (s, 3H, A), 3.83 (s, 3H, B), 3.24 (overlapping ddd's, *J* = 16.7, 7.0 and 1.7 Hz, 1H, A and B), 2.84 (app d, *J* = 16.9 Hz 1H, A and B), 1.97 (td, *J* = 7.5 and 4.5 Hz, 1H, A and B), 1.65 (overlapping dd's, *J* = 8.1 and 4.1 Hz, 1H, A and B), 0.79 (t, *J* = 4.4 Hz, 1H, A and B). ^{13}C NMR (100 MHz, $CDCl_3$) δ 159.7 (A), 159.6 (B), 144.2 (B), 142.4 (A), 139.8 (B), 139.6 (A), 137.8 (A), 136.3 (B), 131.4 (A), 130.7 (B), 129.3, 129.3, 128.3 (2C), 128.3 (2C), 127.1 (B, 2C), 126.3 (A, 2C), 125.7(A), 125.3 (B), 118.7 (B), 117.9 (A), 112.4, 112.3, 111.0, 110.9, 55.2 (2C, A and B), 39.8 (A), 39.7 (B),

37.0 (A), 36.9 (B), 26.9 (A), 26.7 (B), 25.2 (A), 25.1 (B). ESI$^+$-MS *m/z* 263.1 (100%, $[MH]^+$), 213.1 (5%), 150.0 (5%), 131.0 (3%). ESI$^+$-HRMS calcd. for. $C_{19}H_{19}O$ ($[MH]^+$) 263.1430; found 263.1434. {**Isomer A from analysis of crude product:** ^{1}H NMR (400 MHz, $CDCl_3$) δ 7.35-7.18 (m, 6H, ArCH), 7.05 (app. d, *J* = 7.6 Hz, 1H), 6.98 (app s, 1H), 6.80 (dd, *J* = 8.1 and 2.9 Hz, 1H), 6.62 (app s, 1H), 3.83 (s, 3H), 3.23 (ddd, *J* = 16.7, 7.0 and 1.7 Hz, 1H), 2.83 (d , *J* = 16.9 Hz, 1H), 1.96 (td, *J* = 7.5 and 4.5 Hz, 1H), 1.63 (dd, *J* = 8.1 and 4.1 Hz, 1H), 0.80 (t, *J* = 4.4 Hz, 1H).} Data in accordance with the literature (Isomer A).[78]

6-Trimethylsilyl-4-phenyl-1-hexen-5-yne (134)

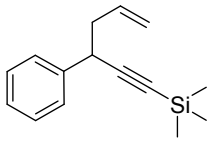

A protocol similar to that used for 4-phenyl-1-hexen-5-yne (**74**), method B, gave the title compound as a colourless oil {from 0.300 g, 1.47 mmol, 1 equiv. of 1-phenyl-3-trimethylsilyl-2-propyn-1-ol (**126**) and 0.503 g, 4.41 mmol, 3 equiv. of allyltrimethylsilane (**127a**)} (0.239 g, 1.05 mmol, 71%). ^{1}H NMR (400 MHz, $CDCl_3$) δ 7.41-7.32 (m, 4H), 7.29-7.24 (m, 1H), 5.87 (m, 1H), 5.09 (m, 1H), 5.06 (t, *J* = 1.2 Hz, 1H), 3.74 (t, *J* = 7.1 Hz, 1H), 2.52 (tt, *J* = 7.1 and 1.1 Hz, 2H), 0.22 (s, 9H). ^{13}C NMR (100 MHz, $CDCl_3$) δ 141.0, 135.3, 128.4, 127.5, 126.7, 117.0, 107.7, 87.8, 42.8, 38.9, 0.15. EI$^+$-MS *m/z* 228 (1%, $[M]^+$), 213 (1%, $[M\text{-}CH_3]^+$), 195 (2%), 187 (86%, $[M\text{-}C_3H_4]^+$), 172 (6%), 159 (100%, $[M\text{-}C_5H_8]^+$), 145 (10%), 131 (5 %), 105 (6%), 83 (11%), 73 (14%, $[Si(CH_3)_3]^+$), 59 (6%). EI$^+$-HRMS calcd. for. $C_{15}H_{20}Si$ ($[M]^+$) 228.1334; found 228.1333. Data in accordance with the literature.[25a]

[(1-Allylcyclohexyl)ethynyl]benzene (136)

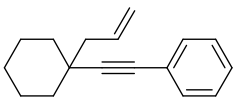

Prepared by a protocol based on that of Zhan *et al.*.[69] 1-Phenylethynyl cyclohexanol (**132o**) (0.50 g, 2.5 mmol, 1 equiv.) and allyltrimethylsilane (**127a**) (1.19 ml, 7.5 mmol, 3 equiv.) were mixed in acetonitrile (5 ml, dry) and $FeCl_3$ (anhydrous, 40 mg, 0.25 mmol, 0.1 equiv.) in acetonitrile (1 ml, dry) was added dropwise. The reaction was stirred at 60 ˚C for 18 hours, reduced *in vacuo* and the product purified by column chromatography, eluting with petroleum ether (40-60), to give the title compound as a colourless oil (0.249 g, 1.11

mmol, 44%). ^{1}H NMR (400 MHz, $CDCl_3$) δ 7.44-7.40 (m, 2H), 7.32-7.23 (m, 3H), 6.05 (ddt, *J* = 12.4, 9.3 and 7.5 Hz, 1H), 5.12 (m, 1H), 5.09 (m, 1H), 2.26 (dt, *J* = 7.2 and 1.3 Hz, 2H), 1.87-1.58 (m, 7H), 1.28-1.12 (m, 3H). ^{13}C NMR (100 MHz, $CDCl_3$) δ 135.0, 131.6, 128.1, 127.4, 124.2, 117.1, 95.1, 83.3, 47.4, 37.6, 37.0, 26.1, 23.1. ESI$^+$-MS *m/z* 301.1 (100%, $[M+Ph]^+$), 279.2 (11%), 245.1 (61%), 225.2 (68%, $[MH]^+$), 195.1 (20%), 167.1 (11%), 149.0 (23%, $[MH_2\text{-}Ph]^+$), 126.0 (30%). ESI$^+$-HRMS calcd. for $C_{17}H_{21}$ ($[MH]^+$) 225.1638; found 225.1633.

(4,4-Dimethylcyclohexa-1,5-dien-1-yl)benzene (135a)

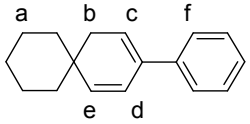

[AuBr(I^{t}Pe)] (**56g**) (3.6 mg, 7.4 □mol, 0.02 equiv.), Ag[Al(OC(CF$_3$)$_3$)$_4$] (**76**) (8.0 mg, 7.4 □mol, 0.02 equiv.) and [(1-allylcyclohexyl)ethynyl]benzene (**136**) (78.3 mg, 0.350 mmol, 1 equiv.) were dissolved in dichloromethane (2 ml) and stirred (0 ˚C - r.t., 15 hours). The reaction mixture was reduced *in vacuo* and purified by column chromatography, eluting with petroleum ether (40-60), to give the title compound as a colourless oil (64.8 mg, 0.289 mmol, 83%). ^{1}H NMR (400 MHz, $CDCl_3$) δ 7.46-7.43 (m, 2H, aromatic C*H*), 7.39-7.34 (m, 2H, aromatic C*H*), 7.31-7.26 (m, 1H, aromatic C*H*), 6.30 (dd, *J* = 9.9 and 1.8 Hz, 1H, alkene C*H* d), 6.05 (app. t, *J* = 4.8 Hz, 1H, alkene C*H* c), 5.97 (d, *J* = 9.9 Hz, 1H, alkene C*H* e), 2.36 (d, *J* = 4.8 Hz, 2H, CH_2 b), 1.64-1.39 (m, 10H, cyclohexyl CH_2). ^{13}C NMR (100 MHz, $CDCl_3$) δ 140.3 (*C*), 137.8 (2 peaks, alkene CH e), 134.9 (*C*), 128.3 (*C*H), 126.8 (*C*H), 125.3 (*C*H), 123.4 (alkene *C*H d), 122.0 (alkene *C*H c), 36.3 (broad, cyclohexyl *C*H_2), 36.2 (alkene *C*H_2 b), 33.4 (cyclohexyl *C*), 26.3 (cyclohexyl *C*H_2), 21.8 (cyclohexyl *C*H_2). EI$^+$-MS *m/z* 224 (100%, $[M]^+$), 181 (7%), 167 (34%), 153 (8%), 142 (7%), 115 (6%), 91 (6%), 49 (34%).

2.5.5. Crystallographic data

Table 38. Crystallographic data for complexes **55a**, **55d** and **57a**.

	55a **[Au(*N*-succ)(I^{t}Bu)]**	**55d** **[Au(*N*-ptm)(I^{t}Bu)]**	**57a** **[Au(*N*-succ)(IMes)]**
formula	$C_{15}H_{24}AuN_3O_2$	$C_{19}H_{24}AuN_3O_2$	$C_{25}H_{28}AuN_3O_2$
M_r	475.34	523.38	599.47
cryst syst	Orthorhombic	Orthorhombic	Monoclinic
space group	*Pca*2(1)	*Pnma*	*P*2(1)/*c*
crystal size/mm^3	0.43 x 0.15 x 0.03	0.15 x 0.13 x 0.04	0.27 x 0.23 x 0.17
cell constants			
a(Å)	11.3451(8)	11.8766(6)	9.6744(4)
b(Å)	10.6675(7)	17.1592(9)	20.2249(9)
c(Å)	27.4051(19)	9.4378(5)	12.7004(6)
□(deg)	90.00	90.00	90.00
□(deg)	90.00	90.00	109.8040(10)
□(deg)	90.00	90.00	90.00
V(Å^3)	3316.7(4)	1923.36(17)	2338.04(18)
Z	8	4	4
□(Å)	0.71073	0.71073	0.71073
□(calcd)(g/cm^3)	1.904	1.807	1.703
□(mm^{-1})	8.879	7.665	6.318
F(000)	1840	1016	1176
T(K)	110(2)	110(2)	110(2)
2□$_{max}$ (deg)	56.60	60.02	60.00
no. of rflns measd	32064	14707	26386
no. of indep rflns	8209	2870	6750
R_{int}	0.0345	0.03091	0.0280
no. of data/restraints/params	8209 / 7 / 392	2870 / 0 / 121	6750 / 0 / 286
Goodness-of-fit on F^2	1.037	1.022	1.047
R indices (all data)	R_1 = 0.0282, ωR_2 = 0.0472	R_1 = 0.0246, ωR_2 = 0.0456	R_1 = 0.0271, ωR_2 = 0.0540
Final R indices [I>2sigma(I)]	R_1 = 0.0213, ωR_2 = 0.0450	R_1 = 0.0200, ωR_2 = 0.0441	R_1 = 0.0229, ωR_2 = 0.0525
max, min □□ (e Å^{-3})	+1.733, -0.686	+1.363, -0.605	+3.317, -0.759

Table 39. Crystallographic data for complexes **66a**, **66d** and **67a.**

	66a	**66d**	**67a**
	[$AuBr_2$(*N*-succ)(I^tBu)]	**[$AuBr_2$(*N*-ptm)(I^tBu)]**	**2[{$AuBr_2$(*N*-succ)(ItPe)}].C_6H_5F**
formula	$C_{15}H_{24}AuBr_2N_3O_2$	$C_{19}H_{24}AuBr_2N_3O_2$	$C_{40}H_{61}Au_2Br_4FN_6O_4$
M_r	635.16	683.20	1422.52
cryst syst	Triclinic	Orthorhombic	Triclinic
space group	*P*-1	*Pnma*	*P*-1
crystal size/mm^3	0.23 x 0.21 x 0.20	0.44 x 0.15 x 0.03	0.44 x 0.20 x 0.07
cell constants			
a(Å)	9.7911(5)	19.8674(17)	11.8901(9)
b(Å)	13.9362(7)	13.3922(11)	14.8899(11)
c(Å)	15.3479(8)	8.3251(7)	15.2604(12)
□(deg)	72.3520(10)	90.00	106.6900(10)
□(deg)	74.0220(10)	90.00	107.2830(10)
□(deg)	86.4790(10)	90.00	96.2640(10)
V($Å^3$)	1918.02(17)	2215.0(3)	2414.6(3)
Z	4	4	2
□(Å)	0.71073	0.71073	0.71073
□(calcd)(g/cm^3)	2.200	2.049	1.957
□(mm^{-1})	11.848	10.267	9.426
F(000)	1200	1296	1364
T(K)	110(2)	110(2)	110(2)
2□$_{max}$ (deg)	60.08	56.56	60.00
no. of rflns measd	22084	20843	27421
no. of indep rflns	10877	2847	13566
R_{int}	0.0333	0.0546	0.0261
no. of data/restraints/params	10877 / 0 / 427	2847 / 0 / 133	13566 / 0 / 525
Goodness-of-fit on F^2	1.007	1.073	1.032
R indices (all data)	R_1 = 0.0421, ωR_2 = 0.0688	R_1 = 0.0352, ωR_2 = 0.0871	R_1 = 0.0300, ωR_2 = 0.0639
Final R indices [I>2sigma(I)]	R_1 = 0.0307, ωR_2 = 0.0654	R_1 = 0.0319, ωR_2 = 0.0845	R_1 = 0.0247, ωR_2 = 0.0617
max, min □□ (e $Å^{-3}$)	+2.371, -1.315	+2.581, -2.380	+2.342, -1.576

Table 40. Crystallographic data for complexes **66a**, **66d** and **67a. 67c**, and **68c**.

	67c	**68c.C_6H_5F**
	[$AuBr_2$(*N*-tfs)(I^tPe)]	**[$AuBr_2$(*N*-ptm)(IMes)] .C_6H_5F**
formula	$C_{17}H_{24}AuBr_2F_4N_3O_2$	$C_{35}H_{33}AuBr_2FN_3O_2$
M_r	735.18	903.43
cryst syst	Orthorhombic	Monoclinic
space group	*Pbca*	*P*2(1)/*c*
crystal size/mm^3	0.44 x 0.33 x 0.13	0.28 x 0.24 x 0.18
cell constants		
a(Å)	13.5158(18)	17.6109(3)
b(Å)	18.242(2)	12.2187(3)
c(Å)	18.874(2)	16.6542(3)
□(deg)	90.00	90.00
□(deg)	90.00	111.8490(10)
□(deg)	90.00	90.00
V($Å^3$)	4653.7(10)	3326.26(12)
Z	8	4
□(Å)	0.71073	0.71073
□(calcd)(g/cm^3)	2.099	1.804
□(mm^{-1})	9.806	6.866
F(000)	2784	1752
T(K)	110(2)	110(2)
2□$_{max}$ (deg)	60.12	54.96
no. of rflns measd	66257	44337
no. of indep rflns	6784	7619
R_{int}	0.0403	0.0509
no. of data/restraints/params	6784 / 91 / 332	7619 / 0 / 456
Goodness-of-fit on F^2	1.439	1.072
R indices (all data)	R_1 = 0.0502, ωR_2 = 0.1011	R_1 = 0.0401, ωR_2 = 0.0613
Final R indices [I>2sigma(I)]	R_1 = 0.0430, ωR_2 = 0.0989	R_1 = 0.0285, ωR_2 = 0.0581
max, min □□ (e $Å^{-3}$)	+1.345, -1.236	+0.634, -1.076

2.6. References

(1) (a) Nolan, S. P. *Nature* **2007**, *445*, 496-497; (b) Hashmi, A. S. K. *Chem. Rev.* **2007**, *107*, 3180-3211; (c) Furstner, A. *Chem. Soc. Rev.* **2009**, *38*, 3208-3221.

(2) (a) Furstner, A.; Davies, P. W. *Angew. Chem., Int. Ed.* **2007**, *46*, 3410-3449; (b) Gorin, D. J.; Sherry, B. D.; Toste, F. D. *Chem. Rev.* **2008**, *108*, 3351-3378; (c) Jimenez-Nunez, E.; Echavarren, A. M. *Chem. Commun.* **2007**, 333-346.

(3) (a) Haug, T. T.; Harschneck, T.; Duschek, A.; Lee, C.-U.; Binder, J. T.; Menz, H.; Kirsch, S. F. *J. Organomet. Chem.* **2009**, *694*, 510-514; (b) Blanc, A.; Alix, A.; Weibel, J.-M.; Pale, P. *Eur. J. Org. Chem.* **2010**, 1644-1647.

(4) (a) Sanz, S.; Jones, L. A.; Mohr, F.; Laguna, M. *Organometallics* **2007**, *26*, 952-957; (b) Roembke, P.; Schmidbaur, H.; Cronje, S.; Raubenheimer, H. *J. Mol. Catal. A: Chem.* **2004**, *212*, 35-42.

(5) Nieto-Oberhuber, C.; Perez-Galan, P.; Herrero-Gomez, E., Lauterbach, T.; Rodríguez, C.; López, S.; Bour, C.; Rosellón, A.; Cárdenas, D. J.; Echavarren, A. M. *J. Am .Chem. Soc.* **2008**, *130*, 269-279.

(6) (a) Witham, C. A.; Mauleon, P.; Shapiro, N. D.; Sherry, B. D.; Toste, F. D. *J. Am. Chem. Soc.* **2007**, *129*, 5838-5839; (b) Marion, N.; Gealageas, R.; Nolan, S. P. *Org. Lett.* **2007**, *9*, 2653-2656.

(7) (a) Ito, H.; Yajima, T.; Tateiwa, J.; Hosomi, A. *Chem. Commun.* **2000**, 981-982; (b) Diez-Gonzalez, S.; Nolan, S. P. *Acc. Chem. Res.* **2008**, *41*, 349-358.

(8) Ray, L.; Katiyar, V.; Barman, S.; Raihan, M. J.; Nanavati, H.; Shaikh, M. M.; Ghosh, P. *J. Organomet. Chem.* **2007**, *692*, 4259-4269.

(9) Guan, B. T.; Xing, D.; Cai, G. X.; Wan, X. B.; Yu, N.; Fang, Z.; Yang, L. P.; Shi, Z. J. *J. Am. Chem. Soc.* **2005**, *127*, 18004-18005.

(10) (a) Fructos, M. R.; Belderrain, T. R.; de Frémont, P.; Scott, N. M.; Nolan, S. P.; Diaz-Requejo, M. M.; Perez, P. J. *Angew. Chem., Int. Ed.* **2005**, *44*, 5284-5288; (b) Hashmi, A. S. K.; Schafer, S.; Wolfle, M.; Gil, C. D.; Fischer, P.; Laguna, A.; Blanco, M. C.; Gimeno, M. C. *Angew. Chem., Int. Ed.* **2007**, *46*, 6184-6187.

(11) Li, X. Q.; Li, C.; Song, F. B.; Zhang, C. *J. Chem. Res.* **2007**, 722-724.

(12) (a) Kovacs, G.; Ujaque, G.; Lledos, A. *J. Am. Chem. Soc.* **2008**, *130*, 853-864; (b) Brouwer, C.; He, C. *Angew. Chem., Int. Ed.* **2006**, *45*, 1744-1747.

(13) (a) Ma, S. M.; Yu, S. C.; Gu, Z. H. *Angew. Chem., Int. Ed.* **2006**, *45*, 200-203; (b) Zhang, L. M.; Sun, J. W.; Kozmin, S. A. *Adv. Synth. Catal.* **2006**, *348*, 2271-2296; (c) Bruneau, C. *Angew. Chem., Int. Ed.* **2005**, *44*, 2328-2334.

(14) (a) Liu, Y.; Qian, J.; Lou, S.; Zhu, J.; Xu, Z. *J. Org. Chem.*, **2010**, *75*, 1309-1312; (b) Zhou, Y.; Feng, E.; Liu, G.; Ye, D.; Li, J.; Jiang, H.; Liu, H. *J. Org. Chem.* **2009**, *74*, 7344-7348; (c) Hildebrandt, D.; Dyker, G. *J. Org. Chem.* **2006**, *71*, 6728-6733.

(15) Luzung, M. R.; Markham, J. P.; Toste, F. D. *J. Am. Chem. Soc.* **2004**, *126*, 10858-10859.

(16) Marion, N.; Nolan, S. P. *Chem. Soc. Rev.* **2008**, *37*, 1776-1782.

(17) Arduengo, III, A. J. US patent 5 182 405, **1993**.

(18) Lin, I. J. B.; Vasam, C. S. *Can. J. Chem.* **2005**, *83*, 812-825.

(19) Huynh, H. V.; Han, Y.; Jothibasu, R.; Yang , J. A. *Organometallics* **2009**, *28*, 5395-5404.

(20) Gaquere, A.; Liang, S.; Hsu, F.-L.; Bu, X. R. T. *Tetrahedron: Asymmetry* **2002**, *13*, 2089-2093.

(21) (a) Zhang, X.; Corma, A. *Chem. Commun.* **2007**, 3080-3082; (b) Zhang, X.; Corma, A. *Dalton Trans.* **2008**, 397-403; (c) Engel, D. A.; Dudley, G. B. *Org. Lett.* **2006**, *8*, 4027-4029; (d) Lemiere, G.; Gandon, V.; Agenet, N.; Goddard, J. P.; de Kozak, A.; Aubert, C.; Fensterbank, L.; Malacria, M. *Angew. Chem., Int. Ed.* **2006**, *45*, 7596-7599; (e) Li, Z. G.; Capretto, D. A.; Rahaman, R. O.; He, C. *J. Am. Chem. Soc.* **2007**, *129*, 12058-12059

(22) (a) Gaillard, S.; Bantreil, X.; Slawin, A. M. Z.; Nolan, S. P. *Dalton Trans.* **2009**, 6967-6971; (b) Komiya, S.; Shibue, A. *Organometallics* **1985**, *4*, 684-687; (c) Jothibasu, R.; Huynh, H. V.; Koh, L. L. *J. Organomet. Chem*. **2008**, *693*, 374-380; (d) Fan, D. M.; Melendez, E.; Ranford, J. D.; Lee, P. P. F.; Vittal, J. J. *J. Organomet. Chem.* **2004**, *689*, 2969-2974.

(23) Aguilar, D.; Contel, M.; Navarro, R.; Soler, T.; Urriolabeitia, E. P. *J. Organomet. Chem.* **2009**, *694*, 486-493.

(24) Hashmi, A. S. K.; Weyrauch, J. P.; Rudolph, M.; Kurpejovic, E. *Angew. Chem., Int. Ed.* **2004**, *45*, 6545-6547.

(25) (a) Georgy, M.; Boucard, V.; Campagne, J-M. *J. Am. Chem. Soc.* **2005**, *127*, 14180-14181; (b) Terrasson, V.; Marque, S.; Georgy, M.; Campagne, J. M.; Prim, D. *Adv. Synth. Catal.* **2006**, *348*, 2063-2067.

(26) Debono, N.; Iglesias, M.; Sanchez, F. *Adv. Synth. Catal.* **2007**, *349*, 2470-2476.

(27) Corma, A.; González-Arellano, C.; Iglesias, M.; Sánchez, F. *Angew. Chem., Int. Ed.* **2007**, *46*, 7820-7822.

(28) Casado, R.; Contel, M.; Laguna, M.; Romero, P.; Sanz, S. *J. Am. Chem. Soc.* **2003**, *125*, 11925-11935.

(29) Lo, V. K.-Y.; Liu, Y.; Wong, M.-K.; Che, C.-M. *Org. Lett.* **2006**, *8*, 1529-1532.

(30) (a) Sromek, A. W.;Rubina, M.; Gevorgyan, V. *J. Am. Chem. Soc.* **2005**, *127*, 10500-10501; (b) Hashmi, A. S. K.; Salathé, R.; Frey, W. *Chem. Eur. J.* **2006**, *12*, 6991-6996; (c) Harkat, H.; Dembelé, A. Y.; Weibel, J.-M.; Blanc, A.; Pale, P. *Tetrahedron* **2009**, *65*, 1871-1879; (d) Mamane, V.; Hannen, P.; Fürstner, A. *Chem. Eur. J.* **2004**, *10*, 4556-4575.

(31) (a) Hashmi, A. S. K.; Blanco, M. C.; Fischer, D.; Bats, J. W. *Eur. J. Org. Chem.* **2006**, 1387-1389; (b) Morita, N.; Krause, N. *Eur. J. Org. Chem.* **2006**, 4634-4641; (c) Komiya, S.; Kochi, J. K. *J. Am. Chem. Soc.* **1976**, *98*, 7599-7607; (d) Komiya, S.; Albright, T. A.; Hoffmann, R.; Kochi, J. K. *J. Am. Chem. Soc.* **1976**, *98*, 7255-7265.

(32) (a) Vogler, A.; Kunkely, H. *Coord. Chem. Rev.* **2001**, *219-221*, 489-507; (b) Kunkely, H.; Vogler, A. *J. Organomet. Chem.* **1997**, *541*, 177-179.

(33) Gammons, C. H.; Yu, Y.; Williams-Jones, A. E. *Geochim. Cosmochim. Ac.* **1997**, *61*, 1971-1983.

(34) Bergamini, G.; Ceroni, P.; Balzani, V.; Gingras, M.; Raimundo, J. M.; Morandi, V.; Merli, P. G. *Chem. Commun.* **2007**, 4167-4169.

(35) Hashmi, A. S. K. *Angew. Chem., Int. Ed.* **2008**, *47*, 6754-6756.

(36) Straub, B. F. *Chem. Commun.* **2004**, 1726-1728.

(37) Gaillard, S.; Slawin, A. M. Z.; Bonura, A. T.; Stevens, E. D.; Nolan S. P. *Organometallics* **2010**, *29*, 394-402.

(38) Hashmi, A. S. K.; Frost, T. M.; Bats, J. W. *Org. Lett.* **2001**, *3*, 3769-3771.

(39) Hashmi, A. S. K**.** *Catal. Today* **2007**, *122*, 211-214.

(40) (a) Brown, T. J.; Dickens, M. G.; Widenhoefer, R. A. *J. Am. Chem. Soc.* **2009**, *131*, 6350-6351; (b) Herrero-Gómez, E.; Nieto-Oberhuber, C.; López, S.; Benet-Buchholz, J.; Echavarren, A. M. *Angew. Chem., Int. Ed.* **2006**, *45*, 5455-5459; (c) Dias, H. V. R.; Wu. J. *Eur. J. Inorg. Chem.* **2008**, 509-522; (d) Brown, T. J.; Dickens, M. G.; Widenhoefer, R. A. *Chem. Commun.* **2009**, 6451-6453; (e) Cinellu, M. A.; Minghetti, G.; Cocco, F.; Stoccoro, S.; Zucca, A.; Manassero, M. *Angew. Chem., Int. Ed.* **2005**, *44*, 6892-6895; (f) Cinellu, M. A.; Minghetti, G.; Stoccoro, S.; Zucca, A.; Manassero, M. *Chem. Commun.* **2004**, 1618-1619; (g) Zuccaccia, D.; Belpassi, L.; Tarantelli, F.; Macchioni, A. *J. Am. Chem. Soc.* **2009**, *131*, 3170-3171; (h) Schmidbaur, H.; Schier, A. *Organometallics*, **2010**, *29*, 2-23; (i) Flügge, S.; Anoop, A.; Goddard, R.; Thiel, W.; Fürstner, A. *Chem. Eur. J.* **2009**, *15*, 8558-8565.

(41) Pazderski, L.; Pawlak, T.; Sitkowski, J.; Kozerski, L.; Szlyk, E. *Magn. Reson. Chem.* **2009**, 47, 932-941.

(42) Gorin, D. J.; Toste, F. D. *Nature* **2007**, *446*, 395-403.

(43) (a) Volz, F.; Wadman, S. H.; Hoffmann-Röder, A.; Krause, N. *Tetrahedron* **2009**, *65*, 1902-1910; (b) Jung, H. H.; Floreancig, P. E. *J. Org. Chem*. **2007**, *72*, 7359-7366; (c) Sawama, Y.; Sawama, Y.; Krause, N. *Org. Biomol. Chem*. **2008**, *6*, 3573-3579; (d) Volz, F.; Krause, N. *Org. Biomol. Chem*. **2007**, *5*, 1519-1521; (e) Nakajima, R.; Ogino, T.; Yokoshima, S.; Fukuyama, T. *J. Am. Chem. Soc*. **2010**, *132*, 1236-1237.

(44) Sethofer, S. G.; Staben, S. T.; Hung, O. Y.; Toste, F. D. *Org. Lett*. **2008**, *10*, 4315-4318.

(45) Lu, R.; Paul, C.; Basar, S.; König, W. A. *Tetrahedron: Asymmetry* **2005**, *16*, 883-887.

(46) Staben, S. T.; Kennedy-Smith, J. J.; Huang, D.; Corkey, B. K.; LaLonde, R. L.; Toste, F. D. *Angew. Chem., Int. Ed*. **2006**, *45*, 5991-5994.

(47) Ishiuchi, K.; Kubota, T.; Morita, H.; Kobayashi, J. *Tetrahedron Lett*. **2006**, *47*, 3287-3289.

(48) Marion, N.; de Frémont, P.; Lemiere, G.; Stevens, E. D.; Fensterbank, L.; Malacria, M.; Nolan, S. P. *Chem. Commun*. **2006**, 2048-2050.

(49) (a) Cabello, N.; Jiménez-Núñez, E.; Buñuel, E.; Cárdenas, D. J.; Echavarren, A. M. *Eur. J. Org. Chem.* **2007**, 4217-4223; (b) Leseurre L.; Toullec P. Y.; Genet, J. P.; Michelet, V. *Org. Lett*. **2007**, *9*, 4049-4052; (c) Ferrer, C.; Raducan, M.; Nevado, C.; Claverie, C. K.; Echavarren, A. M. *Tetrahedron* **2007**, *63*, 6306-6316; (d) Lee, S. I.; Kim, S. M.; Kim, S. Y.; Chung, Y. K. *Synlett* **2006**, 2256−2260; (e) Nieto-Oberhuber, C.; Munoz, M. P.; Bunuel, E.; Nevado, C.; Cardenas, D. J.; Echavarren, A. M. *Angew. Chem., Int. Ed.* **2004**, *43*, 2402-2408.

(50) Cabello, N.; Rodriguez, C.; Echavarren, A. M. *Synlett* **2007**, 1753-1758.

(51) Odabachian, Y.; Gagosz, F. *Adv. Synth. Catal*. **2009**, *351*, 379-386.

(52) Chatani, N.; Morimoto, T.; Muto, T.; Murai, S. *J. Am. Chem. Soc.* **1994**, *116*, 6049-6050.

(53) Trost, B. M.; Tanoury, G. J. *J. Am. Chem. Soc.* **1988**, *110*, 1636-1638.

(54) (a) Fürstner, A.; Szillat, H.; Stelzer, F. *J. Am. Chem. Soc.* **2000**, *122*, 6785-6786; (b) Méndez, M.; Muñoz, M. P.; Nevado, C.; Cárdenas, D. J.; Echavarren, A. M. *J. Am. Chem. Soc.* **2001**, *123*, 10511-10519.

(55) Chatani, N.; Inoue, H.; Morimoto, T.; Muto, T.; Murai, S. *J. Org. Chem.* **2001**, *66*, 4433-4436.

(56) Ota, K.; Lee, S. I.; Tang, J.-M.; Takachi, M.; Nakai, H.; Morimoto, T.; Sakurai, H.; Kataoka, K.; Chatani, N. *J. Am. Chem. Soc.* **2009**, *131*, 15203-15211.

(57) Chatani, N.; Kataoka, K.; Murai, S.; Furukawa, N.; Seki, Y. *J. Am. Chem. Soc.* **1998**, *120*, 9104-9105.

(58) (a) Chatani, N.; Inoue, H.; Kotsuma, T.; Murai, S. *J. Am. Chem. Soc.* **2002**, *124*, 10294-10295; (b) Kim, S. M.; Lee, S. I.; Chung, Y. K. *Org. Lett.* **2006**, *8*, 5425-5427.

(59) Miyanohana, Y.; Chatani, N. *Org. Lett.* **2006**, *8*, 2155-2158.

(60) (a) Miyanohana, Y.; Inoue, H.; Chatani, N. *J. Org. Chem.* **2004**, *69*, 8541-8543; (b) Nakai, H.; Chatani, N. *Chem. Lett.* **2007**, *36*, 1494-1495.

(61) Jiménez-Núñez, E.; Echavarren, A. M. *Chem. Rev.* **2008**, *108*, 3326-3350.

(62) Ezzitouni, A.; Russ, P.; Marquez, V. E. *J. Org. Chem.* **1997**, *62*, 4870-4873.

(63) Axen, U.; Lincoln, F. H.; Thompson, J. L. *J. Chem. Soc. D, Chem. Commun.* **1969**, 303-304.

(64) Ohta, Y.; Sakai, T.; Hirose, Y. *Tetrahedron Lett.* **1966**, 6365-6370.

(65) Fürstner, A.; Hannen, P. *Chem.-Eur. J.* **2006**, *12*, 3006-3019.

(66) Fürstner, A.; Schlecker, A. *Chem.-Eur. J.* **2008**, *14*, 9181-9191.

(67) (a) Nicholas, K. M. *Acc. Chem. Res.* **1987**, *20*, 207-214; (b) Teobald, B. J. *Tetrahedron* **2002**, *58*, 4133-4170.

(68) Müller, T. J. *Eur. J. Org. Chem.* **2001**, 2021-2033.

(69) Zhan, Z.; Yu, J.; Liu, H.; Cui, Y.; Yang, R.; Yang, W.; Li, J. *J. Org. Chem.* **2006**, *71*, 8298-8301.

(70) Srihari, P.; Bhunia, D. C.; Sreedhar, P.; Mandal, S. S.; Reddy, J. S. S.; Yadav, J. S.; *Tetrahedron Lett.* **2007**, *48*, 8120-8124.

(71) Sanz, R.; Martinez, A.; Alvarez-Gutierrez, J. M.; Rodriguez, F. *Eur. J. Org. Chem.* **2006**, *6*, 1383-1386.

(72) Luzung, M. R.; Toste, F. D. *J. Am. Chem. Soc.* **2003**, *125*, 15760-15761.

(73) Zhan, Z.; Yang, W.; Yang, R.; Yu, J.; Li, J.; Liu, H. *Chem. Commun.* **2006**, *31*, 3352-3354.

(74) Kabalka, G .W.; Yao, M.-L.; Borella, S. *J. Am. Chem. Soc.* **2006**, *128*, 11320-11321.

(75) Nishibayashi, Y.; Inada, Y.; Hidai, M.; Uemura, S. *J. Am. Chem. Soc.* **2003**, *125*, 6060-6061.

(76) Yadav, J. S.; Reddy, B. V. S.; Rao, T. S.; Rao, K. V. R. *Tetrahedron Lett.* **2008**, *49*, 614-618.

(77) Georgy, M.; Boucard, V.; Debleds, O.; Dal Zotto, C.; Campagne, J. M. *Tetrahedron* **2009**, *65*, 1758-1766.

(78) Sanz, R.; Martinez, A.; Miguel, D.; Alvarez-Gutierrez, J. M.; Rodriguez, F. *Synthesis* **2007**, *20*, 3252-3256.

(79) Okada, T.; Patterson, B. K.; Ye, S.-Q.; Gurney, M. E. *Virology* **1993**, *192*, 631-642.

(80) Shaw, C. F. *Chem. Rev.* **1999**, *99*, 2589-2600.

(81) Sutton, B. M.; McGusty, E.; Wlatz, D. T.; DiMartino, M. J. *J. Med. Chem.* **1972**, *15*, 1095-1098.

(82) (a) Casini, A.; Diawara, M. C.; Scopelliti, R.; Zakeeruddin, S. M.; Grätzel, M.; Dyson, P. J. *Dalton Trans.* **2010**, 2239-2245; (b) Fregona, D.; Ronconi, L.; Aldinucci, D. *Drug Discovery Today* **2009**, *14*, 1075-1076; (c) Hickey, J. L.; Ruhayel, R. A.; Barnard, P. J.; Baker, M. V.; Berners-Price, S. J.; Filipovska, A. *J. Am. Chem. Soc.* **2008**, *130*, 12570-12571.

(83) (a) Pope, W. J. *Br. Pat.*, 338,506, **1930**; (b) Malik, N. A.; Sadler, P. J.; Neidle, S.; Taylor, G. L. *J. Chem. Soc., Chem. Commun.* **1978**, 711-712; (c) Kilpin, K. J.; Henderson, W.; Nicholson, B. K. *Polyhedron* **2007**, *26*, 204-213.

(84) (a) Tyabji, A. M.; Gibson, C. S. *J. Chem. Soc.* **1952**, 450-452; (b) Kharasch, M. S.; Isbell, H. S. *J. Am. Chem. Soc.* **1931**, *53*, 3059-3065; (c) Bonati, F.; Burini, A.; Pietroni, B. R.; Giorgini, E.; Bovio, B. *J. Organomet. Chem.* **1988**, *344*, 119-135; (d) Berners Price, S. J.; DiMartino, M. J.; Hill, D. T.; Kuroda, R.; Mazid, M. A.; Sadler, P. J. *Inorg. Chem.* **1985**, *24*, 3425-3434; (e) de Frémont, P.; Stevens, E. D.; Eelman, M. D.; Fogg, D. E.; Nolan, S. P. *Organometallics* **2006**, *25*, 5824-5828.

(85) Goodgame, D. M. L.; Omahoney, C. A.; Plank, S. D.; Williams D. J. *Polyhedron* **1993**, *12*, 2705-2710.

(86) de Frémont, P.; Singh, R.; Stevens E. D.; Petersen, J. L.; Nolan S. P. *Organometallics* **2007**, *26*, 1376-1385.

(87) Urbano, J.; Hormigo, A. J.; De Frémont, P.; Nolan, S. P.; Díaz-Requejo, M. M.; Pérez, P. J. *Chem. Commun.* **2008**, 759-761.

(88) Ricard, L.; Gagosz, F. *Organometallics* **2007**, *26*, 4704-4707.

(89) Baker, M. V.; Barnard, P. J.; Brayshaw, S. K.; Hickey, J. L.; Skelton, B. W.; White, A. H. *Dalton Trans.* **2005**, 37-43.

(90) Cui, D.-M.; Meng, Q.; Zheng, J.-Z.; Zhang, C. *Chem. Commun*. **2009**, 1577-1579.

(91) (a) Krossing, I. *Chem. Eur. J.* **2001**, *7*, 490-502; (b) Boing, C.; Francio, G.; Leitner, W. *Adv. Synth. Catal.* **2005**, *347*, 1537-1541.

(92) Jafarpour, L.; Stevens, E. D.; Nolan, S. P. *J. Organomet. Chem.* **2000**, *606*, 49-54.

(93) Arduengo, A. J., III. U.S. Patent 5 007 414, **1991**.

(94) Fairlamb, I. J. S.; Taylor, R. J. K.; Serrano, J. L.; Sanchez, G. *New J. Chem.* **2006**, *30*, 1695-1704.

(95) Tetrafluorosuccinimide possesses very low solubility in CH_2Cl_2.

(96) (a) Roundhill, D. M. *Inorg. Chem.* **1970**, *9*, 254-258; (b) Carturan, G.; Belluco. V.; Grazini, M.; Ros, R. *J. Organomet. Chem.* **1976**, *112*, 243-248; (c) Adams, H.; Bailey, N. A.; Briggs, T. N.; McCleverty, J. A.; Colquhoun, H. M.; Williams, D. J. *J. Chem. Soc. Dalton Trans.* **1986**, 813-819.

(97) (a) Zakrzewski, J. *J. Organomet. Chem.* **1989**, *359*, 215-218; (b) Dubuc, I.; Dubois, M-A.; Bélanger-Gariépy, F.; Zargarian, D. *Organometallics* **1999**, *18*, 30-35.

(98) Bell, R. P.; Higginson, W. C. E. *Proc. Roy. Soc. A* **1949**, *197*, 141-159

(99) Hine, J.; Hahn, S.; Hwang, J. *J. Org. Chem.* **1988**, *53*, 884-887.

(100) Darnall, K. R.; Townsend, L. B.; Robins, R. K. *Proc. Nat. Ac. Sc. USA* **1967**, *57*, 548-553.

(101) Schwarzenbach, G.; Lutz, K. *Helv. Chim. Acta.* **1940**, *23*, 1162-1190.

(102) Clarke, D. A.; Hunt, M. M.; Kemmitt, R. D. W. *J. Organomet. Chem.* **1979**, *175*, 303-313.

(103) de Frémont, P.; Scott, N. M.; Stevens, E. D.; Nolan, S. P. *Organometallics* **2005**, *24*, 2411-2418.

(104) (a) Boule, P.; Lemaire, J. *J. Chim. Phys. Phys.-Chim. Biol.* **1980**, *77*, 161-166; (b) Al-Amoudi, M. A. S.; Vernon, J. M. *J. Chem. Soc., Perkin Trans. 2* **1999**, 2667-2670; (c) Schenck, G. O.; Hartmann, W.; Mannsfeld, S. P.; Metzner, W.; Krauch, C. H. *Chem. Ber.* **1962**, *95*, 1642-1647.

(105) Raubenheimer, H. G.; Olivier, P. J.; Lindeque, L.; Desmer, M.; Hrušak, J.; Kruger, G. J. *J. Organomet. Chem.* **1997**, *544*, 91-100.

(106) Fantasia, S.; Petersen, J. L.; Jacobsen, H.; Cavallo, L.; Nolan, S. P. *Organometallics* **2007**, *26,* 5880-5889.

(107) Radius, U.; Bickelhaupt, F. M. *Coord. Chem. Rev.* **2009**, *253*, 678-686.

(108) Baldwin, J. E. *J. Chem. Soc., Chem. Commun.* **1976**, 734-736.

(109) Kuzmic, P. *Anal. Biochem.* **1996**, 237, 260-273.

(110) (a) McArdle; J. V.; Bossard, G. E. *J. Chem. Soc., Dalton Trans.* **1990**, 2219-2224; (b) Blake, A. J.; Gould, R. O.; Greig, J. A.; Holder, A. J.; Hyde, T.; Schroder, M. *J. Chem. Soc., Chem. Commun.* **1989**, 876-878.

(111) Ojima, I.; Vu, A. T.; Lee, S. Y.; McCullagh, J. V.; Moralee, A. C.; Fujiwara, M.; Hoang, T. H. *J. Am. Chem. Soc.* **2002**, *124*, 9164-9174**.**

(112) Trost, B. M.; Tour, J. M. *J. Am. Chem. Soc.* **1987**, *109*, 5268-5270.

(113) Hahn, K.; Chulbom, L. *J . Am. Chem. Soc.* **2005**, *127*, 10180-10181.

(114) Nieto-Oberhuber, C.; Munoz, M. P.; Lopez, S.; Jimenez-Nunez, E.; Nevado, C.; Herrero-Gomez, E.; Raducan, M.; Echavarren, A. M. *Chem.-Eur. J.* **2006**, *12*, 1677-1693.

(115) Schelwies, M.; Dempwolff, A. L.; Rominger, F.; Helmchen, G. *Angew. Chem., Int. Ed.* **2007**, *46*, 5598-5601.

(116) Florio, S.; Troisi, L. *Tetrahedron Lett.* **1996**, *37*, 4777-4780.

(117) Cai, G.; Zhu, W.; Ma, D. *Tetrahedron* **2006**, *62*, 5697-5708.

(118) Zhang, L.; Kozmin, S. A. *J. Am. Chem. Soc.* **2005**, *127*, 6962-6963.

(119) Wollowitz, S.; Halpern, J. *J. Am. Chem.* Soc. **1988**, *110,* 3112-3120.

(120) (a) Fairlamb, I. J. S.; Tommasi, S.; Moulton, B. E.; Zheng, W.; Lin, Z.; Whitwood, A. C. *Eur. J. Inorg. Chem.* **2007**, 3173-3178; (b) Fairlamb, I. J. S.; Grant, S.; Tommasi, S.; Lynam, J. M.; Bandini, M.; Dong, H.; Lin, Z.; Whitwood, A. C. *Adv. Synth. Catal.* **2006**, *348*, 2515-2530.

(121) Shen, Q.; Mastryukov, V. S.; Boggs, J. E. *J. Mol. Struct.* **1995**, *352-353*, 181-191.

(122) Vilsmaier, E.; Roth, W.; Bergsträßer, U. *J. Mol. Struct.* **1999**, *513*, 21-28.

(123) Vilsmaier, E.; Dotzauer, M.; Wagemann, R.; Tetzlaff, C.; Fath, J.; Schlag, W. R.; Bergsträßer, U. *Tetrahedron* **1995**, *51*, 11183-11198.

(124) (a) Tunge, J. A.; Mellegaard, S. R. *Org. Lett.* **2004**, *6*, 1205-1207; (b) Mellegaard-Waetzig, S. R.; Wang, C.; Tunge, J. A. T*etrahedron* **2006**, *62*, 7191-7198.

(125) Schomaker, J. M.; Pulgam, V. R.; Borhan, B. *J. Am. Chem. Soc.* **2004**, *126*, 13600-13601.

(126) Gansäuer, A.; Fan, C. -A.; Keller, F.; Keil, J. *J. Am. Chem. Soc.* **2007**, *129*, 3484-3485.

(127) Wang, B.; Zhang, H.; Zheng, A.; Wang, W. *Bioorg. Med. Chem.* **1998**, *6*, 417-426.

(128) Huang, C. G.; Beveridge, K. A.; Wan. P. *J. Am. Chem. Soc.* **1991**, *113*, 7676-7684.

(129) Nishibayashi, Y.; Wakiji, I.; Ishii, Y.; Uemura, S.; Hidai, M. *J. Am. Chem. Soc.* **2001**, *123*, 3393-3394.

(130) Kuninobu, Y.; Ueda, H.; Takai, K. *Chem. Lett.* **2008**, *37*; 878-879.

(131) Belting, V.; Krause, N. *Org. Biomol. Chem.* **2009**, *7*, 1221-1225.

(132) Ramón, R. S.; Marion, N.; Nolan, S. P. *Tetrahedron* **2009**, *65*, 1767-1773.

(133) Sun, J.; Conley, M. P.; Zhang, L.; Kozmin, S. A. *J. Am. Chem. Soc*. **2006**, *128*, 9705-9710.

(134) (a) Wang, W.; Xu, B.; Hammond, G. B. *Org. Lett.* **2008**, *10*, 3713-3717; (b) Blaszykowski, C.; Harrak, Y.; Brancour, C.; Nakama, K.; Dhimane, A. L.; Fensterbank, L.; Malacria, M. *Synthesis* **2007**, 2037-2049.

(135) Fukamizu, K.; Miyake, Y.; Nishibayashi, Y. *Angew. Chem., Int. Ed*. **2009**, *48*, 2534 -2537.

(136) Horino, Y.; Yamamoto, T.; Ueda, K.; Kuroda, S.; Toste, F. D. *J. Am. Chem. Soc.* **2009**, *131*, 2809-2811.

(137) (a) Gagosz, F. *Org. Lett.* **2005**, *7,* 4129-4132; (b) Zhang. L.; Kozmin, S. A. *J. Am. Chem. Soc.* **2004**, *126*, 11806-11807.

(138) Baldwin, J. E.; Leber, P. A. *Org. Biomol. Chem.* **2008**, *6*, 36-47.

(139) Hansch, C.; Leo, A.; Taft, R. W. *Chem. Rev.* **1991**, *91*, 165-195.

(140) Doering, W. von E.; Schmidt, E. K. G. *Tetrahedron* **1971**, *27*, 2005-2030.

(141) (a) Cooke, R. S.; Andrews, U. H. *J. Am. Chem. Soc.* **1974**, *96*, 2974-2980; (b) Baldwin, J. E.; Keliher, E. J. *J. Am. Chem. Soc.* **2002**, *124*, 380-381; (c) Suhrada, C. P.; Houk, K. N. *J. Am. Chem. Soc.* **2002**, *124*, 8796-8797; (d) Doubleday, C.; Suhrada, C. P.; Houk, K. N. *J. Am. Chem. Soc.* **2006**, *128*, 90-94.

(142) Doering, W. von E.; Zhang, T.-H.; Schmidt, E. K. G. *J. Org. Chem.* **2006**, *71*, 5688-5693.

(143) Herrmann, W. A.; Böhm, V. P. W.; Gstöttmayr, C. W. K.; Grosche, M.; Reisinger, C. P.; Weskamp, T. *J. Organomet. Chem.* **2001**, *617-618*, 616-628.

(144) Henne, A. L.; Zimmer, W. F. *J. Am. Chem. Soc.* **1951**, *73*, 1103-1104.

(145) Unresolved due to complicated higher order spin-spin coupling (^{13}C-^{19}F).

(146) Davis, S. J.; Rondestvedt, C. S. *Chem. Ind.* **1956**, *845*-846.

(147) Tedaldi, L. M.; Smith, M. E. B.; Nathani, R. I.; Baker, J. R. *Chem. Commun.* **2009**, 6583-6585.

(148) Schwier, T.; Rubin, M.; Gevorgyan, V. *Org. Lett.* **2004**, *6*, 1999-2000.

(149) Harrowven, D. C.; May, P. J.; Bradley, M. *Tetrahedron Lett.* **2003**, *44*, 503-506.

(150) Barluenga, J.; Rodríguez, M. A.; Campos, P. J. *Tetrahedron Lett*. **1990**, *31*, 2751-2754.

(151) Bandini, M.; Cozzi, P. G.; Licciulli, S.; Umani-Ronchi, A. *Synthesis* **2004**, 409-414.

(152) Linares, M. L.; Sanchez, N.; Alajarin, R.; Vaquero, J. J.; Alvarez-Builla, J. *Synthesis* **2001**, 382-388.

(153) Cox, R. J.; Ritson, D.J.; Dane, T. A.; Berge, J.; Charmant J. P. H.; Kantacha, A. *Chem. Commun.* **2005**, 1037-1039.

(154) Alonso, D. A.; Najera, C.; Pacheco, M. C. *J. Org. Chem.* **2004**, *69*, 1615-1619.

(155) Wolf, C.; Liu, S. *J. Am. Chem. Soc.* **2006**, *128*, 10996-10997.

(156) Yao, X.; Li, C.-J. *Org. Lett.* **2005**, *7*, 4395-4398.

(157) Tanaka, K.; Shoji, T. *Org. Lett.* **2005**, *7*, 3561-3563.

(158) Cheng, J.; Sun, Y.; Wang, F.; Guo, M.; Xu, J.-H.; Pan, Y.; Zhang, Z. *J. Org. Chem.* **2004**, *69*, 5428-5432.

(159) Smith, C. D.; Tchabanenko, K.; Adlington, R. M.; Baldwin, J. E. *Tetrahedron Lett*. **2006**, 3209-3212.

(160) Hearn, M. T. *J. Magn. Reson.* **1975**, *19*, 401-404.

Chapter 3: Ru imidate complexes; synthesis and catalytic activity

3.1. Introduction

3.1.1. Ru imidate complexes

There have been several ruthenium imidate complexes reported, including succinimidate, phthalimidate and bis(2-pyrimidyl)carboimidate complexes, although with no applications envisaged. Islam and Uddin[1] have reported triaquaruthenium(III) trisuccinimido and triphthalimido complexes, as well as terpyridine and diethylenetriamine analogues, with monodentate *N*-ligated imidate ligands, by reaction of the relevant imidate with $RuCl_3.3H_2O$. Sahajpal *et al.*[2] have prepared several bridged dinuclear ruthenium succinimidate structures including: $[Ru_2(\mu\text{-Cl})(\mu\text{-H})(\mu\text{-}N,O\text{-succ})_2(CO)(PPh_3)_3]$, $[Ru_2(\mu\text{-Cl})(\mu\text{-H})(\mu\text{-}N,O\text{-succ})_2(CO)_2(PPh_3)_2]$ and $[Ru_2(\mu\text{-Cl})(\mu\text{-H})(\mu\text{-}N,O\text{-succ})_2(PPh_3)_4]$ (**154**), by mixing succinimide with either $[RuCl_2(PPh_3)_3]/NEt_3$ or $[RuCl(H)(PPh_3)_3]$. The hydride ligand may originate from methanol added during workup. The complexes contain *N*,*O*-ligated bidentate bridging succinimidate ligands, and bridging hydride and chloride ligands. Shaver *et al.*[3] have reported phthalimidate complexes (with monodentate *N*-ligated phthalimidate ligands) bearing pentadienyl and thioether ligands, including $[Ru(C_5H_5)(N\text{-ptm})(PPh_3)_2]$ and $[Ru_2(C_5H_5)(N\text{-ptm})_2(\mu\text{-}SCH_3)\{\mu\text{-}SCH(CH_3)_2\}]$ (**155**).

Metcalfe *et al.*[4] have reported (but not isolated) [Ru{bis(2-pyrimidyl)carboimidato}(1,10-phenanthroline)](PF_6) (**156**). This is formed (along with other products) by the reaction of $Ru(phen)_2Cl_2.2H_2O$ with tpymt {2,4,6-tris(2-pyrimidyl)-1,3,5-triazine} in refluxing methanol. The tpymt ligand is hydrolyzed to form the bis(2-pyrimidyl)carboimidato ligand. Selected structures are displayed in Scheme 47.

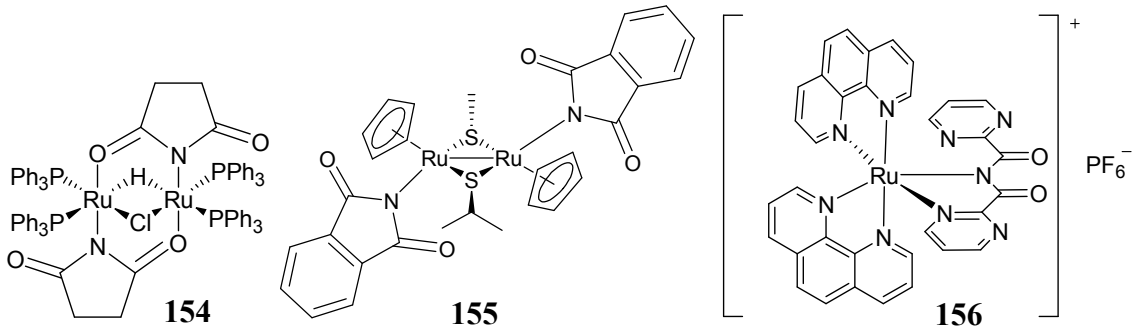

Scheme 47. The structures of $[Ru_2(\mu\text{-Cl})(\mu\text{-H})(\mu\text{-}N,O\text{-succ})_2(PPh_3)_4]$ (**154**), $[Ru_2(C_5H_5)_2(N\text{-ptm})_2(\mu\text{-}SCH_3)\{\mu\text{-}SCH(CH_3)_2\}]$ (**155**) and [Ru{bis(2-pyrimidyl)carboimidato}(1,10-phenanthroline)](PF_6) (**156**).

3.1.2. Diene Metathesis

Alkene metathesis is the transformation of olefins by alkene bond formation and scission, there are several types, including: ring-closing (cyclisation of dienes) (I), ring-opening (formation of dienes from cyclic olefins) (II), cross (also called acyclic diene metathesis, involving the combination of two different olefins to produce two new olefins) (III), ring-rearrangement metathesis (where there are cyclic and acyclic olefins in one molecule) (IV) and ring-opening metathesis polymerisation (formation of polymers from cyclic olefins) (V) (Scheme 48).[5]

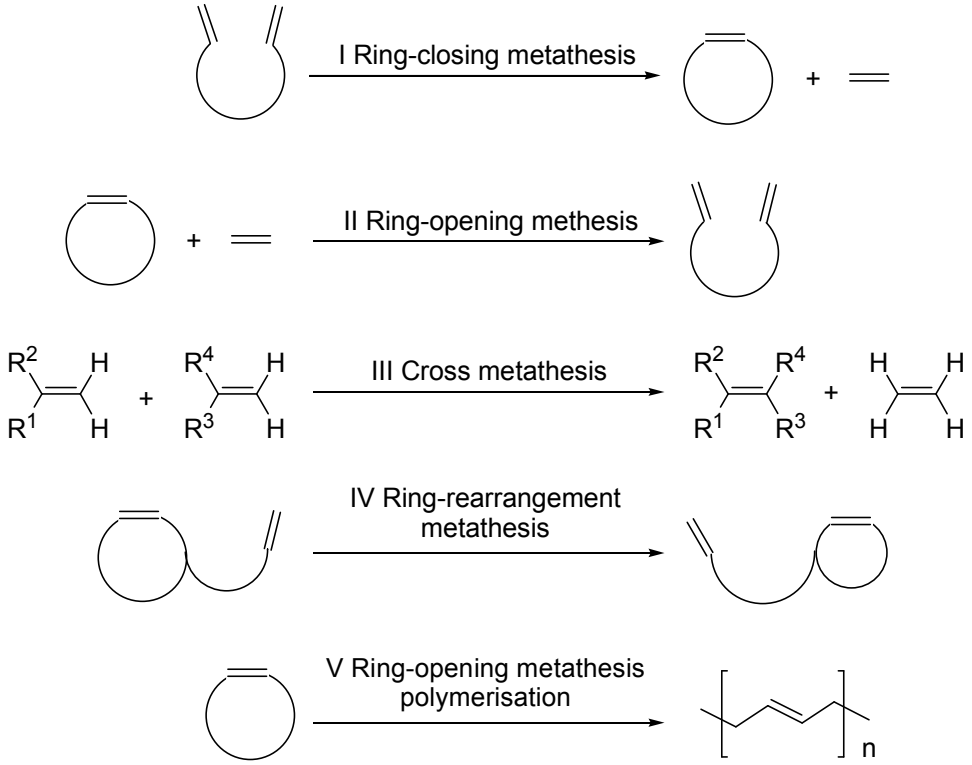

Scheme 48. Types of diene metathesis.

Metathesis is an extremely powerful method for the formation of carbon-carbon bonds and has been widely used industrially in various applications and in natural product synthesis. A major industrial example is that of the Shell Higher Olefins Process (SHOP), which is a method of producing C_{11} to C_{14} linear olefins from ethene for the production of detergents. A key step uses a heterogeneous molybdate catalyst in a cross metathesis reaction as a means of producing linear olefins in the range C_{11}-C_{14} from mixtures of short and long chain olefins. This process is used to produce more than a million tonnes of linear olefins a year.[6]

There are many examples of natural products syntheses which employ metathesis as a key step in the process; ring-closing metathesis (RCM) by homogeneous ruthenium and molybdenum catalysts to form macrocycles is widely used.[7] One example is the use of ring-closing metathesis to create the macrocyclic core in the synthesis of pochonin C (**157**), a natural product with antiviral properties (Scheme 49). The intermediate macrocycle **159** is formed from diene **158** as one regio and stereoisomer, in the presence of ester, enone and epoxide functional groups, demonstrating the broad applicability of this method.[8]

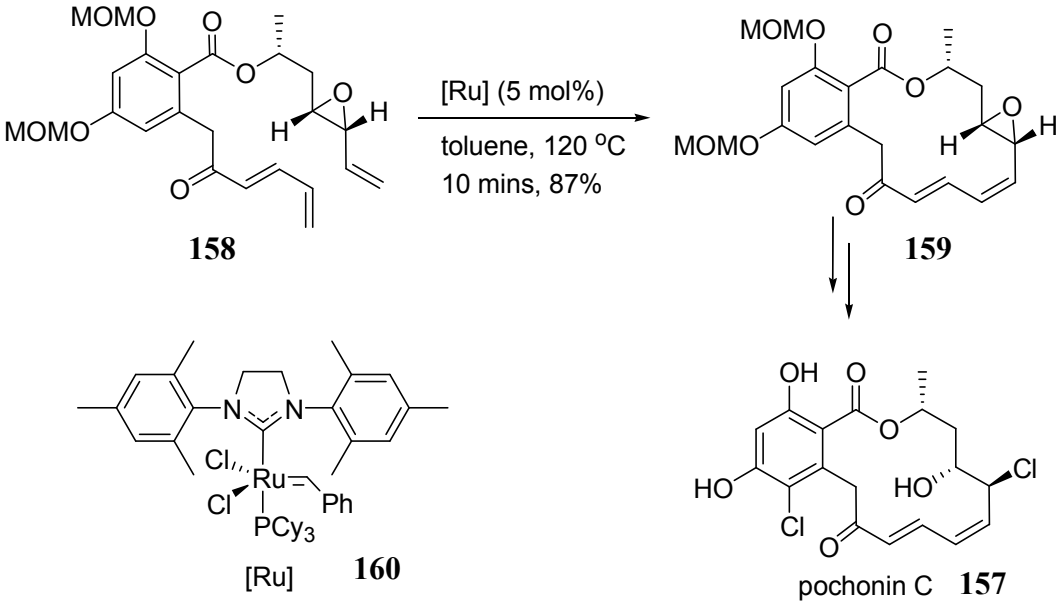

Scheme 49. Macrocyclisation by ring-closing metathesis in the synthesis of pochonin C (**157**).

Ring-opening metathesis polymerisation (ROMP) is also used industrially for the synthesis of polymers.[9]

3.1.3. Metathesis catalysts

3.1.3.1. Ill-defined catalytic systems

Due to the great synthetic and industrial potential of the alkene metathesis reaction there has been a huge amount of research into catalysts that promote the transformation.[10] However, it was only in the 1960's that the metathesis reaction and the first metathesis catalysts were discovered serendipitously during research into Ziegler-Natta catalysis. The first was the so called 'disproportionation' of olefins by Banks and Bailey in 1964 who

used a heterogeneous $M(CO)_6/Al_2O_3$ (M is Mo or W) combination to carry out metathesis of propylene (at 90-315 °C).[11] In the same year Natta reported that a homogenous $MCl_6/AlEt_3$ (M is Mo or W) combination could promote the homopolymerisation (ROMP) of cyclopentene.[12] Calderon *et al.* used a homogenous $WCl_6/EtAlCl_2/EtOH$ system to transform 2-pentene into a statistical mixture of 2-butene, 2-pentene and 3-hexene, coining the term 'Olefin Metathesis' for the reaction.[13] Rh systems were also discovered which used a combination of PPh_3 and $AlEt_3$ with $ReCl_4$ or $ReOCl_3$ to promote metathesis.[14]

Research into a possible mechanism for this class of reactions led to the 'Chauvin mechanism' being reported in 1971.[15] However, the catalysts themselves were ill-defined mixtures which were poorly understood, were very moisture sensitive, intolerant of any functionality in the olefins, required harsh conditions and long initiation times.

3.1.3.2. Well-defined Mo, W and Ta systems

In 1964 Fischer reported the first (unisolated) metal carbene, $[W(COCH_3)(CH_3)(CO)_5]$, this type of heteroatom stabilised carbene has since been termed a 'Fischer carbene'.[16] Schrock isolated the first ylide carbene bearing an alpha hydrogen in 1974, $[Ta(CH_2C(CH_3)_3)_3\{CHC(CH_3)_3\}]$[17] and the first methylene example, $[Ta(C_5H_5)_2(CH_3)(CH_2)]$ in 1975.[18] These types of unstabilised carbenes have since been termed 'Schrock carbenes'. Investigation of the reactions of these complexes with alkenes[19] resulted in the development of the first well-defined organometallic metathesis catalysts by Schrock (with Nb, Ta and W), such as $[Ta(CHCMe_3)Cl(OCMe_3)_2(PMe_3)]$, which were short lived but could metathesise simple alkenes such as *cis*-2-pentene.[20] Other tungsten complexes were prepared and shown to be active metathesis catalysts, such as, $[WCl_2\{CHC(CH_3)_3\}(O)(PEt_3)]$.[21]

Variation of the anionic ligands in complexes using bulky alkoxy groups, such as $[W(OCH_2{}^tBu)_2X_2(CH{}^tBu)]$ (where X is Br or Cl), which when activated by $AlCl_3$, led to highly active catalysts comparable to early ill-defined systems.[22] The use of bulky imido ligands and electron withdrawing alkoxy ligands led to Lewis acid free catalytic systems, such as $[W(NAr)\{OCMe(CF_3)_2\}_2(CH{}^tBu)]$ (Ar = 2,6–diisopropylphenyl).[23] Later analogous Mo complexes were prepared in order to try to improve functional group tolerance, catalyst life time and selectivity at the expense of activity.[24] Variation of the alkylidene ligand resulted in the preparation of the 'Schrock Catalyst',

[Mo(NAr){OCMe(CF_3)$_2$}$_2${CHC(CH_3)$_2$Ph}] (**161**), which has been very widely utilised (Figure 31).[25] This catalyst is highly active and selective, and more tolerant of some functional groups than earlier catalysts, however it is sensitive to air, water and many functional groups, particularly protic groups.

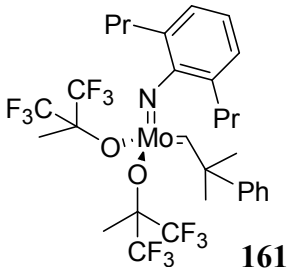

161

Figure 31. Structure of [Mo(NAr){OCMe(CF_3)$_2$}$_2${CHC(CH_3)$_2$Ph}] (**161**) - the 'Schrock' catalyst.

3.1.3.3. Ru catalysts

The intolerance of early Schrock type catalysts to air, water and functionality led to the investigation of Ru and Os complexes as potential metathesis catalysts. Early research by Grubbs *et al.* found that simple Ru and Os complexes ($RuCl_3$, [$RuCl_3$(3,5-COD)] and $OsCl_3$) could carry out ROMP in water[26] and ROMP of unprotected norbornenol derivatives which Schrock type catalysts could not.[27] Grubbs subsequently prepared the first ruthenium alkylidene complex, [$RuCl_2$(CHCH=CPh_2)(PPh_3)$_2$], which could catalyse ROMP in protic media[28] and RCM of functionalised dienes.[29] Ligand variation of halide and phosphine ligands resulted in the finding that a Cl/PCy_3 combination gave the best performance allowing broader metathesis activity and the metathesis of acyclic olefins.[30] Variation of the alkylidene ligand, *via* diazoalkanes, culminated with the preparation of [$RuCl_2$(CHPh)(PCy_3)$_2$] (**162**), since termed Grubbs 1st generation catalyst (Figure 32), which allowed the metathesis of acyclic and functionalised olefins with 20-1000 times higher activity than earlier Ru catalysts. The complex is also remarkably robust, being stable at 60 ˚C in solution and tolerant of water, alcohols and amines, although sensitive to air (O_2 increases the initiation and decomposition rates).[31]

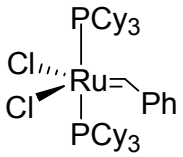

162

Figure 32. The structure of $[RuCl_2(CHPh)(PCy_3)_2]$ (**162**) – 'Grubbs' 1st generation catalyst.

The superior stabilising effect of PCy_3 over PPh_3 (analogues containing PPh_3 decompose in a few hours in solution) led to the investigation of more electron donating ligands, notably *N*-heterocyclic carbenes, to stabilise the catalysts.[32] Three research groups then published the preparation of $[RuCl_2(CHPh)(IMes)(PCy_3)]$, which has a very fast initiation rate and good stability.[33] A further increase in the electron donating ability of the NHC ligand in the form of saturated $IMesH_2$ led to another milestone with the preparation of $[RuCl_2(CHPh)(IMesH_2)(PCy_3)]$ (**160**) - Grubbs 2nd generation catalyst (Figure 33), which is similar to the Schrock catalyst in terms of activity, can yield di, tri and tetra-substituted olefins by RCM and is active at very low catalyst loadings (0.05 mol%).[34]

There have been a number of subsequent modifications which have increased the utility of this type of catalyst. Hoveyda *et al.* synthesised $[RuCl_2(o\text{-}^{i}PrO\text{-}CHPh)(PCy_3)]$ and found it to be stable enough to be purified by silica-gel column chromatography in air,[35] followed by a second generation analogue $[RuCl_2(o\text{-}^{i}PrO\text{-}CHPh)(IMesH_2)]$ - the Grubbs-Hoveyda catalyst (**163**), with increased activity towards electron deficient (such as acrylonitrile) and tri-substituted olefins and greatly improved stability of the precatalyst due to the absence of phosphine ligands (although slower initiation).[36] Grubbs substituted the phosphine ligand in the 2nd generation complex with pyridine[37] and subsequently 3-bromopyridine[38] ligands to yield $[RuCl_2(CHPh)(IMesH_2)(3\text{-}BrPy)_2]$ (**164**) which proved to be a very fast initiator with high activity for acrylonitrile cross-metathesis.

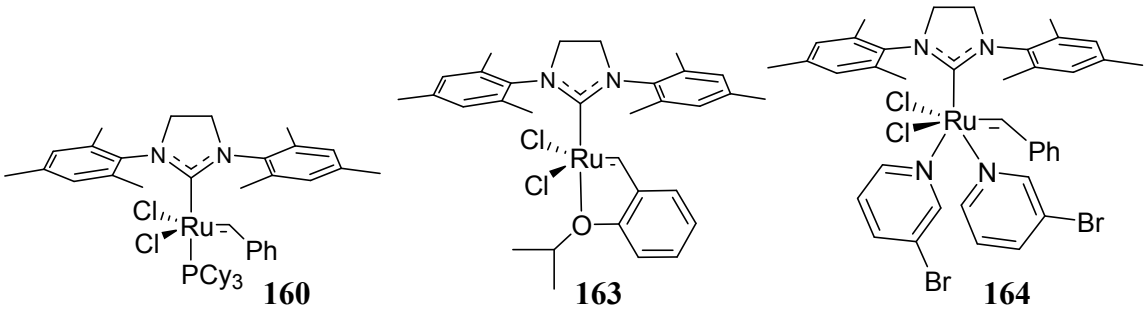

160 **163** **164**

Figure 33. Structures of $[RuCl_2(CHPh)(IMesH_2)(PCy_3)]$ (**160**), $[RuCl_2(o\text{-}^{i}PrO\text{-}CHPh)(PCy_3)]$ (**163**) and $[RuCl_2(CHPh)(IMesH_2)(3\text{-}BrPy)_2]$ (**164**).

Piers *et al.* have prepared a cationic phosphonium alkylidene catalyst (**165**) that has a vacant site rather than a second neutral ligand (Figure). This results in extremely rapid initiation, significantly faster than other Ru and Schrock type catalysts.[39] Other advances include chiral[40] and water/ionic liquid soluble analogues.[41]

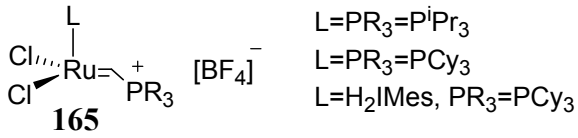

165

Figure 34. Structure of Ru phosphonium alkylidene complexes (**165**) reported by Piers.

3.1.3.4. Ru pseudohalide catalysts

The use of electron withdrawing alkoxy ligands led to the development of Lewis acid free[23] as well as highly efficient chiral[42] catalytic systems for the Schrock series of catalysts described above, however only chloride is routinely used as an anionic ligand in Ru catalysts. The effects of varying the nature of halide ligands in Ru complexes has however been reported, a generic example is the catalyst $[RuX_2(CHCHCPh_2)(PCy_3)_2]$ (**166**) (where X is the halide ligand). The exchange of an iodide ligand for a chloride results in a more than thirteen fold increase in turnover frequency (TOF) in the ring closing metathesis of diethyl diallylmalonate (**167**) (Scheme 50),[43] demonstrating the pronounced effect of the nature of the halide ligand on metathesis activity and the potential for improvement of the catalysts by the use of pseudohalide ligands.

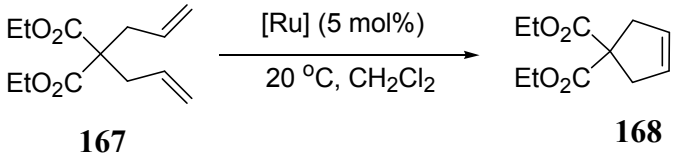

167 **168**

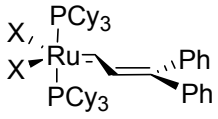

[Ru] **166**

X	TOF (turnovers/hr)
Cl	19.0
Br	15.4
I	1.4

Scheme 50. The effect of varying the nature of the halide ligand in the ring closing metathesis of diethyl diallylmalonate (**167**) by $[RuX_2(CHCHCPh_2)(PCy_3)_2]$ (**166**).

There have been a significant number of pseudohalide ligated Ru benzylidene complexes reported, with fluorinated carboxylates widely used. Buchowicz *et al.* have prepared $[Ru_2(O_2CCF_3)_2(\mu\text{-}O_2CCF_3)_2(CHPh)_2(\mu\text{-}OH_2)(PCy_3)_2]$ (**169**),[44] which is significantly less active than the parent dichloride complex in RCM as the bridging OH_2 ligand is required to dissociate to generate an active monomeric catalyst. A monomeric complex, $[Ru(O_2CCF_3)_2(CHPh)(PCy_3)_2]$ (**170**), can be generated by treatment of **169** with PCy_3 although this too has low metathesis activity (Scheme 51).[45]

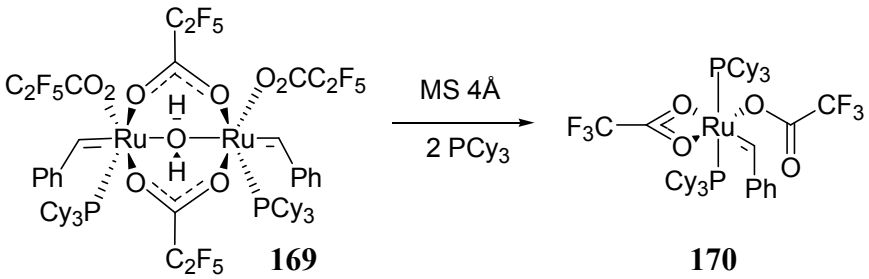

Scheme 51. Preparation of $[Ru(O_2CCF_3)_2(CHPh)(PCy_3)_2]$ (**169**) from $[Ru_2(O_2CCF_3)_2(\mu\text{-}O_2CCF_3)_2(CHPh)_2(\mu\text{-}OH_2)(PCy_3)_2]$ (**170**).

Buchmeiser and co-workers have reported $[Ru(O_2CCF_3)_2(o\text{-}^{i}PrO\text{-}CHPh)(IMesH_2)]$,[46] which has good stability and activity similar to the parent chloride complex, a low activity OSO_2CF_3 analogue, and O_2CCF_3 and $O_2CC_6F_5$ complexes (for use as alkyne metathesis catalysts).[47] Braddock[48] monitored the exchange of Br, Cl, O_2CCF_3 and $O_2CC_2F_5$ ligands between Grubbs-Hoveyda 2nd generation (**163**) type complexes and found that anionic ligand exchange between complexes occurred readily in solution. This was presumed to occur *via* bridged dimers, with exchange between dicarboxylate complexes occurring faster than dihalide complexes.

Perfluorocarboxylate ligands have been used to link Ru benzylidene complexes to solid supports. These have lower activity than the parent dichloride complexes but result in very low Ru residues in the purified product, and allows the recovery and reuse of the catalyst. Mol and co-workers have reported a Grubbs 1st generation analogue linked to a silica support *via* a fluorinated dicarboxylate (**171**) (Figure 35).[49] The Blechert and Buchmeiser[46,50] groups reported the preparation of Grubbs and Grubbs-Hoveyda 1st and 2nd generation complexes containing O_2CCF_3, $O_2CC_2F_5$, OC_6F_5 and fluorinated carboxylates linked to polystyrene supports[51] and found that monosubstituted complexes had better activity than disubstituted complexes (although significantly less than the parent dichloride).[52]

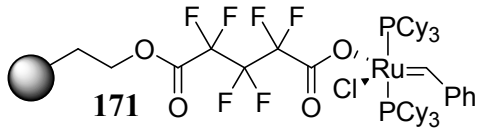

Figure 35. Grubbs 1st generation type Ru benzylidene complex (**171**) linked to a silica support by a fluorinated dicarboxylate ligand reported by Mol.

Fogg and co-workers have prepared a series [Ru(catecholate)(CHPh)(IMes)(Py)] (Py is pyridine) complexes (**172**) with substituted catecholate ligands spanning 4.5 pK_a units (Figure 36). The catecholate ligand allows the variation of electronic parameters without disturbing steric parameters. They found that activity declines with increasing electron withdrawal, with both initiation and particularly propagation rates affected.[53] Increased steric bulk of the ligands may also reduce metathesis activity. They also prepared related complexes containing chelating dichloro *o*-sulfonato aryloxide ligands which possessed good metathesis activity.[54]

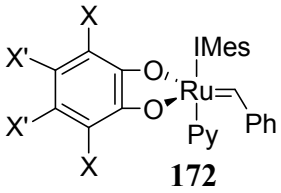

	pK_a		pK_a
X=X'=H	9.36	X=X'=F	6.26
X=H, X'=Me	9.92	X=X'=Cl	5.83
X=H, X'=Cl	8.10	X=X'=Br	5.49
X=H, X'=Br	7.98		

Figure 36. [Ru(catecholate)(CHPh)(IMes)(Py)] (**172**) complexes prepared by Fogg.

Many of the pseudohalide ligands used have been bidentate, *via* linkage to a pendant neutral ligand. These include *N*,*O*-prolinate, *ortho*-diphenylphosphino benzoate and *ortho*-carboxylate substituted furans ligands reported by Grubbs,[55] tridentate *N*,*N*,*O*-heteroscorpionate ligands reported by Burzlaff[56] and bidentate *N*,*O*-coordinated Schiff base ligands reported by Verpoort[57] and Hermann.[58] The use of bi and tridentate *N*,*O*- and *N*,*O*,*O*-amino-benzyloxy ligands by Jensen has resulted in complexes (**173**) with very low activity and poor thermal stability (Figure 37).[59] Related bidentate cyclohexanoxy ligands with pendant pyridine groups have been reported by Vosloo[60] with low activity at room temperature but activity superior to that of the parent complex at 70 ˚C for linear alkene metathesis. Raines[61] has used an *N*,*O*-chelated salicylaldimine ligand in conjunction with Grubbs 1st and 2nd generation type complexes (**174**) resulting in slow initiation but good RCM activity in protic solvents, including the highest reported rate for the RCM of *N*,*N*-diallylamine hydrochloride in water. Fogg has prepared a bidentate iminopyrrole complex (**175**) which mediate RCM in air with high selectivity (for RCM over cross metathesis).[62]

These complexes typically have low activity due to slow initiation but activity can be increased by the use of harsh conditions, phosphine scavengers (*e.g.* CuCl or $TlPF_6$) or Lewis acids, such as $HSiCl_3$, an attribute useful in ROMP processes.

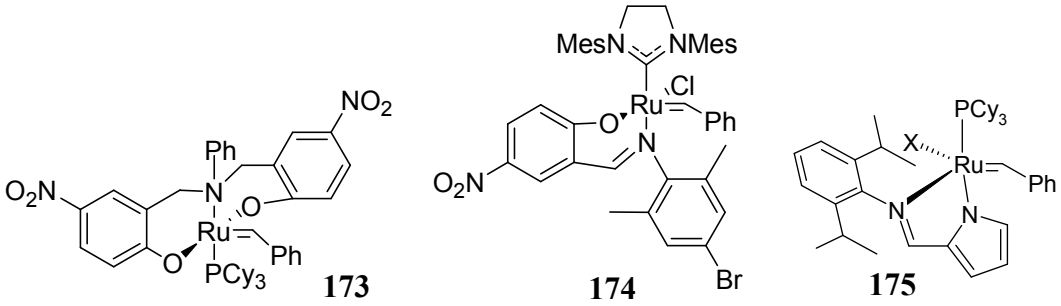

Figure 37. Ru benzylidene complexes bearing; a tridentate *N*,*N*,*O*-amino-benzyloxy (**173**) ligand reported by Jensen, an *N*,*O*-chelated salicylaldimine ligand (**174**) reported by Raines and a bidentate iminopyrrole ligand (**175**) reported by Fogg.

Grela[63] has created a system where a Grubbs-Hoveyda 2nd generation type complex bearing a tridentate *O*,*O*-benzylidene carboxylate ligand (**176**) is activated *in situ* by a protic acid to create a new complex bearing a Cl, O_3SCF_3 or $O_2C(CF_2)_7CF_3$ ligand (**177**) (Scheme 52).

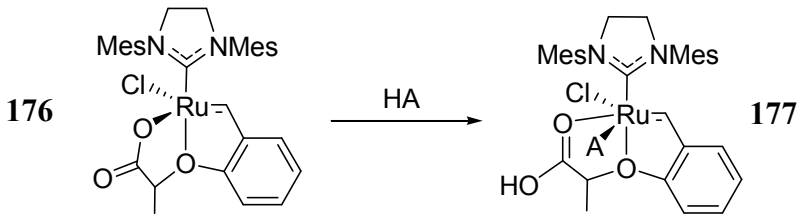

A = Cl, O_3SCF_3, $O_2C(CF_2)_7CF_3$

Scheme 52. Preparation of pseudohalide complexes by reaction of a Ru benzylidene complex bearing a tridentate *O*,*O*-benzylidene carboxylate ligand (**176**) with acid to create a complex bearing a new anionic ligand (**177**).

Hoveyda has prepared a range of chiral Grubbs-Hoveyda 2nd generation complexes (**178**) with chelating binolate substituted NHC ligands which have modest activity but give high *ee* and *trans* selectivity in air (Figure 38).[64]

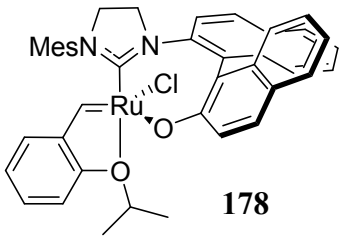

178

Figure 38. The structure of a chiral Ru benzylidene complex (**178**) containing a chelating binolate substituted NHC ligand reported by Hoveyda.

The group of Fogg have prepared [RuCl(OC_6F_5)(CHPh)(IMes)(Py)],[65] which possesses similar activity to the parent dichloride complex and is highly stable, generating turnover numbers in excess of 40,000, significantly more than the parent complex. In addition, the complex is easy to remove from the product with less than 100 ppm Ru residue remaining after column chromatography. They also prepared [Ru(OC_6X_5)Y(CHPh)(IMes)(Py)] (X = Cl, Br, F; Y = Br, Cl) complexes (**179**), which had higher activity but lower lifetimes than the parent complex, and good selectivity for RCM over cross metathesis (Figure 39). They found that, for ligand Y, Br generates a more active catalyst than Cl, in contrast to findings reported for [RuX_2(CHCHCPh_2)(PCy_3)$_2$] (*vide supra*).[43] The halide substituents on the phenoxide ligand are necessary to prevent isomerisation from σ to π ligation, which occurred with unsubstituted phenoxide.[65,66] Grubbs reported [RuX_2(CHPh)(PCy_3)] {X = O^{t}Bu, $OC(CF_3)_2CH_3$, $OC(CF_3)$} complexes, which had essentially no activity in RCM due to the steric congestion in the complex despite having a free coordination site.[67]

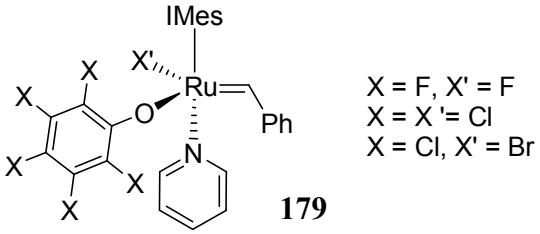

179

Figure 39. Ruthenium benzylidene complexes (**179**) bearing halogenated phenoxy ligands.

3.1.4. Metathesis catalyst design

Despite considerable research and an ever increasing library of ruthenium benzylidene catalysts there are continuing efforts to produce new catalysts driven by several factors. Firstly, catalysts have a limited lifetime and turnover numbers which inhibits commercial application, as despite the fact that the precatalysts are stable, the active catalysts are

sensitive to oxygen and species such as allylic alcohols, as well as soft donors such as alcohols and thiols, which compete for coordination to the metal. Also ruthenium complexes do not have the level of activity of Schrock type catalysts and stereoselectivity, *cis*/*trans* selectivity and cross-metathesis selectivity is still limited. Additionally, it is desirable to develop catalysts that can function in water or ionic liquids for green chemistry, are reusable (recoverable with long lifetimes) and leave low Ru contamination in the final product (by heterogenisation or facile separation). It has been found that specific catalysts are required for specific applications, as no catalyst with all round attributes has yet been developed. The cost of the catalysts is also an issue, with the ever-increasing complexity of ligands, the price of ruthenium and the patenting of many catalyst systems.[10,68]

3.1.5. Metathesis mechanism

The mechanism of a typical Ru-catalysed metathesis reaction has been proposed by Grubbs[43] on the basis of the Chauvin mechanism.[15] The initial step is (in all cases where there are two neutral ligands coordinated to Ru) dissociation of one neutral ligand (Step I) (Scheme 53). The alkene reagent can then bind to the vacant site (Step II) and, providing the alkene and alkylidene have both adopted their active conformations, they can rearrange (*via* [2+2] oxidative cycloaddition) into a ruthena(IV)cyclobutane (Step III). Subsequent [2+2] reductive rearrangement then results in fragmentation and reformation of an olefin and alkylidene (this may be degenerate or create new species) (Step IV). In the case of cross metathesis the olefin can then dissociate (or rearrange again) (Step V) and the new ruthenium alkylidene can carry on reacting in subsequent cycles. In the case of RCM the alkylidene will now have a pendant alkene. Entropically this alkene is then likely to bind to the ruthenium, undergo rearrangement with the alkylidene (Step VI) and generate a cyclic olefin and a methylidene ligand (Step VII). The cycloalkene can then dissociate and the ruthenium methylidene (Step VIII) can catalyse further transformations. This mechanism suggests that the use of less electron donating anionic ligands will allow better alkene binding at the expense of phosphine dissociation. Smaller anionic ligands will have a similar impact.

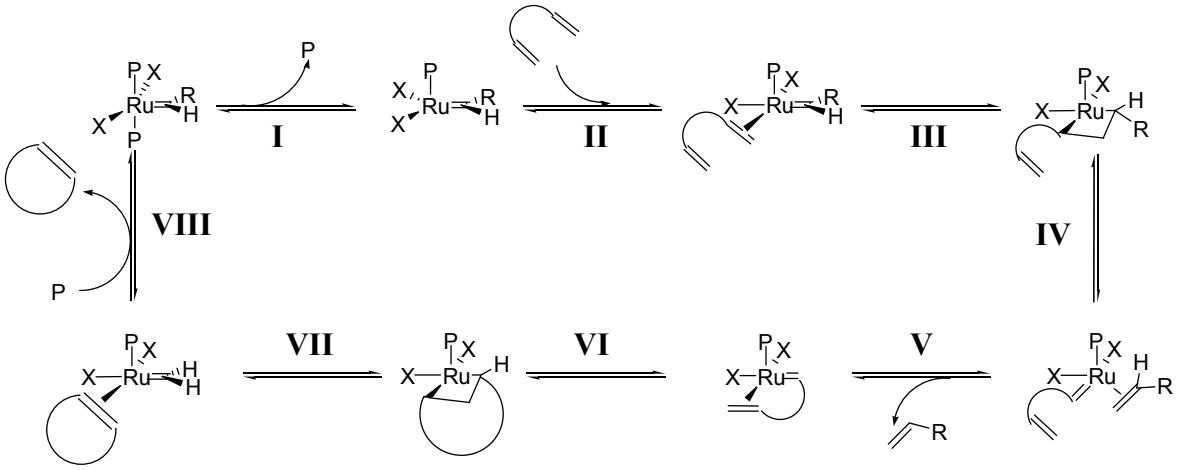

Scheme 53. Mechanism of Ru alkylidene catalysed ring-closing metathesis of dienes proposed by Grubbs.

The dissociation of a neutral ligand, typically a phosphine, pyridine or one part of a bidentate ligand (*e.g.* O^{i}Pr for Grubbs-Hoveyda type complexes) in the first step is essential for catalysis and the ease of dissociation is key to the initiation rate in most cases. The dissociation rate is principally determined by the nucleophilicty (Lewis basicity) of the ligand, the steric constraints upon the ligand, whether it is polydentate and the influence of the neutral ligand *trans* to it in the coordination sphere. The ease of dissociation of the leaving group is in the order:

$$BrPy > Py > PPh_3 > PCy_3 > IMes$$

The nature of the *trans* ligand aids the observed dissociation (and stabilisation of intermediate 14 electron species) in the order:

$$IMesH_2 > IMes > PCy_3 > PPh_3$$

However, computational and thermodynamic calculations[69] and NMR spectroscopic analysis[70] found that the lability of PCy_3 depended on the nature of the *trans* ligand in the order:

$$PPh_3 > PCy_3 > NHC$$

The difference in the observed and calculated initiation rates is proposed to be due to the stabilisation of inactive (**180 a-c**) and active (**181a**) conformations of the alkene and carbene ligands (Figure 40).

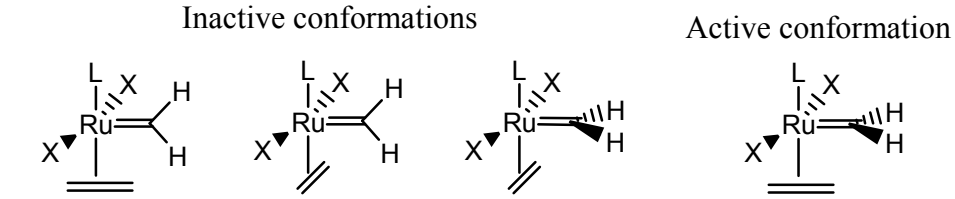

(2a+2s) **180a** (2a+2a) **180b** (2s+2a) **180c** (2s+2s) **181a**

Figure 40. Inactive and active conformations of alkene and carbene ligands in Ru metathesis catalysts.

The geometry of the complex affects the stabilisation of the conformations. A decreased L-Ru-alkene angle (where L is a neutral phosphine or NHC ligand) results in the L-Ru interaction becoming more antibonding, this in turn increases the bonding interaction of the Ru d orbitals with the alkylidene ligand, stabilising the active (2s +2s) conformation of the carbene (**181b**) (Figure 41). More electron donating ligands (*e.g.* NHCs) have a greater influence upon the Ru d orbitals, which in turn leads to increased stabilisation of the active carbene conformation. Steric interaction, such as large NHC mesityl substituents, decreases the L-Ru-alkene angle. In contrast, a decrease in the Cl-Ru-Cl angle leads to an increase in the antibonding interaction between the anionic ligands and the Ru d orbitals, resulting in the stabilisation of an inactive alkylidene conformation (**180d**). As a result smaller, more electron withdrawing, anionic ligands will minimise the interaction between the antibonding orbital and Ru orbitals reducing stabilisation of the inactive conformation (**180d**).[69] In contradiction to this theory, Getty *et al.* have calculated that NHCs are actually weaker σ-donors than phosphines, despite having stronger bonds, due to a significant electrostatic component to the Ru-NHC bond, and they propose that this explains the observations above.[71]

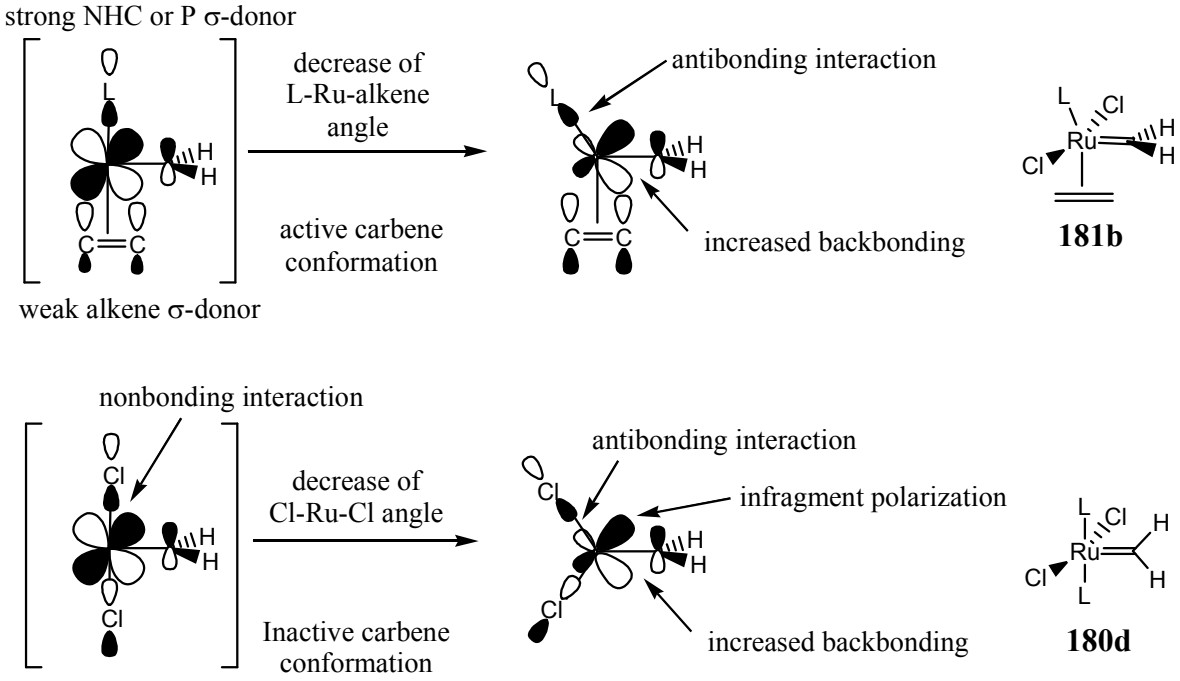

Figure 41. Effect of decreasing L-Ru-alkene and Cl-Ru-Cl angles on orbital interactions in Ru metathesis catalysts and the resultant stabilisation of active (**181b**) and inactive (**180d**) alkylidene conformations.

Straub[72] has carried out computational calculations to determine the effect of different pseudohalide ligands on the efficiency of Ru benzylidene catalysts by studying di-substituted methoxide, methane thiolate, fluoride and mesylate neutral complexes, as well as cationic complexes with water and ammonia ligands. Although no difluoride complexes have been prepared it is logical that they would be more active than dichloride analogues due to the observed order in activity of:

dichloride > dibromide > diiodide

However, it was found that fluoride actually stabilised the inactive carbene conformation, as its compact orbitals overlap well with those of the Ru atom. They found that phosphine dissociation occurred easiest for low activity first generation iodo complexes but high activity second generation complexes had high barriers to dissociation. This anomaly was explained by there being high steric repulsion between chloride and phosphine ligands, whereas the chlorides can fit between NHC substituents resulting in less repulsion. Alkoxides were found to strongly favour the inactive conformation (by 45-60 kJ.mol^{-1}) resulting in poor activity. Thiolate was more active due to more diffuse orbitals but inferior to chloride. Mesylate ($^{-}O_3SCH_3$) ligands have weaker σ donor ability meaning there is no significant stabilisation of the inactive conformation. Additionally, one

of the other O atoms can bind to Ru aiding phosphine dissociation, resulting in very low overall barriers to metathesis. Metal sulfonates however tend to ionise and the free coordination site is filled with water, solvent or functional groups on the substrates. For the cationic complexes water significantly stabilises the active conformation giving very low barriers to catalysis, however activation by ligand dissociation is very unfavourable.

A series describing the ability of ligands to stabilise active relative to inactive conformations was devised. Ligands early in the series actually stabilise the active conformation and later in the series the inactive conformation:

alkyne/alkene (at a free coordination site) > OH_2/OR_2 ≈ NH_3/NR_3 > R_3P > O_3SR > Cl > Br > I > NHC ≈ F ≈ SR > OR > NR_2 > aryl > alkyl

The author came to the conclusion that strong σ donors are required *trans* to the alkene and weak donors *cis* to the alkene. This will stabilize the active carbene conformation and maximise the ability to rearrange ruthenacyclobutanes in order to carry out metathesis.

3.1.6. Decomposition of Ru metathesis catalysts

The impact of decomposition on catalyst efficiency and turnover numbers, and interference of Ru decomposition products in other catalytic cycles (such as alkene isomerisation) has encouraged research into the decomposition of precatalysts and catalysts in the presence and absence of substrate.[73] In the absence of substrate (and to a lesser extent in the presence of substrate) a number of decomposition pathways have been uncovered. Ru propylidenes, such as $[RuCl_2(CHCH_2CH_3)(PCy_3)_2]$, have been found to decompose *via* a presumably bimolecular pathway resulting in the formation of *trans*-3-hexene.[74] Faced bridged dimers were formed derived from $[RuCl_2(CHCHCMe_2)(dcypb)]$ {dcypb is 1,4-bis(dicyclohexylphosphino)butane} which may be the cause of decomposition of the Grubbs precatalyst $[RuCl_2(CHCHCMe_2)(PPh_3)_2]$.[75] Decomposition of Grubbs 1st generation methylidene complex $[RuCl_2(CH_2)(PCy_3)_2]$ is believed to occur *via* a unimolecular route involving incorporation of hydride from the methylidene ligand into the phosphine ligands.[74] Grubbs and co-workers[76] have investigated decomposition of a series of phosphine methylidene complexes, such as **182** (Scheme 54), and found that they all decomposed to form methylphosphonium salts ($R\text{-}PR_3^+.X^-$) (**183**) and inactive binuclear Ru complexes (**185**) *via* the attack of a phosphine ligand on the alkylidene ligand (**184**).

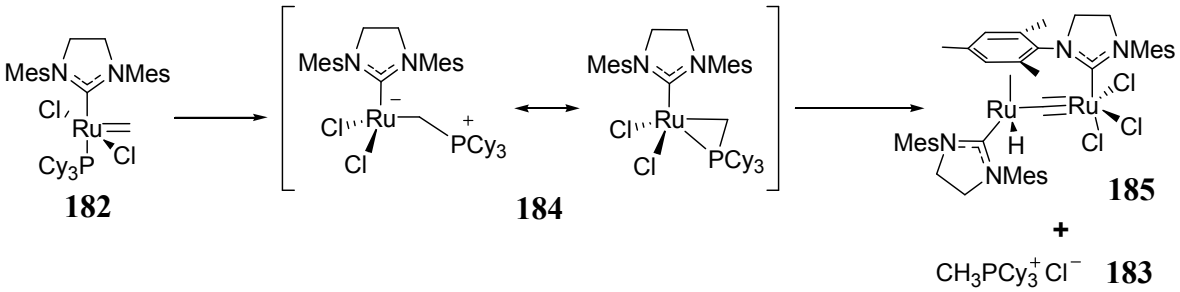

Scheme 54. Decomposition of a Grubbs II type Ru methylidene complex (**182**) *via* phosphine attack on the methylidene ligand.

In the presence of an olefin substrate other decomposition pathways can occur. For example intermediate ruthenacyclobutanes (**186**) can decompose to Ru(IV) allyl hydrides (**187**) and subsequently to Ru(II) propene complexes (**188**) with the complete loss of the alkylidene ligand (Scheme 55).[77]

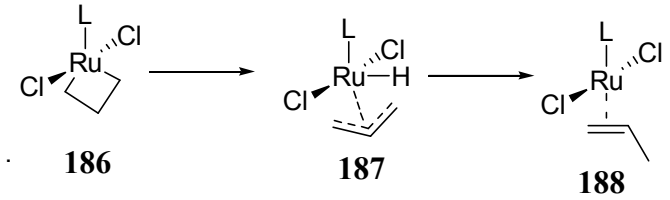

Scheme 55. Decomposition of Ru(IV) ruthenacycles (**186**) *via* allyl hydride formation.

The group of Mol reported that 1st and 2nd generation complexes decomposed in the presence of primary alcohols to carbonyl hydride complexes of the type [RuCl(H)(CO)(PCy_3)L].[78] Grubbs found that the phosphine free Grubbs-Hoveyda 2nd generation complex decomposed in the presence of ethylene to form unidentified Ru hydride species.[76a] It has also been reported that decomposition can occur *via* insertion of Ru into a mesityl methyl C-H bond.[79] Hong *et al.*[80] found a similar decomposition pathway in a related system **189** (Scheme 56), where C-H activation of a phenyl NHC substituent occurs following phosphine dissociation. The resultant hydride (**191**) adds to the benzylidene to give a benzyl ligand (**192**) which combines with the NHC phenyl group to give an inactive Ru(II) species (**193**) which can then also add into the remaining aryl NHC group (**194**).

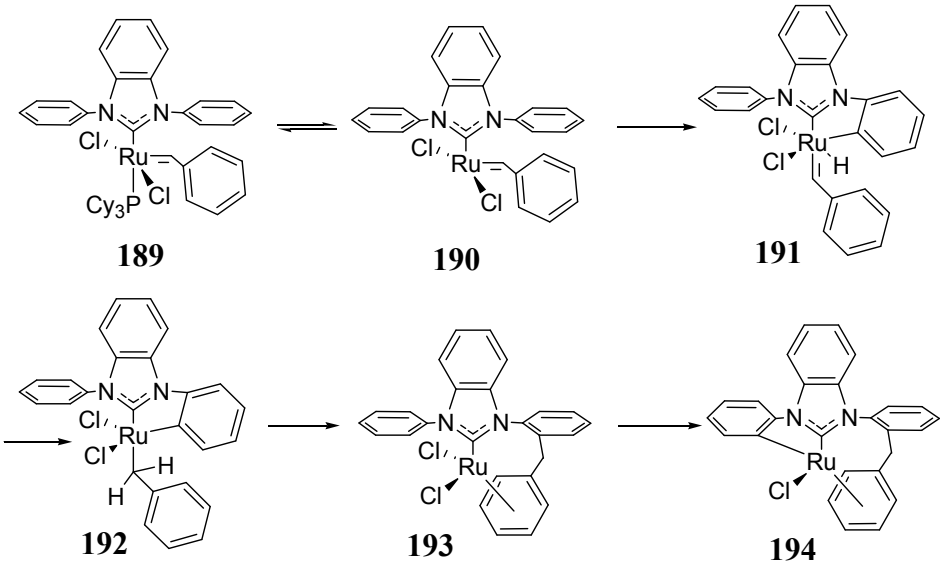

Scheme 56. Decomposition of a Grubbs II type Ru benzylidene complex (**189**) by C-H insertion and hydride formation.

3.1.7. Aims

The initial aim of this study was to investigate the structure and bonding of Ru benzylidene complexes containing imidate ligands (**195**) (Figure 41). The complexes would then be applied to Ru catalysed ring-closing metathesis and ring-opening metathesis polymerisation processes, and the effect of the imidate ligands on these transformations determined. It was envisaged that utilising a series of imidates spanning a range of pK_a values would allow the investigation of the impact of electronic effects on the Ru complexes. Ideally a balance between the stabilisation of active catalytic conformations by highly electron withdrawing imidates and enhanced activation by better electron donors would be obtained.

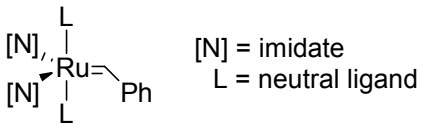

195

Figure 41. The proposed imidate benzylidene complexes (**195**) this study will investigate.

3.2. Results and discussion

3.2.1. Synthesis and characterisation of Ru complexes

3.2.1.1. Strategy for the synthesis of imidato Ru benzylidene complexes

The usual synthesis of Grubbs 1st generation catalyst, $[RuCl_2(CHPh)(PCy_3)_2]$ (**162**), is carried out from $RuCl_3.3H_2O$ (**196**), and the complex is now available commercially along with many other ruthenium benzylidene complexes.[31] $RuCl_3.3H_2O$ is reacted with triphenylphosphine in methanol at reflux to generate $[RuCl_2(PPh_3)_3]$ (**197**). This is then treated with phenyldiazomethane to give $[RuCl_2(CHPh)(PPh_3)_2]$ and *in situ* phosphine exchange yields $[RuCl_2(CHPh)(PCy_3)_2]$ (**162**) (Scheme 57).

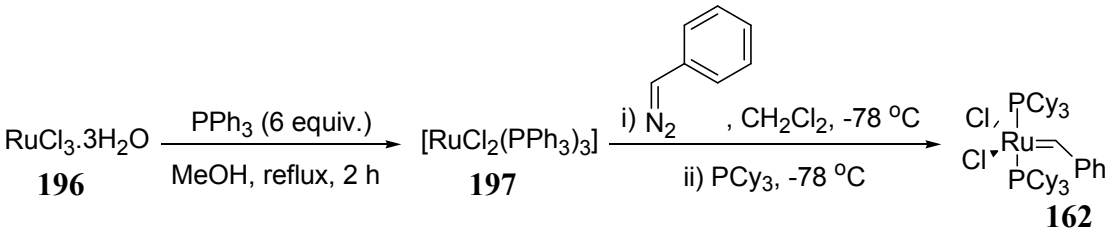

Scheme 57. Synthesis of $[RuCl_2(CHPh)(PCy_3)_2]$ (**162**) from $RuCl_3$ (**196**).

This route allows potential anionic ligand exchange at three points in the synthesis; $RuCl_3.3H_2O$ (**196**), $[RuCl_2(PPh_3)_3]$ (**197**) and the final product $[RuCl_2(CHPh)(PCy_3)_2]$ (**162**). The initial strategy to prepare an imidate ligand containing ruthenium benzylidene complex was to attempt the synthesis of imidate containing analogues of these three complexes.

There have been a number of other synthetic routes to such complexes devised but these have limitations regarding the possibility for anionic ligand exchange. Van der Schaaf *et al.*[81] have reported a synthesis starting from $[RuCl_2(3,5\text{-}COD)]$ (**198**), which progresses *via* $[RuClH(P^iPr_3)_2]$ (**199**), a dihydrogen (**200**) and a vinyl species (**201**) to yield $[RuCl_2(CHPh)(P^iPr_3)_2]$ (**203**) {subsequent phosphine exchange will afford $[RuCl_2(CHPh)(PCy_3)_2]$ (**162**)} (Scheme 58). However, this reaction is carried out in one-pot using HCl as a protic acid and chloride source and so limits the possibility of exploiting imidate ligand exchange.

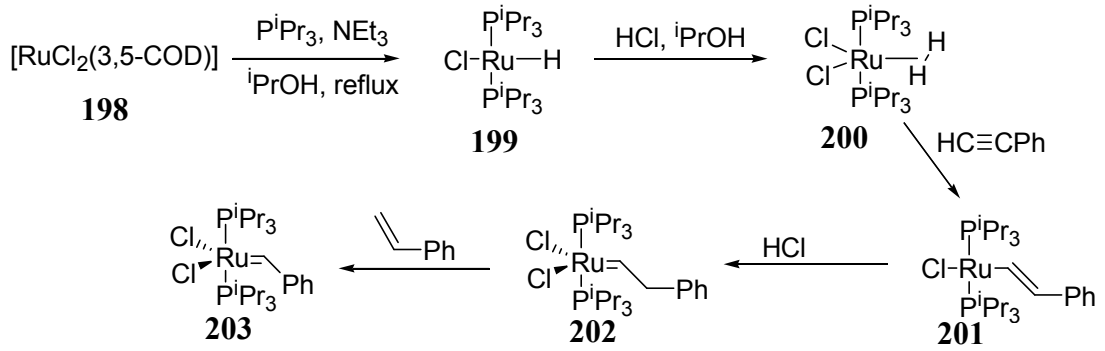

Scheme 58. Synthesis of $[RuCl_2(CHPh)(P^iPr_3)_2]$ (**203**) from $[RuCl_2(3,5\text{-}COD)]$ (**198**).

Another method, developed by the research groups of Werner and Grubbs, also starts from $[RuCl_2(3,5\text{-}COD)]$ (**198**) and proceeds *via* formation of Ru hydride (**204**) and vinyl carbene (**205**) complexes. This system has potential for halide ligand exchange using $[RuCl_2(3,5\text{-}COD)]$ (**198**), although the first step requires the use of hydrogen under pressure which has general synthetic limitations (Scheme 59).[82]

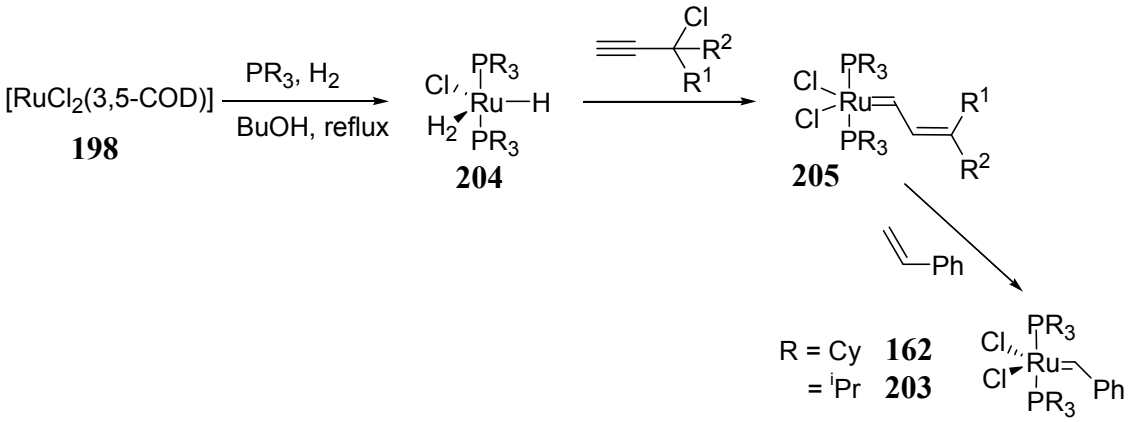

Scheme 59. Synthesis of $[RuCl_2(CHPh)(PR_3)_2]$ (**162** and **203**) *via* $[RuClHH_2(PR_3)_2]$ (**204**).

3.2.1.2. Synthesis and reactivity of $[Ru(N\text{-imidate})_3(OH_2)_3]$ complexes

The synthesis of triaquaruthenium(III) trisuccinimido and triphthalimido complexes, $[Ru(N\text{-succ})_3(OH_2)_3]$ (**206**) and $[Ru(N\text{-ptm})_3(OH_2)_3]$ (**207**), has been reported by Islam and Uddin[1] by refluxing the potassium imidate salt and $RuCl_3.3H_2O$ (**196**) in water. The complexes were successfully prepared by this method, however the solubility in all solvents was extremely low. Attempts to prepare $[Ru(N\text{-imidate})_2(PPh_3)_2]$ complexes by methods similar to the synthesis of terpyridine and diethylenetriamine analogues (6 equivalents of PPh_3 in isopropyl alcohol at 80 ˚C for 15 hours) were unsuccessful due to the low solubility and only starting material was recovered even under forcing conditions.

3.2.1.3. Attempted synthesis of [Ru(*N*-succ)$_2$(PPh$_3$)$_3$]

Synthesis of [Ru(*N*-succ)$_2$(PPh$_3$)$_2$] (**208**) by reaction of [Ru$_2$Cl$_4$(PPh$_3$)$_4$] (**209**) with succinimidate salts was also attempted. Exchange of chloride ligands for pseudohalides in this complex has been reported, for example in [Ru(OAc)$_2$(PPh$_3$)$_2$] (**210**).[83] Attempts using Spencers[83] conditions for the preparation of **210** (treatment of **209** with 10 equivalents of sodium acetate in refluxing *t*-butanol) were unsuccessful due to the formation of a mixture of unidentified products and starting material, as were attempts to exchange the acetate in this complex for imidate directly. Conditions used for the reported preparation of [Ru$_2$(μ-Cl)(μ-H)(μ-*N,O*-succ)$_2$(PPh$_3$)$_4$] (**154**) by Sahajpal *et al.*[2] (1.25 equivalents of succinimide in CH_2Cl_2/NEt_3 at ambient temperature) were employed, with the use of methanol during work-up avoided to prevent hydride formation. However, a mixture of inseparable (by chromatography and recrystallisation) unidentified products and starting material was obtained. Variation of solvent, base and temperature failed to increase the ratio of products to starting material, although there was evidence of small amounts of bound succinimide, these products could not be isolated and quickly decomposed in solution. The use of halide scavenging cations, Ag^+ and Tl^+, gave similar results.

In fact treatment of [RuBr$_2$(PPh$_3$)$_3$] (**211**), [RuCl$_2$(PPh$_3$)$_3$] (**197**) and [Ru$_2$Cl$_4$(PPh$_3$)$_4$] (**209**) with a range of succinimidate salts under various conditions (from room temperature up to 110 ˚C and for 30 minutes up to 48 hours) (Table 41) resulted in a mixture of starting materials, free succinimidate and unidentified products. In most cases small amounts of bound succinimidate were identified amongst a complex mixture of products (by ^{1}H and ^{31}P NMR), however the nature of these products varied depending upon the conditions used. These results show that, although ruthenium succinimidate complexes may be formed in some cases, quantitative conversion and isolation was not possible. The species observed were also unstable in solution.

Table 41. Conditions and reactants used in the attempted synthesis of [Ru(*N*-succ)$_2$(PPh$_3$)$_3$] (**208**).

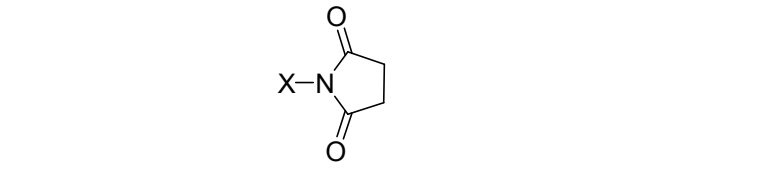

197, **209-211** **208**

Salts/ bases	Solvents	Ru sources
H/NEt$_3$	CH_2Cl_2	[RuCl$_2$(PPh$_3$)$_3$] (**197**)
Li	THF	[Ru$_2$Cl$_4$(PPh$_3$)$_4$] (**209**)
K	Toluene	[Ru(OAc)$_2$(PPh$_3$)$_2$] (**210**)
Na	Methanol	[RuBr$_2$(PPh$_3$)$_3$] (**211**)
Ag	*t*-Butanol	
Tl		

3.2.1.4. Attempted synthesis of [Ru(*N*-succ)$_2$(CHPh)(PCy$_3$)$_2$] and analogues

Reported syntheses of pseudohalide-containing ruthenium benzylidene complexes are generally carried out from the chloride analogue of the complex, *e.g.* [RuCl$_2$(CHPh)(PCy$_3$)$_2$] (**162**), typically using an Ag^{+}[47,48,49] or Tl^{+}[53,54] salt. In order to prepare [Ru(*N*-succ)$_2$(CHPh)(PCy$_3$)$_2$] (**212**), reaction conditions were used based upon those developed by the group of Buchmeiser[51] {2.5 equivalents of Ag(*N*-succ) in CH_2Cl_2 at ambient temperature}, however ^{1}H NMR spectroscopic analysis showed that the desired substitution product had not been formed and there was no longer a signal corresponding to the carbene proton. Benzaldehyde (less than one equivalent with respect to the amount of **162** used) and protonated succinimide were identified in the reaction mixture, no hydride species (down to -25 ppm) were observed. In the ^{31}P spectrum, AgCl.PCy$_3$ and OPCy$_3$ were observed. The resulting black powder had low solubility in most solvents. A similar outcome was obtained with toluene as solvent, with increased Ag(*N*-succ) loading and with shorter reaction times.

In order to avoid loss of PCy$_3$ by AgCl.PCy$_3$ formation, conditions developed by the group of Fogg were employed {3.7 equivalents of Tl(*N*-succ) in toluene for 3 days at ambient temperature} but this yielded similar results. A less reactive and soluble imidate salt, K(*N*-succ), (2.1 equivalents in CH_2Cl_2 for 8 hours at 30 ˚C), as expected resulted in a

slower reaction with little conversion at 30 ˚C after 8 hours, and starting material still remained after 2 hours at reflux. Direct conversion of the carbene signal to the aldehyde signal with no intermediate carbene formation was observed. Sodium succinimidate and potassium maleimidate gave similar results.

To improve the solubility of the imidate salts tetrahydrofuran was used as solvent {with 1 equivalent of Tl(*N*-succ)}. After 2.5 hours 20% decomposition to the aldehyde was observed but there was also 4% (relative to total material) of a new carbene signal in the ^{1}H NMR spectrum at 18.92 ppm (compared to the parent dichloride at 17.78 ppm). After 19 hours the reaction was still incomplete but the new carbene signal has disappeared. Increasing the temperature to 50 ˚C (19 hours) resulted in complete decomposition. Slow addition of the succinimidate salt was also tried under the same conditions but only starting material and decomposition was detected. This suggests that the desired succinimidate complex may form but subsequently decomposes.

Buchowicz *et al.*[44] found that the reaction of $[RuCl_2(CHPh)(PCy_3)_2]$ (**162**) with AgO_2CCF_3 in tetrahydrofuran resulted in complete decomposition of the carbene, but found that $[Ru_2(O_2CCF_3)_2(\mu\text{-}O_2CCF_3)_2(CHPh)_2(\mu\text{-}OH_2)(PCy_3)_2]$ (**169**) could be prepared in hexane (**162** has the lowest metathesis activity and highest stability in hexane). However, the use of Ag(*N*-succ) and Tl(*N*-succ) in hexane and diethyl ether resulted in the typical decomposition. Attempts to carry out ligand exchange on **169** and using Cu_2O to generate Cu(*N*-succ) *in situ* were also unsuccessful.

In view of the decomposition of the carbene ligand in the above reactions, more stable later generation ruthenium benzylidenes were tested. Grubbs 2nd generation complex, $[RuCl_2(CHPh)(IMesH_2)(PCy_3)]$ (**160**), was tested with Ag, Tl, Na and K imidate salts in CH_2Cl_2 and toluene and was found to decompose yielding the corresponding aldehyde. Similar results were observed with the phosphine-free complexes $[RuCl_2(CHPh)(IMesH_2)(Py)]$ (**213**) and $[RuCl_2(o\text{-}^{i}PrO\text{-}CHPh)(IMesH_2)]$ (**163**) with both succinimidate and maleimidate salts (Table 42).

Table 42. Conditions and reactants used in the attempted synthesis of Ru benzylidene imidate complexes.

Salts/ bases	Solvents	Ru sources
Ag	CH_2Cl_2	$[RuCl_2(CHPh)(IMesH_2)(PCy_3)]$ (**160**)
Tl	THF	$[RuCl_2(CHPh)(PCy_3)_2]$ (**162**)
K	Hexane	$[RuCl_2(o\text{-}^{i}PrO\text{-}CHPh)(IMesH_2)]$ (**163**)
Na	Diethyl ether	$[RuCl_2(CHPh)(IMesH_2)(Py)]$ (**213**)
Cu	Toluene	

As the carbene ligand was responsible for the decomposition of the complexes, several Grubbs type ruthenium complexes were tested with alternative carbene ligands, including SPh, O^{n}butyl, and *n*-propyl substituted carbenes (Figure 42). These are easily prepared by treatment of $[RuCl_2(CHPh)(PCy_3)_2]$ (**162**) with the relevant alkene.[84]

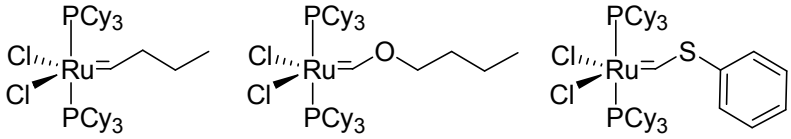

214 **215** **216**

Figure 42. Ruthenium carbene complexes tested for anionic ligand exchange with imidate salts.

Treatment of the *n*-propyl carbene complex **214** with imidate salts {1.1 equivalents of Ag(*N*-succ) in CH_2Cl_2} led to the decomposition of the carbene. However, the O^{n}butyl carbene complex **215** showed trace amounts of other carbene complexes (C*H* carbene signals at 15.69, 15.55 and 15.21 ppm compared with the parent complex at 14.75 ppm in the ^{1}H NMR spectrum) along with significant decomposition. There were a number of alkene signals in the proton spectrum and so the new carbene complexes could be formed by carbene rather than anionic ligand exchange. These new species rapidly decomposed in solution. Using Tl(*N*-succ) (2 equivalents in tetrahydrofuran) only starting material and decomposition products were observed. Treatment of the thioether complex **216** with Tl(*N*-succ) (1.1 equivalents in tetrahydrofuran) resulted in decomposition and starting material recovery only, with the detection of alkene species in the ^{1}H NMR spectrum.

3.2.1.5. Synthesis of [Ru(*N*-tfs)$_2$(*o*-^{i}PrO-CHPh)(IMesH$_2$)]

Buchowicz *et al.*[85] synthesised a range of Grubbs 1st generation complex (**162**) analogues containing carboxylates, including O_2CCF_3, $O_2CC_2F_5$, $O_2CC_6F_5$ and O_2CCl_3, but found that the same reaction with AgO_2CCH_3, TlO_2CCH_3, AgO_3SCF_3 and $AgO_3SC_6H_4Me$ did not yield the benzylidene complex. They concluded that the pK_a of the corresponding acid must lie within the range of -7 to +3 to stabilise the carbene ligand. Succinimide (9.70 in water)[86], maleimide (9.46)[87] and phthalimide (8.30)[88] all lie outside this range which may explain the failure to generate the desired complex. The anion of tetrafluorosuccinimide with an estimated pK_a of 2.1[89] should therefore give better results.

Treatment of [$RuCl_2$(CHPh)(PCy_3)$_2$] (**162**) with tetrafluorosuccinimide (1 equivalent) and copper(I) oxide (2.3 equivalents) in tetrahydrofuran resulted only in decomposition. Subjecting [$RuCl_2$(*o*-^{i}PrO-CHPh)(IMesH$_2$)] (**163**) to the same conditions however led to six new species with trace proton NMR carbene signals at 17.52 (d, J = 0.5 Hz), 17.07, 16.93, 16.91 and a larger broad signal at 16.22 ppm (compared with the parent dichloride at 16.58 ppm), as well as significant decomposition (although only 1% of the aldehyde). Multiple peaks in the ^{19}F NMR spectrum suggest these were tetrafluorosuccinimidate ruthenium benzylidene complexes. In order to improve the selectivity of the reaction Ag(*N*-tfs) (prepared *in situ*) was used (1.05 equivalents) resulting in only three new major species, with carbene signals at 17.81 (19%), 17.52 (34%) and 17.15 (14%) ppm, as well as the starting dichloride and decomposition products, after 5 hours.

In order to prevent the formation of statistical ratios of unsubstituted, monosubstituted and disubstituted complexes during anionic ligand exchange (as reported by Tanaka *et al.*)[48] and encourage the formation of only one species, 4 equivalents of Ag(*N*-tfs) were used. This resulted in a purple solution containing two new species with carbene proton NMR signals at 17.90 (59%) and 17.81 ppm (6%), as well as aldehyde decomposition product (35%), and only one major signal in the ^{19}F spectrum (a singlet at -126.5 ppm). The reaction mixture was subjected to column chromatography on silica-gel under an inert atmosphere, allowing the isolation of an air sensitive purple powder, which was then washed with hexane (to remove the aldehyde). The powder was found to consist of one Ru species, with a carbene proton NMR signal at 18.24 ppm, which was analysed by ^{1}H, ^{19}F and ^{13}C NMR spectroscopy and X-ray diffraction analysis and found to be the disubstituted complex [Ru(*N*-tfs)$_2$(*o*-^{i}PrO-CHPh)(IMesH$_2$)] (**217**) (Scheme 60).

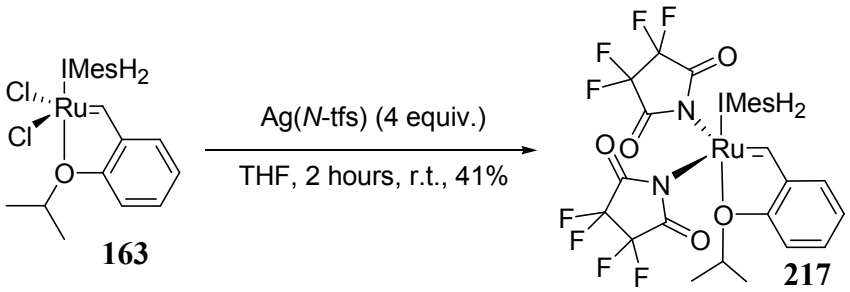

Scheme 60. Reaction of $[RuCl_2(o\text{-}^{i}PrO\text{-}CHPh)(IMesH_2)]$ (**163**) with silver(I) tetrafluorosuccinimidate to give $[Ru(N\text{-}tfs)_2(o\text{-}^{i}PrO\text{-}CHPh)(IMesH_2)]$ (**217**).

Proton NMR spectroscopic analysis (in dry, degassed $CDCl_3$) showed that the tfs complex **217** has a benzylidene carbene CH proton signal (18.24 ppm) that is 1.66 ppm downfield of the parent chloride complex **163** (16.58 ppm). This suggests that the tetrafluorosuccinimidate ligands withdraw significant electron density from Ru, relative to chloride, reducing backbonding from Ru to the carbene and so reducing electron density on the carbene carbon. The signal is also downfield relative to related $[RuXX'(o\text{-}^{i}PrO\text{-}CHPh)(IMesH_2)]$ complexes, where X and X' are anionic ligands such as, Cl/(O_3SCF_3) (**218**) (17.49 ppm),[46] $(O_2CCF_3)_2$ (**219**) (17.38 ppm),[46] $(O_2CC_6F_5)_2$ (**220**) (17.33 ppm),[51] $(OC_6F_5)_2$ (**221**) (17.10 ppm),[51] Cl/$\{O_2CC_3F_6CON(Me)C_3H_6Si(OMe)_3\}$ (**222**) (17.11 and 17.09 ppm)[52b,90] and $\{O_2CC_3F_6CON(Me)C_3H_6Si(OMe)_3\}_2$ (**223**) (17.51 ppm),[52b] however it is upfield relative to $(O_3SCF_3)_2$ (**224**) (18.49 ppm) (Table 43).[46] The remaining proton NMR signals are slightly upfield relative to the dichloride **163**, notably the isopropyl CH signal with a 0.31 ppm shift upfield (4.60 ppm for **217** and 4.91 ppm for **163**) and imidazole CH_2 signals with a 0.20 ppm shift upfield (3.97 ppm for **217** and 4.17 ppm for **163**). The imidazole signal is also more upfield than related pseudohalide complexes, for example **224** (4.16 ppm) and **220** (3.98 ppm).

Table 43. Selected ^{1}H NMR signals of $[RuXX'(o\text{-}^{i}PrO\text{-}CHPh)(IMesH_2)]$ complexes.[a]

Entry	X	Ligand pK_a (in water)	X'		^{1}H NMR chemical shift (ppm)		
					Ru=C*H*Ar	^{i}Pr C*H*	imidazole CH_2
1	Cl	-8.0[91]	Cl	**163**	16.58	4.91	4.17
2	*N*-tfs	2.1[89]	*N*-tfs	**217**	18.24	4.60	3.97
3	Cl	-8.0	O_3SCF_3[46]	**218**	17.49	4.74	4.12
4	O_2CCF_3	-0.25[91]	O_2CCF_3[46]	**219**	17.38	4.55	4.05
5	$O_2CC_6F_5$	1.8[92]	$O_2CC_6F_5$[51]	**220**	17.33	4.57	3.98
6	OC_6F_5	5.5[93]	OC_6F_5[51]	**221**	17.10	3.82[b]	4.10
7[c]	Cl	-8.0	$O_2CC_3F_6R$[d,52b]	**222**	17.11, 17.09	4.68	4.14
8[c]	$O_2CC_3F_6R$[d]	-	$O_2CC_3F_6R$[d,52b]	**223**	17.51	4.55	4.12
9	O_3SCF_3	-14[91]	O_3SCF_3[46]	**224**	18.49	4.72	4.16

[a] In $CDCl_3$ solution. [b] As reported. [c] In CD_2Cl_2 solution. [d] $O_2CC_3F_6R$ is $O_2CC_3F_6CON(Me)C_3H_6Si(OMe)_3$.

The ^{13}C NMR benzylidene carbene carbon signal of [Ru(*N*-tfs)$_2$(*o*-^{i}PrO-CHPh)(IMesH$_2$)] (**217**) is 27.1 ppm downfield of the dichloride complex **163** (324.0 ppm for **217** and 296.9 ppm for **163**) due to the lower electron density on the Ru atom (Table 44). The signal is also downfield relative to related [RuXX'(*o*-^{i}PrO-CHPh)(IMesH$_2$)] complexes **218** (313.8 ppm),[46] **219** (314.7 ppm),[46] **220** (313.5 ppm),[51] **221** (296.3 ppm),[51] **222** (306.9 ppm)[52b] and **223** (316.0 ppm),[52b] although downfield of **224** (332.4 ppm).[46] This mirrors the trend observed for the benzylidene carbene CH proton NMR signal.

There is an 8.5 ppm upfield shift of the NHC carbene carbon signal (202.6 ppm for **217** and 211.1 ppm for **163**) which is consistent with an NHC ligand bound to a more electron deficient metal (the NHC carbene carbon signal is considered an accurate probe for the electron density on the metal).[94] The signal is also upfield of the related pseudohalide complexes **218** (207.1 ppm),[46] **219** (209.1 ppm),[46] **220** (211.6 ppm),[51] **221** (210.4 ppm),[51] **222** (210.9 ppm)[52b] and **223** (210.3 ppm).[52b] In contrast to the benzylidene carbene NMR signals, the NHC carbene carbon signal is also upfield of complex **224** (203.9 ppm).[46]

The mesityl methyl (21.2 and 18.7 ppm) and isopropyl methyl (20.9 ppm) ^{13}C NMR signals for **217** are also significantly upfield relative to the dichloride **163** (30.6, 25.8 and 21.1 ppm, respectively) the reason for which is unclear but is consistent with other pseudohalide complexes.[46,51,52b] Smaller differences are observed for the other signals. The tfs ligand CF_2 signal is a triplet of triplets (*J* is 267 and 22 Hz) which is also observed in the neutral imide and so is not an indication of asymmetric binding, the carbonyl signal however is an unresolved multiplet whereas in the neutral imide it appears as a triplet (*J* is 33 Hz) which may indicate interaction of the carbonyl group with other species.

Table 44. Selected ^{13}C NMR signals of [RuXX'(*o*-^{i}PrO-CHPh)(IMesH$_2$)] complexes.[a]

Entry	X	X'		^{1}H NMR chemical shift (ppm)	
				Ru=C*H*Ar	NHC
1	Cl	Cl	**163**	296.9	211.1
2	*N*-tfs	*N*-tfs	**217**	324.0	202.6
3	Cl	O_3SCF_3[46]	**218**	313.8	207.1
4	O_2CCF_3	O_2CCF_3[46]	**219**	314.7	209.1
5	$O_2CC_6F_5$	$O_2CC_6F_5$[51]	**220**	313.5	211.6
6	OC_6F_5	OC_6F_5[51]	**221**	296.3	210.4
7[b]	Cl	$O_2CC_3F_6R$[c,52b]	**222**	306.9	210.9
8[b]	$O_2CC_3F_6R$[c]	$O_2CC_3F_6R$[c,52b]	**223**	316.0	210.3
9	O_3SCF_3	O_3SCF_3[46]	**224**	332.4	203.9

[a] In $CDCl_3$ solution. [b] In CD_2Cl_2 solution. [c] $O_2CC_3F_6R$ is $O_2CC_3F_6CON(Me)C_3H_6Si(OMe)_3$.

There appears to be a trend for the pseudohalide complexes linking pK_a to the NMR analytical data (the chloride complexes do not fit this trend), however tetrafluorosuccinimidate is a noticeable outlier in each case, suggesting its pK_a is significantly lower than the 2.1 value estimated by Hine *et al.*.[89] The pK_a of tetrafluorosuccinimide was estimated by the authors by comparison of the pK_a of succinimide (a pK_a value of 9.35 in water was used) to pyrrolidinium (11.31) and 3,3,4,4-tetrafluoropyrrolidinium (4.05) ions. Tetrafluorosuccinimidate could also be an outlier due to the differences in σ and π electron donation between the N- and O-coordinated ligands. It is apparent that the tfs complex **217** is very electron deficient relative to other chloride and pseudohalide complexes other than the di substituted O_3SCF_3 complex **224**, to which it appears to have relatively similar properties. The benzylidene carbene carbon and proton NMR signals have a good correlation of increasing chemical shift with decreasing pK_a (Figure 43 and Figure 44) but the NHC carbene carbon signal is not as well correlated with decreasing chemical shift with decreasing pK_a (Figure 45).

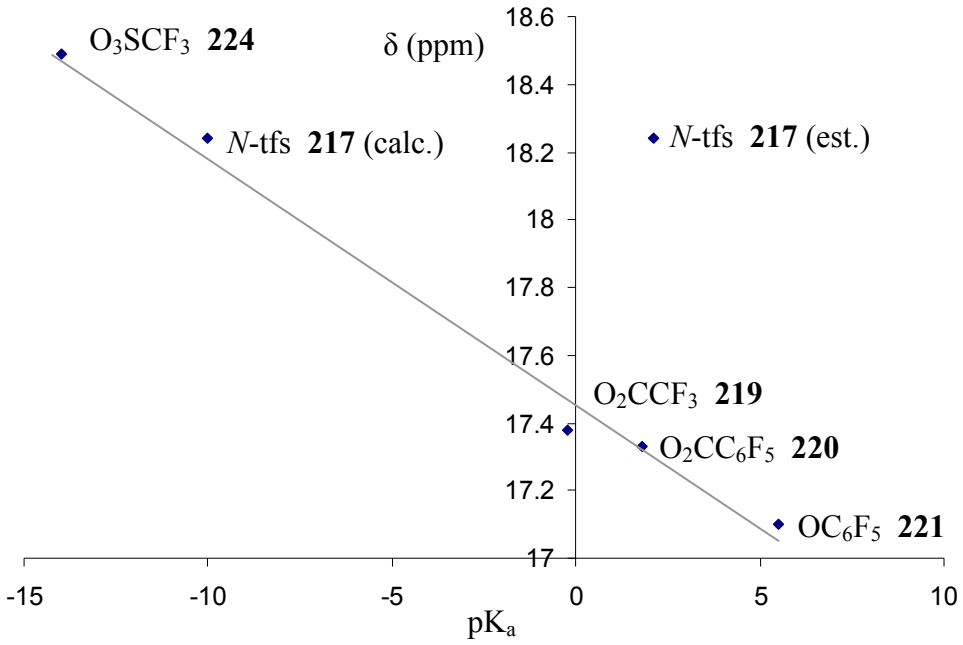

Figure 43. Plot of benzylidene C*H* proton NMR signal against pK_a (in water) of the pseudohalide ligands for $[RuX_2(o\text{-}^{i}PrO\text{-}CHPh)(IMesH_2)]$ complexes.[a]

[a] Line corresponds to line of best fit for complexes **219**-**221** and **224**, $R^2 = 0.991$.

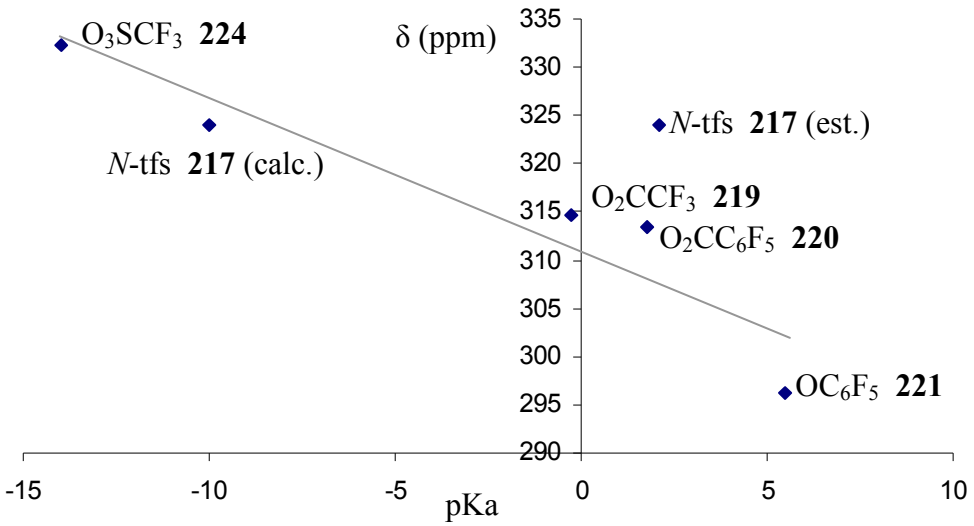

Figure 44. Plot of benzylidene *C*H carbon NMR signal against pK_a (in water) of the pseudohalide ligands for [RuX_2(*o*-^{i}PrO-CHPh)($IMesH_2$)] complexes.[a]

[a] Line corresponds to line of best fit for complexes **219**-**221** and **224**, $R^2 = 0.886$.

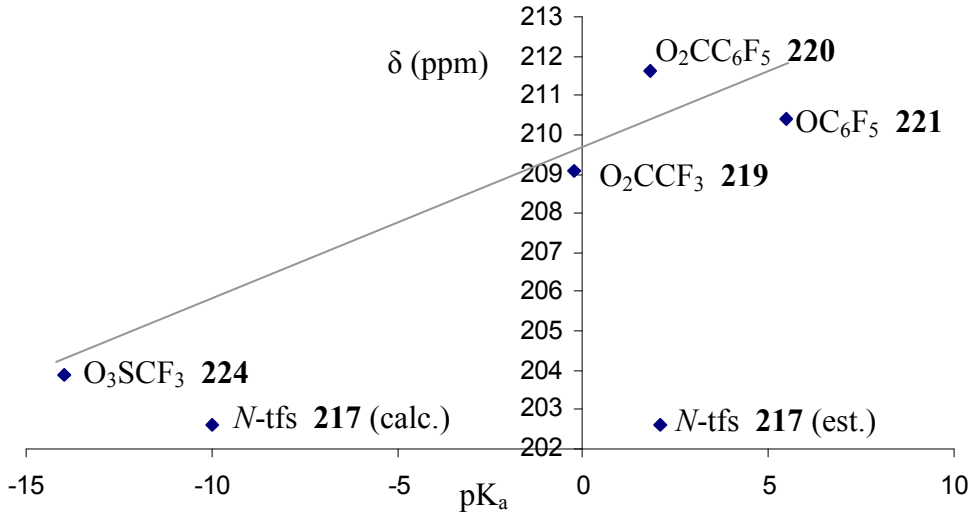

Figure 45. Plot of NHC carbene carbon NMR signal against pK_a (in water) of the pseudohalide ligands for [RuX_2(*o*-^{i}PrO-CHPh)($IMesH_2$)] complexes. [a]

[a] Line corresponds to line of best fit for complexes **219**-**221** and **224**, $R^2 = 0.897$.

In order to determine a more reliable pK_a value for tetrafluorosuccinimide, computational calculations were carried out by collaborators (the group of Zhenyang Lin of the Hong Kong University of Science & Technology) using the method of Fu *et al.*.[95] The geometry of the molecule was calculated in the gas phase using the B3LYP/6-31+G(d) method and the electronic energy using B3LYP/6-311++G-(2df,p) and MP2/6-311++G(d,p) methods. A polarised continuum model (developed by Tomasi and co-workers)[96] was used to calculate solvation free energies for the molecule and so calculate the pK_a.

The pK_a in water of tetrafluorosuccinimide was calculated to be -10.0 which fits well to the lines of best fit (generated form the other complexes) of the plots of pK_a against the benzylidene ligand CH proton and carbon NMR chemical shifts (Figure 43 and Figure 44). It however does not fit as closely to the plot of pK_a against the carbene carbon NMR chemical shift (Figure 45), although the correlation between pK_a and the NMR signal is not as good in this case.

The pK_a value of -10.0 was calculated assuming a simple ionisation process involving the imide dissociating into a proton and an imidate anion. In reality the imide forms hydrogen bonded dimers and higher clusters,[89] which will significantly effect the energy of the ionisation process, and so the calculated pK_a is not the same as would be obtained experimentally. For example, the pK_a of succinimide was calculated by this method as 0.43 and the experimental value is reported as 9.7.[86] However, this pK_a value is a useful indication of the basicity of the tetrafluorosuccinimidate anion, because, as the imidate is ligated to Ru, dimerisation and hydrogen bonding processes will not be relevant. This allows comparison with the other Ru benzylidene complexes (**219**-**221** and **224**), assuming these factors will not be as significant for the carboxylate, triflate and phenolate pseudohalide ligands. Interestingly, the acyclic analogue of tetrafluorosuccinimide, $(CF_3CO)_2NH$, has an experimentally derived pK_a of 1.2 in water and 2.2 in DMSO.[97] The pK_a of the acylic analogue of succinimide, $(CH_3CO)_2NH$, in DMSO is 17.9 (the value in water has not been reported).[98] The difference in these values (15.7) is comparable to the difference between the calculated value for tetrafluorosuccinimide and the experimental value for succinimide in water (19.7).

Complex **217** has a ^{19}F NMR spectrum containing two second order doublets at -126.5 and -125.6 ppm with couplings of 280 Hz (forming an apparent double doublet at -126.0 ppm) in $CDCl_3$. This suggests an asymmetric environment for the *N*-tfs ligands, which

could be due to hydrogen bonding or solvent coordination. The signal is 1.4 ppm downfield of neutral tetrafluorosuccinimide (a singlet at -127.4 ppm)[99] and downfield of *N*-tfs ligated Au(I) (**55-57 b**) and Au(III) (**66c**, **67c**) complexes (Chapter 2).

Complex **217** has a tetrafluorosuccinimidate carbonyl stretching frequency of 1682 cm^{-1} (solid state), which is 69 cm^{-1} lower than the parent imide. This reduction in the stretching frequency on coordination to a metal is typical of imidate ligands.[100] Au(I) (**55-57 b**) and Au(III) (**66c**, **67c**) tetrafluorosuccinimidate complexes have higher frequencies although these are not directly comparable as they were taken in CH_2Cl_2 solution. Reported Pd (**225**, **226**), Ir (**227**) and Rh (**228**) complexes[100c] have similar stretching frequencies in the range 1679-1686 cm^{-1} (Table 45).

Table 45. Carbonyl stretching frequencies of tetrafluorosuccinimidate ligands in transition metal complexes.

Entry	Complex	Carbonyl stretching frequency (cm^{-1})
1	[Ru(*N*-tfs)$_2$(*o*-^{i}PrO-CHPh)(IMesH$_2$)] (**217**)	1682[a]
2	Tetrafluorosuccinimide	1751[a]
3	[Au(*N*-tfs)(I^{t}Pe)] (**56b**)	1704[b]
4	[AuBr$_2$(*N*-tfs)(I^{t}Pe)] (**67c**)	1716[b]
5	[Au(*N*-tfs)(I^{t}Bu)] (**55b**)	1704[b]
6	[AuBr$_2$(*N*-tfs)(I^{t}Bu)] (**66c**)	1718[b]
7	*cis*-[PdCl(*N*-tfs)(Ph$_2$PCH$_2$CH$_2$PPh$_2$)][100c] (**225**)	1682[c]
8	[{Pd(μ-tfs)(C$_6$H$_4$CH=NPh)}$_2$].CH$_2$Cl$_2$[d,100c] (**226**)	1780 (sym.) 1660 (asym.)[c]
9	*trans*-[Ir(*N*-tfs)(CO)(PPh$_3$)$_2$][100c] (**227**)	1686[c]
10	*trans*-[Rh(*N*-tfs)(CO)(PPh$_3$)$_2$][100c] (**228**)	1679[c]

[a] Solid state. [b] CH_2Cl_2 solution. [c] KBr disk. [d] *N*,*O*-bridging tetrafluorosuccinimidate ligand.

Complex **217** was crystallised by layering hexane on a CD_2Cl_2 solution which co-crystallised with [Ru(*N*-tfs)$_3$(IMesH$_2$)(OH$_2$)$_2$] (**229**). This allowed the structure to be determined by X-ray diffraction (Figure 46). Selected bond lengths of these and related complexes are displayed in Table 46. Note: this co-crystal does not represent the bulk material (as observed by NMR spectroscopy).

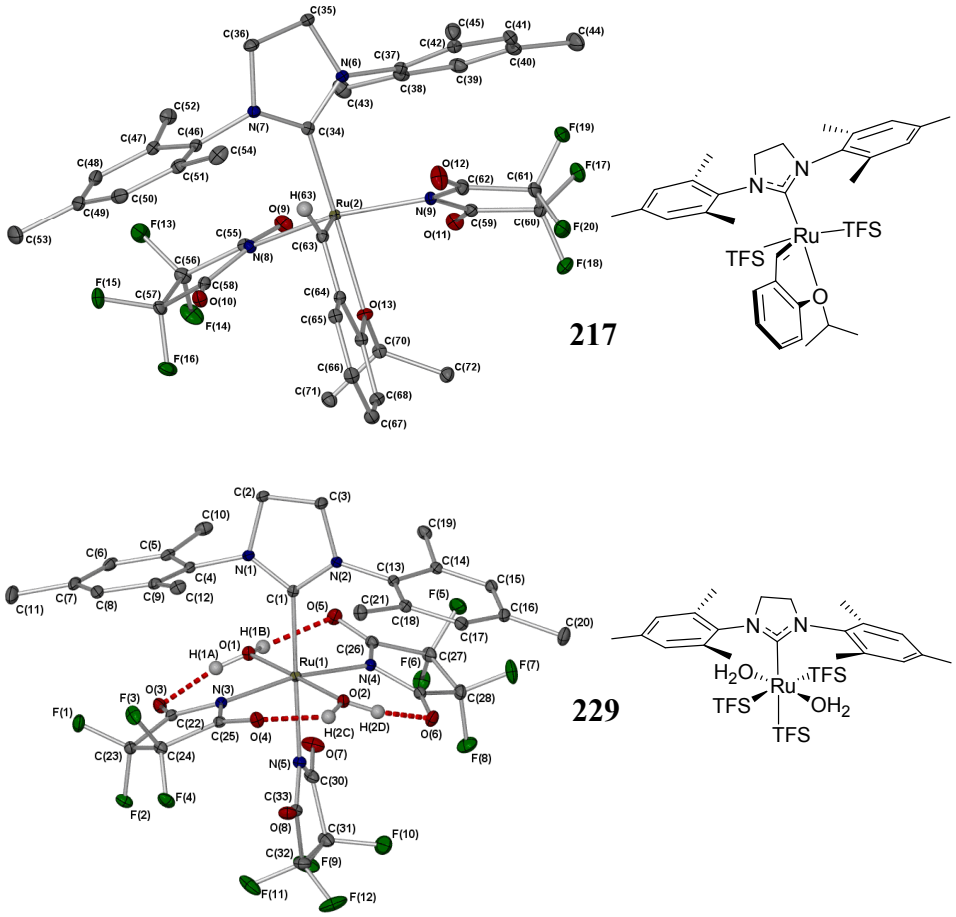

Figure 46. Molecular structure of [Ru(*N*-tfs)$_2$(*o*-^{i}PrO-CHPh)(IMesH$_2$)].[Ru(*N*-tfs)$_3$(IMesH$_2$)(OH$_2$)$_2$] (**217**.**229**). Displacement ellipsoids are shown at the 30% probability level. Hydrogen atoms have been omitted for clarity (except for OH$_2$ and benzylidene carbene protons).

Table 46. Bond lengths in [Ru(*N*-tfs)$_2$(*o*-^{i}PrO-CHPh)(IMesH$_2$)].[Ru(*N*-tfs)$_3$(IMesH$_2$)(OH$_2$)$_2$] (**217**.**229**) and related transition metal complexes.[a]

		Bond length (Å)						
		Anion	*N*-tfs		IMes		Benzylidene	
Entry	Complex	M-Anion	N-C	C=O	Ru-C	C-N	Ru-O	Ru-C
1	[Ru(*N*-tfs)$_2$(*o*-^{i}PrO-CHPh)(IMesH$_2$)] (**217**)	2.090(14), 2.063(14)	1.367(2), 1.369(2), 1.364(2), 1.373(2)	1.215(2), 1.207(2), 1.208(2), 1.202(2)	2.020(17)	1.356(2), 1.355(2)	2.277(12)	1.826(17)
	Average	2.077 (28)	1.368 (8)	1.208 (8)	2.020(17)	1.356 (4)	2.277(12)	1.826(17)
2	[Ru(*N*-tfs)$_3$(IMesH$_2$)(OH$_2$)$_2$] (**229**)	2.120(14), 2.115(15), 2.155(15)	1.369(2), 1.374(2), 1.382(2), 1.371(2), 1.385(2), 1.376(2)	1.221(2), 1.211(2), 1.209(2), 1.219(2), 1.209(2), 1.213(2)	2.112(17)	1.348(2), 1.338(2)	2.005(13) (OH$_2$) 1.999(13) (OH$_2$)	
	Average	2.130(44)	1.376(12)	1.214(12)	2.112(17)	1.343 (4)	2.002(26)	
3	[RuCl$_2$(*o*-^{i}PrO-CHPh)(IMesH$_2$)][36] (**163**)	2.340(12), 2.328(12)			1.981(5)	1.351(6), 1.350(6)	2.261(3)	1.828(5)
	Average	2.334(24)			1.981(5)	1.351(12)	2.261(3)	1.828(5)
4	[RuCl(O$_3$SCF$_3$)(*o*-^{i}PrO-CHPh)(IMesH$_2$)][46] (**218**)	2.0986(19) (O$_3$SCF$_3$), 2.3182(7) (Cl)			1.984(2)		2.2499(17)	1.820(3)
	Average				1.984(2)		2.2499(17)	1.820(3)
5	[Ru(O$_3$SCF$_3$)$_2$(*o*-^{i}PrO-CHPh)(IMesH$_2$)][46] (**224**)	2.0365(16), 2.0258(15)			1.979(2)		2.2458(15)	1.826(2)
	Average	2.0312(31)			1.979(2)		2.2458(15)	1.826(2)
6	[AuBr$_2$(*N*-tfs)(I^{t}Pe)] (**67c**)	2.048(6)	1.367(9), 1.371(10)	1.198(9), 1.11(7), 1.26(3)				
	Average	2.048(6)	1.369(19)	1.189(19)				
7	*trans*-[Ir(*N*-tfs)(CO)(PPh$_3$)$_2$][100c] (**227**)	2.087(4)	1.359(5), 1.365 (8)	1.197(6), 1.202(6)				
	Average	2.087(4)	1.362(13)	1.200(12)				

[a] ESD values are displayed in brackets.

There are no significant bond length differences between [Ru(*N*-tfs)$_2$(*o*-^{i}PrO-CHPh)(IMesH$_2$)] (**217**) and the related dichloride complex **163**, other than the Ru-N bond to the imidate is an average of 2.077(28) Å compared with 2.334(24) Å for the Ru-Cl bond distance, a difference of 0.258 Å. It is however similar to the Ru-O length in [RuCl(O$_3$SCF$_3$)(*o*-^{i}PrO-CHPh)(IMesH$_2$)] (**218**) (2.0986(19) Å) and [Ru(O$_3$SCF$_3$)$_2$(*o*-^{i}PrO-CHPh)(IMesH$_2$)] (**224**) (2.0312(31) Å). The similarity between the complexes is surprising given the differences in NMR chemical shifts.

The Ru(III) complex [Ru(*N*-tfs)$_3$(IMesH$_2$)(OH$_2$)$_2$] (**229**) has longer Ru-N bonds {2.130(44) Å} than **217** {2.077(28) Å} and a longer Ru-IMes bond {2.112(17) Å compared to 2.020(17) Å}, presumably due to the increased hardness of the Ru(III) atom and reduced backbonding. There are no statistically significant differences in the bond lengths between **217** and related tetrafluorosuccinimidato transition metal complexes **67c** and **227**.

In complex **217** there is a close contact between a tetrafluorosuccinimidate carbonyl oxygen and the benzylidene carbene carbon of 2.885 Å (3.027 Å from the other face). It is speculated that this close contact plays a role in the facile decomposition of this complex and the difficulty of synthesizing related imidate complexes, either the carbonyl attacks directly or assists water or oxygen molecules in attacking the carbene.

Complex **229** has a number of hydrogen bonds between the tfs carbonyl groups and H$_2$O ligands. These are O-O 2.579 Å (1.862 Å O-H) for the ligands *cis* to the IMes ligand and 2.979 Å O-O (2.661 Å O-H) for *trans*.

Hydrogen bonding between imidate carbonyl groups and water molecules has also been observed in the crystal structure of *trans*-[Pd(*N*-succ)$_2$(PMe$_2$Ph)$_2$].2H$_2$O (**230**) (Figure 47), obtained within the Fairlamb research group. The two water molecules, which each bridge the two imidate ligands, are approximately 45-47˚ out of the plane of the Pd atom and imidate ligands. The hydrogen bond lengths are O-O 2.826 and 2.858 Å (2.046 and 2.085 Å O-H) which are O-O 0.279 and 0.247 Å (0.184 and 0.223 Å O-H) longer than the hydrogen bonds to the *cis* ligands in **229** and O-O 0.576 and 0.615 Å (0.121 and 0.153 Å O-H) shorter than the bonds to the *trans* ligands.

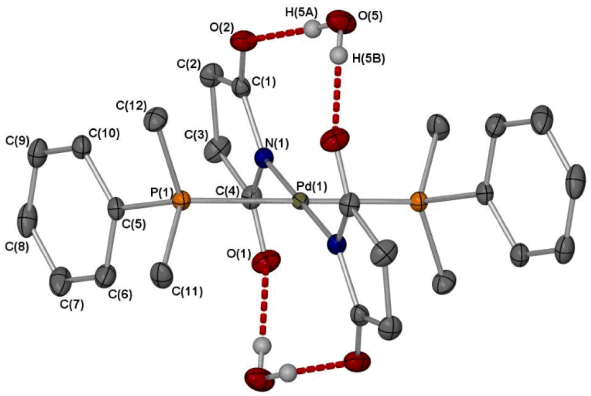

Figure 47. Molecular structure of *trans*-[Pd(*N*-succ)$_2$(PMe$_2$Ph)$_2$].2H$_2$O (**230**). Displacement ellipsoids are shown at the 50% probability level. Hydrogen atoms have been omitted for clarity (except for H$_2$O).

The [Ru(*N*-tfs)$_2$(*o*-^{i}PrO-CHPh)(IMesH$_2$)] complex (**217**) has a distorted square pyramidal geometry, although less distorted than the parent [RuCl$_2$(*o*-^{i}PrO-CHPh)(IMesH$_2$)] complex (**163**). Complex **217** has a smaller C^2-Ru-C^1 bond angle {91.21(7)˚} than **163** {101.5(14)˚} by 10.3˚ (Table 47). The C^1-Ru-O angle is also smaller by 5.98˚ {170.22(6)˚ for **217** and 176.2(14)˚ for **163**}, C^2-Ru-X^2 smaller by 7.37˚ {92.73(7)˚ and 100.1(15)˚, respectively}, X^1-Ru-X^2 larger by 5.57˚ {162.07(6)˚ and 156.5(5)˚} and C^1-Ru-X^2 larger by 3.5˚ {94.40(6)˚ and 90.9(12)˚}. These differences may be caused by steric interactions between the larger anionic ligands in **217** (hence the larger angles between the anionic and other ligands but smaller angles between the neutral ligands). The larger X^1-Ru-X^2 angle is significant as it will result in a reduced antibonding interaction between the anionic ligand orbitals and Ru d orbitals and so reduce stabilisation of the carbene conformation inactive in metathesis.[69,72]

Two other reported pseudohalide [RuXX'(*o*-^{i}PrO-CHPh)(IMesH$_2$)] complexes; [RuCl(O$_3$SCF$_3$)(*o*-^{i}PrO-CHPh)(IMesH$_2$)] (**218**) and [Ru(O$_3$SCF$_3$)$_2$(*o*-^{i}PrO-CHPh)(IMesH$_2$)] (**224**) have bond angles closer to those of the parent dichloride **163** than the tfs complex **217**. Complex **218** has a smaller C^2-Ru-C^1 angle by 11.13˚ than **217** {102.34(11)˚ for **218** and 91.21(7)˚ for **217**} but only 0.8˚ less than **163** {101.5(14)˚} and similarly with the C^1-Ru-O angle {178.17(8)˚ and 170.22 (6)˚, respectively} with a difference of 7.95˚ from **217** and only 2.0˚ from **163** {176.2(14)˚}. The C^1-Ru-X^1 angle {93.50(9)˚ and 98.73(6)˚} is smaller by 5.23˚ than **217** but larger by 3.1˚ than **163** {96.6(12)˚}. Complex **224** has bond angles similar to the monosubstituted analogue **218**.

The [Ru(*N*-tfs)$_3$(IMesH$_2$)(OH$_2$)$_2$] complex (**229**) has a slightly distorted octahedral geometry with bond angles between the IMes ligand and the tetrafluorosuccinimidate ligands *cis* to it of 94.21(6)˚ and 95.92(6)˚ {with an angle of 169.87(6)˚ between the tfs ligands}. Interestingly there have been no similar [RuX$_3$(NHC)] complexes reported.

Table 47. Bond angles in [Ru(*N*-tfs)$_2$(*o*-^{i}PrO-CHPh)(IMesH$_2$)].[Ru(*N*-tfs)$_3$(IMesH$_2$)(OH$_2$)$_2$] (**217**.**229**) and related transition metal complexes.[a]

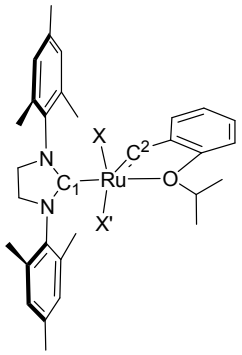

		Bond angle (˚) of [RuXX'(*o*-^{i}PrO-CHPh)(IMesH$_2$)]			
Entry	**Angle**	**X = Cl X' = O_3SCF_3 (218)**	**X = X' = O_3SCF_3 (224)**	**X = X' = Cl (163)**	**X = X' = *N*-tfs (217)**
1	C^2-Ru-C^1	102.34(11)	100.83(9)	101.5(14)	91.21(7)
2	C^2-Ru-X^1	98.87(10)	103.11(8)	100.2(15)	99.12(7)
3	C^1-Ru-X^1	93.50(9)	92.31(7)	96.6(12)	98.73(6)
4	C^2-Ru-O	79.31(10)	79.20(8)	79.3(17)	79.11(6)
5	C^1-Ru-O	178.17(8)	178.93(8)	176.2(14)	170.22(6)
6	X^1-Ru-O	85.43(7)	88.73(7)	86.9(9)	84.29(5)
7	C^2-Ru-X^2	97.21(9)	97.91(8)	100.1(15)	92.73(7)
8	C^1-Ru-X^2	93.12(7)	92.26(7)	90.9(12)	94.40(6)
9	X^1-Ru-X^2	160.87(6)	157.23(6)	156.5(5)	162.07(6)
10	O-Ru-X^2	87.44(5)	86.67(7)	85.3(9)	84.80(5)

[a] ESD values are displayed in brackets.

3.2.2. Catalysis

3.2.2.1. Activity of [Ru(*N*-tfs)$_2$(*o*-^{i}PrO-CHPh)(IMesH$_2$)] in RCM and ROMP processes

The [Ru(*N*-tfs)$_2$(*o*-^{i}PrO-CHPh)(IMesH$_2$)] complex (**217**) was tested for activity in the ring-closing metathesis of dimethyl diallylmalonate (**84**), and compared to the parent dichloride complex (**163**), under the conditions reported by Grubbs *et al*..[101] Complex **163** showed the expected kinetics with 99% conversion after 30 minutes, a k_{obs} value of 2.86 x10^{-3} s^{-1} {Grubbs reported a k_{obs} value of 3.0 x10^{-3} s^{-1} for diethyl diallylmalonate (**167**)} and an initial rate of 2.86 x10^{-4} mol.dm^{-3}.s^{-1} (with a standard error of 1.3% assuming first order kinetics using Dynafit software) (Figure 48). Complex **217** however showed no detectable turnover, or even initiation, after 30 minutes.

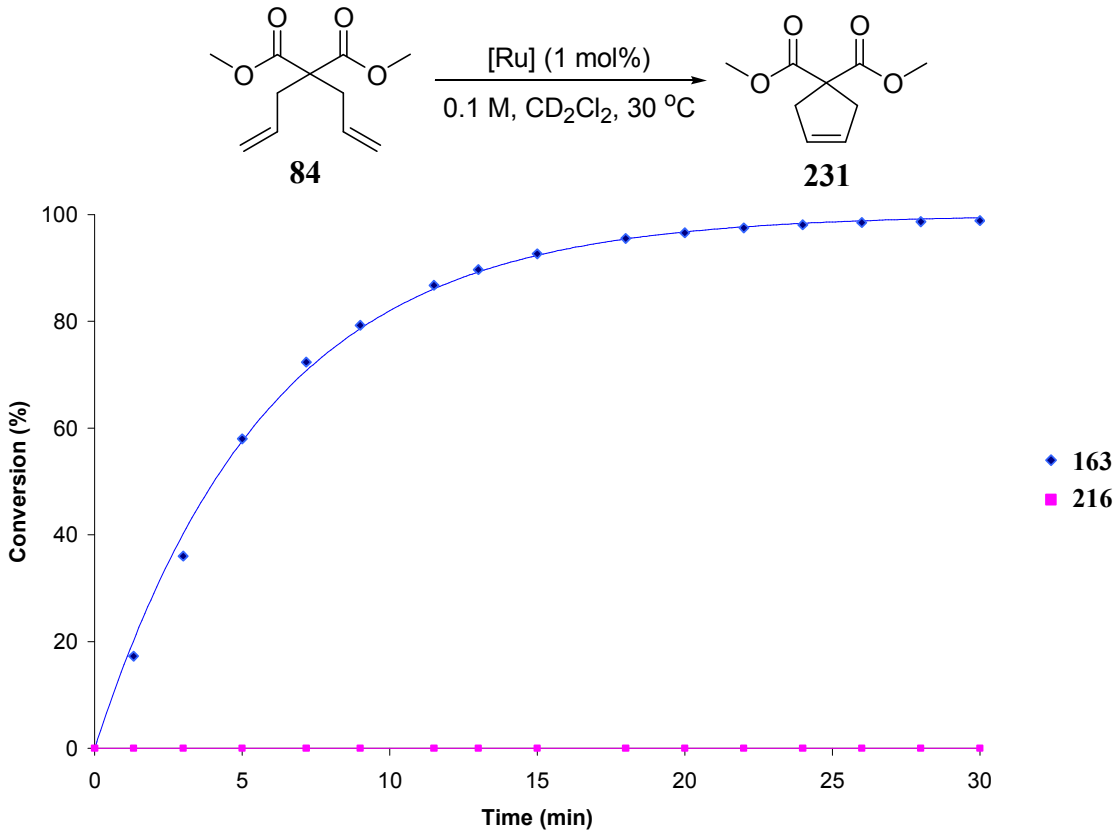

Figure 48. Conversion of dimethyl diallylmalonate (**84**) to dimethyl cyclopent-3-ene-1,1-dicarboxylate (**231**) catalysed by [RuCl$_2$(*o*-^{i}PrO-CHPh)(IMesH$_2$)] (**163**) and [Ru(*N*-tfs)$_2$(*o*-^{i}PrO-CHPh)(IMesH$_2$)] (**217**).[a]

[a] Conditions: 0.1 M solution of dimethyl diallylmalonate (**84**) in CD_2Cl_2, 1 mol% Ru catalyst, 30 ˚C. Anhydrous, oxygen free conditions.

After 20 hours at 30 ^{o}C less than 0.5% turnover was observed for complex **217**. Analysis of the solution after this time by ^{1}H NMR spectroscopy revealed a complex mixture of carbene signals (including triplet and double triplet signal splitting),[102] as well as some decomposition by aldehyde formation, and only a trace of the benzylidene signal corresponding to **217**. Clearly initiation *via* dissociation of the isopropoxy ligand had occurred, followed by metathesis of the benzylidene ligand, resulting in a range of methylidene and alkylidene complexes which must also be essentially inactive in metathesis.

To test the effect of the less electron withdrawing succinimidate ligand, potassium succinimidate (1.9 mol %) was added to a dry degassed solution of [$RuCl_2(CHPh)(PCy_3)_2$] (**162**) (1 mol%) and dimethyl diallylmalonate (**84**) (0.1 M) in CD_2Cl_2 and stirred at 30 ˚C for 2 days. Only 10% conversion occurred compared to 100% for the control with no imidate added. The added succinimidate inhibits the efficiency of the catalyst presumably by mediating decomposition.

The activity of the tfs complex **217** was also tested in the ring-opening metathesis polymerisation of 1,5-cyclooctadiene (**232**) (Scheme 61), but showed less than 5% conversion to **233** over 2 hours compared with quantitative conversion for the dichloride complex **163** (1 mol% loading in 0.5 M CH_2Cl_2 at 30 ˚C for 2 hours).

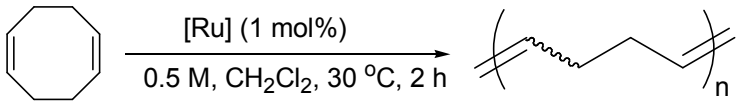

232 **233**

Scheme 61. Ruthenium catalysed ring-opening metathesis polymerisation (ROMP) of 1,5-cyclooctadiene (**232**).

The principal cause of the lack of activity of complex **217** in RCM and ROMP processes is presumably the strong coordination of the isopropyl oxygen to the Ru atom preventing the reagent alkene from coordinating to Ru and initiating the reaction. The tfs ligands withdraw more electron density from the Ru atom relative to chloride increasing the Ru-O bond strength. The activated catalyst was also inactive in the RCM process, which is surprising given the predicted reduced stabilisation of the inactive carbene conformation in the precatalyst (due to a larger X-Ru-X angle and reduced electron donation of the anionic ligand relative to the dichloride complex **163**, *vide supra*).

Fogg and co-workers recently reported that for a series of catecholate Ru complexes (**172**) reducing the electron donation of the catecholate ligand, and consequently the electron density on the ruthenium, reduces the metathesis activity of the catalyst (Figure 36). This may explain why complex **217** containing tfs ligands, which have a significantly lower pK_a than the catecholate ligands, is inactive for these particular metathesis reactions.[53]

Fogg determined that decreased electron density on Ru affects both initiation (by inhibiting ligand dissociation) and propagation (by raising the energy of the Ru(IV) intermediate). Buchowicz *et al.*[85] found that out of the range of Grubbs 1st generation analogues they prepared containing O_2CCF_3, $O_2CC_2F_5$, $O_2CC_6F_5$ and O_2CCl_3 ligands, the $O_2CC_6F_5$ complexes were inactive in metathesis due to insufficient electron density on Ru. In contrast computational studies on gas phase reactions found that reducing electron density on the Ru atom actually increased the activity of complexes in metathesis reactions (although the calculations did not take initiation into account).[103]

Hence, although initiation is inhibited, the effect of reduced Ru electron density on propagation rates is not clear cut. An active catalyst may therefore possibly be obtained by use of a more labile neutral ligand, harsh conditions or an irreversible activation process. The instability of the precatalyst however precludes further investigation.

3.3. Conclusion

In summary, it was possible to prepare the novel tetrafluorosuccinimidate-containing ruthenium benzylidene complex [Ru(*N*-tfs)$_2$(*o*-^{i}PrO-CHPh)(IMesH$_2$)] (**217**). NMR spectroscopic analysis, particularly of the characteristic NHC and benzylidene carbene ^{1}H and ^{13}C signals, showed that this complex was electron deficient due to reduced electron donation by the tetrafluorosuccinimidate ligand, relative to the parent dichloride (**163**). The crystal structure of [Ru(*N*-tfs)$_2$(*o*-^{i}PrO-CHPh)(IMesH$_2$)] (**217**) was obtained {which co-crystallised with [Ru(*N*-tfs)$_3$(IMesH$_2$)(OH$_2$)$_2$] (**229**)} by X-ray diffraction. This showed there to be little difference in bond lengths between complex **217** and the parent dichloride **163**, other than a significantly longer Ru–tfs than Ru-Cl bond length. It was found that there was a greater angle between the tetrafluorosuccinimidate ligands in **217** than the chloride ligands in **163** due to the greater steric bulk of the imidate ligands and shorter Ru-anionic ligand bond lengths. This complex was found to be near-inactive in benchmark ring-closing metathesis and ring-opening metathesis polymerisation reactions. The electron deficiency of the complex would appear to reduce the rate of activation and possibly propagation. The air sensitivity of complex **217** relative to **163** also precludes its practical use as a catalyst.

Unfortunately, it was not possible to prepare Ru(II) alkylidene or benzylidene complexes containing succinimidate, maleimidate or phthalimidate ligands, due to decomposition of the alkylidene and benzylidene ligands. These results show that anionic ligands with relatively low electronegativity result in decomposition of the carbene ligand whereas highly electronegative ligands result in deactivation of the complex in catalysis. Tuning of the electronic properties of the anionic ligand are clearly paramount to the stability and activity of these complexes.

3.4. Future Work

Further investigation of [Ru(*N*-tfs)$_2$(*o*-^{i}PrO-CHPh)(IMesH$_2$)] (**217**) is required in order to develop conditions enabling the activation of the precatalyst, *via* labilisation of the isopropoxy ligand and binding of the alkene reagent, which might be achieved by the use of higher temperature. The use of monodentate benzylidene and neutral ligands, such as 2-bromopyridine, will also aid activation at the expense of complex stability. These developments would allow the activity of the catalyst in the propagation steps of RCM and ROMP processes to be investigated and the determination of whether inhibited activation in electron deficient Ru benzylidene complexes masks high or low propagation activity.

The air sensitivity of complex **217** relative to the parent dichloride **163** ultimately impairs its practicality as a catalyst and so other imidates derived from imides with pK_as intermediate between tetrafluorosuccinimide and succinimide, such as 1,2-dibromosuccinimide and other halogenated imides, should be tested. Complexes with one electron deficient pseudohalide and one halide ligand have in some cases been found to be more active than bis-pseudohalide analogues.[43,52] Complexes such as [RuX(*N*-tfs)(*o*-^{i}PrO-CHPh)(IMesH$_2$)] (where X is Br and Cl), which will have increased electron density on Ru, may therefore prove more catalytically active. This will require an improved synthetic method to prevent the formation of mixtures of products.

Should these studies produce an effective catalyst then the investigation of imidate ligands tethered to solid supports, to produce recyclable catalysts and to reduce Ru contamination of metathesis products, should be undertaken. Chiral imidate ligands {such as those derived from naturally occurring L-(+)-tartaric acid} could be investigated for the preparation of chiral Ru benzylidene complexes for application in enantioselective catalysis.

3.5. Experimental

3.5.1. General Details

All reactions involving ruthenium complexes were carried out using anhydrous, degassed solvents under an inert atmosphere, using Schlenk line or dry box techniques. All reactions involving silver salts were carried out in the absence of light. Solvents were degassed by several freeze-pump-thaw cycles. Dichloromethane, hexane, diethyl ether and toluene were dried by passing through a column of activated alumina. Methanol and *t*-butanol were distilled from magnesium alkoxides, acetone was distilled from calcium chloride and tetrahydrofuran was distilled from sodium benzophenone ketyl. Infra-red spectra were recorded on a Unicam Research Series FT-IR spectrometer. Mass spectrometry was carried out using a Bruker Daltronics micrOTOF instrument. ^{1}H, ^{13}C, ^{19}F and ^{31}P NMR spectra were collected on a JEOL ECX400 spectrometer operating at 400, 101, 376 and 162 MHz, respectively, and referenced to residual solvent signals. ^{13}C NMR signals are singlets unless otherwise stated. ^{1}H-NMR kinetic experiments were carried on a Bruker AMX500 spectrometer operating at 500 MHz. All column chromatography was performed using silica-gel (mesh 220-440) purchased from Fluka Chemicals with the solvent systems specified within the text. All TLC analysis was performed using Merck 5554 aluminium backed silica plates and visualised using UV light (254 nm) or an aqueous solution of potassium permanganate. Melting points were measured in open capillary tubes using a Stuart SMP3 Digital Melting Point Apparatus and are uncorrected. Ruthenium trichloride hydrate was purchased from Precious Metals Online (www.precmet.com.au), tetrabutylammonium bromide, methyltriphenylphosphonium bromide, trifluoroacetic acid, *tert*-butylamine, glyoxal and *tert*-pentylamine were purchased from Alfa Aesar, copper(I)chloride was purchased from Fisons, silver(I)oxide was purchased from Strem Chemicals Inc.. All other chemicals were purchased from Sigma Aldrich Inc. and used without further purification unless otherwise stated. Ag(*N*-mal),[104] Ag(*N*-succ),[105] Tl(*N*-succ),[65] AgO_2CCF_3,[106] $[Ru(N\text{-succ})_3(OH_2)_3]^1$ and $[Ru(N\text{-ptm})_3(OH_2)_3]^1$ were prepared by the reported procedures.

3.5.2. X-Ray crystallography

Diffraction data were collected at 110 K on a Bruker Smart Apex diffractometer with Mo-K_α radiation (λ = 0.71073 Å) using a SMART CCD camera. Diffractometer control, data collection and initial unit cell determination was performed using "SMART" (v5.625

Bruker-AXS). Frame integration and unit-cell refinement software was carried out with "SAINT+" (v6.22, Bruker AXS). Absorption corrections were applied by SADABS (v2.03, Sheldrick). Structures were solved by direct methods using SHELXS-97 (Sheldrick, 1990) and refined by full-matrix least squares using SHELXL-97 (Sheldrick, 1997). All non-hydrogen atoms were refined anisotropically. Hydrogen atoms were placed using a "riding model" and included in the refinement at calculated positions.

3.5.3. Compounds

$[RuCl_2(CHPh)(PCy_3)_2]$ (162)

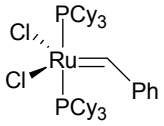

Prepared by a protocol reported by Schwab *et al.*.[31] Benzaldehyde tosylhydrazone (0.302 g, 1.05 mmol, 5 equiv.), potassium methoxide (0.138 g, 1.97 mmol, 9.4 equiv.) and triethylene glycol (2 ml) were stirred *in vacuo* until all methanol was removed. The solution was then stirred (62 °C, 45 mins) to give a deep red solution which was poured into ice water producing a white precipitate. The red solution was extracted with pentane (2 x 5 ml), centrifuged, cold filtered (-40 °C) and the solvent removed *in vacuo* to give a red oil. This was dissolved in dichloromethane (2 ml), cooled to -50 °C and added to a solution of $[RuCl_2(PPh_3)_3]$ (**197**) (196 mg, 204 μmol, 1 equiv.) in dichloromethane (7 ml) at -78 °C. The resultant green solution was stirred at room temperature (5 mins). Tricyclohexylphosphine (125 mg, 448 μmol, 2.2 equiv.) in dichloromethane (4 ml) was added at -78 °C and the solution stirred at room temperature (30 mins) to give a red brown solution. The solution was reduced to 2 ml *in vacuo* and methanol (15 ml) added. The resultant purple precipitate was isolated by cannula filtration and washed with methanol (3 x 1 ml) and acetone (3 x 1 ml) and dried *in vacuo* to give the title compound as a purple powder (99.7 mg, 131 μmol, 64%). ^{1}H NMR (400 MHz, CD_2Cl_2) δ 20.02 (s, 1H, carbene Ru=C*H*Ph), 8.45 (d, *J* = 7.5 Hz, 2H, phenyl *ortho* C*H*), 7.57 (t, *J* = 7.5 Hz, 1H, phenyl *para* C*H*), 7.33 (t, *J* = 7.5 Hz, 2H, phenyl *meta* C*H*), 2.60 (m, 2H, Cy C*H*), 1.68-1.75 (m, 10H, Cy C*H*), 1.48-1.40 (m, 6H, Cy C*H*), 1.25-1.15 (m, Cy C*H*). ^{13}C NMR (101 MHz, CD_2Cl_2) δ 294.7 (m, carbene Ru=*C*HPh), 153.2 (phenyl *C*), 131.2 (phenyl *C*), 129.5 (phenyl *C*), 129.3 (phenyl *C*), 32.5 (t, *J* = 9 Hz, PCy_3 *ipso C*), 30.0 (PCy_3 *meta C*), 28.2 (t, *J* = 5 Hz, PCy_3 *ortho C*), 27.0 (PCy_3 *para C*). ^{31}P NMR (162 Mhz, CD_2Cl_2) δ 36.8 (s,

PCy_3). ESI^+-MS *m/z* 822.4 (9%, $[MH]^+$), 787.4 (100%, $[M\text{-}Cl]^+$), 767.4 (38%), 657.3 (12%), 615.4 (68%), 593.5 (59%), 509.2 (71%). ESI^+-HRMS calcd. for $C_{43}H_{72}ClP_2Ru$ ($[M\text{-}Cl]^+$) 787.3844; found 787.3853. No high resolution signal for $[MH]^+$ due to overlap of the signal with other peaks. Data in accordance with the literature.[31]

Benzaldehyde tosylhydrazone

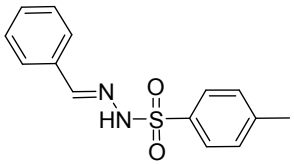

Prepared by a protocol reported by Closs and Moss.[107] *p*-Toluenesulfonhydrazide (5.02 g, 26.9 mmol, 1 equiv.) was dissolved in refluxing methanol (20 ml), cooled to 50 °C and benzaldehyde (2.86 g, 26.9 mmol, 1 equiv.) was added. This was stirred at 50 °C (3 mins) and then at -70 °C (2 hours). The resultant white precipitate was separated by filtration and recrystallised from methanol to yield the title compound as a white powder (5.04 g, 17.5 mmol, 65%). ^{1}H NMR (270 MHz, $CDCl_3$) δ 8.29 (s, 1H, N*H*), 7.88 (d, *J* = 8.3 Hz, 2H, aromatic C*H*), 7.77 (s, 1H, NC*H*Ph), 7.55 (m, 2H, aromatic C*H*), 7.31 (m, 5H, aromatic C*H*), 2.39 (s, 3H, CH_3). ^{13}C NMR (101 MHz, $CDCl_3$) δ 148.0 (N*C*H), 144.2 (CSO_2), 135.1 (Aryl *C*), 133.1 (Aryl *C*), 130.3 (Aryl *C*), 129.7 (Aryl *C*), 128.5 (Aryl *C*), 127.8 (Aryl *C*), 127.3 (Aryl *C*), 21.5 (CH_3). ESI^+-MS *m/z* 297.1 (79%, $[MNa]^+$), 275.1 (100%, $[MH]^+$), 157.0 (14%, $[H_3CPhSO_2H_2]^+$). ESI^+-HRMS calcd. for $C_{14}H_{15}N_2O_2S$ ($[MH]^+$) 275.0849; found 275.0856. Data in accordance with the literature.[107]

Tricyclohexylphosphine

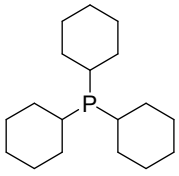

Prepared by a protocol reported by Issleib and Brack.[108] All reagents were distilled and degassed prior to use and all operations were carried out under an inert atmosphere. Cyclohexylbromide (7.51 ml, 61.5 mmol, 6 equiv.) was gradually added to activated magnesium turnings (1.50 g, 61.5 mmol, 6 equiv.) in diethyl ether (20 ml) with cooling. A solution of PCl_3 (0.890 ml, 10.2 mmol, 1 equiv.) in diethyl ether (5 ml) was added dropwise, the solution stirred at room temperature (1 hr) and then refluxed (90 mins) to give a white gelatinous precipitate. A solution of ammonium chloride (2.50 g, 47.2 mmol,

4.6 equiv.) in water (15 ml) was added. The organic layer was extracted (diethyl ether) and reduced *in vacuo* to give a yellow oil. Carbon disulfide (0.460 ml, 7.65 mmol, 0.75 equiv.) was added resulting in a red/brown precipitate. This was separated by filtration, washed with hexane (3 x 5ml) and dried *in vacuo*. The resultant powder was dissolved in methanol (6 ml) and refluxed to give a red solution, carbon disulfide and ethanol were removed by distillation giving the title compound as a white solid (0.683 g, 2.43 mmol, 24%). ^{1}H NMR (400 MHz, CD_2Cl_2) δ 2.04-1.12 (m, 33H). ^{31}P NMR (162 MHz, CD_2Cl_2) δ 11.08 (s). ^{13}C NMR (101 MHz, CD_2Cl_2) δ 31.9, 31.6, 31.5, 31.3, 27.9, 27.8. ESI^{+}-MS *m/z* 297.2 (100%, $[MHO]^{+}$), 281.2 (42%, $[MH]^{+}$). ESI^{+}-HRMS calcd. for $C_{18}H_{34}P$ ($[MH]^{+}$) 281.2393; found 281.2392. Data in accordance with the literature.[108]

[$RuCl_2$(CH-*o*-^{i}PrO-C_6H_4)($IMesH_2$)] (163)

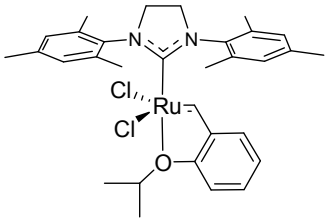

Prepared by a protocol reported by Garber *et al.*.[36] [$RuCl_2$(CHPh)($IMesH_2$)(PCy_3)] (**160**) (103 mg, 122 μmol, 1 equiv.) and CuCl (12.1 mg, 122 μmol, 1 equiv.) were mixed in dichloromethane (2 ml) under an atmosphere of N_2. A solution of 2-isopropoxystyrene (20.1 mg, 124 μmol, 1 equiv.) in dichloromethane (2 ml) was added and the mixture refluxed (2 hours) to give a green solution. The solution was reduced to dryness *in vacuo* and redissolved in a 1:1 mixture of dichloromethane and hexane (5 ml) and filtered through a silica-gel plug, which was washed with dichloromethane. The solution was reduced to dryness *in vacuo* to give the title compound as a green powder (33.7 mg, 53.8 μmol, 44%). ^{1}H NMR (400 MHz, $CDCl_3$) δ 16.58 (s, 1H, carbene Ru=C*H*), 7.49 (m, 1H, aromatic C*H*), 7.05 (s, 4H, mesityl aromatic C*H*), 6.92 (dd, *J* = 7.3 and 1.5 Hz, 1H, aromatic C*H*), 6.85 (dd, *J* = 7.3 and 7.0 Hz, 1H, aromatic C*H*), 6.78 (d, *J* = 8.6 Hz, 1H, aromatic C*H*), 4.91 {septet, *J* = 6.3 Hz, 1H, ^{i}Pr $(CH_3)_2CHOPh$}, 4.17 (s, 4H, imidazole *C*H), 2.48 (s, 12H, mesityl *ortho* CH_3), 2.41 (s, 6H, mesityl *para* CH_3), 1.28 {d, *J* = 5.9 Hz, 6H, ^{i}Pr $(CH_3)_2CHOAr$}. ^{13}C NMR (101 MHz, $CDCl_3$) δ 296.9 (benzyl carbene Ru=*C*H), 211.1 (mesityl carbene Ru=*C*N_2), 152.0, 145.1, 145.0, 138.4, 129.5, 129.4, 129.0, 122.7, 122.1, 112.9, 74.5, 51.2, 30.6, 25.8, 21.1. ESI^{+}-MS *m/z* 592 (14%, $[M\text{-}Cl]^{+}$), 555 (10%), 441 (19%), 405 (100%). Data in accordance with the literature.[36]

2-Isopropoxystyrene

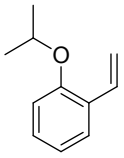

A protocol similar to that reported by Krause *et al.* was used.[46] Methyl triphenylphosphonium bromide (3.28 g, 9.18 mmol, 1 equiv.) was suspended in anhydrous tetrahydrofuran (15 ml) under an atmosphere of N_2. *n*-Butyl lithium (5.87 ml, 9.17 mmol, 1 equiv., 1.56 M in hexanes) was added dropwise at 0 °C and stirred (30 mins, 0 °C) to give a red solution. 2-Isopropoxybenzaldehyde (1.50 g, 9.15 mmol, 1 equiv.) was dissolved in tetrahydrofuran (10 ml, anhydrous) and added dropwise at 0 °C and the solution was stirred (r.t., 3 days). Water (2 ml) was added and the solvent reduced to <10 ml *in vacuo*. The product was extracted with diethyl ether (3 x 5 ml), dried ($MgSO_4$), filtered and reduced *in vacuo*. Purification was achieved by column chromatography, eluting with petroleum ether (40-60):ethyl acetate 98:2, to give the title compound as a colourless oil (0.942 g, 5.81 mmol, 64%). ^{1}H NMR (400 MHz, $CDCl_3$) δ 7.54 (dd, *J* = 7.7 and 1.8 Hz, 1H, aromatic C*H*), 7.24 (m, 1H, aromatic C*H*), 7.11 (dd, *J* = 17.8 and 11.2 Hz, 1H, H_2C=C*H*Ph), 6.93 (m, 2H, aromatic C*H*), 5.80 (dd, *J* = 17.8 and 1.6 Hz, 1H, *trans*-*H*HC=CHPh), 5.29 (dd, *J* = 11.2 and 1.6 Hz, 1H, *cis*-H*H*C=CHPh), 4.57 (septet, *J* = 6.1 Hz, 1H, ^{i}Pr C*H*), 1.40 (d, *J* = 6.1 Hz, 6H, ^{i}Pr CH_3). ^{13}C NMR (101 MHz, $CDCl_3$) δ 155.0, 131.9, 128.6, 127.7, 126.4, 120.5, 114.0, 70.6, 22.1 (1 peak overlapping). EI$^+$-MS *m/z* 162 (32%, $[M]^+$), 120 (100%, $[M-(CH_3)_2C]^+$), 91 (47%), 77 (7%), 65 (12%), 51 (6%), 43 (10%). EI$^+$-HRMS calcd. for $C_{11}H_{14}O$ ($[M]^+$) 162.1045; found 162.1043. Data in accordance with the literature.[46]

2-Isopropoxybenzaldehyde

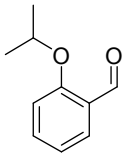

A protocol similar to that reported by Krause *et al.* was used.[46] Salicylaldehyde (2.75 ml, 25.8 mmol, 1 equiv.), tetrabutylammonium bromide (7.69 g, 23.9 mmol, 0.93 equiv.) and isopropyl iodide (6.10 ml, 61.2 mmol, 2.37 equiv.) were dissolved in dichloromethane (90 ml). A solution of sodium hydroxide (1.07 g, 26.8 mmol, 1.04 equiv.) in 50 ml of water was added dropwise with vigorous stirring and the yellow solution stirred at room

temperature (2 days). The product was extracted with dichloromethane (3 x 20 ml), reduced *in vacuo* and dissolved in ethyl acetate. The solution was filtered, dried over Na_2SO_4, filtered and reduced *in vacuo* to give the crude product as a yellow oil. Purification was achieved by Kugelrohr distillation (100 ˚C, 0.7 mm Hg) to give the title compound as a colourless oil (2.15 g, 13.1 mmol, 51%). ^{1}H NMR (400 MHz, $CDCl_3$) δ 10.47 (s, 1H, aldehyde), 7.80 (dd, *J* = 7.9 and 1.8 Hz, 1H, aromatic H), 7.49 (ddd, *J* = 8.4, 7.3 and 1.8 Hz, 1H, aromatic H), 6.98-6.94 (m, 2H, aromatic H), 4.66 (septet, *J* = 6.0 Hz, 1H, isopropyl H), 1.38 (d, *J* = 6.0 Hz, 6H, ispropyl C*H*$_3$). ^{13}C NMR (100 MHz, $CDCl_3$) δ 190.1, 160.5, 135.7, 128.1, 125.6, 120.3, 113.9, 71.0, 21.9. EI$^+$-MS *m/z* 164 (9%, $[M]^+$), 122 (80%), 121 (100%, $[M\text{-isopropyl}]^+$), 104 (13%), 93 (10%), 76 (8%), 65 (16%), 51 (5%). EI$^+$-HRMS calcd. for $C_{10}H_{12}O_2$ ($[M]^+$) 164.0837; found 164.0834. Data in accordance with the literature.[46]

[$Ru_2(O_2CCF_3)_2(\mu\text{-}O_2CCF_3)_2(CHPh)_2(\mu\text{-}OH_2)(PCy_3)_2$] (169)

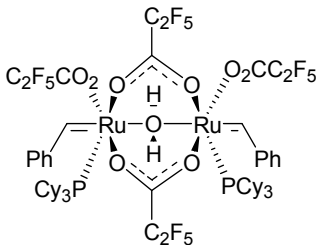

Prepared using a protocol reported by Buchowicz *et al.*.[44] [$RuCl_2(CHPh)(PCy_3)_2$] (**162**) (50.1 mg, 65.9 μmol, 1 equiv.) was dissolved in hexane and cooled to 0 °C. Silver trifluoroacetate (29.7 mg, 134 μmol, 2 equiv.) in tetrahydrofuran (2 ml) was added dropwise and the solution was stirred (0°C, 30 mins) to give a brown precipitate and green solution. The mixture was filtered and the filtrate reduced to dryness *in vacuo* to give the title compound as a green powder (40.8 mg, 28.9 μmol, 88%). ^{1}H NMR (400 MHz, CD_2Cl_2) δ 20.68 (d, *J* = 5.7 Hz, 2H, carbene Ru=C*H*), 11.75 (s, 2H, O*H*$_2$), 8.15 (d, *J* = 7.5 Hz, 4H, phenyl *ortho* C*H*), 7.76 (t, *J* = 7.5 Hz, 2H, phenyl *para* C*H*), 7.44 (t, *J* = 7.8, 4H, phenyl *meta* C*H*), 2.03-0.84 (m, 66H, PCy3). ^{13}C NMR (101 MHz, CD_2Cl_2) δ 327.1 (d, *J* = 16 Hz, carbene Ru=*C*H), 172.7 (q, *J* = 38 Hz, O_2CCF_3), 169.2 (q, *J* = 38 Hz, O_2CCF_3), 158.5 (phenyl *ipso C*), 134.7 (phenyl *C*H), 133.4 (phenyl *C*H), 133.3 (phenyl *C*H), 116.6 (q, *J* = 282 Hz, O_2CCF_3), 35.04 (PCy_3 *ipso C*), 30.85 (d, *J* = 9.8Hz, PCy3 *C*H_2), 29.31 (PCy_3 *C*H_2), 26.12 (PCy_3 *C*H_2). ^{31}P NMR (162 MHz, CD_2Cl_2) δ 43.97 (s, *P*Cy_3). ^{19}F NMR (270 MHz, CD_2Cl_2) δ 75.38 (s, O_2CCF_3), -76.14 (s, O_2CCF_3). Data in accordance with the

literature.[44]

[$RuCl_2(PPh_3)_3$] (197)

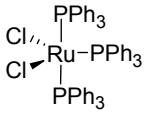

Prepared by a protocol reported by Stephenson and Wilkinson.[109] Ruthenium trichloride trihydrate (**196**) (0.201 g, 0.769 mmol, 1 equiv.) was dissolved in methanol (40 ml) under an atmosphere of N_2 and refluxed (5 mins) to give a purple solution. On cooling to ambient temperature, triphenylphosphine (1.20 g, 4.58 mmol, 6 equiv.) was added and the solution refluxed (3 hours). The resulting brown precipitate was separated by filtration, washed with tetrahydrofuran (3 x 5 ml) and dried *in vacuo* to yield the title compound as a brown powder (0.672 g, 0. 701 mmol, 91%). ^{1}H NMR (400 MHz, CD_2Cl_2) δ 7.65-6.80 (m, 15H, PPh_3). ^{31}P NMR (162 MHz, CD_2Cl_2) δ -4.75 (s, free PPh_3), 28.13 {s, $Ru_2Cl_2(PPh_3)_4$}, 41.73 {br s, $RuCl_2(PPh_3)_3$}. ^{13}C NMR (101 MHz, CD_2Cl_2) δ 135.5 (m), 134.0 (m), 133.9, 132.2 (m), 129.7, 129.0, 128.8 (m), 127.7 (m). ESI^+-MS *m/z* 1095.1 (35%, $[Ru_2Cl_3(PPh_3)_3]^+$), 835.2 (30%, $[Ru_2Cl_3(PPh_3)_2]^+$), 661.0 (54%, $[RuCl(PPh_3)_2]^+$), 625.1 (100%, $[Ru(PPh_3)_2]^+$), 547.2 (52%, $[Ru(PPh_3)(PPh_2)]^+$), 363.1 (42%, $[Ru(PPh_3)]^+$). Data in accordance with the literature.[110]

[$Ru(O_2CCH_3)_2PPh_3)_2$] (210)

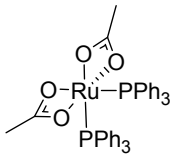

Prepared by a protocol reported by Mitchell *et al.*.[83] $[RuCl_2(PPh_3)_3]$ (**197**) (150 mg, 157 μmol, 1 equiv.) and sodium acetate (130 mg, 1.59 mmol, 10 equiv.) were finely ground together using a pestle and mortar and mixed in *t*-butanol (7.5 ml). The suspension was refluxed (1 hr) and the resulting orange precipitate was separated by filtration, washed with water (1 x 2 ml), methanol (1 x 2 ml) and diethyl ether (1 x 2 ml) and dried *in vacuo* to give the title compound as an orange powder (20.3 mg, 26.0 μmol, 17%). ^{1}H NMR (400 MHz, CD_2Cl_2) δ 7.45 (m, 12H, PPh_3 C*H*), 6.90 (m, 18H, PPh_3 C*H*), 1.38 (s, 6H, CH_3). ^{13}C NMR (101 MHz, CD_2Cl_2) δ 190.7, 137.5 (t, J = 45 Hz), 136.5 (t, J = 5 Hz), 131.6, 129.8 (t, J = 5 Hz), 25.4. ^{31}P NMR (162 MHz, CD_2Cl_2) δ 64.69 (s, *P*Ph_3). ESI^+-MS *m/z* 767.1 (19%, $[MNa]^+$), 726.1 (100%, $[Ru_2(PPh_3)_2]^+$), 685.1 (82%, $[M\text{-}OAc]^+$), 625.1 (4%). Data in

accordance with the literature.[83]

[$RuBr_2(PPh_3)_3$] (211)

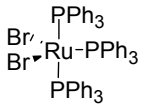

Prepared by a protocol reported by Stephenson and Wilkinson.[109] Ruthenium trichloride trihydrate (**196**) (150 mg, 0.574 mmol, 1 equiv.) and sodium bromide (354 mg, 3.44 mmol, 6.0 equiv.) were dissolved in dry methanol (2.5 ml) under an atmosphere of N_2 and stirred (60 ˚C, 10 hours) to give a red solution. On cooling to ambient temperature, dry methanol (10 ml) was added followed by triphenylphosphine (692 mg, 2.64 mmol, 4.6 equiv.). The solution was refluxed (3 hours) to give a pale yellow solution and brown precipitate. The precipitate was filtered under an atmosphere of N_2, washed with methanol and dried *in vacuo* to give the title compound as a brown powder (0.409 g, 0.391 mmol, 68%). ^{1}H NMR (400 MHz, CD_2Cl_2) δ 7.32-7.24 (m, 27H, Ar*H*), 7.06-7.00 (app. t, *J* = 7.5 Hz, 18H, Ar*H*). ^{13}C NMR (101 MHz, CD_2Cl_2) δ 135.6 (m), 129.8 (s), 127.7 (m). ^{31}P NMR (162 MHz, CD_2Cl_2) δ 42.5 (v. br s), 27.8 (s). ESI$^+$-MS *m/z* 987.2 (4%), 980.2 (1%), 919.2 (4%), 904.2 (1%), 857.2 (13%), 702.1 (1%), 689.1 (1%), 661.1 (5%), 625.1 (3%), 579.2 (100%), 557.2 (7%). Data in accordance with the literature.[109]

[$RuCl_2$(CHPh)($IMesH_2$)(Py)] (213)

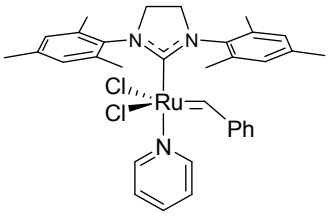

Prepared using a protocol reported by Sanford *et al.*.[37] [$RuCl_2$(CHPh)(PCy_3)($IMesH_2$)] (**160**) (101 mg, 119 μmol, 1 equiv.) was dissolved in toluene (0.5 ml) and pyridine (1.0 ml, 12.3 mmol, 103 equiv.) was added. The green solution was stirred (r.t., 10 mins) and added to pentane (3 ml, -10 °C) by cannula transfer. The resulting green precipitate was separated by filtration, washed with hexane (3 x 5 ml) and dried *in vacuo* to give the title compound as a green powder (52.6 mg, 84.0 μmol, 61%). ^{1}H NMR (400 MHz, C_6D_6) δ 19.70 (s, 1H, carbene Ru=C*H*), 8.88 (br s, 2H, Py C*H*), 8.43 (br s, 2H, Py C*H*), 8.11 (d, *J* = 7.7 Hz, 2H, phenyl C*H*), 7.18 (t, *J* = 7.3 Hz, 1H, phenyl C*H*), 6.93 (t, *J* = 7.7 Hz, 2H, phenyl C*H*), 6.87-6.36 (m, 7H, IMes C*H* and Py C*H*), 6.07 (br s, 2H, phenyl C*H*), 3.41 (br d, *J* = 16.9

Hz, 4H, IMes CH_2), 2.82 (br s, 6H, Mes CH_3), 2.49 (br s, 6H, Mes CH_3), 2.07 (br s, 6H, Mes CH_3). ^{13}C NMR (101 Mhz, C_6D_6) δ 317. 9 (benzyl carbene Ru=*C*H), 220.8 (IMes Ru=*C*N_2), 153.8, 150.9, 139.4, 138.3, 137.7, 135.2, 134.6, 131.1, 129.2, 129.1, 128.3, 124.9, 52.4, 51.7, 21.5, 21.1, 19.5. ESI$^+$-MS *m/z* 605.1 (7%), 585.1 (6%), 569.1 (10%, [M-2Py]$^+$), 509.1 (20%), 495.1 (44%), 453.1 (36%), 435.1 (54%), 423.1 (94%), 405.1 (100%). Data in accordance with the literature.[37]

[$RuCl_2$(CHSPh)(PCy_3)$_2$] (214)

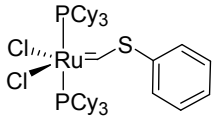

Prepared by a protocol reported by Louie and Grubbs.[84] [$RuCl_2$(CHPh)(PCy_3)$_2$] (**162**) (98.4 mg, 129 μmol, 1 equiv.) was dissolved in dichloromethane (6 ml) and cooled to -20 °C. Anhydrous phenylvinylsulfide (300 μl, 2.30 mmol, 18 equiv.) was added and the solution was stirred (r.t., 30 mins). The red/brown solution was reduced to dryness *in vacuo* and washed with cold methanol (3 x 2 ml) and acetone (3 x 2 ml) to give the title compound as a red/brown powder (55.1 mg, 69.6 μmol, 54%). ^{1}H NMR (400 MHz, CD_2Cl_2) δ 17.78 (s, 1H, carbene Ru=C*H*), 7.40 (m, 5H, phenyl C*H*), 2.61 (m, 6H, PCy_3 *ipso* C*H*), 1.94 (m, 10H, PCy_3 CH_2), 1.74 (m, 18H, PCy_3 CH_2), 1.57-1.25 (m, 32H, PCy_3 CH_2). ^{13}C NMR (101 MHz, CD_2Cl_2) δ 280.4 (t, *J* = 77 Hz, carbene Ru=*C*H), 141.6 (Aryl *C*), 129.8 (Aryl *C*), 129.6 (Aryl *C*), 128.8 (Aryl *C*), 32.7 (t, *J* = 9 Hz, PCy_3 *ipso C*), 30.0 (PCy_3 *meta C*), 28.1 (t, *J* = 5 Hz, PCy_3 *ortho C*), 26.9 (PCy_3 *para C*). ^{31}P NMR (162 MHz, CD_2Cl_2) δ 33.26 (s, *P*Cy_3). ESI$^+$-MS *m/z* 860.4 (46%), 819.4 (100%, [M-Cl]$^+$), 757.4 (90%), 593.5 (64%), 539.1 (17%, [M-PCy_3Cl]$^+$). Data in accordance with the literature.[84]

[$RuCl_2$(CHO(C_3H_6)CH_3)(PCy_3)$_2$] (215)

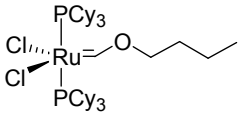

Prepared by a protocol similar to that reported by Schwab *et al.*.[31] [$RuCl_2$(CHPh)(PCy_3)$_2$] (**162**) (0.101 g, 133 μmol, 1 equiv.) was dissolved in dichloromethane (6 ml) and cooled to -20 °C. Anhydrous *n*-butylvinyl ether (200 μl, 2.58 mmol, 19 equiv.) was added and the solution was stirred (r.t., 30 mins). The bright red solution was reduced to dryness *in vacuo* and washed with cold methanol (3 x 2 ml) to give the title compound as an orange powder

(68.1 mg, 90.1 μmol, 68%). ^{1}H NMR (400 MHz, C_6D_6) δ 14.75 (t, *J* = 1.0 Hz, 1H, Ru=C*H*O), 3.82 (t, *J* = 6.4 Hz, 2H, OCH_2), 2.84 (m, 6H, Cy *ipso* C*H*), 2.10 (m, 10H, Cy CH_2, $OCH_2C_2H_4$), 1.76-1.64 (m, 32 H, Cy CH_2, $OCH_2C_2H_4$), 1.31-1.22 (m, 22H, Cy CH_2, $OCH_2C_2H_4$), 0.79 (t, *J* = 7.4 Hz, 3H, CH_3). ^{13}C NMR (101 MHz, CD_2Cl_2) δ 277.6 (t, *J* = 10 Hz, carbene Ru=*C*H), 81.3 (Ru=CHOCH_2), 32.1 (t, *J* = 9 Hz, PCy_3 *ipso C*), 30.3 (OCH_2CH_2), 29.9 (PCy_3 *meta C*), 28.3 (t, *J* = 5 Hz, PCy_3 *ortho C*), 27.0 (PCy_3 *para C*), 19.3 (CH_2CH_3), 13.8 (CH_2CH_3). ^{31}P NMR (162 MHz, C_6D_6) δ 35.24 (s, *P*Cy_3). ESI$^+$-MS *m/z* 856.5 (43%), 824.4 (100%), 783.4 (21%, [M-Cl]$^+$), 757.4 (25%), 725.3 (84%), 691.4 (9%).

[$RuCl_2(CH(CH_2)_2CH_3)(PCy_3)_2$] (216)

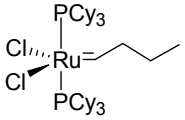

Prepared by a protocol similar to that reported by Schwab *et al.*.[31] [$RuCl_2(CHPh)(PCy_3)_2$] (**162**) (51.2 mg, 61.4 μmol, 1 equiv.) was dissolved in dichloromethane (2 ml) under an atmosphere of N_2 and cooled to -20 °C. Anhydrous 1-pentene (64.1 mg, 916 μmol, 15 equiv.) was added and the solution was warmed to ambient temperature over 20 minutes. The resulting purple/brown solution was reduced to dryness *in vacuo* and washed with cold (0 °C) methanol (3 x 2 ml) to give the title compound as a purple powder (34.1 mg, 43.2 μmol, 70%). ^{1}H NMR (400 MHz, CD_2Cl_2) δ 19.23 (t, *J* = 5.2 Hz, 1H, carbene Ru=C*H*), 2.71 (m, 2H, CHCH_2), 2.65-2.40 (m, 6H, Cy *ipso* C*H*), 1.83-1.09 (m, 66H, Cy CH_2, CH_2CH_3), 1.00 (t, *J* = 7.4 Hz, 3H, CH_3). ^{13}C NMR (100 MHz, CD_2Cl_2) δ 320.6 (m, carbene Ru=*C*H), 62.3 (Ru=CHCH_2), 32.3 (t, *J* = 9 Hz, PCy_3 *ipso C*), 30.0 (PCy_3 *meta C*), 28.4 (t, *J* = 5 Hz, PCy_3 *ortho C*), 27.1 (PCy_3 *para C*), 21.8 (CH_2CH_3), 14.3 (CH_2CH_3). ^{31}P NMR (162 MHz, CD_2Cl_2) δ 36.20 (s, *P*Cy_3). ESI$^+$-MS *m/z* 1082.5 (5%), 911.7 (18%), 802.3 (24%), 667.4 (100%), 615.4 (19%).

[Ru(*N*-tfs)$_2$(CH-*o*-O^{i}Pr-C$_6$H$_4$)(IMesH$_2$)] (217)

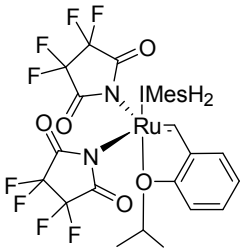

Silver(I) oxide (38.6 mg, 166 μmol, 2.0 equiv.) and tetrafluorosuccinimide (55.4 mg, 324 μmol, 4.0 equiv.) were mixed in tetrahydrofuran (5ml) under an inert atmosphere in the absence of light. The mixture was stirred (r.t., 1 hour) and [RuCl$_2$(CH-*o*-O^{i}Pr-Ph)(IMesH$_2$)] (**163**) (51.0 mg, 81.3 mmol, 1 equiv.) was added and the mixture stirred (6 hours, r.t.). The resultant purple solution was reduced *in vacuo*, redissolved in dry dichloromethane and filtered *via* cannula onto a small column of dried silica-gel under an inert atmosphere. The purple product band was eluted with dichloromethane, reduced to dryness *in vacuo* and washed with dry hexane to give the title compound as a purple powder (30.1 mg, 33.6 μmol, 41%). ^{1}H NMR (400 MHz, $CDCl_3$) δ 18.24 (s, 1H, carbene C*H*), 7.44-7.37 (m, 2H, Ar*H*), 7.01 (app. t, *J* = 7.5 Hz, 1H, Ar*H*), 6.92 (s, 4H, mesityl Ar*H*), 6.76 (d, *J* = 8.3 Hz, 1H, Ar*H*), 4.60 (septet, *J* = 6.3 Hz, 1H, ispropyl C*H*), 3.97 (s, 4H, IMesH$_2$ CH_2), 2.50 (s, 12H, mesityl ortho CH_3), 2.27 (s, 6H, Mes *para* CH_3), 1.13 (d, *J* = 6.3 Hz, 6H, isopropyl CH_3). ^{13}C NMR (101 Mhz, $CDCl_3$) δ 324.0, 202.6, 171.4 (m),[111] 154.1, 141.7, 138.8, 136.3, 136.1, 132.7, 129.8, 124.9, 122.7, 113.8, 77.4, 105.1 (tt, *J* = 267 and 22 Hz), 52.4, 21.2, 20.9, 18.7. ^{19}F NMR (376 Mhz, $CDCl_3$) δ -126.0 (app. dd, *J* = 280 and 59 Hz). IR (solid, cm^{-1}) υ_{max} 2925 (w), 2498 (w), 2160 (m), 2030 (m), 1977 (m), 1682 (s), 1592 (w), 1481 (m), 1455 (w), 1408 (w), 1288 (m), 1262 (m), 1139 (s), 1061 (s), 1014 (s), 925 (m), 852 (w), 749 (m), 623 (m). ESI$^+$-MS *m/z* 919.2 (1%, [MNa]$^+$), 767.2 (100%, [M-tfs+MeCN]$^+$), 726.2 (48%, [M-tfs]$^+$), 701.2 (6%), 676.1 (2%), 619.1 (1%). ESI$^+$-HRMS calcd. for $C_{39}H_{38}F_8N_4NaO_5Ru$ ([MNa]$^+$) 919.1650; found 919.1633. Melting point 95˚C decomposes.

3.5.4. Crystallographic data

Table 48. Crystallographic data for 217.229.

	217.219 **[Ru(*N*-tfs)$_2$(*o*-^{i}PrO-CHPh)(IMesH$_2$)].[Ru(*N*-tfs)$_3$(IMesH$_2$)(OH$_2$)$_2$]**
formula	$C_{72}H_{68}F_{20}N_9O_{13}Ru_2$
M_r	1849.49
cryst syst	Monoclinic
space group	*P2(1)/c*
crystal size/mm^3	0.27 x 0.09 x 0.05
cell constants	
a(Å)	16.0998(7)
b(Å)	17.0984(8)
c(Å)	27.1413(12)
α(deg)	90.00
β(deg)	94.9960(10)
γ(deg)	90.00
V(Å^3)	7443.1(6)
Z	4
λ(Å)	0.71073
ρ(calcd)(g/cm^3)	1.650
μ(mm^{-1})	0.526
F(000)	3740
T(K)	110(2)
$2\theta_{max}$ (deg)	56.60
no. of rflns measd	76376
no. of indep rflns	18517
R_{int}	0.0291
no. of data/restraints/params	18517 / 0 / 1075
Goodness-of-fit on F^2	1.012
R indices (all data)	R_1 = 0.0404, ωR_2 = 0.0709
Final R indices [I>2sigma(I)]	R_1 = 0.0283, ωR2 = 0.0653
max, min Δ*ρ* (e Å^{-3})	+0.533, -0.585

3.6. References

(1) Islam, M. S.; Uddin, M. M. *Synth. React. Inorg. Met.-Org. Chem.* **1992**, *22*, 1303-1315.

(2) Sahajpal, A.; Robinson, S. D.; Hursthouse, M. B.; Mazid, M. A. *J. Chem. Soc., Dalton. Trans.* **1993**, 393-396.

(3) Shaver, A.; El-Khateeb, M.; Lebnis, A.-M. *J. Organomet. Chem.* **2001**, *622*, 1-5.

(4) Metcalfe, C.; Spey, S.; Adams, H.; Thomas, J. A. *J. Chem. Soc., Dalton Trans.* **2002**, 4732-4739.

(5) Handbook of Metathesis, ed. R. H. Grubbs, Wiley-VCH, Weinheim, Germany, **2003**.

(6) Freitas, E. R.; Gum, C.R. *Chem. Eng. Prog.* **1979**, *75*, 667-674.

(7) Nicolaou, K. C.; Bulger, P. C.; Sarlah, D. *Angew. Chem., Int. Ed.* **2005**, *44*, 4490-4527.

(8) Barluenga, S.; Lopez, P.; Moulin, E.; Wissinger, N. *Angew. Chem., Int. Ed.* **2004**, *43*, 3467-3470.

(9) Mol, J. C. *J. Mol. Catal. A: Chemical* **2004**, *213*, 39-45.

(10) Deshmukh, P. H.; Blechert, S. *Dalton Trans.* **2007**, *24*, 2479-2491.

(11) Banks, R. L.; Bailey, G. C. *(I. & E. C.) Prod. Res. Dev.* **1964**, *3*, 170-173.

(12) Natta, G.; Dall'Asta, G.; Mazzanti, G. *Angew. Chem., Int. Ed.* **1964**, *3*, 723-729.

(13) Calderon, N.; Chen, H. Y.; Scott, K. W. *Tetrahedron Lett.* **1967**, *8*, 3327-3329.

(14) Kittleman, E. T.; Zuech, E. A. French Patent 1 561 025, **1967**.

(15) Hérisson, J. L.; Chauvin, Y. *Makromol. Chem.* **1971**, *141*, 161-176.

(16) Fischer, E. O.; Maasbol, A. *Angew. Chem., Int. Ed.* **1964**, *3*, 580-581.

(17) Schrock, R. R. *J. Am. Chem. Soc.* **1974**, *96*, 6796-6797.

(18) Schrock, R. R. *J. Am. Chem. Soc.* **1975**, *97*, 6577-6578.

(19) Wood, C. D.; McLain, S. J.; Schrock, R. R. *J. Am. Chem. Soc.* **1979**, *101*, 3210-3222.

(20) (a) Schrock, R. R.; Rocklage, S. M.; Wengrovius, J. H.; Rupprecht, G. A.; Fellmann, J. D. *J. Mol. Catal.* **1980**, *8*, 73-83; (b) Rocklage, S. M.; Fellmann, J. D.; Rupprecht, G. A.; Messerle, L. W.; Schrock R. R. *J. Am. Chem. Soc.* **1981**, *103*, 1440-1447.

(21) Wengrovius, J. H.; Schrock, R. R.; Churchill, M .R.; Missert, J. R.; Youngs, W. J. *J. Am .Chem. Soc.* **1980**, *102*, 4515-4516.

(22) Kress, J.; Wesolek, M.; Osborn, J. A. *J. Chem. Soc., Chem. Commun.* **1982**, 514-516.

(23) Schaverien, C. J.; Dewan, J. C.; Schrock, R. R. *J. Am. Chem. Soc.* **1986**, *108,* 2771-2773.

(24) Murdzek, J. S.; Schrock, R. R. *Organometallics* **1987**, *6*, 1373-1374.

(25) Schrock, R. R.; Murdzek, J. S.; Bazan, G. C.; Robbins, J.; DiMare, M.; O'Regan, M. *J. Am. Chem. Soc.* **1990**, *112*, 3875-3886.

(26) (a) Novak, B. M.; Grubbs, R. H. *J. Am. Chem. Soc.* **1988**, *110*, 7542-7543; (b) Lu, S. Y.; Quayle, P.; Heatley, F.; Booth, C.; Yeates, S. G.; Padget. J. C. *Macromolecules* **1992**, *25*, 2692-2697; (c) Zenkl, E.; Stelzer, F. *J. Mol. Catal.* **1992**, *76*, 1-14.

(27) Novak, B. M.; Grubbs, R. H. *J. Am. Chem. Soc.* **1988**, *110,* 960-961.

(28) Nguyen, S. T.; Johnson, L. K.; Grubbs, R. H.; Ziller, J. W. *J. Am. Chem. Soc.* **1992**, *114*, 3974-3975.

(29) Fu, G. C.; Nguyen, S. T.; Grubbs, R. H. *J. Am. Chem. Soc.* **1993**, *115*, 9856-9857.

(30) Nguyen, S. T.; Grubbs, R. H.; Ziller, J. W. *J. Am. Chem. Soc.* **1993**, *115*, 9858-9859.

(31) Schwab, P.; Grubbs, R. H.; Ziller, J. W. *J .Am. Chem. Soc.* **1996**, *118*, 100-110.

(32) Weskamp, T.; Schattenham, W. C.; Spiegler, M.; Hermann, W. A. *Angew. Chem., Int. Ed*. **1998**, *37*, 2490-2493.

(33) (a) Huang, J.; Stevens, E. D.; Nolan, S. P.; Petersen, J. L. *J. Am. Chem. Soc.* **1999**, *121*, 2674-2678; (b) Huang, J.; Schanz, H.-J.; Stevens, E. D.; Nolan, S. P. *Organometallics* **1999**, *18*, 5375-5380; (c) Furstner, A.; Thiel, O. R.; Kindler, N.; Bartkowska, B. *J. Org. Chem*. **2000**, *65*, 7990-7995; (d) Scholl, M.; Trnka, T. M.; Morgan, J. P.; Grubbs, R. H. *Tetrahedron Lett.* **1999**, *40*, 2247-2250.

(34) (a) Chatterjee, A. K.; Grubbs, R. H. *Org. Lett.* **1999**, *1*, 1751-1753; (b) Scholl, M.; Ding, S.; Lee, C. W.; Grubbs, R. H. *Org. Lett*. **1999**, *1*, 953-956.

(35) (a) Harrity, J. P. A.; Visser, M. S.; Gleason, J. D.; Hoveyda, A. H. *J. Am. Chem. Soc.* **1997**, *119,* 1488-1489; (b) Harrity, J. P. A.; La, D. S.; Cefalo, D. R.; Visser, M. S.; Hoveyda, A. H. *J. Am. Chem. Soc.* **1998**, *120,* 2343-2351; (c) Kingsbury, J. S.; Harrity, J. P. A.; Bonitatebus, P. J.; Hoveyda A. H. *J. Am. Chem. Soc.* **1999**, *121,* 791-799.

(36) Garber, S. B.; Kingsbury, J. S.; Gray, B. L.; Hoveyda, A. H. *J. Am. Chem. Soc.* **2000**, *122*, 8168-8179.

(37) Sandford, M. S.; Love, J. A.; Grubbs, R. H. *Organometallics* **2001**, *20*, 5314-5318.

(38) Love, J. A.; Morgan, J. P.; Trnka, T. M.; Grubbs, R. H. *Angew. Chem., Int. Ed*. **2002**, *41*, 4035-4037.

(39) (a) Romero, P. E.; Piers, W. E.; McDonald, R. *Angew. Chem., Int. Ed.* **2004**, *43*, 6161-6165; (b) Dubberley, S. R.; Romero, P. E.; Piers, W. E.; McDonald, R.; Parvez, M. *Inorg. Chim. Acta* **2006**, *359*, 2658-2664.

(40) Berlin, J. M.; Goldberg, S. D.; Grubbs, R. H. *Angew. Chem., Int. Ed.* **2006**, *45*, 7591-7595.

(41) (a) Jordan, J. P.; Grubbs, R. H. *Angew. Chem., Int. Ed.* **2007**, *46*, 5152-5155; (b) Rix, D.; Caïjo, F.; Laurent, I.; Gulajski, L.; Grela, K.; Mauduit, M. *Chem. Commun.* **2007**, 3771-3773.

(42) (a) Hoveyda, A. H.; Schrock, R. R. *Chem. Eur. J.* **2001**, *7*, 945-950; (b) Schrock, R. R.; Hoveyda, A. H. *Angew. Chem., Int. Ed.* **2003**, *42*, 4592-4633; (c) Schrock, R. R. *J. Mol. Catal. A* **2004**, *213*, 21-30.

(43) Dias, E. L.; Nguyen, S. T.; Grubbs, R. H. *J. Am. Chem. Soc.* **1997**, *119*, 3887-3897.

(44) Buchowicz, W.; Mol, J. C.; Lutz, M.; Spek, A. L. *J. Organomet. Chem*. **1999**, *588*, 205-210.

(45) Buchowicz, W.; Makal, A.; Wozniak, K. *J. Organomet. Chem.* **2009**, *694*, 3179-3183.

(46) Krause, J. O.; Nuyken, O.; Wurst, K.; Buchmeiser, M. R. *Chem. Eur. J*. **2004**, *10*, 777-784.

(47) (a) Kumar, P. S.; Wurst, K.; Buchmeiser, M. R. *J. Am. Chem. Soc.* **2009**, *131*, 387-395; (b) Dinger, M. B.; Nieczypor, P.; Mol, J. C. *Organometallics* **2003**, *22*, 5291-5296.

(48) Tanaka, K.; Böhm, V. P. W.; Chadwick, D.; Roeper, M.; Braddock, D. C. *Organometallics* **2006,** *25,* 5696-5698.

(49) Nieczypor, P.; Buchowicz, W.; Meester, W. J. N.; Rutjes, F.; Mol, J. C. *Tetrahedron Lett.* **2001**, *42*, 7103-7105.

(50) Yang, L. R.; Mayr, M.; Wurst, K.; Buchmeiser, M. R. *Chem. Eur. J.* **2004**, *10*, 5761-5770.

(51) Halbach, T. S.; Mix, S.; Fischer, D.; Maechling, S.; Krause, J. O.; Sievers, C.; Blechert, S.; Nuyken, O.; Buchmeiser, M. R. *J. Org. Chem.* **2005**, *70*, 4687-4694.

(52) (a) Vehlow, K.; Maechling, S.; Kohler, K.; Blechert, S. *Tetrahedron Lett.* **2006**, *47*, 8617-8620; (b) Vehlow, K.; Maechling, S.; Kohler, K.; Blechert, S. *J. Organomet. Chem.* **2006**, *691*, 5267-5277.

(53) Monfette, S.; Camm, K. D.; Gorelsky, S. I.; Fogg, D. E. *Organometallics* **2009**, *28*, 944-946.

(54) Monfette, S.; Fogg, D. E. *Organometallics* **2006**, *25*, 1940-1944.

(55) (a) Samec, J. S. M.; Grubbs, R. H. *Chem. Commun.* **2007**, 2826-2828; (b) Samec, J. S. M.; Grubbs, R. H. *Chem. Eur. J.* **2008**, *14*, 2686-2692.

(56) Kopf, H.; Holzberger, B.; Pietraszuk, C.; Hübner, E.; Burzlaff, N. *Organometallics* **2008**, *27*, 5894-5905.

(57) (a) Allaert, B.; Dieltiens, N.; Ledoux, N.; Vercaemst, C.; Van Der Voort, P.; Stevens, C. V.; Linden, A.; Verpoort, F. *J. Mol. Catal. A: Chem.* **2006**, *260*, 221-226; (b) Ledoux, N.; Allaert, B.; Schaubroeck, D.; Monsaert, S.; Drozdzak, R.; Van Der Voort, P.; Verpoort, F. *J. Organomet. Chem.* **2006**, *691*, 5482-5486.

(58) Denk, K.; Fridgen, J.; Herrmann, W. A. *Adv. Synth. Catal.* **2002**, *344*, 666-670.

(59) Occhipinti, G.; Bjørsvik, H. R.; Törnroos, K. W.; Jensen, V. R. *Organometallics* **2007**, *26*, 5803-5814.

(60) Jordaan, M.; Vosloo, H. C. M. *Adv. Synth . Catal.* **2007**, *349*, 184-192.

(61) Binder, J. B.; Guzei, I. A.; Raines, R. T. *Adv. Synth. Catal.* **2007**, *349*, 395-404.

(62) Drouin, S. D.; Foucault, H. M.; Yap, G. P. A.; Fogg, D. E. *Can. J. Chem.* **2005**, *83*, 748-754.

(63) Gawin, R.; Makal, A.; Wozniak, K.; Mauduit, M.; Grela, K. *Angew. Chem., Int. Ed.* **2007**, *46*, 7206-7209.

(64) (a) Van Veldhuizn, J. J.; Garber, S. B.; Kingsbury, J. S.; Hoveyda, A. H. *J. Am. Chem. Soc.* **2002**, *124*, 4954-4955; (b) Giudici. R. E.; Hoveyda, A. H. *J. Am. Chem. Soc.* **2007**, *129*, 3824-3825.

(65) Conrad, J. C.; Parnas, H. H.; Snelgrove, J. L.; Fogg D. E. *J. Am. Chem. Soc*. **2005**, *127*, 11882-11883.

(66) (a) Conrad, K. C.; Snelgrove, J. L.; Eeelman, M. D.; Hall, S.; Fogg, D. E. *J. Mol. Catal. A* **2006**, *254*, 105-110; (b) Conrad, J. C.; Amoroso, D.; Czechura, P.; Yap, G. P. A.; Fogg, D. E. *Organometallics* **2003**, *22*, 3634-3636.

(67) Sandford, M. S.; Henling, L. M.; Day, M. W.; Grubbs, R. H. *Angew. Chem., Int. Ed.* **2000**, *39*, 3451-3454.

(68) Conrad, J. C.; Fogg, D. E. *Curr. Org. Chem.* **2006**, *10*, 185-202.

(69) Straub, B. F. *Angew. Chem., Int. Ed.* **2005**, *44*, 5974-5978.

(70) (a) Sanford, M. S.; Ulman, M.; Grubbs, R. H. *J. Am. Chem. Soc.* **2001**, *123*, 749-750; (b) Sanford, S.; Love, J.; Grubbs, R. H. *J. Am. Chem. Soc.* **2001**, *123*, 6543-6554.

(71) Getty, K.; Delgado-Jaime, M. U.; Kennepohl, P. *J. Am. Chem. Soc.* **2007**, *129*, 15774-15776.

(72) Straub, B. F. *Adv. Synth. Catal.* **2007**, 349, 204-214.

(73) van Rensburg, W. J.; Steynberg, P. J.; Kirk, M. M.; Meyer, W. H.; Forman, G. S. *J. Organomet. Chem.* **2006**, *691*, 5312-5325.

(74) Ulman, M.; Grubbs, R. H. *J. Org. Chem.* **1999**, *64*, 7202-7207.

(75) Amoroso, D.; Yap, G. P. A.; Fogg, D. E. *Can. J. Chem.* **2001**, *79*, 958-963.

(76) (a) Hong, S. H.; Day, M. W.; Grubbs, R. H. *J. Am. Chem. Soc.* **2004**, *126*, 7414-7415; (b) Hong, S. H.; Wenzel, A. G.; Salguero, T. T.; Day, M. W.; Grubbs, R. H. *J. Am. Chem. Soc.* **2007**, *129*, 7961-7968.

(77) (a) Janse van Rensburg, W.; Steynberg, P. J.; Meyer, W. H.; Kirk, M. M.; Forman, G. S. *J. Am. Chem. Soc.* **2004**, *126*, 14332-14333; (b) Romero, P. E.; Piers, W. E. *J. Am. Chem. Soc.* **2005**, *127*, 5032-5033.

(78) (a) Banti, D.; Mol, J. C. *J. Organomet. Chem.* **2004**, *689*, 3113-3116; (b) Dinger, M. B.; Mol, J. C. *Eur. J. Inorg. Chem.* **2003**, 2827-2833; (c) Dinger, M. B.; Mol, J. C. *Organometallics* **2003**, *22*, 1089-1095.

(79) (a) Trnka, T. M.; Morgan, J. P.; Sanford, M. S.; Wilhelm, T. E.; Scholl, M.; Choi, T. L.; Ding, S.; Day, M. W.; Grubbs, R. H. *J. Am. Chem. Soc.* **2003**, *125*, 2546-2558; (b) Mathew, J.; Koga, N.; Suresh, C. H. *Organometallics* **2008**, *27*, 4666-4670; (c) DeYonker, N. J.; Foley, N. A.; Cundari, T. R.; Gunnoe, T. B.; Petersen, J. L. *Organometallics* **2007**, *26*, 6604-6611.

(80) Hong, S. H.; Chlenov, A.; Day, M. W.; Grubbs, R. H. *Angew. Chem., Int. Ed.* **2007**, *46*, 5148-5151.

(81) Van der Schaaf, P. A.; Kolly, R.; Hafner, A. *Chem. Commun*. **2000**, 1045-1046.

(82) (a) Wilhelm, T. E.; Belderrain, T. R.; Brown, S. N.; Grubbs, R. H. *Organometallics* **1997**, *16* , 3867-3869; (b) Grunwald, C.; Gevert, O.; Wolf, J.; Gonzalez-Herrero, P.; Werner, H. *Organometallics* **1996**, *15*, 1960-1962.

(83) Mitchell, R. W.; Spencer, A.; Wilkinson, G. *J. Chem. Soc., Dalton Trans.* **1973**, 846-854.

(84) Louie, J.; Grubbs, R. H. *Organometallics* **2002**, *21,* 2153-2164

(85) Buchowicz, W.; Ingold, F.; Mol, J. C.; Lutz, M.; Spek, A. L. *Chem. Eur. J.* **2001**, *7*, 2842-2847.

(86) Schwarzenbach, G.; Lutz, K. *Helv. Chim. Acta.* **1940**, *23*, 1162-1190.

(87) Darnall, K. R.; Townsend, L. B.; Robins, R. K. *Proc. Nat. Ac. Sc. USA* **1967**, *57*, 548-553.

(88) Bell, R. P.; Higginson, W. C. E. *Proc. Roy. Soc. A* **1949**, *197*, 141-159.

(89) Hine, J.; Hahn, S.; Hwang, J. *J. Org. Chem.* **1988**, *53*, 884-887.

(90) This complex possesses *E* and *Z* isomers of the benzylidene bond.

(91) Brownstein, S.; Stillman, A. E. *J. Phys. Chem.* **1959**, *63*, 2061-2062.

(92) Saphier, M.; Burg, A.; Sheps, S.; Cohen, H.; Meyerstein, D. *J. Chem. Soc*., *Dalton Trans*. **1999**, 1845-1849.

(93) Chrystiuk, E.; Jusoh, A.; Santafianos, D.; Williams, A. *J. Chem. Soc., Perkin Trans. 2* **1986**, 163-168.

(94) Huynh, H. V.; Han, Y.; Jothibasu, R.; Yang, J. A. *Organometallics* **2009**, *28*, 5395-5404.

(95) Fu, Y.; Liu, L.; Li, R.-Q.; Liu, R.; Guo, Q.-X. *J. Am. Chem. Soc.* **2004**, *126*, 814-822.

(96) (a) Barone, V.; Cossi, M.; Tomasi, J. *J. Chem. Phys.* **1997**, *107*, 3210-3221; (b) Cammi, R.; Mennucci, B.; Tomasi, J. *J. Phys. Chem. A* **1998**, *102*, 870-875; (c) Cammi, R.; Mennucci, B.; Tomasi, J. *J. Phys. Chem. A* **2000**, *104*, 4690-4698.

(97) Koppel, I.; Koppel, J.; Gal, J.-F.; Maria, P.-C.; Notario, R.; Vlasov, V. M.; Taft, R. W. *Int. J. Mass Spectrom. Ion Processes* **1998**, *175*, 61-69.

(98) Bordwell, F. G. *Acc. Chem. Res.* **1988**, *21*, 456-463.

(99) Zhang, Y.-H.; Dong, M.-H.; Jiang, X.-K.; Chow, Y. L. *Can. J. Chem*. **1990**, *68*, 1668-1675.

(100) (a) Roundhill, D. M. *Inorg. Chem.* **1970**, *9*, 254-258; (b) Carturan, G.; Belluco. V.; Grazini, M.; Ros, R. *J. Organomet. Chem.* **1976**, *112*, 243-248; (c) Adams, H.; Bailey, N. A.; Briggs, T. N.; McCleverty, J. A.; Colquhoun, H. M.; Williams, D. J. *J. Chem. Soc., Dalton Trans.* **1986**, 813-819.

(101) Ritter, T.; Hejl, A.; Wenzel, A. G.; Funk, T. W.; Grubbs, R. H. *Organometallics* **2006**, *25*, 5740-5745.

(102) Larger signals at δ: 26.37 (s), 20.13 (app. td, J = 7.5 and 1.3 Hz), 19.05 (s), 17.65 (app. t, J = 1.2 Hz) and 17.62 ppm (app. td, J = 4.5 and 1.4 Hz).

(103) Adlhart, C.; Hinderling, C.; Baumann, H.; Chen, P. *J. Am. Chem. Soc.* **2000**, *122*, 8204-8214.

(104) Schwartz, A. L.; Lerner, L. M. *J. Org. Chem.* **1974**, *39*, 21-23.

(105) Tao, X.; Li, Y.-Q.; Xu, H.-H.; Wang, N.; Du, F.-L.; Shen, Y.-Z. *Polyhedron* **2009**, *28*, 1191-1195.

(106) Yanagihara, N.; Gotoh, T.; Ogura, T. *Polyhedron* **1996**, *15*, 4349-4354.

(107) Closs, G. L.; Moss, R. A. *J. Am. Chem. Soc.* **1964**, *86*, 4042-4053.

(108) Issleib, K.; Brack, A. *Z. Anorg. Allg. Chem.* **1954**, *277*, 258-270.

(109) Stephenson, T. A.; Wilkinson. G. *J. Inorg. Nucl. Chem.* **1966**, *28*, 945-956.

(110) Shaw, A. P.; Ryland, B. L.; Norton, J. R.; Buccella, D.; Moscatelli, A. *Inorg. Chem.* **2007**, *46*, 5805-5812.

(111) Unresolved due to complicated higher order spin-spin coupling (^{13}C-^{19}F).

Chapter 4: Pd(II) imidate complexes; synthesis and catalytic activity

4.1. Introduction

4.1.1. Pd imidate complexes

Relative to Au and Ru complexes, imidate anions including succinimidate, maleimidate, tetrafluorosuccinimidate, dibromomaleimidate, phthalimidate, o-benzoic sulfimidate, glutarimidate and 1,2,4,5-benzenetetracarboxylic acid diimidate have been widely utilised as ligands in Pd(II) complexes. In 1970 Roundhill[1] reported *trans*-[Pd(*N*-succ)$_2$(PPh$_3$)$_2$] and [Pd(η^2-Hmal)(PPh$_3$)$_2$] in which the maleimide ligand is coordinated to Pd(0) *via* the olefin. Louey *et al.*[2] prepared an interesting chloroform soluble binuclear Pd(II) complex (**234**) containing a bridging pentadentate *N*,*N*,*O*,*O*,*S*-coordinated ligand and also a bidentate *N*,*O*-coordinated bridging maleimidate ligand (Figure 49).

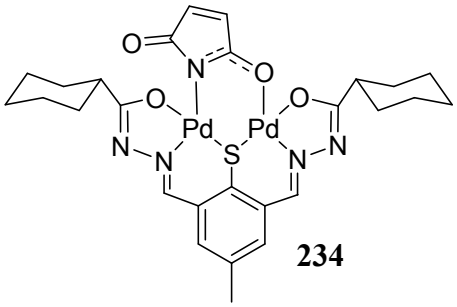

234

Figure 49. Binuclear Pd(II) complex (**234**) containing a bridging *N*,*O*-coordinated maleimidate ligand reported by Louey.

In the early 1980's [PdH(*N*-succ)(PCy$_3$)$_2$] was reported by Yamamoto *et al.*,[3] [Pd(*N*-ptm)$_2$(L)][4] (where L is *N*-(m-tolyl)-*N*'-benzoylthiocarbamide) and *trans*-[Pd(*N*-ptm)$_2$(pyridine)$_2$][5] by Sharma *et al.* and Komorita and Yamada[6] prepared a series of M$_2$[Pd(*N*-imidate)$_4$].nH$_2$O and *trans*-[Pd(*N*-imidate)$_2$(am)$_2$].nH$_2$O complexes (where M is Li^+, Na^+, K^+, Rb^+ or Cs^+; imidate is succ, mal, ptm or the anion of hydantoin; am is ammonia, methylamine or pyridine). Kurosawa *et al.*[7] found that when complexes of the type [Pd(Ar)(allylR)(dppe)] and [Pd(Ar)(η^3-allyl)(PPh$_3$)] {Ar is C_6F_5 or 2,3,5,6-C_6HCl_4; R is H or Me; dppe is 1,2-bis(diphenylphosphino)ethane} were treated with *N*-bromosuccinimide (NBS) [PdAr(*N*-succ)(dppe)] and [Pd(η^3-allyl)(*N*-succ)(PPh$_3$)] complexes were formed, respectively.

Adams *et al.*[8] have prepared *trans*-[Pd(Ph)(*N*-imidate)(PPh_3)$_2$] (where imidate is succ, ptm or tfs) and *cis*-[Pd(Ph)(*N*-imidate)(dppe)].n$CHCl_3$ (**235**) (where imidate is succ or ptm) complexes from the relevant imides and *trans*-[PdCl(Ph)(PPh_3)$_2$] and *cis*-[PdCl(Ph)(dppe)] (**236**), respectively (Scheme 62). Tetrafluorosuccinimide reacted anomalously with *cis*-[PdCl(Ph)(dppe)] (**236**), forming *cis*-[PdCl(*N*-tfs)(dppe)] (**237**), possibly by oxidative addition of the imide and reductive elimination of benzene *via* a Pd(IV) intermediate. Complexes containing *N*,*O*-bridging imidate ligands, [{Pd(*o*-C_6H_4CH=NPh)(μ-*N*,*O*-imidate)}$_2$].CH_2Cl_2 (where imidate is succ or tfs) and [{Pd(*o*-$C_6H_4CH_2NMe_2$)(μ-*N*,*O*-succ)}$_2$], were also prepared by reaction of imides with [{Pd(*o*-C_6H_4CH=NPh)(OAc)}$_2$] and [{PdCl(*o*-$C_6H_4CH_2NMe_2$)}$_2$], respectively.

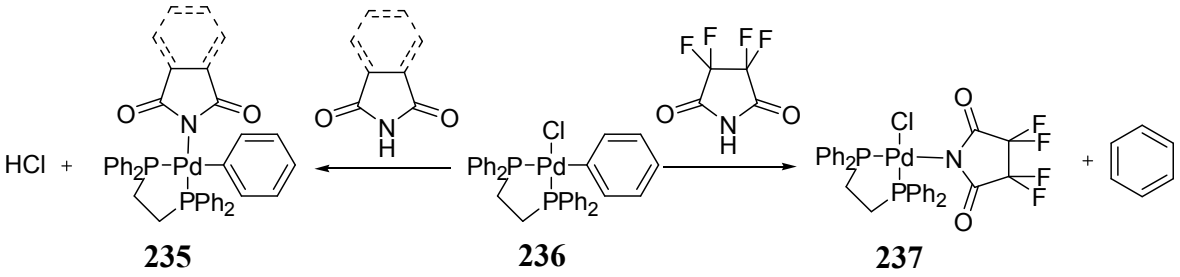

Scheme 62. Divergent reactivity of imides with *cis*-[PdCl(Ph)(dppe)] (**236**).

Colquhoun *et al.*[9] reported an octapalladium box-like structure (**238**) formed from bridging pyromellitimidato (1,2,4,5-benzenetetracarboxylic acid diimidate) ligands prepared by reaction of [Pd_2(μ-Cl)$_2$(1,2-$C_6H_4NMe_2$)$_2$] with pyromellitimide and triethylamine (Figure 50). More recently they have treated the chloro-bridged dimeric complex [Pd{η^5-$C_5H_3CH_2N(CH_3)_2Fe$(η^5-C_5H_5)}(μ-Cl)]$_2$ with succinimide to yield a racemic mixture of the chiral succinimidate bridged analogue [Pd{η^5-$C_5H_3CH_2N(CH_3)_2Fe$(η^5-C_5H_5)}(μ-*N*,*O*-succ)]$_2$. Treatment of the chloride complex with parabanic acid resulted in a homochiral (*R*,*R*,*R*,*R*,*R*,*R* or *S*,*S*,*S*,*S*,*S*,*S*) hexanuclear complex (**239**) in which each parabanato ligand is linked to four Pd atoms by the two N and two O atoms.

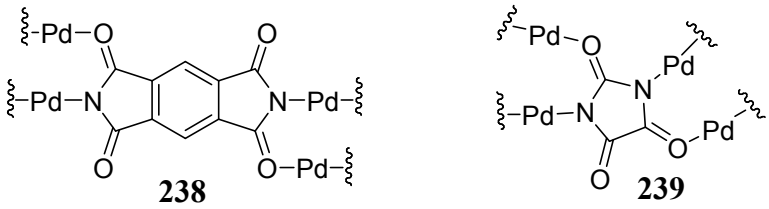

238 **239**

Figure 50. Tetradentate *N*,*N*,*O*,*O*-coordination of pyromellitimidato and parabanate(2-) ligands in Pd(II) complexes (**238** and **239)** reported by Colquhoun *et al.*.

Other Pd imidate complexes reported include *cis*-[Pd(*N*-succ)$_2$(phen)] and *cis*-[Pd(*N*-succ)$_2$(bipy)] (phen is 1,10-phenanthroline; bipy is 2,2'-bipyridine) prepared by Islam *et al.*,[10] *trans*-K_2[PdC1$_2$(*N*-glutarimidate)$_2$].4.5H_2O and *trans*-KNa[PdCl$_2$(*N*-glutarimidate)$_2$].6H_2O prepared by Michalska *et al.*[11] and *trans*-[PdCl(*N*-obs)(PPh_3)$_2$] by Henderson *et al.*.[12] Shimomura *et al.*[13] have prepared *trans*-[Pd(*N*-succ)$_2$LL'] complexes (L is *S*-1-phenylethylamine and L' the *R* or *S* enantiomer) and found three different staggered rotamers around the N-C bond of the phenylethylamine ligand. Aresta *et al.*[14] found that when [PdCl{$CONCH_2(CH_2OCH_2)CH_2$}(L)] and [PdCl{$CON(CH_2)_4CH_2$}(L)] (where L is phen or bipy) were reacted with *N*-chlorosuccinimide, complexes of the type [PdCl(*N*-succ)(L)] were formed (along with $ClC(O)N(CH_2)_4CH_2$ and $ClC(O)NCH_2(CH_2OCH_2)CH_2$, respectively).

Palladium(II) imidate complexes have also been applied catalytically in cross-coupling reactions particularly by the research groups of Fairlamb, Taylor and Serrano. In 1999 Serrano *et al.*[15] reported *cis*-[PdBr(*N*-succ)(PPh_3)$_2$] and [PdBr(*N*-succ)(dppe)] complexes prepared by reaction of [Pd(DBA)$_2$] {DBA is (*E*,*E*)-dibenzylideneacetone} with NBS and PPh_3 or dppe. Crawforth *et al.*[16] found [PdBr(*N*-succ)(PPh_3)$_2$] to be more efficient than other halide and imidate analogues in Stille cross-coupling reactions (Table 1, Chapter 1). It is however only efficient at coupling benzyl type halides not aryl halides, which is opposite to the normal observed selectivity with Pd(II) complexes.

Fairlamb *et al.*[17] found that *trans*-[Pd(*N*-succ)$_2$(PPh_3)$_2$][1] was an efficient catalyst for the Suzuki cross-coupling of aryl halides and organoboronic acids in air and also showed *trans*-[Pd(*N*-ptm)$_2$(PPh_3)$_2$] (prepared by reaction of phthalimide with [Pd(PPh_3)$_4$]) to be an active precatalyst for Suzuki–Miyaura cross-coupling of aryl bromides with aryl and heteroarylboronic acids.[18]

Serrano *et al.*[19] prepared a range of dinuclear cyclometallated [{Pd(phpy)(μ-*N*,*O*-imidate)}$_2$] and [{Pd(azb)(μ-*N*,*O*-imidate)}$_2$] (**240**) complexes {where phpy is 2-

phenylpyridine; azb is azobenzene; imidate is succ (**a**), mal (**b**) or ptm (**c**)} by treatment of the analogous phpy and azb (**241**) acetate complexes with the relevant imide. The succinimidate complexes were then treated with a range of phosphines to prepare mononuclear [Pd(phpy)(*N*-succ)(PR_3)] and [Pd(azb)(*N*-succ)(PR_3)] (**242**) complexes {PR_3 is PPh_3, PPh_2Me, $PPhMe_2$, P(4-F-C_6H_4)$_3$ or P(4-MeO-C_6H_4)$_3$} with monodentate *N*-ligated imidates (Scheme 63).

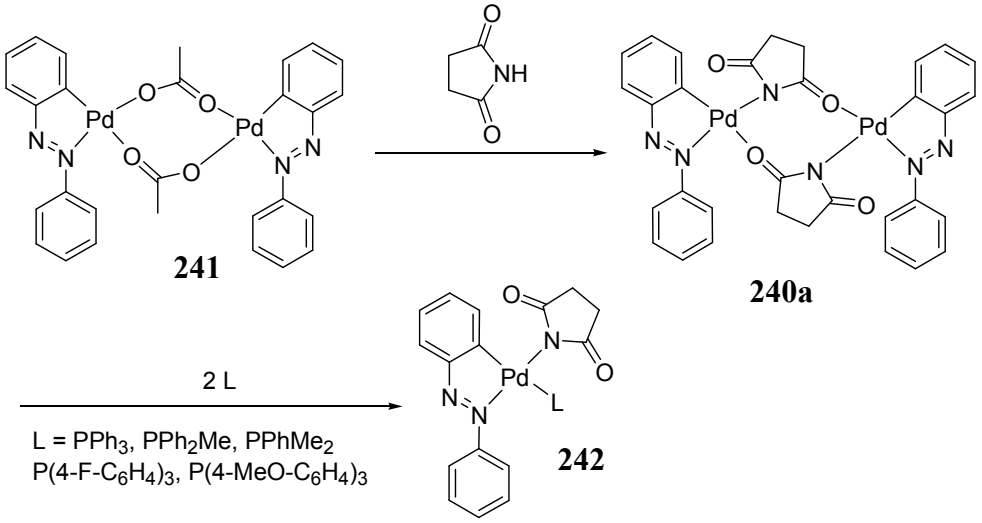

Scheme 63. Preparation of [{Pd(μ-*N*,*O*-succ)(azb)}$_2$] (**240a**) and [Pd(azb)(*N*-succ)(PR_3)] (**242**) complexes reported by Serrano *et al.*.

Fairlamb and co-workers in collaboration with the research group of Serrano[20] prepared an analogous range of [{Pd(bzq)(μ-*N*,*O*-imidate)}$_2$] complexes (where bzq is 7,8-benzoquinolyl; imidate is succ, mal or ptm) and treated these and the azb and phpy series with phosphines to yield [Pd(L)(*N*-imidate)(PR_3)] type complexes (L is azb, bzq or phpy; R is Ph, 4-F-C_6H_4 or 4-MeO-C_6H_4). The nature of the imidate was found to influence the decomposition temperature and (to some extent) the catalytic activity of the dinuclear and mononuclear complexes for the Suzuki–Miyaura cross-coupling reactions of aryl bromides with aryl boronic acids, and the Sonogashira reactions of aryl halides with phenyl acetylene {in the presence and absence of Cu(I) salts}. It was also demonstrated that these catalysts could be recycled several times without loss of activity in a poly(ethylene oxide)/methanol solvent system after removal of non-polar material and products by extraction.

The groups[21] also reported analogous series of [{Pd(μ-*N,O*-imidate)(phox)}$_2$] and [Pd(*N*-imidate)(phox)(PR_3)] complexes {imidate is succ, mal, ptm, 2,3-dibromomaleimidate or

glutarimidate; phox is 2-(2-oxazolinyl)phenyl; R is Ph, 4-F–C_6H_4 or CH_2CH_2CN} (from [{Pd(μ-OH)(phox)}$_2$]) which showed promising activity in Suzuki–Miyaura cross-coupling reactions of aryl bromides with aryl boronic acids. [NBu_4]$_2$[Pd_2{C_4(COOMe)$_4$}$_2$(μ-*N*,*O*-imidate)$_2$] (**243**) and [NBu_4][Pd{C_4(COOMe)$_4$}(*N*-imidate)L] complexes {imidate is succ (**a**), mal (**b**) and ptm (**c**); L is PPh_3, P(4-F-C_6H_4)$_3$, PBu_3, Py, 4-Me$C_6H_4NH_2$ and THT (tetrahydrothiophene)} were prepared in a similar way from [NBu_4]$_2$[Pd_2{C_4(COOMe)$_4$}$_2$(μ-OH_2)$_2$].[22] The complexes were tested for catalytic activity in the cross-coupling of benzyl bromide (**11**) with ethyl (*Z*)-3-(tributylstannyl)propenoate (**12**). The dinuclear imidate complexes had modest activity but were found to be more active than chloro, bromo and hydroxy analogues. The mononuclear complexes were very effective, in particular [NBu_4][Pd{C_4(COOMe)$_4$}(*N*-succ)(Py)], [NBu_4][Pd{C_4(COOMe)$_4$}(*N*-succ)(THT)] and [NBu_4][Pd{C_4(COOMe)$_4$}(*N*-ptm)(THT)], with succinimidate generally superior to maleimidate and phthalimidate and the previously reported [PdBr(*N*-succ)(PPh_3)$_2$] complex. Complexes containing THT ligands were more active than pyridine and phosphine analogues.

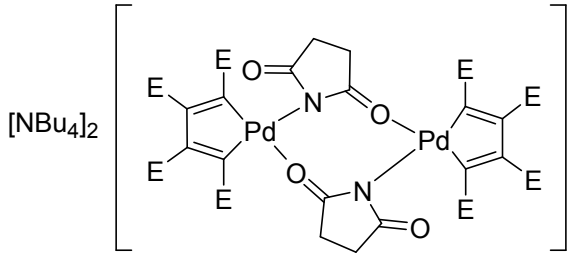

Figure 51. Structure of [NBu_4]$_2$[Pd_2{C_4(COOMe)$_4$}$_2$(μ-*N*,*O*-succ)$_2$] (**243a**) reported by Serrano *et al*..

Ruiz *et al.*[23] have prepared [Pd(C_6F_5)(*N*-imidate)(N–N)] complexes {N–N is 2,2'-bipyridine (bipy), 4,4'-dimethyl-2,2'-bipyridine (Me_2bipy) or *N*,*N*,*N*′,*N*′-tetramethylethylenediamine (tmeda); imidate is succ, mal or ptm}, such as [Pd(C_6F_5)(*N*-succ)(bipy)] (**244a**), from the analogous hydroxy complexes. [NBu_4][Pd(C_6F_5)(*N*-succ)$_2$(H_2O)] and [NBu_4][Pd(C_6F_5)(*N*-succ)$_2$(L)] (**245**) were prepared by reaction of [NBu_4]$_2$[{PdBr(μ-Br)(C_6F_5)}$_2$] and [{Pd(C_6F_5)(μ-Cl)(L)}$_2$] {L is PPh_3 (**a**) and ^{t}BuNC} with succinimide and [NBu_4]OH (Figure 52). The complexes were found to be moderately

active for the Suzuki cross-coupling of aryl bromides and chlorides with phenylboronic acid, and activity was also dependant on the nature of the imidate ligand.

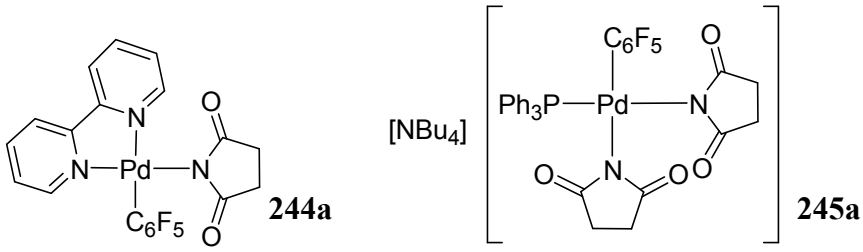

Figure 52. [Pd(C_6F_5)(*N*-succ)(bipy)] (**244a**) and [NBu_4].*cis*-[Pd(C_6F_5)(*N*-succ)$_2$(PPh_3)] (**245a**) reported by Ruiz *et al.*.

More recently Kumar *et al.*[24] reported that the air stable and water soluble complex [Pd_2(μ-Cl)$_2$(*N*-obs)$_2$] (**246**) showed high activity and turnover numbers in Suzuki, Heck and Sonogashira reactions (Figure 53). For example, a 0.00025 mol% catalyst loading for the Heck coupling of 4-bromoanisole with styrene in water gave a 93% yield and turnover number of 372000 compared to 71% yield and a TON of 1,420 for $Pd(OAc)_2$ (**247**).

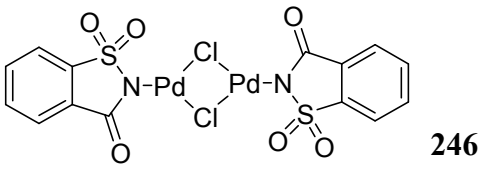

Figure 53. [Pd_2(μ-Cl)$_2$(*N*-obs)$_2$] (**246**) reported by Kumar *et al.*.

Whitfield and Sanford[25] have reported a unique Pd(IV) imidate complex, [PdCl(*N*-succ)(2-phenylpyridine)$_2$] (**248**), formed by reaction of [Pd(2-phenylpyridine)$_2$] (**249**) and *N*-chlorosuccinimide (NCS) (Scheme 64). They propose this as a possible intermediate in the Pd-catalysed conversion of arene C-H bonds into carbon-halogen bonds by *N*-halosuccinimides[26] (and also $PhICl_2$) suggesting a Pd(II)/Pd(IV) catalytic cycle. Heating of the complexes led to reductive elimination, forming Pd(II).

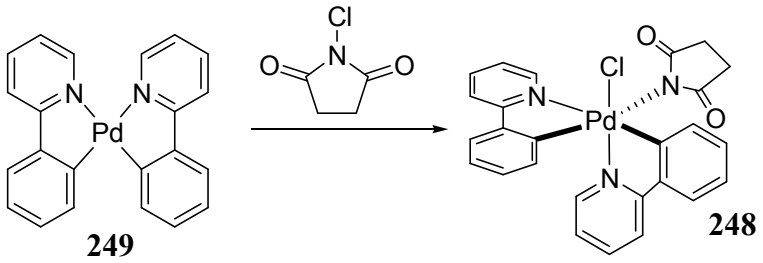

249 **248**

Scheme 64. Preparation of [PdCl(*N*-succ)(2-phenylpyridine)$_2$] (**248**) by Whitfield and Sanford.

4.1.2. Pd-catalysed direct arylation

Since direct arylation was first observed in the 1980's as an unexpected side reaction in attempted Mizoroki-Heck reactions by Ames and Bull,[27] substantial research into direct arylation, the carbon-carbon coupling of an aryl(pseudo)halide with an unactivated arene, has led to the development of efficient procedures for the preparation of a range substituted arenes typically using low oxidation state complexes of Rh, Ru and Pd. It has however only been in the past decade that the true potential of direct arylation has been investigated and exploited.[28] It has the advantage over cross-coupling methodologies of not requiring the prefunctionalisation of one coupling partner as an organometallic compound. This results in a shorter, cheaper and greener synthetic route with good atom economy and reduced metal usage. However, there are significant challenges; the high energy of aryl C-H bonds, selectivity (as there tend to be many aryl C-H bonds in aromatic compounds) and the fact that the C-H bond is typically one of the least reactive functional groups in a molecule.[28]

Direct arylation has been used to form the biaryl motifs of many natural products and biomolecules, particularly *via* the 'lactone method'[29] (an ester linkage is used to join the coupling partners which are coupled intramolecularly to form a lactone which can then be hydrolysed to give a biaryl motif).[28b] For example, Bringmann *et al.*[30] have prepared the 5,8'-coupled naphthylisoquinoline alkaloids, korupensamines (**250**), which have antimalarial properties (and are precursors to anti-HIV1 homo- and hetero-dimeric naphthylisoquinolines), using direct arylation to furnish a lactone (**251**) from aryl bromide **252** as a key step. One atropisomer of the configurationally unstable lactone is subsequently selectively cleaved. The Herrmann-Beller[31] catalyst (**253**) gave a 74% yield whereas a combination of $Pd(OAc)_2$ (**247**) and PPh_3 gave only 26% demonstrating the benefits of catalyst design (Scheme 65).

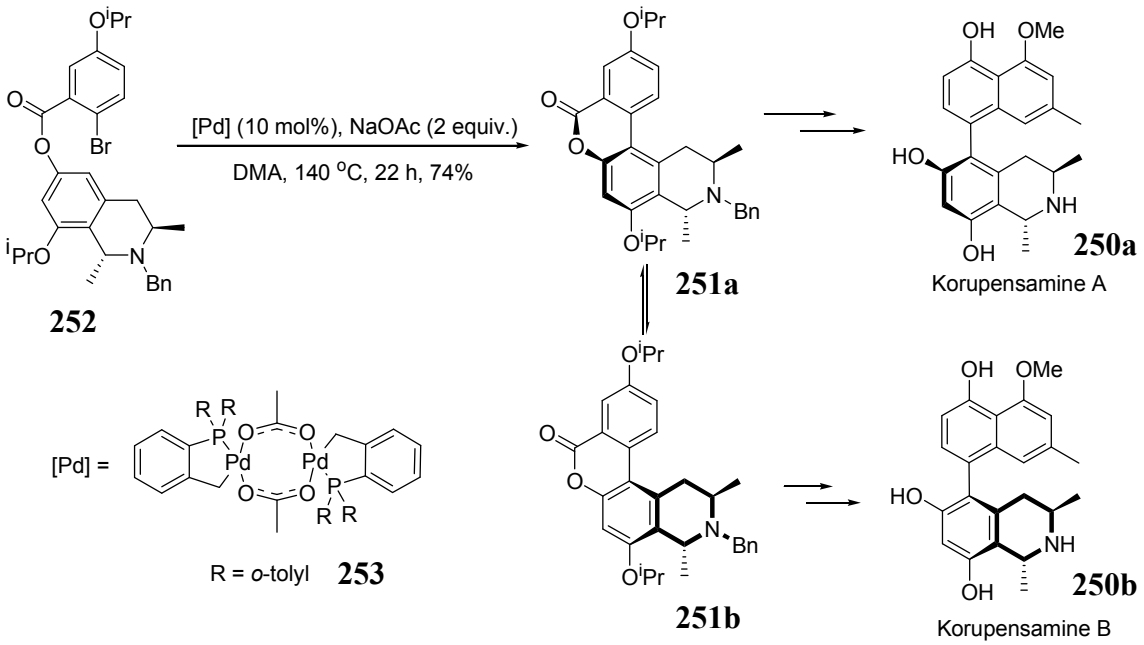

Scheme 65. Key direct arylation step in the synthesis of korupensamines A (**250a**) and B (**250b**) using the Herrmann-Beller catalyst (**253**) as reported by Bringmann *et al.*.

4.1.3. Direct arylation of heterocycles

The direct arylation of heteroarenes with aryl halides has been a significant area of research, due to their prevalence in natural and biologically active molecules. Many different heterocycles, such as thiazoles, oxazoles, pyrimides, pyridines, imidazoles, benzimidazoles and quinolines, have been arylated in this way. An example is that of Gaunthier *et al*. who used direct arylation methodology to prepare a range of $GABA_A$ agonist candidates.[32] These included the direct arylation of an imidazo[1,2-*a*]pyrimidine (**254**) with a biaryl bromide (**255**) as a key step in the synthesis of a R2/3-selective $GABA_A$ agonist (**256**) (Scheme 66).[33] Interestingly, water (<5 mol%) aided the reaction.

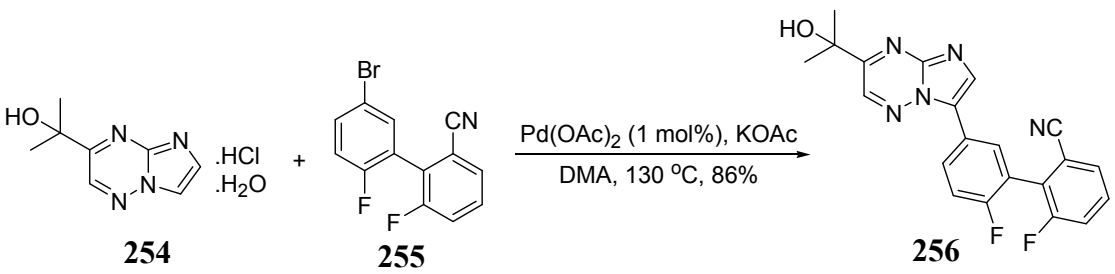

Scheme 66. Direct arylation of an imidazo[1,2-*a*]pyrimidine (**254**) with a biaryl bromide (**255**) in the synthesis of an R2/3-selective $GABA_A$ agonist (**256**) reported by Gaunthier.

Heteroaromatic compounds facilitate arylation, as certain C-H bonds are activated in preference to others, allowing control over regioselectivity and negating the need for tethers or directing groups commonly required for non heteroatom-containing systems. Regioselectivity is also determined by the substrate type, catalyst (electronics and sterics), solvent and additives.[28c] The N-substituent of N-heterocycles can also effect selectivity, which has been observed by Akita *et al.* who found that unsubstituted and alkyl substituted indoles were arylated at C2 where as tosylate substituted indoles were arylated at C3.[34]

Imidazoles are an important class of heterocycles, due to their prevalence in nature, and their arylation has been well studied. The molecule has challenges of C5 *versus* C2 selectivity as well as competition from the nitrogen. The group of Miura[35] carried out initial investigation of the direct arylation of 1,2-dimethylimidazole using $Pd(OAc)_2$ (**247**) and developed optimised conditions (DMF solvent at 140 ˚C) with K_2CO_3 base for aryl bromides and Cs_2CO_3 for iodides. This system worked well for the C5 arylation of imidazoles and other heterocycles using both electron rich and poor, as well as sterically hindered, aryl halides. They also found that using a CuI additive gave increased yields in some cases (particularly with sulfur heterocycles). With *N*-methyl imidazole arylation occurred preferentially at C5 followed by C2, in the presence of CuI and Pd C2 arylation was increased and in the absence of Pd it occurred at C2 exclusively (although in low yields) possibly *via* a Cu(I)/base nucleophilic substitution of the aryl iodide.[36] The group of Sames[37] also investigated arylation of *N*-substituted imidazoles {for example [2-(trimethylsilyl)ethoxy]methyl (SEM) substitution} using a bulky NHC palladium catalyst achieving modest yields but high C5 selectivity.

Bellina *et al.*[38] developed conditions for the arylation of *N*-aryl substituted imidazoles {5 mol% $Pd(OAc)_2$ (**247**), with $AsPh_3$ ligand and CsF base additives, in DMF at 140 ˚C} which gave reasonable yields for neutral and electron rich substituents but did not proceed for electron poor substituents. For the arylation of 1-phenyl-1*H*-imidazole (**257**) with 4-iodoanisole (**258a**), they observed good C5 (**259c**) selectivity with some C2 arylation (**259a**) and C2,C5 diarylation (**259b**) (Entry 1, Table 49). They also observed that added CuI increased selectivity for C2 (**259a**) and optimised the conditions to give high C2 (**259a**) selectivity, in some cases exclusively (although with moderate yields) (Entries 2-4).[39] Bellina *et al.*[40] also managed to develop conditions for selective C2 arylation of unprotected imidazoles (oxazoles, thiazoles, benzimidazoles and indoles) with aryl iodides without the need for added base or donor ligands in reasonable yields. These conditions

also worked well for substituted imidazoles (1-alkyl, 5-aryl and 1,4-diaryl imidazoles), thiazole, oxazole, benzimidazole and benzothiazole (Entry 5).[41] These conditions have been utilised by Besselièvre *et al.*[42] with microwave heating to C2 arylate oxazole with less reactive aryl bromides. Huang *et al.*[43] have managed to modify the Pd/Cu system in order to use low catalyst loadings and catalytic Cu(I) (0.25% Pd and 1 mol% [CuI(Xantphos)] at 100 ˚C for 18 hours in toluene) for the efficient arylation of benzothiazoles and benzoxazole, although yields were moderate for *N*-methyl benzimidazole.

Table 49. Effect of additives on the outcome of the direct arylation of 1-phenyl-1*H*-imidazole (**257**) with 4-iodoanisole (**258a**).[a]

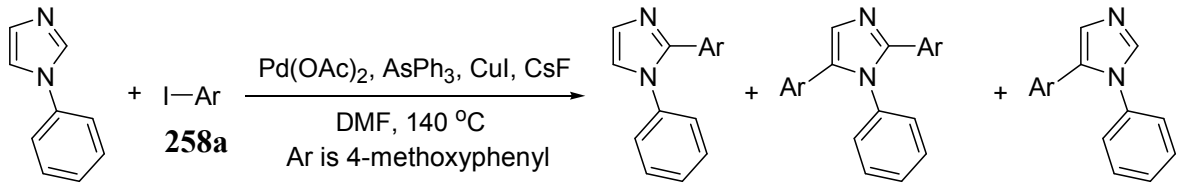

257 C2 **259a** C2, C5 **259b** C5 **259c**

Entry	Loading				Ratio of products			Yield (%)	
	$Pd(OAc)_2$ (mol%)	$AsPh_3$ (equiv.)	CuI (equiv.)	CsF (equiv.)	C2 (259a)	C2, C5 (259b)	C5 (259c)	C2 (259a)	C5 (259c)
1[b]	5	10	-	2	5	0	95	-	49
2[c]	10	-	0.5	2	35	0	65	11	-
3[c]	5	-	2	2	81	18	1	62	-
4[c]	-	-	2	2	100	0	0	26[d]	-
5[e]	5	-	2	-	100	-	-	70	-

[a] Conditions: 1 equiv. 1-phenyl-1*H*-imidazole (**257**) in 0.2 M DMF at 140 ˚C, 2 equiv. 4-iodoanisole (**258a**). [b] 42 hours reaction time. [c] 48 hours reaction time. [d] 44% conversion. [e] 26 hours reaction time.

Another solution to the problem of C2, C5 selectivity in the arylation of imidazoles has been developed by Kondo *et al.*[44] by immobilisation of the aryl iodide on a polymer resin which prevents diarylation. Complete selectivity for C2 or C5 could then be achieved by the presence or absence or CuI, respectively.

The Pd/Cu methodology has been applied to the C8 arylation of nucleosides by the Hocek and Fairlamb groups. Hocek developed conditions for the direct arylation of purines[45] and adapted the technology to C8 arylation of adenosines.[46] The Fairlamb group

have also studied C8 arylation of adenosines and 2'-deoxyadenosines (**260**) in depth to prepare fluorescent biological probes,[47] developing efficient conditions for lower temperature direct arylation. They found that on lowering the temperature from 120 ˚C to 80 ˚C the reaction yield was variable, determining that trace Me_2NH[48] (from DMF decomposition) was required, the concentration of which was affected by reaction temperature and solvent purification conditions.[49] Other secondary amines such as piperidine (0.4 equivalents) had the same effect (Scheme 67).

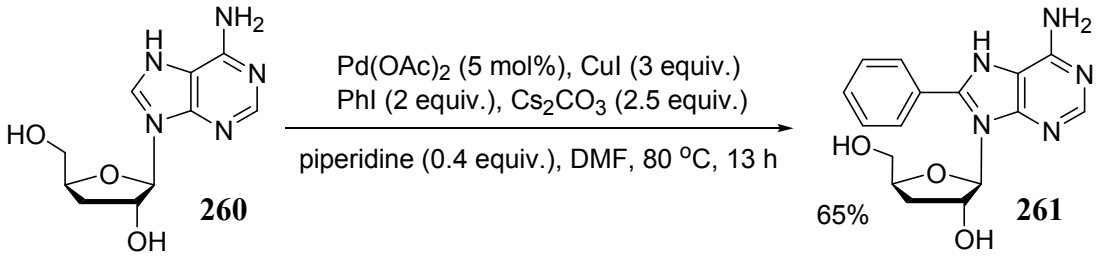

Scheme 67. Conditions for the direct arylation of 2'-deoxyadenosine (**260**) with iodobenzene (**261**) developed by Storr *et al.*.

4.1.4. Direct arylation mechanisms

The typical Pd-catalysed C5 arylation and the C2 Cu/Pd mediated arylation of imidazole are believed to occur *via* separate mechanisms. The first step of the Pd-catalysed mechanism is reduction of the usual $Pd(OAc)_2$ precatalyst (**247**) to the Pd(0) active catalyst (by DMF or phosphine) which is ligated by neutral ligands (typically phosphine) (Step I, Scheme 68). The aryl halide oxidatively adds to the Pd(0) species (Step II), forming a Pd(II) species, which then adds to the imidazole at the C5 position by electrophilic attack with loss of the halide ligand (Step III). Loss of a proton neutralises the resultant carbocation and restores the aromaticity (Step IV), followed by reductive elimination to yield the C5 arylated imidazole and regenerate the Pd(0) catalyst (Step V).[35]

The copper-mediated C2 arylation also proceeds by initial oxidative addition of the aryl halide to the Pd(0) species (Step II), however transmetallation with an organo-C2-cuprate formed from imidazole and CuI then occurs (Step VI). Deprotonation (Step VII) followed by reductive elimination then gives the C2 arylated imidazole and regenerates the active Pd(0) species (Step VIII).[39] The reaction rate is greater with electron withdrawing N-substituents which provides evidence for organocuprate formation due to the increased

acidity of the C2 proton. Lowering CuI or increasing Pd loading reduces selectivity suggesting the organocuprate is in equilibrium with free CuI and imidazole.

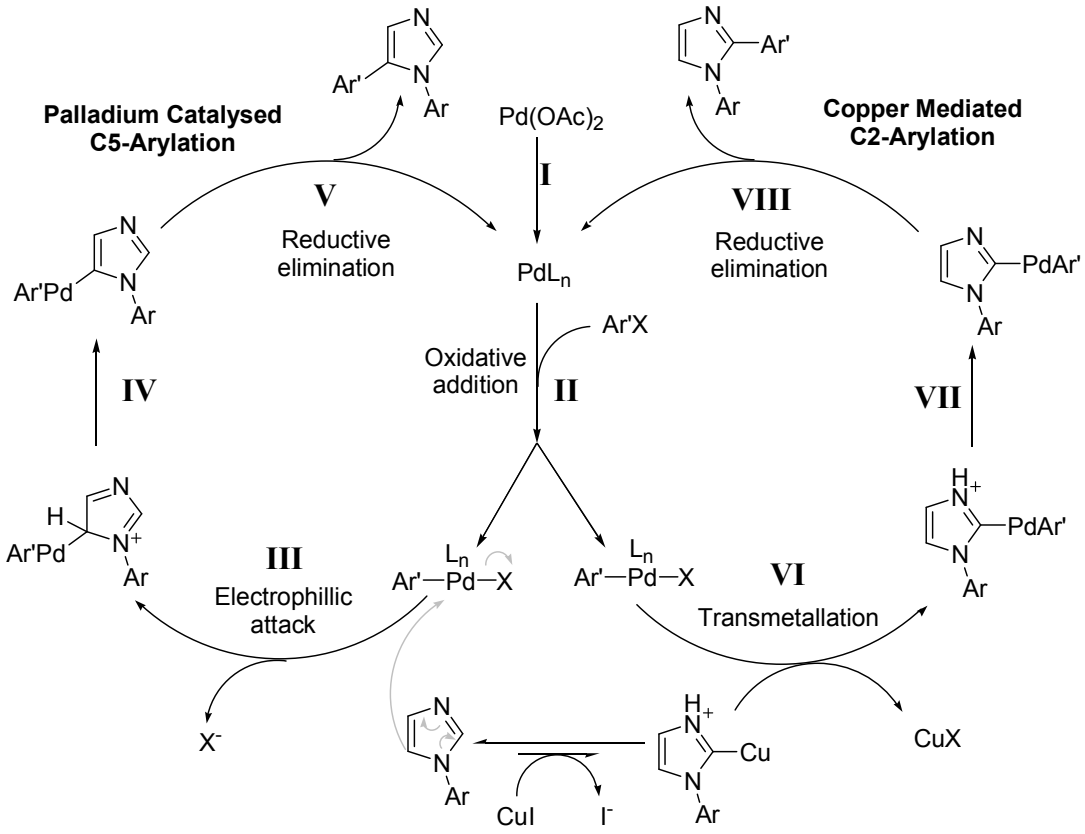

Scheme 68. Proposed mechanisms for the Pd mediated C5 arylation and Pd/Cu mediated C2 arylation of imidazole.

Although electrophilic aromatic substitution (S_EAr) is thought to occur in the Pd catalysed C5 arylation, a number of other mechanisms[28,50] have been proposed for the functionalisation of the C-H bonds in direct arylation reactions including; a concerted S_E3 process,[51] σ-bond metathesis (concerted metallation/deprotonation),[52] Heck-type carbometallation[53] and oxidative addition,[54] depending on the conditions and substrates involved (Scheme 69).[28c,55]

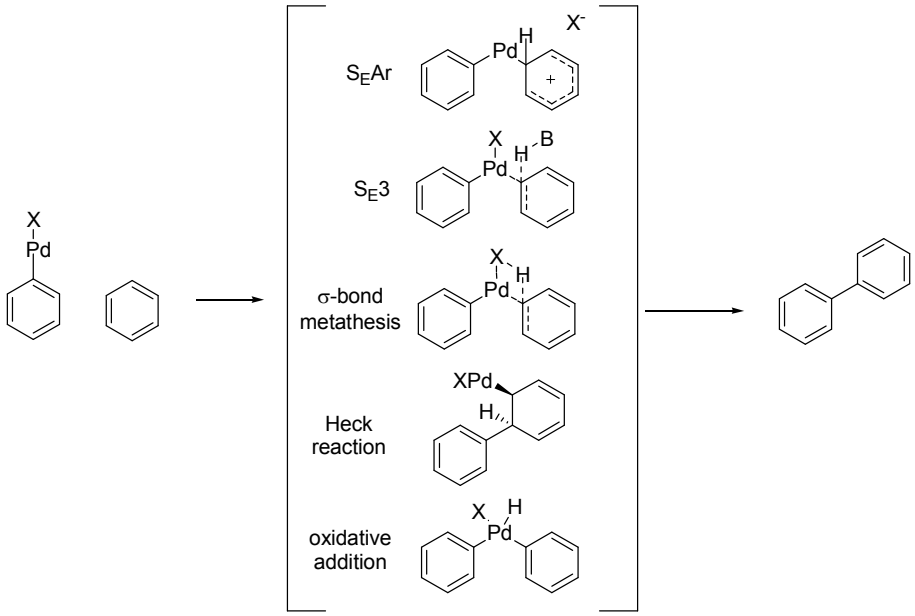

Scheme 69. Possible mechanisms for the functionalisation of C-H bonds in direct arylation reactions.

4.1.5. Anion effects in direct arylation reactions

As described above direct arylation is believed to occur *via* a Pd(0)/Pd(II) mechanism with a Pd(II) complex acting as a stable precatalyst to the active Pd(0) species, the nature of the Pd(II) anionic ligands will affect the rate of reduction to and the stability of the Pd(0) species. Fagnou found that, when using [{$PdCl_2$(IMes)}$_2$] to carry out intramolecular coupling of arenes with pendant aryl chlorides, initiation of this dimeric catalyst was very slow and irreproducible. However, when silver acetate was added the reaction proceeded well and reproducibly with a similar TON to [$Pd(OAc)_2$(IMes)(OH_2)].[56] The further involvement of anionic species in the reaction has also been proposed in a number of cases.

There have been a number of reports of the addition of pivalic acid as a co-catalyst[57] or CsOPiv as a base[54a,58] aiding direct arylation reactions. The pivalate anion is suspected to coordinate to the ArPd(II)X species (after oxidative addition) in place of the halide.[59] It then acts as a proton shuttle in concerted metallation/deprotonation (σ-bond metathesis)[52] of the C-H arene, after which normal reductive elimination occurs and the pivalate anion is regenerated *via* deprotonation by the added base. The *O*,*O*-chelation of the pivalate anion also increases the regioselectivity of the arylation. Fagnou has also utilised the pivalic acid system to arylate nitrobenzene using substoichiometric pivalic acid {30 mol% and 15 mol% HP(^{t}Bu)$_3$$BF_4$}.[60] He also used similar methodology to carry out arylation of

unactivated arenes, such as benzene, with arylbromides,[55] and the room temperature direct arylation of azole N-oxides.[61] Larrosa used a *p*-nitrobenzoic acid/silver(I) oxide base combination for the room temperature direct C2 arylation of indoles.[62]

Pd(II)/Pd(IV) catalytic cycles[63] which intrinsically involve anionic ligands have also been proposed in some direct arylation reactions. Sanford reported the direct arylation of 2-aryl pyridines using $[Ph_2I][BF_4]$ for which mechanistic studies suggested a II/IV cycle.[64] Sanford also reported the C2 arylation of indoles at ambient temperature using this method. The mechanism is proposed to occur *via* electrophilic palladation of the indole C2 position by $Pd(OAc)_2$, followed by oxidative addition of the aryl iodide ($[Ar_2I][BF_4]$) to the Pd(II) species.[65] Daugulis *et al.* used a silver acetate (2.2 equiv.) additive and trifluoroacetic acid solvent combination to carry out the direct arylation of aniline,[66] benzylamine,[67] pyridine and pyrazole[68] using aryl iodides, competition experiments suggested a II/IV mechanism.[66]

Amatore and Jutand[69] have proposed an ionic Pd(0)/Pd(II) cycle operating in addition to the usual neutral cycle in Pd-catalysed cross-coupling reactions, which may also be relevant to direct arylation reactions (Scheme 70). This involves tricoordinate anionic Pd(0) complexes, such as $[Pd(0)Cl(PR_3)_2]^-$ and $[Pd(0)(OAc)(PR_3)_2]^-$ (**262**), in which the anion directly effects the kinetics of oxidative addition of ArI and the reactivity of the resultant Pd(II) species, $[Pd(Ar)I(Cl)(PR_3)_2]^-$ and $[Pd(Ar)I(OAc)(PR_3)_2]^-$ (**263**).

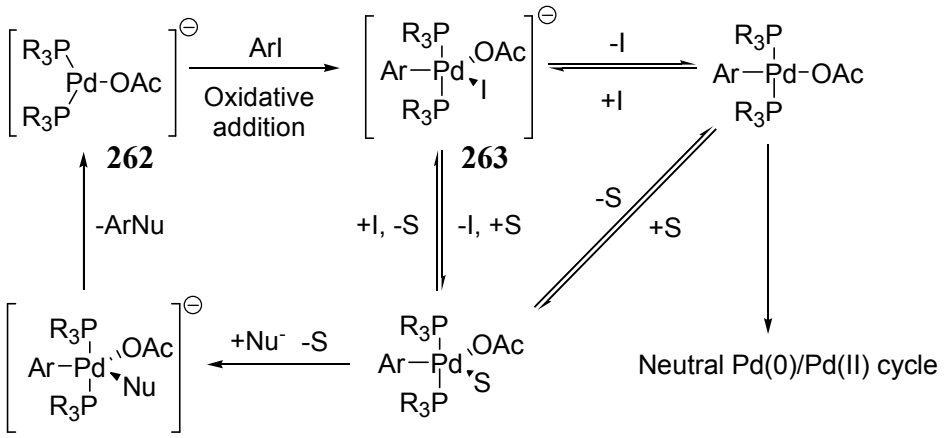

Scheme 70. Anionic Pd(0)/Pd(II) cycle proposed by Amatore and Jutand.

Additionally, the group of Jutand[70] has found that $[Pd(0)(PPh_3)_2]$ in the presence of chloride ions actually consists of a dynamic equilibrium of anionic species; $[\{Pd(0)C1(PPh_3)_2\}_2]^{2-}$, $[Pd(0)C1(PPh_3)_2]^-$ and $[Pd(0)C1_2(PPh_3)_2]^{2-}$ by the use of ^{31}P NMR

spectroscopy and electrochemistry. The presence of the chloride ions stabilises the Pd(0) species although the rate of oxidative addition is reduced. Amatore *et al.*[71] also investigated these effects using acetate and trifluoroacetate ions with the support of DFT calculations. $Pd(O_2CCF_3)_2$ was found to be reduced to $[Pd(0)(O_2CCF_3)(PAr_3)_n]^-$ (n = 2 or 3) species in the presence of triarylphosphines and $[Pd(0)(O_2CCF_3)(PAr_3)_2]^-$ was found to be the active species for oxidative addition of iodobenzene to give *trans*-$[Pd(Ph)(O_2CCF_3)(PPh_3)_2]$ and *trans*-$[Pd(Ph)(DMF)(PPh_3)_2]^+$ in equilibrium. It was found that the rate of formation of $[Pd(0)(O_2CCX_3)(PAr_3)_2]^-$ from $Pd(O_2CCX_3)_2$ and its reactivity towards PhI is higher for triflouroacetate (X=F) than acetate (X=H). The equilibrium constant of *trans*-$[Pd(OCOCX_3)(Ph)(PPh_3)_2]$ and *trans*-$[Pd(Ph)(DMF)(PPh_3)_2]^+$ is also influenced by the nature of X.

4.1.6. Aims

The aim of this study was to investigate the structure and bonding of Pd(II) bisimidate complexes, containing acetonitrile, tetrahydrothiophene and triphenylphosphine ligands, of the type $[Pd(L)_2(imidate)_2]$. These complexes would then be applied to the direct arylation of imidazole using the ligand and base free conditions of Bellina *et al.*[40] and the effect of the nature of the imidate and neutral ligands investigated. Through the investigation of the effect of the nature of the anionic ligand it was hoped that some details of the mechanism of the reaction under these unusual conditions could be elucidated.

4.2. Results and discussion

4.2.1. Synthesis and characterisation of Pd complexes

4.2.1.1. Synthesis of [Pd(imidate)$_2$(L)$_2$] complexes

A range of palladium imidate complexes were prepared on the basis of results obtained previously within the group, those of collaborators and literature reports.[5,10] Initially complexes of the type [Pd(imidate)$_2$(MeCN)$_2$] (**264**) {imidate is succ (**264a**), tfs (**264b**), mal (**264c**), ptm (**264d**) and obs (**264e**)} were prepared. These were synthesised by stirring Pd(OAc)$_2$ (**247**) and two equivalents of the relevant imide in acetonitrile overnight at ambient temperature, which resulted in the precipitation of the desired complexes. In the case of the tfs complex (**264b**) precipitation did not occur spontaneously and diethyl ether was added to the reaction solution resulting in precipitation. Purification was achieved by washing of the crude powders with acetonitrile, petroleum ether (40-60) and diethyl ether. The products were isolated as off-white powders, in 43-84% yield (Table 50), which proved to have very low solubility in all solvents, preventing crystallisation and effective analysis by solution phase spectroscopy, other than ESI-MS, and so solid-state IR and solid-state ^{13}C NMR spectra were obtained.

Tetrahydrothiophene (THT) complexes (**265**) of the type [Pd(imidate)$_2$(THT)$_2$] {imidate is succ (**265a**), ptm (**265b**) and obs (**265c**)} were prepared by treatment of the analogous acetonitrile complexes (**264**) with 2 equivalents of THT in ethanol. These were prepared on the basis of results reported by Serrano *et al.*.[22] Stirring the solutions overnight at ambient temperature again resulted in precipitation of the desired complexes. The products were isolated as off-white powders, in 52-87% yield (Table 50), which had moderate solubility in chloroform allowing solution phase ^{1}H and ^{13}C NMR spectra to be obtained (although signals were broad in ^{1}H and weak in ^{13}C NMR spectra) in addition to IR and ESI-MS spectra.

[Pd(imidate)$_2$(PPh$_3$)$_2$] (**266**) complexes {imidate is succ (**266a**), mal (**266b**), ptm (**266c**) and obs (**266d**)} were obtained to allow comparison with reported complexes and to aid in the analysis of MeCN (**264**) and THT (**265**) analogues. The compounds were prepared by treatment of the analogous acetonitrile complexes (**264**) with 2 equivalents of phosphine at ambient temperature in CDCl$_3$. These complexes were not isolated but analysed directly by ^{1}H and ^{13}C NMR, IR spectroscopy and ESI-MS. The tfs complex however could not be prepared, as no reaction with phosphine was observed under a range of conditions. The

complexes are predicted to have *trans* geometry with *N*-ligated imidate ligands on the basis of reported similar [Pd(*N*-imidate)$_2$L$_2$] complexes.[1,4,5,17]

Table 50. Isolated yields of [Pd(imidate)$_2$(MeCN)$_2$] and [Pd(imidate)$_2$(THT)$_2$] complexes.

Entry	Complex		Yield (%)
1	[Pd(succ)$_2$(MeCN)$_2$]	(**264a**)	58
2	[Pd(tfs)$_2$(MeCN)$_2$]	(**264b**)	43
3	[Pd(mal)$_2$(MeCN)$_2$]	(**264c**)	64
4	[Pd(ptm)$_2$(MeCN)$_2$]	(**264d**)	66
5	[Pd(obs)$_2$(MeCN)$_2$]	(**264e**)	84
6	[Pd(succ)$_2$(THT)$_2$]	(**265a**)	87
7	[Pd(ptm)$_2$(THT)$_2$]	(**265b**)	52
8	[Pd(obs)$_2$(THT)$_2$]	(**265c**)	86

4.2.1.2. Characterisation by NMR spectroscopy

The acetonitrile complexes (**264**) were analysed by solid state ^{13}C NMR and the THT (**265**) and PPh_3 (**266**) complexes by $CDCl_3$ solution phase ^{1}H and ^{13}C NMR spectroscopy (Table 51), although ^{13}C NMR has been infrequently used[12,19,24,25] as a method to characterise the many reported palladium imidate complexes.

Solid-state ^{13}C NMR proved to be a reliable method for analysis of the essentially insoluble [Pd(imidate)$_2$(MeCN)$_2$] complexes (**264**), as analysis of the spectra revealed only signals corresponding to the predicted structures. All complexes had a signal between 125.0-127.5 ppm corresponding to the *C*N carbon of the acetonitrile ligand and at 1.0-5.3 ppm for the methyl carbon (Table 51). The succinimidate complex (**264a**) has a large signal at 2.7 and a smaller peak at 1.0 ppm for the methyl carbon which are significantly upfield of the other imidate complexes (4.5-5.3 ppm) which have only one signal corresponding to the methyl carbon (an upfield shift would be expected as the succinimidate complex is the most electron rich). The additional peak at 1.0 ppm may correspond to a different polymorph or environment in a [Pd(succ)$_2$(MeCN)$_2$] type complex or could be due to acetonitrile ligated to residual acetate complex. There does not

appear to be a clear pattern in the relative order of the acetonitrile peaks as the peaks are broad and generally similar in chemical shift.

The imidate carbonyl signals appear at 164.8-194.4 ppm for the MeCN complexes (**264**), 166.2-188.1 ppm for the THT complexes (**265**) (in $CDCl_3$) and 164.3-186.5 ppm for the PPh_3 complexes (**266**) (in $CDCl_3$). For each series of complexes the carbonyl carbon signals are in the order:

succ > mal > ptm > tfs > obs

This is consistent with Au(I) (**55-57**) and Au(III) (**66-68**) imidate complexes (Chapter 2) and reflects the increasing acidity of the parent imide {with the exception of obs, which does not share the same $N(COR)_2$ structure}.

In each case, with the exception of the obs complexes, the MeCN signals of complexes **264** occur down field relative to THT (**265**) and PPh_3 (**266**) analogues {and related Au(I) (**55-57**) and (III) (**66-68**) imidate complexes}, which may be an effect of the different media. The signals of the THT complexes (**265**) are more upfield than those of the PPh_3 complexes (**264**) by 1.4-1.9 ppm reflecting the weaker donor ability of acetonitrile and THT ligands relative to PPh_3 (sterics may also be a factor). This is also largely true for the other imidate carbon signals.

The ^{13}C NMR spectra of the mal (**264c**) (2 *C*O signals and multiple *C*=*C* signals), succ (**264a**) (3 *C*O and 2 CH_3 signals) and tfs (**264b**) (2 *C*O signals) acetonitrile complexes have more signals than would be expected for single symmetric $[Pd(imidate)_2(MeCN)_2]$ structures. For the maleimidate complex (**264c**) infra-red spectroscopy (*vide infra*) suggests that the imidate ligands are bidentate *N*,*O*-coordinated to Pd. The two carbonyl carbon signals at 186.4 and 181.8 ppm and the broad mulitplet for the imidate *C*H carbons are consistent with this type of coordination.[19] The chemical shifts of the three carbonyl carbon signals in the succinimidate (**264a**) spectrum appear to be consistent with a mixture of (or an equilibrium between) monodentate *N*- and bidentate *N*,*O*-coordination, although there is no evidence of this in the infra-red spectrum. There is only one broad signal for the imidate CH_2 carbons (for *N*,*O*-coordination only a small change in chemical shift would be expected for the two carbons, relative to *N*-coordination).

The phthalimidate complex (**264d**) has only a single carbonyl and single methyl carbon signal but twice as many aromatic signals as would be expected (the signals have very similar chemical shifts) which is not consistent with bidentate *N*,*O*-binding (as confirmed

by the infra-red spectrum). There is also an additional broad signal at the base of the carbonyl carbon signal which may correspond to the extra aromatic peaks. The extra signals may be from an asymmetric structure, the different environments in a oligomeric or cluster structure, impurities such as uncoordinated ligands, residual free or coordinated acetate or different crystalline polymorphs or amorphous material of the same complex. The spectrum of the obs complex (**264e**) contains comparatively sharp signals suggesting a symmetric complex with a crystalline structure.

The tfs complex (**264b**) has a spectrum containing two carbonyl carbon peaks with similar chemical shifts (169.4 and 168.4 ppm) which is not consistent with *N*,*O*-bidentate binding (as confirmed by the infra-red spectrum) and there is only one signal for each MeCN carbon. The imidate *C*F_2 carbon signal is a broad multiplet, which is consistent with some C-F coupling.

Table 51. ^{13}C NMR carbon signals of [Pd(imidate)$_2$(L)$_2$] complexes.

Entry	Complex	^{13}C NMR chemical shift (ppm)		
		Imidate ligand *C*=O	$NCCH_3$ ligand N*C*	$NCCH_3$ ligand *C*H_3
1	[Pd(succ)$_2$(MeCN)$_2$][a] (**264a**)	194.4, 189.9, 188.6	125.4	2.7, 1.0
2	[Pd(tfs)$_2$(MeCN)$_2$][a] (**264b**)	169.4, 168.4	125.0	4.5
3	[Pd(mal)$_2$(MeCN)$_2$][a] (**264c**)	186.4, 181.8	126.0	4.9
4	[Pd(ptm)$_2$(MeCN)$_2$][a] (**264d**)	178.4	125.8	4.3
5	[Pd(obs)$_2$(MeCN)$_2$][a] (**264e**)	164.8	127.5	5.3
6	[Pd(succ)$_2$(THT)$_2$][b] (**265a**)	188.1		
7	[Pd(ptm)$_2$(THT)$_2$][b] (**265b**)	178.3		
8	[Pd(obs)$_2$(THT)$_2$][b] (**265c**)	166.2		
9	[Pd(succ)$_2$(PPh_3)$_2$][b] (**266a**)	186.5		
10	[Pd(mal)$_2$(PPh_3)$_2$][b] (**266b**)	179.9		
11	[Pd(ptm)$_2$(PPh_3)$_2$][b] (**266c**)	176.9		
12	[Pd(obs)$_2$(PPh_3)$_2$][b] (**266d**)	164.3		

[a] Solid state NMR (101 MHz). [b] $CDCl_3$ solution NMR (101 MHz).

^{31}P NMR spectroscopic analysis of the [Pd(imidate)$_2$(PPh_3)$_2$] complexes (**266**) gave a single *P*Ph_3 signal for each complex at 19.3-21.8 ppm (Table 52).

Table 52. ^{31}P NMR chemical shift of PPh_3 ligands in $[Pd(imidate)_2(PPh_3)_2]$ (**266**) complexes.

Entry	Complex	^{31}P NMR chemical shift (ppm)[a]
1	$[Pd(succ)_2(PPh_3)_2]$ (**266a**)	19.9
2	$[Pd(mal)_2(PPh_3)_2]$ (**266b**)	19.3
3	$[Pd(ptm)_2(PPh_3)_2]$ (**266c**)	19.8
4	$[Pd(obs)_2(PPh_3)_2]$ (**266d**)	21.8

[a] In $CDCl_3$ solution (109 MHz).

The mal (**266b**) and ptm (**266c**) complexes have the most upfield signals (19.3 and 19.8 ppm, respectively) which is surprising as the parent imides are more acidic than succinimide (**266a**) (19.9 ppm). This is however consistent with other reported series of palladium imidate complexes, such as, $[NBu_4][Pd\{C_4(COOMe)_4\}(imidate)(PPh_3)]$ (**267**) (Table 53) and $[Pd(imidate)(phox)(PPh_3)]$ (**268**), and the reported chemical shifts for the succ (**266a**) and ptm (**266c**) complexes (20.4 and 20.0 ppm, respectively, in $CDCl_3$ solution). The electron deficient obs complex (**266d**) has the most downfield signal (21.8 ppm). The chemical shifts of these complexes are lower than those reported for related Pd(II) imidate complexes, such as, $[PdBr(N\text{-succ})(PPh_3)_2]$ (**269**) (33.1 and 24.1 ppm) and $[PdCl(obs)(PPh_3)_2]$ (**270**) (24.1 ppm).

Table 53. ^{31}P NMR chemical shifts of PPh_3 ligands in reported palladium imidate complexes.

Entry	Complex	^{31}P NMR chemical shift (ppm)[a]
1	$[NBu_4][Pd\{C_4(COOMe)_4\}(succ)(PPh_3)]$[22] (**267a**)	28.7
2	$[NBu_4][Pd\{C_4(COOMe)_4\}(mal)(PPh_3)]$[22] (**267b**)	28.1
3	$[NBu_4][Pd\{C_4(COOMe)_4\}(ptm)(PPh_3)]$[22] (**267c**)	28.3
4	$[Pd(phox)(succ)(PPh_3)]$[21] (**268a**)	41.9
5	$[Pd(mal)(phox)(PPh_3)]$[21] (**268b**)	41.8
6	$[Pd(phox)(ptm)(PPh_3)]$[21] (**268c**)	41.9
7	*trans*-$[Pd(succ)_2(PPh_3)_2]$[17] (**266a**)	20.4
8	$[Pd(ptm)_2(PPh_3)_2]$[18] (**266c**)	20.0
9	*cis*-$[PdBr(succ)(PPh_3)_2]$[15] (**269**)	33.1 (d, J = 8.8 Hz), 24.1 (d, J = 8.8 Hz)
10	$[PdCl(obs)(PPh_3)_2]$[12] (**270**)	24.1

[a] In $CDCl_3$ solution.

^1H and ^{13}C NMR spectroscopic analysis of the THT ligands of $[Pd(imidate)_2(THT)_2]$ complexes (**265**) showed single sets of broad signals for the ligands suggesting monomeric symmetrical complexes (Table 54).

The ^1H and ^{13}C NMR signals of the CH_2 2 position of THT shift downfield in the order: obs > ptm > succ (by 0.14-0.22 and 5.4-5.8 ppm, respectively), when coordinated to Pd relative to the free ligand, whereas at the 3 position the signals shift upfield in the order: succ > ptm > obs (by 0.10-0.14 and 1.3-1.8 ppm, respectively). This is in agreement with reported $[NBu_4][Pd\{C_4(COOMe)_4\}(imidate)(THT)]$[22] complexes (**271**) reflecting the increased electron donation of succinimidate ligands relative to phthalimidate and especially *o*-benzoic sulfimidate.

Table 54. ^{1}H and ^{13}C NMR chemical shifts of THT ligands in [Pd(imidate)$_2$(THT)$_2$] (**265**) and related reported complexes.

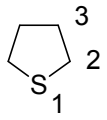

Entry	Compound	^{1}H NMR[a] shift (ppm)		^{13}C NMR[b] shift (ppm)	
		CH_2 2	CH_2 3	C2	C3
1	THT	2.82	1.94	31.8	31.2
2	[Pd(succ)$_2$(THT)$_2$] (**265a**)	2.96	1.92	37.2	29.9
3	[Pd(ptm)$_2$(THT)$_2$] (**265b**)	2.96	1.84	37.3	29.8
4	[Pd(obs)$_2$(THT)$_2$] (**265c**)	3.04	1.80	37.6	29.4
5	[NBu$_4$][Pd{C$_4$(COOMe)$_4$}(succ)(THT)][22] (**271a**)	2.93	1.86	35.1	30.2
6	[NBu$_4$][Pd{C$_4$(COOMe)$_4$}(mal)(THT)][22] (**271b**)	2.91	1.84	34.9	30.1
7	[NBu$_4$][Pd{C$_4$(COOMe)$_4$}(ptm)(THT)][22] (**271c**)	2.98	1.82	35.0	30.1

[a] In $CDCl_3$ solution (400 MHz). [b] In $CDCl_3$ solution (101 MHz).

ESI-mass spectra of the complexes (**264-266**) showed only the desired molecular ion peaks and fragment peaks from sequential loss of ligands. No signals corresponding to complexes containing residual acetate ligands were observed by high resolution ESI-MS.

4.2.1.3. Characterisation by IR spectroscopy

Infra-red spectroscopy is a useful tool for the analysis of palladium imidate complexes as the stretching frequency of the imidate ligand carbonyl bond is characteristic and provides information on the electron density on the coordinated Pd atom and the bonding mode (mono or bidentate) of the imidate. Infra-red spectra of the complexes were taken in the solid state and are displayed in Table 55.

Table 55. The infra-red absorbance frequencies of the imidate carbonyl groups in $[Pd(imidate)_2L_2]$ complexes (**264-266**).

Entry	$[Pd(imidate)_2L_2]$ imidate =	Imidate carbonyl stretching frequency (cm^{-1})[a] L =			
		MeCN	THT	PPh_3	Free imide
1	succ	1633	1632	1642	1683[72]
2	tfs	1716	-	-	1751
3	mal	1616 (1725)	-	1653	1705[73]
4	ptm	1660	1654	1661	1727[74]
5	obs	1686	1677	1675	1725[75]

[a] Solid state.

The bound imidate carbonyl stretching frequencies are 35-89 cm^{-1} lower than the free imides, consistent with related Au, Ru and other reported imidate complexes.[1,8,76] The frequencies are lower than related Au(I) (**55-57**) and Au(III) (**66-68**) imidate complexes (Chapter 2). The frequencies of the $[Pd(imidate)_2(MeCN)_2]$ (**264**) complexes span a large range of 100 cm^{-1} (1616-1717 cm^{-1}), in the order:

$$mal < succ < ptm < obs < tfs$$

The mal complex (**264c**) is anomalous as it has a lower stretching frequency than the succ complex (**264a**) and has the largest shift relative to the free imide. However, there is a second carbonyl stretching signal in the spectrum at 1725 cm^{-1} which is consistent with bidentate *N*,*O*-coordination of the maleimidate ligand to Pd as observed in $[NBu_4]_2[Pd(C_4\{COOMe\}_4(\mu\text{-}N,O\text{-mal})]_2$ (**243b**) (1714 and 1626 cm^{-1}), $[\{Pd(\mu\text{-}N,O\text{-mal})(phpy)\}_2]$ (**272**) (1724 and 1620 cm^{-1}) and $[\{Pd(\mu\text{-}N,O\text{-mal})(bzq)\}_2]$ (**273**) (1720 and 1614 cm^{-1}) (Table 56). Interestingly, the remaining complexes appear to have monodentate *N*-coordination of the imidate ligands to palladium (although the signal for the succinimidate carbonyl is broad suggesting several similar bonding modes). This is surprising given the low solubility of the complexes, although it is typical for $[Pd(imidate)_2(L)_2]$ species bearing two neutral donor ligands.[1,4,5,17]

The frequencies for the $[Pd(imidate)_2(THT)_2]$ complexes (**265**) are slightly lower than those for MeCN complexes (**264**) which is consistent with a more electron rich palladium atom. The frequencies follow the order: succ < ptm < obs, with a range of 45 cm^{-1} (1632-1677 cm^{-1}) as would be expected. The $[Pd(imidate)_2(PPh_3)_2]$ complexes (**266**) are in the

order: succ < mal < ptm < obs, with a range of 33 cm^{-1} (1642-1675 cm^{-1}), consistent with related Au(I) (**55-57**) and (III) (**66-68**) imidate complexes and the previously reported succ (**266a**)[1,17] and ptm (**266c**)[18] complexes. The frequencies are similar to those for the THT complexes (**265**). No pattern emerges when the PPh_3 series (**266**) is compared to the MeCN series (**264**) of complexes.

The stretching frequencies of these complexes are at higher wavenumbers than many reported Pd(II) imidate complexes, such as; *cis*-[PdBr(*N*-succ)$(PPh_3)_2$] (**269**) (1631 cm^{-1}), *trans*-[Pd(Ph)(*N*-succ)$(PPh_3)_2$] (**274a**) (1605 cm^{-1}), *trans*-[Pd(Ph)(*N*-tfs)$(PPh_3)_2$] (**274b**) (1673 cm^{-1}), *trans*-[Pd(Ph)(*N*-ptm)$(PPh_3)_2$] (**274c**) (1640 cm^{-1}), other than [Pd(C_6F_5)(*N*-mal)(L)] complexes, such as [Pd(C_6F_5)(*N*-mal)(tmeda)] (**275**) (1652 cm^{-1}) and [Pd(C_6F_5)(*N*-mal)(bipy)] (**244b**) (1660 cm^{-1}), which have slightly higher frequencies. This would suggest that the [Pd(imidate)$_2$(L)$_2$] complexes (**264-266**) are more electron deficient than these complexes other than those containing the highly electron withdrawing pentafluorophenyl ligands.

Table 56. Infra-red stretching frequencies of imidate carbonyl groups in Pd complexes reported in the literature.

Entry	Complex		Stretching Frequency (cm^{-1})
1	$[NBu_4]_2[Pd(C_4\{COOMe\}_4(\mu\text{-}N,O\text{-mal})]_2$[22]	(**243b**)	1714, 1626[a]
2	$[\{Pd(\mu\text{-}N,O\text{-mal})(phpy)\}_2]$[19]	(**272**)	1724, 1620[a]
3	$[\{Pd(bzq)(\mu\text{-}N,O\text{-mal})\}_2]$[20]	(**273**)	1720, 1614[a]
4	*trans*-[Pd(*N*-succ)$_2(PPh_3)_2$][1]	(**266a**)	1645[a]
5	[Pd(*N*-ptm)$_2(PPh_3)_2$][18]	(**266c**)	1663[c]
6	*cis*-[PdBr(*N*-succ)$(PPh_3)_2$][16a]	(**269**)	1631[b]
7	*trans*-[Pd(Ph)(*N*-succ)$(PPh_3)_2$][8]	(**274a**)	1605[b]
8	*trans*-[Pd(Ph)(*N*-tfs)$(PPh_3)_2$][8]	(**274b**)	1673[b]
9	*trans*-[Pd(Ph)(*N*-ptm)$(PPh_3)_2$][8]	(**274c**)	1640[b]
10	[Pd(C_6F_5)(*N*-mal)(tmeda)][23]	(**275**)	1652[a]
11	[Pd(C_6F_5)(*N*-mal)(bipy)][23]	(**244b**)	1660[a]

[a] Nujol mull. [b] KBr disk. [c] CH_2Cl_2 solution.

A plot of the carbonyl carbon ^{13}C NMR chemical shift against the carbonyl stretching frequency of the imidate ligands reveals that a reasonable linear correlation exists for the PPh_3 (**266**) and particularly the THT (**265**) complexes (Figure 54). For the MeCN analogues (**264**) the succ (**264a**), ptm (**264d**) and obs (**264e**) complexes also follow a linear correlation (although **264a** has multiple ^{13}C NMR signals), the tfs (**264b**) and mal (**264c**) complexes however do not. Complex **264c** is anomalous due to the apparent bidentate *N*,*O*-coordination of the imidate ligand, the reason for the divergence of complex **264b** is less clear.

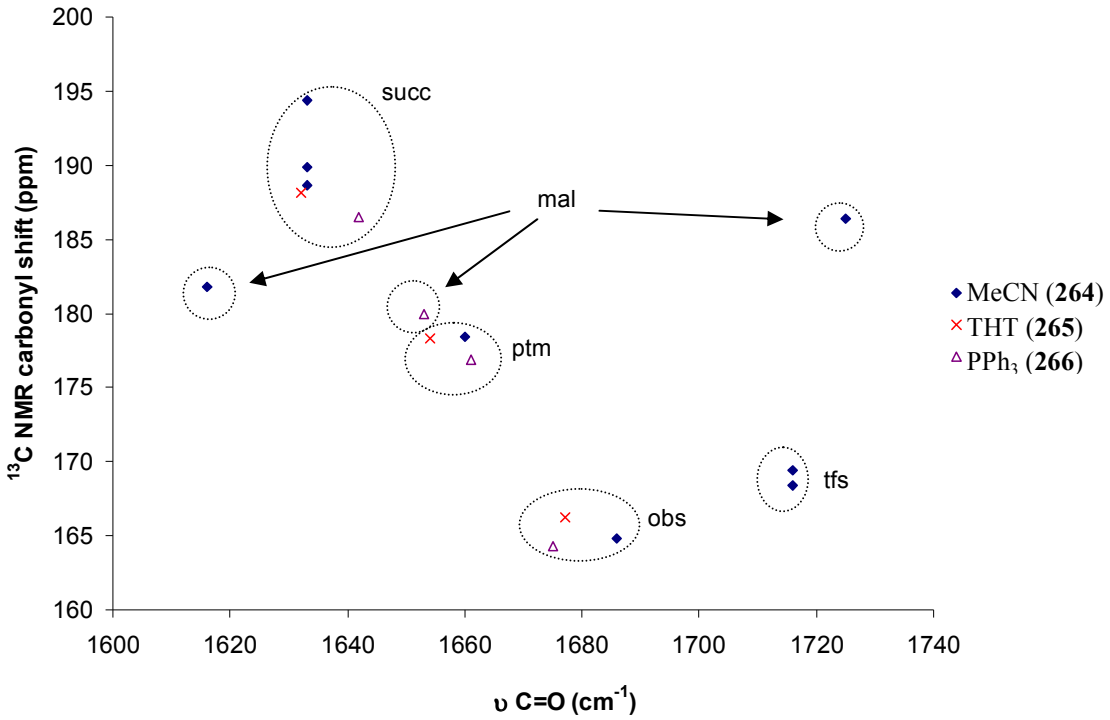

Figure 54. Comparison of $[Pd(imidate)_2(L)_2]$ (**264-266**) carbonyl carbon ^{13}C NMR chemical shift and carbonyl C=O stretching frequency.

4.2.2. Catalysis

4.2.2.1. Direct arylation of imidazole with 4-iodoanisole

Bellina *et al.*[40,41] have developed conditions for the direct arylation of unprotected imidazole (**276a**) with iodoarenes, such as 4-iodoanisole (**258a**), to afford 2-arylated imidazoles **(277**) in reasonable yields (Scheme 71). These conditions do not involve the use of intentionally added base, which is normally required for such reactions, or neutral ligands to stabilize the proposed Pd(0) active species.

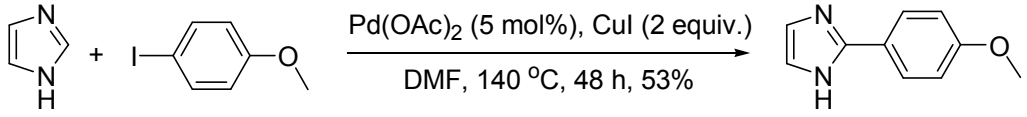

276a **258a** **277a**

Scheme 71. Direct arylation of imidazole (**276a**) with 4-iodoanisole (**258a**) to yield 2-[4-(methyloxy)phenyl]-1H-imidazole (**277a**).

The reaction of imidazole with 4-iodoanisole was used to compare the efficiency of $[Pd(imidate)_2(MeCN)_2]$ (**264**) and $[Pd(imidate)_2(THT)_2]$ (**265**) complexes against $Pd(OAc)_2$ (**247**) and $[Pd(OAc)_2(MeCN)_2]$ (**278**). This reaction was chosen as the moderate 53% yield achieved with **247** under harsh conditions allows for the identification of more active catalysts, the imidazole has three reactive C-H groups as well as the N-H group allowing the testing of selectivity and the exact mechanism and the active catalytic species are unknown.

The reaction was carried out in Radleys carousel apparatus under the reported conditions, with the reactions maintained under a flow of argon in analogy to the reported method (Table 57). No product was isolated using $Pd(OAc)_2$ (**247**), $[Pd(succ)_2(MeCN)_2]$ (**264a**), or $[Pd(ptm)_2(MeCN)_2]$ (**264d**) complexes, although low yields were recorded with tfs (**264b**) (12%), mal (**264c**) (27%) and obs (**264e**) (23%) analogues. The succ (**265a**) and ptm (**265b**) THT complexes were slightly more effective giving 7% and 15%, respectively, but the obs complex (**265c**) gave only 9%.

The complete inefficiency of the reaction with complex **247** is surprising, however it is possible that in these base- and ligand-free conditions the interactions of the DMF solvent may be critical. DMF or the dimethyl amine decomposition product (generated at high temperatures) may act as bases and ligands.[48,77] DMF has been shown to reduce Pd(II) to

colloidal palladium[78] by formation of either CO,[79] formic acid (which requires trace water)[80] or dimethylamine (with trace water)[81] (anaerobic conditions are required for reduction to prevent reoxidation).[82] DMF can also mediate the dehalogenation of aryl iodides and bromides.[83]

It has been observed within the Fairlamb research group[49] that the addition of piperidine to the Pd catalysed C8-phenylation of 2'-deoxyadenosine (**260**) has a beneficial effect. This is presumed to act as a less volatile mimic of the dimethylamine produced by DMF decomposition. Consequently, selected reactions were repeated with 0.1 equivalents (based on 2 mole equivalents of piperidine per Pd complex) and 0.4 equivalents (the optimum loading determined)[49] of added piperidine.

Using $Pd(OAc)_2$ (**247**) it was found that adding 0.1 equivalents of piperidine had a beneficial effect, giving a 25% yield, and using a preformed $[Pd(OAc)_2(piperidine)_2]$ complex (**279**) (reported by Storr *et al.*[49]) a similar 22% yield was achieved. Increasing the loading to 0.4 equivalents increased the yield to 33%. However, the piperidine had a inhibitory effect on the imidate complexes with reduced yields observed for tfs (**264b**) (11%), mal (**264c**) (5%) and obs (**264e**) (6%) complexes using 0.1 equivalents of piperidine, although with 0.4 equivalents a 19% yield was reported for **264c**.

Table 57. Isolated yields obtained in the Pd catalysed direct arylation of imidazole (**276a**) with 4-iodoanisole (**258a**) in unsealed Radleys carousel apparatus.[a]

Entry	Palladium source	Isolated yield (%)		
		0 equiv. piperidine	0.1 equiv. piperidine	0.4 equiv. piperidine
1	$Pd(OAc)_2$ (**247**)	0	25 (22)[b]	33
2	$[Pd(succ)_2(MeCN)_2]$ (**264a**)	0	-	-
3	$[Pd(tfs)_2(MeCN)_2]$ (**264b**)	12	11	-
4	$[Pd(mal)_2(MeCN)_2]$ (**264c**)	27	5	19
5	$[Pd(ptm)_2(MeCN)_2]$ (**264d**)	0	-	-
6	$[Pd(obs)_2(MeCN)_2]$ (**264e**)	23	6	-
7	$[Pd(succ)_2(THT)_2]$ (**265a**)	7	-	-
8	$[Pd(ptm)_2(THT)_2]$ (**265b**)	15	-	-
9	$[Pd(obs)_2(THT)_2]$ (**265e**)	9	-	-

[a] Conditions: 0.2 M solution of imidazole (**276a**) in DMF, 5 mol% Pd complex, 2 equiv. 4-iodoanisole (**258a**), 2 equiv. CuI, 135 ˚C (internal temp.), 48 h. [b] $[Pd(OAc)_2(Py)_2]$ (**279**).

From these results it is clear that the secondary amine aids the reaction mediated by $Pd(OAc)_2$ and so it can be postulated that in the absence of piperidine the formation of dimethylamine by decomposition of DMF is required for the reaction to proceed. Under the reaction conditions dimethylamine (boiling point of 7 ˚C) would be gaseous and so would be rapidly lost in the argon flow. In order to trap the amine the reactions were repeated with the vessels sealed. Under these conditions there was a significant increase in yield (Table 58). With $Pd(OAc)_2$ (**247**) a 33% yield was achieved, identical to that observed with 0.4 equivalents of piperidine, although this is significantly below the 53% reported by Bellina.[40] The imidate complexes also gave improved yields of 29-45%, other than an anomalous 0% yield for the tfs complex (**264b**). The electron deficient obs complex (**264e**) gave a promising 45%, mal (**264c**) 41%, ptm (**264d**) 34% and the more electron rich succ complex (**264a**) just 26%. The results appear to show that, at least for the MeCN imidate complexes, higher yields are achieved with complexes **264c** and **264e** relative to **264a**.

Table 58. Isolated yields obtained in the Pd catalysed direct arylation of imidazole (**276a**) with 4-iodoanisole (**258a**) in sealed Radleys carousel apparatus.[a]

Entry	Palladium source	Isolated yield (%)	
		Commercial laboratory	University laboratory
1	$Pd(OAc)_2$ (**247**)	33	57
2	$[Pd(OAc)_2(MeCN)_2]$ (**278**)	-	43
3	$[Pd(succ)_2(MeCN)_2]$ (**264a**)	26	35
4	$[Pd(ptm)_2(MeCN)_2]$ (**264d**)	34	-
5	$[Pd(mal)_2(MeCN)_2]$ (**264c**)	41	40
6	$[Pd(tfs)_2(MeCN)_2]$ (**264b**)	0	-
7	$[Pd(obs)_2(MeCN)_2]$ (**264e**)	45	49

[a] Conditions: 0.2 M solution of imidazole (**276a**) in DMF, 5 mol% Pd complex, 2 equiv. 4-iodoanisole (**258a**), 2 equiv. CuI, 135 ˚C (internal temp.), 48 h.

These initial results were obtained in a commercial chemistry laboratory (at GlaxoSmithKline laboratories in Harlow) and they were repeated in University laboratories (at the University of York). It was found that the yields were improved at the University laboratories with the highest yield of 57% achieved using $Pd(OAc)_2$ (**247**), comparable to the 53% reported by Bellina, 35% for succ (**264a**) and 49% for the obs complex (**264e**).

$[Pd(OAc)_2(MeCN)_2]$ (**278**) was also tested and a 43% yield observed, suggesting that MeCN ligands actually reduce the efficiency of the Pd complexes. There were a number of variables in the materials and conditions available in the commercial and University laboratories although in both cases Radleys carousel apparatus was used with the same vessel size and heating and stirring rates. Batches of the chemicals used were unchanged, however the DMF solvent batches (form commercial sources) were different, in the commercial laboratory DMF was purchased dry but not degassed and was degassed by bubbling argon through it, whilst in the University laboratory it was purchased dried and degassed. The sources of argon were also different which may have effected the levels of oxygen and water in the reactions. Product purification by column chromatography on silica-gel at the commercial laboratory was carried out using an automated Biotage SP4 system running a CH_2Cl_2/MeOH/NH_3 100/0/0 to 90/10/0.05 gradient solvent system, giving a better chromatographic separation than in the University laboratories where it was carried out manually.

In the University laboratory a series of experiments were carried out to probe the different results obtained in sealed and unsealed conditions and in commercial and University laboratories (Table 59). To test the observation that the reaction worked well in a sealed reaction vessel, the reactions using $Pd(OAc)_2$ (**247**) and the mal complex (**264c**) were carried out under rigorously dry and anaerobic conditions in fully sealed Schlenk tube apparatus, surprisingly only trace product was obtained (Entries 1 and 2). Presumably the Schlenk system is more completely sealed than the Radleys system suggesting a partially sealed system is required for the reaction to progress.

In order to determine why the reaction did not proceed in the Schlenk system, the possible effects of a partially-sealed system were explored using complex **247**. To test if O_2 was required for the reaction 30 ml of air was added *via* syringe, resulting in no product, as did brief exposure of the reaction to air (Entries 3 and 4). Water alone was also added (5 mol%) on the basis of reports which suggest trace water is required to reduce Pd(II) to Pd(0) (*via* formic acid formation[80] or in conjunction with dimethylamine),[81] however this only gave trace product (Entry 5). Changing the solvent to NMP, which has similar properties to DMF but does not as readily decompose, was also tried and again resulted in no product (Entry 6). A Cu(II), $Cu(OAc)_2$, rather than Cu(I) source was used with the same result (Entry 7). On the hypothesis that a moderate pressure of dimethylamine was required for the reaction the pressure was regulated, firstly by the use

of an argon balloon, giving trace product, and secondly using a mineral oil bubbler, which gave only 7% yield (Entries 8 and 9). To test the assumption that reduction of Pd(II) to Pd(0) is required for catalyst activation a Pd(0) source, [Pd(OMe-DBA)$_2$] (**280**) {OMe-DBA is di(4-methoxybenzylidene)acetone}, was used but once again gave only trace product (Entry 10). This reaction was repeated using the Radleys system and gave only a 35% yield, significantly less than the Pd(II) source Pd(OAc)$_2$ (Entry 11). Finally, Pd(0) nanoparticles {poly(*N*-vinyl-2-pyrrolidone, PVP, stabilised} (**281**) were tested in the Radleys system which gave a 67% yield, 10% higher than that achieved with Pd(OAc)$_2$ (Entry 12).

Table 59. Isolated yields obtained in the Pd catalysed direct arylation of imidazole (**276a**) with 4-iodoanisole (**258a**) under various conditions.[a]

Entry	Palladium source	Conditions	Yield (%)
1	Pd(OAc)$_2$ (**247**)		trace
2	[Pd(mal)$_2$(MeCN)$_2$] (**264c**)		trace
3	Pd(OAc)$_2$ (**247**)	30 ml air	0
4	Pd(OAc)$_2$ (**247**)	trace air	trace
5	Pd(OAc)$_2$ (**247**)	H_2O	trace
6	Pd(OAc)$_2$ (**247**)	NMP	0
7	Pd(OAc)$_2$ (**247**)	Cu(OAc)$_2$	0
8	Pd(OAc)$_2$ (**247**)	balloon	trace
9	Pd(OAc)$_2$ (**247**)	bubbler	7
10	[Pd(OMe-DBA)$_2$] (**280**)		trace
11	[Pd(OMe-DBA)$_2$][b] (**280**)		35
12	Nanoparticles[b] (**281**)		67

[a] Conditions: 0.2 M solution of imidazole (**276a**) in DMF, 5 mol% Pd complex, 2 equiv. 4-iodoanisole (**258a**), 2 equiv. CuI, 135 ˚C (internal temp.), 48 h in sealed Schlenk tube apparatus. [b] In Radleys carousel apparatus.

4.2.2.2. Direct arylation of imidazoles with iodoarenes

The most efficient mal imidate complex (**264c**) was used to compare to the benchmark Pd(OAc)$_2$ complex (**247**) with a range of other substrates in the sealed Radleys carousel system (in the commercial laboratory) (Table 60). Firstly the iodoarene was varied, iodobenzene (**258b**) gave a 50% yield of **277b** with **247** and 54% with **264c** compared to

the reported yield of 89%, displaying little difference between the complexes but the deficiency of the conditions. However, with 2-iodotoluene (**258c**) the complex **247** gave 55% and **264c** 46% which compare favourably with the literature yield of 47% of **277c**. With 4-trifluoromethyl iodobenzene (**258d**) yields of 68% and 60% were achieved with complexes **247** and **264c**, respectively, compared with an 84% literature yield of **277d**.[40]

Similar results were observed when the imidazole was varied. With 1-[4-(methyloxy)phenyl]-1H-imidazole (**276b**) the literature 66% yield of **277e** was replicated with complexes **247** (63%) and **264c** (66%). Benzimidazole (**276c**) was tested and yields of 69% and 72% of **277f** were observed with **247** and **264c**, respectively, slightly below the reported yield of 81%.[40,41]

Table 60. Isolated yields obtained in the Pd catalysed direct arylation of imidazoles with iodoarenes.[a]

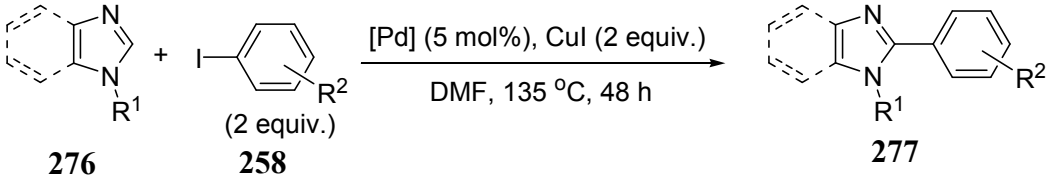

276 **258** **277**

Entry	Reactants		Product	Pd source	Yield (%)
	Imidazole	Iodoarene			
1	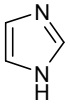 (**276a**)	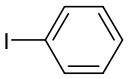 (**258b**)	**277b**	**247** **264c** Lit.[40]	50 54 89
2	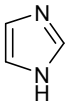 (**276a**)	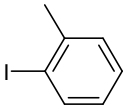 (**258c**)	**277c**	**247** **264c** Lit.[40]	55 46 47
3	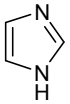 (**276a**)	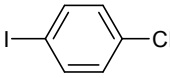 (**258d**)	**277d**	**247** **264c** Lit.[40]	68 60 84
4	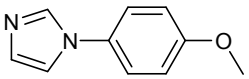 (**276b**)	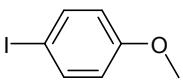 (**258a**)	**277e**	**247** **264c** Lit.[41]	63 66 66
5	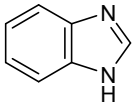 (**276c**)	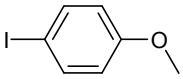 (**258a**)	**277f**	**247** **264c** Lit.[40]	69 72 81

[a] Conditions: 0.2 M solution of imidazole (**276**) in DMF, 5 mol% Pd complex, 2 equiv. iodoarene (**258**), 2 equiv. CuI, 135 ˚C (internal temp.), 48 hrs.

These experiments have shown that there is little difference in the yields obtained with $Pd(OAc)_2$ (**247**) or $[Pd(mal)_2(MeCN)_2]$ (**264c**) complexes as Pd sources. The reduced yield observed with $[Pd(OAc)_2(MeCN)_2]$ (**278**) suggests that lower yields obtained in the reaction of imidazole and iodoanisole using imidate complexes may be a consequence of the MeCN ligands. There did appear to be an effect of the nature of the imidate ligand on the outcome of this reaction, which may be attributable to the rate of reduction of the Pd(II) complex to an active Pd(0) species. The obs complex (**264e**) was most efficient, presumably as its ligand is derived from the most acidic imide which may aid its reduction to the catalytically active Pd(0) species. The mal complex (**264c**) was almost as efficient, despite the less electron withdrawing ligand, which may be related to the bidentate *N*,*O*-coordination of the imidate.

The succ complex (**264a**) was less effective as the more electron rich Pd atom would be less susceptible to reduction. The tfs complex (**264b**) was anomalous in many respects; it failed to precipitate from solution during synthesis, the phosphine analogue could not be prepared and analysis of the ^{13}C NMR chemical shifts and carbonyl bond stretching frequencies did not fit the linear correlation observed with other complexes. Adams *et al.*[8] have also reported that Pd(II) complexes containing tetrafluorosuccinimidate ligands can behave differently to other imidate complexes. This may explain why it was inactive in the sealed Radleys carousel apparatus.

The catalysis of the reaction by the Pd(0) source $[Pd(OMe\text{-}DBA)_2]$ (**280**) in Radleys carousel apparatus and by PVP-stabilised nanoparticles (**281**), as well as the minor differences observed with varied Pd(II) sources, indicates that the reaction proceeds by a Pd(0)/Pd(II) catalytic cycle in which the anionic ligands are not directly involved.

It was found that literature yields could generally be reproduced but only in 'sealed' Radleys carousel apparatus (and more effectively in the University laboratory) and that the apparatus used and the nature of the seal had a significant impact on yields. This may in part be explained by the processes involved in the generation and stabilisation of the catalytically active Pd(0) species. This requires reduction of the Pd(II) complexes to Pd(0) which could be achieved by the DMF[78] solvent *via* CO,[79] dimethylamine[81] or formic acid[80] formation. CO and dimethylamine are volatile species which may be lost in an unsealed reaction vessel. Formation of formic acid requires water, as may the reduction of Pd(II) by dimethylamine, the water may only be able to enter the reaction vessel if it is not completely sealed (such as in the Radleys apparatus), although addition of water to the

reactions did not have a beneficial effect. The addition of piperidine may play the same role as dimethylamine.

The exact nature of the active Pd(0) species in solution is unknown, it may be a monomeric $(L)_nPd(0)$ species (**282**) where L could be DMF, dimethylamine (or piperidine), MeCN or even imidazole ligands. However, in the absence of a strongly coordinating donor ligand (such as phosphine) Pd nanoparticles or clusters (**283**) (specifically surface defect sites)[84] could act as the Pd(0) species to which oxidative addition of arylhalide occurs followed by release of ArPd(II)X (**284**) into solution as a monomeric species.[85] Methoxy-DBA ligands stabilize the Pd(0) monomeric species (**282**) slowing down both oxidative addition and particularly cluster formation, explaining the reduced yields observed with this Pd source (Scheme 72).[85]

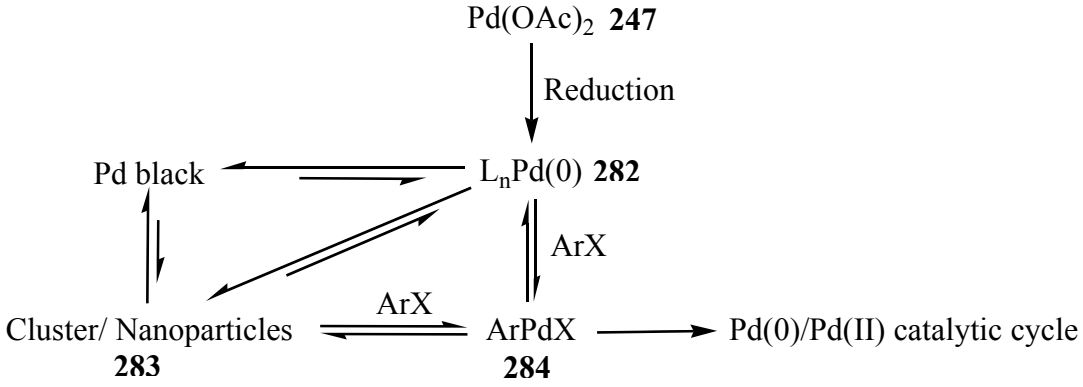

Scheme 72. Reduction of $Pd(OAc)_2$ (**247**) to form catalytically active Pd(0) species.

4.3. Conclusion

A series of [Pd(imidate)$_2$(MeCN)$_2$] (**264**) and [Pd(imidate)$_2$(THT)$_2$] (**265**) complexes have been prepared and characterised by IR and NMR spectroscopy. [Pd(imidate)$_2$(MeCN)$_2$] (**264**) complexes have low solubility but solid-state ^{13}C NMR and IR spectroscopy were found to be effective methods of characterisation. THT (**265**) and PPh_3 (**266**) Pd complexes possess monodentate imidate ligands, whereas [Pd(mal)$_2$(MeCN)$_2$] (**264c**) was found to have *N*,*O*-bidentate bound maleimidate ligands. Succinimidate (**264a**) and tetrafluorosuccinimidate (**264b**) complexes appeared to have asymmetric or multiple bonding modes by ^{13}C NMR spectroscopy but did not appear bidentate by IR spectroscopy.

The application of these complexes to base and ligand-free direct arylation of imidazole (**276a**) with 4-iodoanisole (**258a**) showed that the maleimidate (**264c**) and *o*-benzoic sulfimidate (**265e**) MeCN complexes were the most active and succinimidate (**264a**) the least. The differences in reactivity are likely to be a consequence of different rates of reduction to afford the active Pd(0) species. The substitution of acetate for imidate ligands in this process was not beneficial with the most active maleimidate complex (**264c**) possessing similar activity to Pd(OAc)$_2$ (**247**) in the direct arylation of substituted and unsubstituted imidazoles with iodoarenes. The [Pd(tfs)$_2$(MeCN)$_2$] complex (**264b**) was anomalous in terms of both spectroscopic characteristics (such as carbonyl stretching frequencies) and reactivity.

It was found that the direct arylation of imidazole (**276a**) with 4-iodoanisole (**258a**) under these conditions only proceeded in sealed Radleys carousel apparatus and not in unsealed Radleys or sealed Schlenk apparatus. The addition of sub-stoichiometric piperidine allowed the reaction to proceed under 'unsealed' conditions and variation of the Pd source revealed that the reaction proceeds most efficiently with PVP stabilised nanoparticles (**281**), but slower with [Pd(OMe-DBA)$_2$] (**280**). It is speculated that dimethylamine formed by DMF degradation is required for the reaction to occur and that trace water may also be required in order to aid in the reduction of the Pd(II) precatalyst to the suspected Pd(0) active catalyst. It is not known if the first step of the reaction mechanism proceeds *via* monomeric Pd(0) complexes or Pd(0) nanoparticles, although considering the ligand-free conditions and results observed, a mechanism involving Pd nanoparticles seems likely.

4.4. Future Work

The reason for the differences observed when direct arylation reactions are carried out under base and ligand-free conditions, in sealed and unsealed Radleys carousel and sealed Schlenk apparatus requires investigation. This may be achieved by studying the influence of the concentration of water and secondary amines on the reaction and the specific role played by DMF solvent. The identification of the active catalytic species and the mechanism of its formation will allow the design of improved and more reliable reaction conditions for 'base and ligand-free' processes and other related direct arylation reactions. It also has to be determined whether nanoparticles are involved in the reaction (either as a source of monomeric Pd(0) species or as the reactive species for oxidative addition).

Further analysis of $[Pd(imidate)_2(MeCN)_2]$ (**264**) complexes is required to accurately resolve their structure and bonding, particularly for the tetrafluorosuccinimidate (**264b**) and maleimidate (**264c**) complexes. As $[Pd(OAc)_2(MeCN)_2]$ (**278**) and imidate THT complexes (**266**) were less active than $Pd(OAc)_2$ (**247**) and MeCN (**264**) analogues, respectively, $[Pd(imidate)_2]$ complexes, without neutral ligands, should be prepared and tested in these reactions.

Although not beneficial in this particular process the activity of the imidate complexes (**264** and **265**) relative to $Pd(OAc)_2$ (**247**) should be examined in direct arylation reactions where Pd(II)/(IV) and anionic Pd(0)/(II) mechanisms, in which anionic ligands are integral to the mechanism, are suspected to be involved.

4.5. Experimental

4.5.1. General Details

Acetonitrile was dried by passing through a column of activated alumina, ethanol was distilled from sodium ethoxide. Dimethylformamide was either purchased dry and degassed from Acros or dry from Fischer and degassed by bubbling argon through it. Infra-red spectra were recorded on a Unicam Research Series FT-IR spectrometer. Mass spectrometry was carried out using a Bruker Daltronics micrOTOF or Waters Aquity Ultra Performance LC-MS instrument. ^{1}H, ^{13}C, ^{19}F and ^{31}P NMR spectra were collected on a JEOL ECX400 or Bruker Ultra Shield 400 spectrometer operating at 400, 101, 376 and 162 MHz, respectively, and referenced to residual solvent peaks. ^{13}C NMR signals are singlets unless otherwise stated. Solid-state ^{13}C NMR were collected on a Varian VNMRS spectrometer operating at 101 MHz by the EPSRC national service at the University of Durham. Melting points were measured in open capillary tubes using a Stuart SMP3 Digital Melting Point Apparatus and are uncorrected. All column chromatography was performed using silica-gel (mesh 220-440) purchased from Fluka Chemicals with the solvent systems specified within the text or using prepacked silica-gel columns in a Biotage SP4 automated flash chromatography system. TLC analysis was performed using Merck 5554 aluminium backed silica plates, compounds were visualised using UV light (254 nm) and a basic aqueous solution of potassium permanganate. Palladium(II) acetate was purchased from Precious Metals Online (www.precmet.com.au). All other chemicals were purchased from Sigma Aldrich Inc. or Alfa Aesar and used without further purification unless otherwise stated.

4.5.2. Compounds

$[Pd(succ)_2(MeCN)_2]$ (264a)

Succinimide (90.4 mg, 913 μmol, 2 equiv.) and $Pd(OAc)_2$ (**247**) (103 mg, 457 μmol, 1 equiv.) were placed in a Schlenk tube under an atmosphere of N_2. Acetonitrile (7 ml, dry) was added, the vessel sealed, and the mixture stirred for 15 hours at room temperature. A white precipitate formed which was separated by filtration, washed {acetonitrile, petroleum ether (40-60) and diethyl ether} and dried *in vacuo* to give the title compound as an off-white powder (101 mg, 264 μmol, 58%). ^{13}C NMR (101 MHz, solid) δ 194.4 (s, *C*O), 189.9 (s, *C*O), 188.6 (s, *C*O), 125.4 (br m, *C*N), 31.1 (s, succ *C*H_2), 2.7 (s, *C*H_3), 1.0 (s, *C*H_3). IR (solid, cm^{-1}) υ_{max} 2979 (m), 2921 (m), 2344 (w), 2314 (m), 2160 (br m), 2034

(m), 1978 (w), 1633 (br s), 1437 (w), 1416 (w), 1351 (s), 1284 (m), 1241 (s), 1219 (w), 1032 (w), 1003 (w), l814 (m), 663 (m). ESI^+-MS *m/z* 433.9 (1%), 407.0 (10%, $[MNa]^+$), 385.0 (6%, $[MH]^+$), 366.0 (4%, $[MNa\text{-}MeCN]^+$), 344.0 (10%, $[MH\text{-}MeCN]^+$), 324.9 (9%, $[MNa\text{-}2MeCN]^+$), 302.9 (2%, $[MH\text{-}2MeCN]^+$), 286.0 (100%, $[M\text{-}succ]^+$), 273.0 (10%). ESI^+-HRMS calcd. for $C_{12}H_{14}N_4NaO_4Pd$ ($[MNa]^+$) 406.9942; found 406.9943. Melting point 200 ˚C decomposes.

$[Pd(tfs)_2(MeCN)_2]$ (264b)

Tetrafluorosuccinimide (274 mg, 1.60 mmol, 2 equiv.) and $Pd(OAc)_2$ (**247**) (180 mg, 0.80 mmol, 1 equiv.) were placed in a Schlenk under an atmosphere of N_2, acetonitrile (7 ml, dry) was added, the vessel sealed and the reaction stirred for 15 hours at room temperature to give a pale orange solution. Diethyl ether and petroleum ether were added until a homogenous solution formed. The resultant white precipitate was separated by filtration, washed {cold acetonitrile, petroleum ether (40-60) and diethyl ether} and dried *in vacuo* to give the title compound as a light grey/white powder (181 mg, 343 μmol, 43%). ^{13}C NMR (101 MHz, solid) δ 169.4 (s, *C*O), 168.4 (s, *C*O), 125.0 (m, *C*N), 105.5 (br m, CF_2), 4.5 (s, *C*H_3). IR (solid, cm^{-1}) υ_{max} 3478 (w), 3007 (w), 2936 (w), 2371 (w), 2344 (m), 2317 (w), 2160 (br, m), 2034 (m), 1978 (w), 1784 (w), 1716 (s), 1703 (w), 1303 (s), 1190 (s), 1140 (s), 1063 (s), 1013 (s), 749 (m), 620 (m). ESI^+-MS *m/z* 550.9 (20%, $[MNa]^+$), 528.9 (100%, $[MH]^+$), 509.9 (7%, $[MNa\text{-}MeCN]^+$), 487.9 (5%, $[MH\text{-}MeCN]^+$), 467.9 (1%), 390.0 (7%), 357.9 (59%, $[M\text{-}tfs]^+$). ESI^+-HRMS calcd. for $C_{12}H_7F_8N_4O_4Pd$ ($[MH]^+$) 528.9373; found 528.9378. Anal. calcd. for $C_{12}H_6F_8N_4O_4Pd$ C 27.31, H 1.15, N 10.62; found C 27.10, H 1.21, N 10.27. Melting point 240 ˚C decomposes.

$[Pd(mal)_2(MeCN)_2]$ (264c)

A protocol similar to that used for **264a** gave the title compound as a light grey/white powder {from 168 mg, 0.750 mmol, of $Pd(OAc)_2$ (**247**) and 146 mg, 1.50 mmol, of maleimide} (183 mg, 481 ▫mol, 64%). ^{13}C NMR (101 MHz, solid) δ 186.4 (s, *C*O), 181.8 (s, *C*O), 138.6 (m, mal *C*H), 126.0 (m, *C*N), 4.9 (s, *C*H_3). IR (solid, cm^{-1}) ▫$_{max}$ 3080 (v. br s), 3079 (m), 2933 (m), 2161 (br m), 2033 (m), 1978 (w), 1725 (m), 1616 (br s), 1586 (w), 1359 (s), 1195 (s), 836 (m), 692 (m), 664 (w). ESI^+-MS *m/z* 403.0 (4%, $[MNa]^+$), 361.9 (14%, $[MNa\text{-}MeCN]^+$), 340.0 (38%, $[MH\text{-}MeCN]^+$), 320.9 (49%, $[MNa\text{-}2MeCN]^+$), 301.1 (4%), 284.0 (100%, $[M\text{-}Mal]^+$), 270.9 (44%), 242.9 (6%, $[M\text{-}Mal\text{-}MeCN]^+$). ESI^+-HRMS

calcd. for $C_{12}H_{10}N_4NaO_4Pd$ ([MNa]$^+$) 402.9634; found 402.9634. Melting point 140 ˚C decomposes.

[Pd(ptm)$_2$(MeCN)$_2$] (264d)

A protocol similar to that used for **246a** gave the title compound as a light grey/white powder {from 180 mg, 0.80 mmol, of $Pd(OAc)_2$ (**247**) and 235 mg, 1.60 mmol, of phthalimide} (252 mg, 525 □mol, 66%). ^{13}C NMR (101 MHz, solid) δ 178.4 (s, *C*O), 135.7 (s, aromatic *C*), 134.7 (s, aromatic *C*), 133.6 (s, aromatic *C*H), 130.2 (s, aromatic *C*H), 126.0 (m, *C*N), 121.3 (s, aromatic *C*H), 120.1 (s, aromatic *C*H), 4.30 (s, CH_3). IR (solid, cm^{-1}) □$_{max}$ 2971 (m), 2914 (m), 2345 (w), 2314 (m), 2160 (br m), 2032 (m), 1977 (w), 1660 (s), 1636 (w), 1606 (w), 1464 (w), 1417 (m), 1374 (m), 1349 (w), 1310 (m), 1284 (w), 1186 (m), 1175 (m), 1137 (s), 862 (m), 712 (s), 683 (w). ESI$^+$-MS *m/z* 503.0 (36%, [MNa]$^+$), 481.0 (29%, [MH]$^+$), 462.0 (8%, [MNa-MeCN]$^+$), 440.0 (13%, [MH-MeCN]$^+$), 421.0 (11%, [MNa-2MeCN]$^+$), 413.3 (8%), 375.0 (28%, [M-ptm+MeCN]$^+$), 334.0 (100%, [M-ptm]$^+$), 304.3 (17%), 249.2 (8%), 191.0 (21%). ESI$^+$-HRMS calcd. for $C_{20}H_{15}N_4O_4Pd$ ([MH]$^+$) 481.0123; found 481.0119. Melting point 220 ˚C decomposes.

[Pd(obs)$_2$(MeCN)$_2$] (264e)

A protocol similar to that used for **246a** gave the title compound as a light grey/white powder {from 205 mg, 913 μmol, of $Pd(OAc)_2$ (**247**) and 335 mg, 1.83 mmol, of *o*-benzoic sulfimide} (425 mg, 769 μmol, 84%). ^{13}C NMR (101 MHz, solid) δ 164.8 (s, *C*O), 141.1 (s, aromatic *C*), 134.3 (s, aromatic *C*H), 133.4 (s, aromatic *C*H), 130.3 (aromatic *C*), 127.5 (s, *C*N), 122.5 (s, aromatic CH), 119.8 (s, aromatic *C*H), 5.34 (s, *C*H$_3$). IR (solid, cm^{-1}) υ_{max} 3006 (w), 2937 (w), 2342 (m), 2160 (br m), 2033 (m), 1978 (w), 1686 (s), 1596 (w), 1457 (w), 1328 (w), 1298 (s), 1282 (s), 1241 (s), 1166 (s), 1147 (m), 1124 (m), 1056 (w) 1028 (m), 980 (s), 797 (m), 787 (m), 756 (m), 674 (m). ESI$^+$-MS *m/z* 575.0 (17%, [MNa]$^+$), 552.9 (22%, [MH]$^+$), 512.0 (7%, [MH-MeCN]$^+$), 477.9 (10%), 411.0 (26%, [M-obs+MeCN]$^+$), 369.9 (100%, [M-OBS]$^+$), 321.9 (17%), 233.0 (28%), 191.0 (16%). ESI$^+$-HRMS calcd. for $C_{18}H_{15}N_4O_6PdS_2$ ([MH]$^+$) 552.9462; found 552.9447. Anal. calcd. for $C_{18}H_{14}N_4O_6PdS_2$ C 38.78, H 2.51, N 10.05; found C 38.76, H 2.56, N 9.88. Melting point 220 ˚C decomposes.

[Pd(succ)$_2$(THT)$_2$] (265a)

[Pd(succ)$_2$(MeCN)$_2$] (**264a**) (97.4 mg, 254 μmol, 1 equiv.) was placed in a Schlenk tube under an atmosphere of N_2, ethanol (dry, 5 ml) and tetrahydrothiophene (45 μl, 510 μmol, 2 equiv.) were added and the mixture was stirred for 15 hours at room temperature. The resulting white precipitate was separated by filtration, washed {acetonitrile, petroleum ether (40-60) and diethyl ether} and dried *in vacuo* to give the title compound as a white powder (105 mg, 220 μmol, 87%). ^{1}H NMR (400 MHz, $CDCl_3$) δ 2.96 (br s, 8H, THT CH_2S), 2.61 (s, 8H, succ CH_2), 1.92 (m, 8H, THT CH_2CH$_2$). ^{13}C NMR (101 MHz, $CDCl_3$) δ 188.1 (succ *C*=O), 37.2 (THT *C*H$_2$S), 31.4 (succ *C*H$_2$), 29.9 (THT *C*H$_2$CH$_2$). IR (solid, cm^{-1}) υ_{max} 2963 (w), 2937 (m), 2863 (w), 2320 (w), 2161 (br m), 2033 (m), 1978 (w), 1632 (vs), 1462 (w), 1443 (w), 1340 (s), 1286 (m), 1271 (w), 1222 (s), 1077 (m), 1010 (w), 884 (w), 819 (w), 664 (m). ESI$^+$-MS *m/z* 541.9 (4%, [MNa+MeCN]$^+$), 501.0 (18%, [MNa]$^+$), 479.0 (20%, [MH]$^+$), 454.0 (27%, [MNa-THT+MeCN]$^+$), 413.0 (38%, [MNa-THT]$^+$), 391.0 (41%, [MH-THT]$^+$), 333.0 (17%, [M-succ-THT+MeCN]$^+$), 313.9 (15%), 292.0 (100%, [M-succ-THT]$^+$), 237.0 (11%), 222.9 (6%), 192.9 (3%). ESI$^+$-HRMS calcd. for $C_{16}H_{25}N_2O_4PdS_2$ (MH$^+$) 479.0290; found 479.0277. Anal. calcd. for $C_{16}H_{24}N_2O_4PdS_2$ C 40.08, H 5.01, N 5.85; found C 39.62, H 5.00, N 5.64. Melting point 180 ˚C decomposes.

[Pd(ptm)$_2$(THT)$_2$] (265b)

A protocol similar to that used for **265a** gave the title compound as a white powder (from 98.7 mg, 206 μmol, of **264d**) (61.0 mg, 106 μmol, 52%). ^{1}H NMR (400 MHz, $CDCl_3$) δ 7.70-7.65 (app. dd, *J* = 5.4 and 3.0 Hz, 4H, ptm aromatic C*H*), 7.57-7.53 (app. dd, *J* = 5.4 and 3.0 Hz, 4H, ptm aromatic C*H*), 2.96 (br s, 8H, THT CH_2S), 1.84 (m, 8H, THT CH_2CH$_2$). ^{13}C NMR (101 MHz, $CDCl_3$) δ 178.3 (ptm *C*=O), 136.1 (ptm aromatic *C*), 132.2 (ptm aromatic *C*), 121.5 (ptm aromatic *C*), 37.3 (THT *C*H$_2$S), 29.8 (THT *C*H$_2$CH$_2$). IR (solid, cm^{-1}) υ_{max} 3514 (m), 3455 (w), 2954 (w), 2938 (m), 2160 (br m), 2031 (m), 1978 (w), 1654 (s), 1631 (w), 1603 (w), 1463 (w), 1434 (m), 1352 (s), 1303 (s), 1268 (w), 1175 (m), 1126 (s), 1073 (w), 882 (w), 860 (m), 720 (s), 680 (w). ESI$^+$-MS *m/z* 597.0 (3%, [MNa]$^+$), 575.0 (6%, [MH]$^+$), 550.0 (3%, [MNa-THT+MeCN]$^+$), 509.0 (4%, [MNa-THT]$^+$), 487.0 (6%, [MH-THT]$^+$), 440.0 (3%, [MH-2THT+MeCN]$^+$), 381.0 (2%, [M-ptm-THT+MeCN]$^+$), 361.9 (6%), 340.0 (100%, [M-ptm-THT]$^+$). ESI$^+$-HRMS calcd. for $C_{24}H_{25}N_2O_4PdS_2$ ([MH]$^+$) 575.0293; found 575.0292. Melting point 180 ˚C decomposes.

[Pd(obs)$_2$(THT)$_2$] (265c)

A protocol similar to that of **265a** was used to give the title compound as a white powder (from 103 mg, 187 μmol, of **264e**) (104 mg, 160 μmol, 86%). ^{1}H NMR (400 MHz, $CDCl_3$) δ 7.92-7.89 (m, 2H, obs aromatic C*H*) 7.86-7.83 (m, 2H, obs aromatic C*H*) 7.72-7.67 (m, 4H, obs aromatic C*H*), 3.04 (br s, 8H, THT CH_2S), 1.80 (s, 8H, THT CH_2CH$_2$). ^{13}C NMR (101 MHz, $CDCl_3$) δ 166.2 (obs *C*=O), 142.5 (obs aromatic *C*), 133.1 (obs aromatic *C*), 133.0 (obs aromatic *C*), 130.1 (obs aromatic *C*), 123.9 (obs aromatic *C*), 120.3 (obs aromatic *C*), 37.6 (THT *C*H$_2$S), 29.4 (THT *C*H$_2$CH$_2$). IR (solid, cm^{-1}) υ_{max} 2937 (w), 2160 (br m), 2029 (m), 1978 (w), 1677 (s), 1595 (w), 1463 (m), 1441 (w), 1339 (w), 1297 (s), 1282 (m), 1233 (s), 1160 (s), 1123 (m), 1056 (w), 970 (s), 788 (m), 748 (m), 678 (m). ESI$^+$-MS *m/z* 621.9 (4%, [MNa-THT+MeCN]$^+$), 600.0 (12%, [MH-THT+MeCN]), 580.9 (2%), 552.9 (4%), 505.0 (4%, [M-obs+MeCN]$^+$), 484.9 (2%), 458.0 (8%), 417.0 (100%, [M-obs-THT+MeCN]$^+$), 397.9 (4%), 369.9 (16%), 328.0 (8%), 280.0 (46%), 234.0 (48%), 194.9 (2%). Anal. calcd. for $C_{22}H_{24}N_2O_6PdS_4$ C 40.67, H 3.70, N 4.31; found C 40.13, H 3.65, N 4.38. Melting point 190 ˚C decomposes.

[Pd(*N*-succ)$_2$(PPh$_3$)$_2$] (266a)

[Pd(succ)$_2$(MeCN)$_2$] (**264a**) (50.0 mg, 130 μmol, 1 equiv.) and PPh$_3$ (68.2 mg, 260 μmol, 2 equiv.) were mixed in $CDCl_3$ (10 minutes, r.t.) and NMR spectra taken. The solution was reduced to dryness *in vacuo* for ESI-MS and IR analysis. ^{1}H NMR (400 MHz, $CDCl_3$) δ 7.84-7.78 (m, 12H, Ph aromatic C*H*), 7.43-7.33 (m, 18H, Ph aromatic C*H*), 1.44 (s, 8H, succ CH_2). ^{13}C NMR (101 MHz, $CDCl_3$) δ 186.5 (succ *C*=O), 134.8 (t, *J* = 7 Hz, Ph aromatic *o*-*C*), 130.6 (Ph aromatic *p*-*C*), 129.3 (t, *J* = 24 Hz, Ph aromatic *i*-*C*), 127.9 (t, 5 Hz, Ph aromatic *m*-*C*), 30.4 (succ *C*H$_2$). ^{31}P NMR (162 MHz, $CDCl_3$) δ 19.9 (s). IR (solid, cm^{-1}) υ_{max} 3050 (w), 2926 (w), 2537 (br m), 2372 (w), 2160 (s), 2030 (m), 1977 (m), 1642 (vs), 1572 (w), 1482 (w), 1433 (s), 1348 (m), 1307 (w), 1279 (m), 1231 (s), 1190 (w), 1120 (w), 1092 (m), 743 (m), 693 (s), 656 (m). ESI$^+$-MS *m/z* 849.1 (23%, [MNa]$^+$), 827.1 (85%, [MH]$^+$), 769.1 (100%, [M-succ+MeCN]$^+$), 728.1 (55%, [M-succ]$^+$), 629.1 (6%), 579.2 (8%), 466.0 (13%, [M-succ-PPh$_3$]$^+$), 385.1 (3%), 339.0 (6%), 301.0 (16%). ESI$^+$-HRMS calcd. for $C_{44}H_{39}N_2O_4P_2Pd$ ([MH]$^+$) 827.1430; found 827.1423. Data in accordance with the literature.[1,17]

[Pd(*N*-mal)$_2$(PPh$_3$)$_2$] (266b)

A protocol similar to that of **266a** was used (from 13.2 mg, 34.7 μmol, of **264c**). ^{1}H NMR (400 MHz, $CDCl_3$) δ 7.76-7.71 (m, 12H, Ph aromatic C*H*), 7.39-7.29 (m, 18H, Ph aromatic C*H*), 5.69 (s, 4H, mal C*H*). ^{13}C NMR (101 MHz, $CDCl_3$) δ 179.9 (mal *C*=O), 136.0 (Ph aromatic *p*-*C*), 134.9 (t, *J* = 6.6 Hz, Ph aromatic *o*-*C*), 130.6 (mal *C*H), 129.3 (t, *J* = 23.8 Hz, Ph aromatic *i*-*C*), 128.2 (t, *J* = 5.2 Hz, Ph aromatic *m*-*C*). ^{31}P NMR (162 MHz, $CDCl_3$) δ 19.3 (s). IR (solid, cm^{-1}) υ_{max} 3085 (w), 2356 (w), 2159 (m), 2036 (w), 1966 (w), 1653 (s), 1482 (m), 1434 (m), 1342 (s), 1183 (m), 1093 (m), 998 (w), 830 (m), 740 (m), 691 (s). ESI$^+$-MS *m/z* 845.1 (68%, $[MNa]^+$), 823.1 (96%, $[MH]^+$), 767.1 (100%, $[M\text{-}Mal+MeCN]^+$), 726.1 (69%, $[M\text{-}Mal]^+$), 629.1 (4%), 583.0 (12%, $[MNa\text{-}PPh_3]^+$), 464.0 (18%, $[M\text{-}Mal\text{-}PPh_3]^+$), 339.1 (9%), 315.0 (4%), 301.1 (10%). ESI$^+$-HRMS calcd. for $C_{44}H_{34}N_2NaO_4P_2Pd$ ($[MNa]^+$) 845.0936; found 845.0926.

[Pd(*N*-ptm)$_2$(PPh$_3$)$_2$] (266c)

A protocol similar to that of **266a** was used (from 40.2 mg, 83.6 μmol, of **264d**). ^{1}H NMR (400 MHz, $CDCl_3$) δ 7.77-7.71 (m, 12H, Ph aromatic C*H*), 7.19-7.09 (m, 22H, ptm and Ph aromatic C*H*), 7.07-7.04 (m, 4H, ptm aromatic C*H*). ^{13}C NMR (101 MHz, $CDCl_3$) δ 176.9 (ptm *C*=O), 136.7 (ptm aromatic C*H*), 134.8 (t, *J* = 7 Hz, Ph aromatic *o*-*C*), 130.5 (Ph aromatic *p*-*C*), 130.3 (ptm aromatic C*H*), 129.2 (t, *J* = 24 Hz, , Ph aromatic *i*-*C*), 128.0 (t, *J* = 5 Hz, Ph aromatic *m*-*C*), 120.2 (ptm aromatic C*H*). ^{31}P NMR (162 MHz, $CDCl_3$) δ 19.8 (s). IR (solid, cm^{-1}) υ_{max} 3054 (w), 2529 (br m), 2372 (w), 2161 (s), 2029 (s), 1977 (s), 1661 (vs), 1633 (m), 1606 (m), 1573 (w), 1482 (m), 1462 (w), 1435 (s), 1370 (m), 1356 (m), 1303 (s), 1282 (w), 1176 (m), 1122 (m), 1097 (m), 1073 (w), 999 (w), 860 (w), 743 (w), 721 (m), 691 (s). ESI$^+$-MS *m/z* 945.1 (19%, $[MNa]^+$), 923.1 (100%, $[MH]^+$), 817.1 (10%, $[M\text{-}ptm+MeCN]^+$), 776.1 (13%, $[M\text{-}ptm]^+$), 683.0 (3%), 639.2 (3%), 514.0 (6%, $[M\text{-}ptm\text{-}PPh_3]^+$), 301.0 (6%). ESI$^+$-HRMS calcd. for $C_{52}H_{39}N_2O_4P_2Pd$ ($[MH]^+$) 923.1432; found 923.1445. Data in accordance with the literature.[18]

[Pd(*N*-obs)$_2$(PPh$_3$)$_2$] (266d)

A protocol similar to that of **266a** was used (from 21.0 mg, 38 μmol, of **264e**). ^{1}H NMR (400 MHz, $CDCl_3$) δ 7.93-7.87 (m, 12H, Ph aromatic C*H*), 7.32-7.29 (m, 4H, obs and Ph aromatic C*H*), 7.24-7.12 (m, 20H, obs and Ph aromatic C*H*), 6.97 (d, *J* = 7.6 Hz, 2H, obs aromatic C*H*). ^{13}C NMR (101 MHz, $CDCl_3$) δ 164.3 (obs *C*=O), 143.0 (obs aromatic *C*),

135.4 (t, J = 7 Hz, Ph aromatic *o*-*C*), 131.2 (obs aromatic *C*), 131.1 (obs aromatic *C*), 130.9 (obs aromatic *C*), 130.5 (Ph aromatic *p*-*C*), 129.3 (t, J = 25 Hz, Ph aromatic *i*-*C*), 127.6 (t, J = 5 Hz, Ph aromatic *m*-*C*), 122.7 (obs aromatic *C*), 118.8 (obs aromatic *C*). ^{31}P NMR (162 MHz, $CDCl_3$) δ 21.8 (s). IR (solid, cm^{-1}) υ_{max} 2358 (w), 2160 (m), 2018 (m), 1675 (s), 1435 (s), 1309 (s), 1244 (m), 1173 (s), 1153 (s), 1098 (m), 958 (s), 794 (m), 747 (s), 693 (s). ESI$^+$-MS *m/z* 1118.1 (1%), 1017.1 (2%, $[MNa]^+$), 857.2 (16%), 812.1 (30%, $[M\text{-obs}]^+$), 764.1 (2%), 697.1 (18%), 656.1 (33%), 579.1 (28%), 550.0 (16%, $[M\text{-obs-}PPh_3]^+$), 445.0 (2%), 339.1 (100%, $[PPh_4]^+$), 301.1 (28%, $[OPPh_3Na]^+$). ESI$^+$-HRMS calcd. for $C_{50}H_{38}N_2NaO_6P_2PdS_2$ ($[MNa]^+$) 1017.0590; found 1017.0612.

General procedure for the direct arylation of imidazole (276a) with 4-iodoanisole (258a).

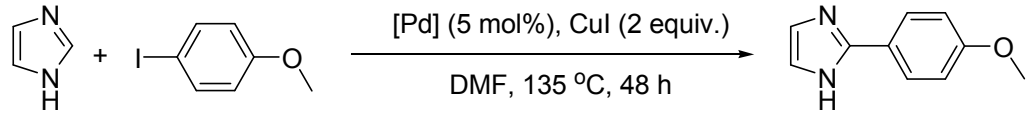

258a **276a** **277a**

Based on a protocol reported by Bellina *et al.*.[40] Imidazole (34.0 mg, 0.500 mmol, 1 equiv.), 4-iodoanisole (234 mg, 1.0 mmol, 2 equiv.), palladium precatalyst (25 μmol, 0.05 equiv) and copper(I) iodide (190 mg, 1.00 mmol, 2 equiv.) were added to a Radleys carousel or Schlenk tube under a stream of argon. The flask was evacuated and filled with argon three times and dry, degassed *N*,*N*-dimethylformamide (DMF) (purchased dry from Acros or Fischer) (2.5 ml) was added *via* syringe. The apparatus was sealed and stirred at 135 ºC (internal temperature) for 48 hours. After cooling to ambient temperature the reaction was diluted with ethyl acetate (10 ml) and poured into a saturated solution of ammonium chloride (10 ml). This was stirred (30 mins) and the organic layer was extracted three times with ethyl acetate. The organic phase was washed (water, 10 ml), dried ($MgSO_4$), filtered and reduced in *vacuo* to give a brown oil. The crude product was added to a silica-gel Biotage SP4 column, eluting with CH_2Cl_2/MeOH/NH_3 100/0/0 to 90/10/0.05 v/v/v, or purified manually by column chromatography on silica-gel. Fractions containing the product by UV visualisation were combined and the solvent removed *in vacuo* to give the title compound as a white powder.

General procedure for the direct arylation of heteroarenes (276) with iodoarenes (258).

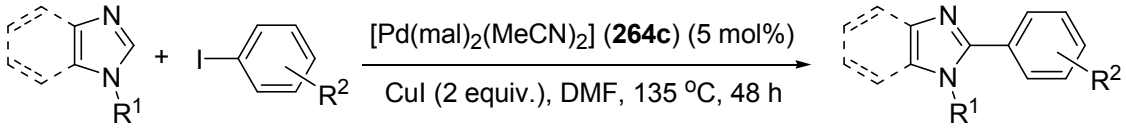

276 **258** **277**

Based on a protocol reported by Bellina *et al.*.[40] The heteroarene (0.500 mmol, 1 equiv.) (if solid), iodoarene (1.00 mmol, 2 equiv.), $[Pd(mal)_2(MeCN)_2]$ (**264c**) (9.5 mg, 25 μmol, 0.05 equiv.) and copper(I) iodide (190 mg, 1.00 mmol, 2 equiv.) were added to a Radleys™ carousel tube under a stream of argon. The flask was evacuated and filled with argon three times and dry, degassed *N*,*N*-dimethylformamide (purchased dry from Fischer) (2.5 ml) (and heteroarene if liquid) was added *via* syringe. The apparatus was sealed and stirred at 135 ºC (internal temperature) for 48 hours. After cooling to ambient temperature, the reaction was diluted with ethyl acetate (10 ml) and poured into a saturated solution of ammonium chloride (10 ml). This was stirred (30 mins) and then the organic layer was extracted three times with ethyl acetate. The organic phase was washed (water, 10 ml), dried ($MgSO_4$), filtered and reduced in *vacuo* to give a brown oil. The crude product was added to a silica-gel Biotage SP4 column and eluted with CH_2Cl_2/MeOH/NH_3 100/0/0 to 90/10/0.05 v/v/v. Fractions containing the product by UV visualisation were combined and the solvent removed *in vacuo* to give the title compound as a white powder.

2-[4-(Methyloxy)phenyl]-1*H*-imidazole (277a)

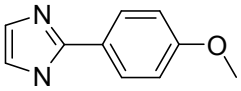

Prepared using the general procedure to give the title compound as a white powder {from 34.0 mg, 0.500 mmol, of imidazole (**258a**) and 234 mg, 1.00 mmol, of 4-iodoanisole (**276a**)} (36.1 mg, 0.207 mmol, 41%). ^{1}H NMR (400 MHz, MeOD) δ 7.77 (app. d, J = 8.9 Hz, 2H, phenyl C*H*), 7.07 (s, 2H, imidazole C*H*), 6.97 (app. d, J = 8.9 Hz, 2H, phenyl C*H*), 3.80 (s, 3H, OCH_3). ^{13}C NMR (101 MHz, MeOD) δ 161.6, 148.1, 127.8, 124.1, 123.4, 115.2, 55.7. ESI$^+$-MS *m/z* 174.97 (100%, $[MH]^+$). ESI$^-$-MS *m/z* 173.01 (100%, $[M-H]^-$). Data in accordance with the literature.[40]

2-Phenyl-1*H*-imidazole (277b)

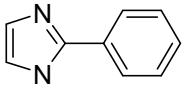

Prepared using the general procedure to give the title compound as a white powder {from 34.0 mg, 0.500 mmol, of imidazole (**276a**) and 0.111 ml, 1.00 mmol, of iodobenzene (**258b**)} (39.1 mg, 0.271 mmol, 54%). ^{1}H NMR (400 MHz, MeOD) δ 7.87-7.84 (m, 2H, aromatic C*H*), 7.45-7.40 (m, 2H, aromatic C*H*), 7.34 (m, 1H, aromatic C*H*), 7.12 (s, 2H, imidazole C*H*). ^{13}C NMR (101 MHz, MeOD) δ 148.0, 131.5, 129.9, 129.7, 126.3 (one peak overlapping). ESI^{+}-MS *m/z* 144.95 (100%, $[MH]^{+}$). ESI^{-}-MS *m/z* 142.99 (100%, $[M-H]^{-}$). Data in accordance with the literature.[40]

2-(2-Methylphenyl)-1*H*-imidazole (277c)

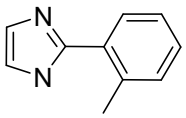

Prepared using the general procedure to give the title compound as a white powder {from 34.0 mg, 0.500 mmol, of imidazole (**276a**) and 0.127 ml, 1.00 mmol, of 1-iodo-2-methylbenzene (**258c**)} (35.2 mg, 0.223 mmol, 46%). ^{1}H NMR (400 MHz, MeOD) δ 7.44 (m, 1H, phenyl C*H*), 7.33-7.22 (m, 3H, phenyl C*H*), 7.13 (s, 2H, imidazole C*H*), 2.41 (s, 3H, CH_3). ^{13}C NMR (101 MHz, MeOD) δ 148.2, 137.9, 131.9, 131.8, 130.5, 130.0, 126.9, 123.5, 20.5. ESI^{+}-MS *m/z* 159.01 (100%, $[MH]^{+}$). ESI^{-}-MS *m/z* 242.75 (11%), 180.96 (18%), 157.01 (100%, $[M-H]^{-}$). Data in accordance with the literature.[40]

2-[4-(Trifluoromethyl)phenyl]-1*H*-imidazole (277d)

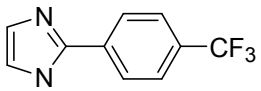

Prepared using the general procedure {from 34.0 mg, 0.500 mmol, of imidazole (**276a**) and 0.147 ml, 1.00 mmol, of 4-iodobenzotrifluoride (**258d**)} to give the title compound as a white powder (63.5 mg, 0.299 mmol, 60%). ^{1}H NMR (400 MHz, MeOD) δ 8.04-8.00 (m, 2H, phenyl C*H*), 7.75-7.71 (m, 2H, phenyl C*H*), 7.19 (s, 2H, imidazole C*H*). ^{13}C NMR (101 MHz, MeOD) δ 126.7 (s), 126.9 (q, J = 4 Hz), 131.2 (q, J = 33 Hz), 135.0 (q, J = 1.3 Hz), 146.3 (s), 125.6 (q, J = 272 Hz) (one peak overlapping). ESI^{+}-MS *m/z* 212.97 (100%, $[MH]^{+}$). ESI^{-}-MS *m/z* 210.96 (100%, $[M-H]^{-}$), 112.81 (23%). Data in accordance with the literature.[40]

1,2-Bis[4-(methyloxy)phenyl]-1*H*-imidazole (277e)

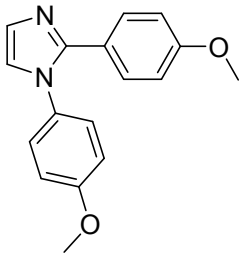

Prepared using the general procedure to give the title compound as a white powder {from 87.0 mg, 0.500 mmol, of 1-[4-(methyloxy)phenyl]-1H-imidazole (**276b**) and 234 mg, 1.00 mmol, of 4-iodoanisole (**258a**)} (97.6 mg, 0.331 mmol, 66%). ^{1}H NMR (400 MHz, MeOD) δ 7.26-7.21 (m, 3H, aromatic C*H*), 7.13-7.10 (m, 3H, aromatic C*H*), 6.94-6.91 (m, 2H, aromatic C*H*), 6.82-6.79 (m, 2H, aromatic C*H*), 3.78 (s, 3H, OCH_3), 3.72 (s, 3H, OCH_3). ^{13}C NMR (101 MHz, MeOD) δ 161.5, 161.0, 148.3, 132.4, 131.2, 128.5, 128.4, 124.2, 123.5, 115.7, 114.8, 56.0, 55.7. ESI$^+$-MS *m/z* 280.98 (100%, [MH]$^+$). ESI$^-$-MS *m/z* 248.96 (16%), 154.78 (100%). Data in accordance with the literature.[41]

2-[4-(Methyloxy)phenyl]-1*H*-imidazole (277f)

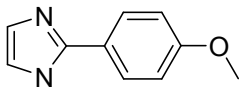

Prepared using the general procedure {from 59.1 mg, 0.500 mmol of benzimidazole (**276c**) and 234 mg, 1.00 mmol, of 4-iodoanisole (**258a**)} to give the title compound as an off-white powder (94.5 mg, 0.358 mmol, 72%). ^{1}H NMR (400 MHz, MeOD) δ 8.02-7.98 (m, 2H, aromatic C*H*), 7.58-7.53 (m, 2H, aromatic C*H*), 7.23-7.19 (m, 2H, aromatic C*H*), 7.06-7.02 (m, 2H, aromatic C*H*), 3.83, (s, 3H, OCH_3). ^{13}C NMR (101 MHz, MeOD) δ 162.9, 153.4, 129.4, 123.6, 123.4, 115.5, 114.7, 55.9 (one peak overlapping). ESI$^+$-MS *m/z* 225.00 (100%, [MH]$^+$). ESI$^-$-MS *m/z* 222.94 (100%, [M-H]$^-$), 207.91 (10%). Data in accordance with the literature.[40]

4.6. References

(1) Roundhill, D. M. *Inorg. Chem.* **1970**, *9*, 254-258.

(2) Louey, M.; Nichols, P. D.; Robson, R. *Inorg. Chim. Acta* **1981**, *47*, 87-96.

(3) Yamamoto, T.; Sano, K.; Yamamoto, A. *Chem. Lett.* **1982**, 907-910.

(4) Sharma, C. L.; Mishra, V. P. *Acta Chim. Hung.* **1983**, *114*, 3-8.

(5) Sharma, C. L.; Narvi, S. S. *Acta Chim. Hung.* **1986**, *123*, 107-114.

(6) Komorita, S.; Yamada, S. *Synth. React. Inorg. Met.-Org. Chem.* **1984**, *14*, 485-500.

(7) Kurosawa, H.; Urabe, A.; Miki, K.; Kasai, N. *Organometallics* **1986**, *5*, 2002-2008.

(8) Adams, H.; Bailey, N. A.; Briggs, T. N.; McCleverty, J. A.; Colquhoun, H. M.; Williams, D. J. *J. Chem. Soc., Dalton Trans.* **1986**, 813-819.

(9) Colquhoun, H. M.; Fairman, R. A.; Tootell, P.; Williams, D. J. *J. Chem. Soc., Dalton Trans.* **1999**, 2651-2652.

(10) Islam, M. S.; Roy, R. K.; Miah, M. A. J. *Synth. React. Inorg. Met.-Org. Chem.* **1991**, *21*, 869-880.

(11) Michalska, D.; Morzyk, B.; Wojciechowski, W.; Glowiak, T. *Inorg. Chim. Acta* **1996**, *248*, 159-166.

(12) Henderson, W.; Nicholson, B. K.; McCaffrey, L. J. *Inorg. Chim. Acta* **1999**, *285*, 145-148.

(13) Shimomura, H.; Komorita, S.; Kuma, H.; Kushi, Y. *Chem. Lett.* **1992**, 913-914.

(14) Aresta, M.; Giannoccaro, P.; Tommasi, I.; Dibenedetto, A.; Lanfredi, A. M. M.; Ugozzoli, F. *Organometallics* **2000**, *19*, 3879-3889.

(15) Serrano, J. L.; Zheng, Y.; Dilworth, J. R.; Sánchez, G. *Inorg. Chem. Commun.* **1999**, *2*, 407-410.

(16) (a) Crawforth, C. M.; Burling, S.; Fairlamb, I. J. S.; Taylor, R. J. K..; Whitwood, A. C. *Chem. Commun.* **2003**, 2194-2195; (b) Fairlamb, I. J. S.; Taylor, R. J. K.; Serrano, J. L.; Sanchez, G. *New J. Chem.* **2006**, *30*, 1695-1704.

(17) Fairlamb, I. J. S.; Kapdi, A. R.; Lynam, J. M.; Taylor, R. J. K.; Whitwood, A. C. *Tetrahedron* **2004**, *60*, 5711-5718.

(18) Chaignon, N. M.; Fairlamb, I. J. S.; Kapdi, A. R.; Taylor, R. J. K.; Whitwood, A. C.; *J. Mol. Catal. A Chem*. **2004**, *219*, 191-200.

(19) Serrano, J. L.; Garcia, L.; Perez, J.; Perez, E.; Vives, J.; Sánchez, G.; López, G.; Molins , E.; Orpen, A. G. *Polyhedron* **2002**, *21*, 1589-1596.

(20) Fairlamb, I. J. S.; Kapdi, A. R.; Lee, A. F.; Sanchez, G.; Lopez, G.; Serrano, J. L.; Garcia, L.; Perez, J.; Perez, E. *Dalton Trans.* **2004**, 3970-3981.

(21) Serrano, J. L.; Garcia, L.; Perez, J.; Perez, E.; Garcia, J.; Sanchez, G.; Lopez, G.; Fairlamb, I. J. S.; Liu, M. *Polyhedron* **2008**, *27*, 1699-1706.

(22) Serrano, J. L.; Fairlamb, I. J. S.; Sanchez, G.; Garcia, L.; Perez, J.; Vives, J.; Lopez, G.; Crawforth, C. M.; Taylor, R. J. K. *Eur. J. Inorg. Chem*. **2004**, 2706-2715.

(23) Ruiz, J.; Vicente, C.; Cutillas, N.; Perez, J. *Dalton Trans.* **2005**, 1999-2006.

(24) Ramesh Kumar, N. S. C.; Raj, I. V. P.; Sudalai, A. *J. Mol. Catal. A Chem.* **2007**, *269*, 218-224.

(25) Whitfield, S. R.; Sanford, M. S. *J. Am. Chem. Soc.* **2007**, *129*, 15142-15143.

(26) (a) Dick, A. R.; Hull, K. L.; Sanford, M. S. *J. Am. Chem. Soc.* **2004**, *126*, 2300-2301; (b) Kalyani, D.; Dick, A. R.; Anani, W. Q.; Sanford, M. S. *Tetrahedron* **2006**, *62*, 11483-11498.

(27) (a) Ames, D. E.; Bull, D. *Tetrahedron* **1982**, *38*, 383-387; (b) Ames, D. E.; Opalko, A. *Synthesis* **1983**, 234-235; (c) Ames, D. E.; Opalko, A. *Tetrahedron* **1984**, *40*, 1919-1925.

(28) (a) Ackermann, L.; Vincent, R.; Kapdi, A. R. *Angew. Chem., Int. Ed.* **2009**, *48*, 9792-9826; (b) McGlacken, G. P.; Bateman, L. M. *Chem. Soc. Rev.* **2009**, *38*, 2447-2464; (c) Alberico, D; Scott, M. E.; Lautens, M. *Chem. Rev.* **2007**, *107*, 174-238.

(29) (a) Bringmann, G.; Pabst, T.; Henschel, P.; Kraus, J.; Peters, K.; Peters, E.-M.; Rycroft, D. S.; Connolly, J. D. *J. Am. Chem. Soc.* **2000**, *122*, 9127-9133; (b) Ohmori, K.; Tamiya, M.; Kitamura, M.; Kato, H.; Oorui, M.; Suzuki, K. *Angew. Chem., Int. Ed.* **2005**, *44*, 3871-3874; (c) Kitamura, M.; Ohmori, K.; Kawase, T.; Suzuki, K. *Angew. Chem., Int. Ed.* **1999**, *38*, 1229-1232.

(30) Bringmann, G.; Ochse, M.; Götz, R. *J. Org. Chem.* **2000**, *65*, 2069-2077.

(31) Herrmann, W. A.; Brossmer, C.; Öfele, K.; Reisinger, C.-P.; Priermeier, T.; Beller, M.; Fischer, H. *Angew. Chem., Int. Ed.* **1995**, *34*, 1844-1848.

(32) (a) Jensen, M. S.; Hoerrner, R. S.; Li, W.; Nelson, D. P.; Javadi, G. J.; Dormer, P. G.; Cai, D.; Larsen, R. D. *J. Org. Chem.* **2005**, *70*, 6034-6039; (b) Cameron, M.; Foster, B. S.; Lynch, J. E.; Shi, Y.-J.; Dolling, Y.-H. *Org. Process Res. Dev.* **2006**, *10*, 398-402; (c) Goodacre, S. C.; Hallett, D. J.; Carling, R. W.; Castro, J. L.; Reynolds, D. S.; Pike, A.; Wafford, K. A.; Newman, R.; Atack, J. R.; Street, L. J. *Bioorg. Med. Chem. Lett.* **2006**, *16*, 1582-1585. (d) Humphries, A. C.; Gancia, E.; Gilligan, M. T.; Goodacre, S.; Hallett, D.; Merchant, K. J.; Thomas, S. R. *Bioorg. Med. Chem. Lett.* **2006**, *16*, 1518-1522.

(33) Gauthier, D. R., Jr.; Limanto, J.; Devine, P. N.; Desmond, R. A.; Szumigala, R. H., Jr.; Foster, B. S.; Volante, R. P. *J. Org. Chem.* **2005**, *70*, 5938-5945.

(34) (a) Akita, Y.; Inoue, A.; Yamamoto, K.; Ohta, A.; Kurihara, T.; Shimizu, M. *Heterocycles* **1985**, *23*, 2327-2333; (b) Akita, Y.; Itagaki, Y.; Takizawa, S.; Ohta, A. *Chem. Pharm. Bull.* **1989**, *37*, 1477-1480.

(35) Pivsa-Art, S.; Satoh, T.; Kawamura, Y.; Miura, M.; Nomura, M. *Bull. Chem. Soc. Jpn.* **1998**, *71*, 467-473.

(36) Pivsa-Art, S.; Fukui, Y.; Miura, M.; Nomura, M. *Bull. Chem. Soc. Jpn*. **1996**, *69*, 2039-2042.

(37) Touré, B. B.; Lane, B. S.; Sames, D. *Org. Lett.* **2006**, *8*, 1979-1982.

(38) Bellina, F.; Cauteruccio, S.; Mannina, L.; Rossi, R.; Viel, S. *J. Org. Chem.* **2005**, *70*, 3997-4005.

(39) Bellina, F.; Cauteruccio, S.; Mannina, L.; Rossi, R.; Viel, S. *Eur. J. Org. Chem*. **2006**, 693-703.

(40) Bellina, F.; Cauteruccio, S.; Rossi, R. *Eur. J. Org. Chem*. **2006**, 1379-1382.

(41) Bellina, F.; Calandri, C.; Cauteruccio, S. Rossi, R. *Tetrahedron*, **2007**, *63*, 1970-1980.

(42) Besselièvre, F.; Mahuteau-Betzer, F.; Grierson, D.; Piguel, S. *J. Org.Chem.* **2008**, *73*, 3278-3280.

(43) Huang, J.; Chan, J.; Chen, Y.; Borths, C. J.; Baucom, K. D.; Larsen, R. D.; Faul, M. M. *J. Am. Chem. Soc.* **2010**, *132*, 3674-3675.

(44) Kondo, Y.; Komine, T.; Sakamoto, T. *Org. Lett.* **2000**, *2*, 3111-3113.

(45) (a) Čerňa, I.; Pohl, R.; Klepetářová, B;. Hocek, M. *Org. Lett.* **2006**, *8*, 5389-5392; (b)Čerňa, I.; Pohl, R.; Klepetářová, B.; Hocek, M. *J. Org. Chem.* **2008**, *22*, 9048-9054.

(46) Čerňa, I.; Pohl, R.; Hocek, M. *Chem. Commun.* **2007**, *45*, 4729-4730.

(47) Storr, T. E.; Firth, A. G.; Wilson, K.; Darley, K.; Baumann, C. G.; Fairlamb, I. J. S. *Tetrahedron* **2008**, *64*, 6125-6137.

(48) Mutzart, J. *Tetrahedron* **2009**, *65*, 8313-8323.

(49) Storr, T. E.; Baumann, C. G.; Thatcher, R. J.; De Ornellas, S.; Whitwood, A. C.; Fairlamb, I. J. S. *J. Org. Chem.* **2009**, *74*, 5810-5821

(50) Seregin, I. V.; Gevorgyan, V. *Chem. Soc. Rev.* **2007**, *36*, 1173-1193.

(51) Zollinger, H. *Adv. Phys. Org. Chem.* **1964**, *2*, 163-200.

(52) (a) Hennessy, E. J.; Buchwald, S. L. *J. Am. Chem. Soc.* **2003**, *125*, 12084-12085; (b) Mota, A. J.; Dedieu, A.; Bour, C.; Suffert, J. *J. Am. Chem. Soc.* **2005**, *127*, 7171-7182; (c) Davies, D. L.; Donald, S. A.; Macgregor, S. A. *J. Am. Chem. Soc.* **2005**, *127*, 13754-13755.

(53) (a) Hughes, C. C.; Trauner, D. *Angew. Chem., Int. Ed.* **2002**, *41*, 1569-1572; (b) Lane, B. S.; Brown, M. A.; Sames, D. *J. Am. Chem. Soc.* **2005**, *127*, 8050-8057.

(54) (a) Campo, M. A.; Huang, Q.; Yao, T.; Tian, Q.; Larock, R. C. *J. Am. Chem. Soc.* **2003**, *125*, 11506-11507; (b) Capito, E.; Brown, J. M.; Ricci, A. *Chem. Commun.* **2005**, 1854-1856.

(55) Lafrance, M. Fagnou, K. *J. Am. Chem. Soc.* **2006**, *128*, 16496-16497.

(56) Campeau, L.-C.; Thansandote, P.; Fagnou, K. *Org. Lett.* **2005**, *7*, 1857-1860.

(57) Zhao, D.; Wang, W.; Lian, S.; Yang, F.; Lan, J.; You, J. *Chem. Eur. J.* **2009**, *15*, 1337-1340.

(58) Campo, M. A.; Larock, R. C. *J. Am. Chem. Soc.* **2002**, *124*, 14326-14327.

(59) Gorelsky, S. I.; Lapointe, D.; Fagnou, K. *J. Am. Chem. Soc.* **2008**, *130*, 10848-10849.

(60) Caron, L.; Campeau, L.-C.; Fagnou, K. *Org. Lett.* **2008**, *10*, 4533-4536.

(61) Campeau, L.-C.; Bertrand-Laperle, M.; Leclerc, J.-P.; Villemure, E.; Goreslky, S.; Fagnou, K. *J. Am. Chem. Soc.* **2008**, *130*, 3276-3277.

(62) Lebrasseur, N.; Larrosa, I. *J. Am. Chem. Soc.* **2008**, *130*, 2926-2927.

(63) (a) Sehnal, P; Taylor, R. J. K.; Fairlamb, I. J. S. *Chem. Rev.* **2010**, *110*, 824-889; (b) Fairlamb, I. J. S. *Tetrahedron* **2005**, *61*, 9661-9662.

(64) Kalyani, D.; Deprez, N. R.; Desai, L. V.; Sanford, M. S. *J. Am. Chem. Soc.* **2005**, *127*, 7330-7331.

(65) Deprez, N. R.; Kalyani, D.; Krause, A.; Sanford, M. S. *J. Am. Chem. Soc.* **2006**, *128*, 4972-4973.

(66) (a) Daugulis, O.; Zaitsev, V. G. *Angew. Chem., Int. Ed.* **2005**, *44*, 4046-4048; (b) Shabashov, D.; Daugulis, O. *Org. Lett.* **2006**, *8*, 4947-4949.

(67) Lazareva, A.; Daugulis, O. *Org. Lett.* **2006**, *8*, 5211-5213.

(68) Shabashov, D.; Daugulis, O. *Org. Lett.* **2005**, *7*, 3657-3659.

(69) (a) Amatore, C.; Jutand, A. *Acc. Chem. Res.* **2000**, *33*, 314-321; (b) Amatore, C.; Jutand, A. *J. Organomet. Chem.* **1999**, *576*, 254-278; (c) Amatore, C.; Azzabi M.; Jutand, A. *J. Organomet. Chem.* **1989**, *363*, C41-C45.

(70) Amatore, C.; Azzabi M.; Jutand, A. *J. Am. Chem. Soc.* **1991**, *113*, 8375-8384.

(71) Amatore, C.; Jutand, A.; Lemaître, F.; Ricard, J. L.; Kozuch, S.; Shaik, S. *J. Organomet. Chem.* **2004**, *689*, 3728-3734.

(72) Hulme, A. T.; Johnston, A.; Florence, A. J.; Fernandes, P.; Shankland, K.; Bedford, C. T.; Welch, G. W. A.; Sadiq, G.; Haynes, D. A.; Motherwell, W. D. S.; Tocher, D. A.; Price, S. L. *J. Am. Chem. Soc.* **2007**, *129*, 3649-3657.

(73) Barnes, A. J.; Le Gall, L.; Madec, C.; Lauransan, J. *J. Mol. Struct.* **1977**, *38*, 109-120.

(74) Krishnakumar, V.; Balachandran, V.; Chithambarathanu, T. *Spectrochim. Acta A* **2005**, *62*, 918-925.

(75) Jovanovski, G.; Spotrajanov, B. *J. Mol. Struct.* **1988**, *174*, 467-472.

(76) Carturan, G.; Belluco. V.; Grazini, M.; Ros, R. *J. Organomet. Chem.* **1976**, *112*, 243-248.

(77) (a) Amatore, C.; Catellani, M.; Deladda, S.; Jutand, A.; Motti, E. *Organometallics* **2008**, *27*, 4549-4554; (b) Álvarez, R.; Pérez, M.; Faza, O. N.; de Lera, A. R. *Organometallics* **2008**, *27*, 3378-3389; (c) Jutand, A. *Chem. Rev*. **2008**, *108*, 2300-2347; (d) Aresta, M.; Pastore, C.; Giannoccaro, P.; Kovács, G.; Dibenedetto, A.; Pápai, I. *Chem. Eur. J.* **2007**, *13*, 9028-9034.

(78) Serp, P.; Hernandez, M.; Richard, B.; Kalck, P. *Eur. J. Inorg. Chem.* **2001**, 2327-2336.

(79) Tsuji, J.; Mandai, T. *Synthesis* **1996**, 1-24.

(80) (a) Pletnev, A. A.; Tian, Q.; Larock, R. C. *J. Org. Chem.* **2002**, *67*, 9276-9287; (b) Cacchi, S.; Felici, M.; Pietroni, B. *Tetrahedron Lett.* **1984**, *25*, 3137-3140.

(81) (a) Penalva, V.; Lavenot, L.; Gozzi, C.; Lemaire, M. *Appl. Catal. A: Gen.* **1999**, *182*, 399-405; (b) Grushin, V. V.; Alper, H. *Organometallics* **1993**, *12*, 1890-1901.

(82) El Kaïm, L.; Gamez-Montaño, R.; Grimaud, L.; Ibarra-Rivera, T. *Chem. Commun.* **2008**, 1350-1352.

(83) (a) Zawisza, A. M.; Muzart, J. *Tetrahedron Lett.* **2007**, *48*, 6738-6742; (b) Satyanarayana, G.; Maier, M. E. *J. Org. Chem.* **2008**, *73*, 5410-5415; (c) Kim, H. S.; Gowrisankar, S.; Kim, S. H.; Kim, J. N. *Tetrahedron Lett.* **2008**, *49*, 3858-3861; (d) Kim, H. S.; Lee, H. S.; Kim, S. H.; Kim, J. N. *Tetrahedron Lett.* **2009**, *50*, 3154-3157.

(84) Ellis, P. J.; Fairlamb, I. J. S.; Hackett, S. F. J.; Wilson, K.; Lee, A. F. *Angew. Chem., Int. Ed.* **2010**, *49*, 1820-1824.

(85) Fairlamb, I. J. S.; Kapdi, A. R.; Lee, A. F.; McGlacken, G. P.; Weissburger, F.; de Vries, A. H. M.; Schmieder-van de Vondervoort, L. *Chem. Eur. J.* **2006**, *12*, 8750 - 8761.

5. Conclusion

In summary, imidate anions have incorporated into stable complexes of Au(I), Au(III), Pd(II) and Ru(II). The succinimidate, maleimidate and phthalimidate ligands displayed similar reactivity during the synthesis of imidate organometallic compounds, forming stable Au(I) (**55-57**) and Au(III) (**66-68**) complexes bearing I^{t}Bu, I^{t}Pe and IMes ligands but not Ru alkylidene or benzylidene complexes (due to destabilisation of the carbene ligand). However, although the three ligands all formed complexes bearing MeCN and PPh_3 ligands with Pd(II), the maleimidate complex $[Pd(mal)_2(MeCN)_2]$ (**264c**) appeared to have bidentate *N*,*O*-coordinated imidate ligands, the succinimidate analogue (**264a**) appeared to have multiple monodentate and bidentate coordination modes and the phthalimidate complex (**264d**) a monodentate *N*-coordination mode.

The tetrafluorosuccinimidate and *o*-benzoic sulfimidate (and to an lesser degree 2,3-dibromosuccimidate) ligands reacted differently to succ, mal and ptm. They formed stable Au(I) complexes bearing I^{t}Bu (**55**), I^{t}Pe (**56**) and IMes (**57**) ligands but only formed stable Au(III) complexes bearing I^{t}Bu (**66**) and I^{t}Pe (**67**) and not IMes ligands. Additionally, the reaction of the Au(III) (*pseudo*)halide complexes (**66-68**) with Ag salts (as observed by AgBr precipitation) appeared to follow the pK_a of the parent imide/acid, with succ and bromide complexes reacting very rapidly and tfs and obs complexes very slowly. The tfs ligand (dbs and obs ligands were not tested) formed a stable (although air sensitive) Ru benzylidene complex, [Ru(*N*-tfs)$_2$(*o*-^{i}PrO-CHPh)(IMesH$_2$)] (**217**), unlike succ, mal and ptm ligands. The tfs ligand also reacted differently with Pd, the acetonitrile complex $[Pd(tfs)_2(MeCN)_2]$ (**264b**), which appeared to possess multiple monodentate *N*-coordination modes, did not spontaneously precipitate from the reaction solution during synthesis and failed to react with triphenylphosphine. The obs ligand however behaved analogously to the succ, mal and ptm ligands, with spontaneous precipitation of the acetonitrile complex (**264e**) from the reaction solution, forming a monomeric, monodentate *N*-coordinated complex, which reacted with PPh_3 to form the expected phosphine complex (**266d**).

By using a range of substituted imidate ligands it has been possible to monitor the electronic impact of the ligands on the metal centre and ancillary ligands by NMR spectroscopy. It was found that succ, mal and ptm ligands have relatively similar electronic properties, such as σ and π bonding parameters, which is reflected in the impact of the

imidate ligands on the NMR signals of the ancillary ligands. Generally of the three ligands ptm is the least electron-donating and succ the most, although due to the similarity of the ligands this trend was not always reflected in NMR chemical shifts values {for example, with the ^{31}P NMR signals of *P*Ph$_3$ ligands in [Pd(imidate)$_2$(PPh$_3$)$_2$] complexes (**266**)}. These three ligands were found to have comparable electronic properties to bromide and chloride analogues in Au(I) (**55-57**) and Au(III) (**66-68**) complexes.

The tfs and obs ligands (and dbs) are much less electron-donating than the other imidates causing large shifts in the NMR signals of the ancillary ligands relative to halide parent complexes. The tetrafluorosuccinimidate ligand consistently reduced the electron density of coordinated metal atoms and ancillary ligands more than the obs ligand. The reported pK_a of 2.1 for tetrafluorosuccinimide was found not to correlate with the electronic effect of the conjugate base as a ligand. The calculated value of -10.0 was found to be a more accurate reflection of the electronic properties (although it is unlikely to reflect the solution phase acidity of the parent imide) which were similar to those of $^{-}O_3SCF_3$.

X-Ray diffraction studies of crystals of the complexes showed that there were no significant differences in bond lengths between analogous imidate complexes {with the exception of a longer metal-imidate bond in the Ru(III) complex [Ru(*N*-tfs)$_3$(IMesH$_2$)(OH$_2$)$_2$] (**229**)}. There was also little difference between the imidate complexes and the halide parent complexes, although the metal-imidate bond length was shorter by 0.24-0.27 Å than directly analogous metal bromide and chloride bonds. The Ru-imidate bond length in [Ru(*N*-tfs)$_2$(*o*-^{i}PrO-CHPh)(IMesH$_2$)] (**217**) was found to be similar to the Ru-O_3SCF_3 bond length in [Ru(O_3SCF_3)$_2$(*o*-^{i}PrO-CHPh)(IMesH$_2$)] (**224**).

The catalytic activity of the imidate complexes only partially reflected the pK_a of the parent imide. The activity of the Au(III) complexes (**66-68**) in cycloisomerisation processes was found to follow the order:

$$\text{mal} > \text{dbs} \geq \text{obs} > \text{tfs} > \text{ptm} > \text{succ} \geq \text{Br}$$

The most electron donating succ and ptm ligands were more active than the parent bromide but less active than the more electron-withdrawing obs and tfs complexes. However, mal, dbs and obs complexes were all more active than the tfs complex. The activity of the mal complexes is particularly surprising, suggesting intermediate basicity of the imidate ligand is required for optimal activity. However, in tandem nucleophillic

substitution-cycloisomerisation processes, which rely on Lewis acidity as well as cycloisomerisation ability, the activity reflected the pK_a of the parent imide:

tfs > dbs > mal > ptm > succ

The Ru benzylidene complex [Ru(*N*-tfs)$_2$(*o*-^{i}PrO-CHPh)(IMesH$_2$)] (**217**) was found to be inactive in diene metathesis processes, whilst the parent dichloride possesses high activity. In this case the tfs ligand appears to be too electron-withdrawing, preventing the formation of the active catalyst by dissociation of the isopropoxy ligand.

The activity of the Pd(II) complexes (**264** and **265**) in direct arylation processes in some ways reflected the effects of the imidate ligands in Au(III)-catalysed cycloisomerisation processes. The succ (**264a**) and ptm (**264d**) complexes were once again the least and the mal (**264c**) and obs (**264e**) complexes the most active, with similar activity to the parent diacetate (**247**). The tfs complex (**264b**) behaved anomalously and was found to be inactive under the most reliable reaction conditions. The role of the basicity of the imidate ligands in the activity may be reflected in the ease of reduction of the complexes to catalytically active Pd(0) species. The relatively high activity of the mal complex (**264c**) despite the moderate pK_a of the parent imide may be caused by the bidentate *N*,*O*-coordination mode of the imidate ligand in this complex. The lack of activity of the tfs complex (**264b**) may be a consequence of its reduced reactivity, reflected in its failure to form a phosphine complex.

Relative to parent bromide complexes, imidate ligands impart greater stability to Au(III) precatalysts (**66**-**68**) and catalysts resulting in improved yields in cycloisomerisation processes (particularly with maleimidate) and the facilitation of the unique nucleophillic substitution-cycloisomerisation reaction (with tetrafluorosuccinimidate) that was not possible with Au(I) and Au(III) bromide analogues. This study highlights the benefits, particularly in terms of stability, of using pseudohalide ligands in Au(III) catalysis, as well as expanding the small number of Au(III) organometallic precatalysts reported.

Imidate ligands either destabilised (succ, mal and ptm) or deactivated (tfs) Ru alkylidene and benzylidene complexes in diene metathesis reactions, and so were clearly not beneficial in this case. The synthesis of an imidate Ru complex however expands the library of known Ru benzylidene pseudohalide complexes, which contains few anions ligated *via* nitrogen. The lack of catalytic activity of the Ru tfs complex (**217**) and the synthetic challenges uncovered with the attempted synthesis of other Ru imidate

complexes demonstrates the limitations of anionic ligand exchange in these complexes but helps to define the range of pK_a values of the anionic ligands for which the catalysts are stable and active.

Imidate ligands were also not beneficial to Pd catalysed direct arylation processes, under the 'base and ligand-free' conditions, relative to the parent acetate complex (**247**). However, there was an effect of the nature of the imidate ligand on the activity of the complexes which may be applicable to other direct arylation processes. The underlying research into the 'base and ligand' free reaction conditions has uncovered more reliable reaction conditions, as well as going someway towards uncovering the active catalyst identity and mechanism of formation in these reactions.

This project has reinforced the validity of imidate ligands as pseudohalides, which should lead to the screening of this range of anions, in conjunction with other pseudohalides, as ligands for further transition metal mediated processes. The highly electron-withdrawing tetrafluorosuccinimidate ligand (and *o*-benzoic sulfimidate as a cheap and stable alternative), as an alternative to commonly used perfluorocarboxylate ligands, and the maleimidate ligand, which has been shown to generate very active catalysts, in particular should prove beneficial.

A1. Appendix 1: Studies to determine the catalytically active species in Au(III) mediated processes

A1.1. Stoichiometric reaction of Au(III) complexes and Ag salts

The exact nature of the catalytically-active species in the Au(III)-mediated cycloisomerisation and nucleophillic substitution reactions reported in Chapter 2 are not known. There is some contention about the role played by Au(III) in these reactions. It is known that Au(III) can be reduced to Au(I) during the course of reactions[1] and so Au(I) may be the catalytically active species in such processes. Both oxidation states could play a role, for example, Au(I) could be the active species where a soft π-acid is required (such as in cycloisomerisations), whereas Au(III) may be the active species where Lewis acidity is required (in neutral or cationic form).[2] Nolan[3] has stated that he suspects that the active catalyst in the reported hydration of alkynes and polymerisation of styrene mediated by the parent [$AuBr_3$(NHC)] complexes is actually an Au(I) species formed by reductive elimination of the halide ligands. A series of studies were therefore carried out to determine whether $Au(I)^+$ or $Au(III)^+$ is the catalytically active species in the cycloisomerisation and nucleophillic substitution reactions in the presence of [$AuBr_2$(*N*-imidate)(NHC)] complexes (**66**-**68**) and silver salts.

It was noticed during catalysis experiments that when [$AuBr_2$(*N*-succ)(I^tPe)] (**67a**) was mixed with one equivalent of AgOTf in CH_2Cl_2 a yellow precipitate was formed (this was not observed with complexes with more electron withdrawing imidates). The yellow colour of the solid suggests it is an Au(III) species and the low solubility suggests a new complex. Presumably an ionic complex, [AuBr(*N*-succ)(I^tPe)]X (**285**) (where X is an anion, such as $^-$OTf), has formed by extraction of a bromide ligand by Ag^+. This precipitate was isolated by filtration and, due to lack of solubility in non-coordinating and instability in coordinating solvents, it was analysed by solid state IR spectroscopy. This showed that the precipitate has a 46 cm^{-1} lower carbonyl stretching frequency (1619 cm^{-1}) than [$AuBr_2$(*N*-succ)(I^tPe)] (**67a**) (1665 cm^{-1}) (Table 61). This frequency is even lower than that of [Au(*N*-succ)(I^tPe)] (**56a**) at 1631 cm^{-1}.

This is surprising, as it would be expected that, following the trend of oxidation from Au(I) to Au(III), the wavenumber would increase due to a more electropositive Au atom if an Au(III) cation had formed. This is because electron density from the nitrogen lone pair

would be donated into the Au-N, rather than the succinimidate C-N, bond which would consequently reduce electron density in the C=O bond. This is supported by X-ray diffraction data in the I^{t}Bu analogues **55a** and **66a**. The Au(I) complex [Au(*N*-succ)(I^{t}Bu)] (**55a**) C=O bond is on average 0.013 Å longer than in the Au(III) complex [AuBr$_2$(*N*-succ)(I^{t}Bu)] (**66a**) (although this is not statistically significant). This anomaly could be explained by the theory of Adams, Dubuc and Zakrewski,[4] which states that as the ionic component of the metal imidate bond increases (due to a harder metal centre) then more electron density is localised on the imidate nitrogen, rather than into the metal imidate bond, which results in a weaker C=O bond. This theory explains why imidate complexes have C=O stretching frequencies 54-59 cm^{-1} lower than the free imides.

Table 61. Carbonyl bond IR stretching frequencies of [Au(*N*-succ)(I^{t}Pe)] (**55a**), [AuBr$_2$(*N*-succ)(I^{t}Pe)] (**66a**) and [AuBr(*N*-succ)(I^{t}Pe)]X (**285**).

Entry	Complex	Carbonyl stretching frequency (cm^{-1})	
		Solid	Solution (CH_2Cl_2)
1	[Au(*N*-succ)(I^{t}Pe)] (**55a**)	1631	1644
2	[AuBr$_2$(*N*-succ)(I^{t}Pe)] (**66a**)	1665	1663
3	[AuBr (*N*-succ)(I^{t}Pe)]X (**285**)	1619	insoluble

It was found that if a coordinating species, such as pyridine, was added to the solution then the precipitate dissolved. In order to try to characterise this species (**285**), believed to be [AuBr(*N*-succ)(I^{t}Pe)][OTf], by NMR spectroscopy [AuBr$_2$(^{15}*N*-succ)(I^{t}Pe)] (**73**) was treated with one equivalent of AgOTf in CD_2Cl_2. The resulting precipitate dissolved on addition of one equivalent of pyridine. ^{15}N NMR spectroscopy revealed a single (low resolution) peak (179.5 ppm) corresponding to the parent complex (179.4 ppm). It would appear that the addition of pyridine converts the new species back to the parent complex, suggesting that [AuBr(*N*-succ)(I^{t}Pe)][OTf] formation by irreversible bromide extraction had not occurred. It is also possible that the pyridine solubilises the AgBr side product allowing the reverse reaction to take place, if this is the case then it would suggest that there would be an equilibrium between [AuBr(*N*-succ)(I^{t}Pe)][OTf] / AgBr and [AuBr$_2$(*N*-succ)(I^{t}Pe)] / AgOTf.

In order to monitor the formation of cationic Au species in solution the reaction of Au complexes and silver salts was monitored by proton NMR spectroscopy. Spectra of **55b**, **67a**, **67c**, **56g** and **67g** in combination with AgOTf and Ag[Al(OC(CF$_3$)$_3$)$_4$] (**76**) were taken over time. The I^{t}Pe imidazole proton signals were followed as these are the most characteristic and most sensitive to changes in the Au electronic configuration. Initially spectra were run in d$_6$-acetone to increase the solubility of the silver salts and any ionic species that are formed (Figure 56).

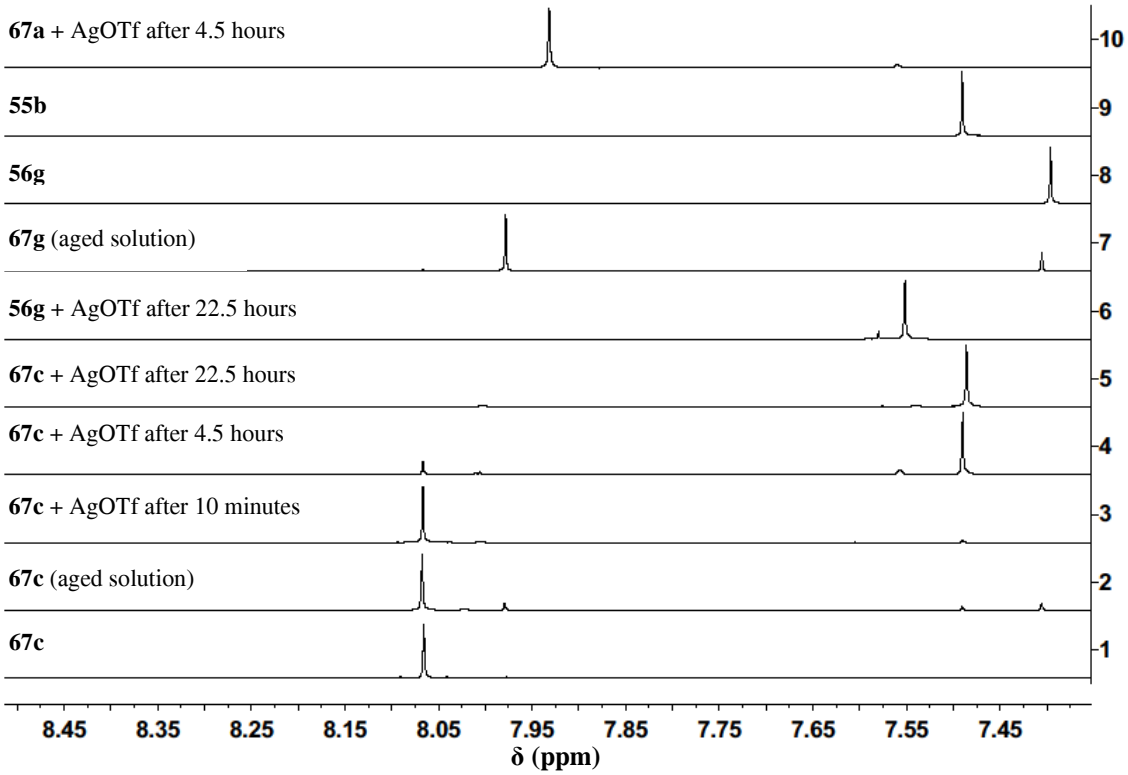

Figure 56. Reaction of **67c** and AgOTf in d$_6$-acetone over time (monitoring the I^{t}Pe imidazole proton signal by ^{1}H NMR spectroscopy, referenced to the residual d$_5$-acetone solvent signal at 2.05 ppm).

The [AuBr(I^{t}Pe)] (**56g**) imidazole signal shifts 0.15 ppm downfield on treatment with AgOTf, which is presumably due to the quantitative formation of an [Au(I^{t}Pe)]$^+$ species (**286**). [AuBr$_2$(*N*-tfs)(I^{t}Pe)] (**67c**) in the presence of AgOTf however degrades almost quantitatively to [Au(*N*-tfs)(I^{t}Pe)] (**56b**) with no observable formation of an Au(III) cationic species, although with a trace amount of the [Au(I^{t}Pe)]$^+$ (**286**) species observable after 4.5 hours. These results would suggest that Br$_2$ is formed {the final solution is brown

and added 1-hexene is brominated to form 1,2-dibromohexane (*vide infra*)}. Ageing of [$AuBr_3$(I^tPe)] (**67g**) over 48 hours in solution in the absence of AgOTf resulted in significant decomposition to **56g**. Ageing of **67c** led to slow formation of **56b**, **56g** and **67g**. [$AuBr_2$(*N*-succ)(I^tPe)] (**67a**) was also treated with AgOTf, only **67a** and the formation of trace **286** were observed.

^{19}F NMR spectroscopy was used to monitor the tetrafluorosuccinimidate ligand fluorine signal (Figure 57). Loss of the signal relating to **67c** occurs along with the formation of **56b**, however a second minor signal at -128.1 ppm, which may relate to free tetrafluorosuccinimidate (or *N*-bromotetrafluorosuccinimide), is observed. Interestingly, this peak has maximum intensity after 4.5 hours and then is reduced after 22.5 hours. A possible explanation is that the free ligand recombined with [Au(I^tPe)]$^+$ (**286**) to form **56b** {or exchanged with [Au(I^tPe)Br] (**56g**)}. This would suggest that reduction of **67c** to **56b** occurs *via* loss of tetrafluorosuccinimidate anion or *N*-bromotetrafluorosuccinimidate. A small amount of hydrolysed tetrafluorosuccinimidate was also observed.

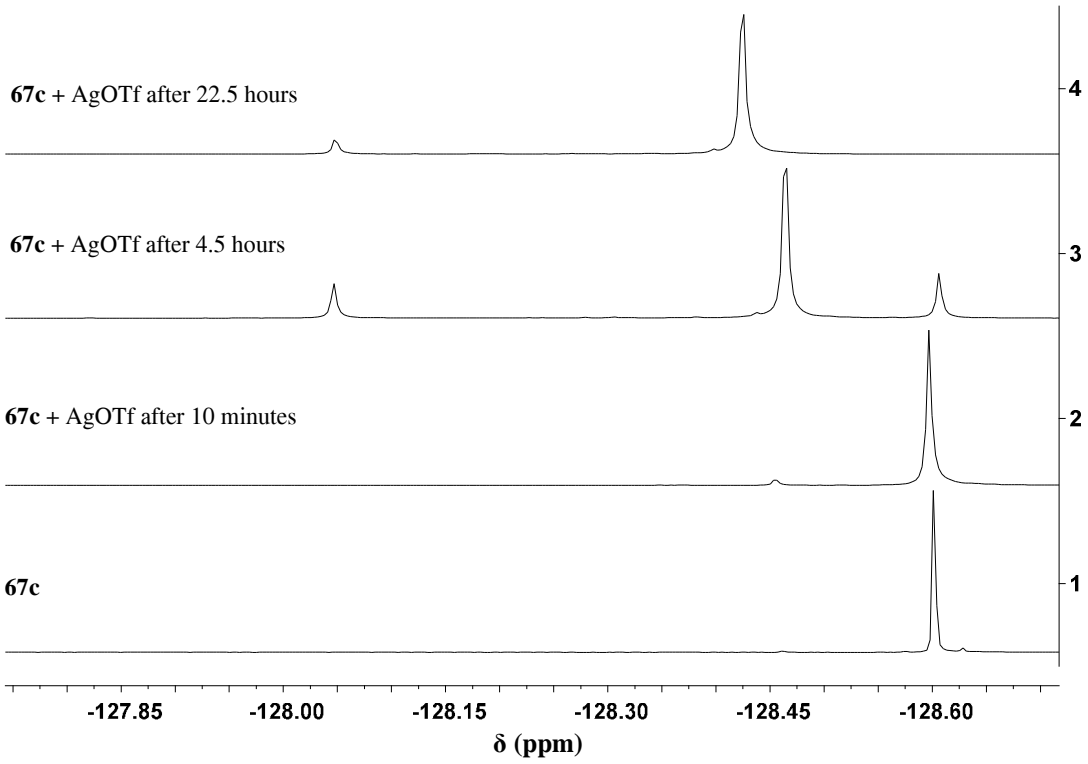

Figure 57. Reaction of **67c** and AgOTf in d_6-acetone over time (monitoring the tfs fluorine signal by ^{19}F NMR spectroscopy).

The same experiment was carried out using Ag[Al(OC(CF$_3$)$_3$)$_4$] (**76**) as the silver source which gives almost identical results (Figure 58). However, there is an additional unidentified broad signal in the Au(I) imidazole region for **67c**.

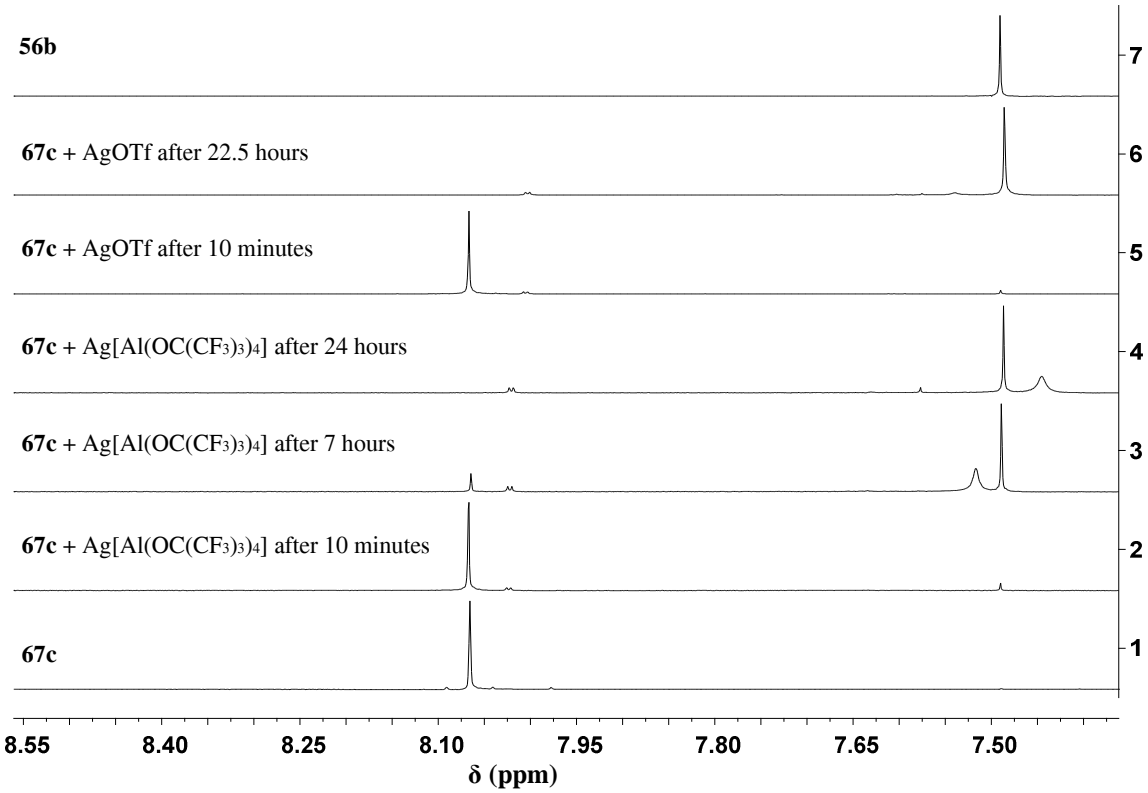

Figure 58. Reaction of **67c** and Ag[Al(OC(CF$_3$)$_3$)$_4$] (**76**) in d$_6$-acetone over time (monitoring the I^{t}Pe imidazole proton signal by ^{1}H NMR spectroscopy, referenced to the residual d$_5$-acetone solvent signal at 2.05 ppm).

In the presence of Ag[Al(OC(CF$_3$)$_3$)$_4$] (**76**) the ^{19}F spectrum again shows the loss of the [AuBr$_2$(*N*-tfs)(I^{t}Pe)] (**67c**) and growth of the [Au(*N*-tfs)(I^{t}Pe)] (**56b**) signal, however the peak at -128.0 ppm is much more significant accounting for more than half of the fluorine signal after 24 hours (Figure 59). This may indicate that the broad signals observed in the ^{1}H spectrum are Au(I) signals from [Au(I^{t}Pe)]$^+$ (**286**) and [AuBr(I^{t}Pe)] (**56g**) species.

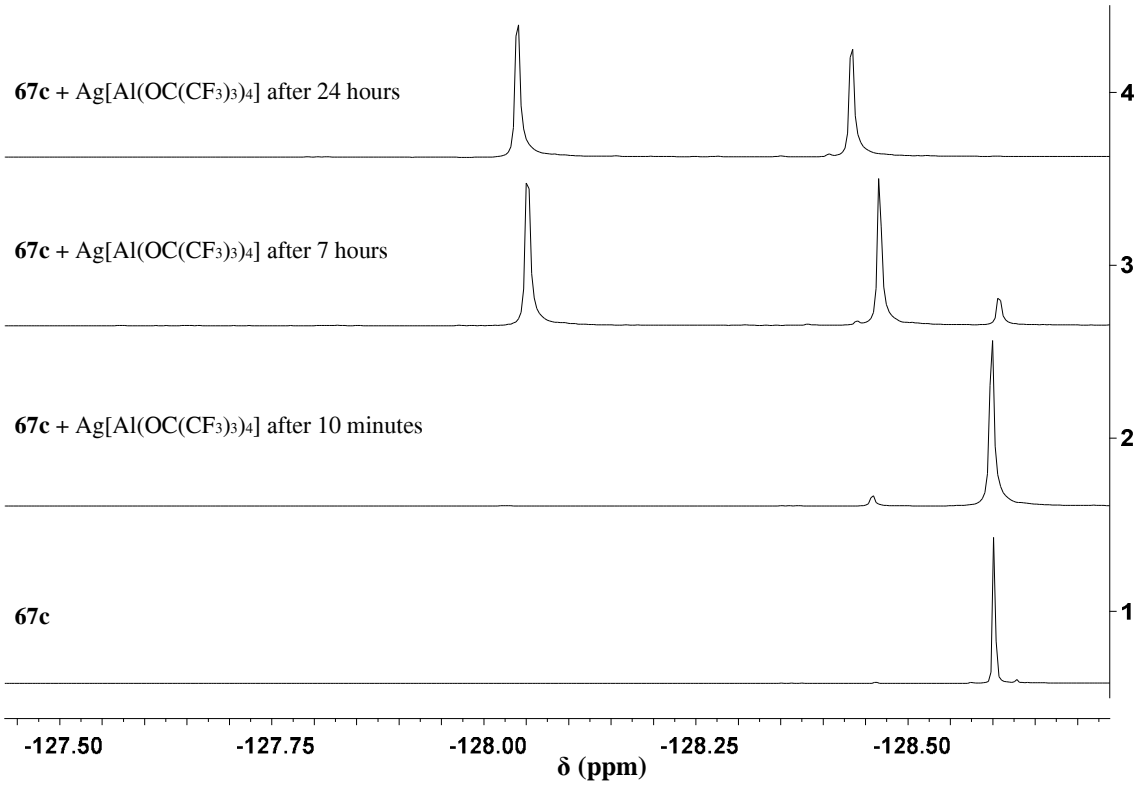

Figure 59. Reaction of **67c** and Ag[Al(OC(CF$_3$)$_3$)$_4$] (**76**) in d$_6$-acetone over time (monitoring the tfs fluorine signal by ^{19}F NMR spectroscopy, referenced to the residual d$_5$-acetone solvent signal at 2.05 ppm).

The experiment was repeated using a 3:1 mixture of CD_2Cl_2 and CD_3CN as solvent, CD_3CN was added to help solubilise ionic species. In this case complex **67c** appears to be relatively stable over 24 hours in the presence of AgOTf and Ag[Al(OC(CF$_3$)$_3$)$_4$] (**76**), with little decomposition over a 24 hour period. There is a small shift in the signal position depending on the silver salt added, possibly due to a close interaction between the silver salt and gold complex (Figure 60). In order to test this theory **67c** was treated with 0.5 equivalents of AgOTf. This gave only one peak, although it was broader than the control and the signal seen with one equivalent of AgOTf and intermediate between them in chemical shift, suggesting this variability is due to an interaction with the silver salt.

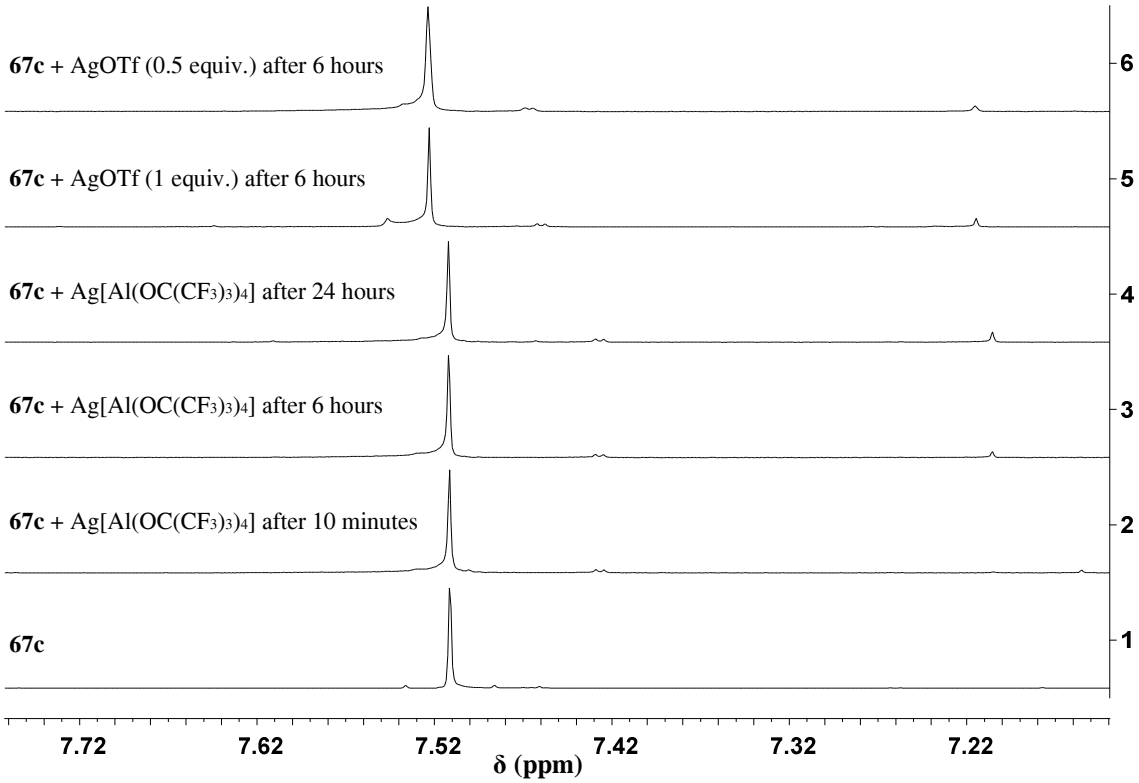

Figure 60. Reaction of **67c** with AgOTf or Ag[Al(OC(CF_3)$_3$)$_4$] (**76**) in 3:1 CD_2Cl_2:d_3-MeCN over time (monitoring the I^{t}Pe imidazole proton signal by ^{1}H NMR spectroscopy, referenced to the residual $CDHCl_2$ solvent signal at 5.31 ppm).

The ^{19}F NMR spectra do not show any significant change over the timeframe, however there is a small **56b** signal, suggesting slow decomposition (Figure 61). There is a small shift in the ^{19}F signal when **67c** is treated with 1 equivalent rather than 0.5 equivalents of AgOTf. This signal also has a small shoulder that could be a new Au(III) species forming by interaction with the silver salt. When 2 equivalents of AgOTf were used the same result was observed but there was also a small amount of an Au(I) species formed.

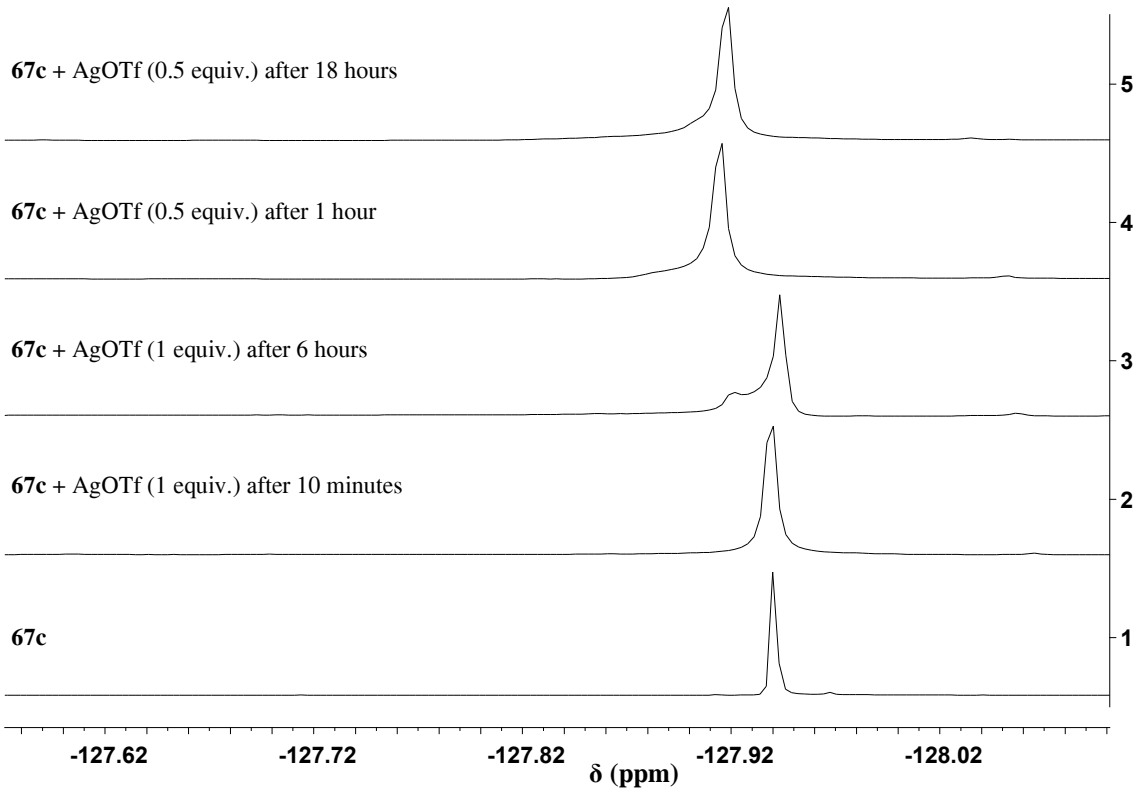

Figure 61. Reaction of **67c** and AgOTf in 3:1 CD_2Cl_2:d_3-MeCN over time (monitoring the tfs fluorine signal by ^{19}F NMR spectroscopy).

Overall these experiments do not provide evidence for the formation of an $Au(III)^+$ species, although there is some evidence for interaction between **67c** and the silver salts. In the CD_2Cl_2/d_3-MeCN solvent system the complexes are stable over 24 hours in the presence of silver salts, however the nucleophilic substitution and cycloisomerisation reactions proceed to completion during this time frame, suggesting either the catalytic species is in trace concentration {as would be expected if the $[Au(III)]^+$/AgBr is in equilibrium with [Au(III)]Br/Ag^+ (*vide supra*)} or that the organic reactants are involved in catalyst activation. In the d_6-acetone solvent system a relatively rapid decomposition of **67c** to **56b** was observed, with some evidence for $[Au(I^tPe)]^+$ (**286**) formation particularly in the presence of $Ag[Al(OC(CF_3)_3)_4]$ (**76**). As **56b** is catalytically inactive small amounts of **286** may be the active catalyst in the cycloisomerisation reactions, but another species must mediate the nucleophillic substitution reactions.

A1.2. Binding of 1-hexene to Au and Ag cations

Binding of 1-hexene[5] and other alkenes and alkynes to Au(I) complexes has been observed spectroscopically and crystallographically.[6] However, there have been no reports of binding to Au(III) and so complexes **67a** and **67c** was treated with 1-hexene and AgOTf in order to observe the effect of the alkene on catalyst activation and to monitor any binding of the alkene to the Au species. The complexes [$AuBr_2$(*N*-tfs)(I^tPe)] (**67a**) and [$AuBr_2$(*N*-tfs)(I^tPe)] (**67c**) and one equivalent of AgOTf were mixed in CD_2Cl_2 for one hour before addition of 1-hexene (1 and 2 equivalents), ^{1}H NMR was then used to monitor the reaction (Figure 62), allowing comparison to the reported Au(I) 1-hexene complex, [Au(μ_2-H_2C=CHC_4H_9)(IPr)][SbF_6] (**287**).[5]

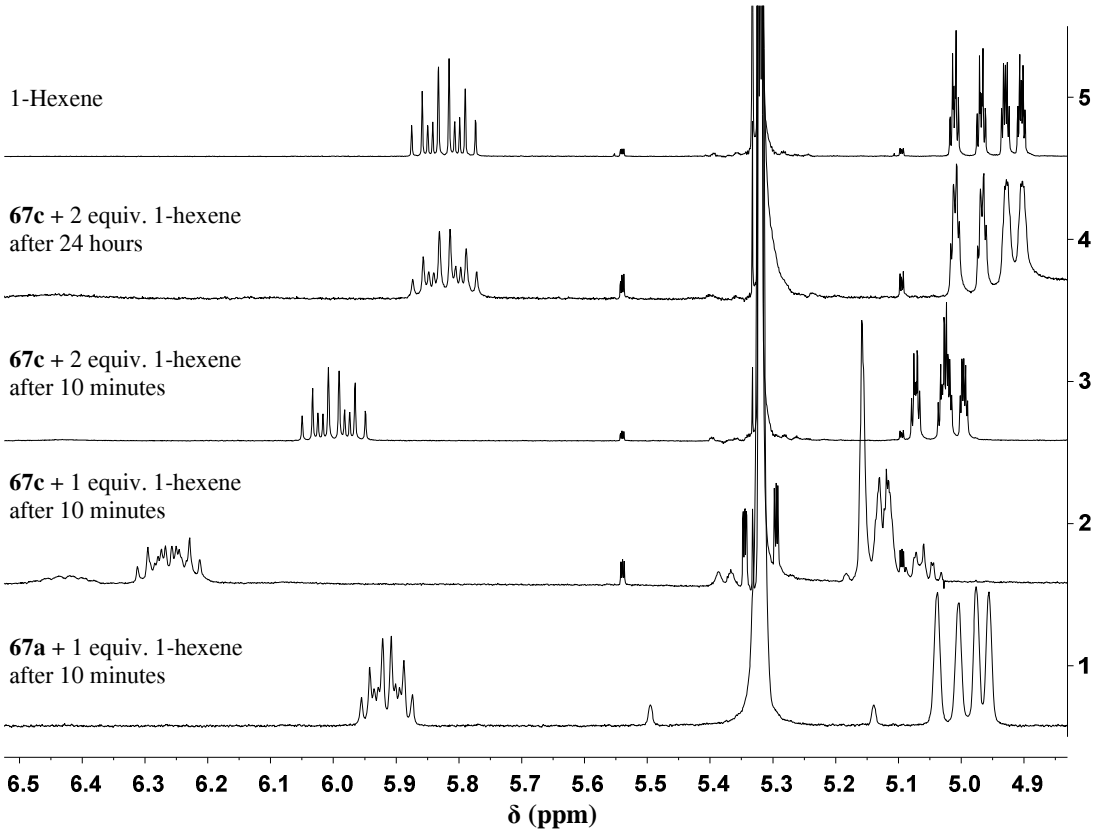

Figure 62. ^{1}H NMR spectra of complexes **67a** and **67c** when treated with AgOTf and 1-hexene in CD_2Cl_2, after 10 minutes and 24 hours (referenced to the residual $CDHCl_2$ solvent signal at 5.31 ppm).

The spectra show that no binding occurs to the neutral Au(III) imidate complexes in the absence of AgOTf (Table 62). Upon mixing of **67a** and AgOTf the expected yellow precipitate formed, addition of 1-hexene (1 equivalent) resulted in settling of the

precipitate. The imidazole signal did not change but there was a small downfield shift (0.09 ppm) in the 1-hexene signals with no change in coupling constants. This shift is typical of simple alkenes bound to a metal where there is little π-back donation from the metal to the alkene antibonding orbitals and is consistent with the reported Au(I) 1-hexene complex.[5] In the reported complex **287** the coupling constants of the alkene protons are reduced by up to 2 Hz, as would be expected due to π-back donation which would increase the p character of the orbitals.

For complex **67c** in the presence of 1 equivalent of 1-hexene and AgOTf there is again no change in the imidazole signal but the alkene signals are shifted even further downfield, by up to 0.44 ppm. Coupling constants of 18.0 Hz for the *trans* coupling and 8.7 Hz for the *cis* coupling were observed. This increased shift relative to **67a** would be expected as the more electron deficient **67c** adduct would withdraw more electron density from the alkene. For complex **67c** in the presence of AgOTf and 2 equivalents of 1-hexene the alkene signals shift downfield by up to 0.18 ppm, with little change in coupling constants relative to free 1-hexene.

Table 62. ^{1}H NMR chemical shifts and coupling constants of 1-hexene alkene proton A in the presence of **67a**, **67c** and AgOTf and for reported complex **287**.[a]

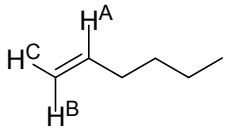

Entry	Complex/ Salt	Equiv. of 1-hexene	δ H^A (ppm)	Coupling constants (Hz)[b]
1	-	-	5.82	17.0, 10.1, 6.7
2	[$AuBr_2$(*N*-tfs)(I^tPe)] (**67c**)	1	5.82	17.0, 10.1, 6.7
3	AgOTf	2	6.21	17.7, 8.9, 6.6
3	[$AuBr_2$(*N*-succ)(I^tPe)] (**67a**) + AgOTf	1	5.91	17.0, 10.0, 6.7
4	[$AuBr_2$(*N*-tfs)(I^tPe)] (**67c**) + AgOTf	1	6.26	18.0, 8.7, 6.5
5	[$AuBr_2$(*N*-tfs)(I^tPe)] (**67c**) + AgOTf	2	6.00	17.0, 10.1, 6.7
6	[Au(μ_2-H_2C=CHC_4H_9)(IPr)][SbF_6] (**287**)	1	6.05	17, 9, 4.5

[a] In CD_2Cl_2 at 400 MHz. [b] Signal observed as a ddt.

Control tests however suggest that the 1-hexene alkene shifts observed in the presence of **67a**, **67c** and AgOTf may be due to Ag^+ binding, with the coupling constants and chemical shifts varying upon the relative amounts of Ag^+ and 1-hexene in solution (reported to bind in a 1:2 ratio) (Figure 63).[7]

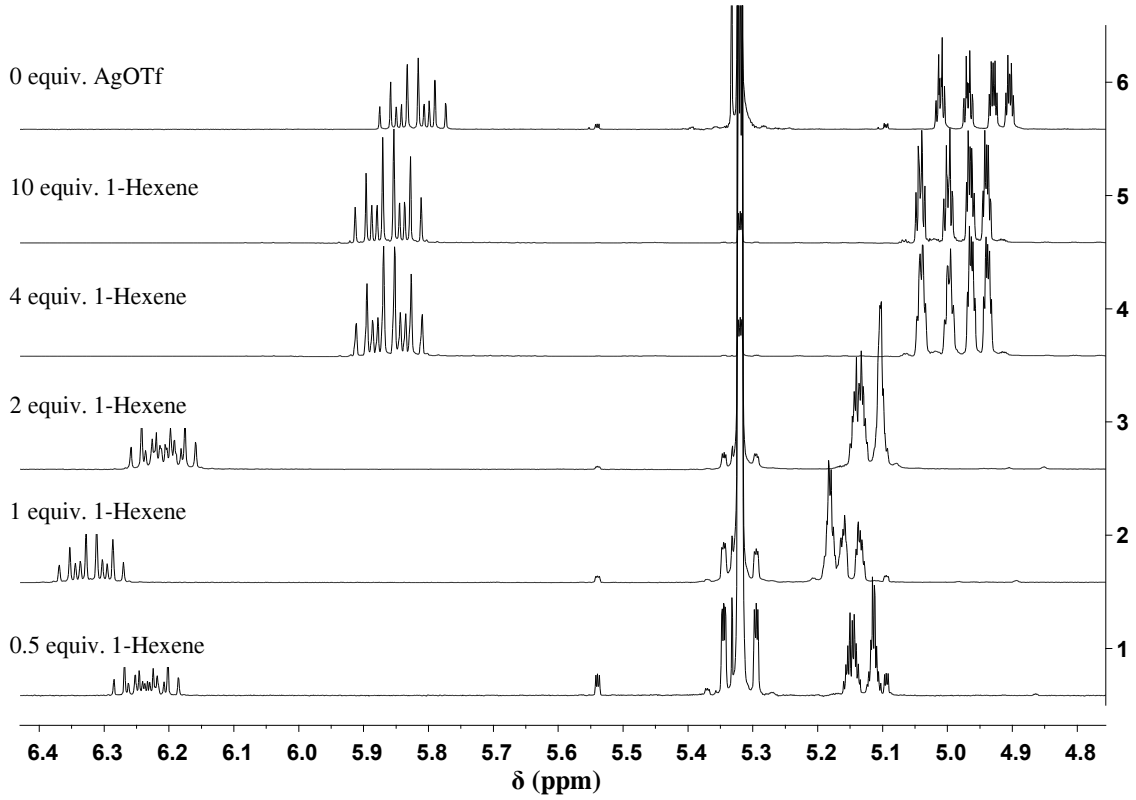

Figure 63. 1-Hexene alkene ^1H NMR signals when treated with increasing equivalents of of AgOTf in CD_2Cl_2 (referenced to the residual $CDHCl_2$ solvent signal at 5.31 ppm).

An additional spectrum of 2 equivalents of 1-hexene in the presence of **67c** and AgOTf was taken after 24 hours and the spectrum had changed significantly, with a number of small I^{t}Pe imidazole signals corresponding to Au(I) and Au(III) species and also a large broad signal (80% of the total imidazole signal) in the Au(I) region. This was also accompanied by a very broad signal (4.45-4.09 ppm) in the 1-hexene alkene region suggesting a fluxional Au(I) alkene complex, of either **56b** or [Au(I^{t}Pe)]$^+$ (**286**). There were also signals corresponding to free 1-hexene and a new set corresponding to 1,2-dibromohexane (about 50% abundance compared to free 1-hexene). There was now no evidence of 1-hexene binding to Ag^+ suggesting this would now have formed AgBr. The ^{19}F NMR spectrum also showed a very large broad signal (-182.2 ppm) suggesting the observed alkene complex is that of **56b**.

These results again do not provide evidence of an $Au(III)^+$ alkene complex, and only Ag^+ binding can be assumed. The alkene does however mediate the relatively rapid decomposition of **67c** to **56b** (not observed in the absence of alkene in CD_2Cl_2), forming a fluxional complex with **56b** and the production of bromine which is trapped by bromination of the alkene. This demonstrates that the unsaturated reagents in the reaction mixture are involved in the solubilisation of the silver salt and the mediation of the decomposition of the Au complex and presumably the formation of the active catalytic species.

Attempts were made to obtain crystals of the complexes in the presence of alkenes and pyridine and silver salts, however these were unsuccessful and resulted in decomposition over time rather than crystal formation.

A1.3. References

(1) (a) Hashmi, A. S. K.; Blanco, M. C.; Fischer, D.; Bats, J. W. *Eur. J. Org. Chem.* **2006**, 1387-1389; (b) Morita, N.; Krause, N. *Eur. J. Org. Chem.* **2006**, 4634-4641; (c) Komiya, S.; Kochi, J. K. *J. Am. Chem. Soc.* **1976**, *98*, 7599-7607; (d) Komiya, S.; Albright, T. A.; Hoffmann, R.; Kochi, J. K. *J. Am. Chem. Soc.* **1976**, *98*, 7255-7265.

(2) Hashmi, A. S. K. *Angew. Chem., Int. Ed.* **2008**, *47*, 6754-6756.

(3) Gaillard, S.; Slawin, A. M. Z.; Bonura, A. T.; Stevens, E. D.; Nolan S. P. *Organometallics* **2010**, *29*, 394-402.

(4) (a) Roundhill, D. M. *Inorg. Chem.* **1970**, *9*, 254-258; (b) Carturan, G.; Belluco. V.; Grazini, M.; Ros, R. *J. Organomet. Chem.* **1976**, *112*, 243-248; (c) Adams, H.; Bailey, N. A.; Briggs, T. N.; McCleverty, J. A.; Colquhoun, H. M.; Williams, D. J. *J. Chem. Soc. Dalton Trans.* **1986**, 813-819; (d) Zakrzewski, J. *J. Organomet. Chem.* **1989**, *359*, 215-218; (e) Dubuc, I.; Dubois, M-A.; Bélanger-Gariépy, F.; Zargarian, D. *Organometallics* **1999**, *18*, 30-35.

(5) Brown, T. J.; Dickens, M. G.; Widenhoefer, R. A. *J. Am. Chem. Soc.* **2009**, *131*, 6350-6351.

(6) (a) Lavallo, V.; Frey, G. D.; Donnadieu, B.; Soleilhavoup, M.; Bertrand, G. *Angew. Chem., Int. Ed.* **2008**, *47*, 5224-5228; (b) Herrero-Gómez, E.; Nieto-Oberhuber, C.; López, S.; Benet-Buchholz, J.; Echavarren, A. M. *Angew. Chem., Int. Ed.* **2006**, *45*, 5455-5459; (c) Dias, H. V. R.; Wu. J. *Eur. J. Inorg. Chem.* **2008**, 509-522; (d) Brown, T. J.; Dickens, M. G.; Widenhoefer, R. A. *Chem. Commun.* **2009**, 6451-6453; (e) Cinellu, M. A.; Minghetti, G.; Cocco, F.; Stoccoro, S.; Zucca, A.; Manassero, M. *Angew. Chem., Int. Ed.* **2005**, *44*, 6892-6895.

(7) Sunderrajan, S.; Freeman, B. D.; Hall, C. K. *Ind. Eng. Chem. Res.* **1999**, *38,* 4051-4059.